

**First Report of the  
Technical Committee on  
Ground Improvement and Geosynthetics  
Indian Geotechnical Society, New Delhi**

**Members of the Committee:**

Prof. G. L. Sivakumar Babu (Chairman), IISc, Bangalore

Prof. G. Madhavi Latha (Convenor), IISc, Bangalore

Prof. M. R. Madhav, J.N.T.U. College of Engineering, Hyderabad

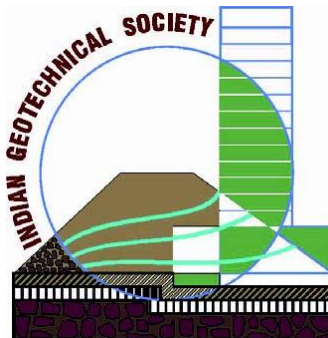
Prof. K. Rajagopal, IIT Madras

Prof. Satyendra Mittal, IIT Roorkee

Prof. D L Shah, M.S.U., Vadodara

Mr. Y. Hari Krishna, Keller Ground Engineering India Pvt. Ltd.

Ms. Minimol Korulla, Maccaferri Environmental Solutions Pvt. Ltd.



**14 November 2016**

**This report contains 446 pages including the cover page**

## Contents

Technical Note on Ground Improvement using Vibro  
Compaction and Stone Columns: Theory & Practice

*-by Keller Ground Engineering India Pvt. Ltd.*

Monograph on Granular Piles and Granular Pile Anchors

*-by Madhav Madhira and Vidyaranya Bandi*

Guidelines for Soil Nailing Technique in Highway Engineering  
Applications

*-by G L Sivakumar Babu*

Technical Note on Ground Improvement using Deep Soil Mixing:  
Theory & Practice

*-by Keller Ground Engineering India Pvt. Ltd.*

Technical Note on Ground Improvement using Grouting  
Techniques: Theory & Practice

*-by Keller Ground Engineering India Pvt. Ltd.*

GEOSYNTHETICS – Glossary & Description

*-by K. Rajagopal*

Design Monograph for Design of Shallow Foundation with  
Geosynthetics

*-by Satyendra Mittal*

Cellular Confinement Systems

*-by Gali Madhavi Latha*

Ground improvement Case studies

*-by Maccaferri Environmental Solutions Pvt. Ltd.*



---

## TABLE OF CONTENTS

<b>1</b>	<b>Background</b> .....	<b>1</b>
1.1	General .....	1
1.2	Technical Committee .....	1
1.3	Brainstorming Session.....	1
<b>2</b>	<b>Deep Vibro Techniques</b> .....	<b>1</b>
2.1	Ground improvement in cohesive and mixed soil.....	1
2.2	Ground Improvement in granular soil .....	2
<b>3</b>	<b>Theory and design approach</b> .....	<b>3</b>
3.1	Vibro Replacement Technique .....	3
3.1.1	Corrections for improvement factor .....	4
3.1.2	Correction for column compressibility .....	5
3.1.3	Correction for Overburden.....	5
3.2	Vibro Compaction .....	6
<b>4</b>	<b>Construction methodology</b> .....	<b>7</b>
4.1	Vibro Replacement .....	7
4.2	Vibro Compaction .....	7
<b>5</b>	<b>Applications and Limitations</b> .....	<b>8</b>
<b>6</b>	<b>Proven performance</b> .....	<b>9</b>
6.1	Case study 1: Settlement control.....	9
6.2	Case study 2: To improve bearing capacity .....	10
6.3	Case study 3: Liquefaction mitigation.....	12
6.4	Case study 4: Enhancement of Lateral Capacity .....	13
<b>7</b>	<b>Observations &amp; suggestions on IS 15284 – Part 1</b> .....	<b>14</b>
<b>8</b>	<b>Bibliography</b> .....	<b>14</b>

## LIST OF FIGURES

Figure 1:	Basic principle of Vibro replacement technique .....	2
Figure 2:	Basic principle of Vibro compaction technique .....	3
Figure 3:	Principle of Ground Improvement.....	3
Figure 4:	Unit cell of SC and typical arrangement of triangular and square grid .....	4
Figure 5:	Priebe's basic improvement factor (reproduced from Priebe, 1995) .....	4
Figure 6:	Consideration of column compressibility .....	5
Figure 7:	Determination of depth factor .....	6
Figure 8	Proposed initial trial points.....	6
Figure 9	Sequence of installation of vibro stone columns (dry bottom feed method).....	7
Figure 10	Sequence of vibro compaction process.....	8
Figure 11	Results of Single column load test and post construction settlements .....	10
Figure 12	Completed view of building.....	10
Figure 13	Typical soil profile and Cross section of Stone column below the tank.....	11
Figure 14	Long term observed settlement .....	11
Figure 15	Completed view of plant .....	12
Figure 16	Compaction in progress & post treatment subsidence.....	12
Figure 17	Pre and post treatment CPT results & plate load test results.....	13
Figure 18:	Typical soil profile .....	13
Figure 19:	Vibro stone columns surrounding BCIS piles .....	14
Figure 20:	Lateral load test on BCIS piles .....	14

## LIST OF TABLES

**No table of figures entries found.**

---

---

## LIST OF ENCLOSURES

- Annexure 1 Technical paper on “Design of Vibro Stone Columns” (1995) & Technical paper on “Vibro replacement to prevent earthquake induced liquefaction” by Heinz J. Priebe (1998)
- Annexure 2 Technical paper on “Optimal Foundations in Soft Ground: An Innovative Approach for Economizing Cost and Time”
- Annexure 3 Technical paper on “Vibro Stone Columns to Support Large Oil Storage Tank Farm on West Coast of India”
- Annexure 4 Technical paper on “Ground Improvement Solutions to Mitigate Liquefaction: Case Studies”
- Annexure 5 Technical paper on “Ground Improvement Using Vibro Techniques in Flyash Deposits”
- Annexure 6 Observations on IS 15284 part 1 Rev 1
-

## **1 Background**

### **1.1 General**

The President Indian Geotechnical Society (IGS) has constituted several Technical Committees (TCs) in order to contribute substantial technical innovations to serve the geotechnical community by publishing guidelines in the field of ground engineering. In this endeavour, IGS formed various TCs to seek support in the preparation of guidelines and publish them on behalf of IGS. In order to form the guidelines, the modus operandi suggested by IGS was to conduct brain-storming sessions in local chapters in each of the selected themes and topics and further to record the proceedings. Each member of the committee shall have to make a presentation followed by a detailed discussion. The chairman of each TC will decide the sub-topics on which the theme paper will be presented by a particular member of the committee, followed by a thorough discussion. The individual TC will develop guidelines with regard to various fields of Geotechnology on behalf of IGS who will contribute in a meaningful way to better geotechnical practices in India.

### **1.2 Technical Committee**

With the above background, IGS has identified Ground Improvement and Geosynthetics is one of the TC and the main objective is to prepare an implementable document for practicing engineers covering Ground Improvement technology, limitations, codal provisions, case histories esp. in India with their performances.

### **1.3 Brainstorming Session**

IGS Hyderabad Chapter has taken initiative to support IGS and conducted one day National Workshop on Ground Improvement and Geosynthetics on 29<sup>th</sup> August 2015 in JNTU premises. Minutes of meeting was prepared and circulated among the TC members. It was agreed in the meeting that design and construction aspects of ground improvement using deep vibro techniques shall be addressed by Keller Ground Engineering Pvt. Limited (Keller).

This document describes concept, theory (developed by Keller), design & construction, performance of ground improvement (esp. deep vibro techniques) for variety of projects executed in India.

## **2 Deep Vibro Techniques**

Ground Improvement is a technique that improves the engineering properties of the weak soil mass treated. Usually, the engineering properties that are improved due to ground improvement are shear strength, stiffness and permeability. Ground improvement has been developed into a sophisticated tool to support foundations for a wide variety of structures. Properly applied, i.e. after giving due consideration to the nature of the ground being improved and the type and sensitivity of the structures being built, ground improvement often reduces direct costs and saves precious construction time.

### **2.1 Ground improvement in cohesive and mixed soil**

Vibro techniques are accepted method of subsoil improvement, in which large-size columns of coarse grained material are installed in the soil by means of high capacity depth vibrators. Performance of this composite system consisting of stone columns as reinforcing elements and the weak soil mass that can be established theoretically can be established by full size field plate load tests.

---

Ground improvement using vibro stone columns have been profoundly increased on local soils (cohesive and mixed soils) which are unable to take large foundation loads. Typically stone column consists of a vertical reinforcement introduced by constructing a column of densely packed stones partially or fully replacing the local weak soil. The construction can either by wet or by dry method. The inclusion of stone columns in a specific grid pattern allows the soil mass behaves like a homogenous layer of improved density and stiffness. This process yields enhancement of load bearing capacity and minimizes the settlements of the treated ground compared to the untreated ground.

Stone columns acts as drainage path allowing for rapid consolidation which in turn improves the strength and deformation characteristics of the ground at a much faster rate. Stone columns constructed using vibro techniques allows full or partial displacement instead of partial or full replacement of the weak soil and then leads to further improvement of displaced weak soil by faster dissipation of construction pore water pressure. Also, the improved drainage capabilities of the stone column treated ground provide a much better resistance to liquefaction of the surrounding soil. The resistance to liquefaction is achieved by densification of surrounding weak soil and also by the much increased capacity for faster dissipation of excess pore water pressure.

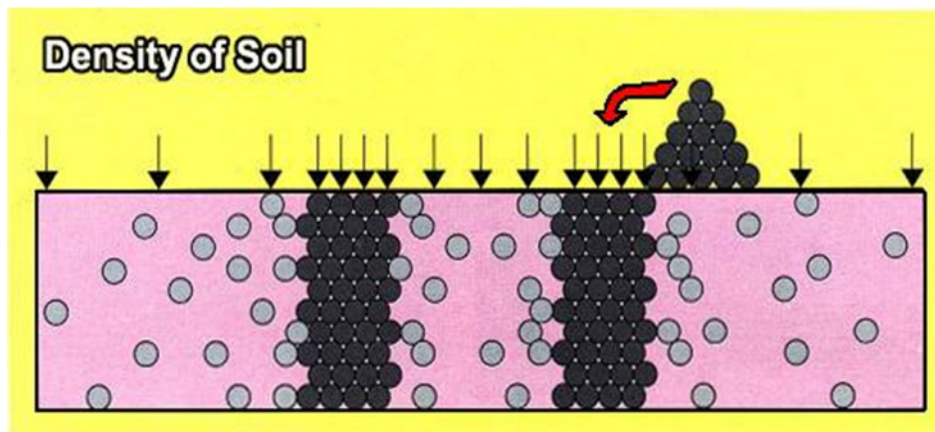


**Figure 1: Basic principle of Vibro replacement technique**

## 2.2 Ground Improvement in granular soil

Vibro Compaction is a technique developed by Keller in the 1930's, designed to induce compaction of granular materials at depth. The basic principle behind the process is that particles of non-cohesive soils can be rearranged into a denser state by means of vibration. A Schematic showing Vibro Compaction technique is shown in Figure 2.

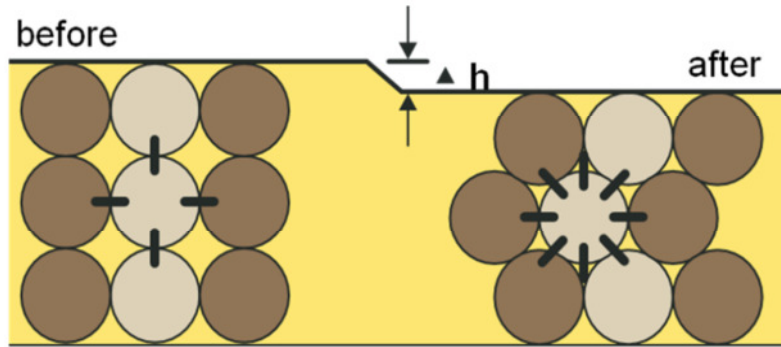


Figure 2: Basic principle of Vibro compaction technique

### 3 Theory and design approach

#### 3.1 Vibro Replacement Technique

Priebe (1995) developed design of vibro stone columns considering a unit cell loaded vertically which can be adopted to different soil conditions. It overcomes the traditional limitation of a stone column being analysed as an isolated column, loaded only on its head.

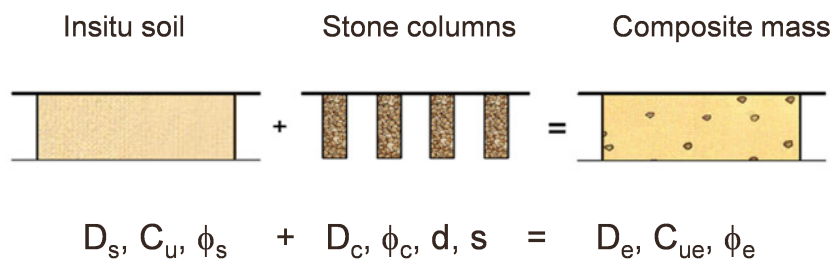
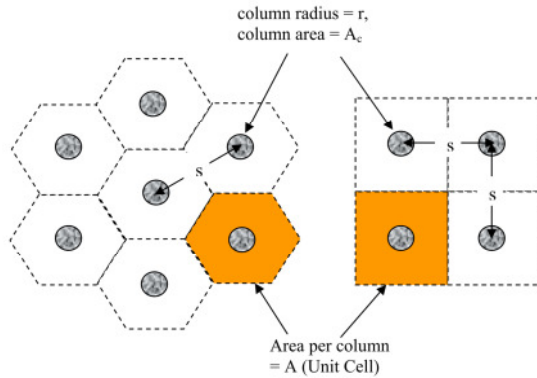


Figure 3: Principle of Ground Improvement

Contrary to vibro compaction which densifies non-cohesive soils due to vibrations, vibro replacement improves cohesive and non-cohesive soils by reinforcing the weak soil with load bearing columns of well compacted, coarse grained material. When the entire weak soil is replaced with a well compacted coarser material, there is no complexity in the understanding of its improved load carrying capacity and corresponding deformations. But, when the weak soil is partially replaced and displaced by the introduction of these stiffer reinforcing elements at regular grid patterns, response of this modified ground becomes complex. There are ways for arriving at an equivalent stiffness matrix of a system that replaces some part with a material of larger stiffness.

Similarly, there are ways and means to establish the modified density and stiffness when the entire soil mass is densified. When the improvement is attributed to both displacement and replacement, the quantification of improvement is difficult to determine. Considerable efforts like large-scale load tests can only prove the effectiveness of the installed stone columns. In a first step, an improvement factor is established by which stone columns improve the performance of the subsoil in comparison to the state without columns just by increasing the overall stiffness. The grid patterns and concept of unit cell is illustrated in Figure 4. Basic improvement factor can be arrived based on the area replacement ratio and the reinforcing material used for stone columns.



**Figure 4: Unit cell of SC and typical arrangement of triangular and square grid**

Improvement factor is presented in Figure 5. According to this improvement factor, the deformation modulus of the composite system can be established due to which settlements will be reduced. Priebe's method is a unit cell approach, which takes into account oedometric conditions. This is very important because the direct use of Priebe's composite parameters for slope stability results in an un-conservative safety factor.

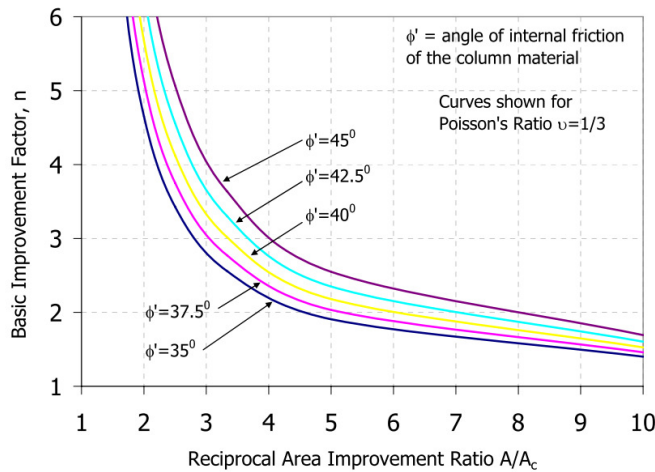


**Figure 5: Priebe's basic improvement factor (reproduced from Priebe, 1995)**

The deformation modulus of the composite system is one of the basic inputs for finalizing the design of stone columns. However, the reality is that in many practical cases the reinforcing effect of stone columns installed by vibro replacement is superposed with the densifying effect of vibro compaction, i.e. the installation of stone columns densifies the soil between grids increasing its  $k_o$  and  $k_p$ . In such case, the densification of the soil has to be evaluated on the basis of original soil data and correspondingly the design of vibro replacement can be modified to suit particular improved site condition.

The basic improvement factor ( $n_0$ ) shall be calculated using the formula.

$$n_0 = 1 + \frac{A_c}{A} \cdot \left[ \frac{5 - A_c/A}{4 \cdot K_{ac} \cdot (1 - A_c/A)} - 1 \right]$$

### 3.1.1 Corrections for improvement factor

Since the column cannot fail in end bearing and any settlement of the load area results in a bulging of the column which remains constant all over its length. The following two corrections need to be applied for improvement factor to get appropriate value.

- Correction for column compressibility
- Correction for overburden

### 3.1.2 Correction for column compressibility

In the case of soil replacement, the actual improvement factor does not achieve an infinite value as determined theoretically for non-compressible material, but it coincides with at best with the ratio of the constrained moduli of column material and soil. Due to compressibility of column material the area of column may get increase and the improvement factor will be reduced. The improvement factor after compressibility correction can be calculated using following relation and Figure 6.

$$n_1 = 1 + \frac{\overline{A}_c}{A} \cdot \left[ \frac{1/2 + f(\mu_s, \overline{A}_c/A)}{K_{ac} \cdot f(\mu_s, \overline{A}_c/A)} - 1 \right]$$

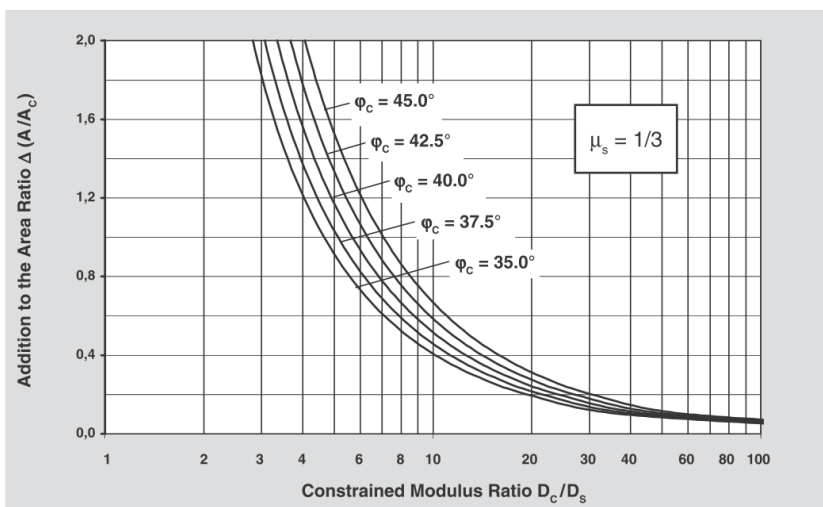


**Figure 6: Consideration of column compressibility**

### 3.1.3 Correction for Overburden

As a result of column installation, the external loads the weights of the columns  $W_c$  and of the soil  $W_s$  which possibly exceed the external loads considerably, has to be added. Under consideration of these additional loads the initial pressure difference decreases asymptotically and the bulging is reduced correspondingly. In other words, with increasing overburden the columns are better supported laterally and therefore, can provide more bearing capacity.

Since the pressure difference is a linear parameter in the derivations of the improvement factor, the ratio of the initial pressure difference and the one depending on depth expressed as depth factor  $f_d$  delivers a value by which the improvement factor  $n_1$  increases to the final improvement factor  $n_2 = f_d \cdot n_1$  on account of the overburden pressure.

$$f_d = \frac{1}{1 + \frac{K_{oc} - 1}{K_{oc}} \cdot \frac{\Sigma(\gamma_s \cdot \Delta d)}{p_c}}$$

$$n_2 = f_d \cdot n_1$$

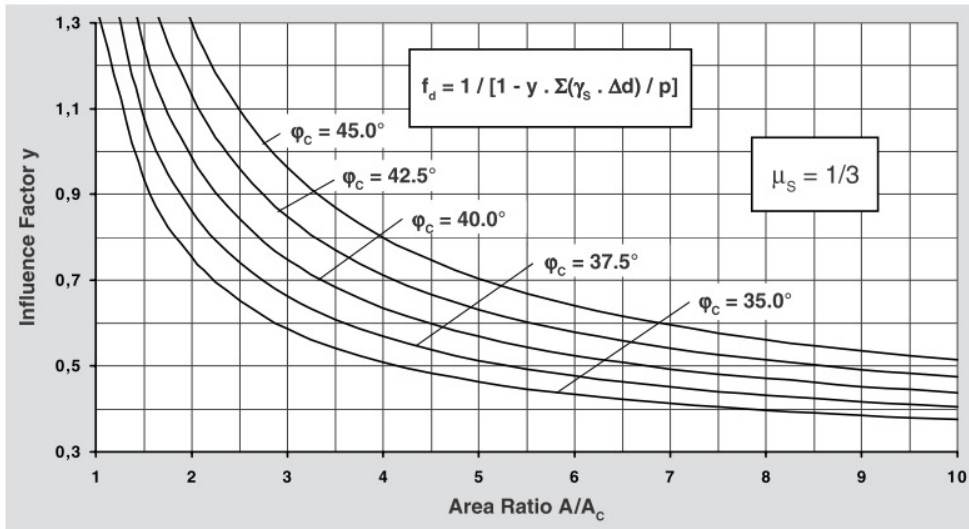


**Figure 7: Determination of depth factor**

The technical paper on “Design of Vibro Replacement” by Heinz J Priebe is enclosed in **Annexure 1**.

### 3.2 Vibro Compaction

Field trials will be carried out prior to the main works to determine the working parameters for Vibro compaction process. A level area of 50m x 50m, to carry out a field trial and necessary area to set-up the plant & equipment is required. The site should preferably be in the vicinity of the main works area. The site will be levelled (by others) prior to commencement of trial works.

The vibro compaction will be carried out at selected trial area by trail & error method with different design parameters like spacings, vibration (amplitude) time & depth of treatment. The typical plan view of initial trial area is shown in Figure 8.

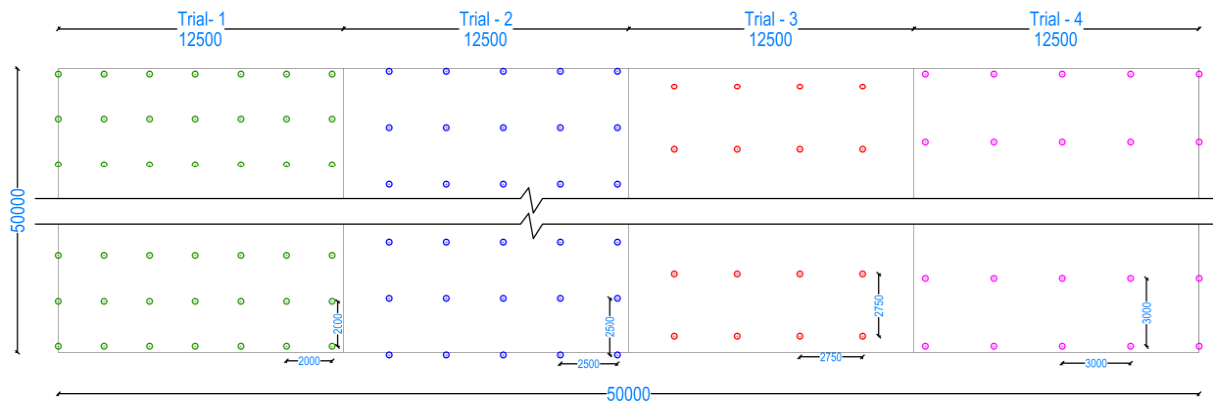


**Figure 8 Proposed initial trial points**

Based on the trial results, the required operating parameters, spacings, quality control procedures, etc. for the vibro compaction will be established and same shall be adopted for main works.

## 4 Construction methodology

### 4.1 Vibro Replacement

Keller has developed the system of custom-built machine called the Vibrocat for installation of vibro stone columns without using water. The Vibrocat comprises a specially constructed track mounted supporting unit, attached with high capacity depth vibrator, which incorporates a stone tube with compression chamber and stone feed hopper ensures properly formed compacted stone columns to the required diameter and depth. A special feature of the dry method is that it does not require water jetting for penetration and hence eliminates the need to handle the collected water.

Furthermore this method can be used most successfully where limited working space is available, especially in developed or urban areas or where no near water source can be found. This technique provides effective drainage paths to ensure rapid consolidation. It also has a built-in real time computer monitoring system to provide quality control on compaction effort throughout the construction process. Sequence of installation of vibro stone columns using dry bottom feed method is illustrated in Figure 9.

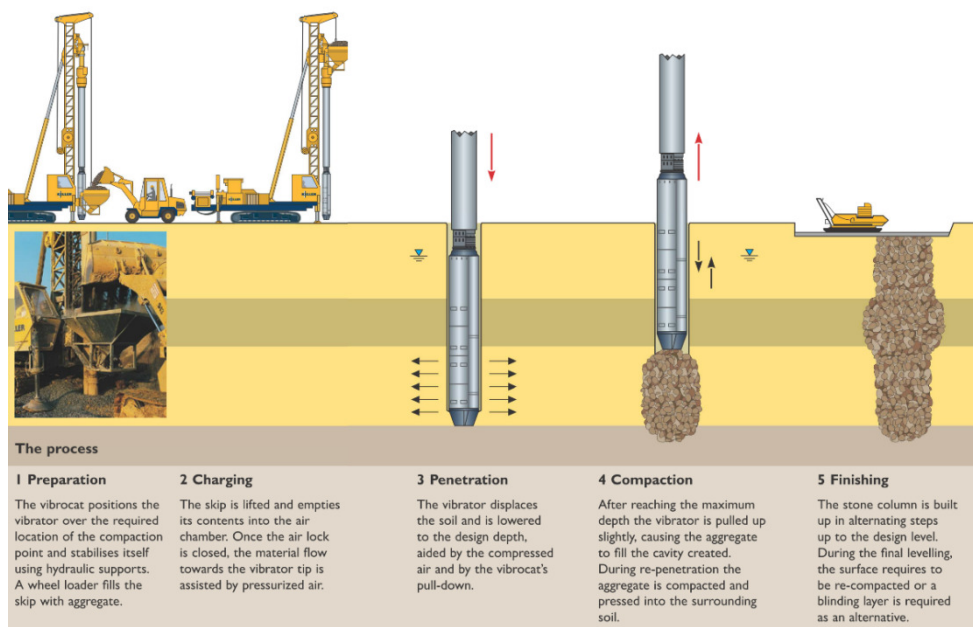


**Figure 9 Sequence of installation of vibro stone columns (dry bottom feed method)**

### 4.2 Vibro Compaction

The essential equipment for this process is a depth vibrator - a long, heavy tube enclosing eccentric weights, driven by an electric motor. The vibrator is connected to a source of electric power and a high-pressure water pump. Extension tubes are added as necessary, depending on the treatment depth, and the whole assemblage is suspended from a crane.

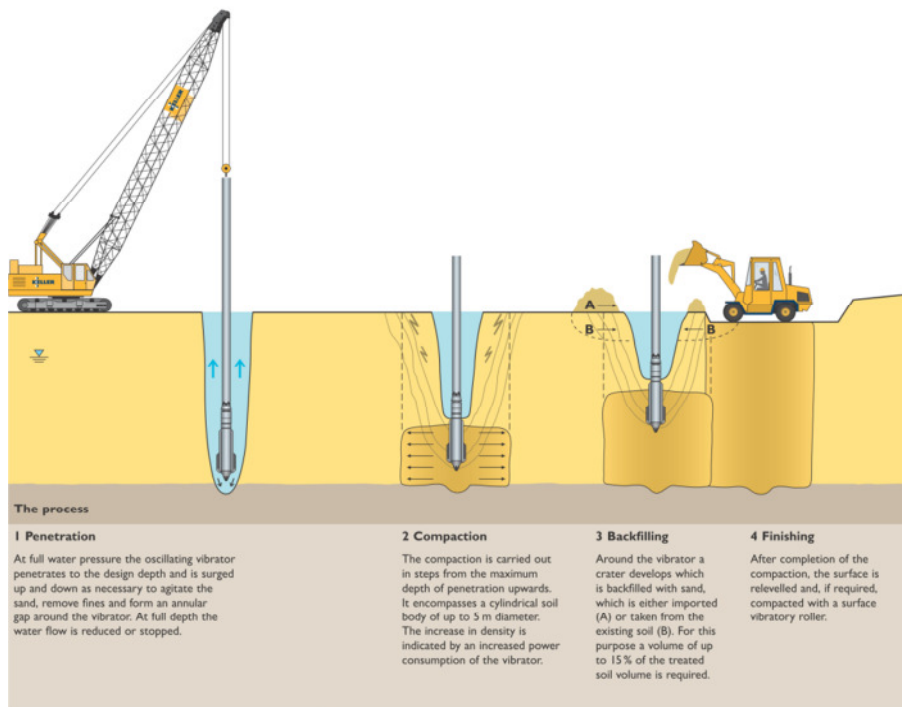


**Figure 10 Sequence of vibro compaction process**

With the electric power and water supply switched on, the vibrator is lowered into the ground. The combination of vibration and high-pressure water jetting causes liquefaction of the soils surrounding the vibrator, which assists in the penetration process. When the required depth is reached, the water pressure is reduced and the vibrator pulled up in short steps. With the inter-particle friction temporarily reduced, the surrounding soil particles then fall back below the vibrator and, subjected to vibratory energy, are rearranged into a denser state. This process is repeated back up to the ground level, leaving on completion, a column of very dense material surrounded by material of enhanced density. The degree of compaction achieved at a particular point depends on the properties of the soil being treated, the amount of time spent at each compaction step and the distance from the vibrator. Vibro compaction is suitable for treating sands with a fines content of less than 10 to 15%. The spacing of probes is designed to ensure that the zones of influence overlap sufficiently to achieve minimum requirements throughout the treated area.

Generally, the effect of the compaction becomes visible at the ground surface in the form of a cone-shaped depression. The depression formed around the vibrator or the extension tubes is continually in-filled with granular materials, which is either imported or obtained from the natural granular deposits at the site. Water required for the penetration and compaction process is obtained either by direct pumping from nearby water source or ground water using well points.

To check that minimum requirements are being met, the normal procedure is to carry out a series of post-compaction deep sounding tests.

## 5 Applications and Limitations

The ground improvement techniques can be adopted for the following ground engineering applications.

- Enhancing the bearing capacity of in-situ soil
- Controlling the larger total & differential settlement

- Mitigating liquefaction potential
- Enhancing lateral confinement for deep foundations

The Ground improvement using vibro replacement / vibro compaction methods being carried out by stone columns / sand, the following limitations are to be thought during design.

- The stone column / vibro compaction is brittle material which will not take any tensile or lateral forces and will take care of only vertical compressive loads.
- Though stone columns /vibro compaction points are carried out at regular intervals, it shall be assumed as the whole soil mass has been improved and same property need to be considered for design.

## **6 Proven performance**

### **6.1 Case study 1: Settlement control**

M/s Urban Tree Infrastructure Private Limited (Urban Tree), Chennai, proposed to develop a residential project in Chennai. The project comprises of 198 units of Stilt + 4 floors and the approximate area of development is about 2.5 acres.

The sub-soil in the project site comprises desiccated clay and medium dense sand up to about 3.50m followed by relatively weak clay and sandy clay up to 6.0m depth. This top 6.0m soil with highly varying consistency is followed by about 8.0m with medium dense sand stiff clay deposits after which there is a 6m thick layer of medium stiff consistency. Denser sand layers and hard clay layers are forming the remaining sub-soil profile. Required loading intensity of the proposed structure on the soft soil is 100kPa.

Considering the project boundary conditions, vibro replacement technique with 20% area replacement ratio (stone columns with dry bottom feed method) up to 6m depth was adopted as a viable method for subsoil improvement and a full raft foundation supported by the treated ground as an alternative foundation system.

Keeping the importance of the post construction performance of the structure, plate load test has been conducted on improved ground and also about 14 locations were identified on the raft foundation to monitor settlements during and post construction.

The results of post construction are shown below.

- Achieved bearing capacity : > 150kPa
- Long term settlement : < 50mm

The measured settlements are substantially lower than the predicted settlement, which proved the efficiency of the raft foundation resting on improved ground.

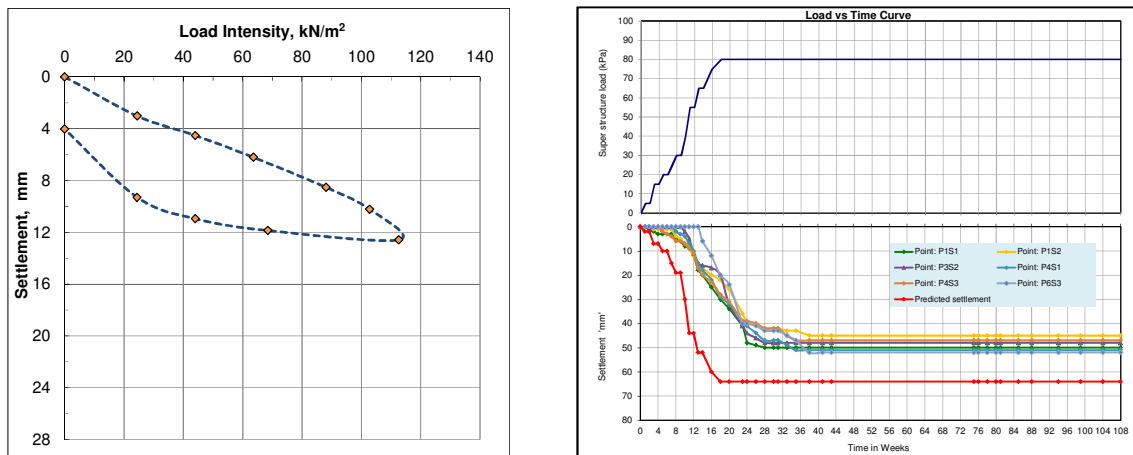


**Figure 11 Results of Single column load test and post construction settlements**



**Figure 12 Completed view of building**

The technical paper explaining project case study on settlement control for residential apartment is enclosed in **Annexure 2**.

## 6.2 Case study 2: To improve bearing capacity

M/s Hindustan Petroleum Corporation Ltd. proposed to develop a tank farm for 18 nos. of floating roof storage tank, 4 nos. of fixed roof storage tank and 3 nos. of fire water tank. The diameter of tank is 32m and height of tank is 15m.

The subsoil consist of top 2.5m flyash fill with the SPT N value NIL followed by soft silty clay of SPT N value of 7 up to 9m depth and this layer is underlain by medium dense sand of SPT 15 up to 25m depth.

The bearing capacity of virgin soil at foundation level of tank is 100kPa. The required bearing capacity of a tank foundation is 200kPa.

To improve the bearing capacity of virgin soil vibro replacement method 25% area replacement ratio up to the depth of 11.5m (stone column using wet top feed method) was proposed.

The typical soil profile and stone column cross section below the tank is shown in Figure 13.

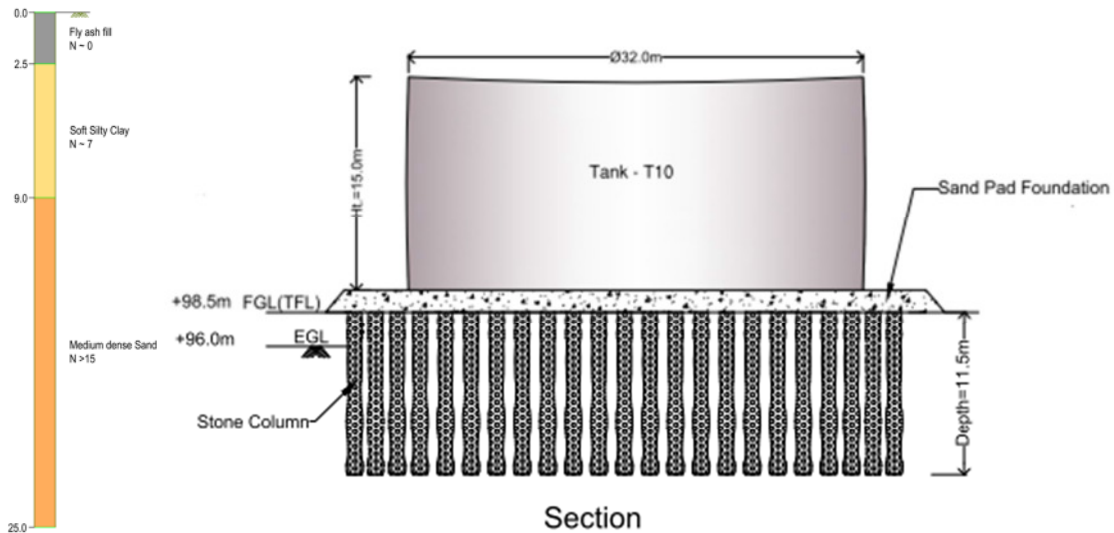


**Figure 13 Typical soil profile and Cross section of Stone column below the tank**

The results of post construction tests are described below.

- Improved bearing capacity : > 200kPa
- Hydro test with full load (water) was carried out and the settlement was recorded. The observed settlement is less than the allowable settlement of tank (< 300mm)

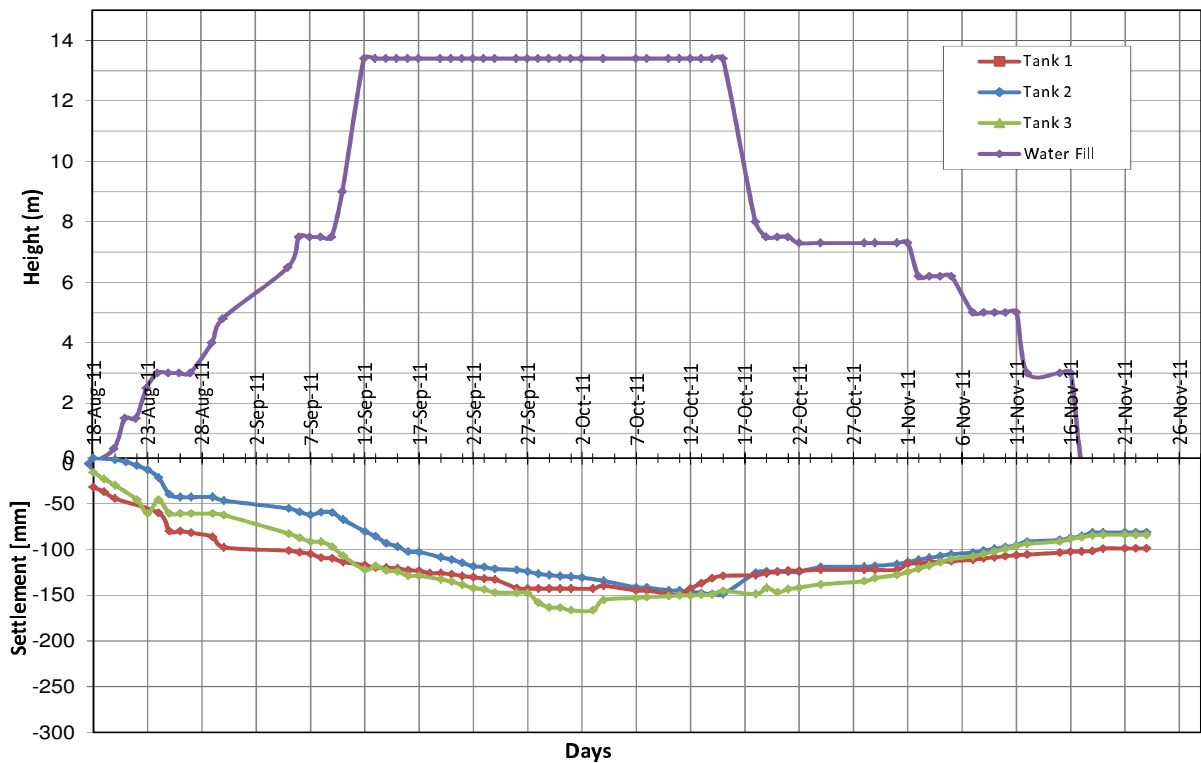


**Figure 14 Long term observed settlement**



**Figure 15 Completed view of plant**

The technical paper published on “Vibro stone columns to support large oil storage tank farms in India” is enclosed in **Annexure 3**.

### **6.3 Case study 3: Liquefaction mitigation**

M/s. GVK Power Ltd. developed the 2x270MW Coal based thermal power station at Goindwal sahib, Punjab and functioning since 2015. The power plant consist of various structures such as power house, boilers, ESPs, switch yard, cooling tower etc. and location comes under the seismic zone of IV with PGA of 2.4g. The subsoil consist of loose sand (relative density < 40%) with fines content 4% - 6% which has a chance of liquefaction.

Being sandy soil and fines content < 10%, vibro compaction method to a treatment depth of 10m was proposed to mitigate mainly liquefaction potential and enhancing bearing capacity of in-situ soil.

Post plate load test & post cone penetration test (CPT) has been carried out at main working area to access the performance of improved ground and results are satisfied as per design requirements.



**Figure 16 Compaction in progress & post treatment subsidence**

The results of improved ground are described as below.

- Relative density after improvement : > 70%
- Improved bearing capacity : > 200kPa
- Backfill consumption : 10%
- Observed subsidence : 1m

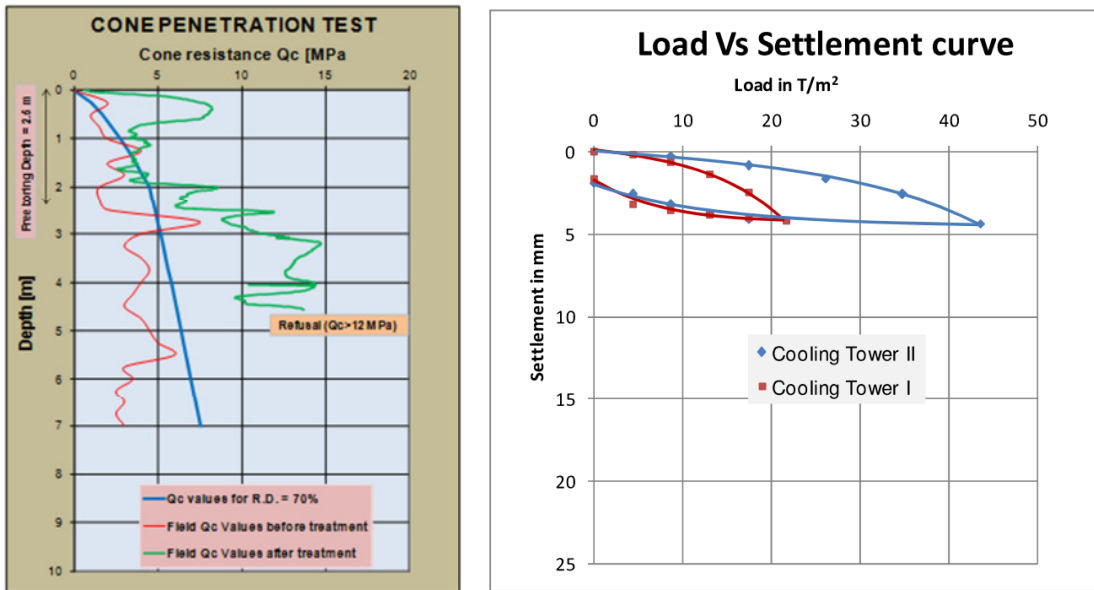


**Figure 17 Pre and post treatment CPT results & plate load test results**

The technical paper describing “Ground improvement solutions to mitigate liquefaction” adopted in India is enclosed in **Annexure 4**.

### 6.4 Case study 4: Enhancement of Lateral Capacity

2x500MW Thermal power plant was proposed at Anpara, Uttar Pradesh. The plant units such as switchyard, crusher house, conveyor and stacker reclaimer are planned to construct on old fly ash pond. The proposed site comprises of top 3 to 13m fly ash deposit followed by silty clay layer.

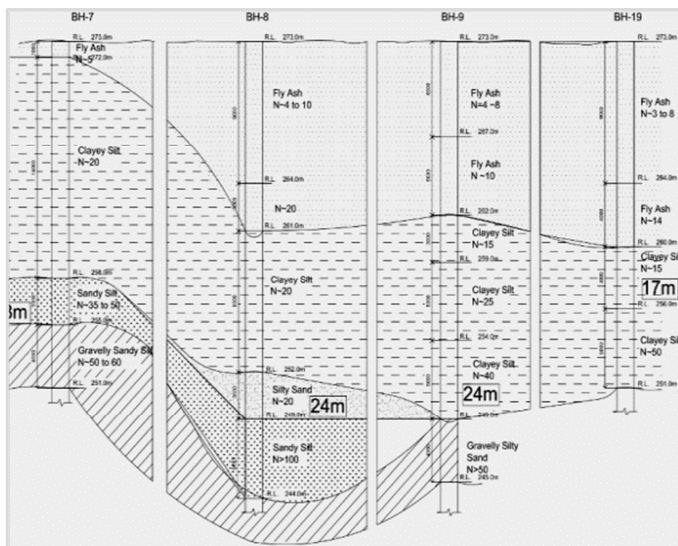


**Figure 18: Typical soil profile**

Because of fly ash deposit the required lateral capacity of pile i.e 7MT is not achieved. Ground improvement using Vibro stone columns are installed at specified pattern surrounding the bored cast-in-situ piles to enhance the density of fly ash deposits which in turn can improve the lateral load carrying capacity. It was required to achieve a design lateral load capacity of 7T with ultimate load of 21T. After the installation of bored cast-in-situ piles and vibro stone columns by bottom feed method, initial lateral load test are conducted on these two grid patterns as illustrated in Figure 19.

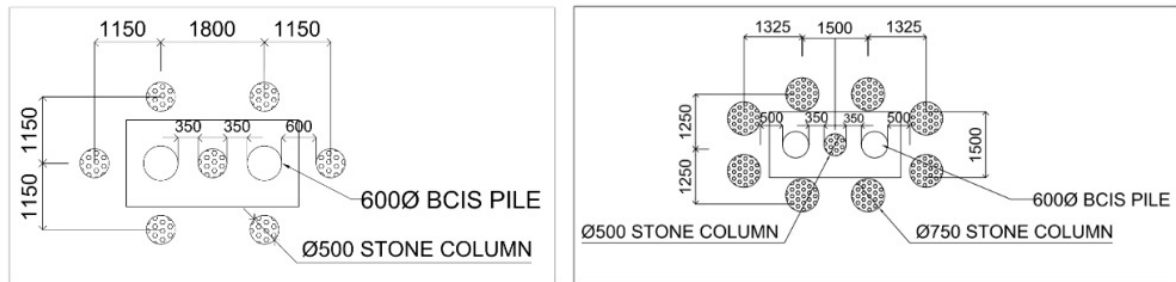


**Figure 19: Vibro stone columns surrounding BCIS piles**

The results of lateral load test on piles are presented in

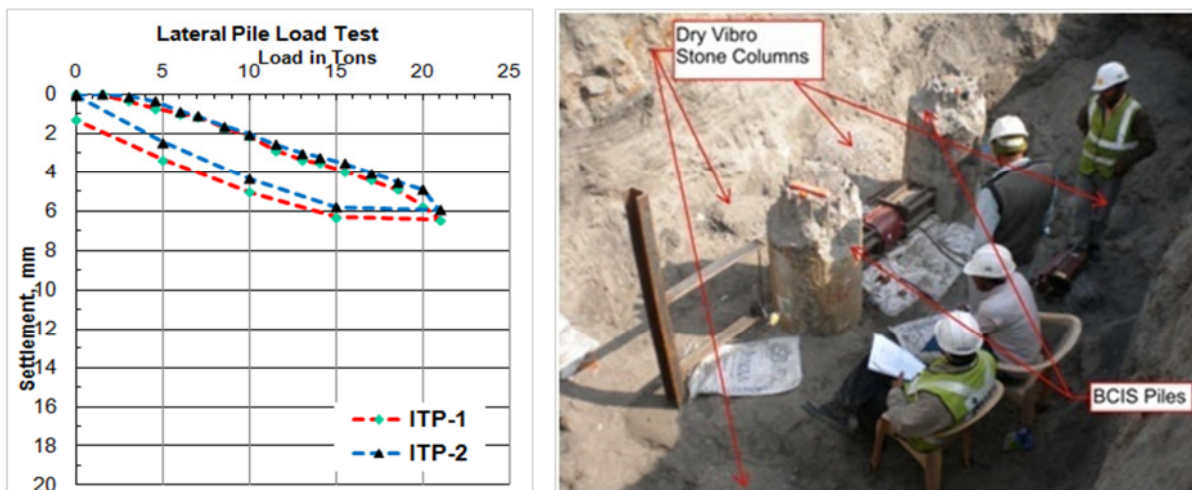


**Figure 20: Lateral load test on BCIS piles**

The results ground improvement are summarised below.

- Achieved lateral capacity : 10 MT
- Stone Column around the pile increases the lateral capacity.

The technical paper describing “Ground Improvement Using Vibro Techniques in Fly Ash Deposits” adopted in India is enclosed in **Annexure 5**.

## 7 Observations & suggestions on IS 15284 – Part 1

In the construction industry as ground improvement has become most common practice in the last 5 to 6 years, this is high time to prepare / revise standard for all types of ground improvement methods. All vibration methods like vibro compaction, vibro replacement and vibro displacement to be added in the present standard IS 15284 (part 1) or a separate standard on “Ground Treatment by Deep Vibrations” may be brought out (similar to BS). In the present standard (IS 15284 – part 1), the few points as appended in **Annexure 6** to be incorporated, which will give more clarity and useful for practicing engineers.

## 8 Bibliography

1. Hughes JMO & Withers N J, 1975, ‘Reinforcing of Soft Cohesive Soils with Stone Columns’, Ground Engineering, Volume 7, Issue No. 3.
2. Seed H.B., and Idriss, I.M (2001). Simplified procedure for evaluating soil liquefaction potential, J. Geotech Engineering. Div., ASCE 97 (9), 1249-1273

3. Seed et. al (2003). Recent advances in soil liquefaction engineering: A unified and consistent framework.
4. Priebe, H.J (1995), The Design of Vibro Replacement, Ground Engineering, December 1995.
5. Priebe, H.J (1998), Vibro Replacement to Prevent Earthquake Induced Liquefaction, Ground Engineering, September 1998.
6. Raju et. al. (2010). Some Environmental Benefits of Dry Vibro Stone Columns in a Gas Based Power Plant Project, Indian Geotechnical Conference, December 2010.
7. Article by Bedanga Bordoloi and Etali Sarmah on "Fly Ash Pond Reclamation" dated May 2010 for Agribusiness Forum.
8. "Study of Effectiveness of Ground Improvement Techniques and Possible Liquefaction Potential" for Anpara-D Thermal Power Project, Department of Earthquake Engineering, IIT Roorkee
9. Raju, V.R. & Sondermann, W., 2005. Ground Improvement using Deep Vibro Techniques. Ground Improvement Case Histories, Indraratna, B & Chu., J. (eds.), 601-638
10. Indian Standard Code (2003). "Design and construction for ground improvement - Guidelines, Part 1: Stone columns", IS 15284 (Part-1): 2003.
11. British Standard (2005). "Execution of Special Geotechnical Works - Ground Treatment By Deep Vibration", BS EN 14731-2005.
12. Building Research Establishment (2000) "Specifying Vibro Stone Columns", BRE - 391.

Annexure 1    Technical paper on “Design of Vibro Stone Columns” (1995) & Technical paper on “Vibro replacement to prevent earthquake induced liquefaction” by Heinz J. Priebe (1998)



# The design of vibro replacement

Dipl.-Ing. Heinz J. Priebe

*Keller Grundbau GmbH*

Presented by

**Keller Grundbau GmbH**

Kaiserleistr. 44

D-63067 Offenbach

Tel. 069 / 80 51 - 0

Fax 069 / 80 51 - 244

E-mail [Marketing@KellerGrundbau.com](mailto:Marketing@KellerGrundbau.com)

[www.KellerGrundbau.com](http://www.KellerGrundbau.com)

Reprint from:

**GROUND ENGINEERING**

December 1995

Technical paper 12-61 E

---

# The Design of Vibro Replacement

Heinz J. Priebe  
*Keller Grundbau GmbH*

Vibro Replacement is an accepted method for subsoil improvement, at which large-sized columns of coarse backfill material are installed in the soil by means of special depth vibrators. The performance of this composite system consisting of stone columns and soil, is not determinable by simple investigation methods like soundings, and therefore, such methods are not suitable for design purposes. However, theoretically, the efficiency of Vibro Replacement can be reliably evaluated. The method elaborated on a theoretical basis and described in this contribution, is easy to survey and adaptable to different conditions due to the separate consideration of significant parameters. Practically, it comprises design criteria for all frequently occurring applications.

## I Introduction

Vibro replacement is part of the deep vibratory compaction techniques whereby loose or soft soil is improved for building purposes by means of special depth vibrators. These techniques as well as the equipment required is comprehensively described elsewhere [1].

Contrary to vibro compaction which densifies noncohesive soil by the aid of vibrations and improves it thereby directly, vibro replacement improves non compactible cohesive soil by the installation of load bearing columns of well compacted, coarse grained backfill material.

The question to what extent the density of compactible soil will be improved by vibro compaction, depends not only on the parameters of the soil being difficult to determine, but also on the procedure adopted and the equipment provided. However, the difficulty of a reliable prognosis is balanced by the fact that the improvement achieved can be determined easily by soundings.

With vibro replacement the conditions are more or less reversed. Considerable efforts only like large-scale load tests can prove the benefit of stone columns. However, a reliable conclusion can be drawn about the degree of improvement which results from the existence of the stone columns only without any densification of the soil between. This is possible because the essential parameters attributable to the geometry of the layout and the backfill material can be determined fairly good. In such a prognosis the properties of the soil, the equipment and the procedure play an indirect role only and that is mainly in the estimation of the column diameter.

Basically, the design method described herewith was developed some twenty years ago and published already [3]. However, in the meantime it came to several adaptations, extensions and supplements which justify a new and comprehensive description of the method. Nevertheless, the derivation of the formulae is renounced with reference to literature.

It may be emphasized: The design method refers to the improving effect of stone columns in a soil which is otherwise unaltered in comparison to the initial state. In a first step a factor is established by which stone columns improve the performance of the subsoil in comparison to the state without columns. According to this improvement factor the deformation modulus of the composite system is increased respectively settlements are reduced. All further design steps refer to this basic value.

In many practical cases the reinforcing effect of stone columns installed by vibro replacement is superposed with the densifying effect of vibro compaction, i.e. the installation of stone columns densifies the soil between. In this cases, first of all the densification of the soil has to be evaluated and only then - on the basis of soil data adapted correspondingly - the design of vibro replacement follows.

Notation			
A	grid area	p	area load resp. foundation pressure
b	foundation width	s	settlement
c	cohesion	W	weight
d	improvement depth	$\alpha$	reduction faktor in earthquake design
$d_{Gr}$	depth of ground failure	$\gamma$	unit weight
D	constrained modulus	$\eta$	safety against ground failure
$f_d$	depth factor	$\mu$	Poisson´s ratio
K	coefficient of earth pressure	$\sigma_{of}$	bearing capacity
m	proportional load on stone columns	$\varphi$	friction angle
n	improvement factor		

Used subscripts, dashes and apostrophes follow from the context. Generally, subscript C means column and S means soil. With the exception of  $K_0$  as coefficient for earth pressure at rest ( $K_a$  for active earth pressure) subscript 0 means a basic respectively an initial value.

## 2 Determination of the Basic Improvement Factor

The fairly complex system of vibro replacement allows a more or less accurate evaluation only for the well defined case of an unlimited load area on an unlimited column grid. In this case a unit cell with the area **A** is considered consisting of a single column with the cross section **A<sub>C</sub>** and the attributable surrounding soil.

Furthermore the following idealized conditions are assumed:

- The column is based on a rigid layer
- The column material is incompressible
- The bulk density of column and soil is neglected

Hence, the column can not fail in end bearing and any settlement of the load area results in a bulging of the column which remains constant all over its length.

The improvement of a soil achieved at these conditions by the existence of stone columns is evaluated on the assumption that the column material shears from the beginning whilst the surrounding soil reacts elastically. Furthermore, the soil is assumed to be displaced already during the column installation to such an extent that its initial resistance corresponds to the liquid state, i. e. the coefficient of earth pressure amounts to  $K = 1$ . The result of the evaluation is expressed as basic improvement factor  $n_0$ .

$$n_0 = 1 + \frac{A_c}{A} \cdot \left[ \frac{1/2 + f(\mu_s, A_c/A)}{K_{ac} \cdot f(\mu_s, A_c/A)} - 1 \right]$$

$$f(\mu_s, A_c/A) = \frac{(1 - \mu_s) \cdot (1 - A_c/A)}{1 - 2\mu_s + A_c/A}$$

$$K_{ac} = \tan^2(45^\circ - \varphi_c/2)$$

A poisson's ratio of  $\mu_s = 1/3$  which is adequate for the state of final settlement in most cases, leads to a simple expression.

$$n_0 = 1 + \frac{A_c}{A} \cdot \left[ \frac{5 - A_c/A}{4 \cdot K_{ac} \cdot (1 - A_c/A)} - 1 \right]$$

The relation between the improvement factor  $n_0$ , the reciprocal area ratio  $A/A_c$  and the friction angle of the backfill material  $\varphi_c$  which enters the derivation, is illustrated in the well known diagram of *Figure 1*.

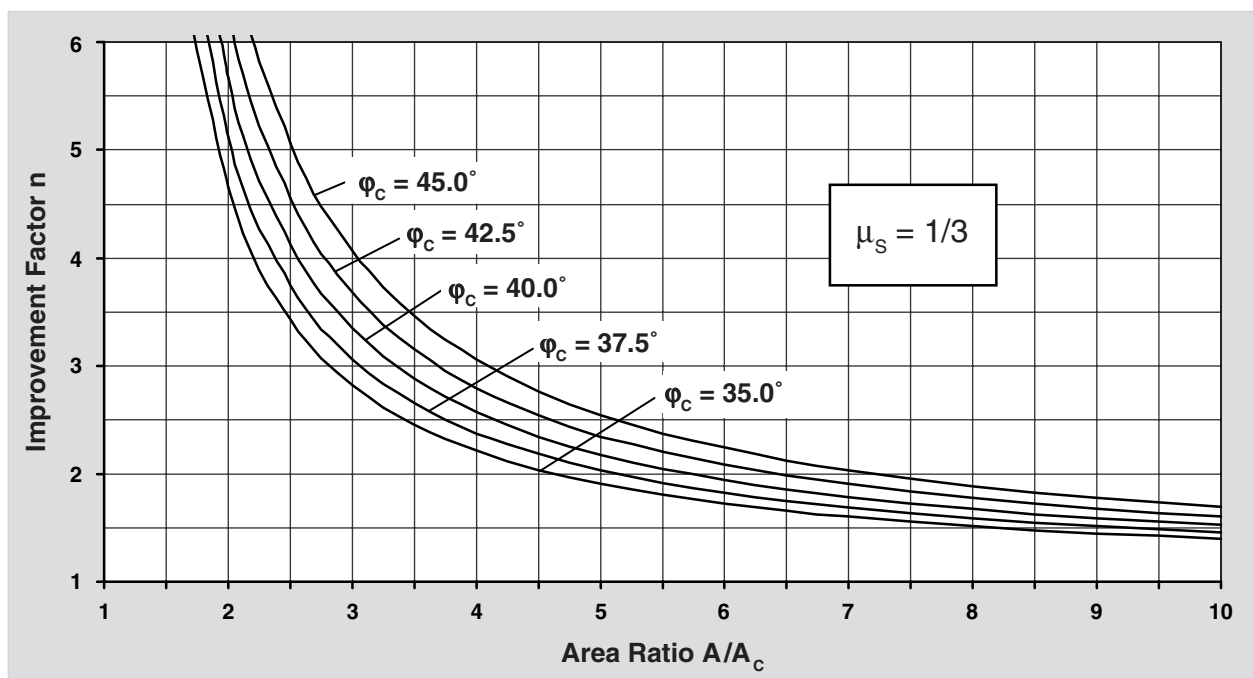


Figure 1: Design chart for vibro replacement

### 3 Consideration of the Column Compressibility

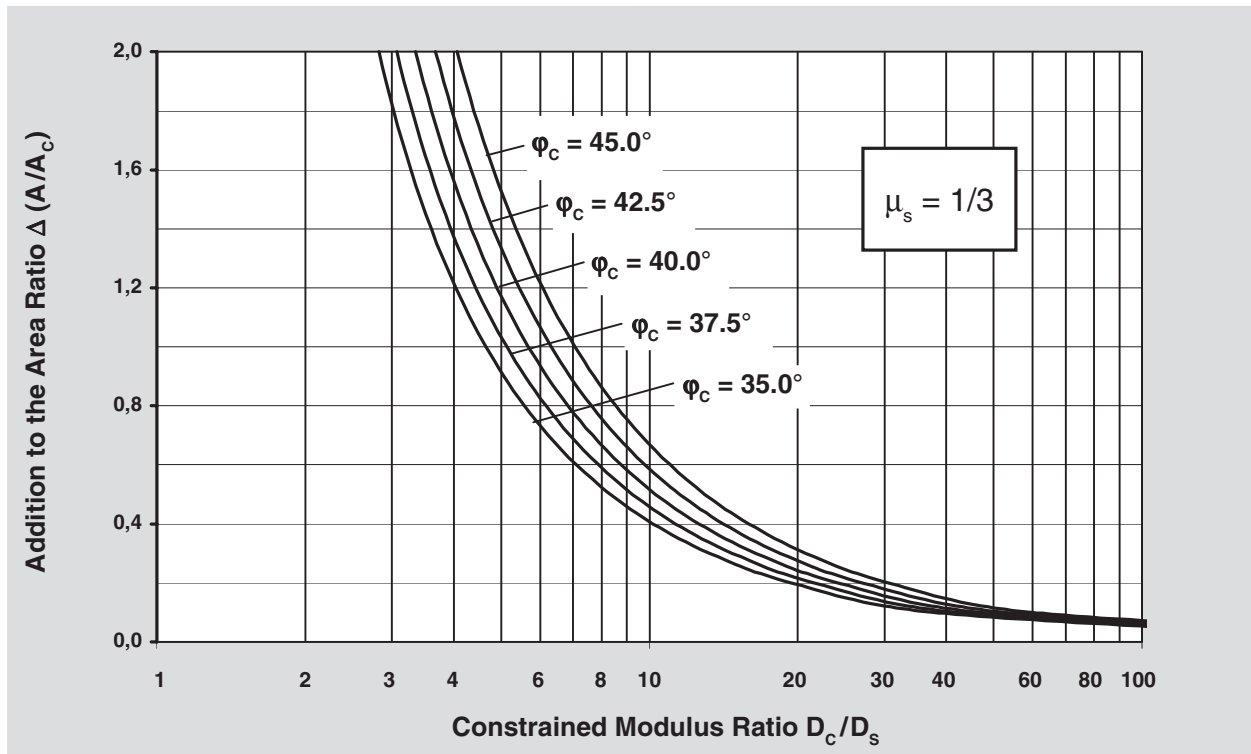


Figure 2: Consideration of column compressibility

The compacted backfill material of the columns is still compressible. Therefore, any load causes settlements which are not connected with bulging of the columns. Accordingly, in the case of soil replacement where the area ratio amounts to  $A/A_c = 1$ , the actual improvement factor does not achieve an infinite value as determined theoretically for non compressible material, but it coincides at best with the ratio of the constrained moduli of column material and soil. In this case for compacted backfill material as well as for soil a constrained modulus is meant as found by large scale oedometer tests. Unfortunately, in many cases soundings are carried out within the columns and wrong conclusions about the modulus are drawn from the results which are sometimes very moderate only.

It is relatively easy to determine at which area ratio of column cross section and grid size  $(A_c/A)_1$  the basic improvement factor  $n_0$  corresponds to the ratio of the constrained moduli of columns and soil  $D_c/D_s$ . For example, at  $\mu_s = 1/3$  the lower positive result of the following expression (with  $n_0 = D_c/D_s$ ) delivers the area ratio  $(A_c/A)_1$  concerned.

$$\left(\frac{A_c}{A}\right)_1 = -\frac{4 \cdot K_{ac} \cdot (n_0 - 2) + 5}{2 \cdot (4 \cdot K_{ac} - 1)} \pm \frac{1}{2} \cdot \sqrt{\left[\frac{4 \cdot K_{ac} \cdot (n_0 - 2) + 5}{4 \cdot K_{ac} - 1}\right]^2 + \frac{16 \cdot K_{ac} \cdot (n_0 - 1)}{4 \cdot K_{ac} - 1}}$$

As an approximation, the compressibility of the column material can be considered in using a reduced improvement factor  $n_1$  which results from the formula developed for the basic improvement factor  $n_0$  when the given reciprocal area ratio  $A/A_C$  is increased by an additional amount of  $\Delta(A/A_C)$ .

$$n_1 = 1 + \frac{\overline{A_C}}{A} \cdot \left[ \frac{1/2 + f(\mu_S, \overline{A_C/A})}{K_{ac} \cdot f(\mu_S, \overline{A_C/A})} - 1 \right]$$

$$\frac{\overline{A_C}}{A} = \frac{1}{A/A_C + \Delta(A/A_C)}$$

$$\Delta(A/A_C) = \frac{1}{(A_C/A)_1} - 1$$

In using the diagram in *Figure 1* this procedure corresponds to such a shifting of the origin of the coordinates on the abscissa which denotes the area ratio  $A/A_C$  that the improvement factor  $n_1$  to be drawn from the diagram, begins with the ratio of the constrained moduli and not with just an infinite value. The additional amount on the area ratio  $\Delta(A/A_C)$  depending on the ratio of the constrained moduli  $D_C/D_S$  can be readily taken from the diagram in *Figure 2*.

#### 4 Consideration of the Overburden

The neglect of the bulk densities of columns and soil means that the initial pressure difference between the columns and the soil which creates bulging, depends solely on the distribution of the foundation load  $p$  on columns and soil, and that it is constant all over the column length. As a matter of fact, to the external loads the weights of the columns  $W_C$  and of the soil  $W_S$  which possibly exceed the external loads considerably, has to be added. Under consideration of these additional loads the initial pressure difference decreases asymptotically and the bulging is reduced correspondingly. In other words, with increasing overburden the columns are better supported laterally and therefore, can provide more bearing capacity.

Since the pressure difference is a linear parameter in the derivations of the improvement factor, the ratio of the initial pressure difference and the one depending on depth - expressed as depth factor  $f_d$  - delivers a value by which the improvement factor  $n_1$  increases to the final improvement factor  $n_2 = f_d \times n_1$  on account of the overburden pressure. For example, at a depth where the pressure difference amounts to 50% only of the initial value, the depth factor comes to  $f_d = 2$ .

The depth factor  $f_d$  is calculated on the assumption of a linear decrease of the pressure difference as it results from the pressure lines  $(p_c + \gamma_c \cdot d) \cdot K_{ac}$  and  $(p_s + \gamma_s \cdot d)$  ( $K_s = 1$ ). However, it has to be considered that with decreasing lateral deformations the coefficient of earth pressure from the columns changes from the active value  $K_{ac}$  to the value at rest  $K_{0c}$ . Up to the depth where the straight line assumed for the pressure difference, meets the actual asymptotic line, the depth factor lies on the safe side. In practical cases the treatment depth is mostly less. However, safety considerations advise not to include the advantageous external load on the soil  $p_s$  in the derivations.

$$f_d = \frac{1}{1 + \frac{K_{oc} - W_s/W_c}{K_{oc}} \cdot \frac{W_c}{p_c}}$$

$$p_c = \frac{p}{\frac{A_c}{A} + \frac{1 - A_c/A}{p_c/p_s}}$$

$$\frac{p_c}{p_s} = \frac{1/2 + f(\mu_s, A_c/A)}{K_{ac} \cdot f(\mu_s, A_c/A)}$$

$$W_c = \Sigma(\gamma_c \cdot \Delta d), \quad W_s = \Sigma(\gamma_s \cdot \Delta d)$$

$$K_{oc} = 1 - \sin \varphi_c$$

The simplified diagram in *Figure 3* considers the same bulk density  $\gamma$  for columns and soil which is not on the safe side. Therefore for safety reasons, the lower value of the soil  $\gamma_s$  should be considered in this diagram always.

$$f_d = \frac{1}{1 + \frac{K_{oc} - 1}{K_{oc}} \cdot \frac{\Sigma(\gamma_s \cdot \Delta d)}{p_c}}$$

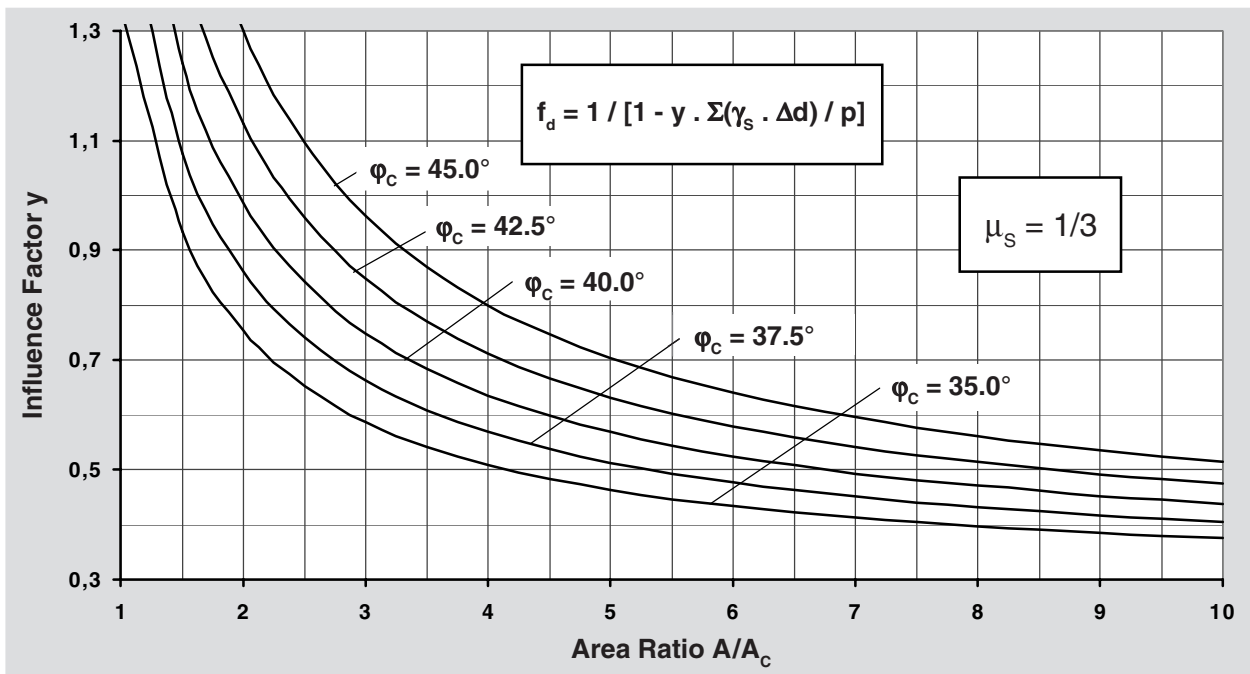


Figure 3: Determination of the depth factor

## 5 Compatibility Controls

The single steps of the design procedure are not connected mathematically and they contain simplifications and approximations. Therefore, at marginal cases compatibility controls have to be performed which guarantee that no more load is assigned to the columns than they can bear at all in accordance with their compressibility.

At increasing depths, the support by the soil reaches such an extent that the columns do not bulge anymore. However, even then the depth factor will not increase to infinity as results from the assumption of a linearly decreasing pressure difference. Therefore, the first compatibility control limits the depth factor and thereby the load assigned to the columns so that the settlement of the columns resulting from their inherent compressibility does not exceed the settlement of the composite system. In the first place this control applies when the existing soil is considered pretty dense or stiff.

$$f_d \leq \frac{D_c/D_s}{p_c/p_s}$$

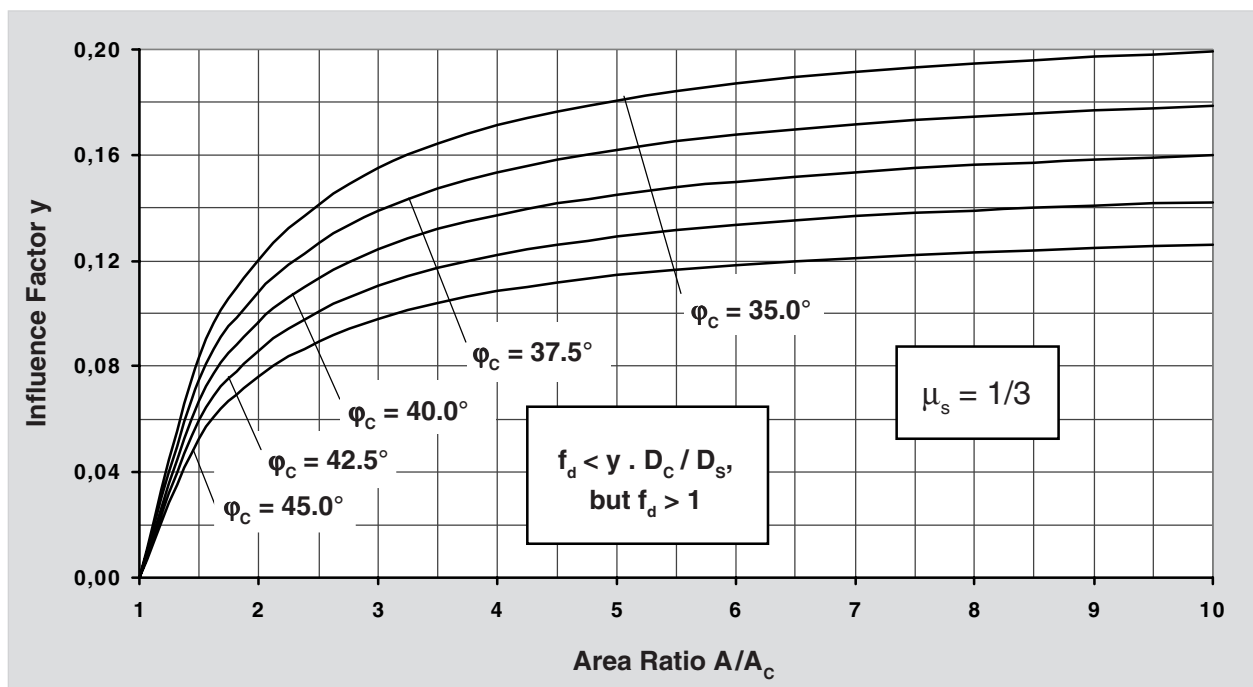


Figure 4: Limit value of the depth factor

The maximum value of the depth factor can be drawn also from the diagram in Figure 4. By the way, a depth factor  $f_d < 1$  should not be considered, even though it may result from the calculation. In this case the second compatibility control is imperatively required which relates to the maximum value of the improvement factor. In a certain way this control resembles the first one. It guarantees that the settlement of the columns resulting from their inherent compressibility does not exceed the settlement of the surrounding soil resulting from its compressibility by the loads which are

assigned to each. In the first place this second control applies when the existing soil is encountered pretty loose or soft.

$$n_{\max} = 1 + \frac{A_c}{A} \cdot \left( \frac{D_c}{D_s} - 1 \right)$$

It has to be observed that the actual area ratio  $A_c/A$  has to be appointed in the formula and not the modified value  $\overline{A_c/A}$ . Because of the simple equation, an independent Diagram is not required.

## 6 Shear Values of Improved Ground

The shear performance of ground improved by vibro replacement is outmost favourable. Whilst under shear stress rigid elements may break successively, stone columns deform until any overload has been transferred to neighbouring columns. For example, a landslide will not occur before the bearing capacity of the total group of columns installed has been activated. The stone columns receive an increased portion of the total load  $m$  thereby which depends on the area ratio  $A_c/A$  und the improvement factor  $n$ .

$$m = (n - 1 + \overline{A_c/A})/n$$

Simplifying, the recommended design procedure does not consider the volume decrease of the surrounding soil caused by the bulging of the columns. Therefore and particularly at a high area ratio, the soil receive a greater portion of the total load than actually calculated. In order not to overestimate the shear resistance of the columns when averaging on the basis of load distribution on columns and soil, the proportional load on the columns has to be reduced. The following approximation seems to be adequate:

$$m' = (n - 1)/n$$

The diagram in *Figure 5* shows in solid lines the proportional load of the columns  $m'$  and in dashed lines the not reduced one  $m$ .

According to the proportional loads on columns and soil, the shear resistance from friction of the composite system can be readily averaged.

$$\tan \bar{\varphi} = m' \cdot \tan \varphi_c + (1 - m') \cdot \tan \varphi_s$$

Since in most practical cases possible lines of sliding cover different depths which is difficult to survey, it is recommended to consider the depth factor in clear-cut cases only, i. e. to calculate usually with a load portion of the stone columns  $m_1'$  related to  $n_1$  and not with  $m_2'$  related to the increased factor  $n_2 = f_d \cdot n_1$ .

The cohesion of the composite system depends on the proportional area of the soil.

$$c = (1 - \overline{A_c/A}) \cdot c_s$$

The installation of stone columns possibly creates damages to the soil structure which are difficult to survey. For safety reasons, it seems to be advisable to consider the cohesion also proportional to the loads, i. e. pretty low, although this proposal is not based on soil mechanical aspects.

$$c' = (1 - m') \cdot c_s$$

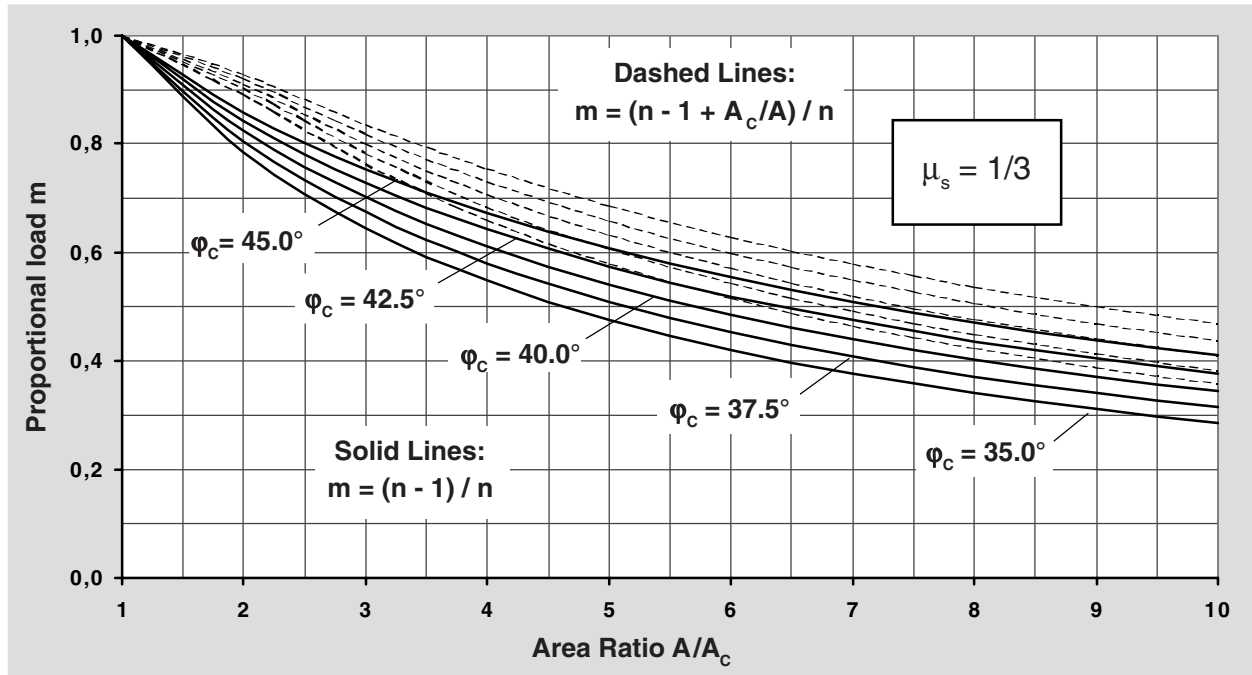


Figure 5: Proportional load on stone columns

## 7 Settlement of Single and Strip Footings

It is not (yet) possible to determine directly the performance of single or strip footings on vibro replacement. The design ensues from the performance of an unlimited column grid below an unlimited load area. The total settlement  $s_\infty$  which results for this case at homogeneous conditions, is readily to determine on the basis of the foregoing description with  $n_2$  as an average value over the depth  $d$ .

$$s_\infty = p \cdot \frac{d}{D_s \cdot n_2}$$

Diagrams which are given in Figure 6 and Figure 7, allow to conclude from this value the settlements of single or strip footings on groups of columns. These diagrams - with the diameter of the stone columns  $D$  as one parameter - are based on numerous calculations which considered load distribution on one side and a lower bearing capacity of the outer columns of the column group below the footing on the other side.

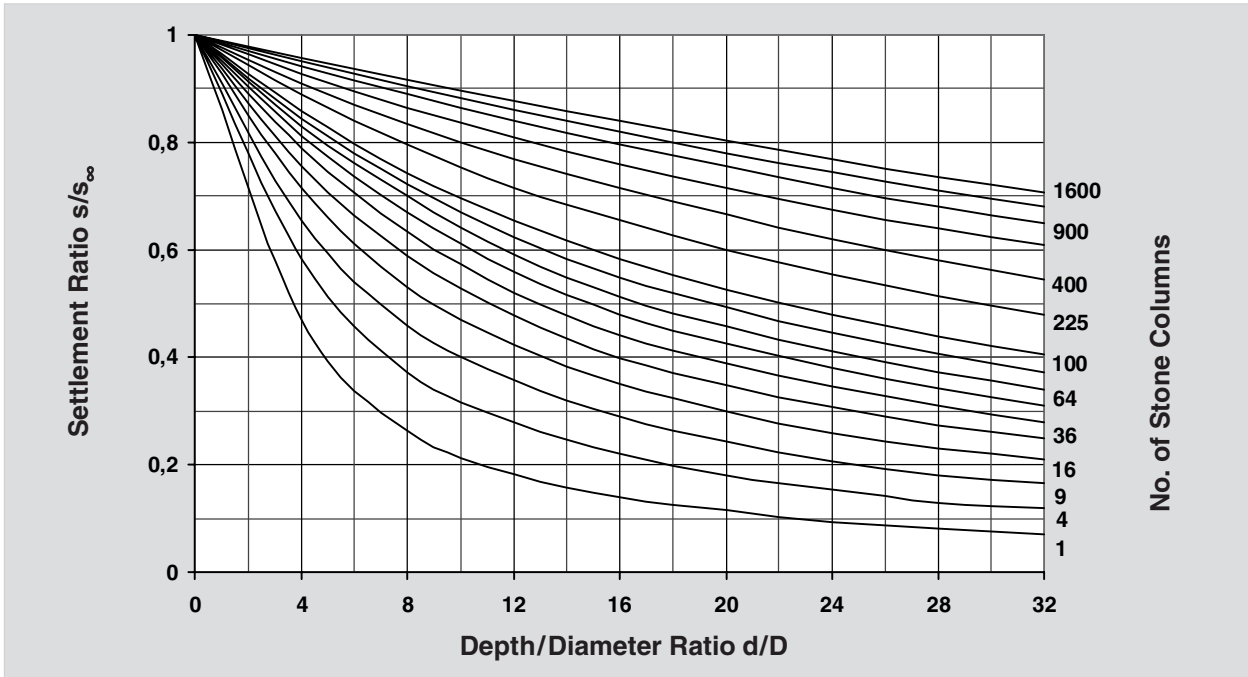


Figure 6: Settlement of single Footings

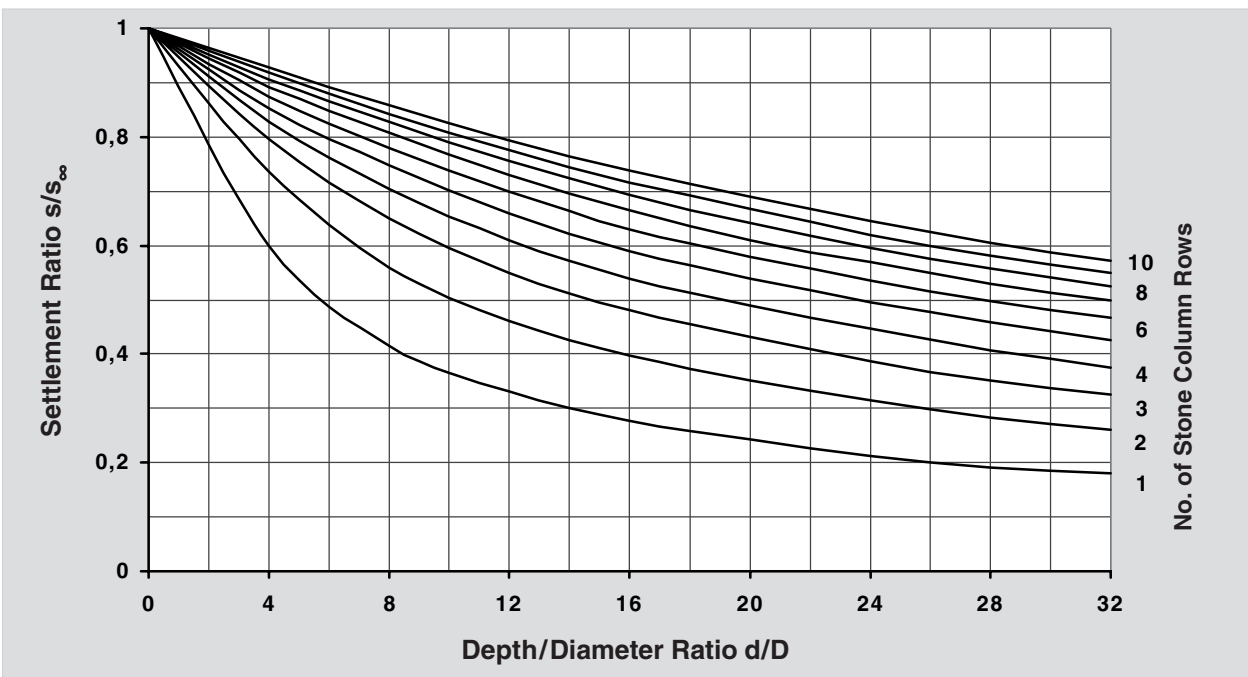


Figure 7: Settlement of strip Footings

The diagrams do not refer directly to footing extensions as to be expected. However, there exists an indirect reference in that the grid area  $A$  required to determine the improvement factor  $n$ , has

to be derived as quotient of the footing area and the number of columns. For example, the settlement reduction which a larger footing experiences normally at the same load, is compensated widely by the lower improvement factor which results from an increased area ratio as follows from a larger footing area on the same number of stone columns. The approximation given for the diagrams by this assumed compensation seems to be acceptable for usually considered area ratios, i. e. up to some  $A/A_C = 10$ .

Quite clear that the diagrams are valid for homogeneous conditions only and refer to the settlement  $s$  up to a depth  $d$  which is the second parameter counting from foundation level. The settlement  $\Delta s$  of any layer at any depth below the footing has to be determined as difference of the settlements up to the depths  $d_l$  and  $d_u$  of the lower and upper bound of the layer concerned with  $n_2$  as an average value over its thickness  $\Delta d$ .

$$\Delta s = \frac{P}{D_S \cdot n_2} \cdot [(s/s_\infty)_l \cdot d_l - (s/s_\infty)_u \cdot d_u]$$

Since  $n_2$  increases with depth on one side due to the depth factor, but becomes less significant with depth on the other side due to the load distribution of a limited footing, it is required even at homogeneous conditions to subdivide greater depths. This avoids settlements being too liberally estimated.

## 8 Bearing Capacity of Single and Strip Footings

A simple method to estimate the bearing capacity of single and strip footings on vibro replacement exists by determining at first a fictitious width  $\bar{b}$  of the footing, using the friction angle  $\bar{\varphi}$  of the improved soil below the footing and the friction angle  $\varphi_s$  of the untreated soil on the outside, which would develop - calculated on the basis of the friction angle  $\varphi_s$  of the untreated soil only - in case of ground failure the same line of sliding outside of the improved area as the actual footing at actual conditions. If the border line of treatment coincide with the edge of the footing - being usually the case but not necessarily - the following formula results:

$$\bar{b} = b \cdot e^{\left[ \arccos(45^\circ - \bar{\varphi}/2) \cdot \tan \bar{\varphi} - \arccos(45^\circ - \varphi_s/2) \cdot \tan \varphi_s \right]} \cdot \frac{\sin(45^\circ + \bar{\varphi}/2)}{\sin(90^\circ - \bar{\varphi})} \cdot \frac{\sin(90^\circ - \varphi_s)}{\sin(45^\circ + \varphi_s/2)}$$

Then, for this fictitious width the bearing capacity is determined by using the friction angle of the untreated ground  $\varphi_s$  and an averaged cohesion according to the proportion of fictitious footing width and failure width outside of the footing. In pure cohesive soil the failure width equals the footing width, thus leading to an average cohesion of  $c'' = (c' + c_s) / 2$ .

For foundations on layered ground the shear values change with depth also. The determination of the bearing capacity, e. g. according to the German Standard DIN 4017, becomes rather complicated with the fictitious width since this width changes at each layer.

A practical approximation can be achieved as follows. At first, safeties  $\eta_0$  and maximum depths of ground failure lines  $d_{Gr,0}$  are calculated applying one after another the soil parameters of every individual layer, e. g. according to DIN 4017.

$$\eta_0 = \overline{\sigma_{of}}/p \quad \overline{\sigma_{of}} = (c_s \cdot N_c \cdot v_c + q \cdot N_d \cdot v_d + \gamma_s \cdot \bar{b} \cdot N_b \cdot v_b) \cdot \bar{b}/b$$

$$d_{Gr,0} = \bar{b} \cdot \sin(45^\circ + \varphi_s/2) \cdot e^{[\arctan(45^\circ + \varphi_s/2) \cdot \tan \varphi_s]}$$

In a second step, the final safety  $\eta$  and maximum depth  $d_{Gr}$  is averaged successively with the values of the individual layers as long as  $d_{Gr(n-1)}$  exceeds  $d_{u(n)}$  being the upper bound of the layer concerned ( $d_{l(n)}$  being the lower bound).

$$\eta_{(n)} = \eta_{0(n)} + [\eta_{(n-1)} - \eta_{0(n)}] \cdot \frac{d_{o(n)}}{d_{Gr(n-1)}}$$

$$d_{Gr(n)} = d_{Gr,0(n)} + [d_{Gr(n-1)} - d_{Gr,0(n)}] \cdot \frac{d_{o(n)}}{d_{Gr(n-1)}}$$

$$n \geq 2 \quad \eta_{(1)} = \eta_{0(1)} \quad d_{Gr(1)} = d_{Gr,0(1)} \quad \text{When } d_{Gr(n-1)} > d_{l(n)} \text{ then } d_{Gr(n-1)} = d_{l(n)}$$

Though little bit uncomfortable, this procedure can still be performed manually in contrast to the iteration as outlined in DIN 4017. The results of both the procedures do not differ much.

## 9 Liquefaction Potential of Improved Ground

Vibro replacement is suitable particularly for ground improvement in seismic areas since stone columns possess a certain flexibility on one side and prevent liquefaction on the other side. The stabilizing effect results from the frictional resistance of the columns which carry a considerable amount of the external load and of the weight of the soil, and their capability to reduce excess porewater pressure in the soil - at least in close vicinity - almost instantly. The steep reduction of porewater pressure towards the column is in so far important as it creates kind of a filter cake effect which maintains the lateral support required for the bearing capacity of the columns and which prevents a higher degree of soil infiltration into the columns although the column material does not fulfill any established filter criteria.

The complex conditions in a seismic event are investigated frequently for more or less homogeneous ground. Nevertheless, practical criteria to evaluate the liquefaction potential were developed rather empirically. For vibro replacement although carried out already many times against earthquake vibrations, even an empirical evaluation is difficult since - fortunately - no damages have been observed so far.

Usually, safety against liquefaction is concluded from the comparison of so-called cyclic stress ratios, namely the one which is provided by the soil on the basis of its density and the one which probably develops in a seismic event.

For a rough estimation of the efficiency of vibro replacement it is proposed to reduce the cyclic stress ratio probably developed in a seismic event, in the same ratio as the load on the soil between the columns is reduced by vibro replacement, i. e. to use a corresponding reduction factor  $\alpha$ .

$$\alpha = p_s/p = 1/n$$

Such a reduction seems to be adequate with regard to the favourable performance of vibro replacement in seismic events. However, from soil mechanical aspects this is not proved and has to be verified ultimately by the increasing number of projects carried out world-wide.

For similar reasons as outlined at the determination of the shear values, it is recommended to use in the formula  $n_1$  rather than  $n_2$ .

A diagram for the reduction factor  $\alpha$  is given in *Figure 8*.

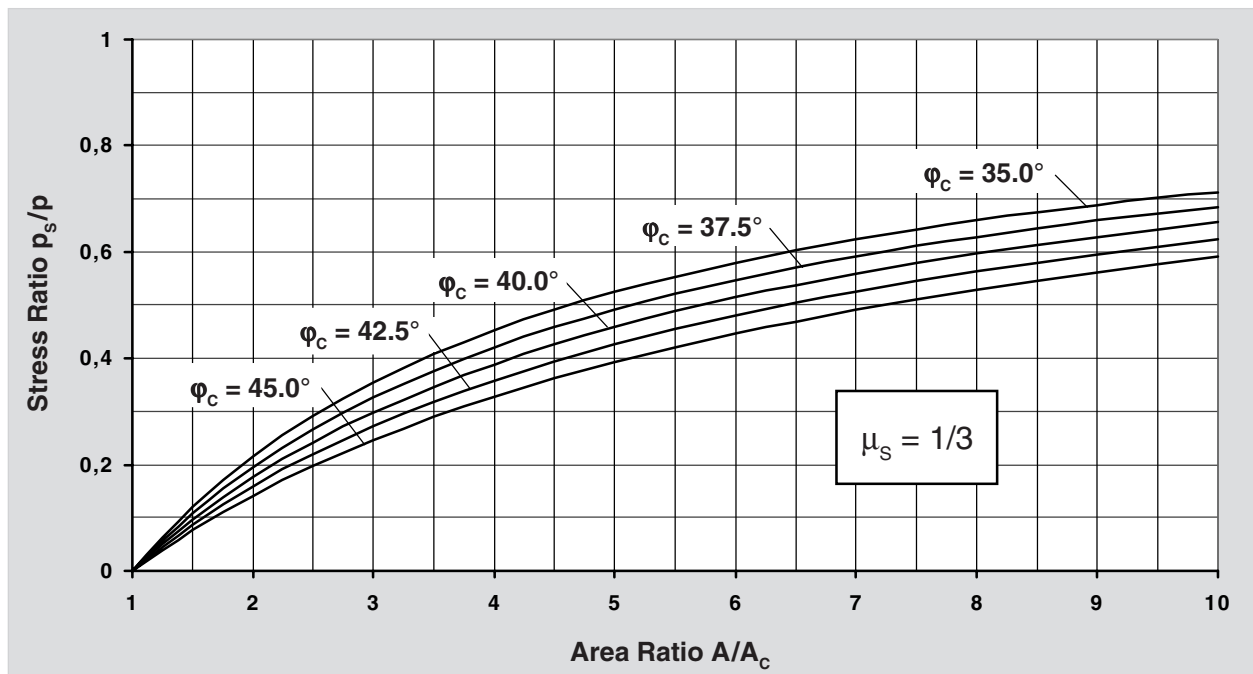


*Figure 8: Residual pressure on the soil after vibro replacement*

## 10 Case Study Worked Example

The design method has been used already frequently in determining the expected behaviour of structures on treated ground. However, in most cases the application is based on parameters indirectly derived from field tests or even just assumed. As long as the actual performance of vibro replacement excels such forecasts, more accurate verifications are usually omitted.

Some full scale field experiments about vibro replacement which comprise measurements beyond common practice are outlined in [2]. For example, enough details of a tank foundation at Canvey Island are given so that the design method can be applied and the results verified.

The diameter of the tank concerned is 36 m. It is founded on a pad of approximately 1 m thickness above soil reinforced by 10 m long stone columns in a grid with triangular spacing of 1.52 m and an average diameter of 0.75 m measured near surface. Including some 0.4 m of top soil the treated strata consist up to 9 m depth of silty and clayey soil occasionally with pockets of peat followed by medium dense silty fine sand in which the columns are embedded. Referred to depths, the given coefficients of volume change  $m_v$  and the constrained moduli  $D_s (= 1 / m_v)$  as used in the design computations are as follows:

Depth [m]	$m_v$ [m <sup>2</sup> /MN]	$D_s$ [MN/m <sup>2</sup> ]	Remarks
-1.0	–	50	pad
0.0		20	top soil
0.4	0.8 - 0.5	2	soft soil
1.0		1	very soft soil
1.6	1.2 - 0.5	1	very soft soil below ground water
8.2	0.3 - 0.06	10	firm soil
9.0		20	medium dense sand

At full loading of 130 kN/m<sup>2</sup> settlements were observed in the range of some 40 cm. A computation according to the design method (s. appendix) shows a final settlement of approximately 38 cm. Taking into consideration the pockets of peat or a possible reduction of column diameter with depth, the value would be higher and in really good agreement. The improvement factors  $n$  as computed on the basis of formulae, can be taken readily also from the diagrams as follows with reference to the first layer below the ground water table which contributes most to the settlements:

$A/A_C$	=	4.53	→	<b>Fig. 1</b>	→	$n_0$	≈	2.35
$D_C/D_s$	=	100	→	<b>Fig. 2</b>	→	$\Delta A/A_C$	≈	0.05
$A/A_C$	=	4.58	→	<b>Fig. 1</b>	→	$n_1$	≈	2.30
$A/A_C$	=	4.58,	$\Sigma(\gamma \cdot d) = 19 \cdot 1.0 + 18 \cdot 0.4 + 16 \cdot 0.6 + 15 \cdot 0.6 + 5 \cdot 6.6/2$					$= 61.3 \text{ kN/m}^2,$
$p$	=	130 kN/m <sup>2</sup>	→	<b>Fig. 3</b>	→	$f_d$	≈	1.38
							→	$n_2 = f_d \cdot n_1 = 3.17$

The discrepancy to the computed value of  $n_2 = 2.94$  is due to the difference between formulae and diagram as outlined in paragraph 4.

## II Conclusions

Out of the deep vibratory compaction techniques vibro replacement covers the widest range with regard to the application in different soils. Whilst vibro compaction is restricted to compactible sand and gravel, the application of vibro replacement extends principally over the total range in grain size of loose soils. Even in most of the noncohesive natural soils suitable for vibro compaction, backfilling with coarse grained material is recommended to increase the compaction efforts - and this means stone column installation. Pure vibro compaction has advanced just lately at gigantic artificial deposits in different coastal regions of the world.

Notwithstanding the importance of vibro replacement, the efficiency of stone columns in soil improvement must not be overestimated. As long as the existing soil is suitable to be densified, this should be the preceding aim of any deep compaction treatment including vibro replacement. However, the achievable densification depends on too many parameters to be calculable. On the contrary the improving effect of stone columns - possibly supplementary to an achieved densification - can be determined pretty reliably.

The application of vibro replacement which was introduced end of the fifties, relied for a long time upon the experience of the contractors. Not before the middle of the seventies first theoretical approaches were submitted. In its fundamentals also the design method outlined afore originates from this time. It has proved its reliability since then. Subsequent supplements imply refinements or extensions of the application range but not a radical alteration on the fundamentals. In respect of the complexity of the matter the design criteria have the advantage to be easy to use and to cover in a closed package all cases practically occurring.

## References

- [1] Kirsch, K.: Die Baugrundverbesserung mit Tiefenrüttlern, 40 Jahre Spezialtiefbau: 1953-1993, Festschrift, Werner-Verlag GmbH, Düsseldorf, 1993.
- [2] Greenwood, D. A.: Load Tests on Stone Columns, ASTM Publication STP 1089, Deep Foundation Improvements: Design, Construction, and Testing, 1991.

*Publications of the author to the design method:*

- [3] Abschätzung des Setzungsverhaltens eines durch Stopfverdichtung verbesserten Baugrundes, Die Bautechnik 53, H.5, 1976.
- [4] Zur Abschätzung des Setzungsverhaltens eines durch Stopfverdichtung verbesserten Baugrundes, Die Bautechnik 65, H.1, 1988.
- [5] Abschätzung des Scherwiderstandes eines durch Stopfverdichtung verbesserten Baugrundes, Die Bautechnik 55, H.1, 1978.
- [6] Vibro Replacement Design Criteria and Quality Control, ASTM Publication STP 1089, Deep Foundation Improvements: Design, Construction, and Testing, 1991.
- [7] The Prevention of Liquefaction by Vibro Replacement, Proc. of the Int. Conf. on Earthquake Resistant Construction and Design, 1990 Balkema, Rotterdam.
- [8] Die Bemessung von Rüttelstopfverdichtungen, Die Bautechnik 72, H.3, 1995

Keller Grundbau GmbH  
 Kaiserleistr. 44, 63067 Offenbach, Tel. 069/8051210, Fax. 069/8051221  
 Program VIBRI, Version 950904, Copyright by KELLER Grundbau GmbH

Vibro Replacement at Canvey Island, Reported 1991 by Greenwood  
 \*\*\*\*\*

Evaluation of the Soil Improvement by Vibro Replacement  
 acc. to Priebe, H.: Die Bautechnik 72, 3/1995  
 below an Area Load on a Regular Triangular Column Grid

Foundation Pressure	130.00 kN/m <sup>2</sup>	Column Material	
Column Distance	1.52 m	Unit Weight	19.00 kN/m <sup>3</sup> , below 1.60 m Depth 12.00 kN/m <sup>3</sup>
Row Distance	1.32 m	Constrained Modulus	100.00 MN/m <sup>2</sup>
Grid Area	2.00 m <sup>2</sup>	Friction Angle	40.00 Degrees
Load Level	-1.00 m	Press. Coefficient	.22
Column Depth	10.00 m		
Considered Depth	20.00 m		

**Subsoil Strata**

No.	TopL. [m]	Dia. [m]	A/AC	DS [MN/m <sup>2</sup> ]	DC/DS	gamma [kN/m <sup>3</sup> ]	my	phi [degree]	c [kN/m <sup>2</sup> ]	Ground Water Table
1	-1.00	.00	****	50.00	2.00	19.00	.33	35.00	.00	1.60 m
2	.00	.75	4.53	20.00	5.00	18.00	.33	25.00	5.00	
3	.40	.75	4.53	2.00	50.00	16.00	.33	.00	25.00	
4	1.00	.75	4.53	1.00	100.00	15.00	.33	.00	20.00	
<b>5</b>	<b>1.60</b>	<b>.75</b>	<b>4.53</b>	<b>1.00</b>	<b>100.00</b>	<b>5.00</b>	<b>.33</b>	<b>.00</b>	<b>20.00</b>	
6	8.20	.60	7.08	10.00	10.00	7.00	.33	.00	30.00	
7	9.00	.60	7.08	20.00	5.00	9.00	.33	30.00	.00	
8	10.00	.00	****	20.00	5.00	9.00	.33	30.00	.00	
9	20.00	.00	****	20.00	5.00	9.00	.33	30.00	.00	

- Top L. = Top Level of Stratum Concerned
- Dia. = Column Diameter
- A = Grid Area Resp. Reference Area
- AC = Cross-sectional Area of Column
- DC = Constrained Modulus of Backfill
- DS = Constrained Modulus )
- gamma = Unit Weight )
- my = Poisson's Ratio ) of Soil
- phi = Friction Angle )
- c = Cohesion )

**Soil Improvement**

No.	n0	d(A/AC)	n1	m1	phi1 [degree]	c1 [kN/m <sup>2</sup> ]	fd	n2	m2	phi2 [degree]	c2 [kN/m <sup>2</sup> ]
1											
2	2.34	1.17	2.01	.50	33.16	2.49	****	1.88	.47	32.67	2.66
3	2.34	.09	2.31	.57	25.41	10.84	1.16	2.68	.63	27.73	9.34
4	2.34	.05	2.32	.57	25.54	8.61	1.21	2.82	.65	28.44	7.09
<b>5</b>	<b>2.34</b>	<b>.05</b>	<b>2.32</b>	<b>.57</b>	<b>25.54</b>	<b>8.61</b>	<b>1.27</b>	<b>2.94</b>	<b>.66</b>	<b>28.98</b>	<b>6.80</b>
6	1.78	.52	1.72	.42	19.35	17.45	1.24	2.13	.53	24.04	14.05
7	1.78	1.17	1.65	.40	34.25	.00	****	1.57	.36	33.90	.00
8											

The Proportional Loads on Columns are Approximated to  $m = 1 - 1/n$

- n0 = Basic Improvement Factor
- d(A/AC) = Addition to the Area Ratio (Column Compressibility)
- n1 = Improvement Factor (with Column Compressibility)  
 (—> Recommended for Failure Analyses if  $n1 < n2$ )
- fd = Depth Factor (Overburden Constraint)  
 (\*\*\*\* —> Overridden by Control Checking!)
- n2 = Improvement Factor (Add. with Overburden Constraint)
- m1,2 = Proportional Load on Columns )
- phi1,2 = Friction Angle of Compound ) Attributable to n1 resp. n2
- c1,2 = Cohesion of Compound )

Settlement	Depth [m]	Infinite Load Area [cm]	w/o Impr. [cm]	Overburden [kN/m <sup>2</sup> ]
	-1.00	.26	.26	.0
	.00	.14	.26	19.0
	.40	1.37	3.66	26.2
	1.00	2.45	6.90	35.8
	1.60	25.81	75.93	44.8
	8.20	.48	1.03	77.8
	9.00	.41	.65	83.4
	10.00	6.46	6.46	92.4
		37.37	95.14	

**Vibro Replacement**

by the **Keller Group**

- the experienced contractors which invented and developed the basic features of the deep vibratory compaction methods.

**VIBRI** - The only software for the design of vibro replacement developed by the author (Priebe) of the design method.

- user friendly
- by graphically supported input
- easy to survey
- by alphanum. and graphic output

For details please contact

**Keller Grundbau GmbH**  
 Technical Department  
 Kaiserleistr. 44  
 63067 Offenbach/Main  
 Tel: 069-8051-218  
 Fax: 069-8051-221  
 GERMANY



# Vibro Replacement to Prevent Earthquake Induced Liquefaction

Dipl.-Ing. Heinz J. Priebe

*Keller Grundbau GmbH*

Presented by

**Keller Grundbau GmbH**

Kaiserleistr. 44

D-63067 Offenbach

Tel. 069 / 80 51 - 0

Fax 069 / 80 51 - 244

E-mail [Marketing@KellerGrundbau.com](mailto:Marketing@KellerGrundbau.com)

[www.KellerGrundbau.com](http://www.KellerGrundbau.com)

**Proceedings of the Geotechnique-Colloquium  
at Darmstadt, Germany, on March 19th, 1998**  
(also published in *Ground Engineering*, September 1998)

**Technical paper 12-57E**

---

# Vibro Replacement to Prevent Earthquake Induced Liquefaction

Dipl.-Ing. Heinz-Joachim Priebe  
Keller Grundbau GmbH, Offenbach

## 1 Introduction

Fortunately, Germany has only a few, localised regions that are at risk from earthquakes, and even here the risk is small. The situation is, however, quite different in the south and south-east of Europe. For example, Assisi in central Italy was hit by an earthquake last year.

Elsewhere, there are regions on earth, often densely populated, where the danger of both severe and very severe earthquakes is quite real. This is of primary concern in south-east Asia and other areas of the Pacific Rim, where approximately 85 per cent of all the world's seismic movements are recorded.

When a building becomes unusable, it does not necessarily mean that the structure has suffered severe damage or a total collapse as a result of seismic shaking. Frequently the ground under and around the building fails and the facility is lost, even though the structure itself might have survived with minor damage. In these cases, failure results from liquefaction.

## 2 The Phenomenon of Liquefaction

Earthquake induced soil liquefaction occurs relatively frequently in areas of more or less level ground. The term phenomenon is used not because the events seldom occur, but because the expression highlights the often astonishing result, such as the overturning of whole apartment blocks or the floating of buried facilities. *Figure 1a* shows a capsized apartment block in Niigata, Japan, resulting from the famous 1964 earthquake (Herzog, 1980).

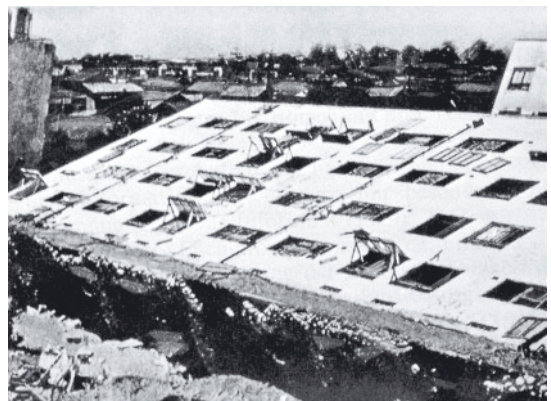


*Figure 1a: Capsized apartment block in Niigata, Japan, 1964*

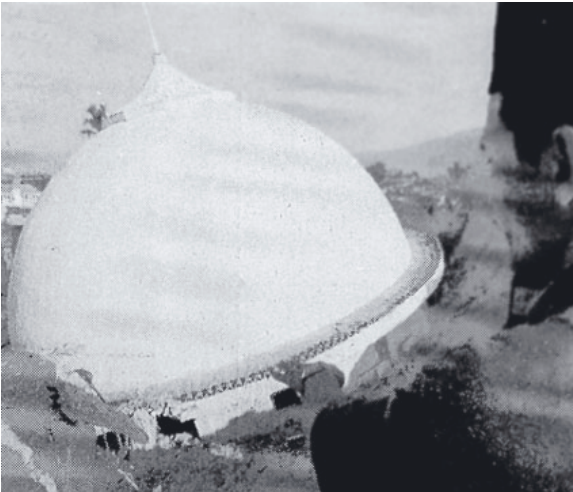


Figure 1b: Subsided mosque near Sungai Penuh, Indonesia, 1994

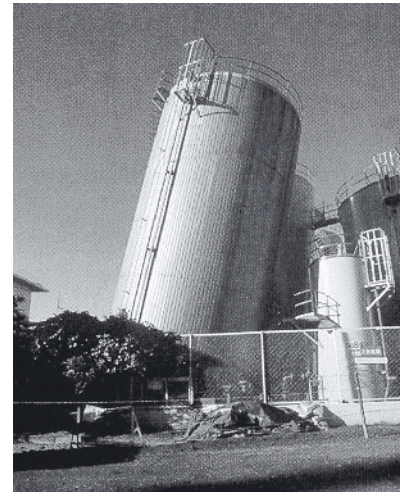


Figure 1c: Tilted tank in Kobe, Japan, 1995

Other spectacular and more recent examples are shown in *figure 1b*, where a mosque in Indonesia subsided during an earthquake in 1994, and in *figure 1c*, where a tank in Kobe, Japan, tilted at the 1995 earthquake (Wenk/Schwarz, 1995).

Liquefaction of this type only occurs in loose to medium dense, saturated soils with fairly uniform grain size distributions, covering the silty sandy range. The most critical soil is fine sandy grained with some silt content. *Figure 2* shows the bandwidth susceptible to liquefaction. It extends from medium to coarse sand to medium to coarse silt. In loose to medium dense conditions, the dynamic forces of a seismic event lead to an adjustment of the grain structure to a denser state. Initially, if the soil does not drain sufficiently, due to a low permeability or long

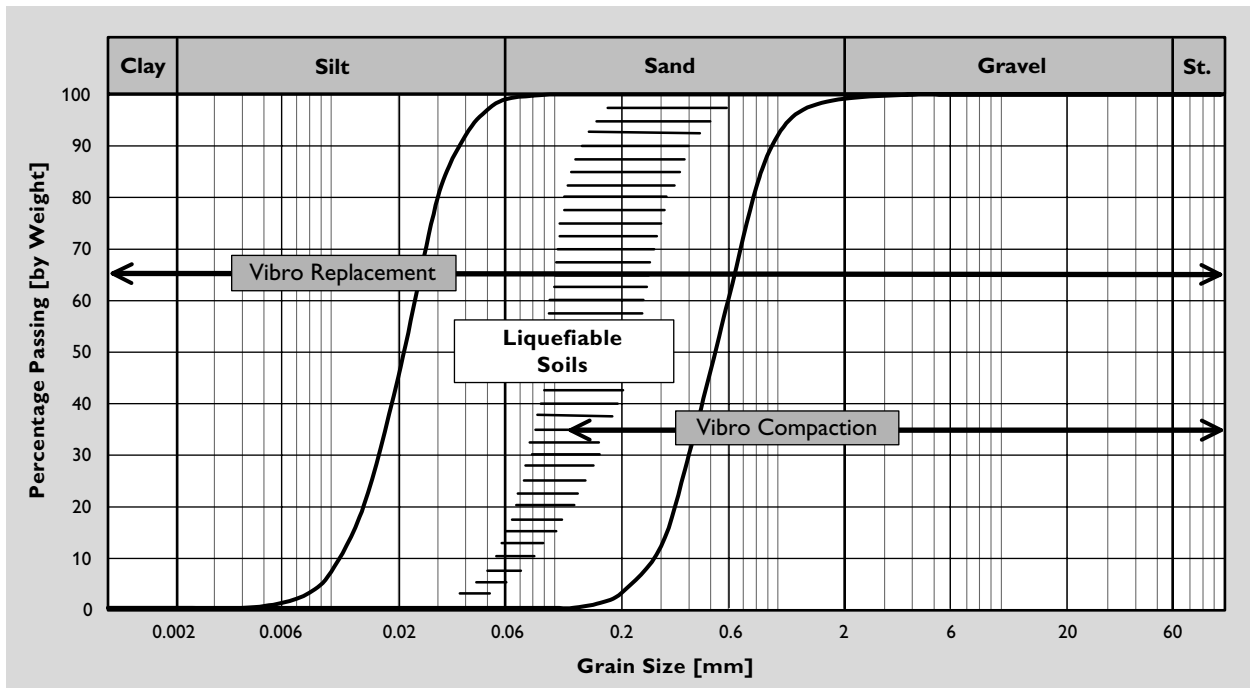


Figure 2: Application ranges of the deep vibratory compaction techniques

drainage paths, effective stresses in the grain structure start to pass to the pore water. The pressure in the pore water, therefore, rises accordingly, and the previously existing shear resistance of the soil diminishes.

In a limit state, the subsoil behaves like a liquid, and loses its bearing capacity. Even if this state lasts only for a short period, extreme deformations may occur, which have little to do with normal ground failure.

### 3 Evaluation of the Liquefaction Potential

In the mid-sixties, extensive efforts were beginning to be made to deal with the engineering problems of soil liquefaction. The reason might have been the 1964 Niigata earthquake, where the phenomenon occurred extensively. However, there were also demands to reduce the risk of liquefaction at the growing number of industrial plants, not only nuclear power stations but also barrages, refineries or chemical plants, where construction or foundation failure could have catastrophic consequences.

Options for evaluating the liquefaction potential at a given earthquake magnitude can be roughly subdivided into three substantial groups: theoretical approaches, laboratory tests and statistical analyses.

With theoretical approaches, the problem that arises is how to consider the prevailing ground conditions properly. In the second group, laboratory tests can at least deal with the material concerned, but problems lie in the difficulty of realistically modelling natural conditions. Although the soil density is the main parameter in evaluating the liquefaction potential, the influence of ageing and naturally occurring anomalies must not be underestimated. This is equally applicable when transmitting model behaviour to actual conditions.

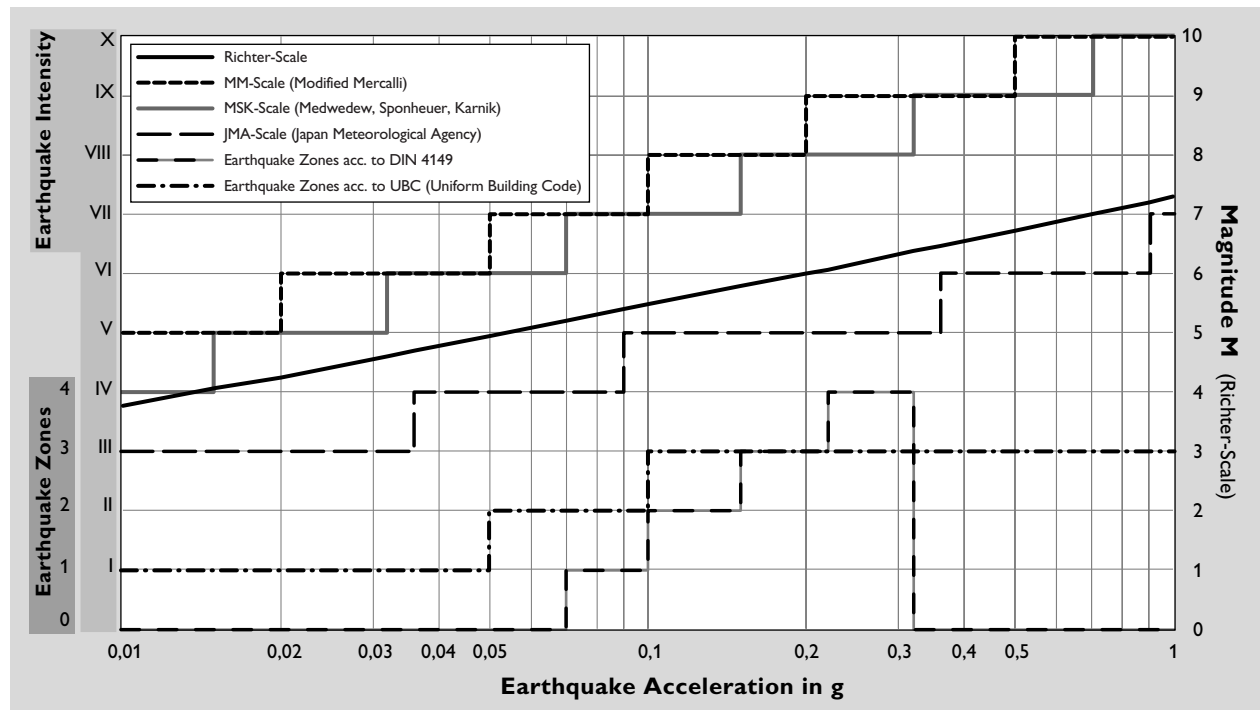


Figure 3: Correlation between common earthquake scales and earthquake acceleration

So far, the simplest and probably most reliable method seems to be the evaluation of the soil liquefaction potential on the basis of statistical analyses. For this, the forces expected during a seismic event are compared with the forces that the subsoil under consideration can actually resist. Generally, the maximum surface acceleration on level ground is used as the characteristic value for the forces developed by an earthquake. In *figure 3*, common earthquake scales, based on subjective perceptions and damage observations, are correlated to each other and to the more objective Richter scale. *Figure 3* also gives an idea of the maximum surface acceleration which is attributable to the various scales and, as such, it can be used as support for design purposes. The diagram shows values at the conservative side (Klein, 1990), at least for higher intensities. This is intentional for safety reasons, as the statistical analyses do not contain any further safety factors.

First, in order to evaluate the liquefaction potential, the Seismic Stress Ratio  $SSR = \tau_h / \sigma'_{v0}$  developed in the field at level ground conditions is determined. This is, depending on depth, the ratio between the shear force created by the assumed earthquake magnitude and the effective overburden pressure (Seed/Idriss/Arango, 1983).

$$\frac{\tau_h}{\sigma'_{v0}} = 0.65 \cdot \frac{a_{\max}}{g} \cdot \frac{\sigma_{v0}}{\sigma'_{v0}} \cdot r_d$$

where

$\tau_h$  = seismic shear force [kN/m<sup>2</sup>]

$\sigma_{v0}$  = total overburden pressure [kN/m<sup>2</sup>]

$\sigma'_{v0}$  = effective overburden pressure [kN/m<sup>2</sup>]

$a_{\max}$  = maximum earthquake acceleration [m/sec<sup>2</sup>]

0.65 = average value of acceleration in comparison to  $a_{\max}$

$g$  = acceleration due to gravity [m/sec<sup>2</sup>]

$r_d$  = reduction value depending on depth [ $\approx 1 - 0.012 \cdot z$ ]

$z$  = depth [m]

The stress ratio that the soil can resist, is found by statistical analyses of a multitude of soundings at earthquake affected subsoils. The first of these analyses, related to a magnitude of  $M = 7.5$ , was originally based on Standard Penetration Tests (Seed/Idriss/Arango, 1983). It was then continued, attuned to the more reliable Static Cone Penetration Tests and refined with regard to the silt content of soils, by other investigators (Robertson/Campanella, 1985; Stark/Olson, 1995).

*Figure 4* shows the relationship between seismic stress ratio and modified cone resistance  $q_{c1}$  at the boundary state.

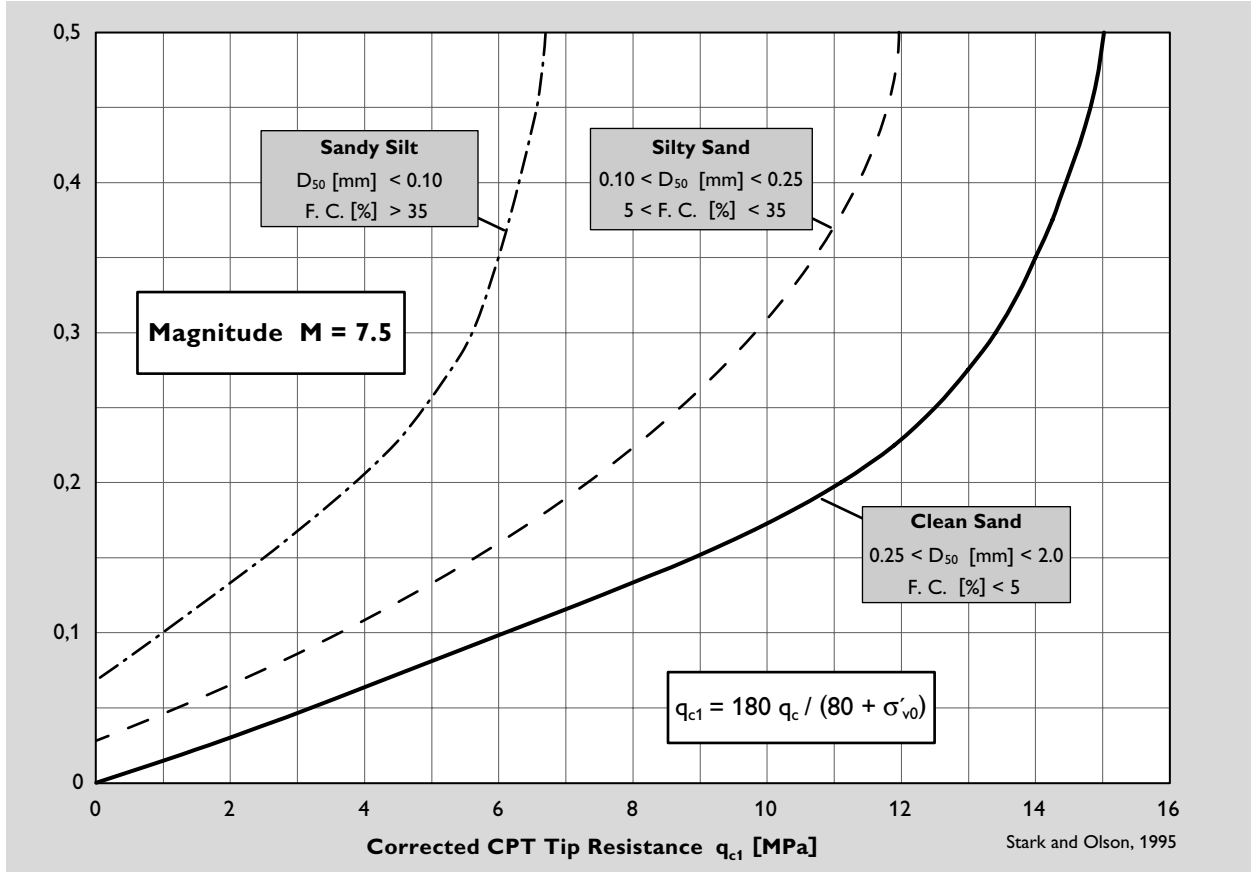


Figure 4: Relationship between seismic stress ratio and CPT tip resistance for sandy soils

$$q_{c1} = C_q \cdot q_c \quad C_q \approx \frac{1.8}{0.8 + \sigma'_{v0}/100}$$

where  $q_c$  = cone resistance [MPa]

The evaluation proposed in the German manual *Grundbau-Taschenbuch* coincides principally with the procedure outlined above (Klein, 1990).

The method was further modified with the introduction of the friction ratio between sleeve friction and cone resistance. In this case, the determination of the grain size distribution can be omitted (Suzuki/Koyamada/Tokimatsu, 1997). In the publication concerned a slightly modified formula, as given below, is used to determine the relevant seismic stress ratio (abbreviations as before).

$$\frac{\tau_h}{\sigma'_{v0}} = 0.1 \cdot (M - 1) \cdot \frac{a_{\max}}{g} \cdot \frac{\sigma_{v0}}{\sigma'_{v0}} \cdot (1 - 0.015 \cdot z)$$

where  $M$  = earthquake magnitude

In this formula, the average value of the acceleration is related to the magnitude  $M$ , and the reduction value  $r_d$  is slightly modified. The diagram shown in figure 5 should be used with modified parameters given below, where sleeve friction and cone resistance is considered via a soil behavior type index  $I_c$ .

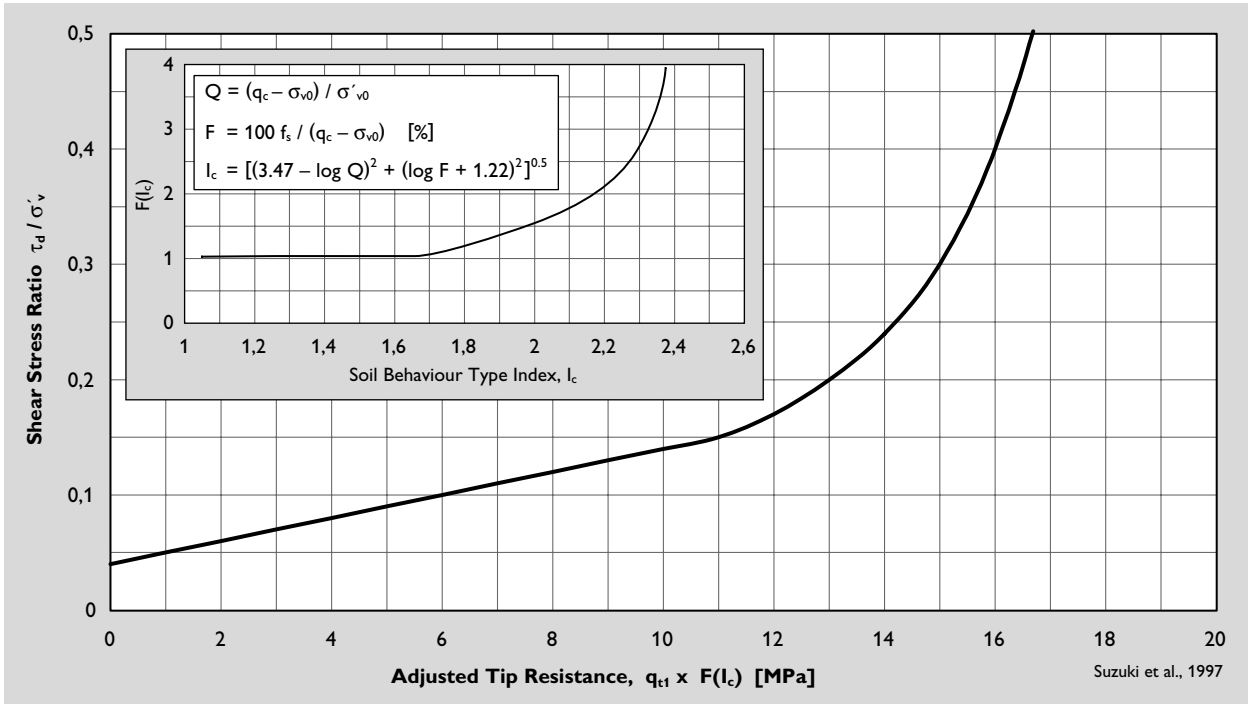


Figure 5: Relationship between seismic stress ratio and CPT tip resistance

$$Q = (q_c - \sigma_{v0}) / \sigma'_{v0}$$

$$F = 100 \cdot f_s / (q_c - \sigma_{v0}) \quad [\%] \qquad f_s = \text{sleeve friction}$$

$$I_c = \left[ (3.47 - \log Q)^2 + (\log F + 1.22)^2 \right]^{0.5}$$

In conclusion, it should be noted that the evaluation of the liquefaction potential by comparing the expected forces of an earthquake with those that the soil can actually resist, is not a safety analysis in the customary way, as the magnitude of an earthquake is a random variable.

#### 4 Performance of Vibro Replacement

Vibro Replacement is more suitable than most other foundation techniques in preventing liquefaction during a seismic event. Generally, the problem can be solved by three alternatives, for which vibro replacement offers the best conditions: soil compaction, drainage and increase in shear resistance.

Which of these prevails with regard to vibro replacement, depends on the grain size distribution of the soil concerned. Figure 2 shows a dashed transition zone relating to deep vibratory compaction techniques, which is located more or less in the middle of the area susceptible to liquefaction, and plays a dominant role.

It is assumed here that the two main compaction techniques, vibro compaction and vibro replacement, are already well known. Therefore, only the main features are described here, in order to understand their performance in soils susceptible to liquefaction. Vibro compaction increases soil density, while vibro replacement, in its pure application, reinforces cohesive, non-compaction soils, using load carrying columns of imported coarse aggregate such as gravel or crushed material. Often, vibro replacement has the combined effect of considerable densification of the surrounding soil by vibrational effects during the installation of stone columns. As in static cases, it is also useful in dynamic events to consider both components of improvement separately, namely the soil densification and the improvement by the stone columns.

Soils with a grain size distribution curve entirely outside the transition zone at the sandy, gravelly side are suitable for treatment solely by vibro compaction. If the distribution curve is totally within the dashed zone, or partly within it with the remainder on the coarse side, it is advisable to add backfill material, that is, install a stone column. The reason for this is to improve transmission of vibrations via the imported material, as the main target is still the densification of the surrounding soil. In all other cases, where the grain size distribution curve is partly or entirely to the left of the transition zone, that is, in the silty clayey area, substantial improvement in the densification due to vibration can not be expected, and stone columns have to be installed which provide considerable improvement due to their stiffness and shear resistance.

Therefore, as shown in *figure 2*, the transition zone between vibro compaction and vibro replacement subdivides the range of soils susceptible to liquefaction into three parts. Generally, as described above, for soils that are within the sandy range, vibro compaction without imported backfill material is suitable for preventing earthquake induced liquefaction. This can be substantiated by cone penetration tests as outlined in section 3 above. In addition, in both the other cases, where vibro replacement is either recommended or definitely required, the improvement by densification can also be substantiated by the same method. However, if the favourable effects of the stone columns with respect to drainage capability and increase in shear resistance are ignored, the result is a very conservative treatment design.

The type of drainage which contributes considerably to the reduction of pore water pressure during the usually very short period of an earthquake, and which thereby reduces the risk of liquefaction, can only be expected in densifiable soils where vibro compaction alone is recommended. In finer grained soils with relatively low permeability, substantiating a reduction in porewater pressure, and hence proving that the risk of liquefaction has been reduced, becomes difficult. However, even if a considerable reduction in the pore water pressure cannot be proved, even at short distances from the column, the high permeability of the columns themselves is decisive for their bearing performance. A high gradient at the periphery of the columns provides the required lateral support, and hence the bearing capacity, even at moments where the soil between the columns could tend to liquefy.

Columns which are laterally supported in the limiting state by the difference in hydraulic pressure provide considerable shear resistance, especially due to load concentration. However, compared to piles, they have the advantage of high flexibility which can absorb the amplitudes occurring during an earthquake, without losing their bearing capacity. This implies that seismic shocks are not reduced significantly by vibro replacement. Therefore, the treatment does not necessarily provide protection for the buildings, but is primarily concerned with the prevention of liquefaction. Any conclusion should not discount that in some cases, buildings which might have otherwise been destroyed by the shaking of non-liquefied soil have remained relatively undamaged solely because of liquefaction.

Since it is difficult to quantify the favourable effects of stone columns in seismic events, in some cases they were not considered in the design at all. In some other cases, where the densification of the soil just missed the specifications, they were given a qualitative consideration only, in the sense that they would compensate for the deficit in soil densification. Such an approach is not satisfying and even rough approximations on a static basis are preferable.

### 5 Evaluation of Liquefaction Potential with Vibro Replacement

It is not possible to estimate, by statistical analyses, the extent to which the risk of liquefaction is reduced by vibro replacement. Fortunately, no failure has occurred so far, even though the application of this method of improvement has been steadily growing. Nevertheless, such analyses for vibro replacement would be difficult to be implemented due to additional variable parameters attributable to the arrangement of the columns.

As the existing analyses collected so far have already proved reliable, a different approach can be made in the design in order to include them. The question does not then become, to what extent have the shear resistance and load bearing capacity been changed by the stone columns, but rather, which part of the forces exerted by an earthquake are borne by the columns without any damages? Such a step, namely reducing the acting forces instead of increasing the resisting ones, is permissible as long as the evaluation, as previously mentioned, is not a customary determination of safety.

It is difficult to determine what amount of the acting forces in a seismic event is taken by the stone columns. Evaluations on the basis of computer simulations or theoretical approaches are more suitable than laboratory tests, in which possibilities are limited. A relatively simple proce-

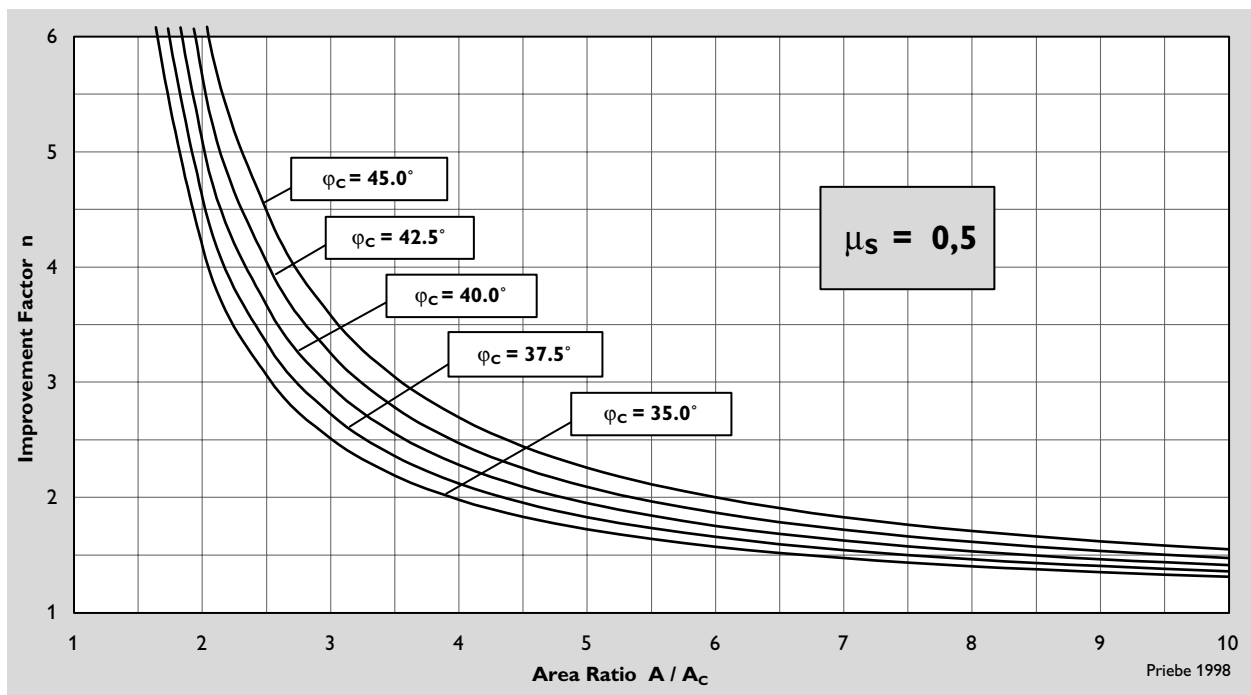


Figure 6: Design chart for vibro replacement

dure for the design of vibro replacement in static cases was outlined comprehensively in *Ground Engineering* (Priebe, 1995). This method was introduced a while ago in Germany and has since proved reliable. Static cases mostly comprise long-term processes, and therefore, as a general approximation, a Poisson's ratio of  $\mu_s = 1/3$  was proposed.

On the other hand, for short-term seismic events, it seems more realistic to consider deformations of the soil with the volume remaining constant, that is, to calculate with  $\mu_s = 0.5$  which also simplifies the formulae. In the above mentioned procedure the improvement factor  $n_0$ , which is the basic value of improvement by vibro replacement, is determined initially using some simplifications and approximations. It is shown in *figure 6*.

$$n_0 = 1 + \frac{A_c}{A} \cdot \left[ \frac{1}{K_{aC} \cdot (1 - A_c/A)} - 1 \right] \quad K_{aC} = \tan^2(45^\circ - \varphi_c/2)$$

where  $A$  = attributable area within the compaction grid  
 $A_c$  = cross section of stone columns  
 $\varphi_c$  = friction angle of column material

The reciprocal value of this improvement factor is merely the ratio between the remaining stress on the soil between the columns  $p_s$ , and the total overburden pressure  $p$  taken as being uniformly distributed without soil improvement and, as such, can be used as a reduction factor. It is simple to calculate this value or it can be taken from *figure 7*.

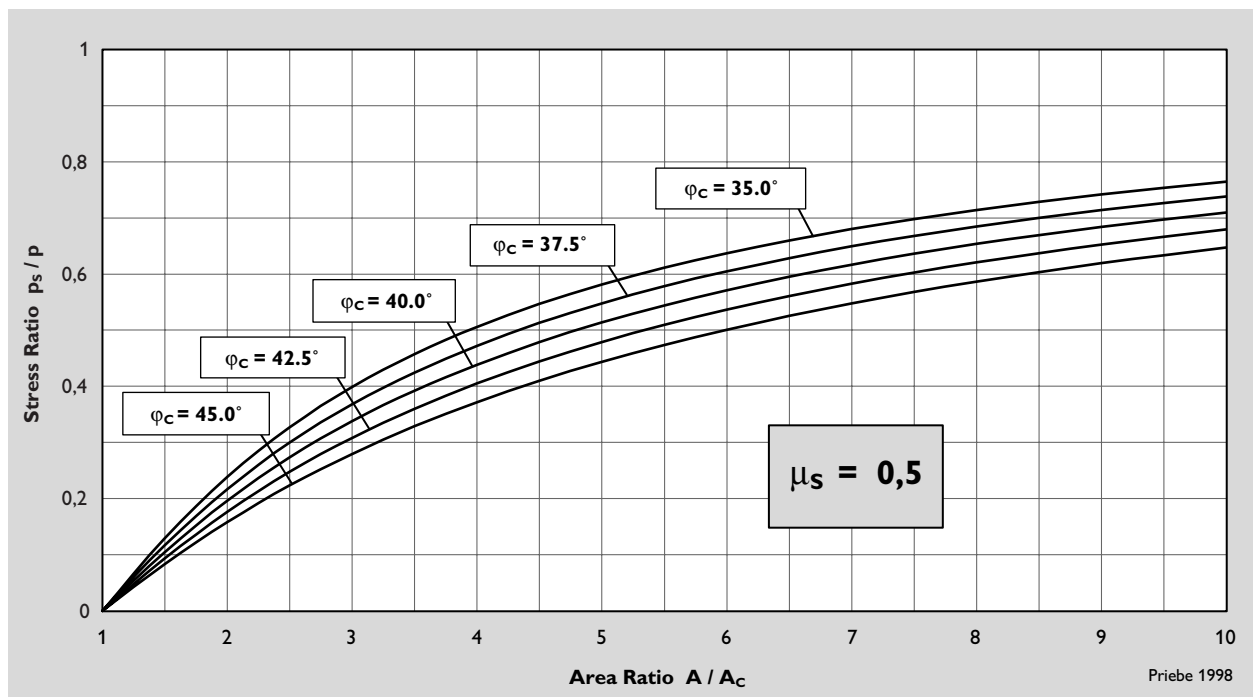


Figure 7: Residual stress on soil between stone columns

$$\alpha = p_s / p = 1/n_0 = \frac{K_{aC} \cdot (1 - A_C/A)}{A_C/A + K_{aC} \cdot (1 - A_C/A)^2}$$

On the understanding that the loads taken by the columns from both the structure and the soil do not contribute to liquefaction, it is proposed to use this factor  $\alpha$  to reduce the Seismic Stress Ratio created by an earthquake, and hence evaluate the remaining liquefaction potential as outlined in section 3.

This procedure represents an approximation which, although not being completely satisfactory from a geotechnical point of view, nevertheless does realistically consider the stabilising effect of vibro compaction.

## 6 Case Histories

The first project where vibro replacement was used to reduce the risk of liquefaction in a seismic event was at the waste water treatment plant of Santa Barbara, in California, USA. This project is relatively well documented and especially interesting, as it has already withstood an earthquake where the acceleration corresponded to the one considered in the design (Mitchell, 1986)

More recently, this improvement technique has been increasingly applied against the risk of earthquakes in a wide range of applications, from bridges and barrages to industrial and marine facilities (Dobson, 1987).

To date, only a few facilities constructed on ground improved by vibro replacement have actually been subjected to earthquakes. However, in such cases, no serious results have been observed, and therefore, at least qualitatively, vibro replacement has proved to be a success (Mitchell / Wentz, 1991).

On a more recent project for oil storage tanks on the Black Sea coast in Georgia, vibro replacement has been carried out to reduce both the settlements and the risk of liquefaction. A soft silty clayey top layer, with thickness ranging from 1 m to 4 m, is underlain by mostly sandy strata with varying silt content up to a depth of approximately 22 m which, in turn, is underlain by calcareous hard clay. The groundwater table lies at around 2 m below ground level.

The tanks, already under construction, have a diameter of 66 m and, in service condition, exert a foundation pressure of up to 150 kN/m<sup>2</sup>. With regard to earthquakes, the design was based on a maximum acceleration of  $a_{\max} = 0.25 \text{ g}$  which corresponds to a magnitude of  $M \approx 6.5$  according to *figure 3*.

For the tank used in the design example below, the soft top layer was completely removed by soil replacement up to a depth of 2.7 m. Vibro replacement was then carried out down to a maximum depth of 11.5 m, with up to 1 m diameter columns placed on a square grid at 3 m spacing.

Calculations for the design, utilising the relevant formulae and diagrams, were performed using a computer program, and the results are shown in *figure 8* below. The upper level of the layers concerned is of main interest with regard to the required cone resistance. For the silty sands beneath the soil replacement, fines contents of 15 per cent were assumed, and the bulk densities

estimated. The measured cone resistance decreased considerably at 8 m depth, most probably due to a silt content higher than the 15 per cent considered, which is also demonstrated by densification of the soil not being achieved by the treatment below this depth. Therefore, in this instance, it is acceptable that the required cone resistance slightly exceeds the measured one. The same also applies at the full depth of treatment. For the rest, the measured values are well above those required and, therefore, there is no concern at all with regard to liquefaction of the upper strata which are generally more crucial.

<b>SUPSA Terminal, Tank D</b>												
<b>Maximum Earthquake Acceleration <math>a_{max} = 0.25 \text{ g}</math></b>						<b>Magnitude <math>M = 6,5</math></b>						
<b>Parameters of Vibro Replacement</b>			Grid Size A			9.00 m <sup>2</sup>						
			Column Diameter D			1.00 m						
			Area Ratio $A_C/A$			0.09						
			Backfill Material $\phi$			42.50°						
			Coeff. of Act. Earth Pressure $K_{aS}$			0.19						
			<b>Reduction Factor <math>\alpha</math> <sup>1)</sup></b>			<b>0.71</b>						
<b>General Parameters</b>			Ground Water Table			2.00 m						
			Surface Load			0.00 kN/m <sup>2</sup>						
<b>Calculation <sup>2)</sup></b>												
F. C.	Depth	$\gamma$	$\gamma'$	$\sigma_{v0}$	$\sigma'_{v0}$	$r_d$	SSR	$\alpha * \text{SSR}$	$q_{c1}$	$C_q$	$q_{c, \text{requ.}}$	$q_{c, \text{meas.}}$
[%]	[m]	[kN/m <sup>3</sup> ]		[kN/m <sup>2</sup> ]					[MPa]		[MPa]	
5	0.00	19.0	11.0	0.0	0.0	1.00	0.000	0.000	0.0	2.250	0.0	0.0
5	2.00	19.0	11.0	38.0	38.0	0.98	0.159	0.113	6.8	1.525	4.5	10.0
15	2.70	18.0	9.0	52.7	45.7	0.97	0.181	0.129	4.7	1.432	3.3	10.0
15	4.00	18.0	9.0	77.4	57.4	0.95	0.209	0.148	5.5	1.310	4.2	10.0
15	8.00	18.0	9.0	153.4	93.4	0.90	0.241	0.172	6.4	1.038	6.2	6.0
15	11.50	18.0	9.0	219.9	124.9	0.86	0.247	0.175	6.6	0.878	7.5	7.0

1) Priebe, Kolloquium Darmstadt, 1998

2) Stark and Olson, Journal of Geotechnical Engineering, 1995

Figure 8: Evaluation of the liquefaction potential at SUPSA Terminal, Tank D

## References

- Department of the Navy, Naval Facilities Engineering Command, Design Manual 7.3 (1983)  
Soil Dynamics, Deep Stabilization, and Special Geotechnical Construction
- Dobson, T. (1987)  
Case Histories of the Vibro Systems to Minimize the Risk of Liquefaction.  
Soil Improvement - A Ten Year Update, Geotechnical Special Publication No. 12
- Engelhardt, K., Golding, H. C. (1975)  
Field testing to evaluate stone column performance in a seismic area. *Geotechnique* 25
- Herzog, M. (1980)  
Zwei Versagensarten des Baugrundes unter Erdbebenwirkung. *Bauingenieur* 55
- Klein, G. (1990)  
Grundbau-Taschenbuch, 4. Auflage, Teil 1
- Mitchell, J. K. (1986)  
Material Behaviour and Ground Improvement.  
International Conference on Deep Foundations, Beijing, Vol. 2
- Mitchell, J. K., Wentz, F. J. 1991  
Performance of Improved Ground during the Loma Prieta Earthquake.  
Report No. UCB/EERC-91/12
- Peck, R. B. (1979)  
Liquefaction Potential: Science Versus Practice.  
ASCE, Journal of the Geotechnical Engineering Division, Vol. 105
- Prater, E. G. (1977)  
Verflüssigung von Bodenschichten infolge Erdbeben.  
Mitteilungen der Schweizerischen Gesellschaft für Boden- und Feldmechanik, Nr. 97
- Priebe, H. J. (1989)  
The prevention of liquefaction by vibro replacement.  
Conference on Earthquake Resistant Construction and Design, Berlin
- Priebe, H. J. (1995)  
Die design of vibro replacement. *Ground Engineering*, Vol. 28, No. 10
- Robertson, P. K., Campanella, R. G. (1985)  
Liquefaction Potential of Sands Using the CPT.  
ASCE, Journal of Geotechnical Engineering, Vol. 111
- Seed, H. B., Booker, J. R. (1977)  
Stabilization of Potentially Liquefiable Sand Deposits Using Gravel Drains.  
ASCE, Journal of the Geotechnical Engineering Division, Vol. 103
- Seed, H. B., Idriss, I. M., Arango, I. (1983)  
Evaluation of Liquefaction Potential Using Field Performance Data.  
ASCE, Journal of Geotechnical Engineering, Vol. 109

Singh, S. (1996)

Liquefaction characteristics of silts. Geotechnical and Geological Engineering

Stark, T. D., Olson, S. M. (1995)

Liquefaction Resistance Using CPT and Field Case Histories.  
ASCE, Journal of Geotechnical Engineering, Vol. 121

Suzuki, Y., Koyamada, K., Tokimatsu, K. (1997)

Prediction of liquefaction resistance based on CPT tip resistance and sleeve friction.  
International Conference on Soil Mechanics and Foundation Engineering, Hamburg

Wenk, T., Schwarz, J. (1995)

Das Große Hanshin-Erdbeben vom 17. Januar 1995. Bautechnik 72

Annexure 2 Technical paper on “Optimal Foundations in Soft Ground:  
An Innovative Approach for Economizing Cost and Time”

# OPTIMAL FOUNDATIONS IN SOFT GROUND: AN INNOVATIVE APPROACH FOR ECONOMIZING COST AND TIME

I.V. ANIRUDHAN<sup>1</sup>, A. MADAN KUMAR<sup>2</sup> and Y. HARI KRISHNA<sup>2</sup>

<sup>1</sup>*Consultant, Geotechnical Solutions, Chennai, India*

<sup>2</sup>*Keller Ground Engineering India Pvt Ltd, Chennai, India*

Improvements of productivity and effective project management procedures have become extremely important for speedy completion of projects with positive results. This paper discusses a milestone project comprising 198 residential units of stilt plus four levels that highlighted the benefits of these key aspects. Success of ground modification procedure benefitting the entire cycle involving End Users, Suppliers, Bankers and Developer is discussed.

Soil profile of the present study comprises weak layers of silty clay and sandy clay with varying consistency for a considerable depth. Deep foundations have been the automatic choice of foundation for major buildings constructed in similar environment. After serious geotechnical appraisal, reconsideration of the foundation system with an alternative solution of Ground Improvement was found to be optimal in terms of Cost and Time. Full raft foundation over the ground improved by installation of Vibro Stone Columns using dry bottom feed technique was found to be the most suitable alternative foundation system.

The ground improvement works were completed within six weeks as against six months to that of pile foundations. This was made possible through effective project management and the raft foundation was cast simultaneously. Full size plate load tests were conducted to ascertain effectiveness of the ground improvement works. Success of the foundation system was proved by full scale monitoring of foundation settlement during and after completion of the project over a span of 2 years. This paper describes design considerations, quality control in the construction of Vibro Stone Columns using dry bottom feed method and performance monitoring of the project thereafter.

## 1. Introduction

Deep foundations like bored cast-in-situ piles and driven piles have historically been the foundation choice for major buildings and other structures constructed in the weak soil deposits. Construction of pile foundations is becoming a challenge due to their high cost, large construction time and also due to severe environmental issues (noise pollution, ground vibrations and carbon footprint). However, given their acceptance in the construction community, driven pile foundations were initially selected as the foundations for the proposed residential project. Since the proposed building complex is located within the close proximity of a well-developed residential locality, severe resistance by the neighborhood to the pile driving activities called for a rethinking on the foundation system.

According to the soil investigations conducted at the proposed project site, the top 6m to 8m of soil profile comprises of silty clay / sandy clay having highly varying consistency. Ground water table was encountered at about 3.0m below the existing ground level. Under the present scenario, the reconsideration of the type of

foundation system with respect to the geotechnical analysis gave a thought to assess feasibility of alternative foundation system using appropriate ground improvement system.

Ground Improvement refers to a technique that improves the engineering properties of the weak soil mass treated. Usually, the properties that are modified are shear strength, stiffness and permeability. Ground improvement has been developed into a sophisticated tool to support foundations for a wide variety of structures. Properly applied, i.e. after giving due consideration to the nature of the ground being improved and the type and sensitivity of the structures being built, ground improvement often reduces direct costs and saves precious construction time

## **2. Acceptability of Ground Improvement Procedures**

For the last two decades, ground improvement using stone columns have been profoundly increased on local soils which are unable to take high foundation loads. Typically stone column consists of a vertical reinforcement introduced by constructing a column of densely packed stones partially or fully replacing the local weak soil. The construction can either by wet or by dry method. The inclusion of stone columns in a specific grid pattern allows the soil mass behaves like a homogenous layer of improved density and stiffness. This process yields enhancement of load bearing capacity and minimizes the settlements of the treated ground compared to the untreated ground.

Stone columns acts as drainage path allowing for rapid consolidation which in turn improves the strength and deformation characteristics of the ground at a much faster rate. Stone columns constructed using vibro techniques allows full or partial displacement instead of partial or full replacement of the weak soil and then leads to further improvement of displaced weak soil by faster dissipation of construction pore water pressure. Also, the improved drainage capabilities of the stone column treated ground provide a much better resistance to liquefaction of the surrounding soil. The resistance to liquefaction is achieved by densification of surrounding weak soil and also by the much increased capacity for faster dissipation of excess pore water pressure.

## **3. Ground Improvement by Vibro Techniques**

Vibro Replacement is an accepted method for subsoil improvement, in which large-size columns of coarse grained material are installed in the soil by means of high capacity depth vibrators. Performance of this composite system consisting of stone columns as reinforcing elements and the weak soil mass that can be established theoretically can also be established by full size field plate load tests. Priebe (1995) developed design of vibro stone columns on theoretical basis which can be adopted to different soil conditions.

Contrary to vibro compaction which densifies non-cohesive soils due to vibrations, vibro replacement improves cohesive and non-cohesive soils by reinforcing the weak soil with load bearing columns of well compacted, coarse grained material. When the entire weak soil is replaced with a well compacted coarser material, there is no complexity in the understanding of its improved load carrying capacity and corresponding deformations. But, when the weak soil is partially replaced and displaced

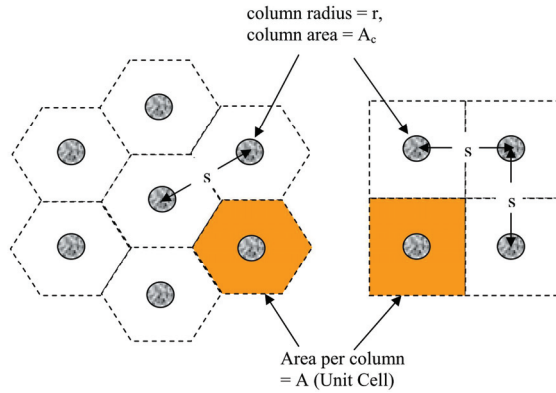


Fig. 1. Unit cell of stone columns and typical arrangement of triangular grid and square grid.

by the introduction of these stiffer reinforcing elements at regular grid patterns, response of this modified ground becomes complex. There are ways for arriving at an equivalent stiffness matrix of a system that replaces some part with a material of larger stiffness. Similarly, there are ways and means to establish the modified density and stiffness when the entire soil mass is densified. When the improvement is attributed to both displacement and replacement, the quantification of improvement is difficult to determine. Considerable efforts like large-scale load tests can only prove the effectiveness of the installed stone columns. In a first step, an improvement factor is established by which stone columns improve the performance of the subsoil in comparison to the state without columns just by increasing the overall stiffness. The grid patterns and concept of unit cell is illustrated in Figure 1. Basic improvement factor can be arrived based on the area replacement ratio and the reinforcing material used for stone columns.

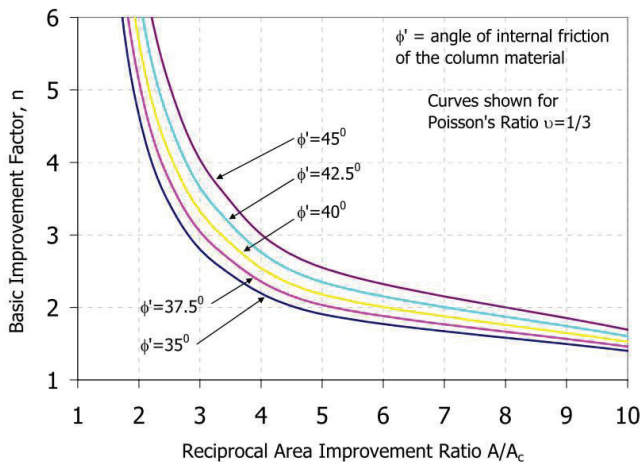


Fig. 2. Priebe's basic improvement factor (reproduced from Priebe, 1995).

Improvement factor (a factor is established by which stone columns improve the performance of the subsoil in comparison to the state without columns) is presented in Figure 2. According to this improvement factor, the deformation modulus of the composite system can be established due to which settlements will be reduced.

The deformation modulus of the composite system is one of the basic inputs for finalizing the design of stone columns. However, the reality is that in many practical cases the reinforcing effect of stone columns installed by vibro replacement is superposed with the densifying effect of vibro compaction, i.e. the installation of stone columns densifies the soil between grids increasing its  $k_0$  (coefficient of earth pressure at rest) and  $k_p$  (coefficient of passive earth pressure). In such case, the densification of the soil has to be evaluated on the basis of original soil data and correspondingly the design of vibro replacement can be modified to suit particular improved site condition.

#### 4. Vibro Stone Columns (Dry Bottom Feed Method)

Keller has developed the system of custom-built machine called the Vibrocat for installation of vibro stone columns without using water. The Vibrocat comprises a specially constructed track mounted supporting unit, attached with high capacity depth vibrator, which incorporates a stone tube with compression chamber and stone feed hopper ensures properly formed compacted stone columns to the required diameter and depth. A special feature of the dry method is that it does not require water jetting for penetration and hence eliminates the need to handle the collected water. Furthermore this method can be used most successfully where limited working

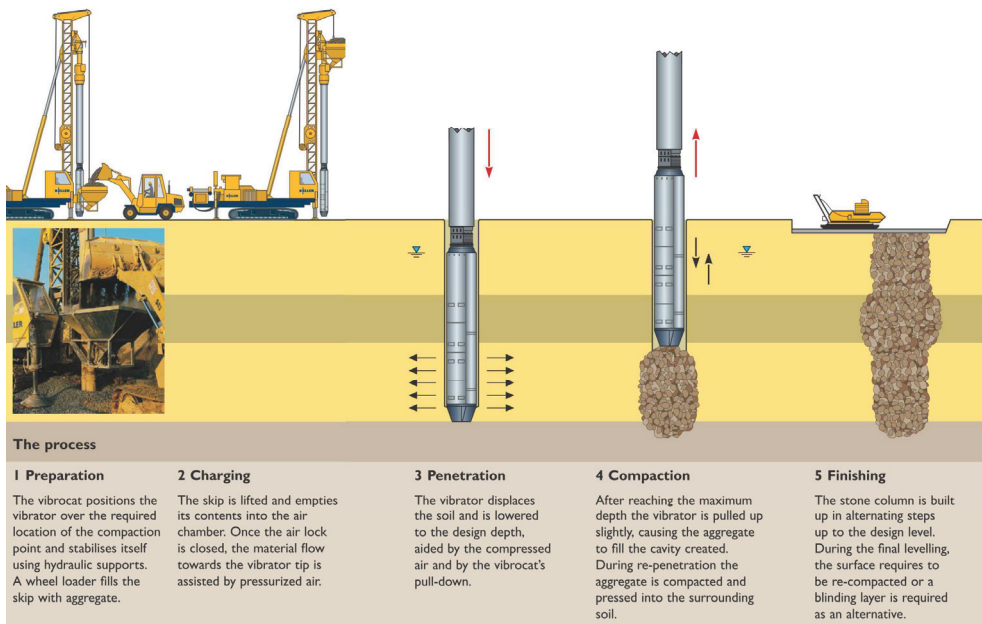


Fig. 3. Sequence of installation of vibro stone columns (dry bottom feed method).

space is available, especially in developed or urban areas or where no near water source can be found. This technique provides effective drainage paths to ensure rapid consolidation. It also has a built-in real time computer monitoring system to provide quality control on compaction effort throughout the construction process. Sequence of installation of vibro stone columns using dry bottom feed method is illustrated in Figure 3.

### 5. About the Project and Subsoil Conditions

Urban Tree Infrastructure Private Limited (Urban Tree), Chennai, proposed to develop a residential project in Chennai. The project comprises of 198 units of Stilt + 4 floors and the approximate area of development is about 2.5 acres. Typical project layout is shown in Figure 4.

The sub-soil in the project site comprises desiccated clay and medium dense sand up to about 3.50m followed by relatively weak clay and sandy clay up to 6.0m depth. This top 6.0m soil with highly varying consistency is followed by about 8.0m with medium dense sand stiff clay deposits after which there is a 6m thick layer of medium stiff consistency. Denser sand layers and hard clay layers are forming the remaining sub-soil profile.

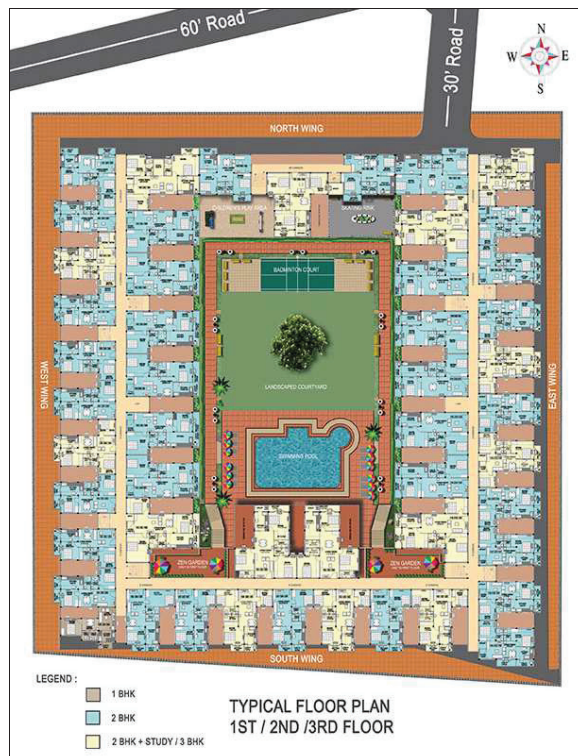


Fig. 4. Overall layout of the proposed project site.

## 6. Design of Foundation System

The performance of individual footings (shallow foundations) would not be effective due to weak to very weak soil layers till 6m depth below the existing ground level. Larger settlements were expected in case of raft foundation due to high structural loads. The range of settlement estimated in the investigation report was about 220mm out of which the top 6m to 8m soil attributing about 115mm. Based on the subsoil conditions, driven cast-in-situ piles resting in hard clay layers below 25m were adopted and, as described earlier, the construction of piles were stopped due to environmental issues.

In this context a possible alternative solution of suitable ground improvement technique in place of already chosen driven cast-in-situ pile foundations resting in hard/competent strata available at about 25m as foundation system is very much advantageous. Under these circumstances, the developer has contacted M/s Keller India to undertake design and execution of the ground improvement works. Considering the project boundary conditions, vibro replacement (stone columns with dry bottom feed method) was selected as a viable method for subsoil improvement and a full raft foundation supported by the treated ground as an alternative foundation system. The selected method of ground improvement satisfied in addressing environmental issues raised at project site. In this method, the stone columns are installed by displacement technique (without removing any soil). Hence, the site environment would be comparatively clean and tidy. In addition, benefits with regard to economizing the foundation cost and optimizing construction time was proven invaluable for the project.

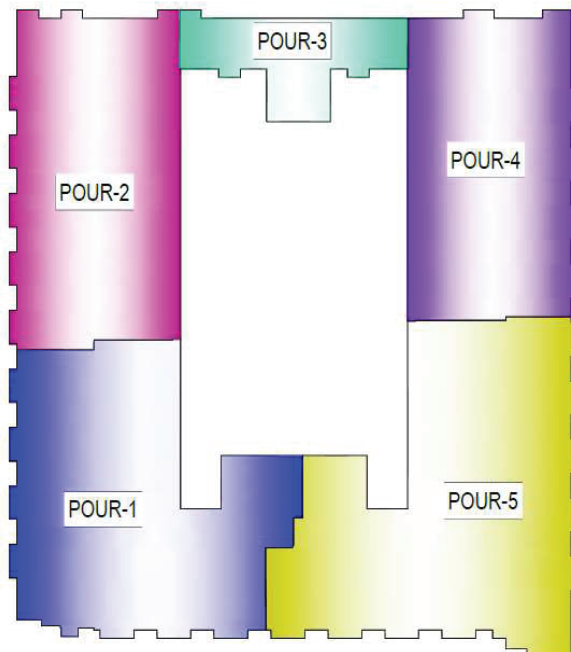


Fig. 5. Footprint of the raft foundation (divided into pours for ease of construction).

As described above, the construction will have stilt plus four floors with average load intensity at the foundation level which is be approximately 75 to 85 kPa. A total footprint area of about 5500m<sup>2</sup> under the raft foundation is to be treated. The foundation raft was divided into six pours for ease in construction. Layout of the proposed building is shown in Figure 5. Individual column loads from the super structure vary from 25 T to 185 T. Though the raft foundation transmits uniform pressure to the bearing soil, denser grid was adopted for pour having large column loads.

Critical review in terms of strength and deformation characteristics for the proposed loading conditions were made using Priebe (1995) design methodology and appropriate geometry (stone column diameter, spacing, pattern and depth) has been chosen. The final scheme was reviewed and vetted by M/s Geotechnical Solutions, Chennai, a third party specialist Geotechnical Consultancy firm for Geotechnical compliance. Typical scheme and cross section of ground improvement using vibro stone columns using dry bottom feed method adopted for the present project is illustrated in Figure 6.

### **6.1. Quality Control and Monitoring**

In order to measure and assure the quality of stone columns being constructed, it is necessary to adopt stringent quality control and quality assurance procedures to meet the specifications and to satisfy the client's requirement at various stages of execution of the project.

### **6.2. During Execution of Ground Improvement**

The installation of each stone column was recorded by the use of an automated computerized recording device fitted to the Vibrocat. This instrument yields a computer record (M4 Graph) of the installation process in a continuous graphical mode, plotting depth versus time and power consumption (compaction effort) versus time. The information provided includes:

- Stone column reference number
- Date of installation
- Start and finish times of installation
- Period required for installation
- Maximum depth
- Compaction effort during penetration and compaction process

The above parameters allow to monitor the quality of the stone columns being installed. Further, diameter of the stone column and consumption of backfill are continuously monitored by the site personnel to estimate the in-situ achieved diameter.

### **6.3. Post Construction**

Full size field plate load test is one of the accepted ways to assess the performance of the improved soil treated with stone columns. The size of the test pad and the magnitude of the test load can vary according to the stone column layout, treatment depth, load and type of structure. Routine Stone Column Load tests were performed

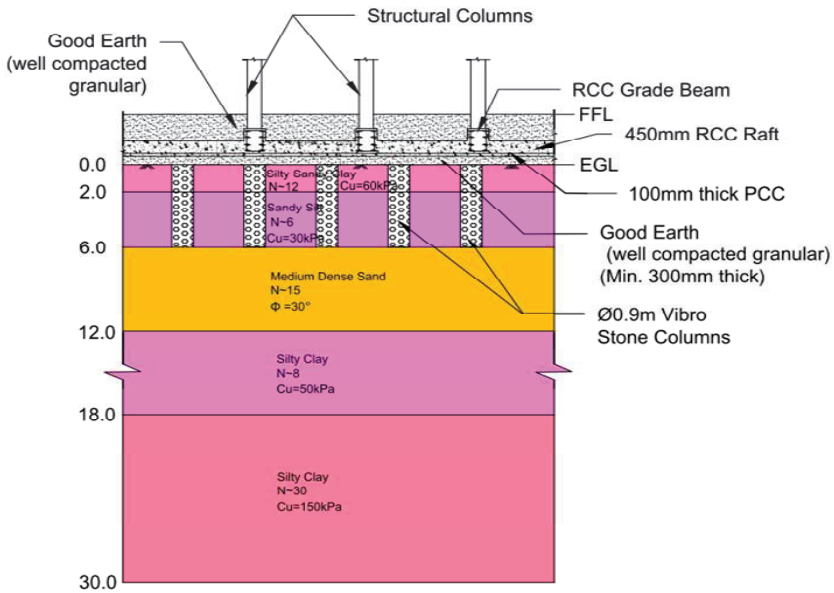


Fig. 6. Typical soil profile showing ground improvement arrangement.

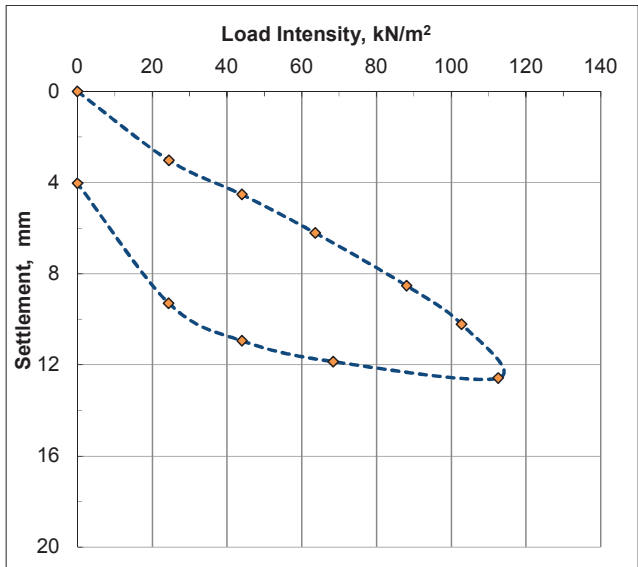


Fig. 7. Results of single column routine plate load test.

to ascertain the effectiveness of design and performance of the ground improvement works. The observed settlements are within the acceptable limits of 75 to 100 mm for raft foundations according to the stipulations specified in Indian Standard Code

of Practice (IS 1904-1986) for the applied design load intensity of 100 kPa. Load test results are presented in Figure 7.

### 7. Real Time Settlement Monitoring

Success of the foundation system needs to be proved by full scale monitoring of foundation settlement during and post completion of the project. Post construction real time monitoring offers confidence on the engineering judgment taken at various stages of the project completion. In this section the predicted design settlements which are calculated using conventional methods are being compared with the actual settlement occurred at the site by adopting proper monitoring systems.

Keeping the importance of the post construction performance of the structure, about 14 locations were identified on the raft foundation to monitor settlements during and post construction. After completion of the installation of the ground improvement works, raft foundation is laid on the treated ground. The entire building foundation area was divided into 6 zones which are delineated based on concrete pour-1 to pour-6. Typical arrangement of the selected locations is shown in Figure 8.

Selection of 14 numbers is based on the number of concrete pours in overall raft foundation i.e., 2 locations per each concrete pour and reduced levels were recorded in regular intervals. Summary of the predicted and observed settlements are shown in Figure 9.

The measured settlements are substantially lower than the predicted settlement, which proved the efficiency of the raft foundation resting on improved ground. It can

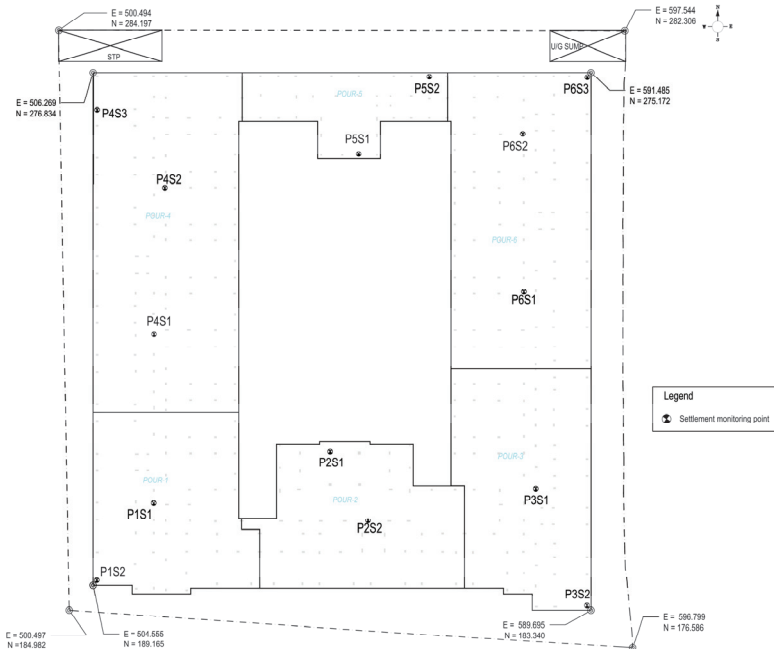


Fig. 8. Settlement monitoring points.

Settlement Points	Designed Settlement (mm)	Observed Settlement (mm)	Settlement recently observed on
P1S1	64	50	29th May 2015
P1S2	64	45	
P2S1	64	13	
P2S2	64	23	
P3S1	64	47	
P3S2	64	51	
P4S1	64	51	
P4S2	64	47	
P4S3	64	47	
P5S1	64	24	
P5S2	64	28	
P6S1	64	39	
P6S2	64	40	
P6S3	64	52	

Fig. 9. Summary of predicted and observed settlements.

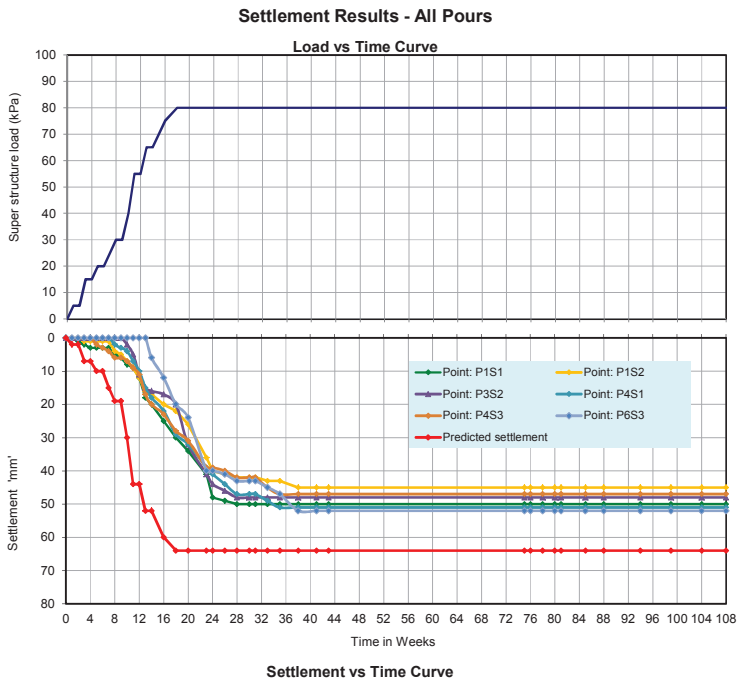


Fig. 10. Results of observed settlements.



Fig. 11. Completed structure (foundation resting on vibro stone columns, dry bottom feed).

be seen from Figure 10 that the load in the super structure increases with increase in number of floors and the corresponding settlements are increased.

The superstructure load is increased from 0 to 80 kPa in 20 weeks and correspondingly predicted settlements (analytical method) increased from the 0 to 64 mm. However, the observed settlements are considerably less than the predicted settlements as well as the allowable settlements of 75 to 100 mm for raft foundations resting in clayey soils. Pattern of the observed settlements at one of the pour is presented in Figure 10. The total settlement observed at the start of maximum loading (after 18 weeks) was about 30mm that was gradually increased to about 50 mm during the next 17 weeks and remained more or less uniform thereafter. It is suggesting that the long term settlements will be of much smaller range than that was expected.

## **8. Conclusions**

Application of vibro replacement proved to be an effective ground improvement solution in varying soil conditions. It is also proven from the results of extensive monitoring results that the required performance was achieved. Vibro stone columns made it possible to support residential buildings on weak deposits. In addition to improving shear strength and compressibility parameters, offered acceleration in the overall construction schedule and enabled the project to be completed within stipulated duration.

The ground improvement works were completed within 6 weeks (as against 6 months to that of pile foundations) that was made possible through effective project management. The project is getting delivered to the end users ahead of time as a result of construction speed of alternative foundation solution (i.e. 6 months vs. 6 weeks) marking a milestone in ground modification. The savings in time is key to success of ground improvement benefitting the entire cycle involving End Users, Suppliers, Bankers and Developer.

### **Acknowledgements**

A project of this nature is possible only with the cooperation and combined efforts of many persons. The authors wish to thank the developer of the project for their kind permission to publish the information contained in this paper. In particular, the authors wish to acknowledge Keller management for their continuous support and encouragement in finalization of theme of this paper including valuable comments and suggestions that helped the authors to refine and improve the quality of the paper. Thanks are also due to Keller India site team for providing photographs and other execution data.

### **References**

1. Hughes JMO & Withers N J, 1975, 'Reinforcing of Soft Cohesive Soils with Stone Columns', *Ground Engineering, Volume 7, Issue No. 3*.
2. Heinz J. Priebe, 1995, *The Design of vibro replacement, Ground Engineering, GT 037-13 E*.
3. IS: 1904 – 1986 (2006), *Code of Practice for Design and Construction of foundations in Soils: General Requirements*.

Annexure 3 Technical paper on “Vibro Stone Columns to Support Large Oil Storage Tank Farm on West Coast of India”

# VIBRO STONE COLUMNS TO SUPPORT LARGE OIL STORAGE TANK FARM ON WEST COAST OF INDIA

SRIDHAR VALLURI<sup>1</sup>, DEEPAK RAJ<sup>2</sup>, and VISHAL SHUKLA<sup>3</sup>

<sup>1</sup> *Geotechnical Manager, Keller Ground Engineering (I) Pvt. Ltd, Mumbai, India.*

*E-mail: sridhar@kellerindia.com*

<sup>2</sup> *Director, Keller Ground Engineering (I) Pvt. Ltd, Mumbai, India.*

*E-mail: deepak@kellerindia.com*

<sup>3</sup> *Civil Manager, Vijay Tanks and Vessels Pvt. Ltd, Vadodara, India.*

*E-mail: vishal@vijaytanks.com*

A large oil storage terminal is being constructed on the west coast of India at Pipavav port, in the state of Gujarat along the Arabian Sea. Proposed terminal has a storage capacity of 250,000 kilolitres to handle classified petroleum products A, B, C as well as non-classified products. The terminal comprises of 48 number of steel storage tanks with diameter varying from 12m to 25m and heights varying from 18 m to 20 m with slenderness ratio varying from 0.8 to 1.5. The storage tanks comprises of floating and fixed roof tanks with ring beam foundation to support the tank shell.

Extensive soil investigation has been carried out by exploring boreholes, conducting standard penetration tests and cone penetration tests. The subsoil consists of six to ten meters thick soft to firm silty clay layer. Ground improvement using Vibro Stone Columns is done to reduce the total settlements, control the differential settlements and increase the bearing capacity of the subsoil. Area replacement ratios varying from 16 to 23% were used with column diameters in the range of 1 m and treatment depths up to 10 m to support the tank foundations. More than twenty field load tests are conducted across the site in the foot print of the tank as one of the quality control measure. Settlement monitoring was carried out during the hydrostatic tests for all the 48 tanks.

This paper summarizes the details of proposed tanks, subsoil conditions, design scheme of vibro stone columns, quality control measures taken during the construction, hydrostatic test results and their analysis.

*Keywords:* Storage tanks, Slenderness ratio, Soft clay, Vibro stone columns, Quality control, Load tests, Hydrostatic tests.

## 1. Introduction and Project Background

Demand for petroleum and non-petroleum products is on rise due to rapid industrialization and growth in Indian subcontinent. A number of refineries and storage terminals are being constructed across the country, in order to cater to India's growing demand.

Gulf Petrochem (I) Pvt. Ltd. is developing an 'Oil Storage Terminal' at Pipavav Port. The terminal is located in Saurashtra in the state of Gujarat, 152 nautical miles northwest of Mumbai on the west coast of India and 140 km southwest of Bhavnagar. The proposed oil storage terminal will handle Class A, B and C as well as non-classified products with an annual storage capacity of 250,000kL. The terminal on commissioning will have complete flexibility for storing any type of oil product. The proposed terminal site is spread over eight (8) hectares area. The subsoil at the site

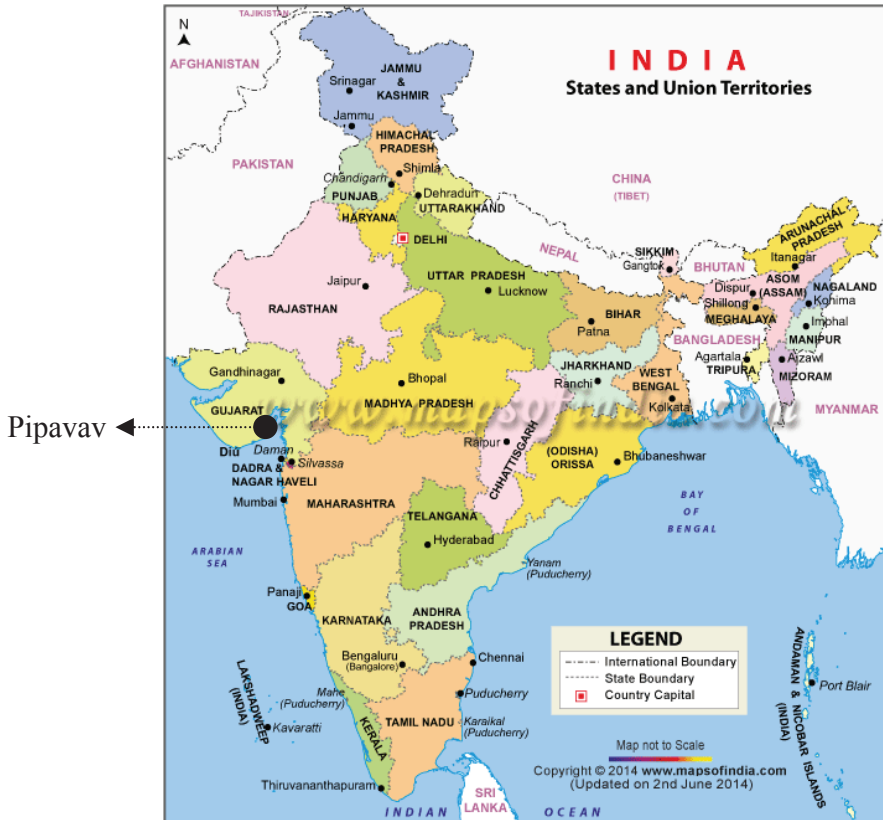


Fig. 1. Project Location - Oil Storage Terminal at Pipavav, Gujarat.

consists soft to firm clayey silt followed by stiff soils. The subsoil soil is expected to settle excessively under the imposed foundation loads. Hence, ground improvement using vibro stone columns is done to support the tank and the associated utility building foundations to increase the shear resistance of the soil, to control post construction long term and differential settlements.

**2. Details of the Structures at Proposed Tank Farm**

The proposed Oil Storage Terminal consists of construction of 48 no’s of steel storage tanks and associated utility structures like Office buildings, truck loading facilities and weigh bridges. Based on the storage type of the liquid, the tanks are arranged under six (6) enclosures as shown in Figure 2. Enclosure-1 comprises of floating roof tanks while the rest of the enclosures are having fixed roof tanks including two (2) no’s of fire water tanks. The diameter (D) and height (H) of the proposed tanks are varying from 12 m to 26 m and 18 m to 20 m, respectively. Due to higher slenderness ratio (H/D) and the uplift forces arising from tank design, ring beam foundation with anchor bolts were proposed as foundation interface for all the tanks. Details of tanks and utility structures proposed on ground improvement at the facility are provided in Table 1.

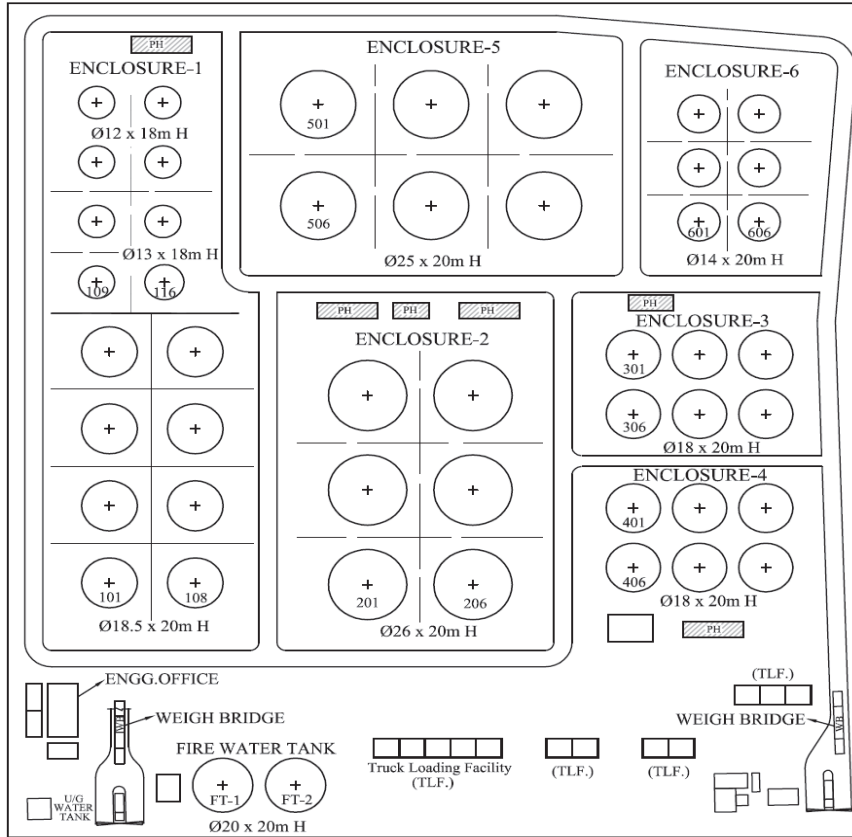


Fig. 2. Layout of Oil Storage Terminal at Pipavav, Gujarat.

Table 1. Details of the Tank Farm and Structures

Enclosure	No	D / L (m)	H / B (m)	Type of Roof	Storage Product	Storage Capacity (KL)
Enclosure-1	8	18.5	20	Floating	Class A	56,648
	7	12	18			
	1	13	18			
Enclosure-2	6	26	20	Fixed	Class C	60,000
Enclosure-3	6	18	20	Fixed	Non - Classified	30,000
Enclosure-4	6	18	20	Fixed	30,000	
Enclosure-5	6	25	20	Fixed	Class B	55,950
Enclosure-6	6	14	20	Fixed	Class C	17,538
Fire Water Tanks	2	20	20	Fixed	Water	12,560
Engineering office	1	20	10	RCC (G+3)	—	—
Weigh Bridge	2	12	3	—	—	—

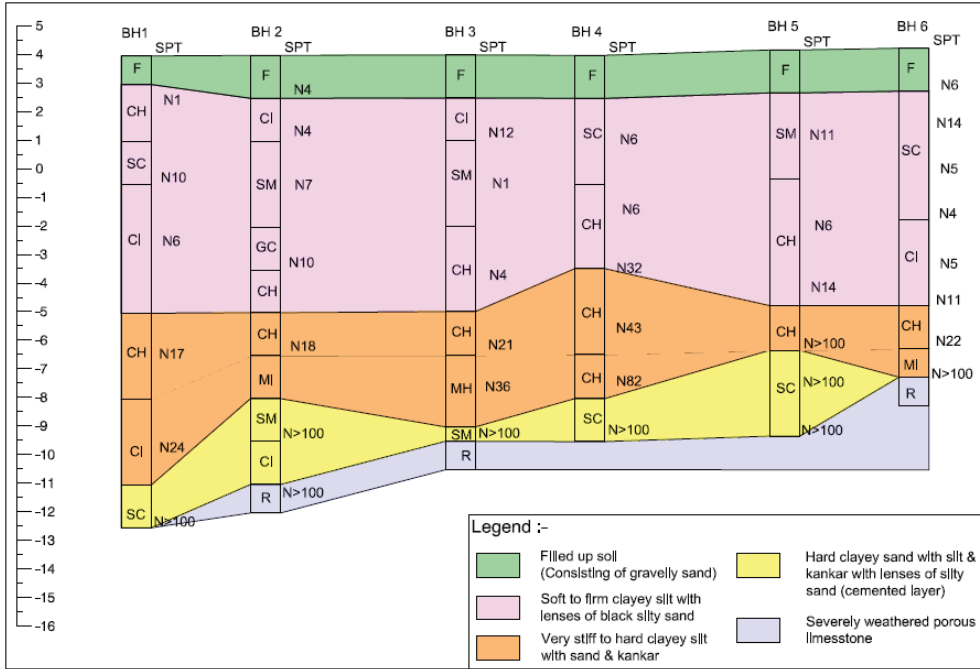


Fig. 3. Typical sub soil profile.

### 3. Subsoil Profile

The existing ground level (EGL) at the proposed site is varying from RL +4.6 m to RL +3.8 m. Extensive soil investigation was carried out at the proposed oil storage terminal site by exploring 15 number of boreholes and 46 number of electric Cone Penetration Tests (CPT) up to the refusal levels. This included an extensive field and laboratory tests on the disturbed and undisturbed soil samples obtained during the investigation. The subsoil in general consists of 1 m to 1.5 m thick fill from EGL, followed by 6.5 m to 9 m thick soft to firm silty clay/clayey silt layer with SPT, N values ranging from 4 to 10. This layer is underlain by 1.5 m to 3 m stiff to very stiff clayey silt/silty clay with SPT - N values ranging from 20 to 50, followed by the 1.5 m to 3 m thick clayey sand layer and below this rock is encountered. Typical subsoil stratification is shown in Figure 3.

### 4. Design Criteria

The design loading intensity of the proposed steel storage tanks is varying from 20 to 22 T/m<sup>2</sup>. Allowable long term total settlement at edge is 300 mm and 150 mm for fixed roof tanks and floating roof tanks, respectively. The allowable maximum differential settlement along the periphery between any two points is 1 in 300 and 1 in 500 for fixed roof tanks and floating roof tanks, respectively. For the utility buildings and associated structures the required design loading intensity was 15 T/m<sup>2</sup> with an allowable post construction long term settlements of 40 mm.

**5. Proposed Ground Improvement Solution**

The silty clay/ clayey silt in the top layers were expected to settlement excessively under the imposed foundation loads and also the soil capacity was not adequate to support the tank foundations. Hence, ground improvement using Vibro stone column is proposed to support the foundations of the storage tanks and associated terminal structures.

Using Vibro stone column technique, the following geotechnical improvements are achievable:

- Improvement in the stiffness of the subsoil to decrease settlements
- Improvement in the shear strength of the subsoil to increase bearing capacity
- Rapid consolidation of the subsoil
- To mitigate liquefaction potential

**5.1. Concept of Vibro Stone Columns**

Vibro Stone Column (Vibro replacement) technique introduces a coarse grained material as load bearing elements consisting of gravel or stone aggregate as a backfill medium. The stone column and the in situ soil form an integrated system having low compressibility and high shear strength. The excess pore water pressure can dissipate through the stone column, which also acts as a vertical drain. The settlement expected for the treated soil is reduced while the rate of settlement is increased when compared with the untreated soils.

**5.2. Design of Vibro Stone Column Works**

The design analysis of Vibro stone columns is carried out according to Priebe’s (1995) design methodology to meet the technical performance criteria as summarized in

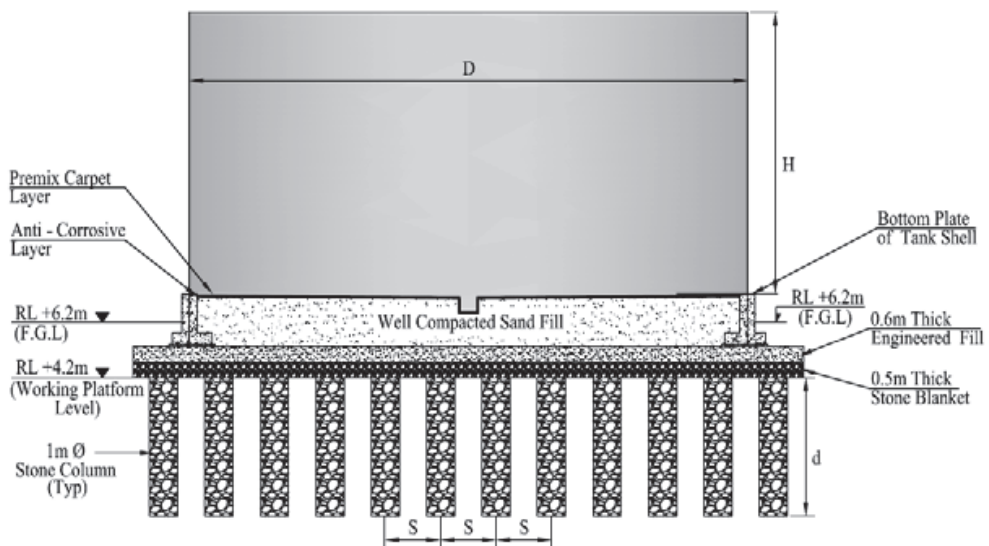


Fig. 4. Typical cross section of tank with vibro stone columns.

section 4. Vibro stone columns of 1 m diameter with an area replacement ratio varying from 16% to 23% were used across the site to meet the design requirements of floating as well as fixed roof tanks. Columns were designed to be terminated in the stiff layers. Depth of the columns was varying from 9.5 m to 10.5 m below EGL across the site. Treatment of stone columns was extended beyond the foot print area of the ring beam to provide confinement and to take care of the edge stability. Figure 4 shows typical cross section of tank with vibro stone columns foundation.

## 6. Construction Methodology

Top feed wet method was used for the installation of the vibro stone columns. In this method, the depth vibrator and extension tubes are suspended from a crawler crane. The vibrator penetrates the ground with the help of water jets at the side of vibrator,

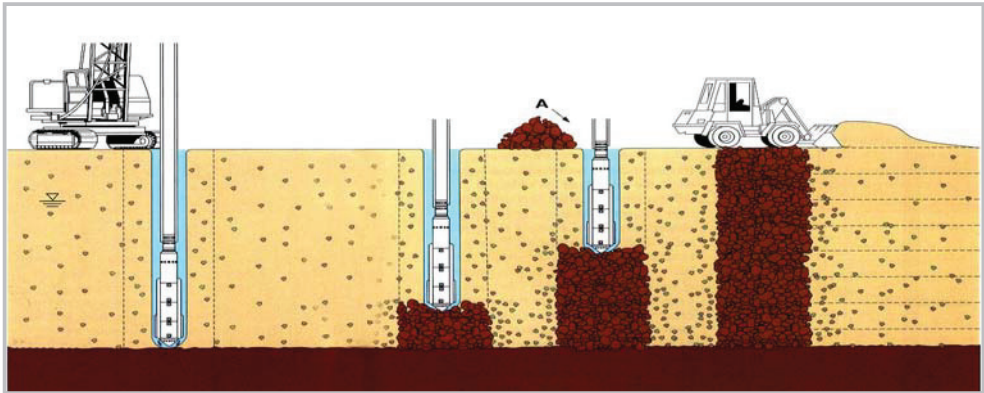


Fig. 5. Step wise illustration of vibro stone column installation by top feed wet method.



Fig. 6. Installation of Vibro stone columns by top feed wet method.

its self-weight and horizontal vibrations. An annular space is created between the vibrator and borehole walls through which stone is fed from the top, to the tip of the vibrator. The up-down motion of the vibrator compacts the stone laterally into the surrounding soil. This results in a well compacted stone column that has a diameter larger than original hole. Wheel loaders were used to continuously supply the stone from the stockpiles at site. Figure 5 shows step wise installation process of vibro stone columns by top feed wet method.

Two (2) vibro stone column rigs were used to treat the areas proposed on ground improvement. Works were carried out during the period from November, 2012 to July, 2013 to treat 16,600 m<sup>2</sup>. A typical picture taken during the installation of vibro stone columns is presented in Figure 6.

### 7. Quality Control and Quality Assurance

In the execution of vibro stone column works quality is assured by implementing various control measures at different stages as per the comprehensive field quality control procedures outlined and submitted during the design stage.

The same has been summarized below:

- Pre-Construction: Soil investigation, stone aggregate source approval and testing.
- During Construction : Monitoring of construction parameters
- After Construction : Testing by means of load tests (single and group)

Prior to commencement of works, an extensive soil investigation program was carried out as detailed in section 3 of the paper. The design is carried out considering the subsoil data in the foot print of the tank to arrive at the optimum design of vibro stone columns. The material used for the stone columns was checked from the source prior to start of works at approved and accredited national laboratories. Tests include included crushing, abrasion, sulphate resistance, water absorption and grain size analysis as per the specifications outlined in BS EN 14731:2005 and BRE-391. Material testing was carried at periodic intervals for the samples collected from site and source to see that sound stone aggregate material is used for the construction of vibro stone columns. Typical stone aggregate specifications are outlined in Table 2.

During construction the vibro stone column, installation process is monitored using real time computerized monitoring system. The vertical position and the current drawn by the depth vibrator is continuously measured (in real time) and displayed to the operator. This data is printed in the form of graph and which was reviewed

Table 2. Stone aggregate specification for vibro stone columns.

S.No	Tests	Criteria
1	Specific Gravity	> 2.5
2	Aggregate Crushing Value	< 30%
3	Los Angeles Abrasion Value	< 30%
4	Water Absorption	< 2%
5	Soundness	< 12%
6	Aggregate Size	75 mm to 12 mm

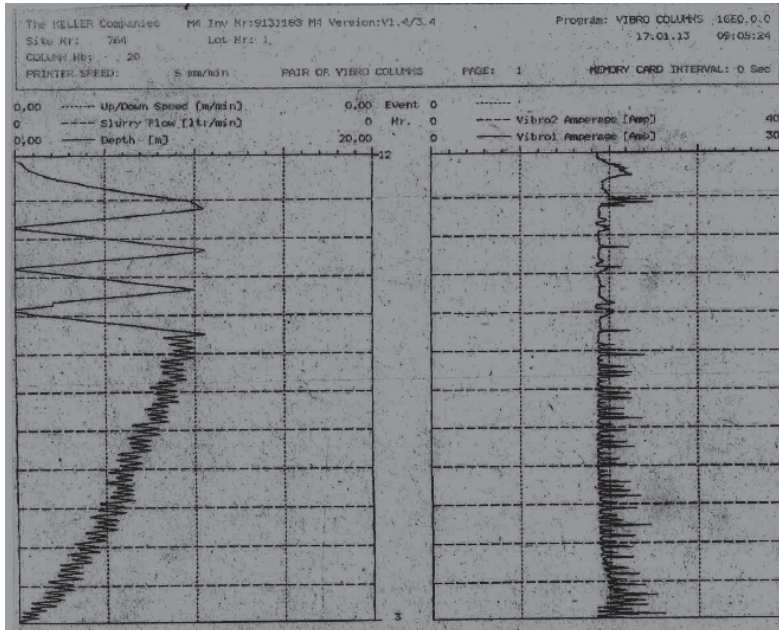


Fig. 7. Typical quality control graph output of vibro stone column.

by the engineer daily. The quality control graph provides the information of stone column number, date of installation, start and finish date of installation, period taken to install the column, maximum depth and compaction effort during penetration and compaction process. A typical quality control graph of vibro stone column for enclosure 1 is presented in Figure 7.

After installation of vibro stone columns load tests are conducted to check the load carrying capacity of the improved ground. Total fifteen (15) routine single column load tests and five (5) routine three column group load tests were done on the installed vibro stone columns, in order to check the design capacity of the stone columns in turn to check the safe bearing capacity of soil after ground improvement. The tests were conducted as per the guidelines specified in the Indian standard code, IS 15284 (Part-1): 2003.

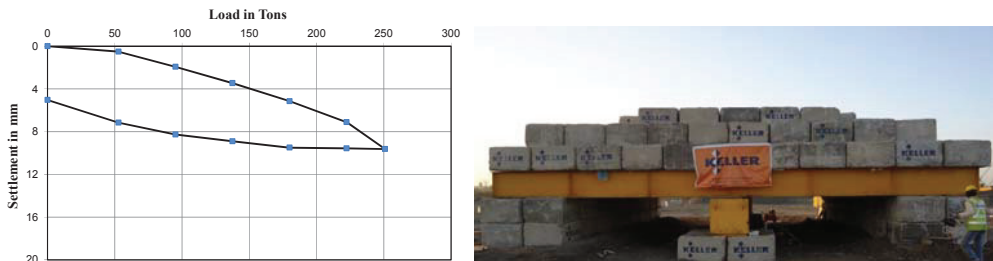


Fig. 8. Load vs settlement plot for routine three column group load test.

A typical result showing the load vs settlement plot for a routine group column load test is presented in Figure 8. The result of the load tests were well within the permissible limit indicating the columns were built with good quality and work man ship.

**8. Performance of Tanks - Hydrotest Results**

Hydrotest was carried out for all the 48 no’s of tanks and settlement monitoring was carried out as per the procedure outlined in the design report. Slow stage hydrotest was carried out for the tanks founded on vibro stone columns to control

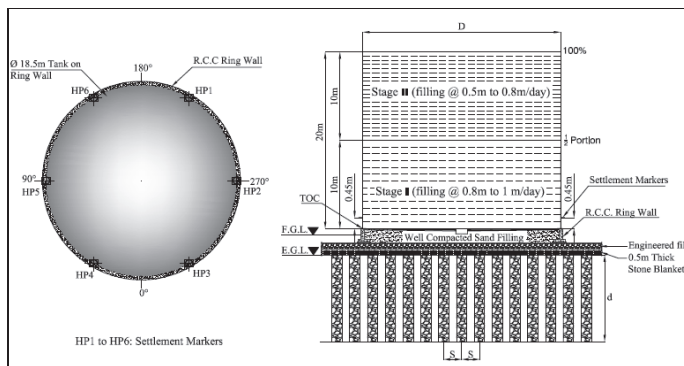


Fig. 9. Details of water filling rate for slow stage hydro test and location of settlement markers along the tank periphery.

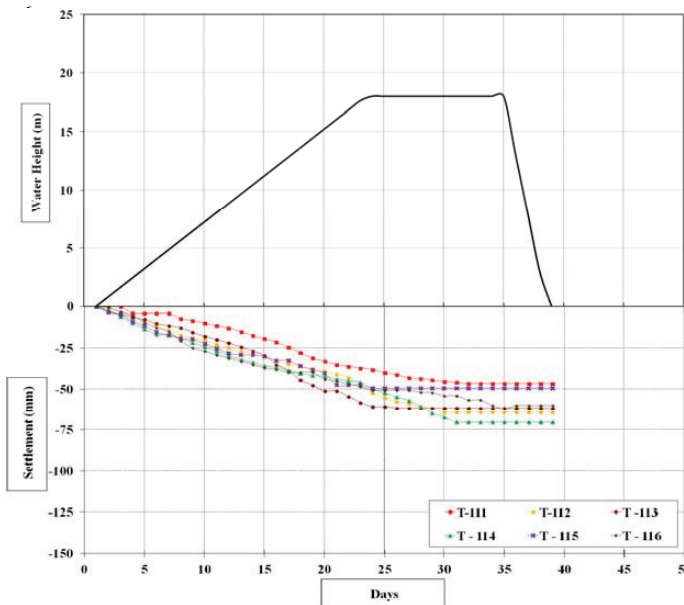


Fig. 10. Average Peripheral Settlement plot during Hydrotest for Enclosure 1 (Floating Roof).

the differential settlements and control the long term post construction settlements.

Settlement of tanks was measured using a series of survey points established on the tank shell prior start of hydrotest. Details of the filling rate adopted for the hydrotest and the settlement observation points for the tanks are presented in the Figure 9.

The final load (full water height) was maintained till the rate of settlements was stabilized. A clear trend of stabilization of settlement was seen in the entire tank farm within seven (7) days of reaching full stage water load. Typically, the duration for

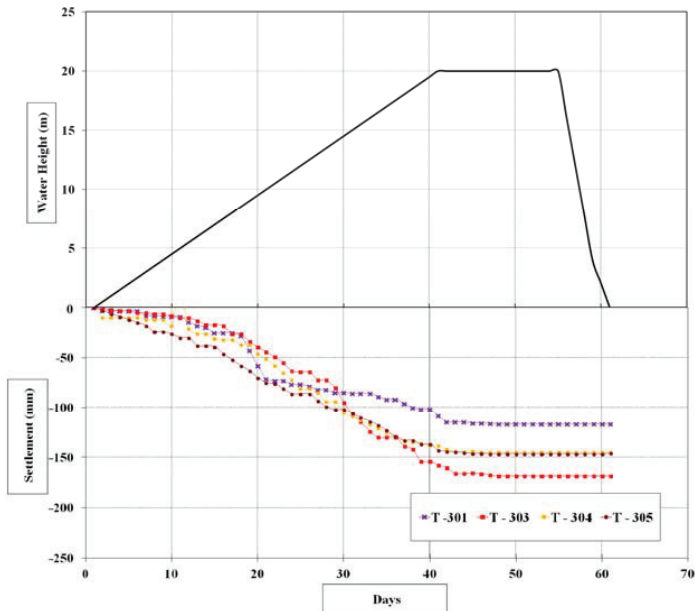


Fig. 11. Average Peripheral Settlement plot during Hydrotest for Enclosure 3 (Fixed Roof).



Fig. 12. Completed Oil Storage Terminal.

the hydrotest for each tank was in the range of 35 to 50 days which was sufficient to reach the estimated degree of consolidation and to control the long term settlements post hydrotest. The average settlement of the tanks recorded during hydrotest for enclosure E-1 and E-5 are presented in Figure 10 and Figure 11, respectively.

Measured peripheral settlements of tanks ranged from 50 to 75 mm in enclosure-1 (floating roof tanks) while the same was 125 to 175 mm for the tanks in enclosure-3 (fixed roof). Settlements were also monitored for the Engineering office building (G+3 storied) building. Measured settlements were in the range of 18 to 23 mm for the building.

The measured settlements of the tanks and the buildings were well within the allowable limits in terms total and differential settlements indicating very good performance of vibro stone columns.

## **9. Conclusions**

An Oil Storage Terminal is being developed in Pipavav in Gujarat. The terminal development consists of construction of 48 No's of storage tanks and associated utility facilities. Ground improvement using vibro stone columns is proposed to support the foundations at the terminal. Vibro stone columns are proposed to enhance the shear strength and compressibility parameters of the subsoil and also accelerate the consolidation of the soft soils.

Success for a project of this kind is only possible with quality control at each stage of construction which is implemented for this project. Settlement monitoring results have shown the effectiveness of vibro stone columns to support the tank foundations and ancillary buildings. The settlements were uniform and well within the tolerable limits. Ground improvement with Vibro stone columns has resulted in homogenizing the subsoil which helped in controlling the differential settlements.

The Oil storage terminal is commissioned successfully in the month of February, 2015.

## **Acknowledgements**

The authors wish to thank the developer M/s Gulf Petrochem and the EPC contractor M/s Vijay Tanks & Vessels for their kind permission to publish the information contained in this paper. The authors also wish to acknowledge Keller management for their continuous support and encouragement in finalization of theme of this paper including valuable comments and suggestions that helped the authors to refine and improve the quality of the paper. Thanks are also due to design and execution team of M/s Keller and M/s Vijay Tank & Vessels for providing hydrotest monitoring data at regular intervals.

## **References**

1. Building Research Establishment (2000). "Specifying Vibro Stone Columns", BRE - 391.
2. British Standard (2005). "Execution of Special Geotechnical Works - Ground Treatment By Deep Vibration", BS EN 14731-2005.
3. Indian Standard Code (2003). "Design and construction for ground improvement - Guidelines, Part 1: Stone columns", IS 15284 (Part-1): 2003.
4. Priebe, H.J. (1996). "The Design of Vibro Replacement", Ground Engineering, December 1995.

Annexure 4 Technical paper on “Ground Improvement Solutions to Mitigate Liquefaction: Case Studies”

## GROUND IMPROVEMENT SOLUTIONS TO MITIGATE LIQUEFACTION: CASE STUDIES

Madan Kumar Annam, Technical Manager, Keller India, [madankumar@kellerindia.com](mailto:madankumar@kellerindia.com)

V. R. Raju, Managing Director, Keller Asia, [vrraju@kellersing.com.sg](mailto:vrraju@kellersing.com.sg)

**ABSTRACT:** There have been major advances occurred in the past in understanding as well as practicing of engineering treatment of seismic soil liquefaction and assessment of seismic site response. While research on liquefaction continues, the geotechnical engineering practice has developed various techniques for site improvement that can mitigate the potential effects of liquefaction. The first part of this paper address soil liquefaction and second part concentrates on the case histories where ground improvement methods using vibro techniques were implemented to mitigate liquefaction-induced damages in major infrastructure projects.

### INTRODUCTION

Liquefaction is defined as the transformation of a granular material from a solid to a liquefied state as a consequence of increased pore-water pressure and reduced effective stress. Liquefaction is one of the critical problems in geotechnical engineering. High ground water levels and alluvial soils have a high potential risk for damage due to liquefaction, especially in seismically active regions. The most critical soil is fine sand with some silt content.

### Evaluation of the Liquefaction Potential

A large part of India lies in potentially hazardous earthquake prone zones. A large portion of eastern, western and northeastern part of the country comes under Zone V and Zone IV (Refer Fig. 1).

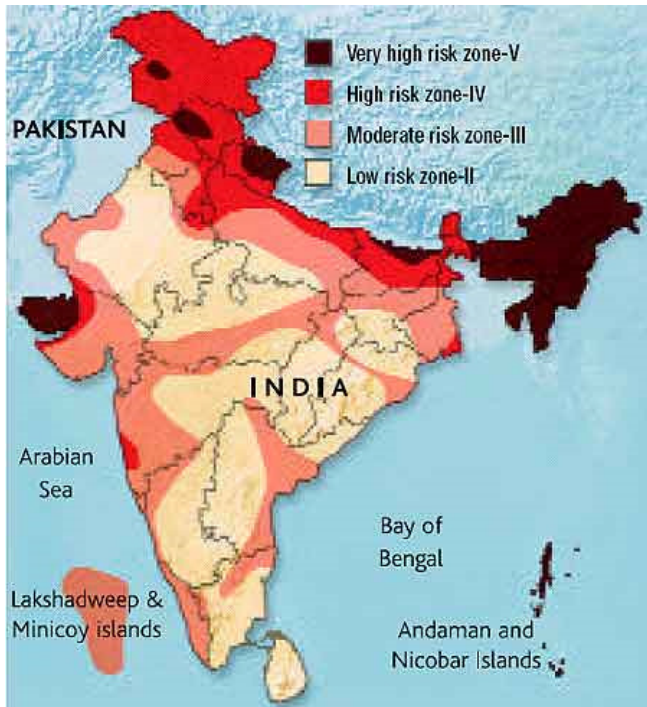


Fig. 1 Seismic Zone Map of India

The simplest and probably most reliable method to evaluate the soil liquefaction potential is statistical analyses from the past history. For this, the forces expected during a seismic event are compared with the forces that the subsoil under

consideration can actually resist. Generally, the maximum surface acceleration on level ground is used as the characteristic value for the forces developed by an earthquake.

Estimation of two variables for evaluation of liquefaction resistance of soils is expressed in terms of Cyclic Stress Ratio (CSR), the seismic demand on a soil layer and Cyclic Resistance Ratio (CRR), the capacity of the soil to resist liquefaction. One of the most widely accepted and used SPT based correlations is the “deterministic” relationship proposed by Seed, et al (1984, 1985) represented in Fig. 2. Seed and Idriss (1971) formulated the following equation for calculation of the Cyclic Stress Ratio:

$$CSR = (\tau_{av}/\sigma'_{vo}) = 0.65(a_{max}/g)(\sigma_{vo}/\sigma'_{vo})r_d$$

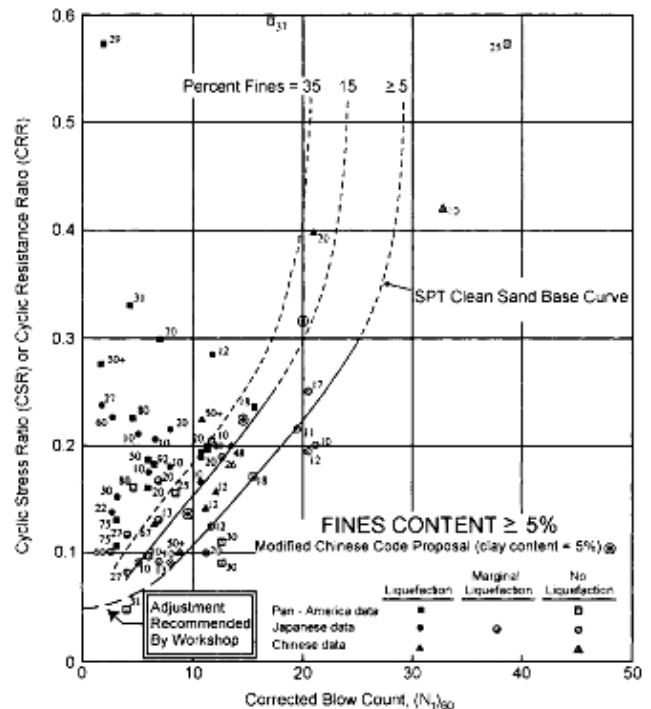


Fig. 2 SPT Clean-Sand Base Curve for Magnitude 7.5 Earthquakes

Where,  $a_{max}$  = peak horizontal acceleration at the ground surface generated by the earthquake (discussed later);  $g$  = acceleration of gravity;  $\sigma_{vo}$  and  $\sigma'_{vo}$  are total and effective

vertical over burden stresses, respectively; and  $r_d$  = stress reduction coefficient which accounts for flexibility of the soil profile. Seed and Idriss (2001) used the approximated equation for CRR for clean-sands that used a base curve and fitting the following equation:

$$CRR_{7.5} = [1/ \{34-(N_1)_{60}\}] + [(N_1)_{60}/135] + [50/ (10(N_1)_{60}+45)]$$

Where  $(N_1)_{60}$  is SPT N value projected for clean sand obtained after corrections on measured field SPT N value. The above equation is valid for  $(N_1)_{60} < 30$ . For  $(N_1)_{60} > 30$ , clean granular soils are too dense to liquefy and are classed as non-liquefiable (Refer Seed and Idriss 2001).

**GROUND IMPROVEMENT TECHNIQUES**

The liquefaction potential of weak deposits can be mitigated with ground improvement techniques such as vibro replacement (vibro stone columns) and vibro compaction. These techniques use vibratory energy to densify loose soils at depth by backfilling. Principles of vibro replacement and vibro compaction techniques are discussed in this paper.

**Deep Vibro Techniques**

Vibro technique offers the weak deposits to get compaction, drainage and increase in shear resistance. Fig. 3 shows transition zone of soils tends to liquefiable and possible techniques of ground improvement with deep vibro compaction or replacement.

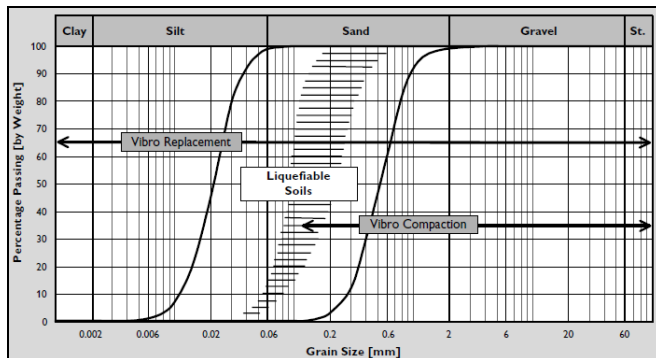


Fig. 3 Application ranges of the deep vibro techniques

**Vibro Compaction**

The basic principle behind the vibro compaction process is that particles of non-cohesive soils can be rearranged into a denser state by means of vibration.

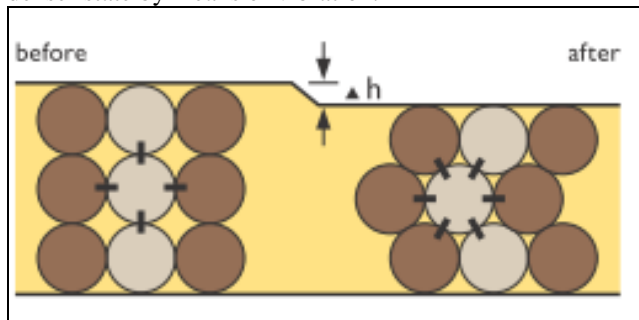


Fig. 4 Schematic showing vibro compaction technique

Vibration is achieved by means of powerful vibrator at deeper depths. The vibrator is connected to a source of electric power and a high-pressure water pump. Extension tubes are added as necessary, depending on the treatment depth, and the whole assemblage is suspended from a crane. A Schematic showing Vibro Compaction technique is presented in Fig. 4.

**Vibro Replacement**

The stabilization of weak deposits by displacing the soil radially with the help of a depth vibrator, refilling the resulting space with granular material and compacting the same with the vibrator is referred to as Vibro Replacement.

The resulting matrix of compacted soil and stone columns has improved load bearing and settlement characteristics. A schematic showing the basic principle of the vibro replacement technique, explained in Fig. 5. Keeping the site conditions in view vibro stone columns can be installed either wet method (top feed) or dry method (bottom feed). Technically and functionally, vibro stone columns installed in both methods serve similar.

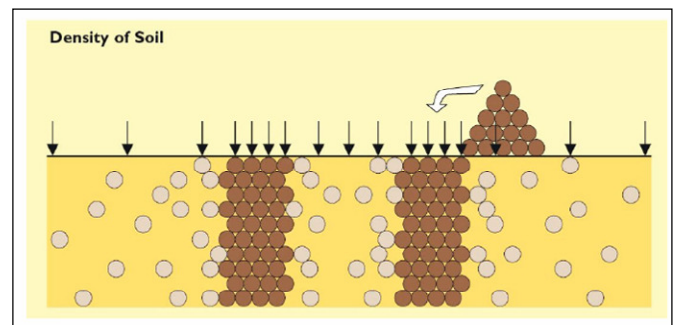


Fig. 5: Schematic showing vibro replacement technique

The above ground improvement techniques were adopted in various infrastructure projects to mitigate liquefaction potential across India.

Few case studies of the executed projects falls under seismic Zone IV and V as per IS 1893 Part 1 (2002) are discussed in the following sections.

**CASE STUDIES**

**Power Plant at Goindwal Sahib, Punjab**

A power plant of capacity 2 x 270 MW coal based Thermal Power Plant was built at Goindwal Sahib, near Amritsar, Punjab. Power plant structures such as Boiler, Electro Static Precipitator (ESP), Switch Yard, Power House Building, etc. were planned as part of development of power plant.

Soil at this project site is primarily sandy silt / silty sand to about 1.5m to 2m depth, followed by fine sands with fines content of about 6% to the final explored depth of about 30m. The average SPT N value is 10 up to a depth 4m to 6m from the existing ground level and SPT N value ranges from 15 to 25 to a depth of about 15m. Medium dense to dense sand

layers were encountered beyond 15m depth with SPT N values are generally > 25.

The existing natural soils (fine sands) at the proposed site being loose were susceptible to liquefaction in an event of an earthquake. Hence, Ground Improvement by Vibro Compaction Technique was proposed to mitigate liquefaction and to enhance the bearing capacity.

Vibro Compaction for main works has been carried out to a depth of 8m.



Fig. 6 Twin Vibrators in action.



Fig. 7 The difference in levels achieved (about 1m) as a result of vibro compaction

Post Cone Penetration Tests (CPT) were conducted after completion of the vibro compaction for various structures, as part of QA/QC procedures. Based on the analysis of the post CPT results, a Relative Density of more than 70% was achieved. Pre and post cone resistance ( $Q_c$ ) values are shown in Fig. 8 in which the target relative density is also presented. The target relative density is evaluated based on correlations proposed by Schmertmann with respect to  $Q_c$ . In addition to

the above, 2nos plate load tests ( $20 \text{ t/m}^2$  &  $40 \text{ t/m}^2$ ) were conducted at cooling tower I & II area to assess the load vs settlement behavior of the improved ground for required safe bearing capacity of  $10 \text{ t/m}^2$ . The plate load test results indicate that the settlements are less than 5mm in both cases.

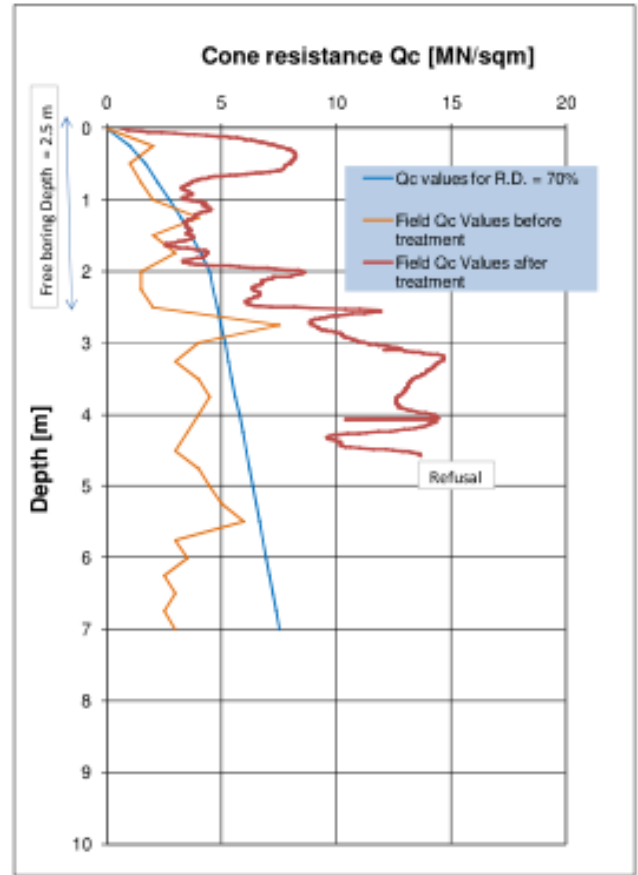


Fig. 8 Pre and Post CPT results at ESP area.

#### A School Building, Noida

One of the reputed educational societies in Noida, Uttar Pradesh has proposed to build a school building. The soil investigation at the proposed site revealed that loose to medium dense fine sand exists to a depth of 9m which is susceptible to liquefaction. Since the project location falls under Seismic Zone IV, the required field SPT (Standard Penetration Test) shall be more than 20 (performance criteria requirement by the designer), to mitigate liquefaction and to achieve bearing capacity.

Ground improvement technique using vibro compaction was proposed as treatment to mitigate liquefaction and to enhance the safe bearing capacity of the loose sand deposit till 9 m depth below the existing ground level.

About three boreholes prior to and two boreholes after the commencement of vibro compaction works were carried out in the project area to assess the effect of vibro compaction. It can be seen from Fig. 9 that the post treatment SPT N values (shown in discontinuous lines) are larger than the

performance line confirming the effect of the ground improvement.

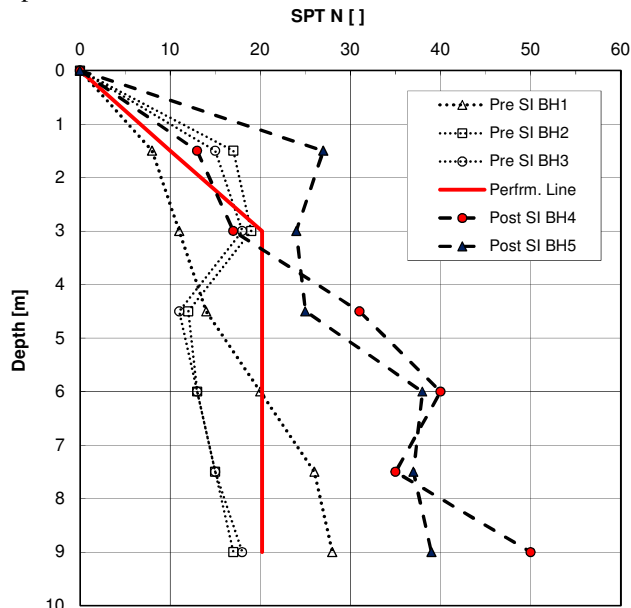


Fig. 9 Graph showing performance of vibro compaction

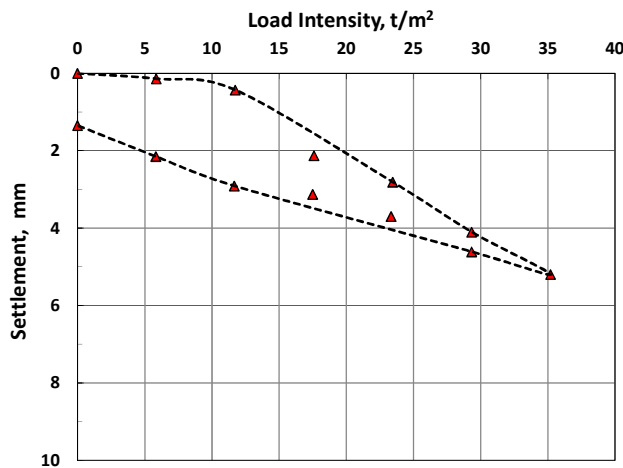


Fig. 10 Graph showing Load Intensity vs Settlement

Further, a field plate load test was also performed at site to assess bearing capacity of the treated ground. The observed settlements were within the acceptable limits for the applied load intensity as illustrated in Fig. 10.

**Sewage Treatment Plant, Noida**

Greater Noida Development Authority was constructing a 137 MLD Sewage Treatment Plant in Greater Noida, Uttar Pradesh. Various structures such as Chlorination tanks, SBR basins, Air blower, Grit chambers etc. were proposed. The project location falls under seismic Zone IV, however as per the requirements of the Client the ground improvement techniques were adopted to satisfy liquefaction effects of Zone V conditions.

The soil profile comprise of silty sand layer of 3m to 4m thick with SPT N ranging from 6 to 8 followed by fine, loose

to medium dense sand up to a depth of 10m below the existing ground level with SPT N ranging from 11 to 18. A clayey silt / silty clay layer was encountered up to 20 m depth with SPT N more than 20. A load intensity of 10 t/m<sup>2</sup> to 15 t/m<sup>2</sup> was anticipated due to various structures. The top soil layers up to 10m depth were susceptible to liquefaction.

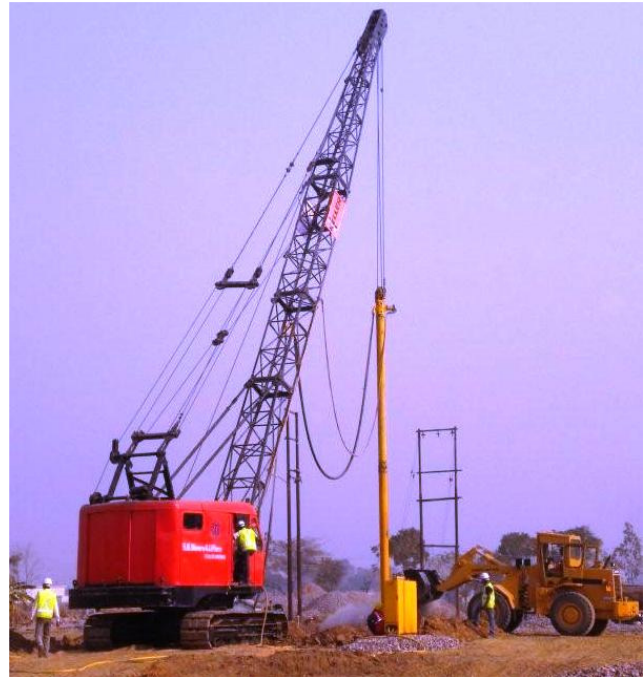


Fig. 11 Installation of vibro stone columns at STP, Noida

Vibro Stone Columns were installed in triangular grids of different spacing under strip and raft foundation to a depth of 10m from existing ground level to mitigate the liquefaction and to enhance the bearing capacity.

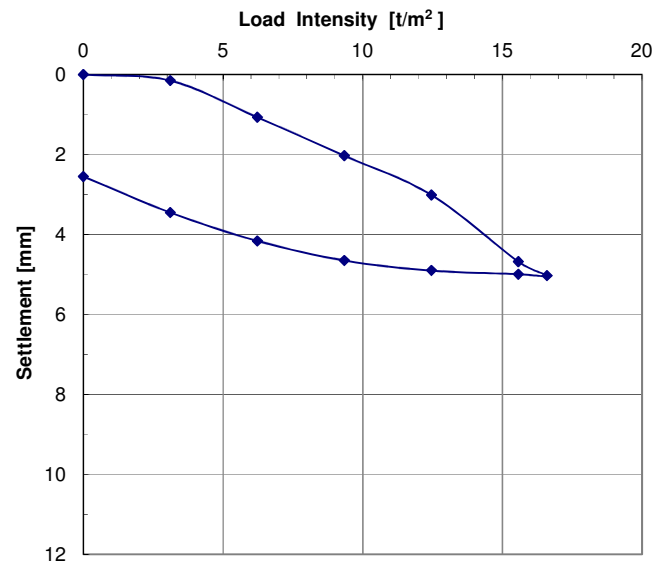


Fig. 12 Load Intensity vs. Settlement curve at STP, Noida

A field plate load test was performed at site to assess bearing capacity of the treated ground. The observed settlements were found within the acceptable limits for the applied load intensity as shown in Fig. 12.

**LNG Terminal, Hazira**

Two liquefied natural gas storage tanks were constructed in Hazira LNG Terminal Project of each 84 m in diameter and with a filling level of approximately 35 m. The site is located at an estuary on the coast of the Khambhat Gulf in India.

The subsoil profile at the project site consists of loose to medium dense silty sand up to a depth of 16 m below the existing ground level. The upper 4 to 5 m was recently reclaimed material. The fines content of the sand was in the range of 15% on average, sometimes slightly higher. Very dense sand with SPT > 50 was encountered below 16m from existing ground level.

A peak ground acceleration (PGA) of  $a = 0.24g$  confirming to seismic Zone IV conditions were assumed in the design of ground improvement system. Analysis and design was carried out using the method stipulated by Priebe (1998) for the initial in-situ density conditions. Ground improvement using vibro replacement technique was adopted to mitigate liquefaction.

Vibro stone columns of 16 m long were installed in a square grid pattern. Additional strips of stone columns were installed around the periphery of the tank to provide additional stability to the treatment area in case of a seismic event.

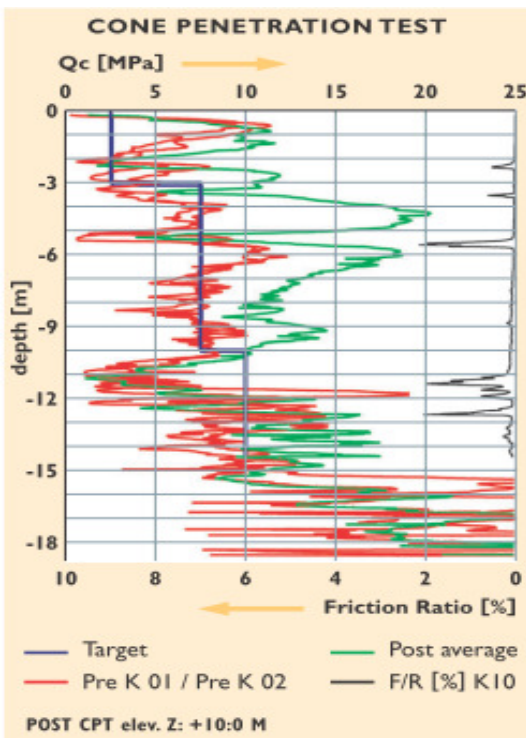


Fig. 13 Pre and Post CPT results

Pre and Post CPT at site on trial stone columns were carried out. Post treatment results showed a two-fold increase in the CPT values of the sand zones as shown in Fig. 13. Hydro tests were performed on the installed tanks and the expected settlements were in the range of 120 mm, well within the limits at the centre of tank under full tank load of  $23.0 \text{ t/m}^2$ .



Fig. 14 Tanks commissioned after successful Hydro Test and in operation for last 8 years

**Power Plant in North Delhi**

A gas based combined cycle power generating capacity of 108 MW was constructed at North Delhi. Main plant structures were proposed to be built on deep foundations whereas lightly loaded ancillary structures such as clariflocculator, storage tanks, switchyard etc. (loading intensity of about  $10 \text{ t/m}^2$ ) was proposed to be placed on shallow foundations.

The soil profile at the project site in general consists of loose to medium dense sandy soils with N values ranging between 5 and 10 to a depth of about 10 to 12m followed by dense silty sands / sandy silt ( $N > 15$  to 30) to about 30m. This project site falls under Zone IV with peak ground acceleration of  $0.24g$ . The native loose sandy soil deposits were susceptible to liquefaction to a depth of about 10 to 12m below existing ground level.

Vibro replacement technique using dry vibro stone columns (bottom-feed displacement method) was adopted to ensure required bearing capacity to eliminate pile foundations. In addition, the proposed ground improvement technique was designed to mitigate the liquefaction potential in the event of earthquake.

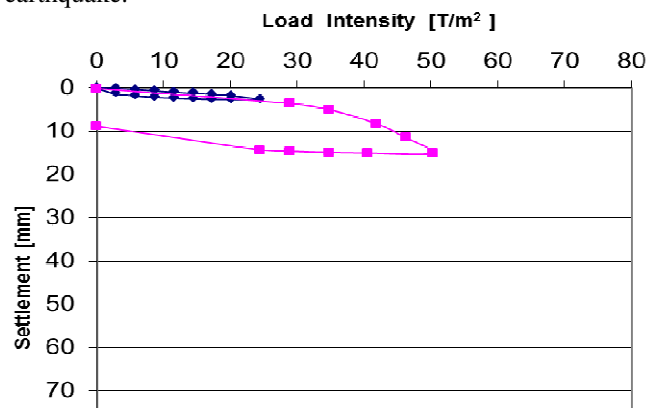


Fig. 15 Load Intensity vs. Settlement Curve

The proposed technique allowed fast construction in a congested site avoiding usage of water and subsequent muck removal. Single column plate load test was conducted on the installed dry vibro stone columns to a maximum load intensity 50 t/m<sup>2</sup>. Settlement under the ultimate test load was observed to be less than 16mm (Refer Fig. 15).

In addition to the technical performance and commercial benefits, an embodied CO<sub>2</sub> calculation showed an environmental benefit (lower greenhouse gas emissions) of the Vibro stone column solution as shown in Table 1.

**Table 1** Embodied Carbon Comparison

Sl. No.	Item	Embodied CO <sub>2</sub> [kg]	
		BCIS Piles	Stone Columns
1	Concrete (incl. wastage)	667,516	-
2	Stone aggregates (incl. wastage)	-	42,412
3	Reinforcement Steel	382,373	-
4	Fuel consumption for installation	199,354	118,350
Total		1,249 T	161 T

**Product Packaging Unit at Babrala, Uttar Pradesh**

Expansion of the existing Product Packaging Unit was under development at Babrala, Uttar Pradesh. As part of expansion, various structures such as Conveyor Belts, MCC cum Control room and the Wagon Loading Platform were to be constructed.

The soils at the project site consisted of loose to medium dense sand with fines less than 10% to about 12 m depth from EGL with top 3.0 to 4.0m of clayey silt. The ground water table was encountered at a depth of 3.0 m from EGL. The site was prone to liquefaction during an event of earthquake as it falls under seismic Zone IV.

Ground improvement using vibro compaction/vibro replacement technique was proposed to mitigate the liquefaction potential of the soil to enhance safe bearing capacity of soil and reduce the estimated total and differential settlement of the soil to a depth of 12 m below EGL.

Vibro stone columns were installed for conveyor belt foundations and the transfer towers. A combination vibro stone columns and vibro compaction has been used to support the foundations of MCC room which is the most interesting aspect of the project.

The vibro stone columns were constructed in the top 4m followed by vibro compaction up to 12m. An illustrative sketch is shown in Fig. 17.

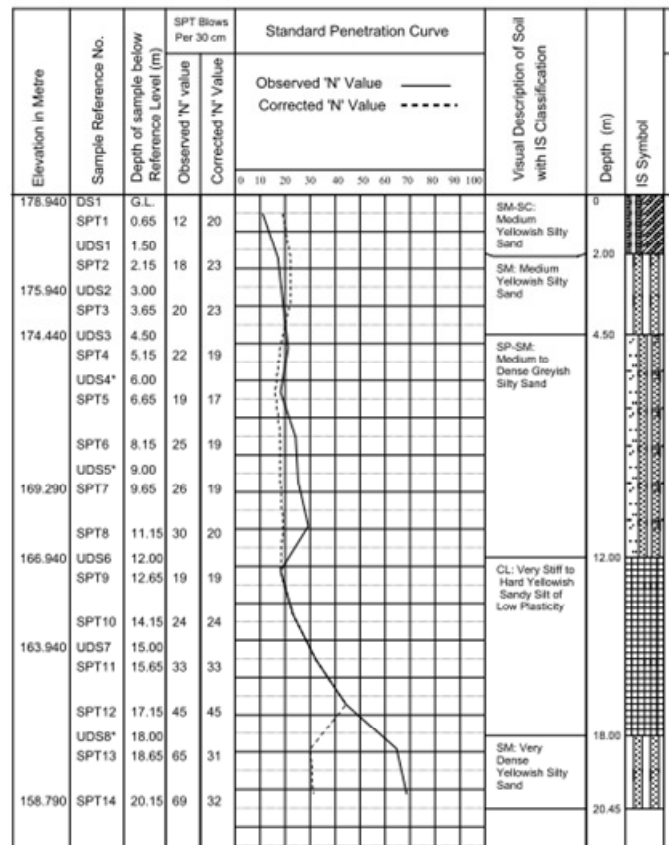


**Fig. 16** Typical borehole log at Babrala

Plate load tests were performed over the treated area and results confirmed that the settlements at design loads were within the allowable limits.

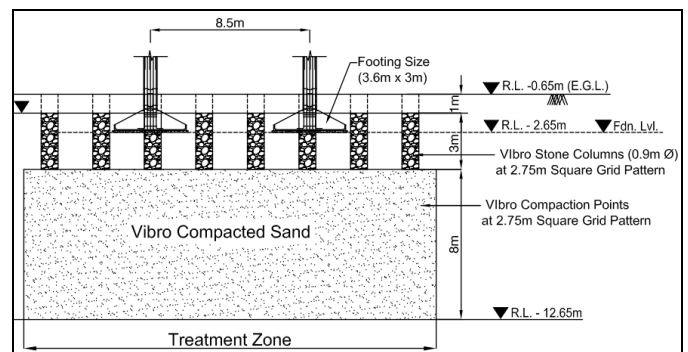


**Fig. 17** Sketch showing ground improvement with combination of vibro techniques at MCC Room of the plant

Post treatment CPTs' were also executed which proved an average improvement of two folds in the Q<sub>c</sub> values and of 70% relative density was achieved. Also, post treatment SPTs showed a considerable improvement in SPT N values to about 2 to 3 times in the treated area as shown below in Fig. 18.

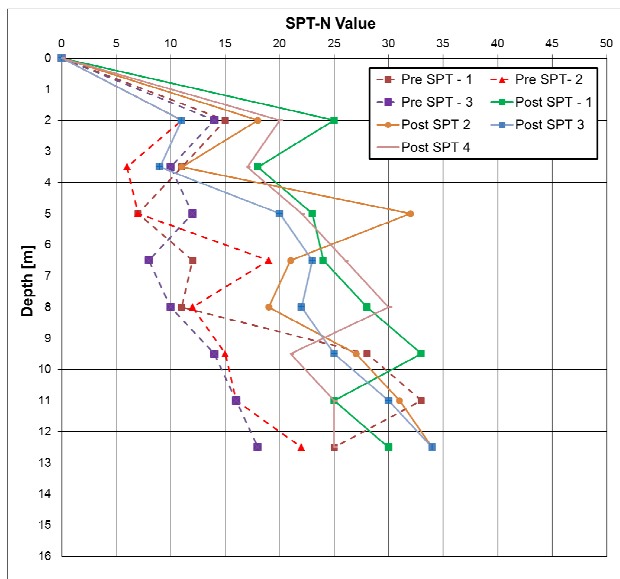


Fig. 18 Pre and Post SPT comparison

## CONCLUSIONS

The presence of liquefaction soil does not mean that one has to abandon the site or to install deep foundations. In seismic zones with liquefiable soils, ground improvement technique provides technically sound and cost effective solutions.

Efficient and economic solutions to problems caused by soil conditions require a thorough evaluation of project conditions, project needs, method capabilities and a field test program.

Six projects have been described in which vibro methods have been successfully used to accomplish the required ground improvement to mitigate liquefaction and to enhance bearing capacity requirements. The success is measured in terms of either load tests or by the comparison of results of pre and post soil investigation done at particular sites.

## REFERENCES

1. Seed H.B., and Idriss, I.M (2001). Simplified procedure for evaluating soil liquefaction potential, *J. Geotech Engineering. Div.*, ASCE 97 (9), 1249-1273
2. Seed et. al (2003). Recent advances in soil liquefaction engineering: A unified and consistent framework.
3. Priebe, H.J (1995), The Design of Vibro Replacement, *Ground Engineering*, December 1995
4. Priebe, H.J (1998), Vibro Replacement to Prevent Earthquake Induced Liquefaction, *Ground Engineering*, September 1998
5. Raju et. al. (2010). Some Environmental Benefits of Dry Vibro Stone Columns in a Gas Based Power Plant Project, *Indian Geotechnical Conference*, December 2010

Annexure 5 Technical paper on “Ground Improvement Using Vibro Techniques in Flyash Deposits”

# Ground Improvement Using Vibro Techniques in FlyAsh Deposits

Dr V R Raju

Keller Ground Engineering (I) Pvt Ltd, India

## ABSTRACT

Ash ponds are extensively located in India. Unavailability of suitable construction site for extension of existing power plants or to build a new plant makes it worthwhile to consider the ash pond as one of the options. Ash ponds in general are not consistent with the depth and density characteristics of the hydraulically deposited fly ash across the site. The traditional methods of foundation design in such situations may result in commercially unviable solution. Ground improvement in such case provides a techno-commercially feasible solution. Anpara Thermal Power Plant by Uttar Pradesh Rajya Vidyut Utpadan Nigam Ltd (UPRVUNL) is one such classic example. The site allocated for the proposed development of Unit D of the power plant is an abandoned ash pond. An extensive research has been done and was established that ground improvement using stone columns (dry bottom feed method) shall be adopted to not only mitigate the liquefaction potential but also to enhance the bearing capacity of the hydraulically deposited fly ash deposits. The stone columns are also installed to enhance the lateral capacity of bored cast-in-situ piles. This paper illustrates the soil conditions, proposed ground improvement technique to address the geotechnical applications of bearing capacity, liquefaction mitigation and enhancing the lateral capacity of piles and discuss the pre and post treatment testing.

## 1. INTRODUCTION

Ash ponds are extensively located in India. The area occupied by the ash ponds is more than 250sq.km and it is likely to cross 1,000sq.km by 2012 (Bedanga Bordoloi and Etali Sarmah, 2010). Unavailability of suitable construction site for extension of existing power plants or to build a new plant makes it worthwhile to consider the ash pond as one of the options. Ash ponds in general are not consistent with the depth and density characteristics of the hydraulically deposited fly ash across the site. This results in inadequate bearing capacity and lateral capacities of deep pile foundations. The traditional methods of foundation design in such situations may result in commercially unviable solution. Ground improvement in such case provides a techno-commercially feasible solution.

Anpara Thermal Power Plant in Uttar Pradesh is a classic example for such case. Uttar Pradesh Rajya Vidyut Utpadan Nigam Ltd (UPRVUNL) is expanding the existing power plant by setting up Unit-D of 2 x 500 MW capacity at Anpara, near Sonebhadra. The site allocated for the proposed development is an abandoned ash pond of area approximately 5,400 acres. The depth of ash varies across the site and ranges between 3m and 13m and is loose to medium dense in condition. It was found out during the initial soil investigation that the existing bearing capacity of the fly ash deposits is the less than the required i.e., 10T/m<sup>2</sup>

for open foundations of structures like pump house, cable gallery etc at coal handling plant. Also, site falls under Zone –III according to the IS 1893 (Part 1):1982, making it susceptible to liquefaction in an event of an earthquake. An extensive research has been done (study of effectiveness of ground improvement techniques and possible liquefaction potential for Anpara D Thermal Power Project, IIT Roorkee) and was established that ground improvement using stone columns (dry bottom feed method) shall be adopted to not only enhance the bearing capacity but also to mitigate the liquefaction potential of the fly ash deposits. Further, the stone columns are also installed surrounding the bored cast-in-situ piles to enhance the lateral capacity for structures like stacker reclaimer, crusher house etc of coal handling plant, which otherwise was giving low lateral capacity.

## 2. SOIL CONDITIONS

The project site is an old ash pond. Depth and density characteristics of fly ash vary across the site. The depth generally ranges between 3m and 13m underlain by clayey silt / silty clay to about 23m depth. Below this dense sandy silt or hard clayey silt was found and occasionally weathered rock (granitic gneiss) is encountered.

Density characteristics vary considerably within the depth of fly ash. The SPT N values recorded are as low as 2 to as high as 30, but generally vary from 3 to 8. This is followed by stiff to hard clayey silt with SPT N values ranging between 9 and 30. The following figure-1 illustrates the cross sectional profile of the site indicating the variation in depth and density characteristics of fly ash.

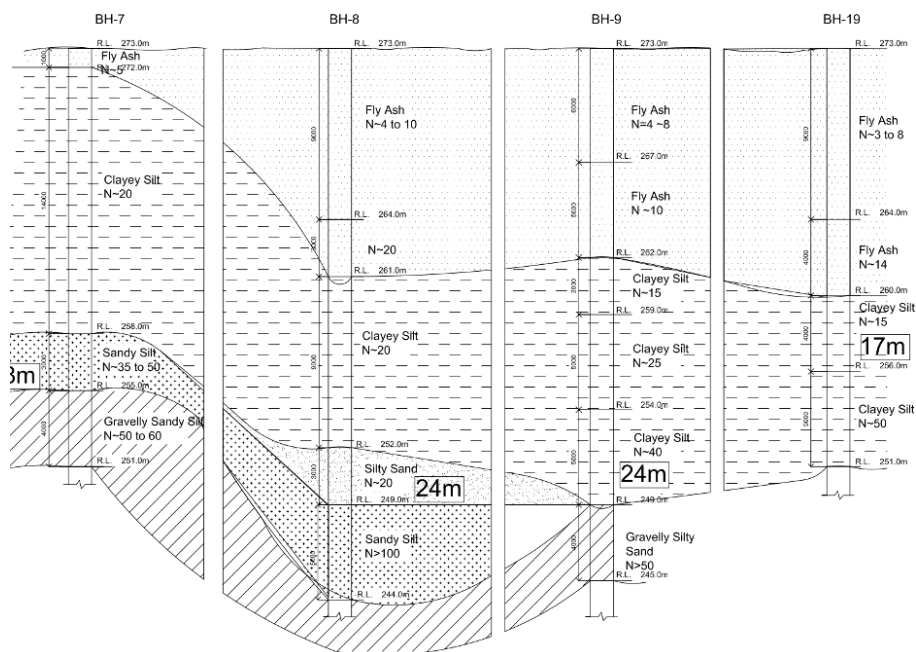


**Fig. 1** Typical sectional profile illustrating the soil conditions at Coal Handling Plant location

### 3. GROUND IMPROVEMENT TECHNIQUE

Vibro Stone columns using bottom feed method is adopted as a ground improvement technique. This method does not require water for penetration, which avoids the need to handle and dispose large quantities of muck and also makes it environment friendly. It is also well suited for a congested site, with many simultaneous activities. For this method of installation, a rig called Vibrocat is used. It consists of a bottom-feed depth vibrator mounted on a crawler-rig. An operational advantage of the Vibrocat is that it is able to exert a pull-down force, improving penetration speed and hence productivity. A typical Vibrocat unit, used on site, is shown in Fig. 2.



**Fig. 2** A typical Vibrocat unit

The Vibrocat feeds the coarse granular material to the tip of the vibrator with the aid of pressurized air. The installation method consists of alternative steps of penetration and retraction. During the retraction, gravel runs from the vibrator tip into the annular space created and are then compacted using vibrator thrusts and compressed air. Fig. 3 illustrates the schematic of this process.

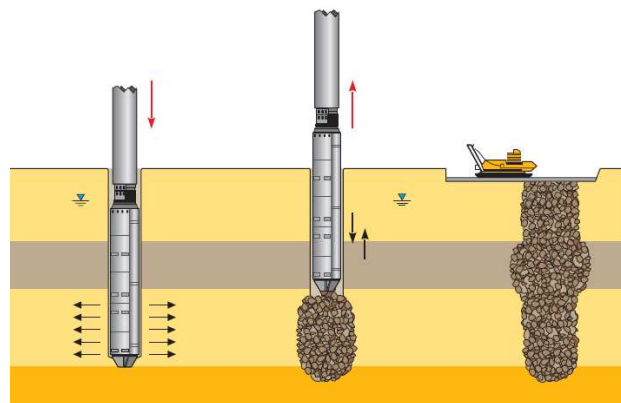


**Fig. 3** Schematic of stone column installation (Dry bottom feed method)

## **4. GEOTECHNICAL APPLICATION**

Ground improvement using vibro stone columns by bottom feed has been adopted to achieve the following objectives:

### **4.1 Improve Bearing Capacity of Open Foundations**

The density characteristics of fly ash vary across the site as a result the net safe bearing capacity for open foundations is less than the desired value of  $10T/m^2$ . It is proposed to install stone columns to at least 0.5m into the underlying stiff clayey silt / silty clay layer to achieve the desired bearing capacity for open foundations.

### **4.2 Enhance Lateral Capacity of Piles**

The existence of loose fly ash deposits resulted in less than the desired lateral capacity of bored cast-in-situ piles. Stone columns were installed around the bored cast-in-situ piles to enhance the density characteristics of the fly ash surrounding the piles there by improving the lateral capacity to 7T (working load).

### **4.3 Mitigate Liquefaction Potential**

According to IS 1893 (Part 1):1982, the site falls under Zone –III making it susceptible to liquefaction in an event of an earthquake under the possible excitation or peak ground acceleration of 0.16g. According to Table 1, Note 4 of IS 1893 (Part 1):1982, soils with SPT N values less than 20 for Zone III are liable to liquefy.

The SPT N values obtained range between 3 and 8 within the fly ash depth indicating the possibility of liquefaction in an event of an earthquake. The proposed stone columns increases the density characteristics of the fly ash, there by not only enhance the bearing capacity (section 3.1) but also mitigate the liquefaction potential.

It was proposed to adopt dry bottom feed method for installation of stone columns to achieve above applications. Extensive initial field trials were carried out before carrying out the main works to assess the suitability of the technique as well as to assess the required grid pattern to achieve post performance criteria.

## 5. INITIAL FIELD TRIALS

Initial field trials were carried out to assess the bearing capacity and also the lateral capacity of bored cast-in-situ pile foundations as a result of stone column installation. The following sections illustrate the field trials carried out elaborately to address the above listed geotechnical applications.

### 5.1 Bearing Capacity

Vibro stone columns of 0.9m diameter at 2m centre to centre spacing in a triangular grid pattern, terminating at least 0.5m into the underlying stiff silty clay or clayey silt is proposed as treatment scheme to achieve the target bearing capacity of  $10T/m^2$ . According to the guide lines stipulated in IS 15284 (Part 1): 2003 – “Design and Construction for Ground Improvement – Guide Lines”, single and group column initial load tests are performed at site to assess the increase in bearing capacity as well as the settlements characteristics of stone columns. The following figure 4 illustrate the results of plate load tests conducted on single and group of 3 columns at coal handling plant location.

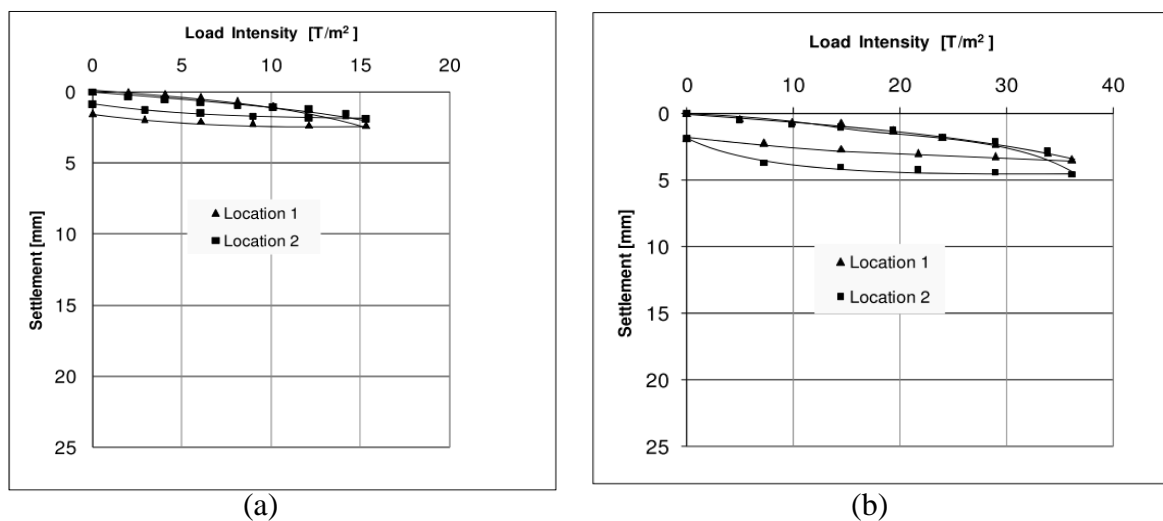


Fig. 4 Load Vs Settlement plot of (a) Load Test on Single Column (b) Load Test on Group of 3 columns

### 5.2 Lateral Capacity of Piles

Vibro stone columns are installed at specified pattern (as illustrated in figure 5) surrounding the bored cast-in-situ piles to enhance the density of fly ash deposits which in turn can improve the lateral load carrying capacity. It was required to achieve a design lateral load capacity of 7T with ultimate load of 21T. After the installation of bored cast-in-situ piles and vibro stone columns by bottom feed method, initial lateral load test are conducted on these two grid patterns.

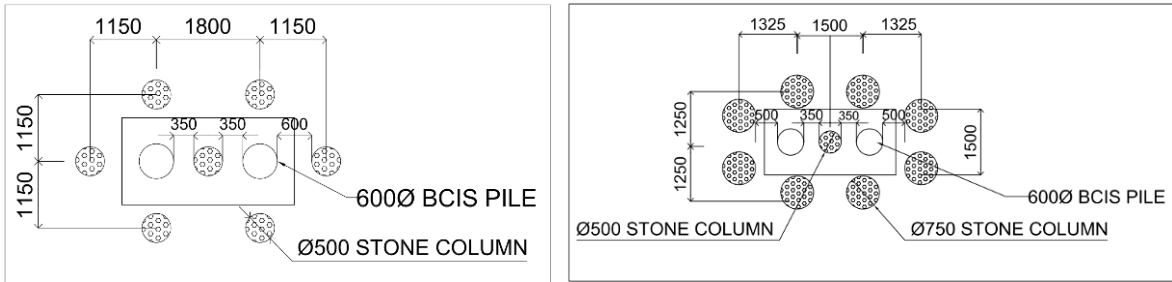


Fig. 5 Initial field trials layout for lateral load (a) Stone Column of 500mm dia. (b) Stone Columns of 750mm diameter surrounding the piles with 0.5m dia stone column at the centre

The results indicated that the deformations are within the allowable limits of 5mm at the design load of 7T (according to IS 2911, Part 4, Cl. 7.4) even for 0.5m grid pattern shown in fig 5(b). The following figure 6 illustrates the observations made during the initial lateral load tests (load vs deflection plot).

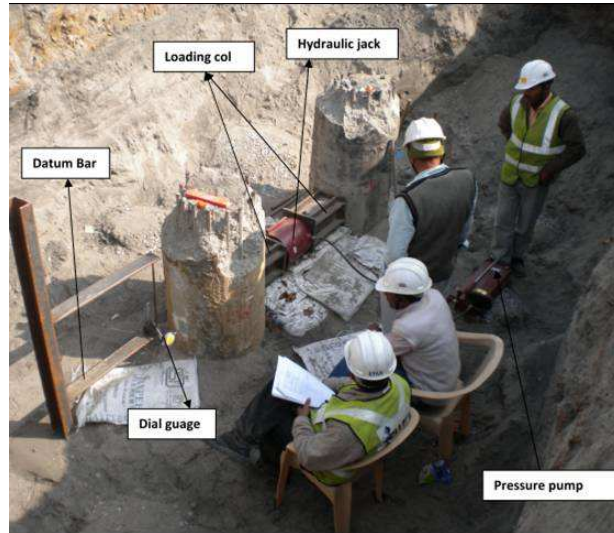
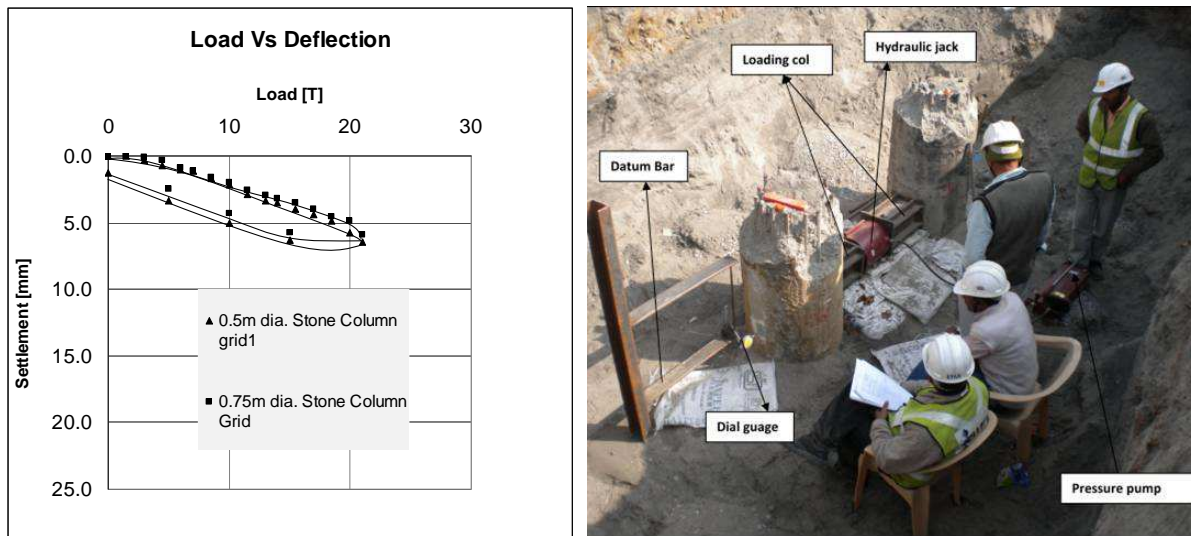


Fig. 6 Load Vs deflection plot of initial lateral load test on bored cast-in-situ piles

## 6. EXECUTION OF MAIN WORKS

Upon successful execution of initial field trials to assess the improvement in density characteristics of fly ash deposits after ground improvement, main works have been carried out. Ground improvement using vibro stone columns (dry bottom feed method) is carried out for open foundations of the structures like pump house, cable gallery, drive house etc at coal handling plant. About 34,000lin.m of vibro stone columns 0.9m dia are installed for open foundations of various structures of coal handling plant.

The following figure 7 illustrates the typical drawing of stone columns installed for open foundations of pump house structure of coal handling plant.

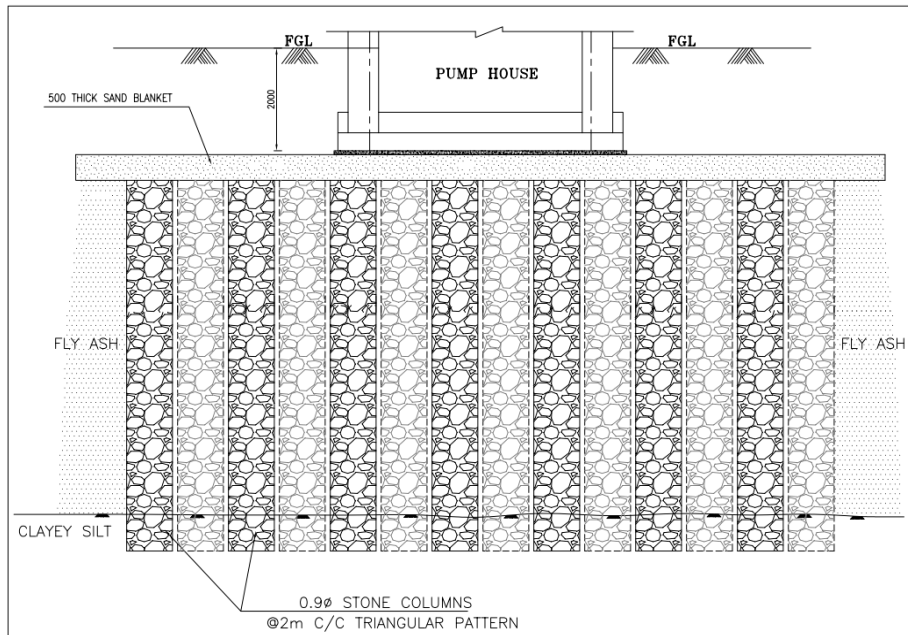


Fig. 7 Details of Stone Columns installed for open foundations of pump house Structure

Similarly, to enhance the lateral load carrying capacity of bored cast-in-situ piles of structures like conveyor, crusher house etc of coal handling plant, 45,000 lin.m of 0.5m diameter vibro stone columns are installed. The following figure 8 illustrates the schematic of stacker reclaimer at coal handling plant, where stone columns are used to enhance the lateral capacity of piles.

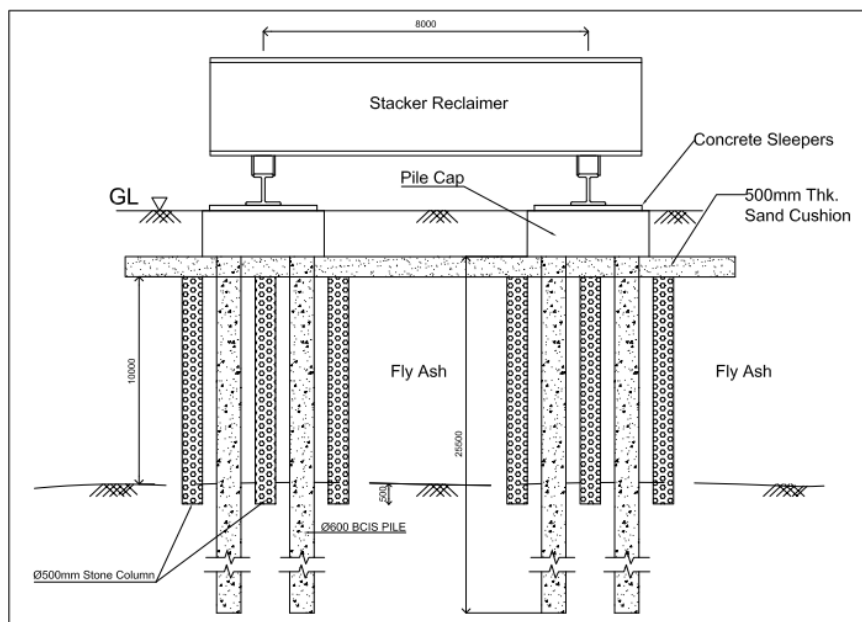


Fig. 8 Typical details of Stone columns installed surrounding the piles to enhance the lateral capacity

The following pictures (figure 9) illustrate the works in progress at coal handling plant locations.

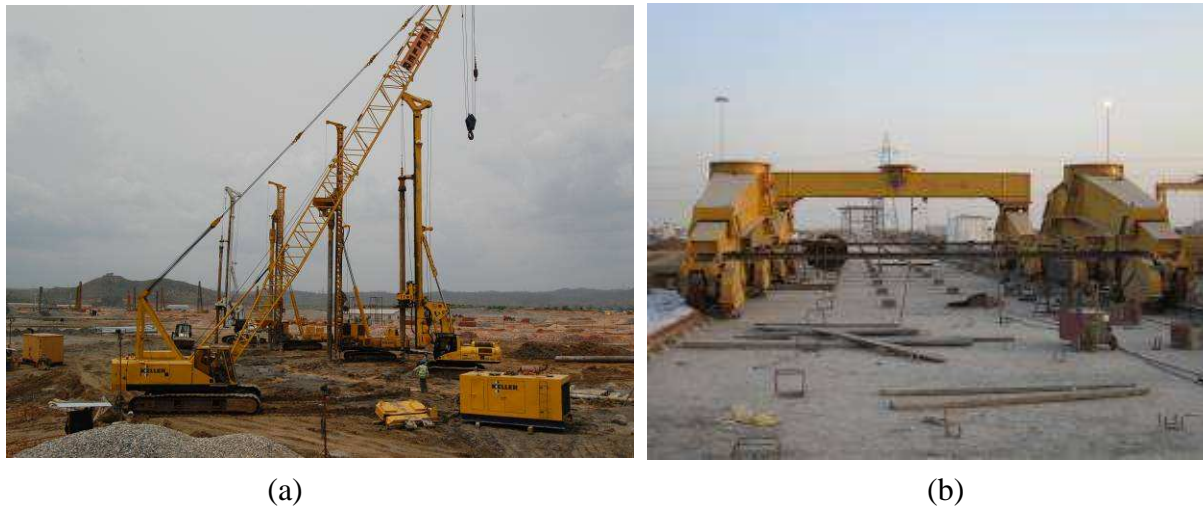


Fig. 9 (a) Installation of Stone Columns and Bored Cast-in-situ Piles using Hydraulic rigs in progress  
 (b) Conveyor 9A Structure under construction – here piles in combination with 500mm dia piles are used as foundation

## 6. QUALITY CONTROL AND QUALITY ASSURANCE

Quality control procedures are important firstly to assure the client that the product he receives is of a high standard, secondly to prevent costly re-work for the contractor and most importantly to ensure public safety. Generally, quality control is applied pre-construction, during construction and post-construction. Various standards can be used to aid in the formulation of good contract specifications and quality control procedures.

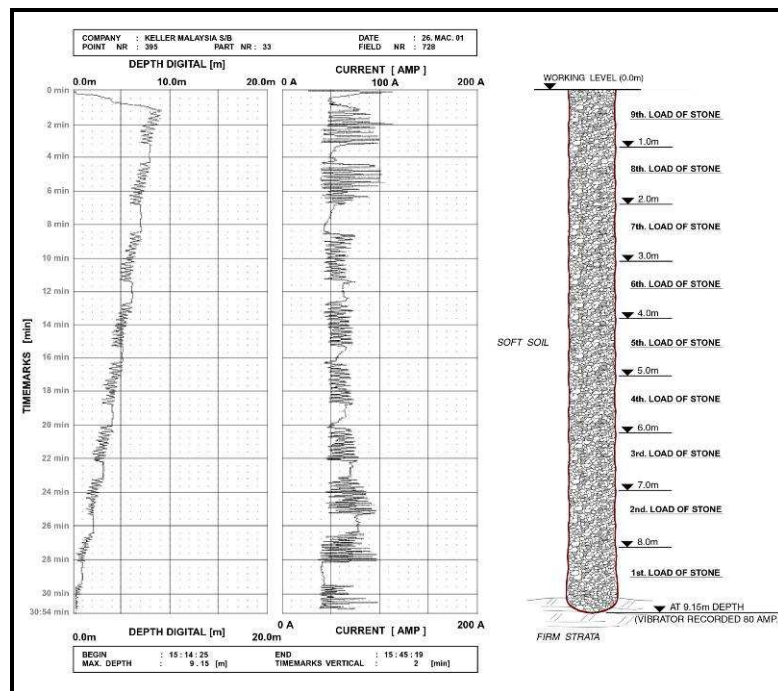


Fig. 10 Typical quality control record print out generated simultaneously during installation of stone columns

For Vibro Stone Columns, it is essential to ensure that columns are built to the right depth, to the right diameter and are properly compacted. Computerized monitoring (as shown in figure 10) of the penetration depth of the vibrator easily ensures that the design depth is reached. Sensors within the depth vibrator can readily measure the amperage drawn by the motor, giving an indication of the compaction effort of the depth vibrator. IS 15284 (Part 1): 2003 gives guidelines on the estimation of the column diameter based on fill consumption. In the case of dry bottom-feed stone columns (See Raju & Sondermann, 2005), even the location of each charge of stone along the depth of the column may be determined from the record of depth vs. amperage. Post-construction, load tests are routinely performed as a quality control measure. Another useful general standard for stone column construction and testing is EN 14731:2005.

## **7. CONCLUSIONS**

In view of the unavailability or scarcity of the suitable construction site ash ponds form one of the options to consider for the proposed development. Detailed study is required to carry out to check the suitability of the ash pond for the proposed development. In general it has been noticed that the geotechnical characteristics i.e., density of hydraulically deposited fly ash is not consistent with depth which may pose challenges with regards to bearing capacity and pile lateral load carrying capacity. In such a situation, ground improvement using dry vibro stone columns provides a techno-commercially feasible solution. It is evident from the experience in Coal Handling Plant structures at Anpara D Thermal Power Plant in Uttar Pradesh that the ground improvement using stone columns (dry bottom feed method) can be successfully adopted to enhance the bearing capacity of the fly ash deposits. Stone columns also ensured mitigation of liquefaction potential of the site under an event of earthquake as the site falls under zone III. Further, the stone columns also helped in enhancing the lateral capacity of deep pile foundations. With this experience, similar application is adopted at other structures of the power plant such as Switchyard and for the Water Treatment Plant structures, which is currently under construction.

## **References**

1. Article by Bedanga Bordoloi and Etali Sarmah on “Fly Ash Pond Reclamation” dated May 2010 for Agribusiness Forum.
2. IS 1893 (Part 1):1982 “Criteria for Earthquake Resistant Design of Structures - Part 1 : General Provisions and Buildings”

3. “Study of Effectiveness of Ground Improvement Techniques and Possible Liquefaction Potential” for Anpara-D Thermal Power Project, Department of Earthquake Engineering, IIT Roorkee
4. IS 15284 (Part 1): 2003 – “Design and Construction for Ground Improvement – Guide Lines”
5. IS 2911 (Part 1) Section 2- “Code of practice for design and construction of pile foundations: Part 1 Concrete piles, Section 2 Bored cast-in-situ piles”
6. IS 2911, Part 4, “Code of practice for design and construction of pile foundations: Part 4 Load test on piles”
7. Raju, V.R. & Sondermann, W., 2005. Ground Improvement using Deep Vibro Techniques. *Ground Improvement Case Histories*, Indraratna, B & Chu., J. (eds.), 601-638
8. EN 14731:2005, “Execution of special geotechnical works. Group treatment by deep vibration”

## Annexure 6 Observations on IS 15284 part 1 Rev 1



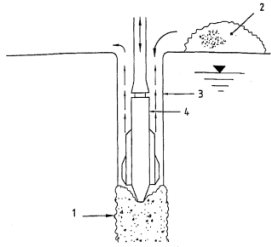
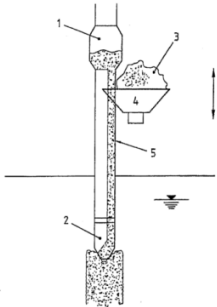
**Note on observations of Keller Ground Engineering India Pvt. Ltd. on practices of ground improvement using stone columns and suggestions in present standard (IS 15284 – Part 1)**

- In the construction industry as ground improvement has become most common practice in the last 5 to 6 years, this is high time to prepare /revise standard for all types of ground improvement methods.
- All vibration methods like vibro compaction, vibro replacement and vibro displacement to be added in the present standard IS 15284 (part 1) or a separate standard on “Ground Treatment by Deep Vibrations” may be brought out (similar to BS).
- In the present standard (IS 15284 – part 1) we feel that the following points to be incorporated, which will give more clarity and useful for practicing engineers.

S. No.	Description	Present practice (as per IS 15284 (part 1): 2003)	Recommended
1	Diameter of Stone column	In the present standard (Clause 7.1) there is no specific recommendation for the diameter of stone columns	It is recommended that the diameter of vibrated stone column shall be in the range of 0.8m to 1.2m
2	Area of treatment	Present standard (Clause 6.4) specifies that the application of stone columns is limited to embankments, tanks etc.	In practice vibro stone columns are being used extensively for buildings, industrial structures, infrastructure projects like railways, airports, port facilities, power plant structures etc. to improve bearing capacity, to reduce settlements and to mitigate liquefaction potential
3	Treatment depth	Present standard says that the average depth of treatment may be around 15m	In practice with the present equipment availability, the depth of stone column shall be as given below <ol style="list-style-type: none"> <li>1. The depth of stone column using wet top feed method is 25m to 30m</li> <li>2. Using dry bottom-feed method can construct a column of 15m to 20m depth</li> </ol>
4	Spacing	In Clause 7.3 of present standard, it is mentioned that the column spacing broadly ranges from 2 to 3. It is not clear	It is usual practice that spacing of stone column broadly ranges from 1.5 to 2.5 times of stone column diameter based on design Area Replacement Ratio



S. No.	Description	Present practice (as per IS 15284 (part 1): 2003)	Recommended
5	Area Replacement Ratio	In the present code there is no specific ranges of Area Replacement Ratio	In practice the Area Replacement Ratio of 10% to 30% is being used widely based on the soil condition, loading condition and design performance criteria
6	Installation techniques	In Annexure C-1.2 of present standard explained about the installation of stone column using <b>“Direct mud circulation method”</b> in which bentonite slurry is used for <b>stabilizing the borehole</b> and it shall be <b>pumped out</b> .	The specified method is practically not feasible so it shall be removed
7	Installation techniques	Annexure C of present standard gives the following methods for the installation of stone column  C-1 Non- displacement method C-2 Displacement method C-3 Vibro replacement method a) Wet process b) Dry process	It shall be modified as below  C-1 Non- displacement method C-2 Displacement method C-3 Vibro method 3.1. Displacement method 3.2. Vibro replacement method a) Wet process (Replacement: top feed method) b) Dry process (Displacement: bottom feed method)
8	Vibro replacement method	Annexure C-3 (b) of present standard explains that Dry process is suitable for soils relatively high initial strength with relatively low water table where the hole can be stand of its own upon extraction of the probe, such as unsaturated fills	Dry process (bottom feed method) is displacement method and the stone shall be delivered at the tip of vibrator through bottom feed mechanism and shall be used for all type of soils and irrespective of water table as the vibrator string will go into the required depth of treatment and remains in the hole during column construction
9	Measurement of stone column diameter	After installation of stone column there is no specific method/practice is mentioned to measure the diameter of column	It is common practice that the stone volume consumed for making a single column is used for confirm the diameter as the depth of column is known

S. No.	Description	Present practice (as per IS 15284 (part 1): 2003)	Recommended
10	Estimation of load capacity	In the present standard (Clause 9.3.2) it is mentioned that any other alternative methods can be used	Alternative methods like Heinz J. Priebe methods (the design of vibro replacement) can be used for the estimation of load capacity which is accepted internationally
11	Installation techniques	For wet and dry method, the installation process is not explained in the standard	<p>The installation process and method explained in British standard (below picture) shall be included for more clarity</p> <p><b>Wet method (Top feed):</b> EN 14731:2005 (E)</p>  <p>Key 1 Stone column 2 Stone stockpile 3 Water feeding 4 Vibrator</p> <p>Figure B.2 – Wet process</p> <p><b>Dry method (Bottom feed)</b></p>  <p>Key 1 Pressure chamber 2 Vibrator 3 Stone stockpile 4 Stone feed bucket 5 Stone delivery tube</p> <p>Figure B.3 – Dry bottom-feed process</p>
12	Grading of stones	The present standard there is no specific grading for different methods of stone column	<p>The common practice and as per BS the following grading shall be adopted</p> <ol style="list-style-type: none"> <li>1. For wet process the grade of stone is 12 to 75mm</li> <li>2. For dry process (bottom feed) the grade of stone is 12 to 40mm</li> </ol>



**References:**

1. BS EN 14731: 2005, "Execution of special geotechnical works –Ground treatment by deep vibrations".
2. BRE Garston, Watford, WD2 7 JR, "Specifying vibro stone columns".

**MONOGRAPH ON**  
**GRANULAR PILES AND GRANULAR PILE ANCHORS**

<sup>1</sup>Madhav Madhiraand <sup>2</sup>Vidyaranya Bandi

1 Prof. Emeritus, JNT University and Visiting Professor, IITH, Hyderabad, 500085, India

2 Engineering Manager, L&T TI-IC, Mumbai 400097, India.

## **1. INTRODUCTION**

Granular piles are often constructed through soft soils fully penetrating to an end bearing stratum or as floating piles in deep deposits, the tips resting at depths where the strength of the soil is adequate.

Failure mechanisms (Fig. 1) for a single granular pile are bulging, general shear and pile failure though probable failure is by bulging or pile failure. Methods to estimate the ultimate capacity of granular piles corresponding to general shear, bulging and pile failures are presented in Table 1. In pile failure mode, the total load applied on the granular pile is resisted by shaft resistance generated along the shaft length and the bearing resistance at the base of the GP while the resistance generated by lateral confinement of the granular fill material near the top in GP limits its bulging capacity.

The functional utility of the granular pile to carry the compressive load is extended to resist the uplift or pullout forces generated in foundations by a simple modification of connecting the base of the foundation to a plate, pedestal or geogrid at the tip of the granular pile by a cable or rod to transfer the pullout load (Fig. 2).

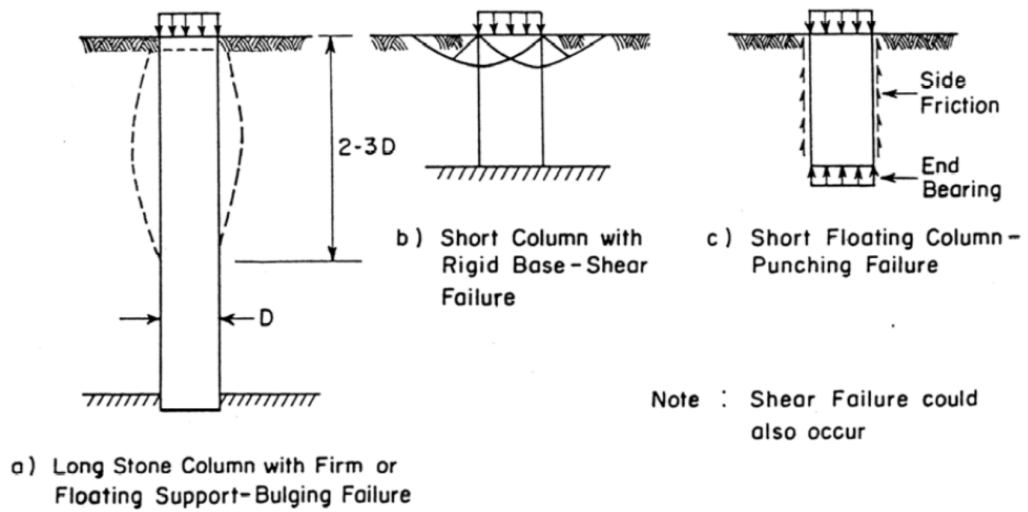


Fig. 1 (a) Bulging, (b) General Shear and (c) Pile Failure Mechanisms for Single Granular Pile

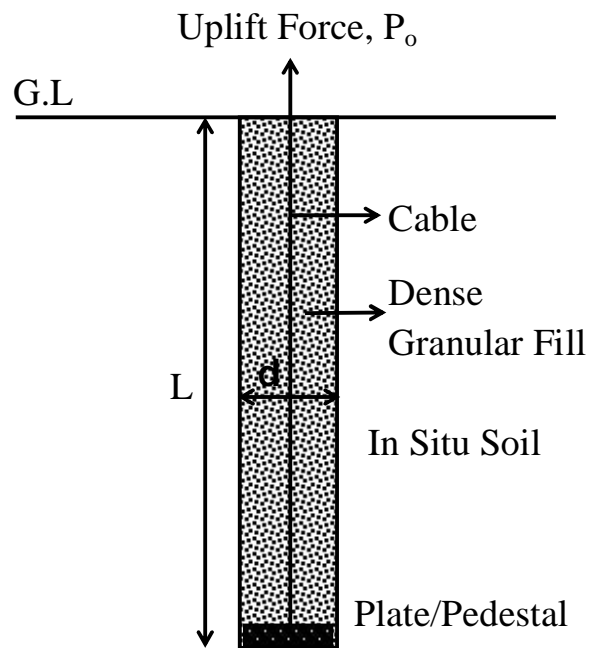


Fig. 2 Granular Pile Anchor.

Table 1 Estimation of Ultimate Load (Aboshi and Suematsu, 1985)

Mode of Failure	Derived Formula	References
Bulging	$q_{ult} = \left( \gamma_c z k_{pc} + 2c_o \sqrt{k_{pc}} \right) \frac{1 + \sin \phi_s}{1 - \sin \phi_s},$ <p>where <math>k_{pc}</math> is the passive earth pressure coefficient of column and <math>\phi_s</math> is the frictional resistance of soil</p>	Greenwood (1970)
	$q_{ult} = \left( F_c^1 C_o + F_q^1 Q_o \right) \frac{1 + \sin \phi_s}{1 - \sin \phi_s},$ <p>where <math>F_c^1</math> and <math>F_q^1</math> are the cavity expansion factors and <math>Q_o</math> is the surcharge stress</p>	Vesic (1972), Datye & Nagaraju (1975)
	$q_{ult} = (\sigma_{ro} + 4C_o) \frac{1 + \sin \phi_s}{1 - \sin \phi_s},$	Hughes and Withers (1974)
	$q_{ult} = \frac{1 + \sin \phi_s}{1 - \sin \phi_s} (4C_o + \sigma_{ro} + K_o q_s) \left( \frac{W}{B} \right)^2 + \left( 1 - \left( \frac{W}{B} \right)^2 \right) q_s$ <p>where W and B are diameters of stone column and footing respectively.</p>	Madhav et al. (1979)
General Shear	$q_{ult} = C_o N_c + \left( \frac{1}{2} \gamma_c B N_\gamma \right) + \gamma_c D_f N_q,$ <p>where <math>N_c</math>, <math>N_q</math> and <math>N_\gamma</math> are the dimensionless parameters that depend on the trench and soil parameters.</p>	Madhav and Vitkar (1978)
	$q_{ult} = \left( \frac{1}{2} \gamma_c B \tan^3 \psi \right) + 2C_o \tan^2 \psi + 2(1 - a_s) C_o \tan \psi$ $\psi = 45^\circ + \frac{\tan^{-1}(\mu_s a_s \tan \phi_s)}{2}$	Barksdale and Bachus (1983)
Sliding Surface	$q_{ult} = (1 - a_s) C_o + (\gamma_s z + \mu_{s\sigma_z}) a_s \tan \phi_s \cos^2 \theta$ $\mu_s = \frac{n}{1 + (n - 1) a_s},$ <p>where <math>a_r</math> is area replacement ratio and <math>\phi_s</math> &amp; <math>\gamma_s</math> are column parameters</p>	Aboshi et al. (1979)

## 2. ULTIMATE CAPACITY OF GRANULAR PILE (GP) IN HOMOGENOUS GROUND

Ultimate capacity of granular pile in compression is estimated for homogenous ground, i.e., the undrained strength,  $c_u$ , of the in situ soil is constant with depth.

### 2.1 Single Granular Pile in Compression

A granular pile of diameter,  $d$ , and length  $L$ , is considered (Fig.3). The saturated unit weight, the undrained strength and the shear modulus of the in situ soil assumed constant with depth are  $\gamma_s$ ,  $c_u$  and  $G$  respectively while  $\phi_{gp}$  and  $\gamma_{gp}$  are respectively the angle of shearing resistance and unit weight of the granular pile material.

The ultimate pile capacity,  $P_{comp}$ , is limited by the interface shear stresses,  $\tau$ , acting on the cylindrical boundary and the ultimate bearing stress,  $q_b$ , at the base of the GP (Fig. 4a). The ultimate shear stresses,  $\tau$ , equals the undrained shear strength,  $c_u$ , while the limiting bearing stress,  $q_b$ , equals  $N_c.c_u$  (Fig. 4b). The ultimate capacity,  $P_{ult}$ , of GP in compression

by pile capacity after normalization with  $\frac{\pi.d^2}{4}.c_u$  reduces to

$$P_{pf}^* = 4 \frac{L}{d} + N_c \quad (1)$$

where  $P_{pf}^* = P_{ult, pf} / \{\pi d^2/4\}c_u$  and  $N_c$  – bearing capacity factor that varies from 6.2 to 9 for  $L/d$  increasing from 0 to 5 or more.

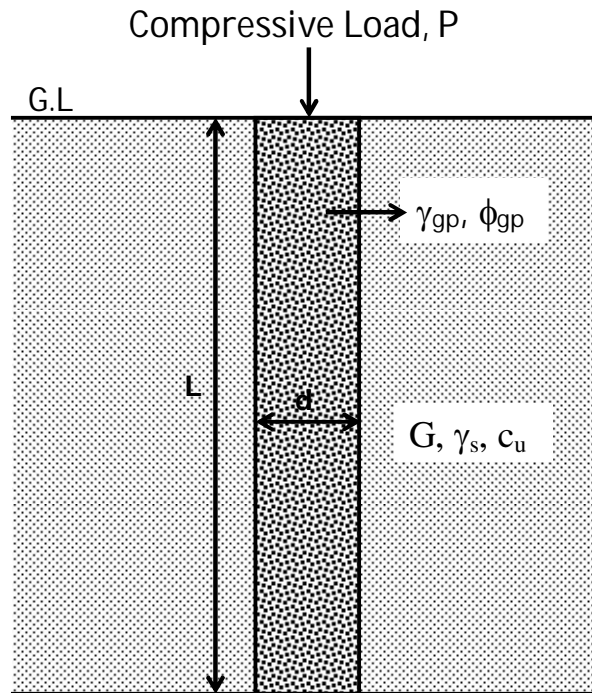


Fig. 3 Granular Pile under Compression.

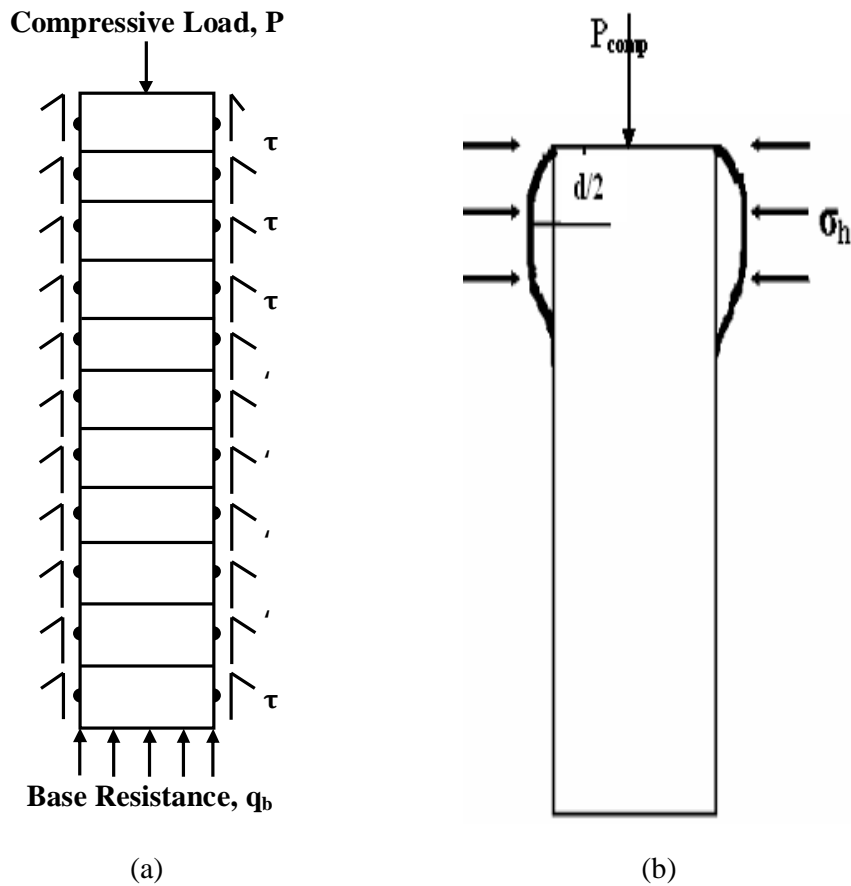


Fig. 4(a) Pile & (b) Bulging Failures for GP.

For bulging failure, following Gibson and Anderson (1961), Hughes and Withers (1974) and Hughes et al. (1975), for expansion of a cavity near the top (at a depth of  $d/2$  from the top) of the GP,  $P_{ult, bf}$  is

$$P_{ult, bf} = \frac{\pi \cdot d^2}{4} N_{\Phi} \{c_u \cdot N_c^* + \sigma_{ho}\} \quad (2)$$

where the lateral confining pressure  $\sigma_{ho}$ , is the horizontal total stress at depth equal to half the diameter ( $d/2$ ) of GP,  $N_c^* = 1 + \ln\left(\frac{G}{c_u}\right)$  and  $N_{\Phi} = \frac{(1 + \sin \phi_{gp})}{(1 - \sin \phi_{gp})}$ . Normalizing  $P_{ult, bf}$

with  $\frac{\pi \cdot d^2}{4} \cdot c_u$  Eq. (2) reduces to

$$P^* = \frac{4P_{comp}}{\pi d^2 c_u} = N_{\Phi} [N_c^* + \beta] \quad (3)$$

$$\text{where } \beta = \left[ \frac{\gamma_w \cdot d}{c_u} \left( \frac{K_o \cdot \gamma_{sub}}{\gamma_w} + 1 \right) \right]$$

The critical length,  $(L/d)_{cr}$  defined as is the length at which the ultimate capacities by pile and bulging failures equal. The ultimate capacity is governed by pile failure for  $L/d$  smaller than the critical length and by bulging failure for  $L/d$  greater than the critical length.

## 2.2 Ultimate Pullout Capacity of Granular Pile Anchor (GPA) – Homogenous Ground

The applied pullout load is transferred to the base through the cable or steel rod attached to the base plate, pad or sheet placed prior to the installation of the granular pile material (Fig. 5).

The ultimate pullout capacity of the GPA is the lesser of the loads at which it is either pulled out by pile (Fig. 6a) or by bulging (Fig. 6b) failure. The normalized ultimate capacity,  $P^*$  of GPA by pile capacity is

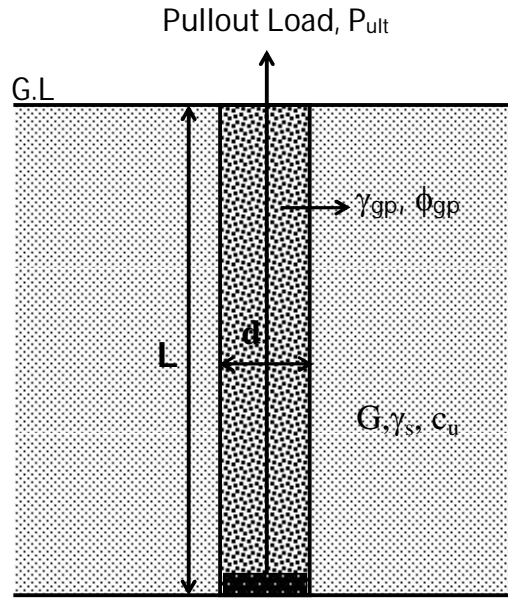


Fig. 5 GPA under Pullout

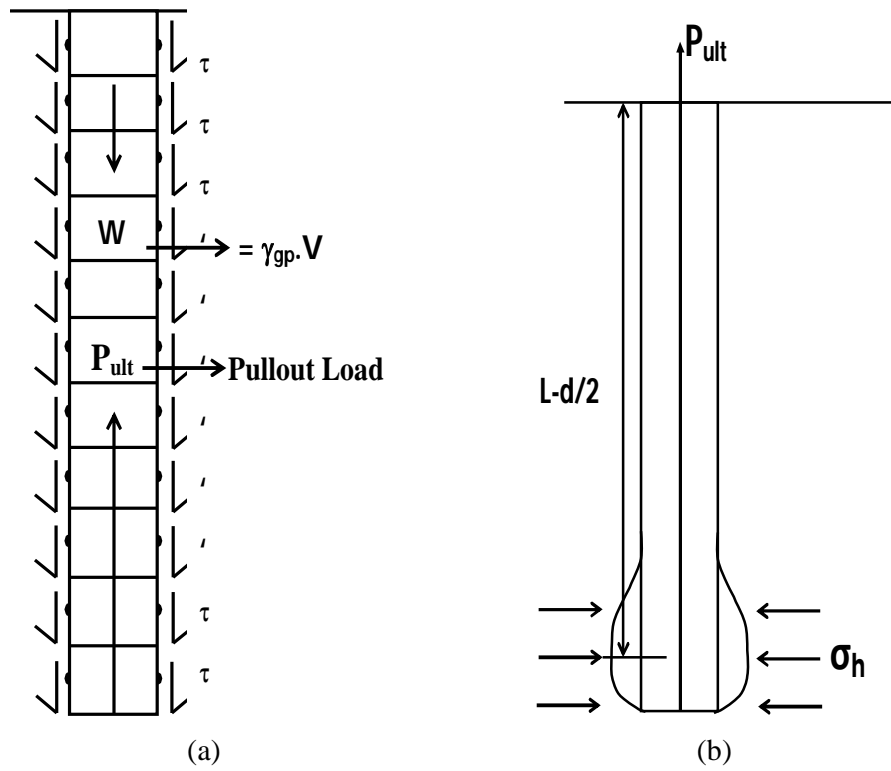


Fig. 6 Pullout (a) and Bulging (b) Failures of GPA.

$$P^* = \frac{4P_{ult}}{\pi d^2 c_u} = \frac{L}{d}(4 + \lambda) \tag{4}$$

where  $\lambda = \frac{\gamma_{gp} \cdot d}{c_u}$

Bulging is considered likely to occur at a distance of half-diameter of the GPA from the tip instead of from the top as was considered for bulging capacity of granular piles in compression. The bulging capacity of the GPA is

$$P_{ult} = \frac{\pi \cdot d^2}{4} \cdot N_{\Phi} \{c_u \cdot N_c^* + \sigma_{h_0}\} \quad (5)$$

The total horizontal stress,  $\sigma_{h_0}$ , is considered at depth  $z = (L - d/2)$  assuming groundwater level to be at ground level. The normalized ultimate pullout load by bulging,  $P^*$  is

$$P^* = \frac{4P_{ult}}{\pi d^2 c_u} = N_{\Phi} \left[ N_c^* + \beta \cdot \left( \frac{L}{d} - \frac{1}{2} \right) \right] \quad (6)$$

where  $\beta = \frac{\gamma_w \cdot d}{c_u} \left\{ \frac{K \cdot \gamma_{sub}}{\gamma_w} + 1 \right\}$  - a lateral confining stress parameter that depends particularly

on lateral earth pressure coefficient,  $K$ , of the in situ soil. The critical length,  $(L/d)_{cr}$  defined as is the length at which the ultimate capacities by pile and bulging failures equal. The ultimate capacity is governed by pile failure for  $L/d$  smaller than the critical length and by bulging failure for  $L/d$  greater than the critical length.

### 2.3 Results

The ultimate capacity of GP in compression and the ultimate pullout capacity of GPA are estimated for both the pile and bulging failure mechanisms using Eqs. 1 & 3 for GP and 4 & 6 for GPA for the following ranges of the parameters:  $\gamma_s$ : 14 to 16 kN/m<sup>3</sup>;  $\gamma_{gp}$ : 18 to 21 kN/m<sup>3</sup>;  $c_u$ : 10 to 60 kPa;  $L/d$ : 1 to 25;  $\phi_{gp}$ : 30<sup>0</sup> to 45<sup>0</sup>;  $G/c_u$ : 50 to 500;  $\gamma_s d/c_u$ : 0.1-2;  $\lambda (= \gamma_{gp} d/c_u)$ : 0.1-2.5;  $\gamma_{sub} d/c_u$ : 0.03 to 0.7;  $\gamma_w d/c_u$ : 0.08 to 1.2,  $\beta = 0.1 - 1.6$  and  $K_0 = 0.5-1.0$ .

The ultimate capacity of GP is presented in Fig. 7 as a function of  $L/d$  for  $\phi_{gp}$  in the range of  $30^\circ$  to  $45^\circ$ , for  $G/c_u = 100$  &  $200$ , and  $\beta = 1.0$ .

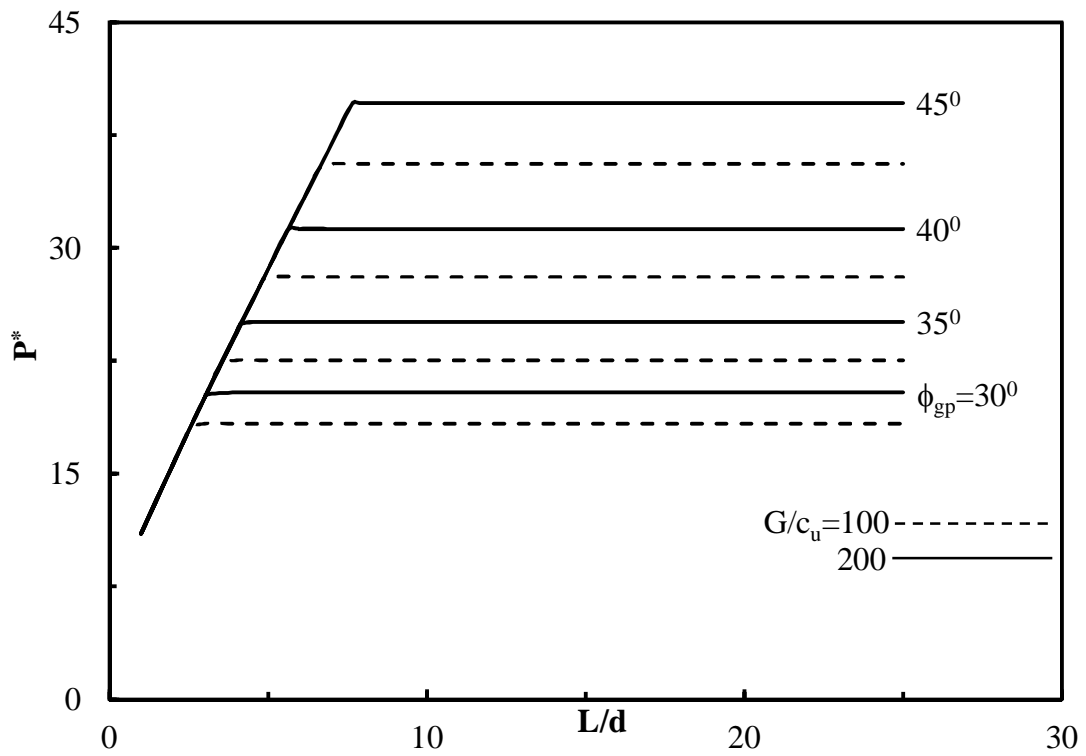


Fig. 7 Ultimate capacity,  $P^*$  of GP - Effect of  $\phi_{gp}$  for  $G/c_u = 100$  and  $200$  &  $\beta = 1.0$ .

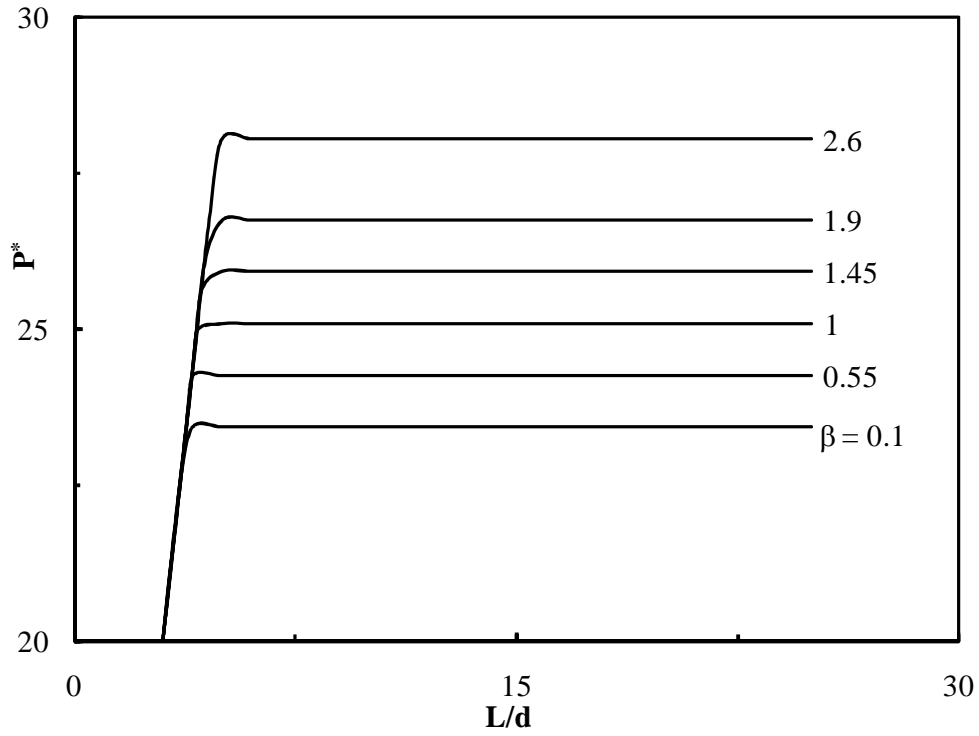


Fig. 8 Ultimate capacity,  $P^*$  of GP - Effect of  $\beta$  for  $\phi_{gp} = 35^\circ$  &  $G/c_u=200$ .

Fig. 8 depicts the effect of the lateral stress parameter,  $\beta$ , on the ultimate capacity of the GP.

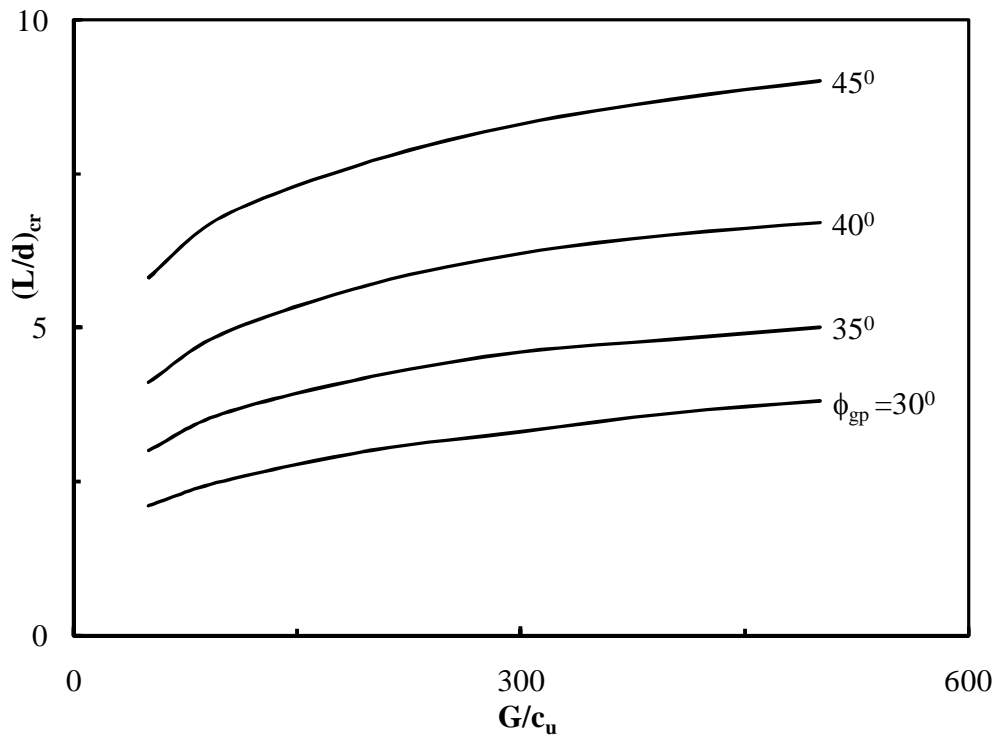


Fig.9 Critical length,  $(L/d)_{cr}$  for GP in compression – Effect of  $\phi_{gp}$  for  $\beta = 1.0$ .

The effects of  $G/c_u$  and  $\phi_{gp}$  on the critical length,  $(L/d)_{cr}$  of GP are shown in Fig. 9.

The variation of ultimate pullout capacity,  $P^*$  with  $L/d$  showing the effect of  $\lambda$  for  $\beta=1$ ,  $G/c_u=200$  &  $\phi_{gp}=35^\circ$  is depicted in Fig. 11.

The ultimate pullout capacity of GPA is presented in Fig. 10 as a function of  $L/d$  and includes the effects of  $G/c_u$  &  $\phi_{gp}$  for  $\lambda=1.3$  &  $\beta=1.0$ . It may be noted that the ultimate pullout capacity increases with  $L/d$  even for bulging failure mode since bulging is expected to occur near the tip of GPA.

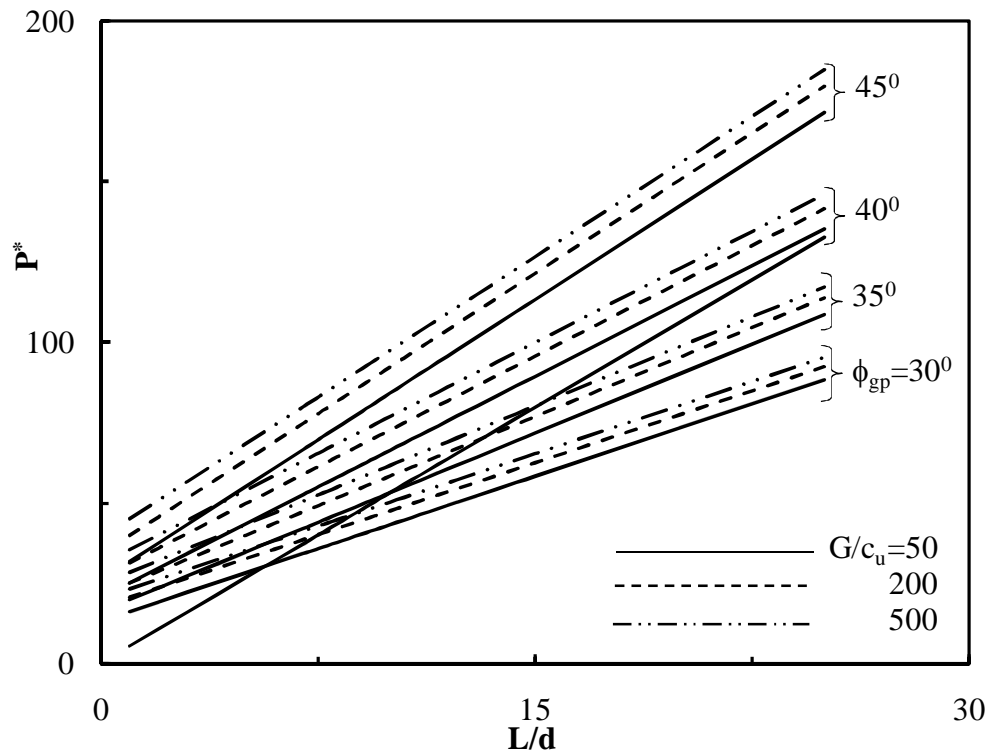


Fig. 10 Ultimate pullout capacity,  $P^*$  vs  $L/d$  for GPA – Effect of  $G/c_u$  &  $\phi_{gp}$  for  $\lambda=1.3$  &  $\beta=1.0$ .

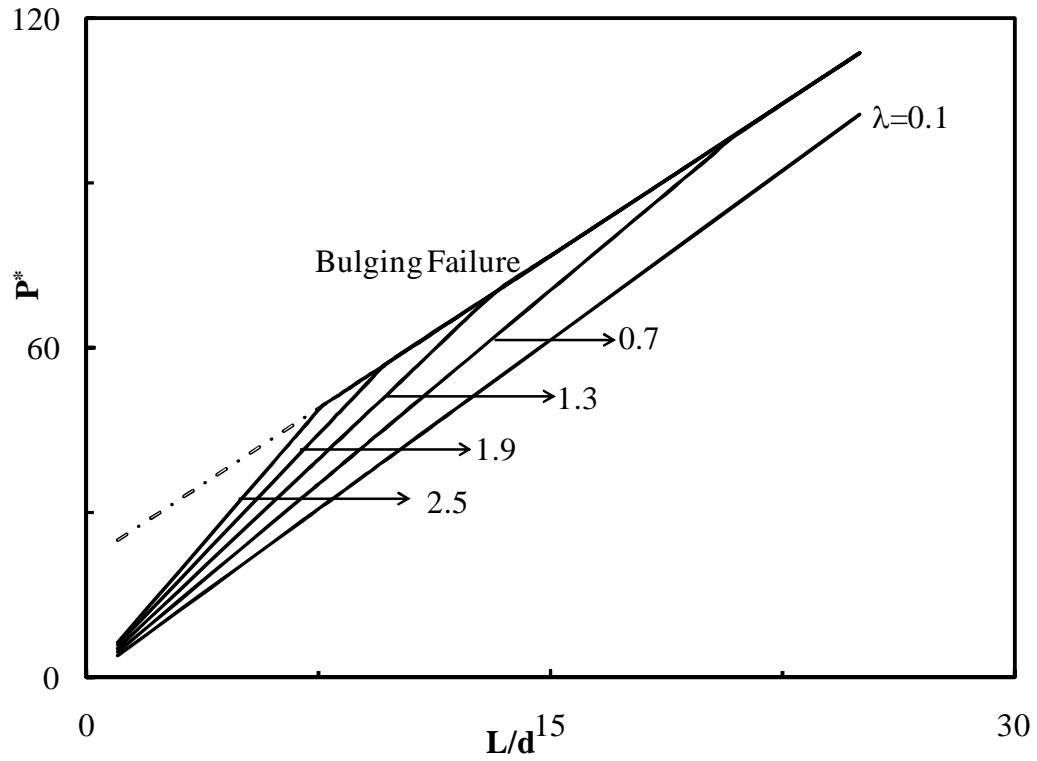


Fig. 11 Ultimate pullout capacity,  $P^*$  vs  $L/d$  for GPA – Effect of  $\lambda$  for  $\beta=1$ ,  $G/c_u=200$  &  $\phi_{gp}=35^\circ$ .

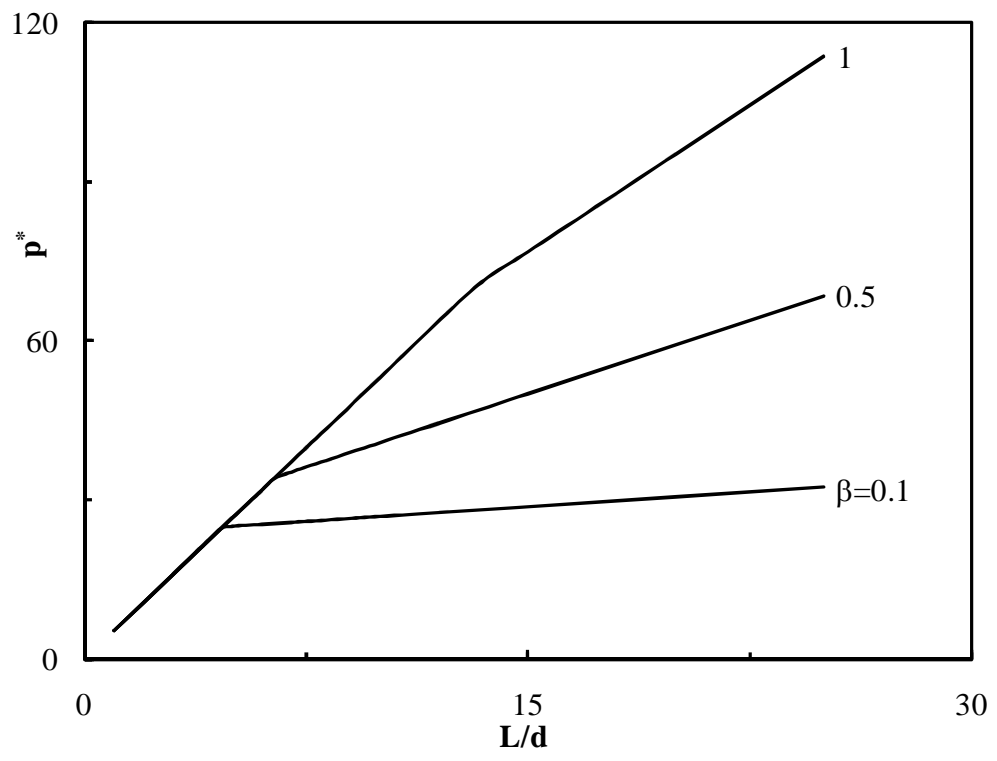


Fig. 12 Ultimate pullout capacity,  $P^*$  vs  $L/d$  for GPA – Effect of  $\beta$  for  $\lambda=1.3$ ,  $G/c_u=200$  &  $\phi_{gp}=35^\circ$ .

The effect of the lateral stress parameter,  $\beta$ , on ultimate pullout capacity of GPA is depicted in Fig. 12.

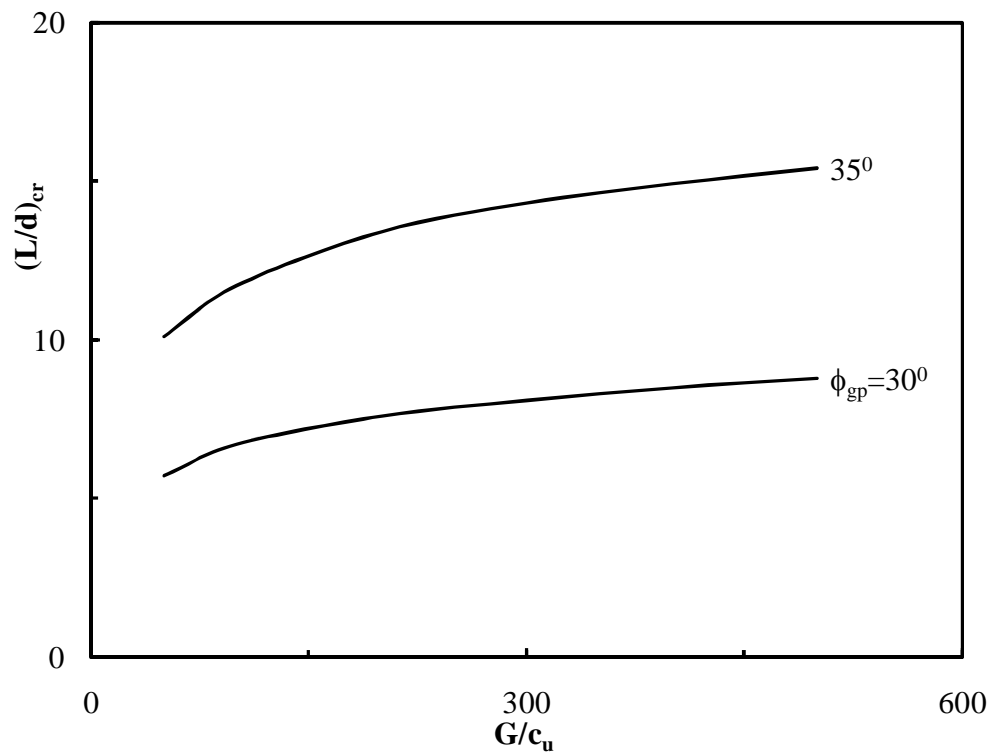


Fig. 13 Critical length,  $(L/d)_{cr}$  vs  $G/c_u$  for GPA -Effect of  $\phi_{gp}$  for  $\lambda=1.3$  &  $\beta = 1.0$  in GPA.

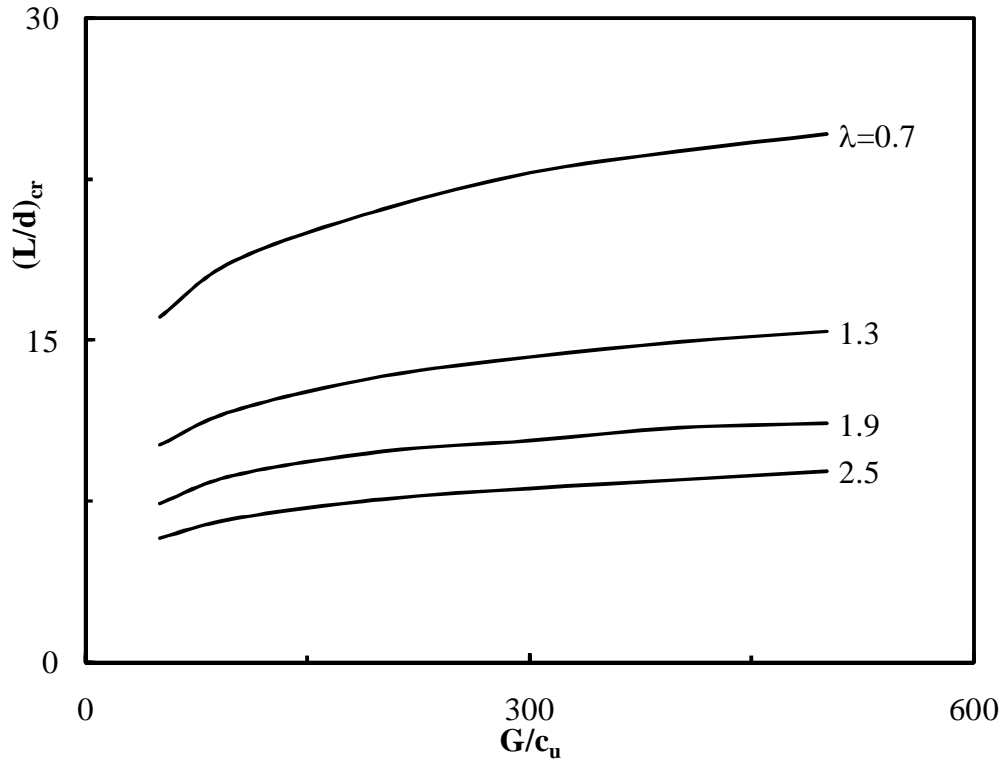


Fig. 14 Critical length,  $(L/d)_{cr}$  vs  $G/c_u$  for GPA - Effect of  $\lambda$  for  $\beta=1.0$  &  $\phi_{gp}=35^\circ$ .

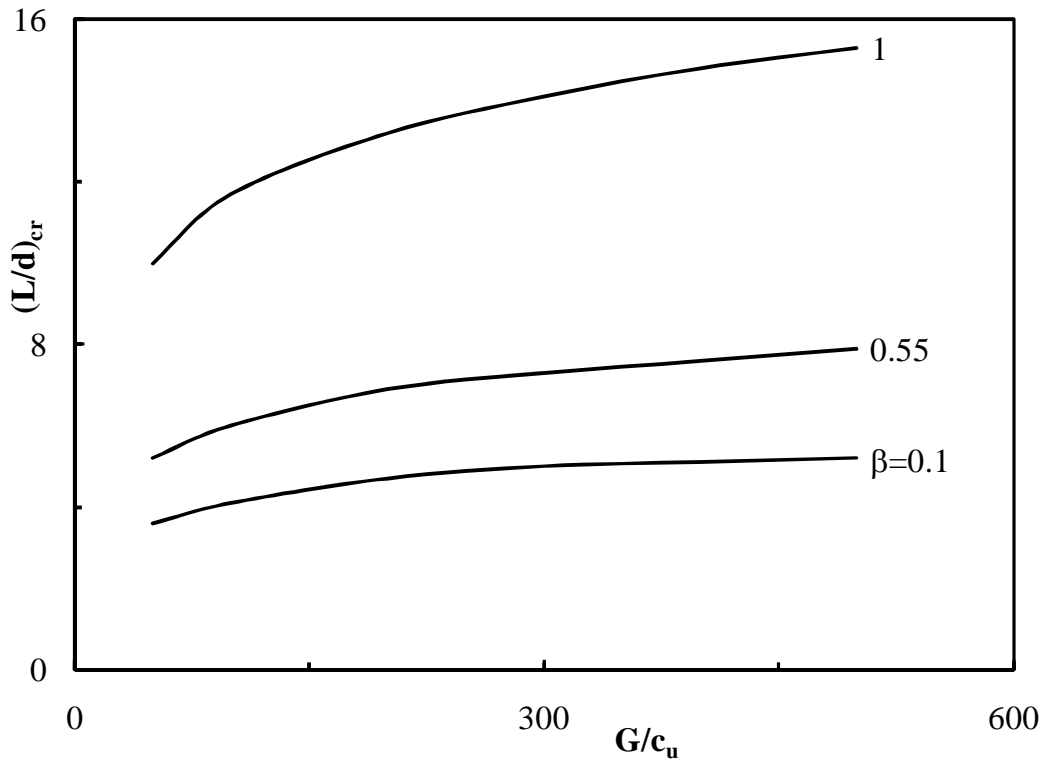


Fig. 15 Critical length,  $(L/d)_{cr}$  vs  $G/c_u$  for GPA - Effect of  $\beta$  for  $\lambda=1.3$  &  $\phi_{gp}=35^\circ$ .

The variation of critical length,  $(L/d)_{cr}$  of GPA with  $G/c_u$  for  $\phi_{gp}$  varying from  $30^\circ$  to  $45^\circ$  is shown in Fig. 13 while the variations with  $\lambda$  and  $\beta$  in Figs 14 and 15 respectively.

### 3. NON-HOMOGENOUS GROUND

The undrained shear strength of in situ soil is considered (Fig.16) to increase linearly with depth (non-homogenous ground), and the ultimate capacities of the GP and GPA estimated. The variation of undrained shear strength of normally consolidated soil with depth normalized with length of the granular pile, is expressed as

$$c_u(z) = c_{uo} \left[ 1 + \alpha_c \frac{z}{L} \right] \quad (7)$$

where  $\alpha_c$ , non-homogeneity strength parameter expresses the rate of increase of undrained shear strength with depth.

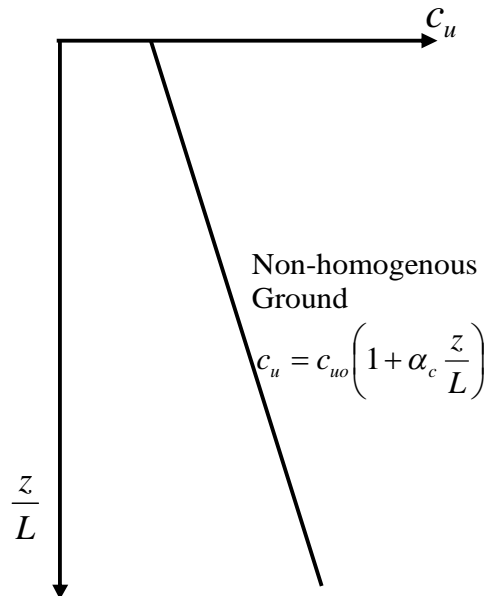


Fig. 16 Profile of undrained shear strength of the soil with normalized depth

### 3.1 Ultimate Capacity of Granular Pile (GP)

The ultimate compressive capacity,  $P_{ult}$  of GP by pile capacity normalized with  $\frac{\pi.d^2}{4}.c_{uo}$  is

$$P^* = \left(4 \cdot \frac{L}{d} + N_c\right) \left(1 + \frac{\alpha_c}{2}\right) \quad (8)$$

where the normalized compressive capacity,  $P^*$ , of GP,  $P^* = \frac{P_{ult}}{\left\{\frac{\pi.d^2}{4} c_{uo}\right\}}$  is

The normalized ultimate capacity,  $P^*$ , of GP for bulging failure in non-homogeneous ground is

$$P^* = \frac{4P_{comp}}{\pi d^2 c_{u0}} = N_\Phi \left[ \left(1 + \alpha_c \frac{d}{2L}\right) N_c^* + 0.5\beta \right] \quad (9)$$

### 3.2 Ultimate Pullout Capacity of Granular Pile Anchor (GPA)

The normalized of ultimate pullout capacity,  $P^*$  of GPA for pile failure is

$$P^* = \frac{L}{d} \{4(1 + 0.5\alpha_c) + \lambda\} \quad (10)$$

where  $\lambda = \frac{\gamma_{gp} d}{c_{uo}}$  - function of the density of the granular fill material.

The undrained strength of the soil at distance  $d/2$  from the tip of GPA where bulging is expected to occur, is

$$c_u = c_{uo} \left(1 + \alpha_c \frac{(L-d/2)}{L}\right) = c_{uo} \left(1 + \frac{\alpha_c}{(L/d)} \cdot \left(\frac{L}{d} - \frac{1}{2}\right)\right) \quad (11)$$

The normalized ultimate pullout load,  $P^*$ , of GPA for bulging failure, is

$$P^* = \frac{4P_{ult}}{\pi d^2 c_{uo}} = N_{\Phi} \left[ \left( 1 + \frac{\alpha_c}{(L/d)} \cdot \left( \frac{L}{d} - \frac{1}{2} \right) \right) N_c^* + \beta \cdot \left( \frac{L}{d} - \frac{1}{2} \right) \right] \quad (12)$$

where  $\beta = \frac{\gamma_w \cdot d}{c_{uo}} \left\{ \frac{\gamma_{sub} \cdot K_o}{\gamma_w} + 1 \right\}$  - lateral confining pressure parameter

### 3.3. Results

The ultimate compressive and pullout resistances of GP & GPA in non-homogenous ground are estimated for both the pile and bulging failure mechanisms using Eqs. 8 &10, and 12 & 14 respectively for the following ranges of the parameters:  $\gamma_s$ : 14 to 16 kN/m<sup>3</sup>;  $\gamma_{gp}$ : 18 to 21 kN/m<sup>3</sup>;  $c_{uo}$ : 10 to 60 kPa; L/d: 1 to 25;  $\phi_{gp}$ : 30<sup>0</sup> to 45<sup>0</sup>; G/c<sub>uo</sub>: 50 to 500;  $\gamma_s d/c_{uo}$ : 0.1-2;  $\lambda$  ( $=\gamma_{gp} d/c_{uo}$ ): 0.1-2.5;  $\gamma_{sub} d/c_{uo}$ : 0.03 to 0.7;  $\gamma_w d/c_{uo}$ : 0.08 to 1.2,  $\alpha_c = 0.5 - 1.0$ ,  $\beta = 0.1 - 1.6$  and  $K_0 = 0.5-1.0$ .

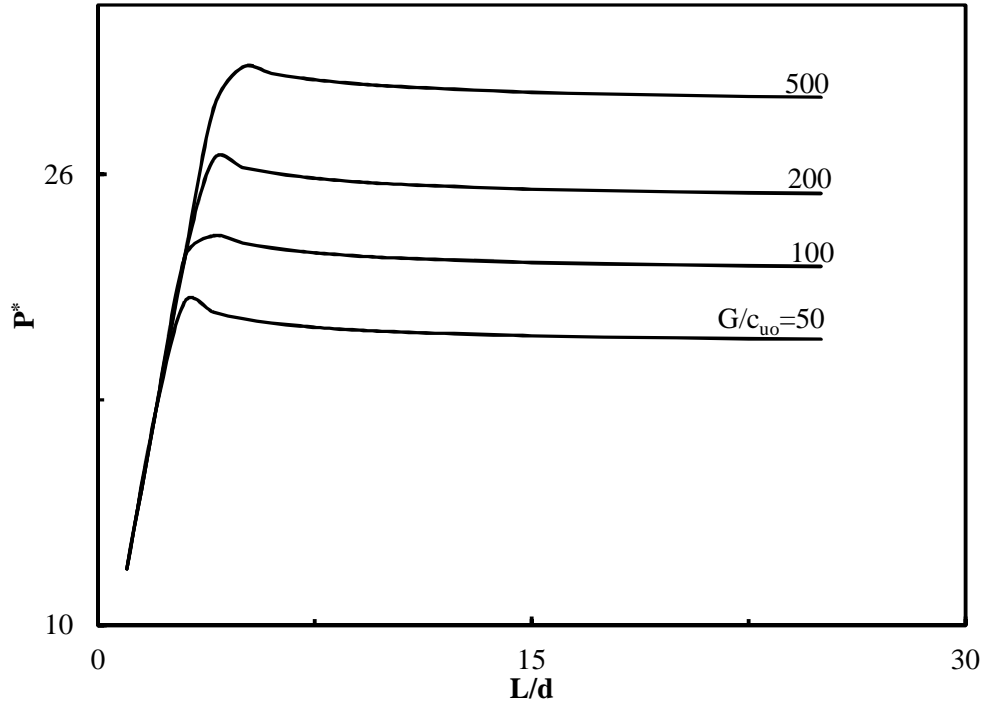


Fig. 17 Ultimate compressive capacity,  $P^*$  for GP vs. L/d - Effect of G/c<sub>u</sub> for  $\phi_{gp} = 35^0$ ,  $\beta = 1.0$  &  $\alpha_c = 0.5$  in non-homogenous ground.

The variations of ultimate capacity of GP in non-homogeneous ground (undrained strength increasing linearly with depth) with  $L/d$  for different  $G/c_u$  and non-homogeneity parameter,  $\alpha_c$  are given in Figs. 17 and 18.

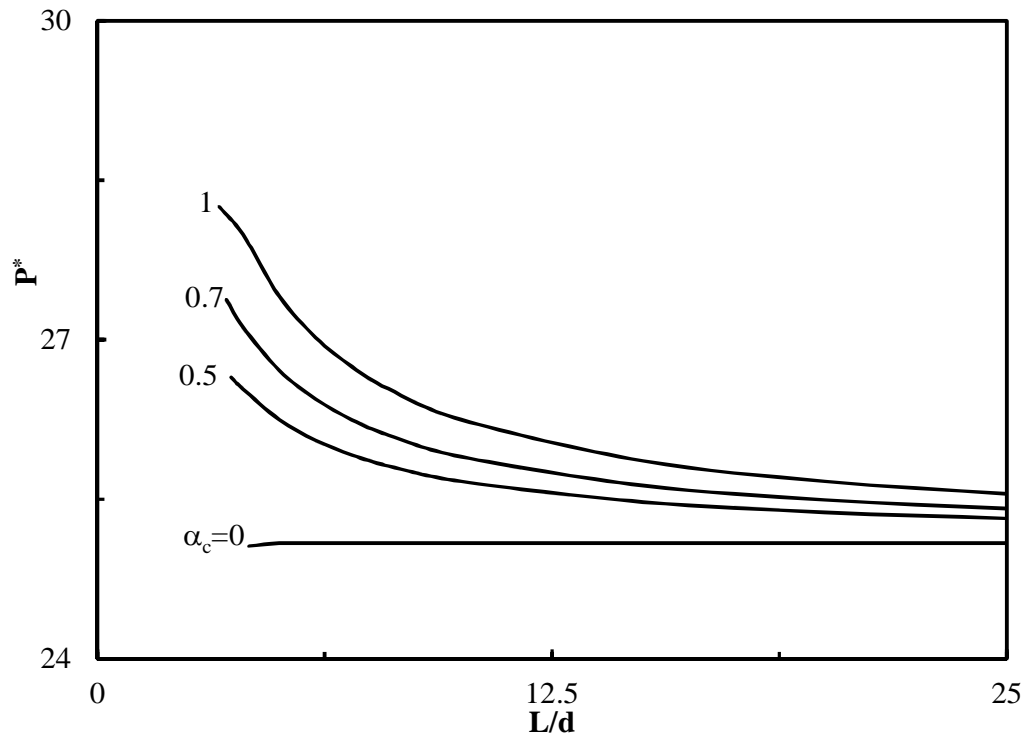


Fig. 18 Ultimate compressive capacity,  $P^*$  for GP vs  $L/d$ – Effect of  $\alpha_c$  for  $G/c_{u0} = 200$ ,  $\phi_{gp} = 35^\circ$  &  $\beta = 1.0$  in non-homogenous ground.

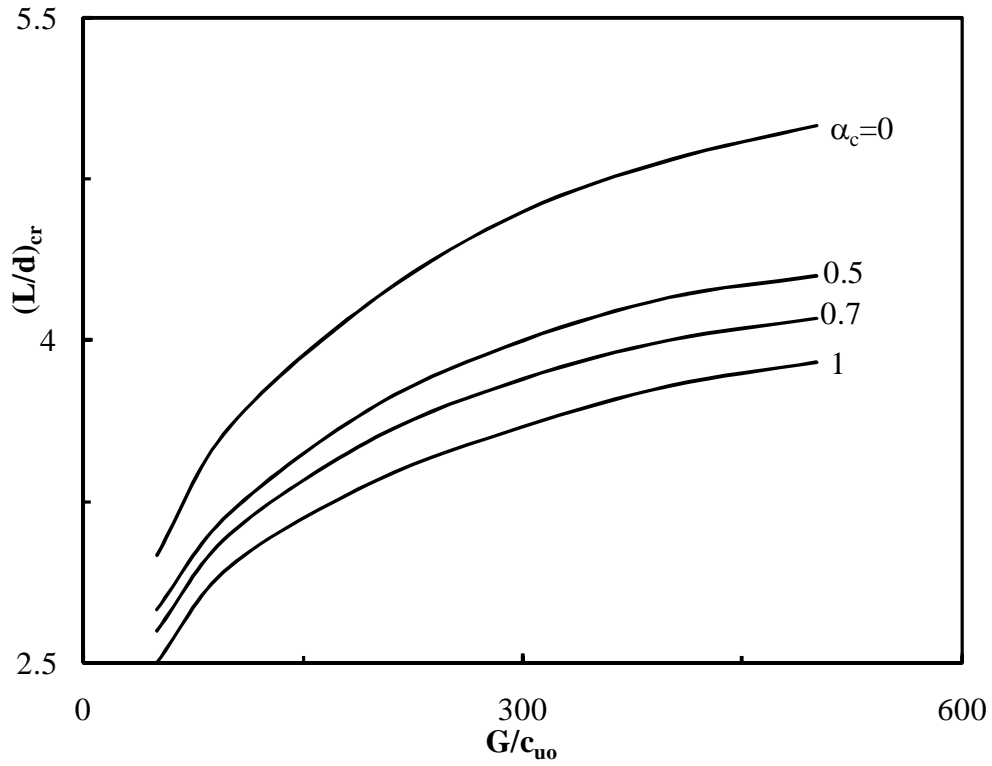


Fig. 19 Critical length,  $(L/d)_{cr}$  vs.  $G/c_{uo}$  for GP – Effect of  $\alpha_c$  for  $\phi_{gp} = 35^\circ$  &  $\beta = 1.0$  in non-homogenous ground.

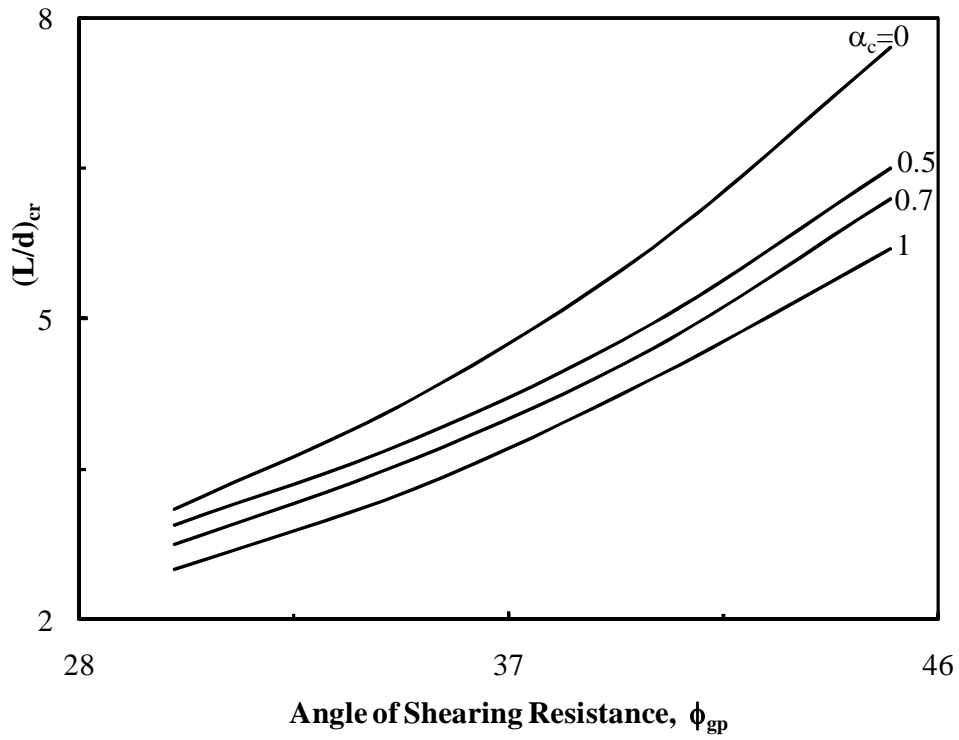


Fig. 20 Critical length,  $(L/d)_{cr}$  vs.  $\phi_{gp}$  for GP – Effect of  $\alpha_c$  for  $G/c_{uo}=200$  &  $\beta = 1.0$  in non-homogenous ground.

The effects of non-homogeneity parameter,  $\alpha_c$ , as effecting the variations of critical length,  $(L/d)_{cr}$  of GP with  $G/c_{u0}$  and  $\phi_{gp}$  are given in Figs. 19 and 20.

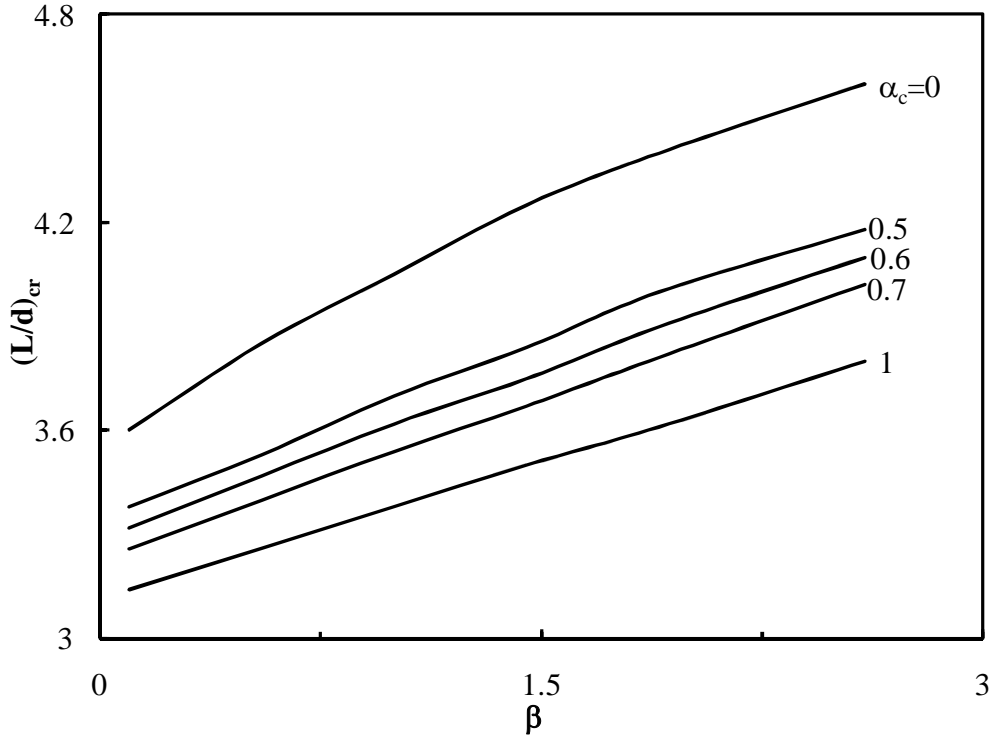


Fig. 21  $(L/d)_{cr}$  vs.  $\beta$  for GP—Effect of  $\alpha_c$  for  $G/c_{u0}=200$  &  $\phi_{gp}=35^\circ$  in non-homogenous ground.

Fig. 21 depicts the effect of non-homogeneity parameter,  $\alpha_c$  on the variation of  $(L/d)_{cr}$  for GP with  $\beta$  for  $G/c_{u0}=200$  &  $\phi_{gp}=35^\circ$ .

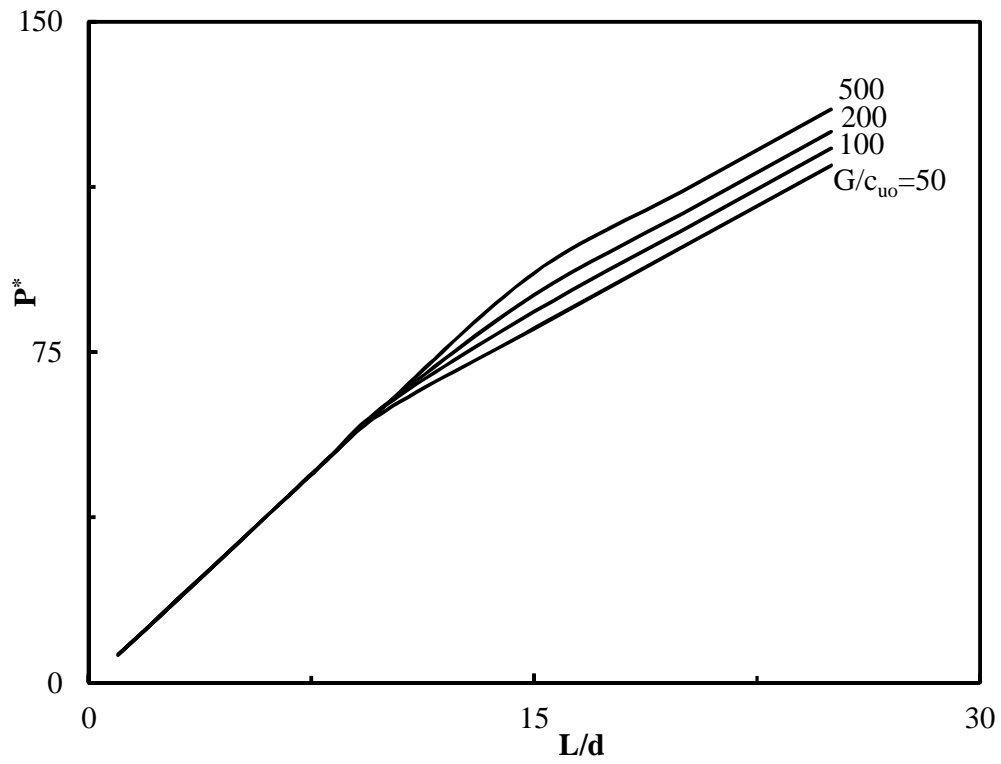


Fig. 22 Ultimate pullout capacity,  $P^*$  for GPA vs.  $L/d$  -Effect of  $G/c_u$  for  $\phi_{gp}=35^\circ$ ,  $\lambda=1.3$ ,  $\beta = 1.0$  &  $\alpha_c=0.5$  in non-homogenous ground.

Figs. 22 and 23 present the variations of ultimate pullout load of GPA with  $L/d$  for different  $G/c_u$  and  $\alpha_c$ .

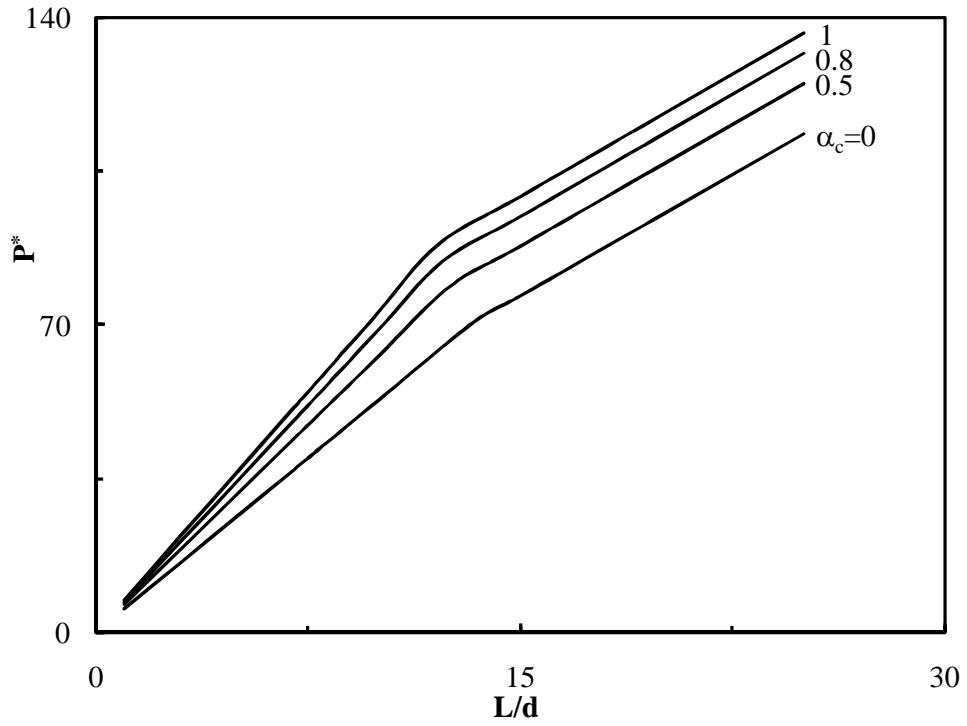


Fig. 23 Ultimate pullout capacity,  $P^*$  for GPA vs.  $L/d$ – Effect of  $\alpha_c$  for  $G/c_{u0}=200$ ,  $\varphi_{gp}=35^\circ$ ,  $\lambda=1.3$  &  $\beta = 1.0$  in non-homogenous ground.

Figs. 24 and 25 show variations of  $(L/d)_{cr}$  with  $(G/c_{u0})$  and  $\varphi_{gp}$  and show the effect of non-homogeneity parameter,  $\alpha_c$ .

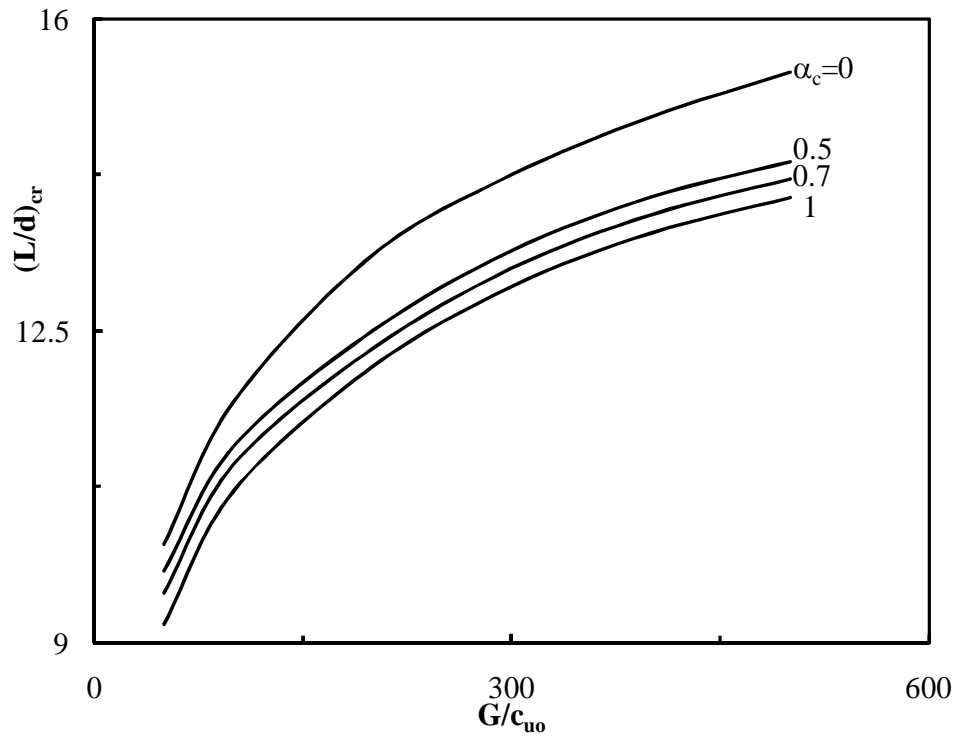


Fig. 24 Critical length,  $(L/d)_{cr}$  vs.  $G/c_{u0}$  for GPA – Effect of  $\alpha_c$  for  $\phi_{gp} = 35^\circ$ ,  $\lambda=1.3$  &  $\beta = 1.0$  in non-homogenous ground.

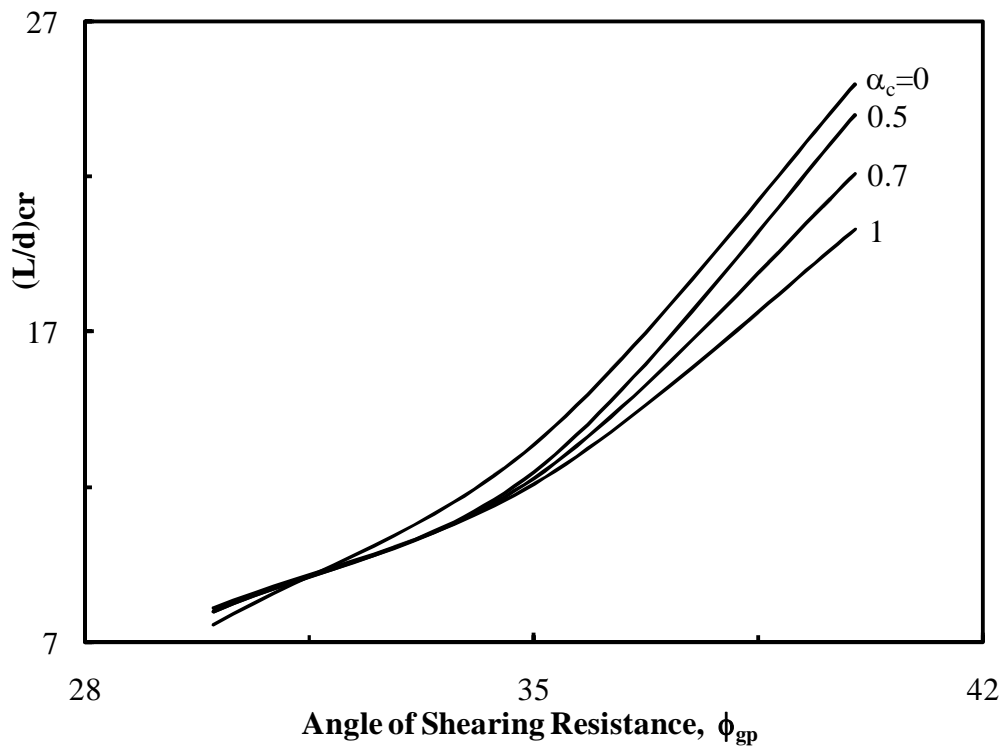


Fig. 25 Critical length,  $(L/d)_{cr}$  vs.  $\phi_{gp}$  for GPA—Effect of  $\alpha_c$  for  $G/c_{u0}=200$ ,  $\lambda=1.3$  &  $\beta = 1.0$  in non-homogenous ground.

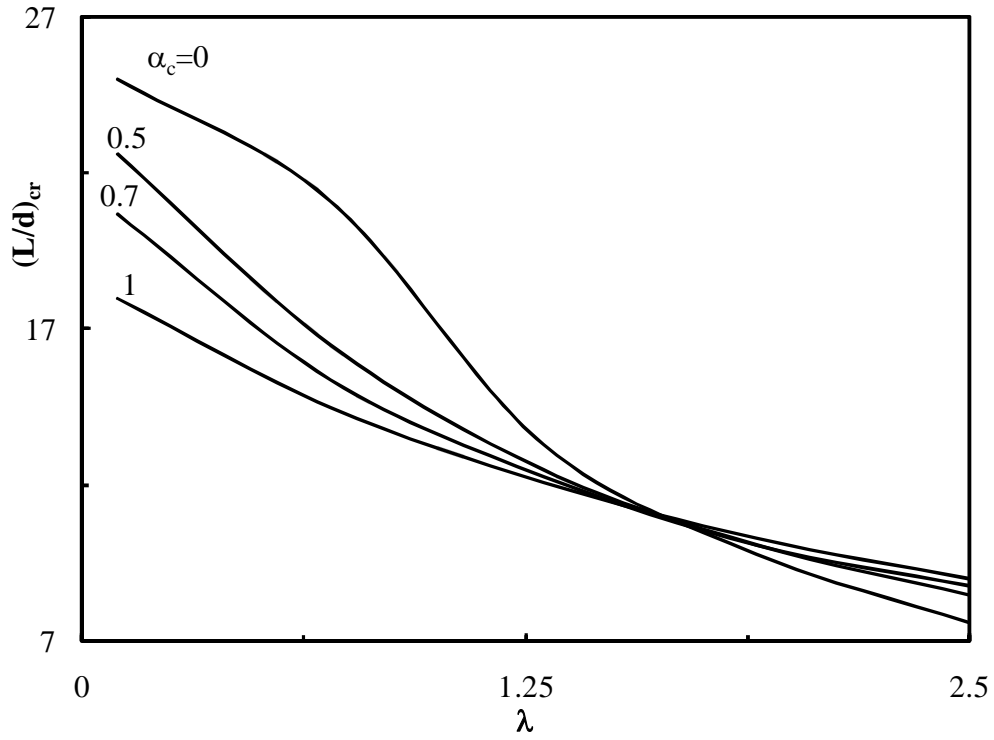


Fig. 26 Critical length,  $(L/d)_{cr}$  vs.  $\lambda$  for GPA –Effect of  $\alpha_c$  for  $G/c_{u0}=200$ ,  $\phi_{gp}=35^\circ$  &  $\beta=1.0$  in non-homogenous ground.

The variations of the critical length,  $(L/d)_{cr}$  of GPA with the parameters  $\lambda$  and  $\beta$  for different non-homogeneity parameter,  $\alpha_c$ , can be seen in Figs. 26 and 27 respectively.

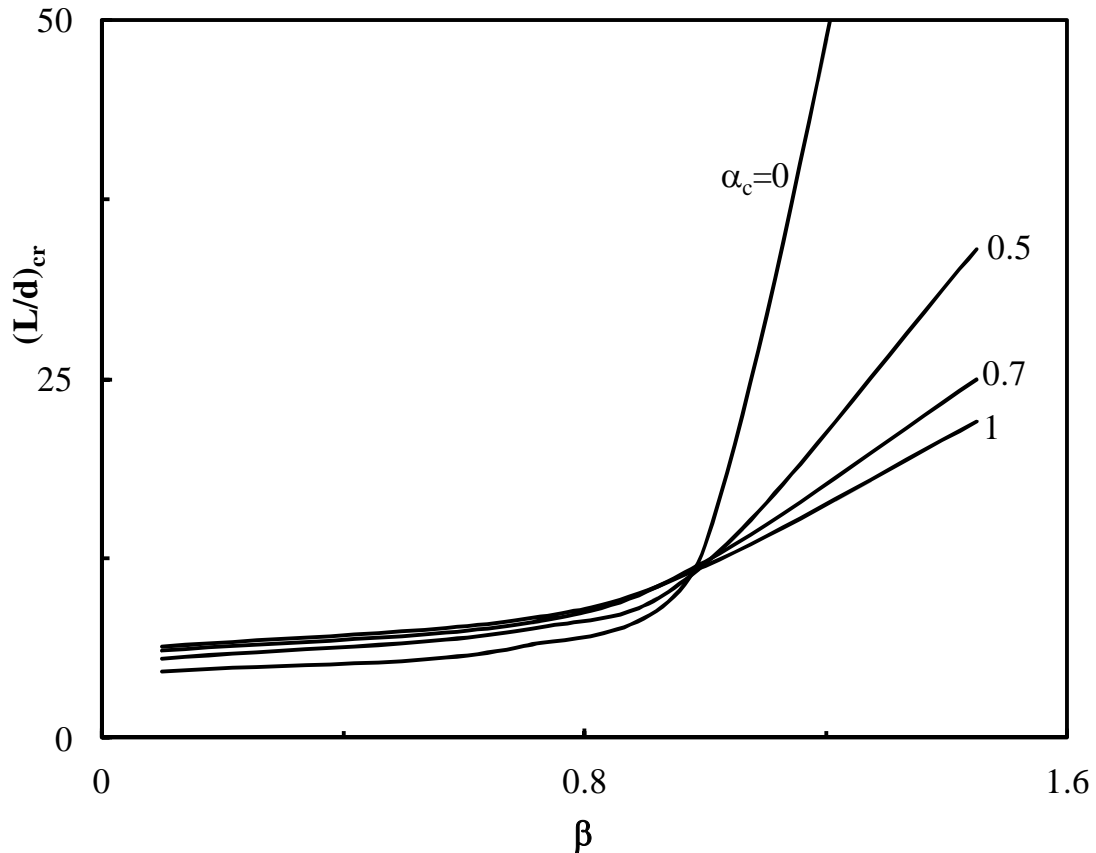


Fig. 27 Critical length,  $(L/d)_{cr}$  vs.  $\beta$  for GPA –Effect of  $\alpha_c$  for  $G/c_{uo} = 200$ ,  $\phi_{gp} = 35^\circ$  &  $\lambda = 1.3$  in non-homogenous ground.

#### 4. LOAD - DISPLACEMENT RESPONSE OF GP ANDGPA

Settlement of a granular pile under working loads is similar to that of incompressible floating pile in a half space, with correction for the effect of pile compressibility and is given (Poulos and Davis 1980) as

$$\rho = \frac{P \cdot I}{K_s \cdot d} \quad (13)$$

where  $I = I_o \cdot R_k \cdot R_h \cdot R_v$ ,  $\rho$  - settlement at top of GP,  $P$  - applied axial load,  $I_o$  - settlement influence factor for incompressible pile in semi-infinite mass, for  $\nu_s = 0.5$ ,  $R_k$  - correction factor for pile compressibility,  $R_h$  - correction factor for finite depth of layer on

a rigid base, and  $R_v$  - correction factor for soil Poisson's ratio,  $\nu_s$ . Plot of  $I_o$  is given in Fig. 28 while those for  $R_K$ ,  $R_b$ , and  $R_v$  in Figs. 29, 30 & 31.

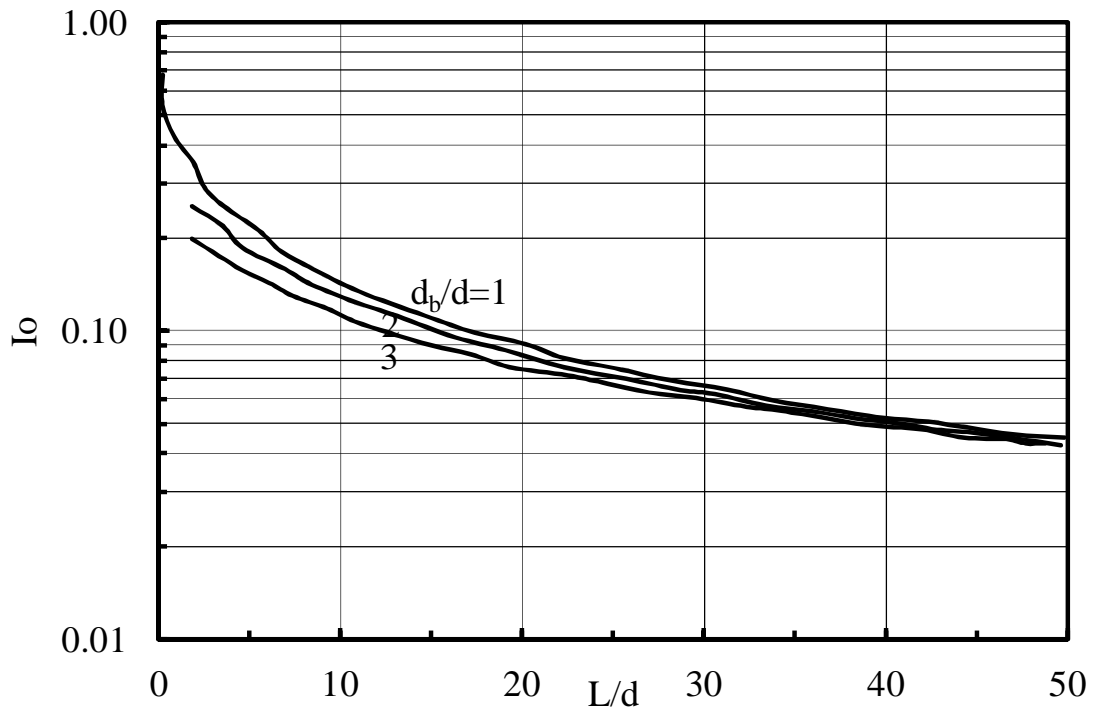


Fig. 28 Settlement Factor  $I_o$  for  $L/d=100$  and  $\nu_s=0.5$  for Incompressible Pile (Poulos and Davis, 1980)

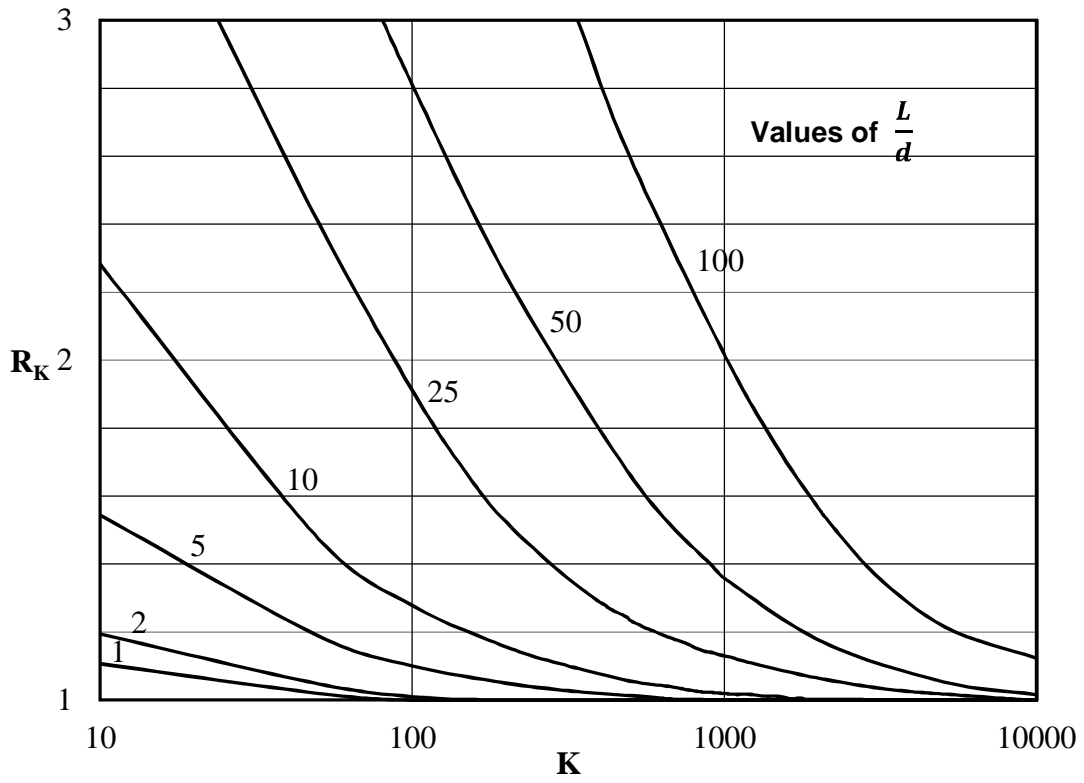


Fig. 29 Correction factor for compressibility,  $R_K$  for  $\nu_s=0.5$  (Poulos and Davis, 1980)

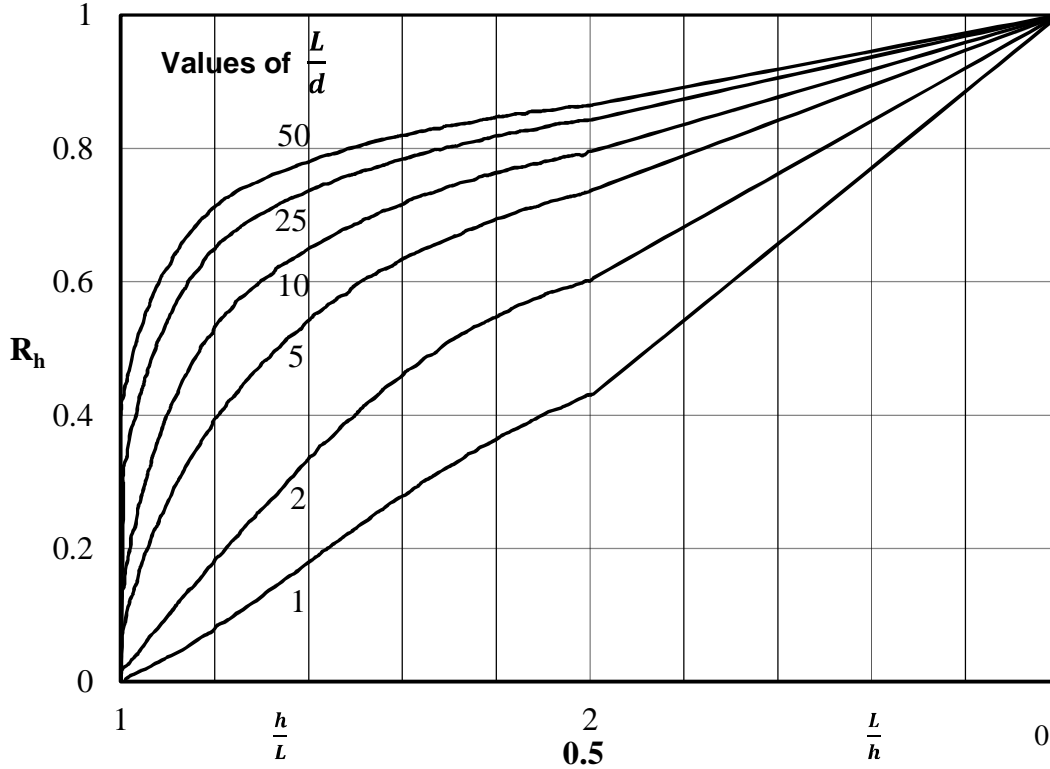


Fig. 30 Correction factor for Finite Layer,  $R_h$  (Poulos & Davis, 1980).

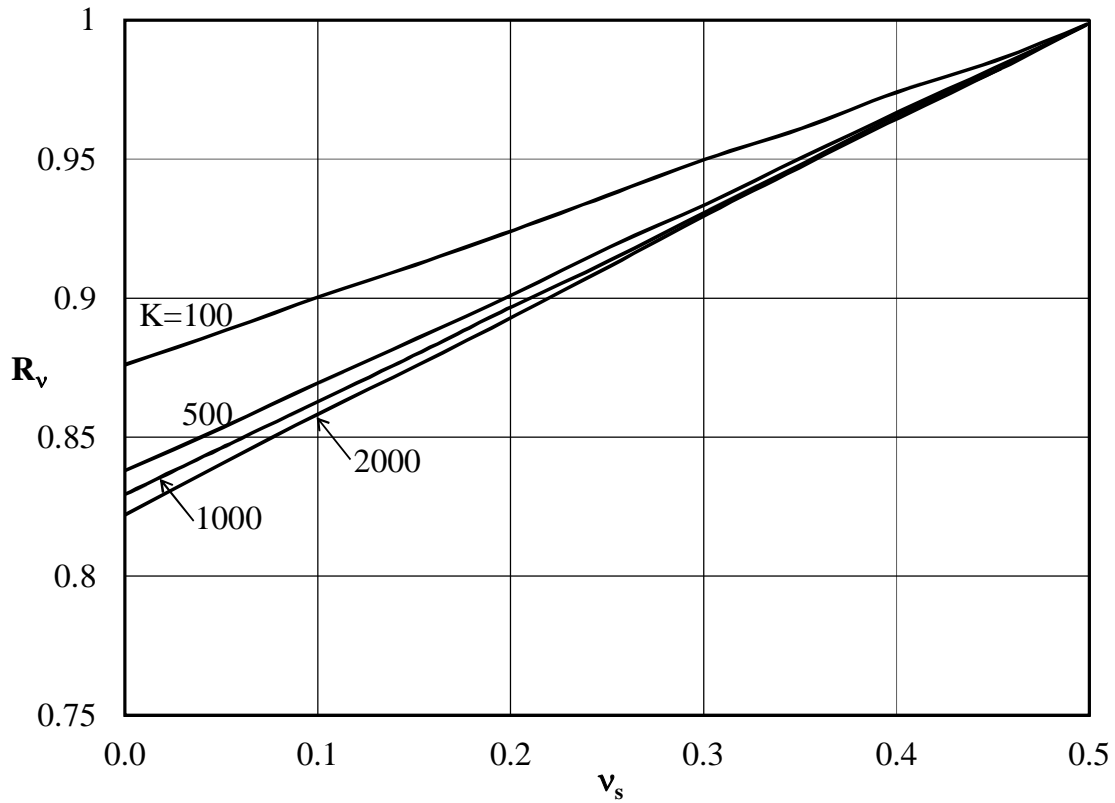


Fig. 31 Correction factor for Poisson's ratio,  $R_v$  (Poulos & Davis, 1980).

Displacements,  $\rho_u$ , of GPA under working loads are estimated in a similar manner as that for GP, i.e., treating it as a compressible pile subjected to pullout.

$$\rho_u = \frac{P \cdot I}{E_s \cdot d} \quad (14)$$

where  $P$  is the pullout load and  $I$  the influence coefficient for upward displacement. The top  $\rho_{u0}$  and tip displacements,  $\rho_{uL}$  are represented respectively by the displacement influence coefficients  $I_{U0}$  and  $I_{UL}$ .

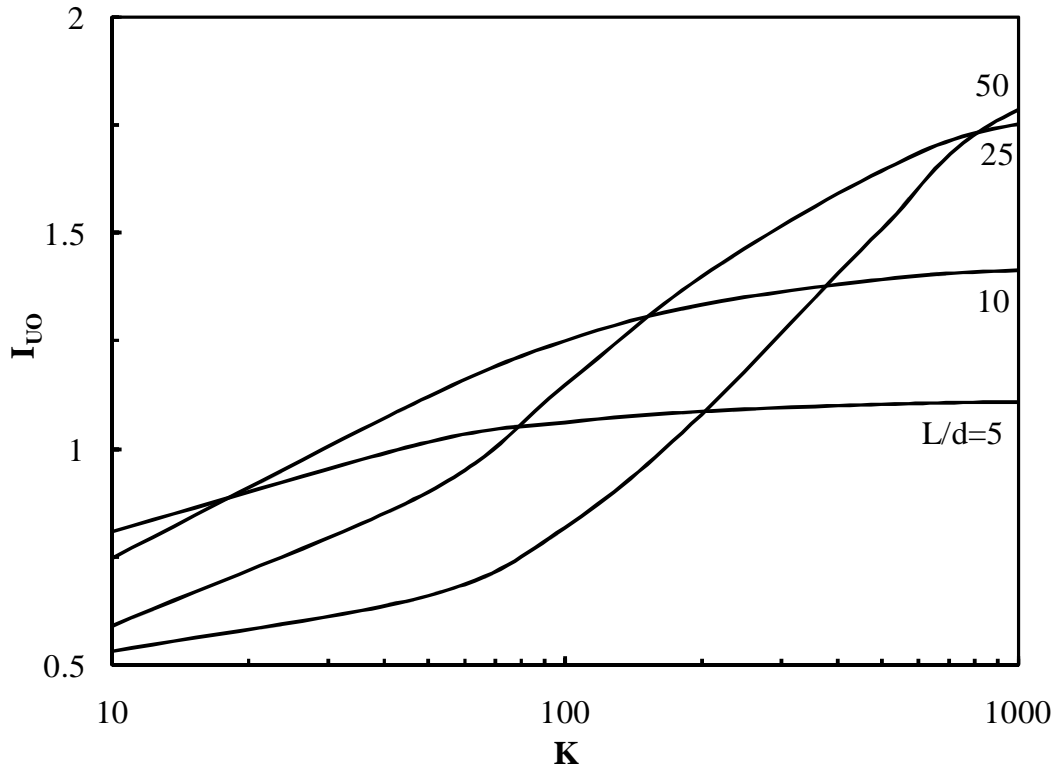


Fig. 32 Normalized tip displacement,  $I_{UO}$  vs.  $K$ , for  $v_s=0.5$  – Effect of  $K$ .

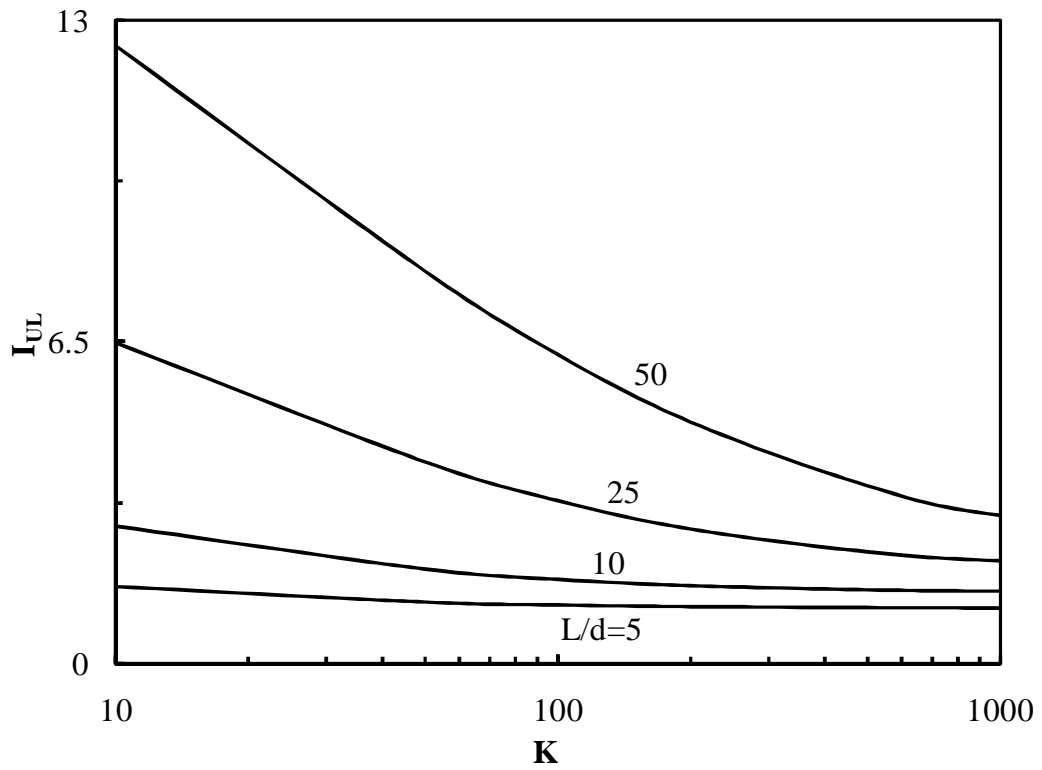


Fig. 33 Normalized top displacement,  $I_{UL}$ , vs.  $K$ , for  $v_s=0.5$  – Effect of  $L/d$ .

The variations of displacement influence coefficients of GPA at the tip,  $I_{UO}$  and at the top,  $I_{UL}$ , with relative pile stiffness,  $K$  for different  $L/d$  are given in Figs. 32 and 33.

## CONCLUSIONS

Solutions and results for the ultimate capacities of GP in compression and GPA in pullout are presented for homogenous (undrained shear strength constant with depth) and non-homogenous (undrained shear strength increasing linearly with depth) ground conditions. The ultimate capacities are reported as the lesser of the pile and bulging capacities. The ultimate capacities of GP and GPA are functions of granular pile and in-situ ground properties, viz., the unit weight,  $\gamma_{gp}$  and angle of shearing resistance,  $\phi_{gp}$  of granular pile material; and unit weight,  $\gamma_s$ , undrained strength,  $c_u$ , the rigidity modulus,  $G$  and the non-homogeneity strength parameter,  $\alpha_c$  of the soil.

Variations of ultimate capacities in GP and GPA with  $L/d$  are presented as functions of  $G/c_u$ ,  $\phi_{gp}$ , unit weight parameter,  $\lambda$  and lateral confinement pressure parameter,  $\beta$  for homogenous and non-homogeneous ground conditions. The transition from pile to bulging capacity with the  $L/d$  is termed as the critical length,  $(L/d)_{cr}$ . Variations of  $(L/d)_{cr}$  as functions of relevant parameters including the non-homogeneity strength parameter,  $\alpha_c$  are presented.

Displacements of GP and GPA are presented considering them as compressible pile, in situ soil to behave linearly and the in situ ground to be homogeneous. The elastic continuum approach of Poulos & Davis (1980) is extended to predict displacement responses of GP and GPA. The variations of normalized displacement influence coefficients with  $L/d$  and  $K$  are presented.

## REFERENCES

- Aboshi H., Ichimoto E., Enoki M. and Harda K. (1979).The Composer-A Method to Improve Characteristics of Soft Clays by Inclusion of Large Diameter Sand Columns. Proceedings of International Conference on Soil Reinforcement: Reinforced Earth and Other Techniques, Paris, Vol.1: pp. 211-216.
- Aboshi, H. and Suemastu N. (1985). The Sand Compaction Pile Method: State-of-The-Art-Paper. Proceedings of 3<sup>rd</sup> International Geotechnical Seminar on Soil Improvement Methods, Nanyang Technological Institution, Singapore.
- Barksdale R. D. and Bachus R. C. (1983).Design and Construction of Stone Columns. Report No. FHWA/RD-83/026, U. S. Department of Transportation, Federal Highway Administration, Washington, D. C., pp. 194.
- Datye K.R. and Nagaraju S.S. (1975).Installation and Testing of Rammed Stone Columns. Proceedings of Indian Geotechnical Society Specialty Sessions, 5<sup>th</sup> ARC on SMFE, Bangalore, pp. 101-104.
- Gibson R. E. and Anderson W. F. (1961).In Situ Measurement of Soil Properties with the Pressuremeter. Civil Engineering Publication Works Revision 56, pp. 615-618.
- Greenwood D.A. (1970).Mechanical Improvement of Soft Soils below Ground Surface. Proceedings of the Ground Engineering Conference, Institute of Civil Engineers, London, June 11-12, pp. 9-20.
- Hughes J.M.O. and Withers N.J. (1974). Reinforcing of Soft Cohesive Soils with Stone Columns. Ground Engineering Journal, Vol. 7, No. 3, pp. 42-49.
- Hughes J.M.O., Withers N.J. and Greenwood D.A. (1975). A Field Trial of the Reinforced Effect of Stone Column in Soil. Geotechnique, Vol. 25, No.1, pp. 31-44.
- Madhav, M.R. and Vitkar, P.P. (1978). Strip Footing on Weak Clay Stabilized with Granular Trench or Piles. Canadian Geotechnical Journal, Vol.15, No.2, pp. 605-609.
- Madhav M. R., Iyengar N. G. R., Vitkar P. P. and Nandi S. A. (1979). Increased Bearing Capacity and Reduced Settlements due to Inclusions in Soil. Symposium on Reinforcements of Soils, Paris, Vol. 2: pp. 329-333.
- Vesic A.S. (1975). Bearing Capacity of Shallow Foundations. Foundation Engineering Handbook, Van Nostrand Reinhold, pp. 121-144.

# **Guidelines for Soil Nailing Technique in Highway Engineering Applications**

Submitted to

**Technical Committee  
on Ground Improvement and geosynthetics  
Indian Geotechnical Society, New Delhi**

**Dr. GL Sivakumar Babu**  
Professor



**Department of Civil Engineering  
Indian Institute of Science, Bangalore – 560 012  
Karnataka, India**

**Date: November , 2015**

## PREFACE

This document provides interim guidelines for the analysis, design and construction of soil nail walls in highway engineering applications. Recommended guidelines are the outcome of the research carried out at Civil Engineering Department, Indian Institute of Science, Bangalore towards research project “*Guidelines for Soil Nailing Technique in Highway Engineering, Research Scheme (R-86)*” financially supported by Ministry of Shipping, Road Transport and Highways, Government of India New Delhi. Document is divided into 6 main sections addressing different issues related to soil nailing technique in the following manner:

Section 1: Provides a customary introduction to the soil nailing technique.

Section 2: Provides information and guidelines about methods of construction and selection of materials for soil nail walls.

Section 3: Discusses allowable stress design method based analysis of failure modes of soil nail walls and provide recommendations and methodology to evaluate factors of safety against various failure modes.

Section 4: Provides general steps and other considerations for the design soil nail walls.

Section 5: Illustrates step-by-step the design methodology for soil nail walls (discussed in sections 3 and 4) with the help of a design example.

Section 6: Provides procedures and requirements for conducting field pullout testing of soil nails.

Additionally, frequently required information regarding design of soil nail walls is presented in tabular form in Appendix A. A format for preparing database of typical soil nail wall project is also presented in Appendix B.

Recommendations of the Federal Highway Administration (FHWA 2003) report “*Geotechnical Engineering Circular No. 7: Soil Nail Walls*”, being an exhaustive and most prevalently used manual for soil nail walls in practice; has been appraised analytically and using finite element based rigorous computational tool and are suitably considered as the key reference in the preparation of these interim guidelines. It is believed that the document fulfills the requirements in professional works.

**GL Sivakumar Babu**

# CONTENTS

	<b>Page No.</b>
<i>Acknowledgments</i>	<i>ii</i>
<i>Preface</i>	<i>iii</i>
<i>Contents</i>	<i>iv</i>
<i>List of Tables</i>	<i>vii</i>
<i>List of Figures</i>	<i>viii</i>
<i>List of Symbols</i>	<i>ix</i>

## **SECTION 1: INTRODUCTION**

1.1 DEFINITION	01
1.2 ORIGIN	01
1.3 DESIGN METHODS	02
1.4 SOIL NAILING APPLICATIONS IN HIGHWAY ENGINEERING	02
1.5 ADVANTAGES AND LIMITATIONS	04
1.5.1 Advantages	04
1.5.2 Limitations	04

## **SECTION 2: CONSTRUCTION MATERIALS AND METHODS**

2.1 INTRODUCTION	05
2.2 SOIL NAIL INSTALLATION METHODS	05
2.3 COMPONENTS OF A TYPICAL SOIL NAIL WALL	05
2.4 CONSTRUCTION SEQUENCE	07
2.5 GEOTECHNICAL ASPECTS	09
2.5.1 Soil investigation	09
2.5.2 Bond strength	10
2.5.3 Suitable in-situ ground conditions	11

## **SECTION 3: ANALYSIS OF FAILURE MODES**

3.1 INTRODUCTION	12
3.2 FAILURE MODES OF SOIL NAIL WALLS	12
3.3 EXTERNAL FAILURE MODES	13
3.3.1 Global stability	13
3.3.2 Sliding Stability	16

3.3.3 Bearing capacity (or base heave) failure	18
3.4 INTERNAL FAILURE MODES	19
3.4.1 Soil nail pullout failure mode	20
3.4.2 Nail tensile strength failure mode	21
3.5 FACING DESIGN AND FAILURE MODES	21
3.5.1 Facings design procedure	22

## **SECTION 4: GENERAL DESIGN CONSIDERATIONS**

4.1 INTRODUCTION	29
4.2 GENERAL DESIGN STEPS	29
4.2.1 Initial soil nail wall considerations	29
4.2.2 Preliminary design	31
4.2.3 Final design	32
4.3 OTHER DESIGN CONSIDERATIONS	33
4.3.1 Loads and load combinations	33
4.3.2 Permissible soil nail wall deformations	33
4.3.3 Drainage measures	33
4.3.4 Corrosion protection	34

## **SECTION 5: DESIGN EXAMPLE**

5.1 INTRODUCTION	35
5.2 INITIAL DESIGN CONSIDERATIONS	35
5.3 PRELIMINARY DESIGN	36
5.4 FINAL DESIGN	38
5.4.1 EXTERNAL FAILURE MODES	38
5.4.1.1 Global stability	38
5.4.1.2 Sliding stability	40
5.4.1.3 Bearing capacity (or basal heave) failure	42
5.4.2 INTERNAL FAILURE MODES	42
5.4.2.1 Soil nail pullout failure	42
5.4.2.2 Soil nail tensile strength failure	42
5.4.3 FACING DESIGN AND CHECKS	44
5.4.4 GENERAL CONSIDERATIONS AND DESIGN SUMMARY	49
5.4.4.1 General considerations	49
5.4.4.2 Design summary	49

## **SECTION 6: FIELD PULLOUT TESTING OF SOIL NAILS**

6.1 INTRODUCTION	52
6.2 FIELD PULLOUT TEST APPARATUS	52
6.3 TYPES OF FIELD PULLOUT TESTS	53
6.3.1 Verification test	54
6.3.2 Proof test	54
6.3.3 Creep test	54
6.4 TEST PROCEDURE	55
6.4.1 Procedure for verification test	55
6.4.2 Procedure for proof test	56
6.5 TEST ACCEPTANCE CRITERIA	57
6.5.1 Acceptance criteria for verification test	57
6.5.2 Acceptance criteria for proof test	58
6.5.3 Acceptance criteria for creep test	58
6.6 TYPICAL TEST DATA SHEET	58
APPENDIX A: GENERAL DESIGN TABLES	60
APPENDIX B: TYPICAL SOIL NAIL WALL PROJECT SUMMARY	65

## LIST OF TABLES

<b>Table caption</b>	<b>Pg. No.</b>
Table 5.1 Desired minimum recommended factors of safety for permanent soil nail walls.	36
Table 5.2 Maximum axial tensile force developed in each nail from top.	37
Table 5.3 Allowable axial force carrying capacity of nails at different levels.	39
Table 5.4a Factor of safety against soil nail pullout failure (static case).	43
Table 5.4b Factor of safety against soil nail pullout failure (seismic case).	43
Table 5.5 Factor of safety against soil nail tensile strength failure.	44
Table 5.6 Summary of important design parameters.	50
Table 5.7 Summary of factors of safety attained for various failure modes.	50
Table 5.8 Summary of facing design (temporary and permanent).	50
Table 6.1 Loading schedule for verification test.	56
Table 6.2 Loading schedule for proof test.	57

## LIST OF FIGURES

<b>Figure caption</b>	<b>Pg. No.</b>
Fig. 1.1 Example applications of soil nail walls in highway engineering.	03
Fig. 2.1 Components of a typical soil nail wall (FHWA 2003).	06
Fig. 2.2 Typical construction sequence of soil nail walls (FHWA 2003).	08
Fig. 2.3 Soil investigation boring layout for soil nail walls (FHWA 2003).	10
Fig. 3.1 Principal failure modes of soil nail walls.	12
Fig. 3.2 Global stability of soil nail walls: (a) simplified single wedge failure mechanism; (b) forces acting on the failure plane.	13
Fig. 3.3 Failure wedge triangle.	15
Fig. 3.4 Sliding stability of soil nail walls.	17
Fig. 3.5 Excavation base heave failure for soil nail walls (FHWA 2003).	19
Fig. 3.6 Pullout failure of soil nails.	20
Fig. 3.7 Punching shear failure mode: Bearing plate connection used in temporary facing (FHWA 2003).	26
Fig. 3.8 Punching shear failure mode: Headed stud connection used in permanent facing (FHWA 2003).	26
Fig. 5.1 General outline of designed soil nail wall.	38
Fig. 5.2 Details of facing reinforcement.	51
Fig. 6.1 Field pullout test set up (FHWA 2003).	53
Fig. 6.2 Typical format of soil nail field pullout test data sheet.	59

## LIST OF SYMBOLS

$\Delta L_{\min}$	Minimum acceptable movement
$(L_P)_z$	Pullout (effective bond) length of nail at depth $z$
$(T)_z$	Axial tensile force in nail at depth $z$
$A_H$	Cross-sectional area of the stud head
$A_{SH}$	Cross-sectional area of the headed-stud shaft
$A_{st}$	Cross-sectional area of tensile reinforcement (i.e. nail)
$A_t$	Nail bar cross-sectional area
$a_{vm}, a_{hm}$	Reinforcement cross sectional area per unit width in the vertical and horizontal directions at the at mid-span
$a_{vn}, a_{hn}$	Reinforcement cross sectional areas per unit width in the vertical and horizontal directions at the nail head
$A_{vw}, A_{hw}$	Total cross sectional area of waler bars in the vertical and horizontal directions
$B'$	Width of influence in an excavation
$B_e$	Width of excavation
$B_L$	Base width of sliding failure surface
$c$	In-situ soil cohesion
$C_F$	Factor that considers the non-uniform soil pressures behind the facing
$D$	Maximum of $D_N$ and $D_{DH}$
$D'_c$	Effective diameter of assumed conical failure surface at the center of the section
$D_B$	Depth of strong deposit from bottom of excavation
$D_{DH}$	Grout (drill) hole diameter
$D_H$	Diameter of the stud head
$D_S$	Diameter of the headed-stud shaft
$DTL$	Design test load
$E$	Young's modulus of steel
$f_{ck}$	Characteristic yield strength of concrete
$F_h$	Horizontal seismic inertia force
$FS_{FF}$	Factor of safety against facing flexure failure
$FS_{FP}$	Factor of safety against facing punching failure
$FS_{FT}$	Factor of safety against facing tensile failure
$FS_G$	Factor of safety for global stability
$FS_H$	Factor of safety against excavation base heave (bearing capacity) failure
$FS_{HT}$	Factor of safety against headed-stud tensile failure
$FS_P$	Factor of safety against nail pullout failure
$FS_{SL}$	Factor of safety for sliding stability
$FS_T$	Factor of safety against nail tensile strength failure
$F_v$	Vertical seismic inertia force
$f_y$	Characteristic yield strength of steel

$h$	Temporary/permanent facing thickness
$H$	Vertical wall height
$H_1$	Effective height of soil mass that considers sloping ground
$h_c$	Effective depth of conical surface
$H_{eq}$	Equivalent wall height
$i$	Nail inclination with respect to horizontal
$K$	Active earth pressure coefficient
$K_A$	Static active earth pressure coefficient
$K_{AE}$	Seismic active earth pressure coefficient
$k_h$	Horizontal seismic coefficient
$k_v$	Vertical seismic coefficient
$L$	Length of soil nail
$L_1$	Length of top nail required to cross failure plane
$L_2$	Length of top nail required to satisfy pullout criterion
$L_B$	Soil nail bonded length (for load testing)
$L_{BP}$	Length of bearing plate
$L_e$	Length of excavation
$L_F$	Length of inclined failure surface
$L_P$	Pullout (effective bond) length
$L_S$	Headed-stud length
$N_c$	Bearing capacity factor
$N_F$	Normal force acting on the failure surface
$N_H$	Number of headed-studs in the connection
$P$	Maximum applied test load
$P$	Active lateral earth force
$P_A$	Active lateral earth force for static case
$P_{AE}$	Active lateral earth force for seismic case
$Q_{all}$	Allowable pullout resistance per unit length
$q_s$	Uniformly distributed surface loading
$Q_T$	Total surcharge load
$q_u$	Ultimate bond strength
$Q_u$	Ultimate pullout capacity per unit length
$R_{FP}$	Facing punching shear capacity
$R_{HT}$	Tensile failure of the headed-studs
$R_P$	Nail pullout resistance (capacity)
$R_T$	Nail bar tensile capacity
$S_F$	Shear force on failure surface
$S_h$	Horizontal nail spacing
$S_{HS}$	Headed-stud spacing
$S_u$	Undrained shear strength of fine grained soils
$S_v$	Vertical nail spacing

$S_{v1}$	Vertical spacing of first nail (topmost nail)
$T_1$	Axial tensile force in first nail (topmost nail)
$T_{all}$	Allowable axial tensile nail force
$T_{eq}$	Equivalent axial tensile nail force
$t_H$	Headed-stud head thickness
$T_{max}$	Maximum axial tensile nail force
$T_o$	Axial tensile nail force at nail head
$t_p$	Thickness of bearing plate
UL	unbonded length of nail (test)
W	Weight of rigid failure block ABC
z	Arbitrary depth measured from ground surface
$\alpha$	Wall face batter angle (from vertical)
$\beta$	Backslope angle
$\beta_{eq}$	Equivalent backslope angle
$\gamma$	In-situ soil unit weight
$\Delta H$	Slope rise up to bench (if present)
$\Delta H$	Equivalent overburden
$\rho$	Provided reinforcement ratio
$\rho_{max}$	Maximum limit of reinforcement ratio
$\rho_{min}$	Minimum limit of reinforcement ratio
$\Sigma D$	Sum of driving forces along failure plane
$\Sigma R$	Sum of resisting forces along failure plane
$\phi$	In-situ soil angle of internal friction
$\psi$	Inclination of failure plane
$\omega$	An angle relating the horizontal and vertical seismic coefficients

## **SECTION 1: INTRODUCTION**

### **1.1 DEFINITION**

Soil nailing is an innovative earth retaining technique. It is innovative in the sense that, unlike other earth retaining techniques, such as conventional retaining walls and geosynthetic reinforced slopes, its construction proceeds from the top to bottom with reinforced soil being in-situ. In principle, soil nailing consists of the passive reinforcement of existing ground by installing closely spaced steel bars (i.e. nails), which may be subsequently encased in grout. A shotcrete facing is then applied at the wall face to provide continuity. This ground support technique relies on the mobilization of the tensile strength of the steel reinforcement at relatively small deformations in the surrounding ground. In a soil nail wall, the properties and material behaviour of three components—the native soil, the reinforcement (nails) and the facing element—and their mutual interactions significantly affect the performance of the structure. Additionally, various other factors such as the construction sequence, the installation method of nails, the connection between the nails and the facing are also likely to influence the behaviour of soil nail walls.

### **1.2 ORIGIN**

The origin of soil nailing can be traced since 1960s when it was used as a support system for underground excavations in rock referred to as the New Austrian Tunneling Method. Since then, soil nailing technique has been widely utilised for various slope stability applications in developed countries like USA, France, UK, etc. In India, over the last decade, soil nailing technique has been considerably used for the applications such as, stabilization of road/rail side slopes, basement excavations, additional support for bridge abutments and side walls of the approaches for subways.

### **1.3 DESIGN METHODS**

Since its inception, various analysis approaches such as: limit equilibrium analysis, multi-criteria analysis, kinematical limit analysis, strain compatibility analysis, discrete element analysis, nonlinear programming and finite element analysis have been developed to study behaviour of soil nail walls. However, for practical purposes, the available analysis and design methods for soil nail walls can be broadly classified into two main categories:

- (a) *Limit equilibrium design* methods, which are used to evaluate the global safety factor of the nailed structures with respect to a rotational or translational failure along potential sliding surfaces, taking into account the shearing, tension, or pull-out resistance of the inclusions crossing the potential failure surface.
- (b) *Working stress design* methods which are used to estimate the tension and shear forces generated in the nails during construction under the design loading conditions and evaluate the local stability at each level of nails.

Limit equilibrium based methods have attracted the attention of the researchers because of their simplicity, reasonable accuracy and popularity among the practicing engineers. The main shortcoming of limit equilibrium based methods is that they fail to address deformation behaviour of soil nail walls adequately. Deformation estimates are generally obtained empirical relations based on the past experiences. Rigorous computational tools based on numerical techniques such as: finite element and finite difference methods are often employed to study overall stability and deformation estimates of soil nail walls. In this document, allowable stress design method (ASD) for the analysis and design of soil nail structures is used and recommended.

### **1.4 SOIL NAILING APPLICATIONS IN HIGHWAY ENGINEERING**

Soil nail walls are particularly well suited to excavation applications for ground conditions that require vertical or near-vertical cuts. Soil nail walls have been used

successfully in highway cuts; end slope removal under existing bridge abutments during underpass widening; for the repair, stabilization, and reconstruction of existing retaining structures; and tunnel portals. Some of the example applications of soil nail walls in highway engineering are shown in **Fig. 1.1**.



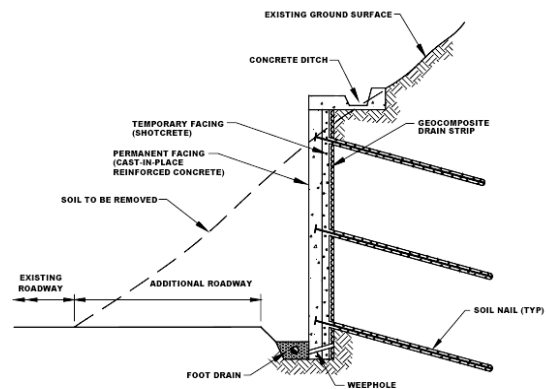
**(a) Roadside slope**



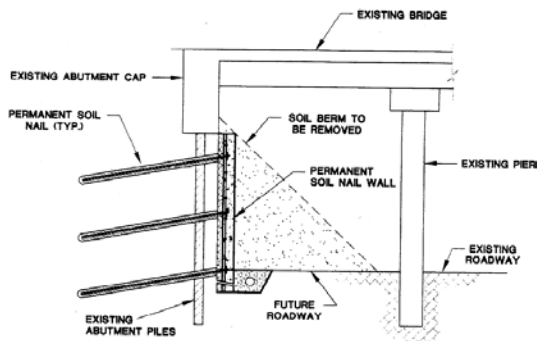
**(b) Approaches to subway**



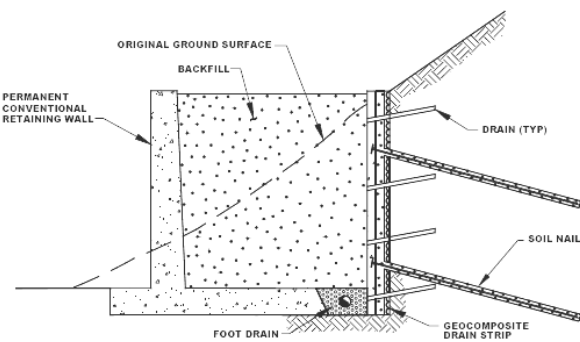
**(c) Bridge abutment**



**(d) Highway widening**



**(e) Widening under existing bridge**



**(f) Temporary shoring**

**Fig. 1.1** Example applications of soil nail walls in highway engineering.

## **1.5 ADVANTAGES AND LIMITATIONS**

### **1.5.1 Advantages**

Soil nail walls exhibit numerous advantages when compared to ground anchors and alternative top down construction techniques. Soil nailing is less disruptive to traffic and causes less environmental impact, require smaller right-of-way, relatively flexible and can accommodate relatively large total and differential settlements. Soil nail walls have performed well during seismic events owing to overall system flexibility; and are more economical than conventional concrete gravity walls when conventional soil nailing construction procedures are used.

### **1.5.2 Limitations**

Soil nail walls may not be appropriate for applications where very strict deformation control is required for structures and utilities located behind the proposed wall, as the system requires some soil deformation to mobilize resistance. Also, occurrence of utilities may place restrictions on the location, inclination, and length of soil nails in the upper rows. Soil nail walls are not well-suited where large amounts of groundwater seep into the excavation because of the requirement to maintain a temporary unsupported excavation face. Moreover, construction of soil nail walls requires specialized and experienced contractors.

## **SECTION 2: CONSTRUCTION MATERIALS AND METHODS**

### **2.1 INTRODUCTION**

Various aspects such as: basic elements of the typical soil nail wall; construction methodology; construction materials; extent of geotechnical investigation and favorable conditions have been presented in the subsequent sections.

### **2.2 SOIL NAIL INSTALLATION METHODS**

Two most prevalently used soil nail installation techniques in practice are: (i) drilled and grouted soil nails and (ii) driven soil nails.

Drilled and grouted soil nails, also known as grouted nails, are approximately 100 mm to 200 mm diameter nail holes drilled in the soil mass to be retained, typically, at a spacing of about 1.5 m apart. Steel bars are then placed and the holes are grouted. Grouted nails can be used for both temporary and permanent applications. On the other hand, driven soil nails are relatively small in diameter (20 mm to 25 mm) and are mechanically driven into the ground. They are usually spaced approximately 0.5 m to 1.0 m apart. The use of driven soil nails allows for a faster installation (as compared to drilled and grouted soil nails); however, this method of installation cannot provide good corrosion protection other than by sacrificial bar thickness.

Grouted nails are recommended for all types of soil nail walls applications; and in particular, for walls with vertical height more than 5 m. Driven nails shall only be used for temporary excavation support purposes, and when wall heights are smaller (less than or upto 5.0 m).

### **2.3 COMPONENTS OF A TYPICAL SOIL NAIL WALL**

Various components of a typical soil nail wall are shown in **Fig. 2.1**.

**(a) Nail bars:** Threaded solid or hollow steel reinforcing bars are commonly used for soil nails. Bars generally have a nominal tensile strength of 415 MPa or higher. Minimum recommended diameter of reinforcement bar (tendon) is 20 mm.

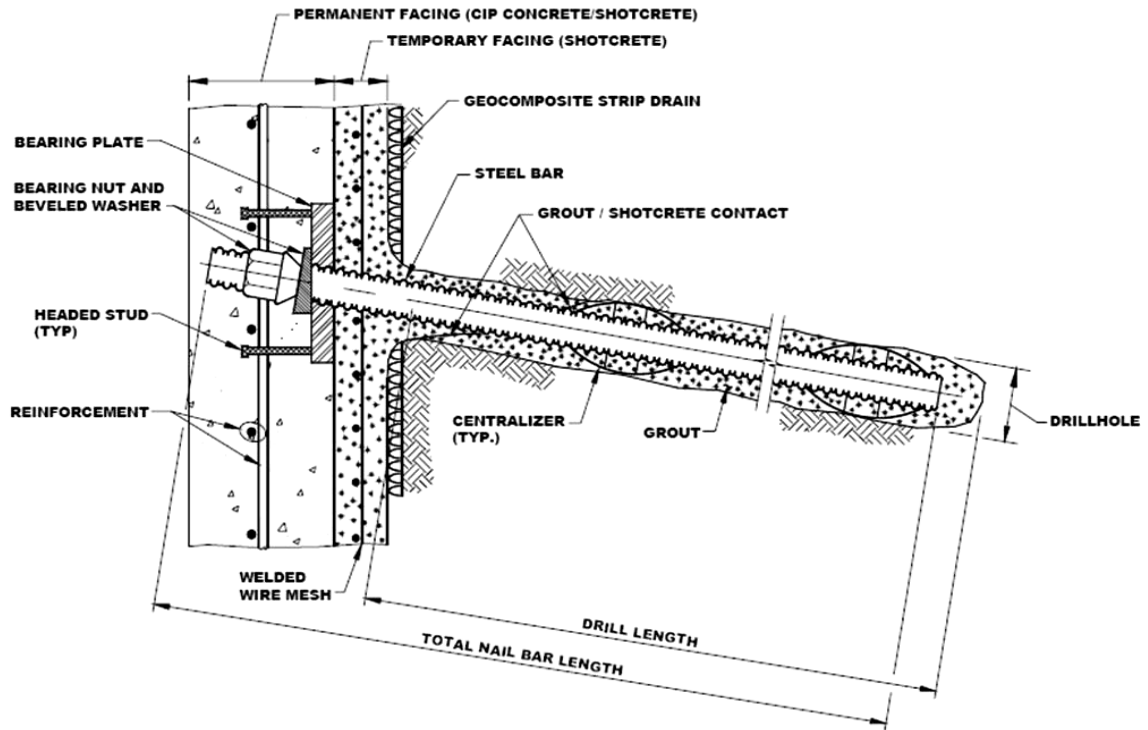


**Fig. 2.1** Components of a typical soil nail wall (FHWA 2003).

**(b) Nail head:** The nail head comprises of following main components: the bearing-plate, hex nut, and washers; and the headed-stud (*see Fig. 2.1*). The bearing plate is made of Grade 250 MPa steel and is typically square, 200 to 250 mm side dimension and 19 mm thick. The purpose of the bearing plate is to distribute the force at the nail end to the temporary shotcrete facing and the ground behind the facing. The bearing plate has a central hole, which is inserted over the nail bar. Beveled washers are then placed and the nail bar is secured with a hex nut or with a spherical seat nut. Washers and nuts are steel with a grade consistent with that of the nail bar commonly of 415 MPa or higher. Nuts are tightened with a hand-wrench. The headed-stud connection may

consist of four headed studs that are welded near the four corners of the bearing plate to provide anchorage of the nail head into the permanent facing. For temporary walls, the bearing plate is on the outside face of the shotcrete facing.

- (c) **Grout:** Grout for soil nails is required to fill the annular space between the nail bar and the surrounding ground, and for shotcreting of the temporary facing. Grout for soil nail walls is commonly a neat cement grout with the water/cement ratio typically ranging from 0.4 to 0.5. Grout mix shall be prepared in accordance with IS: 9012 – 1978 “*Recommended practice for shotcreting*”. Grout shall have a minimum 28 days characteristic strength of 20 MPa. For filling up nail holes, grout shall be pumped shortly after the nail bar is placed in the drillhole to reduce the potential for hole squeezing or caving. In solid nail bar applications, the grout may be injected by tremie methods through a grout pipe, which is previously inserted to the bottom of the drillhole, until the grout completely fills the drillhole.
- (d) **Centralizers:** Centralizers are devices made of polyvinyl chloride (PVC) or other synthetic materials that are installed at various locations along the length of each nail bar to ensure that a minimum thickness of grout completely covers the nail bar. They are installed at regular intervals, typically not exceeding 2.5 m, along the length of the nail and at a distance of about 0.5 m from each end of the nail.
- (d) **Other components:** Other main component of soil nail wall includes corrosion protection elements; wall facings and drainage system (*see Sections 3 and 4* for details).

## 2.4 CONSTRUCTION SEQUENCE

Typical sequence of construction of a soil nail wall include following steps as shown in

**Fig. 2.2:**

Step 1: Excavation of initial cut;

Step 2: Drilling hole for nail;

Step 3: Installation of nails followed by grouting and placing of drainage strip;

Step 4: Placing of construction facing and installation of bearing plates;

Step 5: Repetition of process till final level is reached; and

Step 6: Placing of final facing.

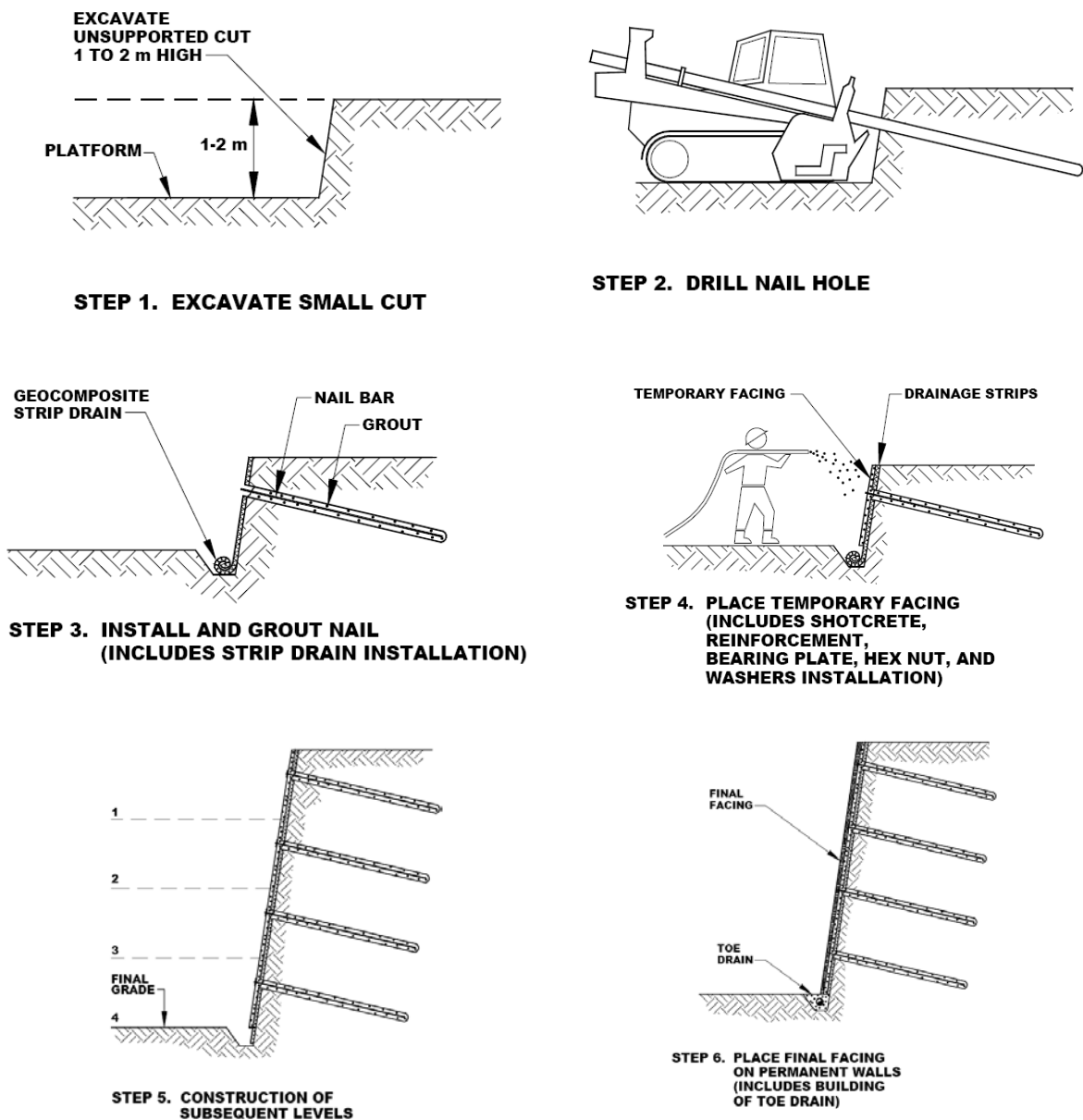


Fig. 2.2 Typical construction sequence of soil nail walls (FHWA 2003).

## 2.5 GEOTECHNICAL ASPECTS

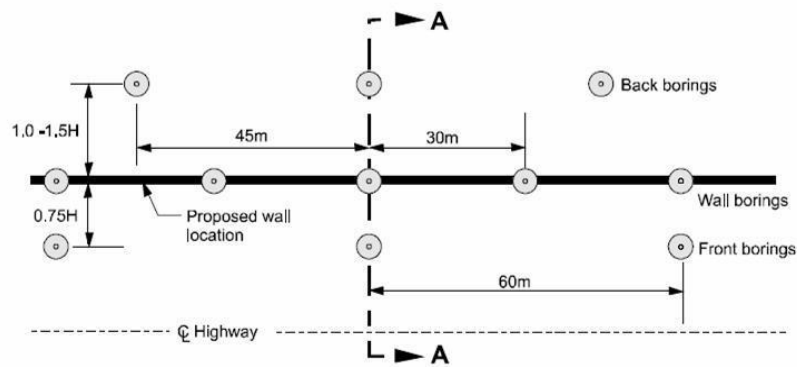
### 2.5.1 Soil investigation

Exploratory borings shall be performed for the design of soil nail walls to obtain: (1) SPT N-values to classify soil and delineate the stratigraphy, (2) both disturbed and undisturbed soil samples for laboratory soil testing, and (3) observations of groundwater. Laboratory testing of soil samples collected during borings enable judicious selection of soil parameters for the design of soil nail walls. **Fig. 2.3** can be used as a preliminary guide to help designers plan the number, location, and frequency of borings for soil nail wall applications.

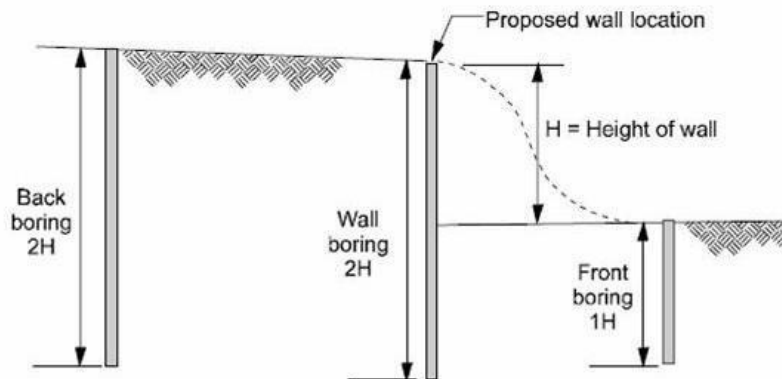
For soil nail walls more than 30 m long, borings should be spaced between 30 to 60 m along the proposed centerline of the wall. For walls less than 30 m long, at least one boring is necessary along the proposed centerline of the wall. Borings are also necessary in front and behind the proposed wall. Borings behind the wall should be located within a distance up to 1 to 1.5 times the height of the wall behind the wall and should be spaced up to 45 m along the wall alignment. If the ground behind the proposed wall is sloping, the potentially sliding mass behind the wall is expected to be larger than for horizontal ground. Therefore, borings behind the proposed wall should be located farther behind the wall, up to approximately 1.5 to 2 times the wall height. Borings in front of the wall should be located within a distance up to 0.75 times the wall height in front of the wall and should be spaced up to 60 m along the wall alignment.

The depth of borings should extend at least one full wall height below the bottom of the excavation (*see Fig. 2.3*). Borings should be deeper when highly compressible soils (i.e., soft to very soft fine-grained soils, organic silt, and peat) occur at the site behind or under the proposed soil nail wall. The required boring depths for soil nail wall projects may be greater if deep loose, saturated, cohesionless soils occur behind and under the

proposed soil nail wall and the seismic risk at the site require that the liquefaction potential be evaluated. The subsurface investigation depths may need to be deep at proposed sites of soil nail walls where seismic amplification is of concern, particularly in deep, soft soils. If rock is encountered within the selected depth, a core at least 3 m long retrieved in two 1.5 m long runs should be obtained to inspect the nature of the rock and its discontinuities.



(a) Typical plan (distances shown are recommended maximum)



(b) Section A-A

**Fig. 2.3** Soil investigation boring layout for soil nail walls (FHWA 2003).

### 2.5.2 Bond strength

Bond strength of the nail-soil interface is an extremely important parameter required for the design, analysis and performance assessment of soil nail walls. The pullout capacity of a soil nail installed in a grouted nail hole is affected by the size of the nail (i.e., perimeter and length) and the ultimate bond strength  $q_u$ . The bond strength is the

mobilized shear resistance along the soil-grout interface. For drilled and grouted nails, the bond strength is a function of ground conditions around the nail (i.e. soil type and conditions); soil nail installation type including drilling method, grouting procedure, grout nature, grout injection (e.g. gravity or under pressure); and the size of the grouted zone.

The bond strength adopted for the design of soil nails is commonly based on conservative estimates obtained from field correlation studies and local experience in similar conditions. Consequently, some percentage of the soil nails shall be load tested (pullout tests) in the field to verify bond strength design. Procedure for conducting field pullout tests on soil nails is described in **Section 6**. As a preliminary estimate bond strength for various soil conditions and construction methods based on the literature may be adopted from **Table A.2** of Appendix A.

### **2.5.3 Suitable in-situ ground conditions**

Following are the in-situ conditions considered favorable for the prospective use of soil nailing technique.

- (a) Soil shall be able to stand unsupported to a depth of about 1 m – 2 m high vertical or nearly vertical cut for 24-48 hours.
- (b) Groundwater table shall be sufficiently below level of the lowermost soil nail at all cross-sections.
- (c) Favorable soils: Stiff to hard fine –grained soils, dense to very dense granular soils with some apparent cohesion, weathered rock with no weakness planes and glacial soils.

## SECTION 3: ANALYSIS OF FAILURE MODES

### 3.1 INTRODUCTION

Allowable stress design (ASD) methodology is recommended for the analysis of potential failure modes of soil nail walls. Governing equations for the analysis and design of soil nail walls in consideration of each potential failure mode have been described for the most general case, and hence, designer may suitably simplify the governing equations to suit project specific conditions. Design example presented in **Section 5** may be referred for better understanding.

### 3.2 FAILURE MODES OF SOIL NAIL WALLS

Failure modes of soil nail walls can be broadly classified into three distinct groups as external, internal and facing failure modes (*see Fig. 3.1*). Recommended minimum factors of safety for the design of soil nail walls using ASD method are presented in **Table A.1**.

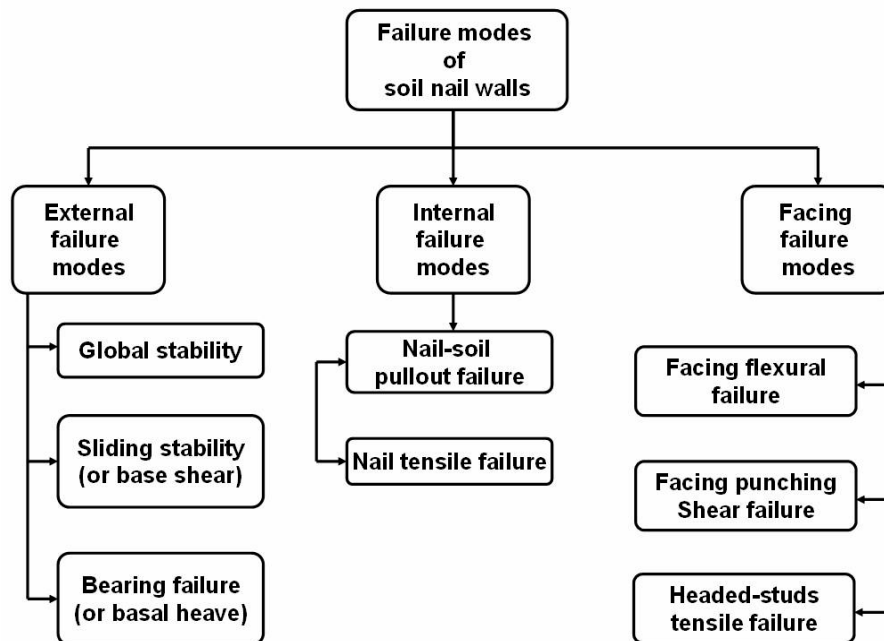


**Fig. 3.1** Principal failure modes of soil nail walls.

### 3.3 EXTERNAL FAILURE MODES

#### 3.3.1 Global stability

Global stability of the soil nail walls refers to the overall stability of the reinforced soil nail wall mass. In this failure mode, along the slip surface (i.e. potential failure plane), the driving force due the self weight and external loading on the retained mass exceeds the resisting force provided by the in-situ soil and the nails.

##### Simplified global stability analysis

Global stability analysis for soil nail walls can be carried out using a simple, single wedge failure mechanism (see **Fig. 3.2**) with failure plane assumed to be inclined at an angle  $\psi = 45 + (\phi/2)$  (in degrees) with respect to the horizontal. The factor of safety for global stability  $FS_G$  is expressed as the ratio of the resisting forces  $\Sigma R$  and driving forces  $\Sigma D$ , which acts tangentially to the potential failure plane:

$$FS_G = \frac{\sum R}{\sum D} \quad (3.1)$$

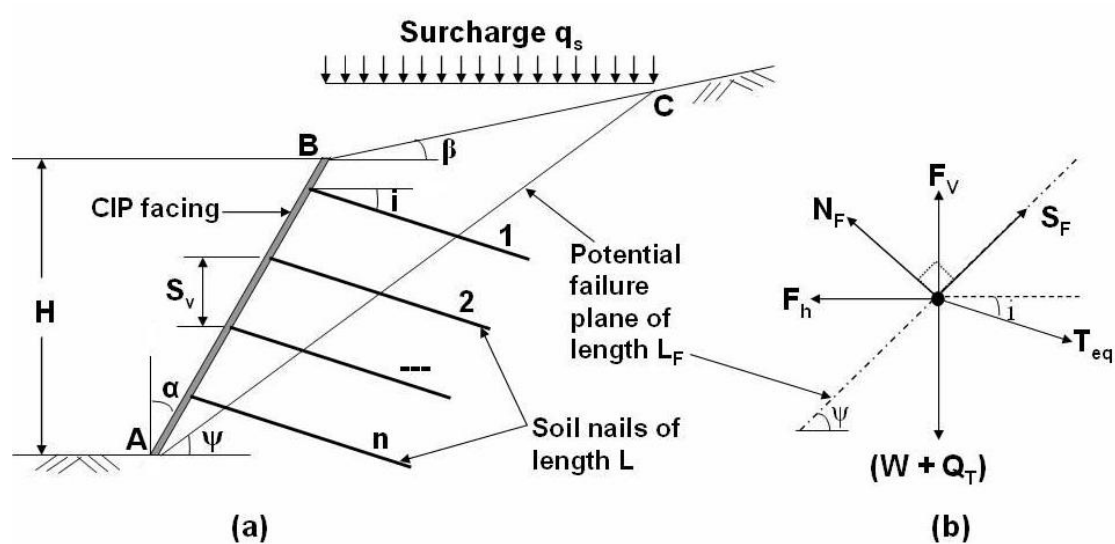


**Fig. 3.2** Global stability of soil nail walls: (a) simplified single wedge failure mechanism; (b) forces acting on the failure plane.

Considering the equilibrium of forces (*see Fig. 3.2b*) acting along the failure plane and rearranging the terms, factor of safety for global stability  $FS_G$  can be determined as

$$FS_G = \frac{cL_F + T_{eq} \cos(\psi - i) + [(W + Q_T - F_v) \cos \psi + T_{eq} \sin(\psi - i) - F_h \sin \psi] \tan \phi}{(W + Q_T - F_v) \sin \psi + F_h \cos \psi} \quad (3.2)$$

where:  $c$  [kPa] = in-situ soil cohesion;

$\phi$  [degrees] = in-situ soil angle of internal friction;

$i$  [degrees] = nail declination with respect to horizontal;

$\alpha$  [degrees] = wall face batter with respect to vertical;

$\beta$  [degrees] = backslope angle with respect to horizontal;

$H$  [m] = vertical height of the soil nail wall;

$$L_F \text{ [m]} = \frac{H \cos(\alpha + \beta)}{\cos \alpha \sin(\psi - \beta)} = \text{length of the potential failure plane;}$$

$$Q_T \text{ [kN/m]} = \frac{q_s H \cos(\psi + \alpha)}{\cos \alpha \sin(\psi - \beta)} = \text{total surcharge load; and}$$

$q_s$  [kPa] = distributed surcharge loading.

*Determination of weight of failure wedge, W*

Using sine rule for  $\Delta ABC$  (*see Fig. 3.2a and Fig. 3.3*), we get

$$\frac{a}{\cos(\psi + \alpha)} = \frac{b}{\cos(\alpha + \beta)} = \frac{c}{\sin(\psi - \beta)} \quad (3.3)$$

Using Hero's formula

$$\text{Area of } \Delta ABC = \sqrt{s(s-a)(s-b)(s-c)} \quad \text{where } s = (a+b+c)/2 \quad (3.4)$$

$$\text{Therefore, weight of failure wedge, } W \text{ [kN/m]} = \gamma \times \Delta ABC \quad (3.5)$$

where:  $\gamma$  [kN/m<sup>3</sup>] = in-situ soil unit weight.

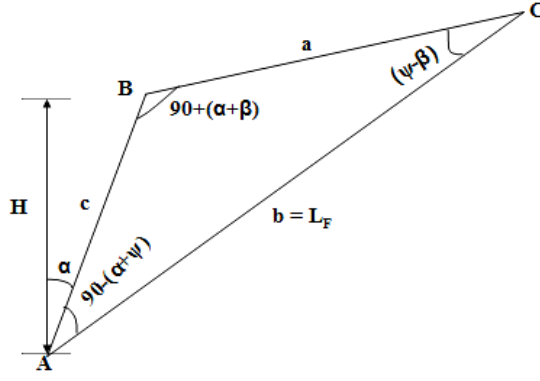


**Fig. 3.3** Failure wedge triangle.

*Determination of equivalent nail force  $T_{eq}$*

Allowable axial force carrying capacity  $T_{all}$  of any particular soil nail embedded at depth  $z$  below the ground surface can be determined as the *minimum* of its pullout capacity  $R_P$  and tensile capacity  $R_T$  given by Eqs. (3.6) and (3.7) respectively.

$$(R_P)_z \text{ [kN]} = (\pi D L_P q_u) / 1000 \quad (3.6)$$

$$(R_T)_z \text{ [kN]} = (0.25 \pi d^2 f_y) / 1000 \quad (3.7)$$

where:  $D$  [mm] = effective diameter of nail (equal to  $d$  [mm] i.e. diameter of reinforcement bar (nail) for driven nails and equal to  $D_{DH}$  [mm] i.e. drillhole diameter in case of grouted nails);  $q_u$  [kPa] = ultimate bond strength (*see Table A.2*);  $f_y$  [MPa] = characteristic yield strength of reinforcement bar;  $L_P$  [m] = effective bond length (i.e. nail length in the passive zone), given by Eq. (3.8).

$$(L_P)_z \text{ [m]} = L - \left[ \frac{(H - z) \cos(\psi + \alpha)}{\cos \alpha \sin(\psi + i)} \right] \quad (3.8)$$

where:  $L$  [m] = length of the soil nail.

If,  $S_v$  [m] is the vertical spacing of soil nails, total number of nails  $n$  provided in a given cross-section of the soil nail wall can be determined. Knowing,  $S_h$  [m] i.e. horizontal (out-of-plane) spacing of soil nails, the equivalent nail force  $T_{eq}$  per meter length of the soil nail can be obtained using Eq. (3.9).

$$T_{eq} [\text{kN/ m}] = \frac{1}{S_h} \sum_{j=1}^n (T_{all})_j \quad (3.9)$$

*Determination of seismic inertia forces  $F_h$  and  $F_v$*

Pseudo-static approach can be adopted for seismic stability analysis of soil nail walls. In this method, the earthquake-induced, time-varying forces of inertia acting within a potentially sliding rigid block involving the soil nail wall system are replaced by equivalent pseudo-static force acting at the center of gravity of the analyzed block. The horizontal and vertical components of this equivalent pseudo-static force are expressed as:

$$\text{Horizontal seismic inertia force, } F_h [\text{kN/ m}] = k_h (W + Q_T) \quad (3.10a)$$

$$\text{Vertical seismic inertia force, } F_v [\text{kN/ m}] = k_v (W + Q_T) \quad (3.10b)$$

It is to be noted that the horizontal inertia force  $F_h$  should be directed away from the slope and the vertical inertia force  $F_v$  should be directed upwards (*see Fig. 3.2*). The appropriate values of seismic coefficients  $k_h$  and  $k_v$  can be evaluated using IS: 1893 Part I (2002) “Code of practice for earthquake resistant design of structures”. For practical applications the vertical inertia force is generally disregarded, however, for particular cases, in accordance with IS: 1893 Part I (2002), vertical seismic coefficient  $k_v$  can be taken equal to two-thirds of the horizontal seismic coefficient  $k_h$  for the evaluation of the vertical inertia force  $F_v$ .

### **3.3.2 Sliding stability**

Sliding stability considers the ability of the soil nail wall to resist sliding along the base of the retained system in response to lateral earth pressures behind the soil nails. Sliding failure may occur when additional lateral earth pressures, mobilized by the excavation, exceed the sliding resistance along the base. To evaluate the factor of safety for sliding stability, soil nail wall is considered as a rigid block of width  $B_L$  against which lateral

earth force from retained soil are applied (see Fig. 3.4). It is assumed that the displacements of the soil block along its base are large enough to mobilize the active pressure acting on it.

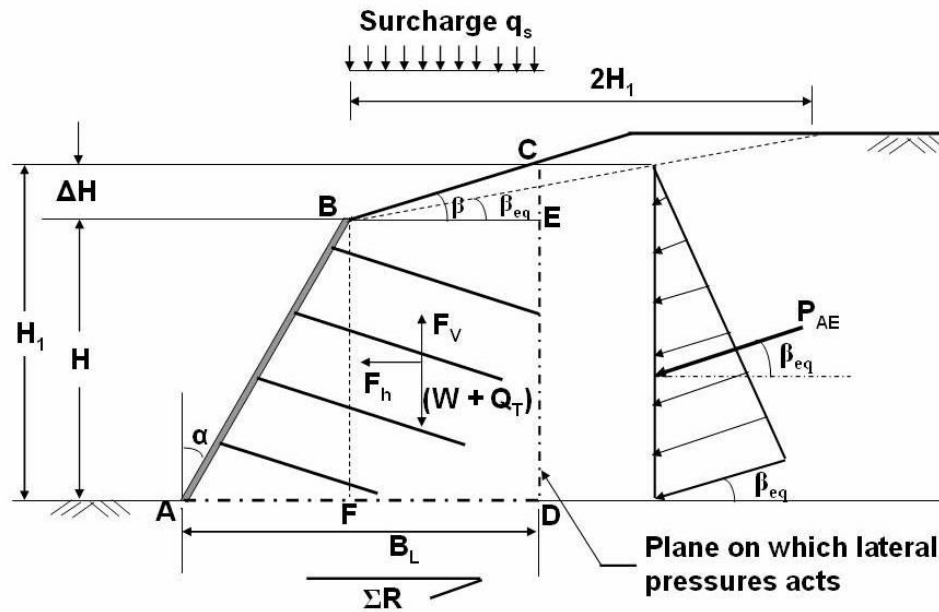


Fig. 3.4 Sliding stability of soil nail walls.

The factor of safety against sliding  $FS_{SL}$  is calculated as the ratio of horizontal resisting forces  $\Sigma R$  to the applied driving horizontal forces  $\Sigma D$ , i.e.

$$FS_{SL} = \frac{\Sigma R}{\Sigma D} = \frac{c_b B_L + (W + Q_T - F_v + P \sin \beta_{eq}) \tan \phi_b}{F_h + P \cos \beta_{eq}} \quad (3.11)$$

where:

$c_b$  and  $\phi_b$  = soil strength parameters along the base of rigid sliding block (AD);

$\beta_{eq}$  = equivalent backslope angle [for broken slopes  $\beta_{eq} = \tan^{-1}(\Delta H/2H_1)$ , for infinite slopes  $\beta_{eq} = \beta$ ];

$B_L$  [m] =  $L + H \tan \alpha$  = base width of the rigid sliding block (AD);

$H_1$  [m] =  $H + \Delta H = H + L \tan \beta$  = effective height over which earth pressure acts (CD);

$Q_T$  [kN/m] =  $q_s L$  = total surcharge load;

$$W [\text{kN/ m}] = W_{\text{ABF}} + W_{\text{BCE}} + W_{\text{BEDF}} = \frac{1}{2} \gamma H^2 \left[ \tan \alpha + 2 \left( \frac{L}{H} \right) + \left( \frac{L}{H} \right)^2 \tan \beta \right] = \text{total weight}$$

of the rigid sliding block (ABCD);

$$F_h [\text{kN/ m}] = k_h (W + Q_T) = \text{horizontal seismic inertia force; and}$$

$$F_v [\text{kN/ m}] = k_v (W + Q_T) = \text{vertical seismic inertia force.}$$

*Determination of total active thrust P*

The total lateral active thrust P acting behind the wall-nailed soil block is expressed as:

$$P = \frac{\gamma H_1^2}{2} K (1 - k_v) \left\{ 1 + \frac{2q_s}{\gamma H_1} \left[ \frac{\cos \alpha}{\cos(\beta - \alpha)} \right] \right\} \quad (3.12)$$

where: K = coefficient of lateral active earth pressure which can be determined using Eq. (3.13).

$$K = \frac{\cos^2(\phi - \alpha - \omega)}{\cos \omega \cos^2 \alpha \cos(\alpha + \beta + \omega) \left[ 1 + \sqrt{\frac{\sin(\phi + \beta) \sin(\phi - \beta - \omega)}{\cos(\alpha + \beta + \omega) \cos(\beta - \alpha)}} \right]^2} \quad (3.13)$$

where:  $\omega$  [degrees] = an angle relating the horizontal and vertical seismic coefficients such that  $\phi - \beta \geq \omega$ , given by Eq. (3.14).

$$\omega = \tan^{-1} \left( \frac{k_h}{1 - k_v} \right) \quad (3.14)$$

### 3.3.3 Bearing capacity (or base heave) failure

Bearing capacity failure, though not a prominent failure mode, may be of concern when a soil nail wall is excavated in fine-grained or soft soils. Because the wall facing do not extend below the bottom of the excavation the unbalanced load caused by the excavation may cause the bottom the excavation to heave and cause a bearing capacity failure of the foundation (see **Fig. 3.5**).

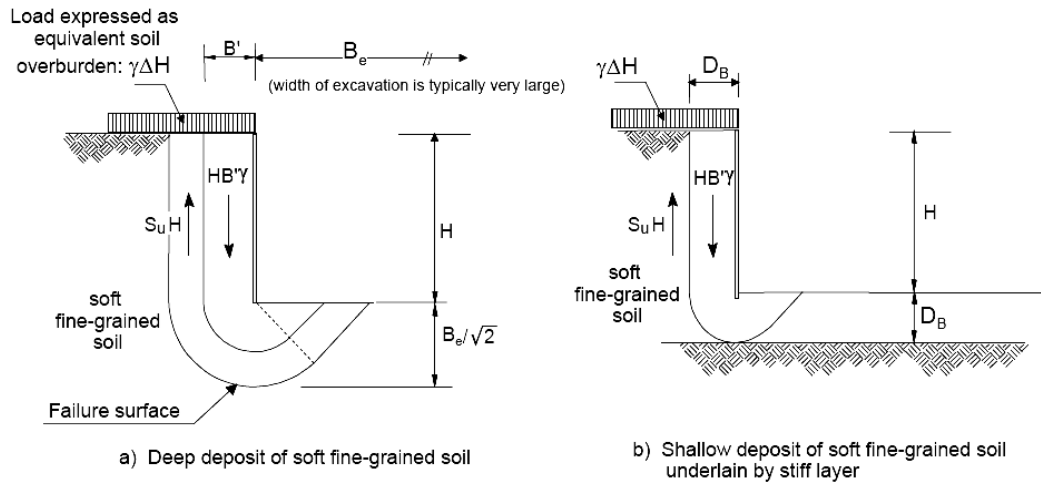


**Fig. 3.5** Excavation base heave failure for soil nail walls (FHWA 2003).

The factor of safety against heave  $FS_H$  is given by:

$$FS_H = \frac{S_u N_c}{H_{eq} \left( \gamma - \frac{S_u}{B'} \right)} \quad (3.15)$$

where:  $S_u$  [kPa] =  $cN_c \left( 1 + \frac{B_e}{L_e} \right)$  = undrained shear strength of the soil

$$N_c = \cot \phi \left[ e^{\pi \tan \phi} \tan^2 \left( 45 + \frac{\phi}{2} \right) - 1 \right] = \text{bearing capacity factor}$$

$H_{eq}$  [m] = equivalent wall height =  $H + \Delta H$ , with  $\Delta H$  [m] as an equivalent overburden;

$B'$  [m] = width of influence,  $B' = B_e / 2$ , where:  $B_e$  [m] = width of excavation.

When a strong deposit underlying the soft layer and occurring at a depth  $D_B < 0.71B_e$  below the excavation bottom is encountered (*see Fig. 3.5b*),  $B'$  in Eq. (3.15) must be replaced by  $D_B$  [m].

### 3.4 INTERNAL FAILURE MODES

Internal stability of soil nails shall be checked at each nail level. Pullout failure and nail tensile strength failure are the two important internal failure modes of soil nail walls.

Following procedure shall be followed to determine the factors of safety of soil nails against internal failure modes.

### 3.4.1 Soil nail pullout failure mode

Nail pullout failure is a failure along the soil-grout or soil-nail (in case of driven nails) interface due to insufficient intrinsic bond strength and / or insufficient nail length. It is the primary internal failure mode in a soil nail wall. For any particular nail embedded at depth  $z$  (see **Fig. 3.6**), factor of safety against pullout failure  $FS_p$  can be determined as the ratio of its pullout capacity  $R_p$  to the maximum axial force  $T$  developed in the nail.

$$(FS_p)_z = \left( \frac{R_p}{T} \right)_z \quad (3.16)$$

where:  $(R_p)_z$  is as determined by Eq. (3.6); and knowing the value of coefficient of lateral earth pressure  $K$  from Eq. (3.13), maximum axial force  $T$  at depth  $z$  can be obtained as:

$$(T)_z [\text{kN}] = K(q_s + \gamma z)S_h S_v \quad (3.17)$$

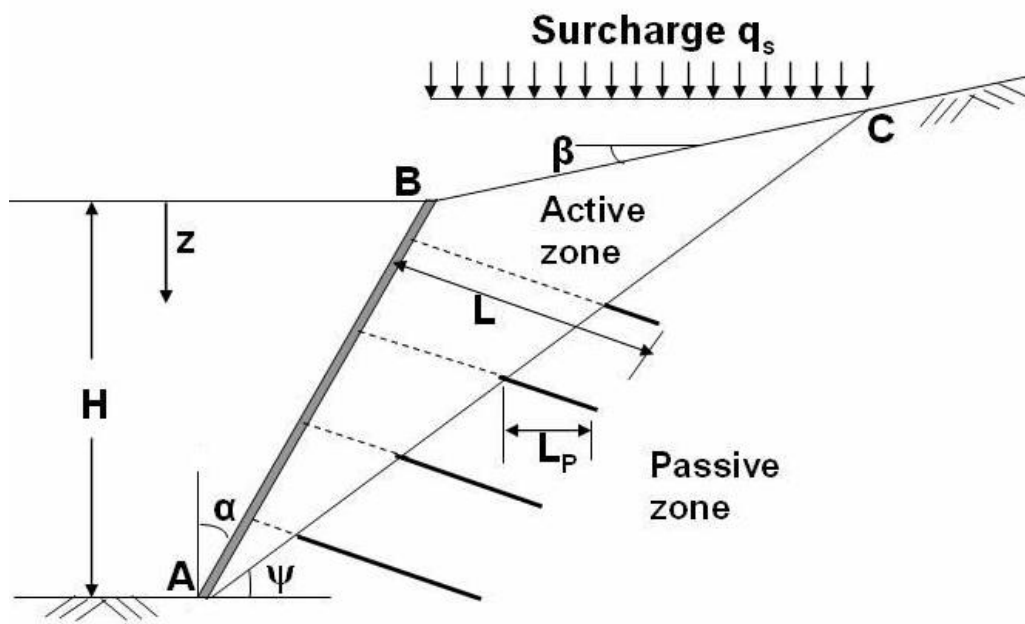


**Fig. 3.6** Pullout failure of soil nails.

### 3.4.2 Nail tensile strength failure mode

Tensile failure of a soil nail takes place when the axial force along the soil nail  $T$  is greater than the nail tensile capacity which may lead to the break-up of the tensile member. Factor of safety against nail tensile strength failure  $FS_T$  for any nail embedded at depth  $z$  can be calculated as the ratio of maximum axial tensile load capacity  $R_T$  of nail to the maximum axial force  $T$  developed in the nail at depth  $z$ .

$$(FS_T)_z = \left( \frac{R_T}{T} \right)_z \quad (3.18)$$

where:  $(R_p)_z$  and  $(T)_z$  are as determined by Eq. (3.7) and Eq. (3.17) respectively.

### 3.5 FACING DESIGN AND FAILURE MODES

Soil nail walls are generally provided with two types of facings: (a) temporary facing and (b) permanent facing. Temporary facing is usually constructed by providing reinforcement in the form of welded wire mesh throughout the wall face, and by additional bearing plates and waler bars at the nail heads; which is, subsequently shotcreted. On the other hand, permanent facing is usually constructed as cast-in-place reinforced cement concrete. However, reinforcement in the permanent facing may be adopted in the form of welded wire mesh or reinforcement bars in either direction. Most of the times temporary facing resists major portion of the loads transferred from soil nails at nail head at the wall face, while permanent facing serves the purpose of improving aesthetic of the wall face. Connection between temporary facing and permanent facing is usually provided by means of headed-studs (usually four numbers per plate) welded on the bearing plates. Following section presents the step-by-step procedure for designing conventional facing system for soil nail walls along with recommended checks for various facing failure modes.

### 3.5.1 Facings design procedure

*Step 1: Determine design nail head tensile force at the wall face  $T_o$*

$$T_o \text{ [kN]} = T_{\max} [0.6 + 0.2(S_{\max} - 1)] \quad (3.19)$$

where:  $T_{\max}$  [kN] = maximum axial force developed in the soil nails; and

$S_{\max}$  [m] = maximum of the  $S_v$  and  $S_h$

*Step 2: Select facing thicknesses*

Temporary facing thickness h: [e.g., 100, 150, 200 mm].

Permanent facing thickness h: [e.g., 200 mm].

*Step 3: Select appropriate facing materials*

(a) Adopt steel reinforcement grade Fe 415 (or Fe 500) with characteristic strength  $f_y = 415$  MPa (or  $f_y = 500$  MPa).

(b) Adopt suitable welded wire mesh (WWM) (*see Table A.3*) and reinforcement bar (*see Table A.4*).

(c) Adopt suitable concrete/shotcrete grade between M20 to M30 with characteristic compressive strength  $f_{ck}$  between 20-30 MPa.

(d) Adopt suitable headed-stud characteristics (*see Table A.5*).

(e) Adopt bearing plate geometry: minimum size 200 × 200 mm x 19 mm.

*Step 4: Check for minimum and maximum reinforcement requirements*

(a) Calculate the minimum and the maximum reinforcement ratios as:

$$\rho_{\min} [\%] = 20 \frac{\sqrt{f_{ck} \text{ [MPa]}}}{f_y \text{ [MPa]}} \quad (3.20)$$

$$\rho_{\max} [\%] = 50 \frac{f_{ck} \text{ [MPa]}}{f_y \text{ [MPa]}} \left( \frac{600}{600 + f_y \text{ [MPa]}} \right) \quad (3.21)$$

Therefore, the placed reinforcement shall be  $\rho_{\min} \leq \rho \leq \rho_{\max}$ . In addition the ratio of the reinforcement in the nail head and mid-span zones should be less than 2.5 to ensure comparable ratio of flexural capacities in these areas.

(b) Select reinforcement area per unit length of WWM for temporary/permanent facing (see **Table A.3**) at the nail head  $a_n$  and at mid-span  $a_m$  in both the vertical and horizontal directions. Usually, the amount of reinforcement at the nail head is adopted same as the amount of reinforcement at the mid-span (i.e.,  $a_n = a_m$ ) in both vertical and horizontal directions.

However, for temporary facing, if waler bars are used at the nail head in addition to the WWM, recalculate the total area of reinforcement at the nail head in the vertical direction and horizontal direction using Eqs. (3.22) and (3.23) respectively.

$$a_{vn} = a_{vm} + \frac{A_{vw}}{S_h} \quad (3.22)$$

$$a_{hn} = a_{hm} + \frac{A_{hw}}{S_v} \quad (3.23)$$

where:  $a_{vn}$  and  $a_{hn}$  are the reinforcement cross sectional areas per unit width in the vertical and horizontal directions at the nail head respectively;  $a_{vm}$  and  $a_{hm}$  are the reinforcement cross sectional area per unit width in the vertical and horizontal directions at the at mid-span respectively; and  $A_{vw}$  and  $A_{hw}$  are the total cross sectional area of waler bars in the vertical and horizontal directions respectively.

Note: If rebar is used in permanent facings instead of WWM, the total area of reinforcement must be suitably converted to a per unit length basis.

(c) Calculate the reinforcement ratio at the nail head and the mid-span as:

$$\rho_n [\%] = \frac{a_n}{0.5h} 100 \quad (3.24)$$

$$\rho_m [\%] = \frac{a_m}{0.5h} 100 \quad (3.25)$$

(d) Verify that the reinforcement ratio of the temporary and permanent facing at the mid-span and the nail head are greater than the minimum reinforcement ratio (i.e.,  $\rho_{\min} \leq \rho$ ), otherwise increase the amount of reinforcement ( $a_n$  and/or  $a_m$ ) to satisfy this criterion.

(e) Verify that the reinforcement ratio of the temporary and permanent facing at the mid-span and the nail head are smaller than the maximum reinforcement ratio (i.e.,  $\rho \leq \rho_{\max}$ ), otherwise reduce the amount of reinforcement ( $a_n$  and/or  $a_m$ ) to satisfy this criterion.

*Step 5: Verify facing flexural resistance  $R_{FF}$  for temporary and permanent facings*

(a) Calculate facing flexural resistance  $R_{FF}$  for the temporary and permanent facing as the minimum of:

$$R_{FF} [\text{kN}] = \frac{C_F}{265} \times (a_{vn} + a_{vm}) [\text{mm}^2 / \text{m}] \times \left( \frac{S_h}{S_v} h [\text{m}] \right) \times f_y [\text{MPa}] \quad (3.26)$$

$$R_{FF} [\text{kN}] = \frac{C_F}{265} \times (a_{hn} + a_{hm}) [\text{mm}^2 / \text{m}] \times \left( \frac{S_v}{S_h} h [\text{m}] \right) \times f_y [\text{MPa}] \quad (3.27)$$

where:

$C_F$  = factor that considers the non-uniform soil pressures behind the facing. For permanent facing  $C_F$  is adopted taken equal to 1, whereas, for temporary facings with thickness: 100 mm, 150 mm and 200m,  $C_F$  shall be adopted as 2.0, 1.5 and 1.0 respectively.

(h) Determine the safety factor against facing flexural failure using Eq. (3.28) and if minimum recommended factor of safety against facing flexural failure is not achieved, redesign the facing with increased thickness of facing, steel

reinforcement strength, concrete strength, and/or amount of steel and repeat the facing flexural resistance calculations.

$$FS_{FF} = \frac{R_{FF}}{T_o} \quad (3.28)$$

*Step 6: Verify facing punching shear resistance  $R_{FP}$*

Punching shear failure of the facing can occur around the nail head and must be evaluated at: (1) bearing-plate connection (used in temporary facings), and (2) headed-stud connection (commonly used in permanent facings).

As the nail head tensile force increases to a critical value, fractures can form a local failure mechanism around the nail head resulting in a conical failure surface. This failure surface extends behind the bearing plate or headed studs and punches through the facing at an inclination of about 45 degrees (*see Figs. 3.7 and 3.8*). The size of the cone depends on the facing thickness and the type of the nail-facing connection (i.e., bearing-plate or headed-studs). For practical purposes, punching shear capacity  $R_{FP}$  is assessed similar to the concrete structural slabs subjected to concentrated loading and is evaluated as:

$$R_{FP} \text{ [kN]} = 330\sqrt{f_{ck} \text{ [MPa]}} \pi D'_c \text{ [m]} h_c \text{ [m]} \quad (3.29)$$

where:

$D'_c$  = effective diameter of conical failure surface at the center of section (i.e., considering an average cylindrical failure surface)

$h_c$  = effective depth of conical surface

*For temporary facing (see Fig. 3.7)*

$D'_c = L_{BP} + h$  and  $h_c = h$ ; where:  $L_{BP}$  = length of bearing plate and  $h$  = thickness of temporary facing.

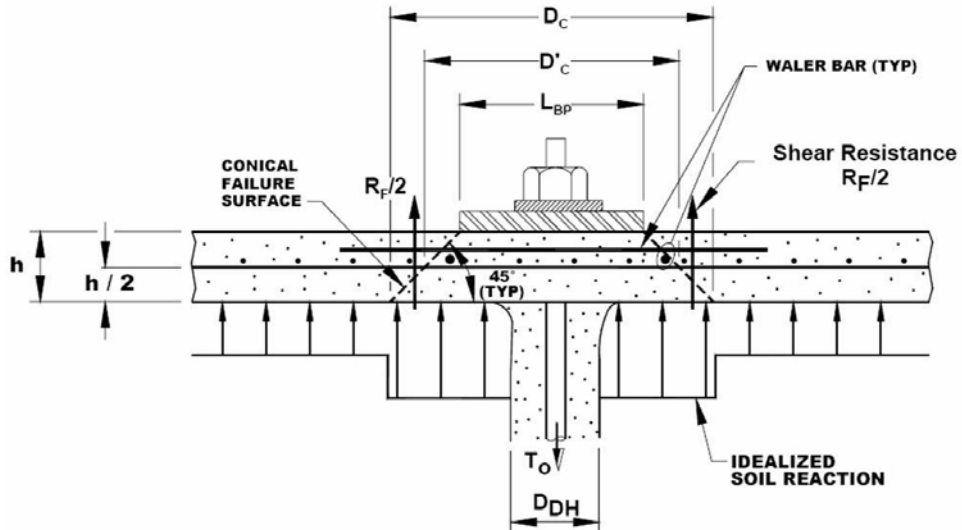


**Fig. 3.7** Punching shear failure mode: Bearing plate connection used in temporary facing (FHWA 2003).

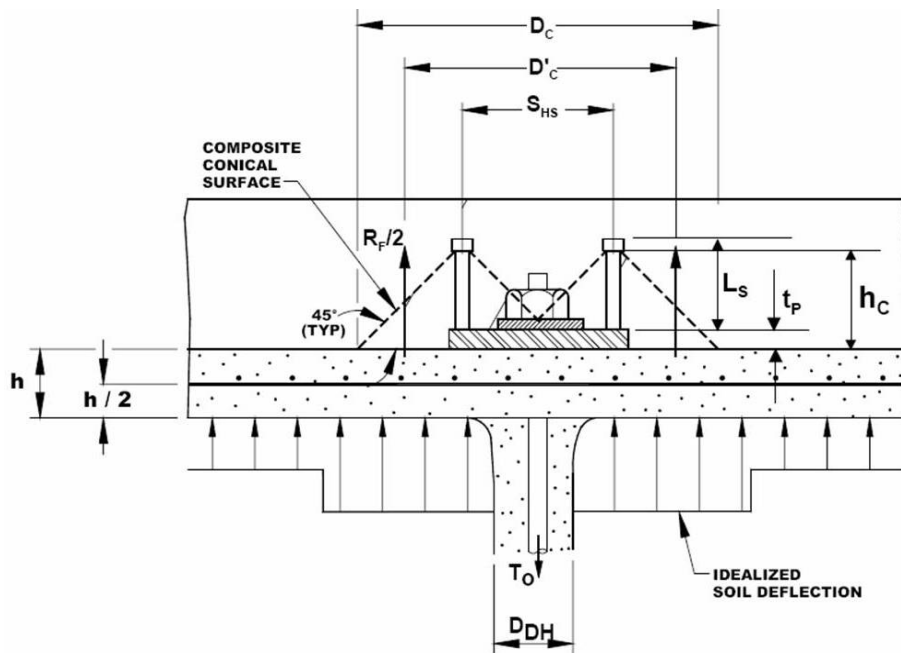


**Fig. 3.8** Punching shear failure mode: Headed stud connection used in permanent facing (FHWA 2003).

For permanent facing (see **Fig. 3.8**)

$$D'_c = \text{minimum of } (S_{HS} + h_c \text{ and } 2h_c) \text{ and } h_c = L_S - t_H + t_P$$

where:  $S_{HS}$  = headed-stud spacing,  $L_S$  = headed-stud length,  $t_H$  = headed-stud head thickness, and  $t_P$  = bearing plate thickness (see **Table A.5**).

Knowing the punching shear capacity  $R_{FP}$  of the facing and the axial force at nail head  $T_o$ , factor of safety against facing punching shear failure modes  $FS_{FP}$  can be determined as:

$$FS_{FP} = \frac{R_{FP}}{T_o} \quad (3.30)$$

If capacity for the temporary/permanent facing is not adequate, then implement larger elements or higher material strengths and repeat the punching shear resistance calculations.

*Step 7: Verify headed-stud resistance  $R_{HT}$  (Permanent facing)*

(a) The tensile capacity of the headed-studs connectors providing anchorage of the nail into the permanent facing (also providing connection between both temporary and permanent facings) must be verified. The nail head capacity against tensile failure of the headed-studs  $R_{HT}$  can be computed as:

$$R_{HT} = N_H A_{SH} f_y \quad (3.31)$$

where:

$N_H$  = number of headed-studs in the connection (usually 4);  $A_{SH}$  = cross-sectional area of the headed-stud shaft; and  $f_y$  = tensile yield strength of the headed-stud.

Knowing the nail head capacity against tensile failure of the headed-studs  $R_{HT}$  and the axial force at nail head  $T_o$ , factor of safety against the tensile failure of the headed-studs  $FS_{HT}$  can be determined as:

$$FS_{HT} = \frac{R_{HT}}{T_o} \quad (3.32)$$

(b) Also verify that compression on the concrete behind headed-stud is within tolerable limits by assuring that:

$$A_H \geq 2.5A_{SH} \text{ and } t_H \geq 0.5(D_H - D_S) \quad (3.33)$$

where:

$A_H$  = cross-sectional area of the stud head;  $t_H$  = head thickness;  $D_H$  = diameter of the stud head; and  $D_S$  = diameter of the headed-stud shaft.

**Note:** Provide sufficient anchorage to headed-stud connectors and extend them at least to the middle of the facing section and preferably behind the mesh reinforcement in permanent facing. Also, provide a minimum 50 mm of cover over headed-studs.

*Step 8: Other facing design considerations*

To minimise the likelihood of a failure at the nail head connection: (1) bearing plates should be mild steel with a minimum yield stress  $f_y$  equal to 250 MPa, (2) nuts should be the heavy-duty, hexagonal type, with corrosion protection, and (3) beveled washers (if used) should be steel or galvanized steel.

## SECTION 4: GENERAL DESIGN CONSIDERATIONS

### 4.1 INTRODUCTION

This section summarises general steps for the design of soil nail walls for practical applications. Salient design considerations have been highlighted to facilitate designers in arriving at the desired soil nail wall configuration ensuring stability and performance requirements.

### 4.2 GENERAL DESIGN STEPS

Design example presented in **Section 5** shall be considered helpful in understanding the step-by-step design procedure for the most common applications of soil nail walls in highway engineering (such as: stabilization of vertical cuts for approaches to subways). In general, the design procedure for soil nail walls includes the following steps:

#### 4.2.1 Initial soil nail wall considerations

- (a) **Wall layout:** Establish the layout of the soil nail wall, including: (1) wall height; (2) length of the wall; (3) backslope; and (4) wall face batter. Wall face batter typically ranges from  $0^\circ$  to  $10^\circ$ . The evaluation of the wall layout also includes developing longitudinal profile of the wall, locating wall appurtenances (e.g., traffic barriers, utilities, and drainage systems), and establishing ROW limitations.
- (b) **Soil nail vertical and horizontal spacing:** Typically, same nail spacing can be adopted in both horizontal  $S_h$  and vertical  $S_v$  directions. Nail spacing ranges from 1.25 to 2 m (commonly 1.5 m) for conventional drilled and grouted soil nails, and as low as 0.5 m for driven nails. As a general rule, soil nail spacing in horizontal and vertical direction must be such that each nail has an influence area  $S_h \times S_v \leq 4 \text{ m}^2$ . Though, soil nail spacing may get affected by the presence of existing underground structures,

the design engineer should specify a minimum horizontal soil nail spacing of about 1.0 m.

- (c) **Soil nail pattern on wall face:** The soil nail pattern on wall face may be adopted as one of the following: (1) square (or rectangular); (2) staggered in a triangular pattern; and (3) irregular (at limited locations) depending upon the ease of construction and site-specific constraints.
- (d) **Soil nail inclination:** Soil nails are typically installed at an inclination ranging from 10 to 20 degrees from horizontal with a typical inclination of 15 degrees. Inclination of soil nails in this range helps in proper flow of grout as well as better provides reinforcing effect.
- (e) **Soil nail length and distribution:** The distribution of soil nail lengths in a soil nail wall can be selected as either uniform (i.e., only one nail length is used for the entire wall), or variable, where different nail lengths may be used for individual soil nail levels within a wall cross section. Uniform nail pattern is recommended for most applications; however, provision of longer nail lengths in upper two-thirds to three-quarters of the wall height significantly reduces wall deformations. Also, variable nail lengths may become inevitable in presence of underground utilities which imposes restriction on designed nail length.
- (e) **Soil nail materials and soil properties:** Shall be adopted as specified in **Section 2**.
- (f) **Other initial considerations:** Evaluate corrosion potential; explore drilling methods likely to be adopted by the prospective contractors (this will provide necessary help in the appropriate selection of the design ultimate bond strength of soil nails); estimate drillhole diameter based on previous experience in similar ground conditions; select desired factors of safety for the different failure modes; and define loadings required to be considered in the design.

#### 4.2.2 Preliminary design

(a) For the specific project application, obtain general parameters as mentioned in **Section**

**4.2.1**. For known drilling method and soil conditions, from **Table A.2** adopted suitable value of ultimate bond strength  $q_u$ , which may otherwise, be obtained by conducting field pullout tests on soil nails as described in **Section 6**.

(b) Determine tensile force  $T$  developed in nail at depth  $z$  using Eq. (4.1)

$$T[\text{kN}] = K(q_s + \gamma z)S_h S_v; \text{ where: } K = K_a = \frac{1 - \sin \phi}{1 + \sin \phi} \quad (4.1)$$

and note the maximum value of axial tensile force  $T_{\max}$ .

(c) For a minimum factor of safety of against nail tensile failure  $FS_T = 1.80$ , determine required cross-sectional area  $A_t$  of the nail bar can be determined as:

$$A_t [\text{mm}^2] = \frac{T_{\max} FS_T}{f_y} \quad (4.2)$$

choose closest commercially available bar size that has a cross-sectional area at least that evaluated using Eq. (4.2).

(d) Determine minimum nail length  $L$  as the maximum of  $L_1$  and  $L_2$

$$L_1 = \frac{(H - S_{v1}) \cos \psi}{\sin(\psi + i)} + \frac{2T_1}{\pi D_{DH} q_u} \text{ and } L_2 = 0.6H \quad (4.3)$$

where:  $T_1$  and  $S_{v1}$  are the axial force and vertical spacing of top nail respectively;  $\psi$  = inclination of failure plane;  $i$  = nail inclination;  $L_2$  = minimum recommended length and  $L_1$  is the length obtained to satisfy following two criteria:

(i) Length of the top nail (i.e. first nail) should be such that it crosses the failure surface.

(ii) Length of the top nail (i.e. first nail) gives a factor of safety against nail pullout failure is more than 2.0.

Note: Minimum nail length  $L$  shall be evaluated for the static case considering vertical height  $H$  of the soil nail wall (i.e. assuming face batter  $\alpha = 0$  degrees) irrespective of the actual wall geometry.

#### **4.2.3 Final design**

Final design of soil nail wall requires following steps:

- (a) Check for external failure modes: (i) Global stability, (ii) Sliding stability and (iii) Basal heave or bearing capacity. Global stability and sliding stability for static and seismic (if required) conditions of the soil nail walls may be evaluated using the procedure stated in **Sections 3.3.1 and 3.3.2** respectively. Basal heave or bearing capacity failure mode shall be considered prominent only in cases where soil nail walls are founded on soft soils. Basal heave or bearing capacity failure mode may be evaluated with reference to the **Section 3.3.3**.

Note: For the evaluation of the global stability, use of rigorous computational tools in addition to the proposed conventional methodology is strongly recommended.

- (b) Check for internal failure modes: (i) Soil-nail pullout failure and (ii) Nail tensile failure. Both of these internal failure modes shall be evaluated at each nail level under static and seismic (if required) conditions with reference to the **Section 3.4**.
- (c) Facing design and checks: For both temporary and permanent soil nail wall facings, design and recommended checks shall be conducted under static and seismic (if required) conditions with reference to the **Section 3.5**.
- (d) Other design considerations such as: permissible wall deformations (may be verified using suitable computational tools), internal and surface drainage, corrosion protection and any site-specific issues shall be adequately addressed in accordance with relevant standards and bye-laws.

## **4.3 OTHER DESIGN CONSIDERATIONS**

### **4.3.1 Loads and load combinations**

Soil nail walls used on typical highway projects are typically subjected to the following different loads during their service life: (i) Dead loads DL (e.g., weight of the soil nail wall system, lateral earth pressure, weight of a nearby above-ground structure); (ii) Live loads LL (e.g., traffic loads); (iii) impact loads IL (e.g., vehicle collision on barriers above soil nail wall); and (iv) earthquake loads EQ. Following load combinations are recommended to assess the most critical loading condition:

- (a) DL + LL
- (b) DL + LL + IL
- (c) DL + EQ

For earthquake loads, allowable stresses shall be increased by 133 percent from the values obtained with factors of safety for static loads.

### **4.3.2 Permissible soil nail wall deformations**

The maximum permissible lateral deformation at the top of the soil nail walls constructed in weathered rock and stiff soils is 0.1%H; sandy soils is 0.2%H and for fine-grained soils is 0.3%H. Under no circumstances maximum permissible lateral deformation shall exceed 0.3% H, where: H is the vertical height of the soil nail wall. Permissible vertical deformation (i.e., settlement) shall be considered to be same as the permissible horizontal deformation.

### **4.3.3 Drainage measures**

- (a) **Short term drainage measures:** Surface water and groundwater must be controlled both during and after construction of the soil nail wall. A surface water interceptor ditch, excavated along the crest of the excavation and lined with concrete, is a

recommended element for controlling surface water flows. Additionally, if ground water impacts are temporary or localized, suitable dewatering measures may be taken for lowering the groundwater table

- (b) **Long term drainage measures:** By means of the drainage system comprising of: (i) vertical geo-composite drain strips placed suitably along the face of wall; (ii) weep holes in the form of PVC pipes of typical diameter as 300-400 mm placed through the face at the location of expected localised seepage; (iii) provision of horizontal or slightly inclined drain pipes of typical diameter 50 mm installed at the locations where it is necessary to control the groundwater pressures imposed on the retained soil mass; (iv) installation of permanent interception ditch behind the wall at its crest to prevent surface water runoff from infiltrating behind the wall or flowing over the wall edge; and (v) provision of a vegetative protective cap to reduce or retard water infiltration into the soil.

#### **4.3.4 Corrosion protection**

Corrosion potential of the soil must be evaluated for all permanent soil nail walls and, in some cases, for temporary walls. Corrosion potential of soil can be evaluated based on tests results of the following properties: pH (potential of hydrogen); electrical resistivity; chloride content; sulfate content; and presence of stray currents.

*Corrosion protection measures:* (a) Specify a minimum grout cover of 25 mm between the reinforcement nail bar and the soil; (b) recommend epoxy coating of minimum thickness 0.4 mm on the nail bars shall be applied by the manufacturer prior to shipment of nails to the construction site, which is, subsequently to be encased in grout cover; and (c) adopt other site-specific suitable corrosion protection measures.

## SECTION 5: DESIGN EXAMPLE

### 5.1 INTRODUCTION

This section illustrates the step by step design methodology of soil nail walls with the help of an example. It is intended to provide field practitioners an exposure to the design methodology of soil nail structures with reference to the various failure modes and design considerations described in the **Sections 3 and 4**.

*Problem statement:* A permanent soil nail is designed to support a vertical cut for the side wall of the approach road for a subway. The maximum design vertical height of the side wall to be supported is 8 m. Groundwater table is considered to be significantly below the zone of influence. Backslope of the wall is assumed to be flat. Site is considered to be at an urban location with the possibility of commercial establishments in the vicinity of the soil nail wall. Peak horizontal ground acceleration is assumed to be 0.15g for seismic considerations. It is also assumed that the project do not have specific construction restrictions and particular requirements such as aesthetics, deformation control etc.

### 5.2 INITIAL DESIGN CONSIDERATIONS

- (a) Vertical height of wall:  $H = 8$  m
- (b) Face batter:  $\alpha = 0.0$  degrees; Backslope angle:  $\beta = 0.0$  degrees
- (c) Soil nail spacing:  $S_h = S_v = 1.5$  m (Note: vertical spacing of first nail  $S_{v1} = 0.75$  m)
- (d) Soil nail spacing pattern at wall face: Square
- (e) Soil nail inclination:  $i = 15$  degrees
- (f) Soil nail length distribution: Uniform
- (g) Soil nail material: Grade Fe 415;  $f_y = 415$  MPa
- (h) Representative soil properties from soil investigation report:

Soil type: dense to very dense silty sands; Cohesion:  $c = 5$  kPa; Friction angle:

$$\phi = 35^\circ; \text{ Unit weight: } \gamma = 18.9 \text{ kN/m}^3.$$

Adopt ultimate bond strength:  $q_u = 100$  kPa (*see Table A.2*)

(i) Loads considered:

$$\text{Self weight of the structure and surcharge load: } q_s = 20 \text{ kN/m}^2$$

$$\text{Seismic loading: } k_h = 0.15 \text{ and } k_v = 0.0$$

(j) Drilling method: rotary drilling; Drillhole diameter:  $D_{DH} = 130$  mm

(k) Desired minimum factors of safety for various failure modes under static and seismic conditions are shown in **Table 5.1**.

**Table 5.1** Desired minimum recommended factors of safety for permanent soil nail walls.

Failure mode	Resisting component	Symbol	Factor of safety	
			Seismic	Static
External stability	Global	$FS_G$	1.10	1.5
	Sliding	$FS_{SL}$	1.10	1.5
Internal stability	Pull-out resistance	$FS_P$	1.50	2.0
	Nail bar tensile strength	$FS_T$	1.35	1.8
Facing failure	Facing flexure	$FS_{FF}$	1.10	1.5
	Facing punching failure	$FS_{FP}$	1.10	1.5
	Headed stud tensile	$FS_{HT}$	1.50	2.0

### 5.3 PRELIMINARY DESIGN

(a) Determine maximum axial force  $T_{max}$

Tensile force T developed in nail at depth z is given by

$$T[\text{kN}] = K(q_s + \gamma z)S_h S_v; \text{ for static case: } K = K_a = \frac{1 - \sin \phi}{1 + \sin \phi} = \frac{1 - \sin 35}{1 + \sin 35} = 0.27$$

On substituting values of various parameters,  $T[\text{kN}] = 12.2 + 11.53z$  (*see Table 5.2*)

**Table 5.2** Maximum axial tensile force developed in each nail from top.

Nail No. j	Depth of nail z [m]	Axial force T [kN]
01	0.75 ( $z = S_{v1}$ )	20.85
02	2.25	38.14
03	3.75	55.54
04	5.25	72.73
05	6.75	90.00

Therefore, maximum axial force:  $T_{\max} = 90.0 \text{ kN}$

(b) Determine minimum nail length  $L$  and nail diameter  $d$

Minimum length of soil nail  $L$  is adopted as the maximum of  $L_1$  and  $L_2$ :

$$L_1 = \frac{(H - S_{v1}) \cos \psi}{\sin(\psi + i)} + \frac{2T_1}{\pi D_{DH} q_u} \text{ and } L_2 = 0.6H$$

Here:  $\psi = 45 + (35/2) = 62.5^\circ$ ;  $i = 15^\circ$ ;  $q_u = 100 \text{ kPa}$ ;  $D_{DH} = 130 \text{ mm}$ ;  $T_1 = 20.85 \text{ kN}$

$S_{v1} = 0.75$  and  $H = 8 \text{ m}$ . On substituting these values in above equation

$$L_1 = \frac{(8 - 0.75) \cos 62.5}{\sin(62.5 + 15)} + \frac{2 \times 20.85}{\pi \times 0.13 \times 100} = 4.44 \text{ m and } L_2 = 0.6 \times 8 = 4.80 \text{ m.}$$

Hence, adopt nail length:  $L = 4.80 \text{ m}$ .

For a minimum factor of safety of against nail tensile failure  $FS_T = 1.80$ , the required cross-sectional area  $A_t$  of the nail bar can be determined as:

$$A_t \left[ \text{mm}^2 \right] = \frac{T_{\max} FS_T}{f_y} = \frac{90 \times 1000 \times 1.80}{415} = 390$$

Select reinforcement bar of diameter  $d = 25 \text{ mm}$  providing cross sectional area  $A_t = 490 \text{ mm}^2 (> 390 \text{ mm}^2)$ . This bar can be installed with no difficulty in the drillhole. Available grout cover is at least  $(100 - 25) / 2 = 37.5 \text{ mm} > \text{minimum cover} = 25 \text{ mm}$ .

General layout of the soil nail wall is shown in **Fig. 5.1** and is used as the reference in the following calculations.

## 5.4 FINAL DESIGN

Final design consists of (i) evaluation of external and internal failure modes under static and seismic conditions (if considered), and (ii) facing design and checks against facing failure modes.

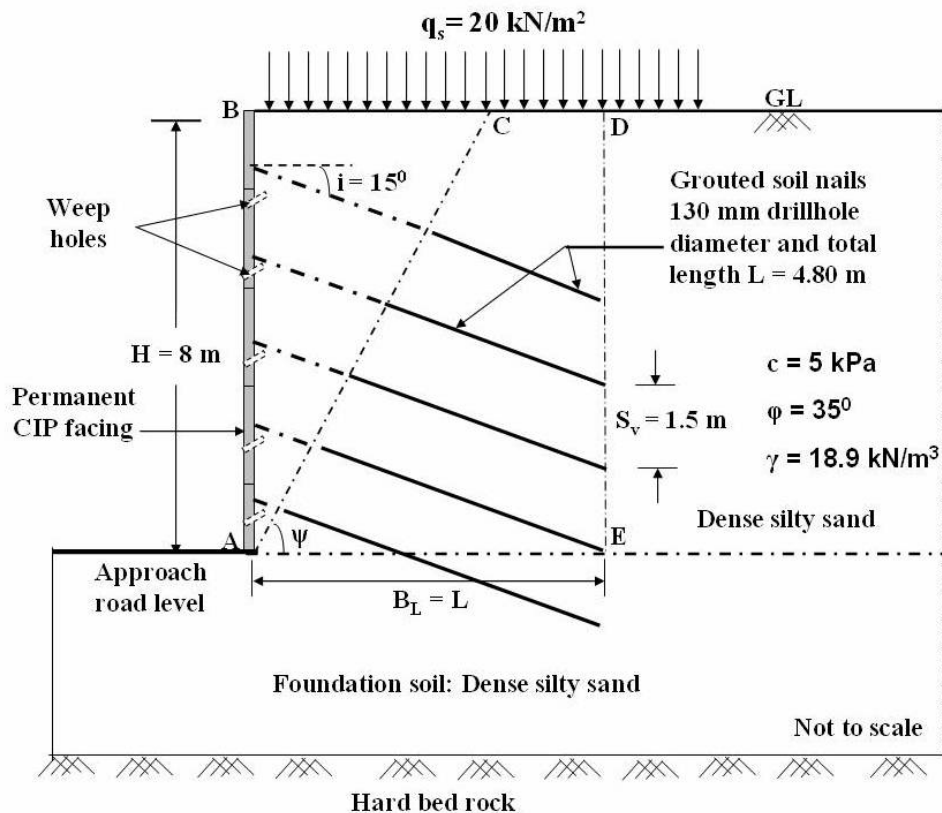


Fig. 5.1 General outline of designed soil nail wall.

### 5.4.1 EXTERNAL FAILURE MODES

#### 5.4.1.1 Global stability

##### (a) Static global stability

Determination of length of failure plane  $L_F$

$$L_F [\text{m}] = \frac{H}{\sin \psi} = \frac{8}{\sin 62.5} = 9.02$$

Determination of equivalent nail force  $T_{eq}$

$$R_P [\text{kN}] = \pi D_{DH} L_P q_u = \pi \times 0.13 \times L_P \times 100 = 40.84 L_P$$

$$\text{where: } L_p [\text{m}] = L - \left[ \frac{(H - z) \cos \psi}{\sin(\psi + i)} \right] = 4.80 - \left[ \frac{(8 - z) \cos 62.5}{\sin(62.5 + 15)} \right] = 1.02 + 0.47z$$

$$R_T [\text{kN}] = \frac{\pi d^2 f_y}{4 \times 1000} = \frac{\pi \times 25^2 \times 415}{4 \times 1000} = 203.71$$

Allowable axial force carrying capacity  $T_{\text{all}}$  [kN] of nail embedded at depth  $z$  is the minimum of  $R_P$  and  $R_T$ .

For  $S_h = 1.5$  m, equivalent nail force  $T_{\text{eq}}$  can be determined as:

$$T_{\text{eq}} [\text{kN/m}] = \frac{1}{S_h} \sum_{j=1}^n (T_{\text{all}})_j = \frac{1}{1.5} \times 568.08 = 378.72; \text{ Here: } n = 5 \text{ and } \sum_{j=1}^5 (T_{\text{all}})_j \text{ is obtained}$$

from **Table 5.3**.

**Table 5.3** Allowable axial force carrying capacity of nails at different levels.

Nail No. j (from top)	Depth of nail $z$ [m]	Effective pullout length $L_p$ [m]	Nail pullout capacity $R_P$ [kN]	Nail tensile capacity $R_T$ [kN]	Allowable axial force carrying capacity of nail $T_{\text{all}}$ [kN]
01	0.75	1.37	55.95	203.71	55.95
02	2.25	2.08	84.95	203.71	84.95
03	3.75	2.78	113.53	203.71	113.53
04	5.25	3.49	142.53	203.71	142.53
05	6.75	4.19	171.12	203.71	171.12
				$\sum_{j=1}^5 (T_{\text{all}})_j =$	<b>568.08</b>

*Determination of weight of failure wedge  $W$*

With reference to the **Fig. 5.1**, weight of failure wedge ABC can be determined as:

$$W [\text{kN/m}] = \gamma \times (\text{Area of } \Delta ABC) = 0.5 \gamma H^2 \cot \psi$$

$$\text{Therefore, } W [\text{kN/m}] = 0.5 \times 18.9 \times 8^2 \times \cot 62.5 = 314.84$$

*Determination of total surcharge load  $Q_T$*

$$Q_T [\text{kN/m}] = q_s H \cot \psi = 20 \times 8 \times \cot 62.5 = 83.29$$

$$\text{Therefore, term } (W + Q_T) = 314.84 + 83.29 = 398.13 \text{ kN/m}$$

Global stability safety factor  $FS_G$  under static conditions is given by:

$$FS_G = \frac{cL_F + T_{eq} \cos(\psi - i) + [(W + Q_T) \cos \psi + T_{eq} \sin(\psi - i)] \tan \phi}{(W + Q_T) \sin \psi}$$

Substituting the values of various parameters  $FS_G$  under static condition is obtained as:

$$FS_G = \frac{(5 \times 9.02) + 378.72 \cos(62.5 - 15) + [(398.13) \cos 62.5 + 378.72 \sin(62.5 - 15)] \tan 35}{(398.13) \sin 62.5}$$

$$FS_G = 1.77 (> 1.50 \text{ safe for static case})$$

### **(b) Seismic global stability**

For  $k_h = 0.15$  and  $k_v = 0.0$

Horizontal seismic inertia force,  $F_h [\text{kN/m}] = k_h (W + Q_T) = 0.15 \times 398.13 = 59.72$

Vertical seismic inertia force,  $F_v [\text{kN/m}] = k_v (W + Q_T) = 0.0$

Global stability safety factor  $FS_G$  under seismic conditions is given by:

$$FS_G = \frac{cL_F + T_{eq} \cos(\psi - i) + [(W + Q_T - F_v) \cos \psi + T_{eq} \sin(\psi - i) - F_h \sin \psi] \tan \phi}{(W + Q_T - F_v) \sin \psi + F_h \cos \psi}$$

On substitution of values of various parameters  $FS_G$  under seismic condition is obtained as:

$$FS_G = \frac{588.10}{380.71} = 1.54 (> 1.10 \text{ safe for seismic case})$$

### **5.4.1.2 Sliding stability**

#### **(a) Static sliding stability**

Factor of safety for sliding stability of soil nail wall  $FS_{SL}$  in static condition is given by:

$$FS_{SL} = \frac{c_b B_L + (W + Q_T + P \sin \beta_{eq}) \tan \phi_b}{P \cos \beta_{eq}}$$

Here:  $c_b = c = 5 \text{ kPa}$ ;  $\phi_b = \phi = 35^\circ$ ;  $\beta_{eq} = \beta = 0.0$ ;  $B_L = L = 4.80 \text{ m}$

For static case total active lateral earth pressure  $P = P_A$  can be determined as:

$$P_A \text{ [kN/m]} = \frac{\gamma H^2}{2} K \left[ 1 + \frac{2q_s}{\gamma H} \right] = \frac{18.9 \times 8^2}{2} \cdot 0.27 \left[ 1 + \frac{2 \times 20}{18.9 \times 8} \right] = 206.57$$

where: coefficient of lateral active earth pressure:  $K = K_a = 0.27$

$$W \text{ [kN/m]} = \text{Unit weight} \times \text{Area of sliding wedge ABDE} = 18.9 \times (8 \times 4.8) = 725.76$$

$$Q_T \text{ [kN/m]} = \text{Surcharge load} \times \text{Length AD} = q_s \times B_L = 20 \times 4.8 = 96$$

Therefore, term  $(W + Q_T) = 725.76 + 96 = 821.76 \text{ kN/m}$

Substituting of values of various parameters,  $FS_{SL}$  under static condition is obtained as:

$$FS_{SL} = \frac{(5 \times 4.8) + (821.76 + 206.57 \sin 35) \tan 35}{206.57 \cos 0} = 2.90 (> 1.50 \text{ safe for static case})$$

### **(b) Seismic sliding stability**

Factor of safety for sliding stability of soil nail wall  $FS_{SL}$  in seismic condition is given by:

$$FS_{SL} = \frac{c_b B_L + (W + Q_T - F_v + P \sin \beta_{eq}) \tan \phi_b}{F_h + P \cos \beta_{eq}}$$

For  $k_h = 0.15$  and assumed  $k_v = 0.0$

For seismic case total active lateral earth pressure  $P = P_{AE}$  can be determined as:

$$P_{AE} \text{ [kN/m]} = \frac{\gamma H^2}{2} K (1 - k_v) \left[ 1 + \frac{2q_s}{\gamma H} \right]$$

where: coefficient of lateral active earth pressure:  $K = K_{ae}$ , which can be evaluated as:

$$K = \frac{\cos^2(\phi - \omega)}{\cos^2 \omega \left[ 1 + \sqrt{\frac{\sin \phi \sin(\phi - \omega)}{\cos \omega}} \right]^2} = \frac{\cos^2(35 - 8.53)}{\cos^2 8.53 \left[ 1 + \sqrt{\frac{\sin 35 \sin(35 - 8.53)}{\cos 8.53}} \right]^2} = 0.36$$

$$\text{where: } \omega \text{ [deg]} = \tan^{-1} \left( \frac{k_h}{1 - k_v} \right) = \tan^{-1} \left( \frac{0.15}{1 - 0} \right) = 8.53$$

$$\text{Therefore, } P_{AE} \text{ [kN/m]} = \frac{18.9 \times 8^2}{2} \cdot 0.36 (1 - 0) \left[ 1 + \frac{2 \times 20}{18.9 \times 8} \right] = 275.33$$

$$\text{Horizontal seismic inertia force: } F_h \text{ [kN/m]} = k_h (W + Q_T) = 0.15 \times 821.76 = 123.26$$

Vertical seismic inertia force:  $F_v [\text{kN/m}] = k_v(W + Q_T) = 0.0$

Substituting values of various parameters,  $FS_{SL}$  under seismic condition is obtained as:

$$FS_{SL} = \frac{(5 \times 4.8) + (821.76 - 0 + 275.33 \sin 0) \tan 35}{123.26 + 275.33 \cos 0} = 1.50 (> 1.10 \text{ safe for seismic case})$$

#### **5.4.1.3 Bearing capacity (or basal heave) failure**

Since, the soil nail wall is founded in dense silty sand, basal heave or bearing capacity failure of the soil nail wall is not likely to occur and hence, not evaluated in this example.

### **5.4.2 INTERNAL FAILURE MODES**

#### **5.4.2.1 Soil nail pullout failure**

For any particular nail embedded at depth  $z$ , factor of safety against pullout failure  $FS_P$  can be obtained as:

$$(FS_P)_z = \left( \frac{R_P}{T} \right)_z$$

where:  $R_P$  and  $T$  are determined similarly as in **Table 5.3**. While determining  $T$ , value of earth pressure coefficient  $K = K_a$  (here:  $K_a = 0.27$ ) for static case and  $K = K_{ae}$  (here:  $K_{ae} = 0.36$ ) for seismic case shall be used. Results of the soil nail pullout failure analysis for seismic and static cases are shown in **Tables 5.4a** and **5.4b** respectively. The minimum recommended  $FS_P$  for static case is 2.0 and for seismic case is 1.50. It may be observed from **Tables 5.4a** and **5.4b** that for the bottom two nails (04 and 05)  $FS_P$  values are marginally less than the minimum recommendations, though practically insignificant.

#### **5.4.2.2 Soil nail tensile strength failure**

Factor of safety against nail tensile strength failure  $FS_T$  for any nail embedded at depth  $z$  can be obtained as:

$$(FS_T)_z = \left( \frac{R_T}{T} \right)_z$$

where:  $R_T$  and  $T$  are determined similarly as in **Table 5.3**. While determining  $T$ , value of earth pressure coefficient  $K = K_a$  (here  $K_a = 0.27$ ) for static case and  $K = K_{ae}$  (here  $K_{ae} = 0.36$ ) for seismic case shall be used. Results of the soil nail tensile failure analysis for seismic and static cases are shown in **Table 5.5**. It may be observed from **Table 5.5** that the factors of safety against nail tensile strength failure are well above the minimum recommended  $FS_T$  for static case is 1.80 and for seismic case is 1.35.

**Table 5.4a** Factor of safety against soil nail pullout failure (static case).

Nail No. j (from top)	Depth of nail z [m]	Effective pullout length $L_p$ [m]	Nail pullout capacity $R_p$ [kN]	Axial force developed in nail T [kN]	Factor of safety against nail pullout failure $FS_p$
01	0.75	1.37	55.95	20.85	2.68
02	2.25	2.08	84.95	38.14	2.22
03	3.75	2.78	113.53	55.54	2.04
04	5.25	3.49	142.53	72.73	1.95
05	6.75	4.19	171.12	90.00	1.90

**Table 5.4b** Factor of safety against soil nail pullout failure (seismic case).

Nail No. j (from top)	Depth of nail z [m]	Effective pullout length $L_p$ [m]	Nail pullout capacity $R_p$ [kN]	Axial force developed in nail T [kN]	Factor of safety against nail pullout failure $FS_p$
01	0.75	1.37	55.95	27.68	2.02
02	2.25	2.08	84.95	50.64	1.68
03	3.75	2.78	113.53	73.61	1.54
04	5.25	3.49	142.53	96.57	1.48
05	6.75	4.19	171.12	119.53	1.43

**Table 5.5** Factor of safety against soil nail tensile strength failure.

Nail No. j (from top)	Depth of nail z [m]	Nail tensile capacity $R_T$ [kN]	Axial force developed in nail T [kN]		Factor of safety against nail tensile failure $FS_T$	
			Static	Seismic	Static	Seismic
01	0.75	203.71	20.85	27.68	9.77	7.36
02	2.25	203.71	38.14	50.64	5.34	4.02
03	3.75	203.71	55.54	73.61	3.66	2.76
04	5.25	203.71	72.73	96.57	2.80	2.11
05	6.75	203.71	90.00	119.53	2.26	1.70

### 5.4.3 FACING DESIGN AND CHECKS

#### Step 1: Calculate design nail head tensile force at the face $T_o$

For  $T_{max} = 90.0$  kN (static case);  $T_{max} = 119.53$  kN (seismic case) and  $S_{max} = 1.5$  m, nail head tensile force at the wall face  $T_o$  can be obtained as:

$$T_o \text{ [kN]} = T_{max} [0.6 + 0.2(S_{max} - 1)] = 90[0.6 + 0.2(1.5 - 1)] = 63.0 \text{ (for static case)}$$

$$T_o \text{ [kN]} = T_{max} [0.6 + 0.2(S_{max} - 1)] = 119.53[0.6 + 0.2(1.5 - 1)] = 83.67 \text{ (for seismic case)}$$

#### Step 2: Adopt wall facing thickness

Temporary facing thickness h: 100 mm

Permanent facing thickness h: 200 mm

#### Step 3: Adopt appropriate facing materials

(a) Steel reinforcement: Grade Fe 415 with characteristic strength:  $f_y = 415$  MPa

(b) Concrete/shotcrete: Grade M20 with characteristic compressive strength:  $f_{ck} = 20$  MPa

(c) Welded wire mesh (temporary facing): WMM 102 x 102–MW19 x MW19 (*see Table A.3*)

(d) Horizontal and vertical waler bars (temporary facing): 2 x 10 mm diameter, ( $f_y = 415$  MPa,  $A_{vw} = A_{hw} = 2 \times 78 = 156 \text{ mm}^2$ ) in both directions.

(e) Bearing plate (temporary facing): Grade 250 ( $f_y = 250$  MPa); Shape: Square; Length:  $L_{BP} = 225$  mm; Thickness:  $t_p = 25$  mm.

(f) Reinforcement bar (permanent facing): 16 mm diameter @ 300 mm both ways.

(g) Headed-studs: 4 numbers; Size:  $\frac{1}{2} \times 4 \frac{1}{8}$ ;  $L_S = 100$  mm;  $D_H = 25$  mm;  $D_S = 13$  mm;  $t_H = 8$  mm;  $S_{HS} = 150$  mm (*see Table A.5*)

#### Step 4: Checks for facing reinforcement

Determine the minimum and the maximum reinforcement ratios as:

$$\rho_{\min} [\%] = 20 \frac{\sqrt{f_{ck} [\text{MPa}]}}{f_y [\text{MPa}]} = 20 \frac{\sqrt{20}}{415} = 0.21$$

$$\rho_{\max} [\%] = 50 \frac{f_{ck} [\text{MPa}]}{f_y [\text{MPa}]} \left( \frac{600}{600 + f_y [\text{MPa}]} \right) = 50 \frac{20}{415} \left( \frac{600}{600 + 415} \right) = 1.42$$

Therefore, the adopted reinforcement shall be  $\rho_{\min} \leq \rho \leq \rho_{\max}$ . In addition the ratio of the reinforcement in the nail head and mid-span zones should be less than 2.5 to ensure comparable ratio of flexural capacities in these areas.

#### Temporary facing

Reinforcement in vertical  $a_{vm}$  and horizontal  $a_{hm}$  directions in mid-span:

$$a_{vm} = a_{hm} = 184.2 \text{ mm}^2/\text{m} \text{ for WWM } 102 \times 102 - \text{MW19} \times \text{MW19} \text{ (see Table A.3)}$$

Reinforcement in vertical  $a_{vn}$  and horizontal  $a_{hn}$  directions around soil nail head:

Since same amount of reinforcement is provide in both directions (*see Step 3d*),  $a_{vn} = a_{hn}$

$$a_{vn} = a_{hn} = a_{vm} + \frac{A_{vw}}{S_h} = 184.2 + \frac{156}{1.5} = 288.2 \text{ mm}^2 / \text{m}$$

Reinforcement ratio  $\rho$  at nail head and mid-span in vertical direction

$$\rho_n [\%] = \frac{a_{vn}}{0.5h} 100 = \frac{(288.2/1000)}{0.5 \times 100} \times 100 = 0.58$$

$$\rho_m [\%] = \frac{a_{vm}}{0.5h} 100 = \frac{(184.2/1000)}{0.5 \times 100} \times 100 = 0.37$$

checks:

$$\rho_n = 0.58\% > \rho_{\min} = 0.21\% \quad \dots \text{ ok}$$

$$\rho_n = 0.58\% < \rho_{\max} = 1.42\% \quad \dots \text{ ok}$$

$$\rho_m = 0.37\% > \rho_{\min} = 0.21\% \quad \dots \text{ ok}$$

$$\rho_m = 0.37\% < \rho_{\max} = 1.42\% \quad \dots \text{ ok and } \rho_n / \rho_m = 1.56 < 2.5 \quad \dots \text{ ok}$$

Permanent facing

Total area of 16 mm diameter @ 300 mm c/c is equal to 670 mm<sup>2</sup>/m (see **Table A.4**).

This area of reinforcement is provided in both vertical and horizontal directions, therefore,  $a_{vn} = a_{hn} = a_{vm} = a_{hm} = 670 \text{ mm}^2/\text{m}$  (no waler bars are provided in permanent facing).

Reinforcement ratio  $\rho$  at nail head and mid-span in vertical direction

$$\rho_n [\%] = \rho_m [\%] = \frac{a_{vn}}{0.5h} 100 = \frac{(670/1000)}{0.5 \times 200} \times 100 = 0.67 \quad (\text{satisfies both } \rho_{\min} = 0.21\% \text{ and}$$

$$\rho_{\max} = 1.42\% \text{ and } \rho_n / \rho_m = 1.0 < 2.5)$$

**Step 5: Verify facing flexural resistance  $R_{FF}$**

Temporary facing

Calculate facing flexural resistance  $R_{FF}$  as:

$$R_{FF} [\text{kN}] = \frac{C_F}{265} \times (a_{vn} + a_{vm}) [\text{mm}^2 / \text{m}] \times \left( \frac{S_h}{S_v} h [\text{m}] \right) \times f_y [\text{MPa}]$$

For temporary facing with thickness  $h = 100 \text{ mm} (= 0.1 \text{ m})$ , adopt  $C_F = 2.0$

$$(a_{vn} + a_{vm}) = 288.2 + 184.2 = 472.4 \text{ mm}^2 / \text{m} ; \text{ nail spacing ratio: } S_h/S_v = 1.0.$$

$$\text{Therefore, } R_{FF} [\text{kN}] = \frac{2}{265} \times 472.4 \times (1 \times 0.1) \times 415 = 148$$

Safety factor against facing flexural failure  $FS_{FF}$  is given by

$$FS_{FF} = \frac{R_{FF}}{T_o} = \frac{148}{63} = 2.35 (> 1.50 \text{ safe for static case})$$

$$FS_{FF} = \frac{R_{FF}}{T_o} = \frac{148}{83.67} = 1.76 (> 1.10 \text{ safe for seismic case})$$

Permanent facing

For permanent facing with thickness  $h = 200 \text{ mm} (= 0.2 \text{ m})$ , adopt  $C_F = 1.0$

$$(a_{vn} + a_{vm}) = 670 + 670 = 1340 \text{ mm}^2 / \text{m}; \text{ nail spacing ratio: } S_h/S_v = 1.0.$$

$$\text{Therefore, } R_{FF} [\text{kN}] = \frac{1}{265} \times 1340 \times (1 \times 0.2) \times 415 = 420$$

Safety factor against facing flexural failure  $FS_{FF}$  is given by

$$FS_{FF} = \frac{R_{FF}}{T_o} = \frac{420}{63} = 6.67 (> 1.50 \text{ safe for static case})$$

$$FS_{FF} = \frac{R_{FF}}{T_o} = \frac{420}{83.67} = 5.02 (> 1.10 \text{ safe for seismic case})$$

**Step 6: Verify facing punching shear resistance  $R_{FP}$**

Temporary facing: Check for bearing-plate connection

Facing punching shear capacity  $R_{FP}$  is given by:

$$R_{FP} [\text{kN}] = 330 \sqrt{f_{ck} [\text{MPa}]} \pi D_c' [m] h_c [m]$$

$$\text{Here: } f_{ck} = 20 \text{ MPa}; h_c = h = 0.1 \text{ m}; D_c' = L_{BP} + h = 225 + 100 = 325 \text{ mm} = 0.325 \text{ m}$$

Substituting values of various parameters, temporary facing punching shear capacity  $R_{FP}$

is calculated as

$$R_{FP} [\text{kN}] = 330 \times \sqrt{20} \times \pi \times 0.325 \times 0.1 = 150$$

Safety factor against facing punching shear failure  $FS_{FP}$  is given by

$$FS_{FP} = \frac{R_{FP}}{T_o} = \frac{150}{63} = 2.38 (> 1.50 \text{ safe for static case})$$

$$FS_{FP} = \frac{R_{FP}}{T_o} = \frac{150}{83.67} = 1.79 (> 1.10 \text{ safe for seismic case})$$

Permanent facing: Check for headed-stud connection

Here:  $f_{ck} = 20$  MPa;  $L_S = 100$  mm;  $D_H = 25$  mm;  $D_S = 13$  mm;  $t_H = 8$  mm;  $S_{HS} = 150$  mm;

$t_p = 25$  mm.

$h_c = L_S - t_H + t_p = 100 - 8 + 25 = 117$  mm = 0.117 m;  $2h_c = 0.234$  m

$D'_c = \text{minimum of } (S_{HS} + h_c \text{ and } 2h_c)$

$S_{HS} + h_c = 150 + 117 = 267$  mm = 0.267 m

Therefore,  $D'_c = 0.234$  m (minimum of  $S_{HS} + h_c$  and  $2h_c$ )

Substituting values of various parameters, permanent facing punching shear capacity  $R_{FP}$  is calculated as:

$$R_{FP} [\text{kN}] = 330 \times \sqrt{20} \times \pi \times 0.234 \times 0.117 = 127$$

Safety factor against facing punching shear failure  $FS_{FP}$  is given by

$$FS_{FP} = \frac{R_{FP}}{T_o} = \frac{127}{63} = 2.01 (> 1.50 \text{ safe for static case})$$

$$FS_{FP} = \frac{R_{FP}}{T_o} = \frac{127}{83.67} = 1.52 (> 1.10 \text{ safe for seismic case})$$

**Step 7: Verify headed-stud resistance  $R_{HT}$  (only for permanent facing)**

Tensile capacity of the headed-studs

$$\text{For: } N_H = 4; A_{SH} = \frac{\pi D_S^2}{4} = \frac{\pi \times 13^2}{4} = 132.73 \text{ mm}^2; f_y = 0.415 \text{ kN/mm}^2$$

Nail head capacity against tensile failure of the headed-studs  $R_{HT}$  can be computed as:

$$R_{HT} [\text{kN}] = N_H A_{SH} f_y = 4 \times 132.73 \times 0.415 = 220.33$$

Safety factor against headed-stud tensile failure  $FS_{HT}$  is given by

$$FS_{HT} = \frac{R_{HT}}{T_o} = \frac{220.23}{63} = 3.49 (> 1.50 \text{ safe for static case})$$

$$FS_{HT} = \frac{R_{HT}}{T_o} = \frac{220.23}{83.67} = 2.63 (> 1.10 \text{ safe for seismic case})$$

Check for tolerable limits of compression on the concrete behind headed-stud

$$A_H = \frac{\pi D_H^2}{4} = \frac{\pi \times 25^2}{4} = 490.87 \text{ mm}^2 \text{ and } A_{SH} = \frac{\pi D_S^2}{4} = \frac{\pi \times 13^2}{4} = 132.73 \text{ mm}^2$$

To assure that the compression on the concrete behind headed-stud is within tolerable limits, following two conditions shall be satisfied:

(a)  $A_H \geq 2.5A_{SH} \Rightarrow 490.87 \geq 2.5(132.73) = 490.87 \text{ mm}^2 \geq 331.82 \text{ mm}^2 \dots\dots\text{ok}$

(b)  $t_H \geq 0.5(D_H - D_S) \Rightarrow 8 \geq 0.5(25 - 13) = 8 \text{ mm} \geq 6 \text{ mm} \dots\dots\text{ok}$

#### **5.4.4 GENERAL CONSIDERATIONS AND DESIGN SUMMARY**

##### **5.4.4.1 General considerations**

*(a) Permissible lateral deformation*

Depending on the soil type, permissible lateral deformation of the soil nail wall shall be within 0.1-0.3% of the vertical height H. For sandy soils (in present example), permissible lateral wall deformation = 0.002H = 0.002 x 8000 = 16 mm.

*(b) Drainage and corrosion resistance*

Since the groundwater table at the construction site is well below the zone of influence, internal drainage can be considered sufficient in the form of geocomposite drain strips, weepholes and toe drains. For surface drainage, suitable provisions shall be made in agreement with opinion of contractor and the site-engineer. Although, the ground corrosion potential is unknown in the present example, suitable measures against corrosion protection shall be adopted. A minimum grout thickness of 25 mm over nail bars shall be provided.

##### **5.4.4.2 Design summary**

**Tables 5.6-5.8** presents the summary of soil nail wall design example presented above. Further, **Fig. 5.2** shows the details of reinforcement in both temporary and permanent facings.

**Table 5.6** Summary of important design parameters.

Parameter	Value
Number of nails per section	5.0
Nail inclination $i$ [degrees]	15.0
Drillhole diameter $D_{DH}$ [mm]	130.0
Diameter of nails $d$ [mm]	25.0
Length of nails $L_N$ [m]	4.8
Spacing $S_h \times S_v$ [m x m]	1.5 x 1.5
Maximum axial tensile force $T_{max}$ [kN] (seismic case)	90.0 (119.53)

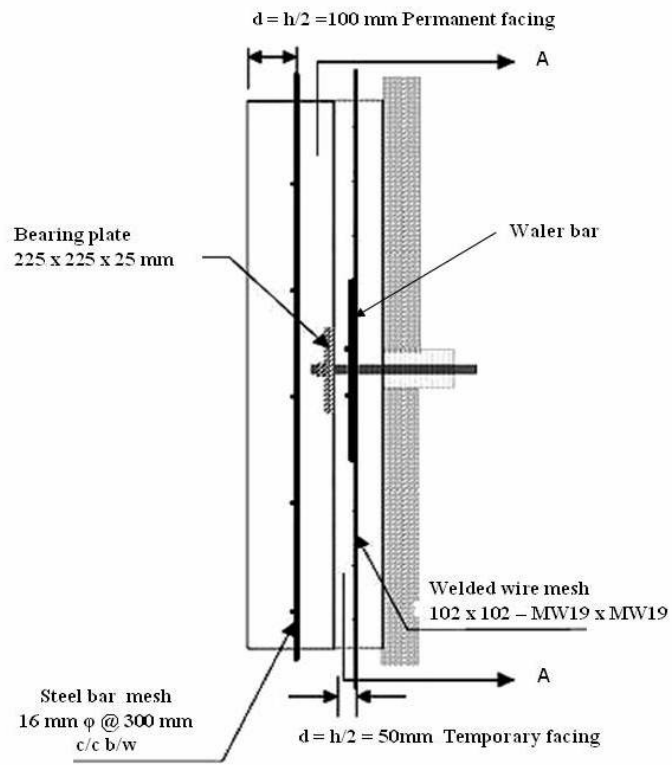
**Table 5.7** Summary of factors of safety attained for various failure modes.

Failure mode	Remarks	Factor of safety	
		Seismic	Static
Global $FS_G$	--	1.77	1.54
Sliding $FS_{SL}$	--	2.90	1.50
Pull-out resistance $FS_P$	Minimum	1.90	1.43
Nail bar tensile strength $FS_T$	Minimum	2.26	1.70
Facing flexure $FS_{FF}$	Temporary facing	2.35	1.76
	Permanent facing	6.67	5.02
Facing punching $FS_{FP}$	Temporary facing	2.38	1.79
	Permanent facing	2.01	1.52
Headed stud tensile $FS_{HT}$	--	3.49	2.63

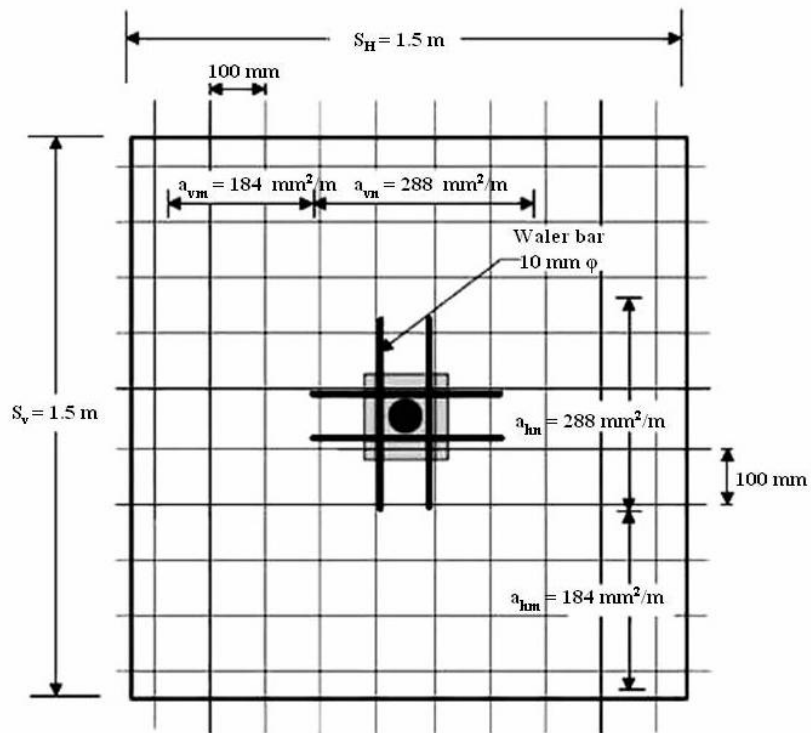
**Table 5.8** Summary of facing design (temporary and permanent).

Element	Description	Temporary facing	Permanent facing
General	Thickness $h$	100	200
	Facing type	Shotcrete	CIP concrete
	Concrete grade	M20	M20
Reinforcement	Type	Welded wire mesh (WWM)	Steel bars
	Steel grade	Fe415	Fe415
	Denomination	102 x 102 – MW19 x MW19	16 $\phi$ @ 300 b/w
Other reinforcement	Type	Waler bars 2 - 10 $\phi$ b/w	--
Bearing plate	Type	Square	4H-Studs 1/2 x 4 1/8
	Steel	Fe250	--
	Dimensions	225 x 225 x 25	--
Headed studs	Dimensions	--	Nominal length, $L_S = 100$
		--	Head diameter, $D_H = 25$
		--	Shaft diameter, $D_S = 13$
		--	Head thickness, $t_H = 08$
		--	Spacing, $S_{HS} = 150$

All dimensions are in mm



(a) Side view



(b) Section A-A

**Fig. 5.2** Details of facing reinforcement.

## **SECTION 6: FIELD PULLOUT TESTING OF SOIL NAILS**

### **6.1 INTRODUCTION**

Field pullout testing of soil nails shall be conducted (a) to verify that the nail design loads can be carried without excessive movements and with an adequate safety factor for the service life of the structure, and (b) to verify the adequacy of the contractor's drilling, installation, and grouting operations prior to and during construction of production soil nails.

### **6.2 FIELD PULLOUT TEST APPARATUS**

A center-hole hydraulic jack and hydraulic pump shall be used to apply a test load to a nail bar. The axis of the jack and the axis of the nail must be aligned to ensure uniform loading. Typically, a jacking frame or reaction block is installed between the shotcrete or excavation face and the jack. The jacking frame should not react directly against the nail grout column during testing. Once the jack is centered and aligned, an alignment load should be applied to the jack to secure the equipment and minimize the slack in the set-up. The alignment load should not be permitted to exceed 5 percent of the maximum test load.

Movement of the nail head should be measured with at least one, and preferably two, dial gauges mounted on a tripod or fixed to a rigid support that is independent of the jacking set-up and wall. The use of two dial gauges provides: (1) an average reading in case the loading is slightly eccentric due to imperfect alignment of the jack and the nail bar, and (2) a backup if one gauge malfunctions. The dial gauges should be aligned within 5 degrees of the axis of the nail, and should be zeroed after the alignment load has been applied. The dial gauges should be capable of measuring to the nearest 0.02 mm. The dial

gauges should be able to accommodate a minimum travel equivalent to the estimated elastic elongation of the test nail at the maximum test load plus 25 mm, or at least 50 mm.

A hydraulic jack is used to apply load to the nail bar while, a pressure gauge is used to measure the applied load. A center-hole load cell may be added in series with the jack for use during creep tests. For extended load hold periods, load cells are used as a means to monitor a constant applied load while the hydraulic jack pump is incrementally adjusted. Over extended periods of time, any load loss in the jack will not be reflected with sufficient accuracy using a pressure gauge. Recent calibration data for the jack, pressure gauge, and load cell must be obtained from the contractor prior to testing. **Fig. 6.1** shows schematically a test set up for field testing of soil nails.

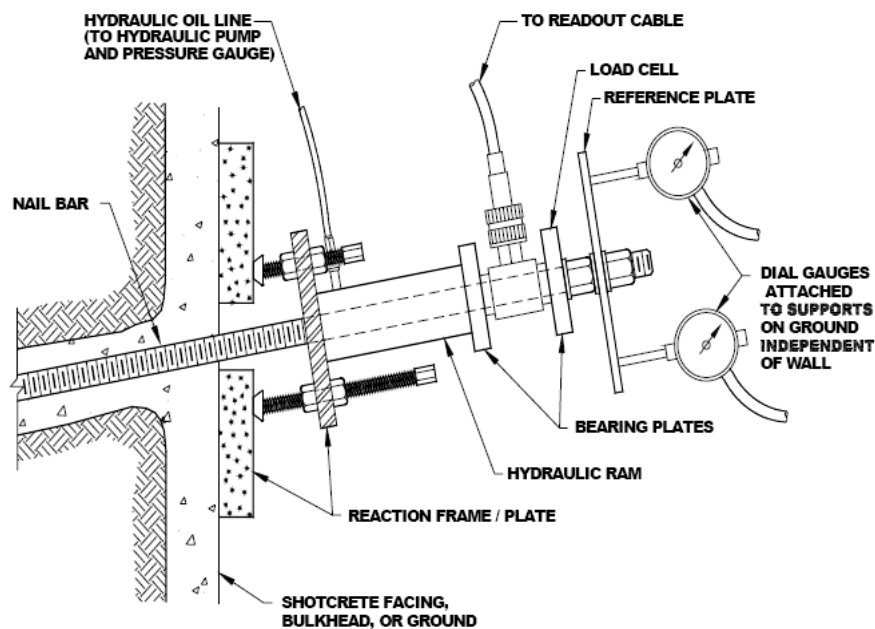


**Fig. 6.1** Field pullout test set up (FHWA 2003).

### 6.3 TYPES OF FIELD PULLOUT TESTS

Depending upon the type of test being performed, the maximum test load, the load increments, and the time that each load increment is held shall be determined. To prevent chances of explosive failure of the steel, in no case, the soil nail tendon be stressed to

more than 80 percent of its minimum ultimate tensile strength for grade Fe415 steel, or more than 90 percent of the minimum yield strength for grade Fe500 steel.

### **6.3.1 Verification test**

A verification test on soil nail is performed: (a) to determine the ultimate bond capacity (if carried to pullout failure); (b) verify the design bond factor of safety, and (c) to determine the soil nail load at which excessive creep occurs. In general, the maximum verification test load shall verify 200 percent of the design bond capacity to ensure a minimum factor of safety of 2.0 against pullout failure of soil nails. Verification tests are generally conducted on non-production “sacrificial” nails as a first order of work prior to construction. Verification test when conducted to failure is known as ultimate test. Verification test nails shall have both bonded and (temporary) unbonded lengths i.e. nail length without grout cover.

### **6.3.2 Proof test**

A proof test is typically performed on a specified number of the total number of production soil nails installed. Typically, successful proof tests shall be performed on 5 percent of the production nails in each row or a minimum of 1 test per row. This test is a single cycle test in which the load is applied in increments until a maximum test load, typically 125 to 150 percent of the design bond capacity, is achieved. Proof tests provide information necessary to evaluate the ability of production soil nails to safely withstand design loads without excessive structural movement or long-term creep over the structure’s service life.

### **6.3.3 Creep Test**

Creep tests are typically performed as part of a verification or proof test. Creep testing is conducted at a specified, constant test load, with movement recorded at specified time

intervals. The deflection-versus-log-time results are plotted on a semi-log graph, and are compared with the acceptance criteria specified in the contract documents.

## 6.4 TEST PROCEDURE

### 6.4.1 Procedure for verification test

(a) Calculate design test load as:

The design test load DTL shall be determined by the following equation:

$$DTL = L_B \times Q_{all} \quad (6.1)$$

where:

$L_B$  = soil nail bonded length; which shall be not be less than 3 m and more than  $(L_B)_{max}$  (so as to ensure that the nail load does not exceed 80 percent of the allowable nail bar tensile strength during verification test) given by Eq. (6.2).

$$(L_B)_{max} = \frac{0.8 \times A_t \times f_y}{Q_{all} \times (FS_T)_{ver}} \quad (6.2)$$

where:  $A_t$  = nail bar cross-sectional area;  $f_y$  = nail bar yield strength;  $Q_{all}$  = allowable pullout resistance per unit length ( $Q_{all} = Q_u / FS_P$ );  $(FS_T)_{ver}$  = factor of safety against tensile failure of nail during verification tests (generally 2.5 or 3.0).

*Note: The unbonded length of test nail shall be at least 1 m.*

(b) The verification test shall be conducted by measuring and recording the incremental test load applied to the verification soil nail and the movement of the soil nail head at each load increment. Verification test nail may be loaded to failure or a maximum test load of 300 percent of the DTL in accordance with the loading schedule shown in **Table 6.1**.

(c) Each increment of load shall be held for at least 10 minutes. Monitor the verification test nail for creep at the 1.50DTL load increment. Measure and record

nail movements during creep portion of the test at 1 minute, 2, 3, 4, 5, 6, 10, 20, 30, 40, 50, and 60 minutes. Maintain the load during the creep test within 2 percent of the intended load by use of the load cell.

**Table 6.1** Loading schedule for verification test.

Test load	Hold time
0.05 DTL max. (AL)	1 minute
0.25 DTL	10 minutes
0.50 DTL	10 minutes
0.75 DTL	10 minutes
1.00 DTL	10 minutes
1.25 DTL	60 minutes
1.50 DTL (Creep test)	10 minutes
1.75 DTL	10 minutes
2.00 DTL	10 minutes
2.50 DTL	10 minutes max.
3.00 DTL or Failure	10 minutes max.
0.05 DTL max. (AL)	1 minute (record permanent set)

Note: The alignment load AL should not exceed 5 percent of DTL and dial gages should be set to zero after the application of AL.

#### 6.4.2 Procedure for proof test

(a) Calculate design test load DTL using Eqs. (6.1) and (6.2) by adopting factor of safety against tensile failure of nail for proof production test equal to 1.5.

*Note: Production proof test nails shorter than 4 m in length may be tested with bond length less than 3 m.*

(b) Perform proof tests by incrementally loading the proof test nail to 150 percent of the DTL in accordance with the loading schedule shown in **Table 6.2**. Record the soil nail movements at each load increment.

(c) The creep period shall start as soon as the maximum test load 1.50 DTL is applied and the nail movement shall be measured and recorded at 1 minute, 2, 3, 5, 6, and 10 minutes. Where the nail movement between 1 minute and 10 minutes exceeds 1 mm, maintain the maximum test load for an additional 50 minutes and record movements

at 20 minutes, 30, 50, and 60 minutes. Maintain all load increments during creep test period within 5 percent of the intended load.

**Table 6.2** Loading schedule for proof test.

Test load	Hold time
0.05 DTL max. (AL)	Until movement stabilizes
0.25 DTL	Until movement stabilizes
0.50 DTL	Until movement stabilizes
0.75 DTL	Until movement stabilizes
1.00 DTL	Until movement stabilizes
1.25 DTL	Until movement stabilizes
1.50 DTL (max. test load)	Start creep test

Note: The alignment load AL should not exceed 5 percent of DTL and dial gages should be set to zero after the application of AL.

## 6.5 TEST ACCEPTANCE CRITERIA

Preliminary requirement of field pullout testing is that the both test nails and the production nails shall have the same method of installation, the soil/rock conditions, equipment, and the operator. Moreover, testing should be completed in each row of nails prior to excavation and installation of the underlying row. If inadequate test results indicate faulty construction practice or bond capacities less than required, the contractor should be required to alter nail installation/construction methods. In the event that required design adhesion capacities are still not achievable, redesign may be necessary.

### 6.5.1 Acceptance criteria for verification test

The verification test acceptance criteria require that:

- (a) no pullout failure occurs at 200 percent of the design load where pullout failure is defined as the inability to maintain constant test load without excessive movement; and
- (b) the total measured movement  $\Delta L$  at the test load of 200 percent of design load must exceed 80 percent of the theoretical elastic movement of the unbonded length UL i.e.

$$\Delta L_{\min} = 0.8 \frac{P \times UL}{EA} \quad (6.3)$$

where:  $\Delta L_{\min}$  = minimum acceptable movement; P = maximum applied test load; UL = unbonded length of test nail (measure from the back of reference plate to top of the grouted length); A = cross-sectional area of the nail bar; and E = Young's modulus of steel (typically 200 GPa).

This criterion ensures that load transfer from the soil nail to the soil occurs only in the bonded length and not in the unbonded length.

### **6.5.2 Acceptance criteria for proof test**

The acceptance criteria for proof test require that no pullout failure occurs and that the total movement at the maximum test load of 150 percent of design load must exceed 80 percent of the theoretical elastic movement of the unbonded length. Again, the measured movement must be  $\Delta L \geq \Delta L_{\min}$ , where  $\Delta L_{\min}$  is as defined in Eq. (6.3).

### **6.5.3 Acceptance criteria for creep test**

*For verification tests*, the total creep movement should be less than 2 mm between the 6- and 60-minute readings and the creep rate should show linear or decreasing trend throughout the creep test load hold period. *For proof tests*, the total creep movement should be less than 1 mm during the 10-minute readings or the total creep movement should be less than 2 mm during the 60-minute readings and the creep rate should show linear or decreasing trend throughout the creep test load hold period.

## **6.6 TYPICAL TEST DATA SHEET**

**Fig. 6.2** shows the typical format for soil nail field pullout test data sheet.



**APPENDIX A**  
**GENERAL DESIGN TABLES**

**Table A.1**  
**Minimum Recommended Factors of Safety for the Design of Soil Nail Structures using the ASD Method**

Failure mode	Resisting component	Symbol	Factors of safety		
			Static		Seismic (Temporary and permanent structures)
			Temporary structures	Permanent structures	
External stability	Global stability	FS <sub>G</sub>	1.35	1.5	1.1
	Sliding stability	FS <sub>SL</sub>	1.3	1.5	1.1
	Bearing capacity	FS <sub>H</sub>	2.5 <sup>(1)</sup>	3.0 <sup>(1)</sup>	2.3 <sup>(1)</sup>
Internal stability	Pullout resistance	FS <sub>P</sub>	2.0	2.0	1.5
	Nail bar tensile strength	FS <sub>T</sub>	1.8	1.8	1.35
Facing strength	Facing flexure	FS <sub>FF</sub>	1.35	1.5	1.1
	Facing punching shear	FS <sub>FP</sub>	1.35	1.5	1.1
	Headed-stud tensile	FS <sub>HT</sub>	1.5-1.8	1.7-2.0	1.3-1.5

Source: FHWA (2003)

Note:

(1) The safety factors for bearing capacity are applicable when using standard bearing-capacity equations. When using stability analysis programs to evaluate this failure mode, the factors of safety for global stability apply.

**Table A.2**  
**Estimated Bond Strength of Soil Nails in Soil and Rock**

Material	Construction method	Soil/rock type	Ultimate bond strength, $q_u$ [kPa]
Rock	Rotary drilled	Marl/limestone	300 -400
		Phyllite	100 -300
		Chalk	500 -600
		Soft dolomite	400 -600
		Fissured dolomite	600 - 1000
		Weathered sandstone	200 -300
		Weathered shale	100 -150
		Weathered schist	100 -175
		Basalt	500 -600
		Slate/hard shale	300 -400
Cohesionless soils	Rotary drilled	Sand/gravel	100 - 180
		Silty sand	100 - 150
		Silt	60 - 75
		Piedmont residual	40 - 120
		Fine colluvium	75 - 150
	Driven casing	Sand/gravel low overburden	190 - 240
		high overburden	280 - 430
		Dense moraine	380 - 480
		Colluvium	100 - 180
	Augered	Silty sand fill	20 - 40
		Silty fine sand	55 - 90
		Silty clayey sand	60 - 140
Jet grouted	Sand	380	
	Sand/gravel	700	
Fine-grained soils	Rotary drilled	Silty clay	35 -50
	Driven casing	Clayey silt	90 -140
	Augered	Loess	25 - 75
		Soft clay	20 - 30
		Stiff clay	40 - 60
		Stiff clayey silt	40 - 100
Calcareous sandy clay	90 - 140		

Source: FHWA (2003)

**Table A.3**  
**Welded Wire Mesh Dimensions**

Mesh designation <sup>(1), (2)</sup> (mm x mm –mm <sup>2</sup> x mm <sup>2</sup> )	Wire cross-sectional area per unit length <sup>(3)</sup> (mm <sup>2</sup> /m)	Weight per unit area (kg/m <sup>2</sup> )
102x102 - MW9xMW9	88.9	1.51
102x102 -MW13xMW13	127.0	2.15
102x102 -MW19xMW19	184.2	3.03
102x102 -MW26xMW26	254.0	4.30
152x152 - MW9xMW9	59.3	1.03
152x152 -MW13xMW13	84.7	1.46
152x152 -MW19xMW19	122.8	2.05
152x152 -MW26xMW26	169.4	2.83

Source: FHWA (2003)

Notes:

- (1) The first two numbers indicate the mesh opening size, whereas the second pair of numbers following the prefixes indicates the wire cross-sectional area.
- (2) Prefix M indicates metric units. Prefix W indicates plain wire. If wires are pre-deformed, the prefix D shall be used instead of W.
- (3) This value is obtained by dividing the wire cross-sectional area by the mesh opening size.

**Table A.4**  
**Area of Reinforcement Bars at given Spacings**  
**(Values in cm<sup>2</sup> per Meter width)**

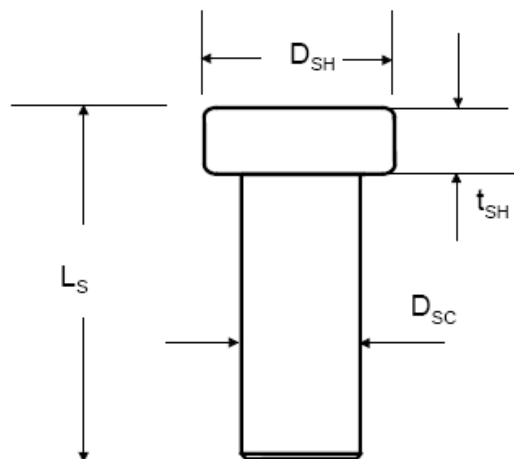
Spacing (cm)	Reinforcement bar diameter (mm)											
	6	8	10	12	14	16	18	20	22	25	28	32
<b>5</b>	5.65	10.05	15.71	22.62	30.79	40.21	50.89	62.83	76.03	98.17	123.15	160.85
<b>6</b>	4.71	8.38	13.09	18.85	25.66	33.51	42.41	52.36	63.36	81.81	102.63	134.04
<b>7</b>	4.04	7.18	11.22	16.16	21.99	28.72	36.35	44.88	54.30	70.12	87.96	114.89
<b>8</b>	3.53	6.28	9.82	14.14	19.24	25.13	31.81	39.27	47.52	61.36	76.97	100.53
<b>9</b>	3.14	5.59	8.73	12.57	17.10	22.34	28.27	34.91	42.24	54.54	68.42	89.36
<b>10</b>	2.83	5.03	7.85	11.31	15.39	20.11	25.45	31.42	38.01	49.09	61.58	80.42
<b>11</b>	2.57	4.57	7.14	10.28	13.99	18.28	23.13	28.56	34.56	44.62	55.98	73.11
<b>12</b>	2.36	4.19	6.54	9.42	12.83	16.76	21.21	26.18	31.68	40.91	51.31	67.02
<b>13</b>	2.17	3.87	6.04	8.70	11.84	15.47	19.57	24.17	29.24	37.76	47.37	61.87
<b>14</b>	2.02	3.59	5.61	8.08	11.00	14.36	18.18	22.44	27.15	35.06	43.98	57.45
<b>15</b>	1.88	3.35	5.24	7.54	10.26	13.40	16.96	20.94	25.34	32.72	41.05	53.62
<b>16</b>	1.77	3.14	4.91	7.07	9.62	12.57	15.90	19.63	23.76	30.68	38.48	50.27
<b>17</b>	1.66	2.96	4.62	6.65	9.06	11.83	14.97	18.48	22.36	28.87	36.22	47.31
<b>18</b>	1.57	2.79	4.36	6.28	8.55	11.17	14.14	17.45	21.12	27.27	34.21	44.68
<b>19</b>	1.49	2.65	4.13	5.95	8.10	10.58	13.39	16.53	20.01	25.84	32.41	42.33
<b>20</b>	1.41	2.51	3.93	5.65	7.70	10.05	12.72	15.71	19.01	24.54	30.79	40.21
<b>21</b>	1.35	2.39	3.74	5.39	7.33	9.57	12.12	14.96	18.10	23.37	29.32	38.30
<b>22</b>	1.29	2.28	3.57	5.14	7.00	9.14	11.57	14.28	17.28	22.31	27.99	36.56
<b>23</b>	1.23	2.19	3.41	4.92	6.69	8.74	11.06	13.66	16.53	21.34	26.77	34.97
<b>24</b>	1.18	2.09	3.27	4.71	6.41	8.38	10.60	13.09	15.84	20.45	25.66	33.51
<b>25</b>	1.13	2.01	3.14	4.52	6.16	8.04	10.18	12.57	15.21	19.63	24.63	32.17
<b>26</b>	1.09	1.93	3.02	4.35	5.92	7.73	9.79	12.08	14.62	18.88	23.68	30.93
<b>28</b>	1.01	1.80	2.80	4.04	5.50	7.18	9.09	11.22	13.58	17.53	21.99	28.72
<b>29</b>	0.97	1.73	2.71	3.90	5.31	6.93	8.77	10.83	13.11	16.93	21.23	27.73
<b>30</b>	0.94	1.68	2.62	3.77	5.13	6.70	8.48	10.47	12.67	16.36	20.53	26.81
<b>32</b>	0.88	1.57	2.45	3.53	4.81	6.28	7.95	9.82	11.88	15.34	19.24	25.13
<b>34</b>	0.83	1.48	2.31	3.33	4.53	5.91	7.48	9.24	11.18	14.44	18.11	23.65
<b>36</b>	0.79	1.40	2.18	3.14	4.28	5.59	7.07	8.73	10.56	13.64	17.10	22.34
<b>38</b>	0.74	1.32	2.07	2.98	4.05	5.29	6.70	8.27	10.00	12.92	16.20	21.16
<b>40</b>	0.71	1.26	1.96	2.83	3.85	5.03	6.36	7.85	9.50	12.27	15.39	20.11

**Table A.5**  
**Headed-Stud Dimensions**

Headed-Stud Size	Nominal Length	Head Diameter	Shaft Diameter	Head Thickness
	$L_s$ (mm)	$D_H$ (mm)	$D_S$ (mm)	$t_H$ (mm)
$\frac{1}{4} \times 4 \frac{1}{8}$	105	12.7	6.4	4.7
$\frac{3}{8} \times 4 \frac{1}{8}$	105	19.1	9.7	7.1
$\frac{3}{8} \times 6 \frac{1}{8}$	156	19.1	9.7	7.1
$\frac{1}{2} \times 4 \frac{1}{8}$	105	25.4	12.7	7.9
$\frac{1}{2} \times 5 \frac{5}{16}$	135	25.4	12.7	7.9
$\frac{1}{2} \times 6 \frac{1}{8}$	156	25.4	12.7	7.9
$\frac{5}{8} \times 6 \frac{9}{16}$	162	31.8	15.9	7.9
$\frac{3}{4} \times 3 \frac{11}{16}$	89	31.8	19.1	9.5
$\frac{3}{4} \times 4 \frac{3}{16}$	106	31.8	19.1	9.5
$\frac{3}{4} \times 5 \frac{3}{16}$	132	31.8	19.1	9.5
$\frac{3}{4} \times 6 \frac{3}{16}$	157	31.8	19.1	9.5
$\frac{7}{8} \times 4 \frac{3}{16}$	102	34.9	22.2	9.5
$\frac{7}{8} \times 5 \frac{3}{16}$	127	34.9	22.2	9.5
$\frac{7}{8} \times 6 \frac{3}{16}$	152	34.9	22.2	9.5

Source: FHWA (2003)

Note: Locally available headed-studs may be used in-lieu of those mentioned in above table.



**Reference figure for dimensions of Headed-stud**

## APPENDIX B: TYPICAL SOIL NAILING PROJECT SUMMARY

Project No..... Report Date.....

Project Title.....

Project Site.....

Client..... Contractor.....

Type of structure.....

Purpose of structure.....

Duration of project..... (Start date..... Completion Date.....)

### Attachments

Sl.No.	Item	Yes	No	Remark (s), if any
1	Soil testing report			
2	Field pullout test report			
3	Photographs			
4	Other (if any)			
5	Other (if any)			

**TABLE B.1 TECHNICAL INFORMATION**

Parameter	Symbol	Unit	Value	Remark (s), if any
<i>Wall Layout</i>				
Vertical height of soil nail wall	H	m		
Maximum longitudinal stretch	L	m		
Face batter (wrt vertical)	$\alpha$	Degrees		
Slope of backfill	$\beta$	Degrees		
Surcharge (if any)	$q_s$	kPa		
<i>Soil Properties (adopted from soil testing data)</i>				
Cohesion	c	kPa		
Friction angle	$\phi$	Degrees		
Unit weight	$\gamma$	kN/m <sup>3</sup>		
<i>Nail (or Reinforcement) Properties</i>				
Type				
Installation method				
Steel grade				

<i>Reinforcement or Nail Properties Continued</i>				
Length	$L_N$	m		
Nail diameter	D	mm		
Drill hole diameter	$D_{DH}$	mm		
Nail spacing (vertical x horizontal)	$S_V \times S_H$	m x m		
Nail inclination (wrt horizontal)	i	Degrees		
Compressive strength of grout	$f_{ck}$	MPa		

**TABLE B.2 WALL FACING COMPONENTS**

<b>Element</b>	<b>Description</b>	<b>Temporary Facing</b>	<b>Permanent Facing</b>
<b>General</b>	Thickness (mm)		
	Facing type		
	Concrete grade		
<b>Reinforcement</b>	Type		
	Steel grade		
	Size / Denomination		

<b>Bearing Plate</b>	Type		
	Steel		
	Dimensions		
<b>Other Information (s), If any</b>			

**TABLE B.3 FIELD PULLOUT TEST SUMMARY**

<b>Parameter</b>	<b>Test 1</b>	<b>Test 2</b>	<b>Test 3</b>	<b>Remark (s), if any</b>
Depth of test nail (m)				
Maximum pullout load (kN)				
Maximum nail displacement (mm)				

Prepared by

Name.....

Signature.....

Designation.....

Date.....

Place.....



---

## TABLE OF CONTENTS

<b>1</b>	<b>Background</b> .....	<b>1</b>
1.1	General .....	1
1.2	Technical Committee .....	1
1.3	Brainstorming Session .....	1
<b>2</b>	<b>Deep Soil Mixing (DSM)</b> .....	<b>1</b>
2.1	Introduction .....	1
2.2	Design Philosophy .....	3
2.2.1	Mix Design of Grout Slurry.....	4
2.2.2	Process Design.....	4
2.3	Application and Process of DSM .....	4
2.3.1	Bearing Capacity Improvement & Settlement Control (Wet DSM) .....	5
2.3.2	Bending Rigidity for Excavation Support (Gravity & CDSM- Compound DSM) .....	7
2.3.3	General Soil improvement for shallow depth (Mass stabilisation).....	8
2.3.4	Quality control and testing of DSM .....	9
<b>3</b>	<b>Case studies</b> .....	<b>11</b>
3.1	Improvement of Bearing Capacity & Settlement Control (Wet DSM) .....	11
3.1.1	Case study 1: Optimized Foundation for 6 Storey Condominium, Singapore.....	11
3.1.2	Case study 2: Optimised Foundation Systems for Jelutong Sewage Treatment Plant in Penang Island, Malaysia.....	12
3.2	Bending rigidity for excavation support (Gravity wall and CDSM) .....	13
3.2.1	Case Study 1: Black soil Strengthening of Slime for Deep Excavation at Bunus Sewerage treatment plant, Kuala Lumpur, Malaysia .....	13
3.2.2	Case Study 2: Deep Excavation support for Basement of 3-storey commercial complex with 2-level basement, Kuala Lumpur, Malaysia.....	14
3.2.3	Case Study 3: Deep Excavation support for Music Academy Poznan, Poland. ....	15
3.2.4	Case Study 4: Excavation Support for TBM Retrieval Shaft using Deep Soil Mixing Technique, Kuala Lumpur.....	16
3.3	Ground treatment for shallow depth .....	18
3.3.1	Case Study 1: Mass Stabilisation of Peat and Mud for a Road Embankment Gärtnavägen, Sodertälje, Sweden.....	18
<b>4</b>	<b>Bibliography</b> .....	<b>19</b>

## LIST OF FIGURES

Figure 1:	Basic concept of Deep Soil Mixing (Source: Broms, 2004) .....	2
Figure 2:	Single and Multi-shaft mixing .....	2
Figure 3:	Soil mixing patterns in DSM .....	3
Figure 4:	Geomechanical design philosophy for deep stabilisation .....	3
Figure 5:	Wet DSM machine & Ejection of the binder (wet form) from the machine .....	5
Figure 6:	Mixing operations in Wet DSM process .....	6
Figure 7:	Overall process in Wet DSM .....	6
Figure 8:	Typical cross section of gravity DSM wall .....	7
Figure 9:	Typical arrangements of DSM columns .....	8
Figure 10:	Process of installing Steel H sections & Overall view of CDSM arrangements .....	8
Figure 11:	Types of mixing in Shallow depth .....	9
Figure 12:	Typical computer record of the Wet DSM .....	10
Figure 13:	Typical testing methods (Unconfined compressive strength testing on backflow samples) .	10
Figure 14:	Visual examination of exposed columns by means of excavation .....	11
Figure 15:	Pressure vs settlement curve & Completed view of building .....	11
Figure 16:	Plan layout and Proposed foundation system of SBR .....	12
Figure 17:	Settlement monitoring & UCS test results of SBR .....	12
Figure 18:	Completed SBR tanks during hydro test.....	13
Figure 19:	Typical plan & cross section of Treatment scheme and SPT results of Digester tank .....	14
Figure 20:	Typical exposed DSM and Structure after DSM installation .....	14
Figure 21:	Schematic of DSM gravity wall block.....	15

---

Figure 22 Completed excavation.....	15
Figure 23: Typical CDSM scheme and exposed CDSM columns.....	16
Figure 24: Completed structure of Music Academy Poznan.....	16
Figure 25 Typical cross section of the tunnel.....	17
Figure 26: DSM scheme and exposed columns after excavation.....	17
Figure 27: DSM Core Sample UCS Strength Test Results.....	17
Figure 28 Typical cross section of Mass stabilisation .....	19

## LIST OF TABLES

**No table of figures entries found.**

## LIST OF ENCLOSURES

Annexure I	Technical paper on “Soil mixing - Challenges of Application ranging from Ground Improvement to Structural Elements” by Topolnicki M, 2006.
Annexure II	Technical paper on “Quality Control of Wet Deep Soil Mixing with reference to Polish Practices and Applications”.
Annexure III	Technical paper on the project case study on Deep Soil Mixing in Mine tailing for 8m Deep Excavation”, Y. W Yee, V.R. Raju, H K Yandamuri, Kuala Lumpur
Annexure IV	Technical paper on the project case study on “Excavation Support for TBM Retrieval Shaft using Deep Soil Mixing Technique, Kuala Lumpur”, Ir. Yew Weng, Yee and Ir. Yean Chin & Tan.

## **1 Background**

### **1.1 General**

The President Indian Geotechnical Society (IGS) has constituted several Technical Committees (TCs) in order to contribute substantial technical innovations to serve the geotechnical community by publishing guidelines in the field of ground engineering. In this endeavour, IGS formed various TCs to seek support in the preparation of guidelines and publish them on behalf of IGS. In order to form the guidelines, the modus operandi suggested by IGS was to conduct brain-storming sessions in local chapters in each of the selected themes and topics and further to record the proceedings. Each member of the committee shall have to make a presentation followed by a detailed discussion. The chairman of each TC will decide the sub-topics on which the theme paper will be presented by a particular member of the committee, followed by a thorough discussion. The individual TC will develop guidelines with regard to various fields of Geotechnology on behalf of IGS who will contribute in a meaningful way to better geotechnical practices in India.

### **1.2 Technical Committee**

With the above background, IGS has identified Ground Improvement and Geosynthetics is one of the TC and the main objective is to prepare an implementable document for practicing engineers covering Ground Improvement technology, limitations, codal provisions, case histories esp. in India with their performances.

### **1.3 Brainstorming Session**

IGS Hyderabad Chapter has taken initiative to support IGS and conducted one-day National Workshop on Ground Improvement and Geosynthetics on 29<sup>th</sup> August 2015 in JNTU premises. Minutes of meeting was prepared and circulated among the TC members. It was agreed in the meeting that design and construction aspects of ground improvement using Deep Soil Mixing (DSM) shall be addressed by Keller Ground Engineering Pvt. Ltd (Keller).

This document describes concept, theory, design & construction, performance of ground improvement using Deep Soil Mixing for variety of projects executed in Asia.

## **2 Deep Soil Mixing (DSM)**

### **2.1 Introduction**

Ground improvement using deep soil mixing is accepted world-wide in order to enhance the engineering properties such as increase strength, lower permeability and reduced compressibility of soils. The experiences have been positive and deep soil mixing methods are undergoing rapid development, particularly with regard to the explicabilities and cost effectiveness.

The roots of Deep Soil Mixing (DSM) go back to the mid-1950s, when the Mixed in Place (MIP) piling technique was developed. In this method a mechanical mixer was used to mix cementitious grout such as lime, cement or a combination of both in different proportion into the soil for the purpose of creating foundation elements and retaining walls. The grout was injected from the tip of the mixing tool consisting of a drilling head and separated horizontal blades. The technique forms columns within the treated zone whilst improving shear and compressibility parameters of the in-situ loose/soft soils. The basic concept of Deep Soil Mixing is illustrated in Figure 1.

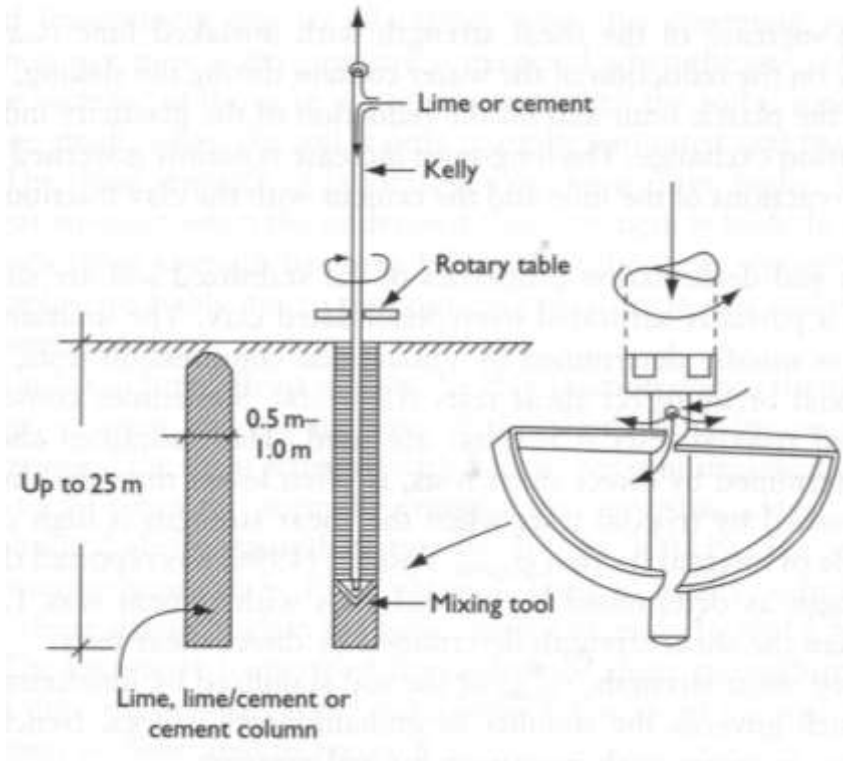


**Figure 1: Basic concept of Deep Soil Mixing (Source: Broms, 2004)**

In general, single or multi shaft are used for mixing process that needs primarily cement-based slurries to create isolated elements, continuous walls or blocks. The different mixing process are shown in Figure 2



**Figure 2: Single and Multi-shaft mixing**

Depending on the purpose of deep mixing works, specific condition of the site, stability calculations and costs of treatment, different patterns of column installations are used to achieve desired results by utilising spaced or overlapping & single or combined columns. Typical patterns of DSM in practice are shown in Figure 3.

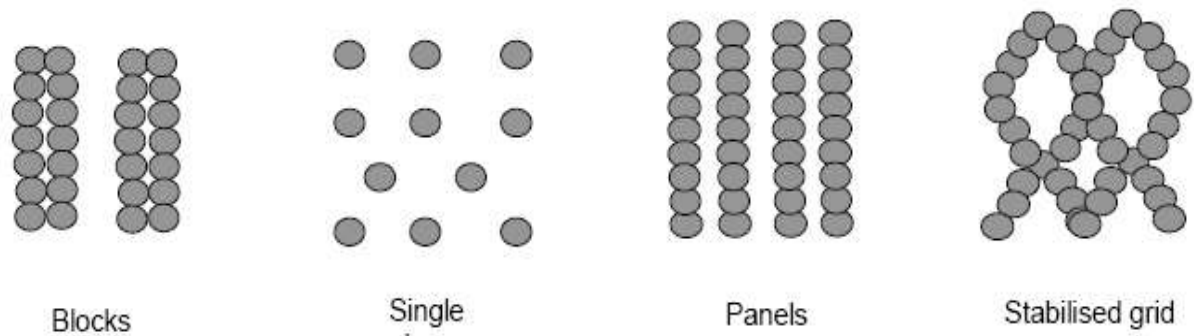


**Figure 3: Soil mixing patterns in DSM**

DSM method is best suited in cohesive soil with high moisture contents & loose, saturated & fine granular soils. It is also used in less cohesive soils, but not feasible in very dense/ stiff materials/ in ground with obstructions characteristics such as cobbles, boulders etc.

## 2.2 Design Philosophy

The design philosophy for DSM is to produce a relatively rigid and high strength pile-like column that mechanically interacts with the surrounding natural soil. The applied load is partly carried by the columns and partly by the unstabilised soil between the columns. Therefore, a too stiffly stabilised material is not necessarily the best solution since such a material will behave like a pile. Instead, the increased stiffness and strength of the stabilised soil should not prevent an effective interaction and load distribution between the stabilised and natural soil. This philosophy is schematically described in Figure 4.

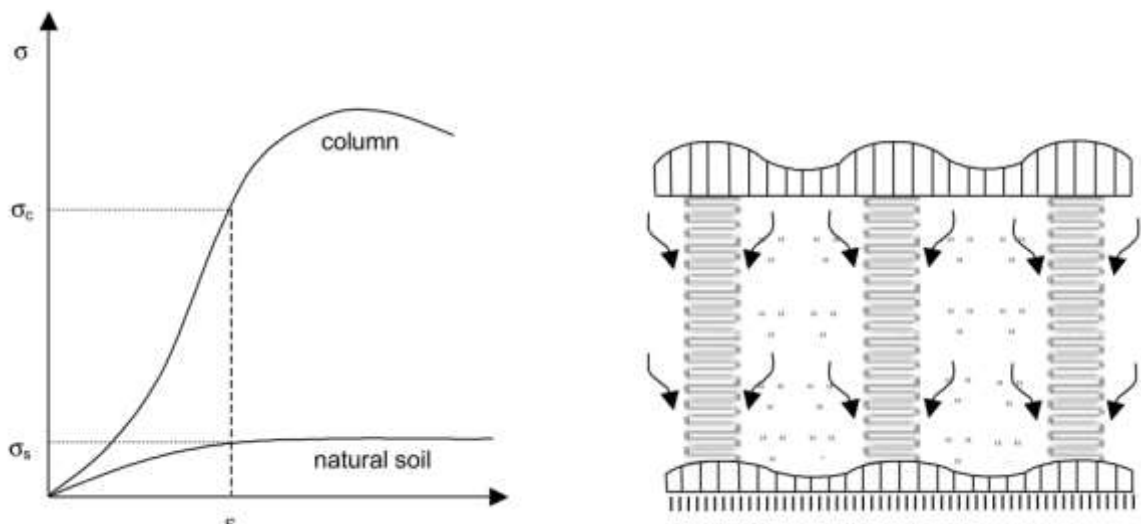


**Figure 4: Geomechanical design philosophy for deep stabilisation**

To compare various column patterns in terms of the treatment area and to evaluate composite properties of the treated elements and surrounding untreated soil, a purposely defined ratio of area improvement ( $a_p$ ) is used

$$a_p = \frac{\text{Net area of soil mixing}}{\text{Respective total area}}$$

For group of columns, to avoid too risky designs with low  $a_p$  values and high strength elements, it has been generally recommended that the width of the improved ground should

be larger than the thickness of soft soil. Depending upon the application, the DSM are frequently designed with area improvement ratios between 15% to 50 %.

### 2.2.1 Mix Design of Grout Slurry

The grout slurry has to be designed after evaluating the natural moisture content in the in-situ soil, desired viscosity / flow rate of grout slurry to suit available equipment and curing period for hydration process. Typically, water-cement (W/C) ratio ranges between 0.8 and 1.2 with grout slurry densities in the range of 1.4 to 1.6 t/m<sup>3</sup>.

### 2.2.2 Process Design

The objective of process design is to achieve efficient mixing of grout slurry and in-situ soil whilst delivering design quantities of grout slurry per cubic meter of soil. The process operating parameters has to be designed to achieve design binder content and also to suit available equipment (i.e. torque of base machine, maximum rotation speed of mixing tool, type of grout pump, achievable maximum flow rates and flow pressures, diameter and position of nozzles, no. of nozzles and mixing blades, no. of cycles etc.).

Based on the process operating parameters, the blade rotation number (T) is defined as the total number of effective mixing/cutting blades passing during 1m of single shaft movement through the soil (Topolnicki, 2004), and is expressed as follows,

$$T = \Sigma M \times \left( \frac{R_p}{V_p} + \frac{R_w}{V_w} \right)$$

Where,

- ΣM is total number of effective mixing/cutting blades;
- R<sub>p</sub> is rotation speed during penetration;
- V<sub>p</sub> is rate of penetration;
- R<sub>w</sub> is rotation speed during withdrawal;
- V<sub>w</sub> is rate of withdrawal.

## 2.3 Application and Process of DSM

The Deep Soil Mixing techniques can be adopted for the following ground engineering applications

- Enhances the bearing capacity of weak and problematic soil types such as loose sands, soft marine clays, ultra-soft slimes, weak silty clays & sandy silts.
- Control Settlements
- Foundations of embankment fill for highways, railways & runways.
- Slope stabilisation, stabilisation of cuts and excavations.
- Excavation support walls.
- Ground treatment.
- Hydraulic cut-off walls.
- In-situ reinforcement piles and gravity walls.
- Environmental remediation.

Technical paper on “Soil mixing- the challenges of application ranging from ground improvement to structural elements” is attached in Annexure I.

Different methods of DSM used for the above applications are listed below

- Wet Deep Soil Mixing
- Gravity Wall/Compound Deep Soil Mixing (CDSM - I Sections)
- Mass Stabilisation

### 2.3.1 Bearing Capacity Improvement & Settlement Control (Wet DSM)

Wet DSM is used to enhance the bearing capacity and to reduce the settlement of the soft soils. A typical wet DSM unit consists of an installation rig fitted with a mast and a drill motor as shown in Figure 5. The wet binder is mixed separately at a mixing plant (consists of high speed colloidal mixers and agitators) and transported to the rig point in a slurry form with desired flow rate and grout pressure using custom-built pumps. The grout slurry is delivered in the ground through nozzles located below mixing blades.

Mixing is achieved by using an auger-mixing tool connected to the drill motor by a kelly bar. The mixing tool is drilled down to firm ground or intended depth whilst delivering and mixing of required quantity of grout slurry with in-situ soil uniformly. Once at the required depth, the tool is drilled out with the simultaneous injection of grout slurry. Depending on the process design, one or two cycles of mixing operations can be executed. The rotation speed during penetration and withdrawal, rate of penetration and withdrawal, flow rate of grout slurry and grout pressure are adjusted such that the desired amount of grout slurry is thoroughly mixed with the in-situ soil. The rotation speed ranges between 40 and 70 rpm; the rate of penetration ranges between 0.6 and 1.2 m/min and rate of withdrawal ranges between 2 and 3 m/min. Typically, the flow rate of grout slurry ranges between 60 and 120 lit/min with grout pressures of 30 to 60 bars.



**Figure 5: Wet DSM machine & Ejection of the binder (wet form) from the machine**

The process of efficient mixing of grout slurry with in-situ soil is shown in Figure 6. The amount of slurry injected into the ground is continuously monitored by flow sensors to verify whether the required amount of grout slurry has actually been utilised uniformly over the length of the column.



**Figure 6: Mixing operations in Wet DSM process**

The overall Wet DSM process is illustrated in Figure 7. The execution method of the soil mixing process is laid down in the European Standard prEN14679 (2003).



**Figure 7: Overall process in Wet DSM**

The amount of cement in the grout slurry is usually in the range of 250 to 400 kg/m<sup>3</sup> of soil. The final result of the Wet DSM process is a relatively rigid soil mass in the shape of a cylindrical column with improved deformation and shear strength characteristics. Typically, undrained shear strength of the columns ranges between 500 and 2000 kPa. The rate of strength gain is dependent on soil conditions but typically requires about 2 to 4 weeks of minimum curing period. Typical column diameter ranges from 0.8m to 1.5m and maximum treatment depth from 15m to 20m.

### 2.3.2 Bending Rigidity for Excavation Support (Gravity & CDSM- Compound DSM)

Gravity type structures are subjected to large horizontal forces caused by earth pressure. For this type of structures DSM techniques that utilize an array of soil/cement columns arranged in the native soil in a manner that creates a gravity block. This block resists the sliding and overturning loads and thus eliminated the need for bracing or tieback anchors for stability. All the support elements are placed prior to any excavation, thus speeding the construction schedule. Because it is a gravity block, no steel reinforcement is needed. Typical gravity wall cross section is shown Figure 8.



**Figure 8: Typical cross section of gravity DSM wall**

Retention systems comprise applications associated with restraining the earth pressure mobilised during deep excavations and vertical cuts in soft ground, with protection of structures surrounding excavations measures against base heave and prevention of landslides and slope failures. In these applications blocks wall column patters are mainly used while the soil binder mix is typically engineered to have strength and stiffness. To overcome soil and water lateral pressures the DSM columns should have adequate internal shear.

Steel pipes or H beams can be installed in DSM columns executed with the wet method to increase the bending resistance and create a structural wall for excavation support. Elongated mixing time and /or full restroking are usually applied to ensure easier installation of soldier elements immediately after mixing. Panels of mixed soil between H beam reinforcement are designed to work in arching. Concrete facing, tieback anchors or stage struts are typically used in combination with the DM walls. Drainage media may be required behind the wall to prevent build up excess hydrostatic pressures. Deep circular shafts can be constructed using 2 to 3 concentric rings of overlapping DSM columns acting together in hoop compression.

The typical arrangement of DSM excavation support walls is illustrated in Figure 9. Steel reinforcement is installed in every other DSM column after mixing and the accessible face of each column is trimmed off once the excavation is complete. The wall system is supported with at least one level of struts or anchors and walers for horizontal support. It is common for DSM excavation systems to have multiple levels of support.

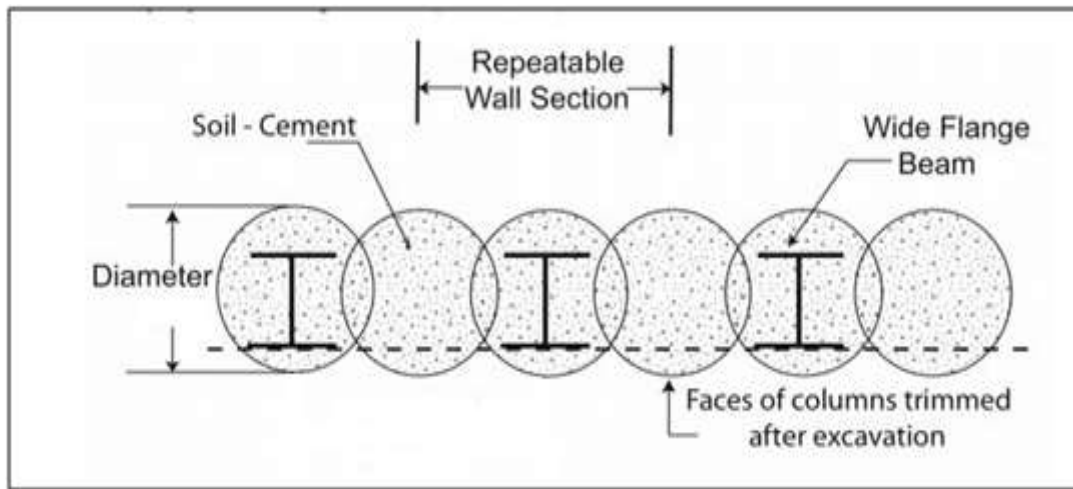


**Figure 9: Typical arrangements of DSM columns**

The use of CDSM is to produce blocks of over lapping piles for nailed or self supporting gravity retaining structures. Steel H sections are installed as structural reinforcement in retaining walls prior to the hardening of the soil-cement mixture. The soil-cement is designed to arch between adjacent steel H sections. The process of installing steel H sections & overall view of CDSM arrangements is shown in Figure 10.



**Figure 10: Process of installing Steel H sections & Overall view of CDSM arrangements**

### 2.3.3 General Soil improvement for shallow depth (Mass stabilisation)

The Complementary Shallow Mixing Method (SMM) has been specially developed to reduce the costs of improving loose or soft superficial soils overlying substantial areas, including land disposed dredged sediments and wet organic soils a few meters thick. It is also a suitable method for in-situ remediation off contamination soils and sludges. In such applications, the soils have to be thoroughly mixed in-situ with an appropriate amount to binders to ensure stabilisation of the entire volume of treated soil. Therefore, this type of soils mixing is often referred to as mass stabilisation. Mass stabilisation can be used to a depth of about 5 meters.

In this method special mixing tools are used, which are in most cases fixed to an excavator's rig arm. Mixing is executed vertically or horizontally, with mixing tools that resemble screw propellers having a centrally provided nozzle for binder. The binder is fed from a separate unit which houses the pressurised binder container, compressor, air dryer and supply control unit.

Stabilisation is executed in phases, according to the operational range of the drilling rig, which generally comprises an area of 8 to 10 m<sup>2</sup> and depth up to 4 m. Once the required binder volume has been applied, mixing is continued to assure the optimum mixing properties. The different type of mixing is shown in Figure 11.

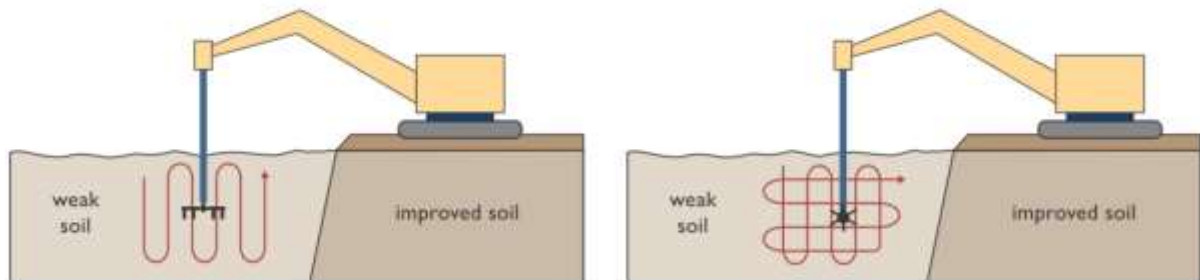


**Figure 11: Types of mixing in Shallow depth**

The total soil volume is stabilised in order to create a block that can carry the load of the embankment. The binder generally consists of cement, quick lime, slag or a mixture of the above. After mass stabilisation the stabilised block is much stiffer than the original soil, which will reduce the settlements and improve stability. Mass-stabilisation (MS) is usually used in combination with lime/cement (LC) columns where the top very soft (primary organic) soils are mass-stabilised and the underlying soft clay is stabilised with lime/cement columns. The mass-stabilisation production rate is highly depended on the type of project and the amount of binder. Generally, the production rate varies between 300-500 m<sup>3</sup>/16 hrs shift.

Mass stabilization can be achieved by installing vertical overlapping columns with up and down movements of rotating mixing tools, as in the case of DSM and is most cost effective when using large diameter mixing augers or multiple shaft arrangements.

#### **2.3.4 Quality control and testing of DSM**

Quality assessment of the DSM products is regarded as one of the pressing issues confronting the implementations of soil mixing. Quality assessment is obtained from the installation records of the columns and from the results of appropriate laboratory and field verification tests.

Quality control during execution is important for DSM also to ensure uniform improvement of the soil. The mixing units are equipped with computerized recording devices to measure real time depth of mixing tool; amount of grout slurry used; flow rate of grout; grout pressure; rotation speed during penetration and withdrawal; and rate of penetration and withdrawal. Typical computer record showing relevant quality control parameters is shown in the Figure 12.

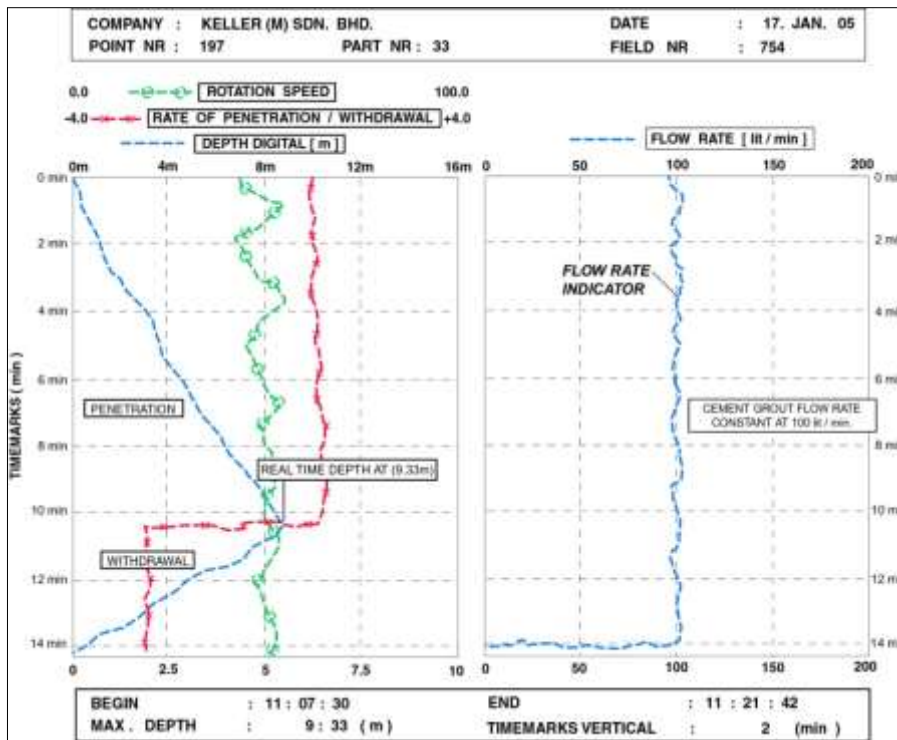


**Figure 12: Typical computer record of the Wet DSM**

After allowing for sufficient curing time, the columns of DSM also can be tested using single and group column plate load tests, unconfined compressive strength on cored and backflow samples, visual examination on exposed columns by means of excavation etc. Typical testing methods are represented in following Figure 13. The visual examinations of the exposed columns are shown in Figure 14. The technical paper on “Quality control of wet deep soil mixing with reference to polish practices and applications” are enclosed in Annexure II.

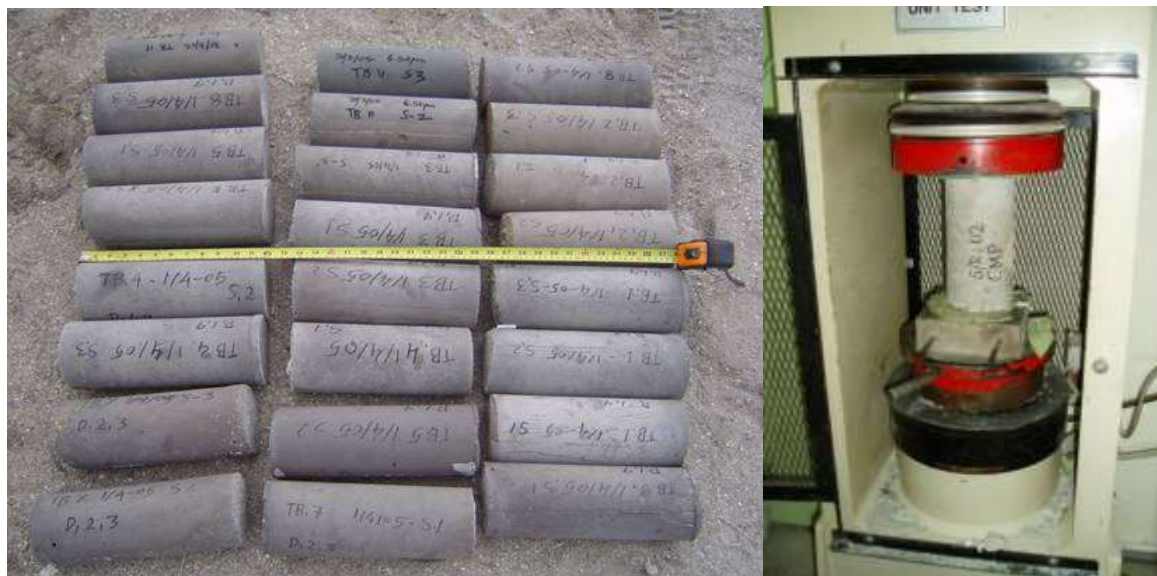


**Figure 13: Typical testing methods (Unconfined compressive strength testing on backflow samples)**



Figure 14: Visual examination of exposed columns by means of excavation

### 3 Case studies

#### 3.1 Improvement of Bearing Capacity & Settlement Control (Wet DSM)

##### 3.1.1 Case study 1: Optimized Foundation for 6 Storey Condominium, Singapore.

M/s Prestigious W- Residences at Sentosa Cove, Singapore proposed to develop a condominium in Singapore. The project comprises of 6 storey condominiums and the approximate area of development is about 1120 m<sup>2</sup>.

The sub soil in the project site comprises of sand for top 2m followed by soft clayey silt up to 10m. This layer was underlying by stiff clay up to 50m. The loading intensity of the proposed structure on the soft soil is 180kPa.

Considering the project boundary conditions, DSM technique with 25 % to 35 % area replacement ratio (Wet DSM) up to maximum of 8 m was adopted as a viable method for subsoil improvement and a full raft foundation supported by the treated found as an alternative foundation system.

Keeping the importance of post performance of the structure, plate load test has been conducted on the improved ground. The graph showing settlement from plate load test and completed structures are shown in Figure 15.

The results of post construction are shown below

- Achieved bearing capacity : > 180kPa
- Settlement : 10mm @ max 180 kPa loading intensity

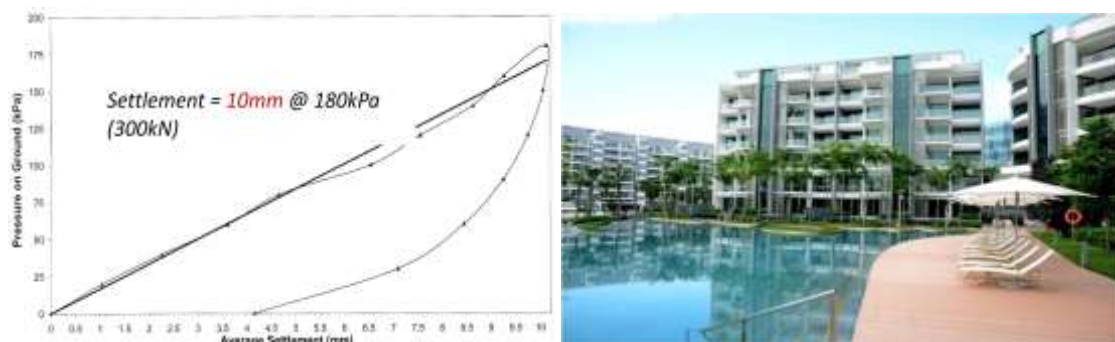


Figure 15: Pressure vs settlement curve & Completed view of building

### 3.1.2 Case study 2: Optimised Foundation Systems for Jelutong Sewage Treatment Plant in Penang Island, Malaysia.

A Jelutong Sewage Treatment plant is under construction in Penang Island and when completed will cater for an ultimate capacity of 1.2 million populations equivalent. The project will serve as a centralized sewage treatment facility and will include 12 nos. of Sequential Batch Reactor (SBR) tanks and associated process tanks.

The subsoil primarily consists of 3m to 5m thick reclaimed fill / domestic waste dumps followed by 5m to 7m thick soft marine clay. This is followed by stiff to very stiff cohesive deposits to over 50m depth. The ground water table varied between 1m and 2m below existing ground level.

The foundation system was designed to ensure adequate bearing capacity (to support loading intensity of 92kPa), limit the total settlement of the structure to be less than 75mm and differential settlement to be less than 1(V):360(H).

DSM technique with 8 % to 12 % area replacement ratio (Wet DSM) up to maximum of 14 m was adopted. The plan layout and proposed foundation system using cement mix piles at SBR is shown in Figure 16.

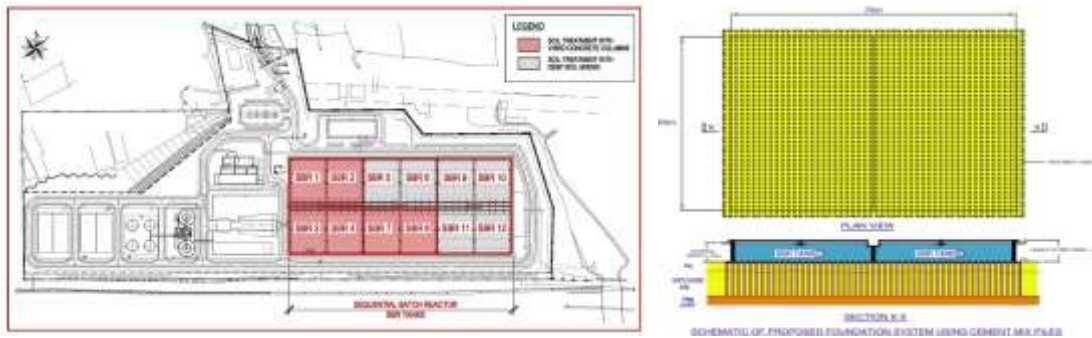


Figure 16: Plan layout and Proposed foundation system of SBR

The settlements were monitored using precise survey instruments during and after Hydro tests and UCS results are shown in Figure 17. The completed SBR tanks during hydro test is shown in Figure 18.

The results of post construction are shown below

- Achieved bearing capacity : > 90kPa
- Settlement : 5 to 20mm (During hydro test)

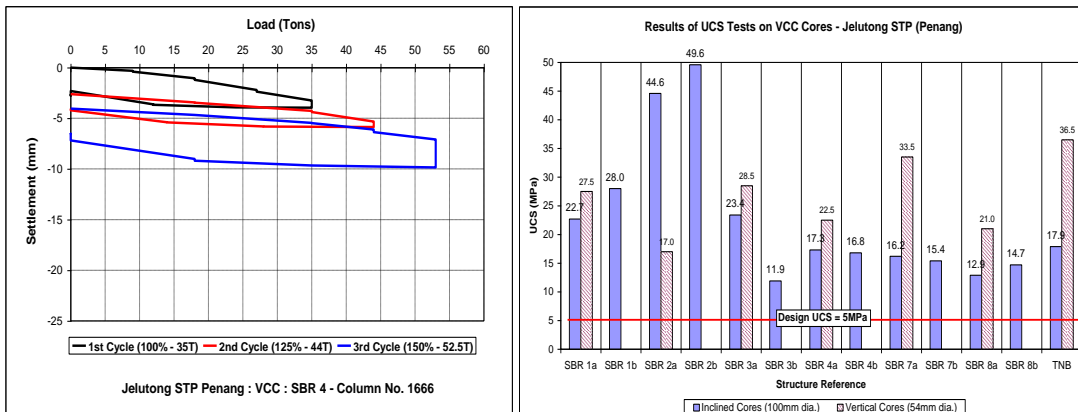


Figure 17: Settlement monitoring & UCS test results of SBR



**Figure 18: Completed SBR tanks during hydro test**

## **3.2 Bending rigidity for excavation support (Gravity wall and CDSM)**

### **3.2.1 Case Study 1: Black soil Strengthening of Slime for Deep Excavation at Bunus Sewerage treatment plant, Kuala Lumpur, Malaysia**

The Sewage Services Department of the Ministry of Housing and Local Government, Malaysia proposed to construct a Sewage Treatment Plant in Kuala Lumpur. As part of the treatment process, four (4) numbers of 23m diameter digesters were constructed at equi-distance from each other. Each digester is essentially a 15m high tank with a coned shaped (45 degree) base buried 8m below ground.

Being a former tin mining area, the site is underlain by highly variable soil conditions. Very soft slime was found at the foot-prints of 3 of the digesters while loose sand with slime layers was found at one of the digesters. The depth of limestone bedrock typically varied between 7m and 13m below ground. The groundwater table was about 2m below ground.

To support the excavation gravity DSM has adopted to the maximum depth of 12m. The DSM block was also designed to be sufficiently massive to overcome potential uplift forces. Wet DSM columns of 0.87m diameter were interlocked at 0.75m spacing was adopted as an effective solution. The columns were designed to achieve an unconfined compressive strength of 0.3 Mpa.

The solid cored samples were tested in a laboratory and showed more than acceptable UCS (Unconfined Compressive Strength) between 1MPa and 3MPa about 1 to 2 months after installation. Standard Penetration Tests (SPT) were carried out for some columns and were used to confirm increase in stiffness of the soil. Typical results are presented shear strength of the soil was increased by more than 50 times after 1 to 2 months of curing period. The typical plan, cross section of treatment scheme and SPT N value after treatment is shown in Figure 19.

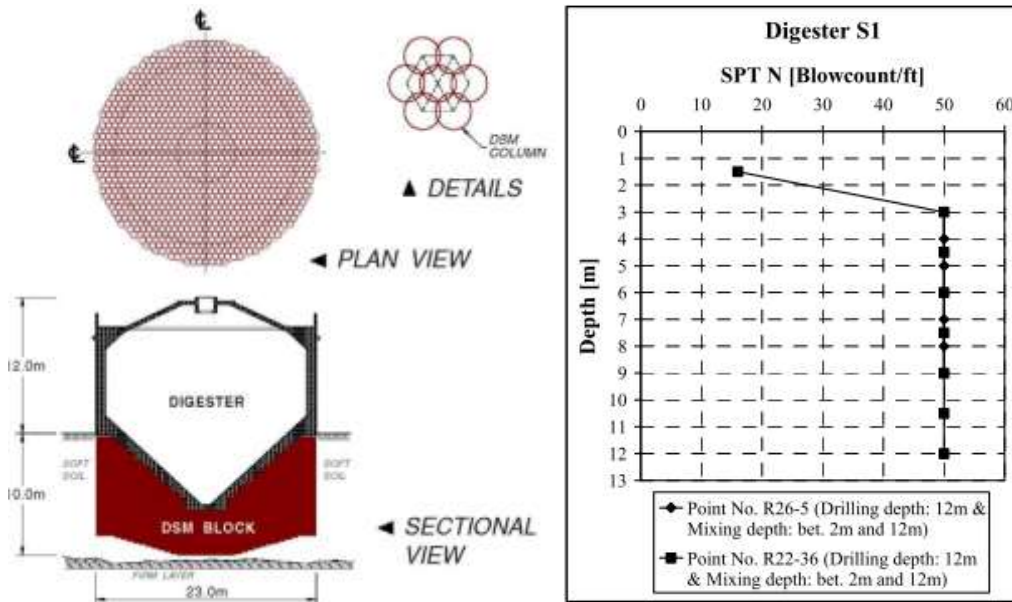


**Figure 19: Typical plan & cross section of Treatment scheme and SPT results of Digester tank**

The typical exposed DSM after excavation and digester after installation of DSM as shown in Figure 20.



**Figure 20: Typical exposed DSM and Structure after DSM installation**

The technical paper explaining the project case study on “Deep Soil Mixing in mine Tailings for an 8m Deep Excavation” is enclosed in Annexure III.

### 3.2.2 Case Study 2: Deep Excavation support for Basement of 3-storey commercial complex with 2-level basement, Kuala Lumpur, Malaysia.

A project comprising 3-storey commercial complex with 2-level basement car park floors (about 7m depth below existing ground level) is under construction in the middle of Kuala Lumpur City Centre. The proposed 2-level basement construction required 7m deep excavation with underlying limestone interface for a total perimeter length of about 690m.

The subsoil comprised of loose silty sand deposits and ex-mining soils with SPT values in the range of 5 blows/ft to 12 blows/ft. Underlying this loose soil layers, karstic limestone formation was found with extremely varying rock-head levels ranging between 3m and 15m below existing ground level. The ground water table was found to be at about 1m to 2m below existing ground level.

The gravity wall block was designed to ensure adequate resistance against lateral earth pressure to support the intended depth of excavation, whilst reducing seepage water inflow

and thus, minimise the possible risk of drawdown and consequent ground subsidence to the surroundings. Wet DSM columns of 0.85m diameter were interlocked at 0.75m centres to form the rigid gravity wall block. The columns were designed to achieve an unconfined compressive strength of 1.0Mpa.

The cores from DSM columns were extracted and tested in a laboratory for UCS. The test results indicated an UCS in the range of 1MPa to 3MPa. In addition, wall movement was monitored during excavation works, which showed a maximum horizontal movement of about 30mm to 40mm. The schematic of DSM gravity wall block is shown in Figure 21.

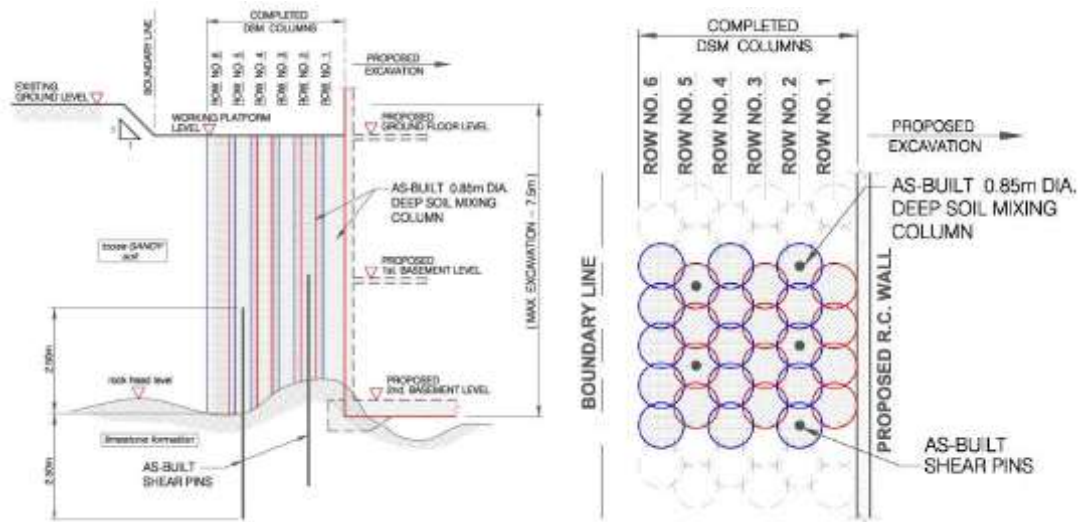


**Figure 21: Schematic of DSM gravity wall block.**

The Completed excavation of Gravity wall is shown in Figure 22.



**Figure 22 Completed excavation**

### 3.2.3 Case Study 3: Deep Excavation support for Music Academy Poznan, Poland.

The Music Academy Poznan (PL) planned in 2005 new construction of a 5-storey concert hall "I.J. Paderewski" with circular cross-section ( $\phi=46$  m). The building with a basement was in 8 m distance to the neighbouring building built at a road junction.

The building is under a low powerful up dividend to a depth of 4m from easy to medium densely packed sands. Among them is clay with a Basalt Stone Liner on. The water table is about 3.5m above the deepest excavation bottom. was for the creation of 6.7m below ground level a 0.8m thick base plate provided.

In cooperation with the company GT project Keller Polska developed a variant in which the excavation by 248 overlapped and reinforced TBV-pillars as well as by a ring beam (80 x 80 cm) in the head region is secured. Despite an intermediate layer of Basaltstei-NEN with 30 to 50cm diameter could the I-beam easily in the freshly prepared lagerich- TBV columns be installed tig. Before excavation the excavation was from the ring beam.

Reinforced concrete for the ablation of the bending moment elements and transverse forces completed. With the production of waterproof sheeting was in April 2005 started. The columns with lengths of 8.2m and a diameter of 70cm were placed in a Centre distance of 55cm produced. The embedment in the impermeable sandy loam was 3.5m. Each second column was reinforced with an IPE 300 profile. The typical CDSM scheme and exposed columns after excavation is shown in Figure 23.

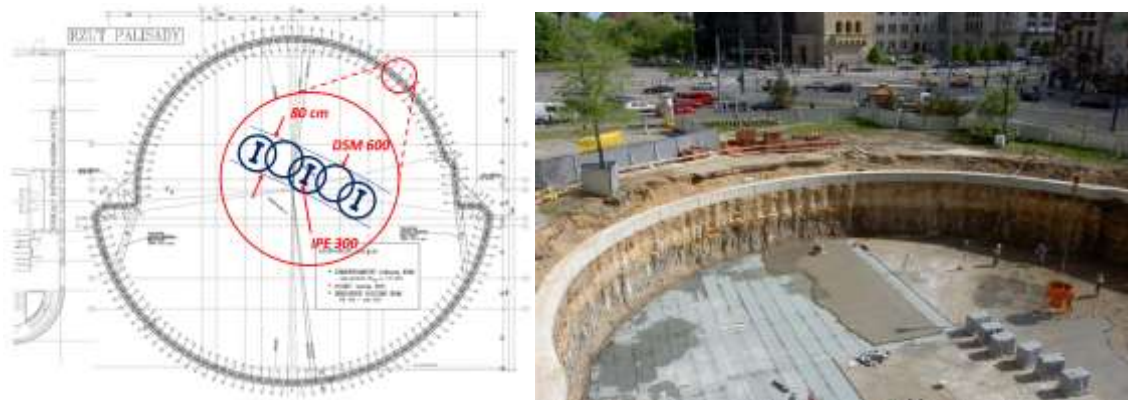


**Figure 23: Typical CDSM scheme and exposed CDSM columns**

The completed structure of Music Academy Poznan is shown in Figure 24



**Figure 24: Completed structure of Music Academy Poznan**

### **3.2.4 Case Study 4: Excavation Support for TBM Retrieval Shaft using Deep Soil Mixing Technique, Kuala Lumpur**

The Klang Valley Mass Rapid Transit (KVMRT) Project when completed will cover a distance of 51km and comprise of 31 passenger stations. The South Portal structure at Taman Maluri, Kuala Lumpur (KL) acted as the transition point between the elevated and underground sections of the Sungai Buloh - Kajang line and also, as the shaft for retrieval of the Tunnel Boring Machines (TBM) from Cochrane Station. The rail level is about 15m below the existing ground level. The ensuing 15m deep excavation required an earth support system.

Seven (7) boreholes were conducted on the site during the design stage. These showed that thickness of overburden soil varied between 7m and 10m below existing ground level. The soil generally comprised of sandy silt with interbedded layers of soft clay. This is typical of former tin mining soil. The typical cross section & scheme of DSM, exposed columns after installation are shown in Figure 25 & Figure 26.

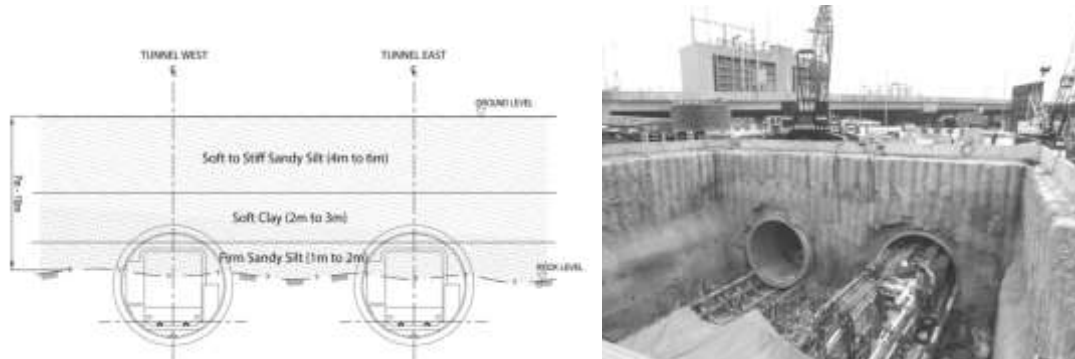


Figure 25: Typical cross section of the tunnel

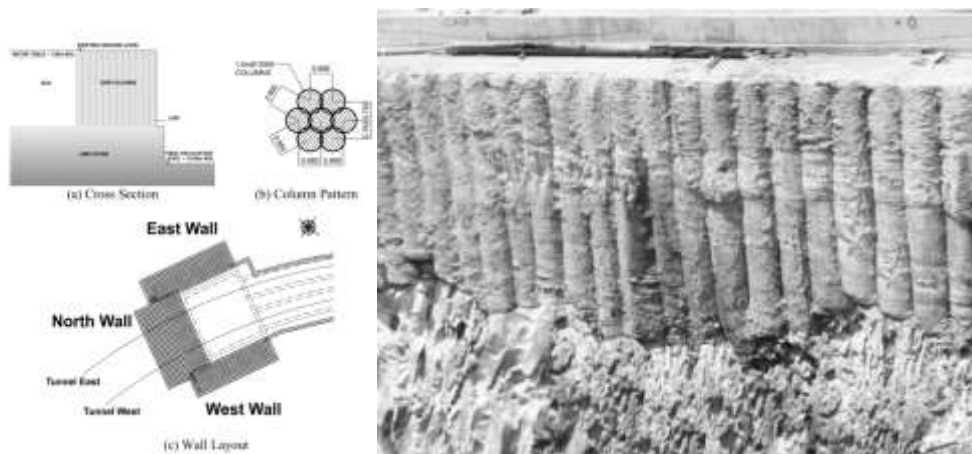


Figure 26: DSM scheme and exposed columns after excavation

Core samples were collected to examine consistency of the columns and to recover sections for unconfined compressive strength (UCS) tests. Cores were done in both the centre and the edge of the columns (where the columns intercept). As shown in Figure 27, test results show UCS strength consistently above 1.5 MPa after 28 days.

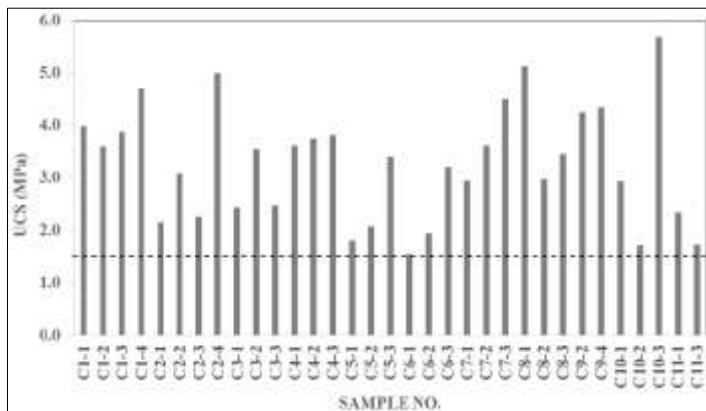


Figure 27: DSM core sample UCS strength test results

Wall movement was monitored during excavation works using both inclinometers and settlement markers. Three inclinometers were installed, one on each wall face, and twenty-one settlement markers on the ground surface. Maximum wall movement was observed at East wall, showing a reading of 10 to 15mm (less than 0.15% wall height).

The shape of the deflection implied that there was some sliding movement, albeit small. This is well within widely accepted wall deflection criterion of 0.5%. The maximum ground subsidence of 2mm to 6mm was observed behind West wall, and this was probably caused by construction load. Back-analyses imply a stiffness modulus of the block between 35 and 100 times of UCS.

In Annexure IV, the technical paper explaining the project case study on “Excavation Support for TBM Retrieval Shaft using Deep Soil Mixing Technique, Kuala Lumpur” is enclosed.

### **3.3 Ground treatment for shallow depth**

#### **3.3.1 Case Study 1: Mass Stabilisation of Peat and Mud for a Road Embankment Gärtunavägen, Sodertälje, Sweden.**

The project was a general contract, where Peab in cooperation with Keller Grundläggning AB and SWECO received the work to construct a continuation of road 225 between Södertälje and Nynäshamn. The new road was to be built upon a peat bog with underlying clay. Keller Grundläggning AB made the design for the mass- and deep stabilisation.

The Ground Investigation Report showed 0.5 – 3m organic soil (peat) and underneath from 3 to 15m a soft silty clay, laying upon moraine. The peat had a water content of up to 1200%. The organic soil had a water content of 300 – 500% and a shear strength of 3 to 7kPa. The clay had a shear strength of 10 – 25 kPa with increasing strength towards the depth.

Mass stabilisation was chosen for the organic soil and lime-cement columns for the underlying clay. Laboratory tests and field tests were executed and the proposed binder content was 175kg/m<sup>3</sup> cement for the peat and 80kg/m<sup>3</sup> lime/cement (50%/50%) for the clay. The dimensioning shear strength in the peat was 50kPa and 100 kPa for the clay. The achieved shear strength in the project was from 50kPa in the peat and 200kPa in the clay. The settlements in the peat stopped after approximately one month.

Keller’s specially designed mass stabilisation machine was used in combination with the ordinary lime column rig. The mass stabilisation work was executed in a grid pattern with blocks of 3x4m. This was to ensure that the right amount of binder was mixed into the soil. Shortly after stabilisation a layer of 0.8m fill and geogrid was laid over the block to preload the peat layer. The rigs could use the stabilised area after 24 hours. The final fill-height of the embankment was applied after 1 month. The typical cross section of mass stabilisation is shown in Figure 28.

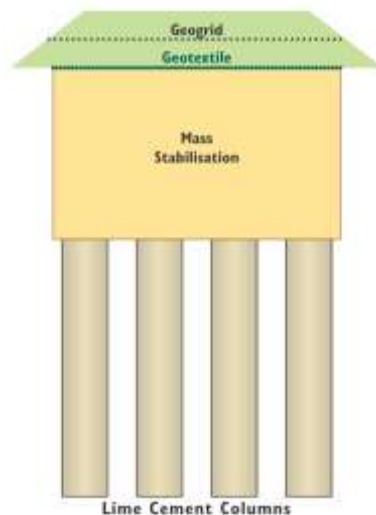


**Figure 28: Typical cross section of Mass stabilisation**

## 4 Bibliography

1. Federal Highway Administration Design manual (2013): Deep mixing for embankment and foundation support., FHWA-HRT-13-046.
2. Raju V.R & Hari Krishna Y “Deep soil mixing”, Institute of Engineers Malaysia (2005)
3. Broms, B.B. (1999) “Design of lime, lime/cement and cement columns”, *Proceedings of the International Conference on Dry Mix Methods for Deep Soil Stabilisation*, Stockholm, Sweden, pp. 125-153.
4. Broms, B.B. (2004) “Lime and Lime/cement Columns”, *Ground Improvement (2<sup>nd</sup> Edition)*, Edited by Moseley, M.P. and Kirsch, K, Spon Press. 2004, pp. 252-330.
5. prEN 14679 (2003) “Execution of Special Geotechnical Works – Deep Mixing”, *European Standard*.
6. Euro Soil Stab (2002) “Development of Design and Construction Methods to Stabilise Soft Organic Soils”, *Design Guide Soft Soil Stabilisation*, CT97-035I, European Commission Project BE 96-3177.
7. Larsson, S. (2005) “On the Use of CPT for Quality Assessment of Lime Cement Columns”, *Proceedings of the International Conference on Deep Mixing Best Practice and Recent Advances*, Stockholm, Sweden.
8. LCM Brochure “Dry Soil Mixing”, Sweden.
9. Raju, V.R. and Abdullah, A. (2005) “Ground Treatment Using Dry Deep Soil Mixing for a Railway Embankment in Malaysia”, *Proceedings of the International Conference on Deep Mixing Best Practice and Recent Advances*, Stockholm, Sweden.
10. Swedish Geotechnical Society (1997) “Lime and Lime Cement Columns”, *SGF Report 4:95E: Guide for Project Planning, Construction and Inspection*, Linkoping, Sweden.
11. Topolnicki, M. (2004) “In-situ Soil Mixing”, *Ground Improvement (2<sup>nd</sup> Edition)*, Edited by Moseley, M.P. and Kirsch, K, Spon Press. 2004, pp. 331-428.
12. V.R Raju and Y Hari Krishna, (2008) “Ground improvement Techniques for infrastructure projects in Malaysia”, *Proceedings of 12<sup>th</sup> International conference of International Association for computer methods and Advances in Geomechanics*, Goa.

Annexure I      Technical paper on “Soil mixing - Challenges of Application ranging from Ground Improvement to Structural Elements” by Topolnicki M, 2006.



# Soil mixing - challenges of applications ranging from ground improvement to structural elements

**M. Topolnicki, prof. dr hab. inż.,  
Gdańsk University of Technology & Keller  
Polska Sp. z o.o.**

Presented by

**Keller Grundbau GmbH**  
Kaiserleistraße 44  
D-63067 Offenbach  
Tel. +49 69 8051-0  
Fax +49 69 8051 244  
E-mail: [Info@KellerGrundbau.com](mailto:Info@KellerGrundbau.com)  
[www.KellerGrundbau.com](http://www.KellerGrundbau.com)

**XIII. Danube-European Conference on  
Geotechnical Engineering, Ljubljana,  
29.-31.05.2006**

**Technical paper 32-55 E**

# Soil mixing - challenges of applications ranging from ground improvement to structural elements

**M. Topolnicki**

Gdańsk University of Technology & Keller Polska Sp. z o.o.

## ABSTRACT

The current state of development of the wet method of deep Soil Mixing (SM) is presented, based on experience gained in Poland, where the use of wet SM is seeing continuous growth which began in 1999. Considered case histories refer to ground improvement, foundation support, retention systems and cut-off walls. They demonstrate not only a unique flexibility of the application of SM, but also prove that deep soil mixing should be considered as a competitive solution to a number of different geotechnical problems. Challenges of SM application are connected with varying properties of the stabilised soil, as well as with appropriate geotechnical design. Stiff, rigid SM columns interact in a different way with the soil than the more flexible columns. It is therefore important that design engineers are aware of these differences. Specialised soils mixing in relation to environmental projects is not touched upon.

## I. INTRODUCTION

The use of in situ Soil Mixing (SM) in Europe to improve the engineering properties of soft or contaminated ground is increasing rapidly, indicating growing interest and acceptance of this relatively new technology in civil engineering. The extent of applications of SM across European countries differs considerably, as reviewed recently by Massarsch and Topolnicki (2005). Outside Scandinavia the total number of implemented projects is still relatively small compared with other relevant geotechnical methods, however industrial, social and environmental developments in Europe offer major commercial opportunities for an increase in SM applications. In Poland, for instance, the wet soil mixing method is now in regular use. Typical applications of SM involve ground improvement and hydraulic cut-off walls. However, structural supports, such as pad and strip foundations and retaining structures, have also been founded on soil mixing elements installed in various patterns ranging from individual columns to grids, walls and blocks of stabilised soil (e.g. Topolnicki, 2004). Consequently, the strength of soil mixing elements may differ significantly within the range determined by low

capacity columns, with a compressive strength of about 0.3 to 0.5 MPa, and high capacity individual or combined structural elements, having unconfined compressive strength in the order of 2 to 5 MPa, which perform similar to piles or block foundations. The external loads are usually transferred down to the bearing layer resulting in a fixed type improvement, but can be also partly or wholly transferred to the foundation soil when a more interactive or even a floating type of improvement is desired. The choice of the required strength and of the load transfer system is dictated by the purpose of the deep mixing application, and reflects the mechanical capabilities and characteristics of the particular mixing method used. In the following sections, selected examples of soil mixing applications are presented to illustrate the current practice, based on the experience gained in Poland, where the use of wet soil mixing has grown rapidly since 1999. Considered case histories refer to ground improvement, hydraulic cut-off wall, support of slab and individual foundations and retention systems. They demonstrate not only a unique flexibility of the application of SM, but also prove that deep soil mixing should be considered as a competitive solution for a number of different geotechnical problems.

## **2. APPLICATIONS**

### **2.1 Ground improvement for city highway**

SM columns of diameter 0.8 m were applied to support a road embankment overlying weak soils found to the depth of 3 to 8 m below the ground surface (Fig. 1). The subsoil consisted of loose anthropogenic fill, underlined by peat and organic clay. The organic soils were 1 to 4 m thick. The embankment height was 1.3 to 2.5 m and the equivalent live load was 30 kPa. A triangular column spacing of 2m×2m was selected, resulting in the design compressive stress of 480 to 676 kPa, assuming column diameter reduced to 0.7 m. The required unconfined compressive strength (UCS) of the stabilised soil material was 1.5 MPa. Altogether, 2402 columns with a total length of 15,532 m were constructed. The final embankment was strengthened with two layers of geogrid, resulting in the so-called Load Transfer Platform design (cf. Topolnicki, 1999).

### **2.2 Hydraulic cut-off wall**

A hydraulic cut-off wall is constructed by installing intercut SM columns to intercept potential seepage flow paths. Since the hydraulic conductivity and continuity of the cut-off wall are the most important design considerations, the slurry mixes must be tailored to soil conditions, and adequate control of columns' overlapping zones and verticality are required. This is especially important when cut-off walls are executed to a large depth with single shaft mixing equipment, as shown in Fig. 2.

For SM cut-off walls, the unconfined compressive strength is typically in the range of 0.7 to 3 MPa, and even higher if steel reinforcement is installed. The permeability is normally between  $10^{-8}$  to  $10^{-9}$  m/s. When bentonite and/or clayey stone dust and/or fly ash are added to the slurry mix, the permeability can be reduced to  $10^{-9}$  to  $10^{-10}$  m/s, with the associated decrease of the unconfined compressive strength usually below 1 MPa.

### **2.3 Support of a slab foundation**

A multistory building was located in heterogeneous soil conditions. Under superficial mixed fill, organic clay and some peat were locally present, extending from 3.5 to about 6.7 m be-

low the foundation level. Organic soils were underlined by fine sand and silt layers of varying thickness, making ordinary piling very expensive due to the necessary pile length. Early calculations also indicated, that direct placement of the foundation slab on the existing soil would lead to large and unequal settlements, ranging from 7 to about 50 cm.

In this situation a wet SM option was investigated and finally accepted by the client. The design was based on 3D FEM calculation, allowing for slab-soil interaction and elastic behavior of columns. The resulting arrangement of 461 SM columns is shown in Fig. 3. For the outlined design it was essential to make a good estimate of the expected compressive strength of the stabilised soil since significant variation in column strength was anticipated. For this reason, maximum factored load acting on a single column was limited to 430 kN, resulting in design compressive stress of 0.86 MPa, and a special mixing procedure was adopted at the construction site. With a safety factor of 2.5, applied to the maximum factored design stress, the 28-days UCS of the stabilised soil was required to be 1.9 MPa.

## 2.4 Support of strip and pad foundations

Strip and pad foundations of a commercial centre Megaplex were initially designed for CFA piles because excessive settlement differences were expected. The subsoil consisted of a thin fill material, underlying sandy and silty clays, and a coarse sand layer in a dense state. Loads acting on strip foundations ranged between 230 and 729 kN/m, with resulting vertical stresses of 230 to 430 kPa. Twelve types of rectangular footings were also designed for loads between 1170 and 5670 kN, yielding vertical stress of 310 to 677 kPa (Fig. 4).

The initial piling design was successfully converted into a competitive SM project. Pad and strip foundations were supported on closely spaced SM columns of 0.8 m diameter, and were consequently designed as direct foundations, resulting in cost savings since less steel reinforcement was needed. The number of columns under the footings ranged from 3 to 14, and was determined by taking into account the expected strength of the stabilised soil as well as the allowable settlement difference of 5mm over 6 m span, specified by the client. The maximum design load acting on a single column, with slightly reduced diameter due to aggressive groundwater, was limited to 512 kN, corresponding to compressive design stress of 1330 kPa. Exposed columns on the bottom of foundation pits are shown in Fig. 5.

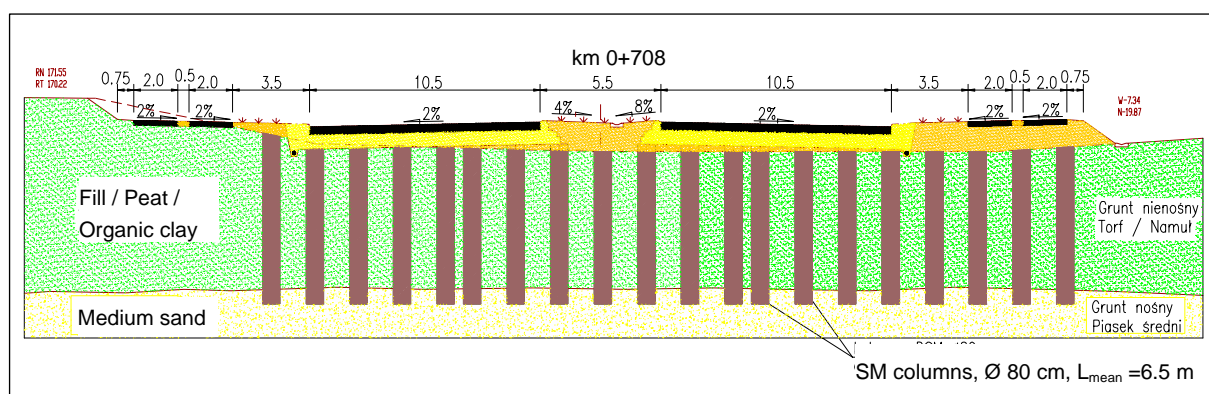


Figure 1. Road embankment supported on SM columns (Trasa Zielona, Lublin, Poland).

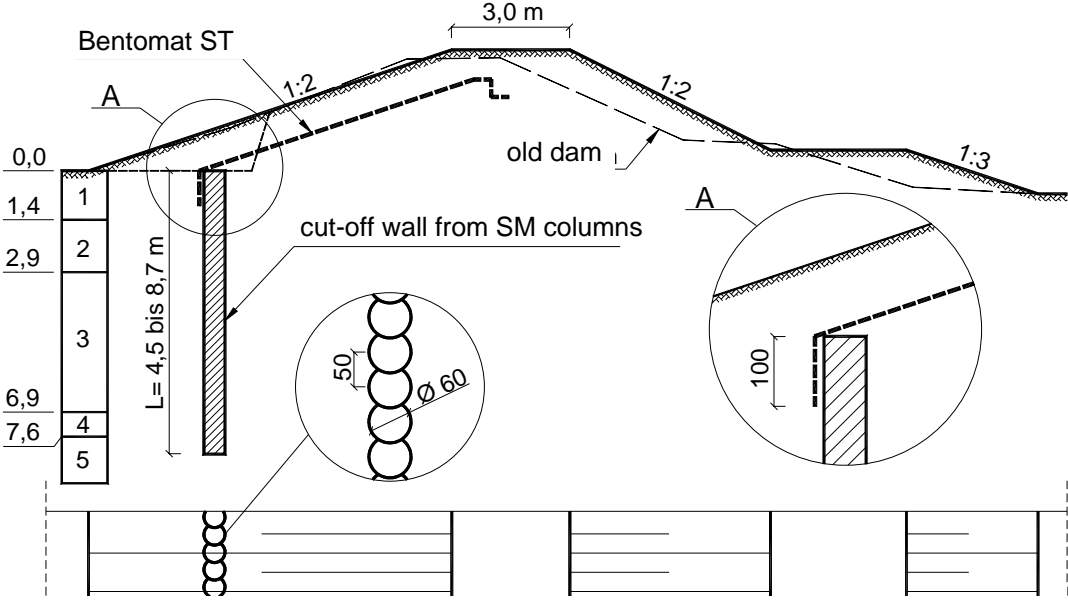


Figure 2. Soil mixing cut-off wall to intercept seepage flow paths under river bank embankment (The Vistula river near Tarnobrzeg, Poland).



Figure 3. Arrangement of SM columns under the foundation slab of multistory building (Kielce, Poland).

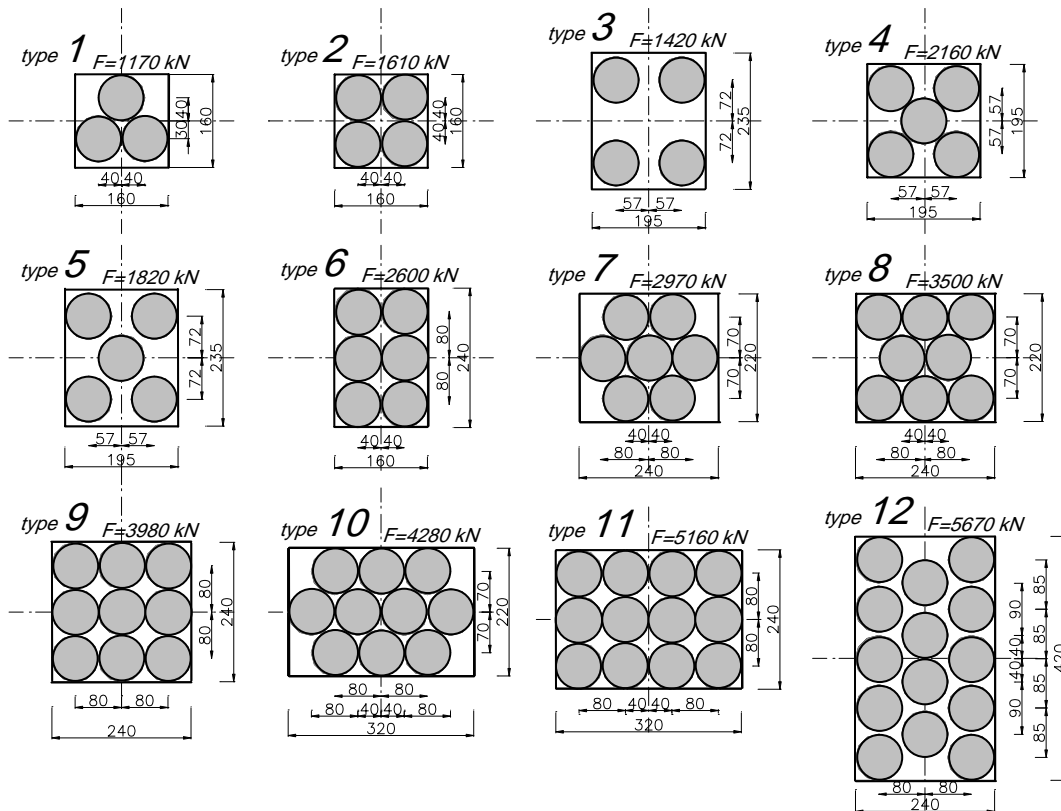


Figure 4. Arrangement of SM columns under pad foundations of a commercial centre (Megaplex, Katowice, Poland).



Figure 5. Exposed SM columns under pad foundation of a commercial centre (Megaplex, Katowice, Poland).



Figure 6. Soil mixing works and exposed columns for a bridge support foundation (A2 highway near Poznań, Poland).



Figure 7. Temporary SM wall with embedded steel H-beams for excavation support (Music Academy, Poznań, Poland).



Figure 8. Permanent soil mixing retention wall with embedded steel H-beams and concrete facing (Oświęcim, Poland).

## 2.5 Bridge supports

Construction work on the A2 highway in Poland led to interesting applications of wet SM. Careful analysis revealed that certain road bridges, originally designed on large diameter piles, can be supported on SM columns, fulfilling all stability and settlement requirements and offering substantial savings on foundation costs.

The solution adopted for bridge WD-23 provides a good example of this application. The subsoil consisted of boulder sandy clays, with an average CPT cone resistance of 2 MPa. The geotechnical design included a total of 200 columns for the five bridge supports. The applied arrangement of 46 SM columns under bridge abutment foundation is shown in Fig. 6. The allowed maximum characteristic design compressive stress was 830 kPa, and the requested compressive strength was 2.5 MPa. The observed settlement of this support was 12 mm. It is interesting to note that since 2002 about 80 road bridges have been founded on SM columns in Poland.

## 2.6 Temporary and permanent retention systems

Retention systems using SM are mostly comprised of applications associated with restraining the earth pressure mobilised during deep excavations. In these applications wall-type column patterns are used, while the soil-cement mix is typically engineered to have high strength and stiffness. To overcome soil and water lateral pressures the SM columns should also have adequate shear resistance. Other key requirements for successful construction are a high degree of column homogeneity and maintaining verticality tolerance to achieve the minimum required designed thickness of columns effectively in continuous contact.

For the projects shown in Figs. 7 and 8, steel H-beams were installed in fresh SM columns to increase the bending resistance and create a structural wall for excavation support.

Elongated mixing time and full restroking were required to ensure easier installation of soldier elements immediately after mixing. Panels of mixed soil between H-beam reinforcement were designed to work in arching. Tieback anchors or stage struts are typically used in combination with the SM walls. In case of circular excavations or shafts peripheral concrete cap beams working in hoop compression can be constructed instead, as shown in Fig 7.

For permanent SM walls, concrete facing is needed to prevent the soil-cement mix from long-term deterioration and damage and to provide smooth wall surface. Concrete facing is easily constructed, with the reinforcing bars welded to exposed H-beams, as shown in Fig. 8.

### 3. CONCLUSIONS

When soil mixing is applied to support shallow embankments or foundation slabs usually to reduce excessive or differential settlement, the quality of individual columns is less important and the overall performance depends mainly on the combined interaction between the supported structure, soil, and strengthening elements (i.e. columns). This soil-structure interaction design concept is frequently applied in the case of low strength soil mixing and is often combined with preloading to accelerate strength gain and consolidation settlement. This concept has proved to be efficient and cost-effective. On the other hand, when soil mixing is performed to support high embankments or heavily loaded pad or strip foundations, and where horizontal loads, shear forces, or bending moments may appear, the quality of load-bearing columns is essential to prevent progressive failure mechanisms. The same applies for economically attractive low values of the area improvement ratio, and for retention systems with steel reinforced soil mixing columns. Consequently, a good assessment of the expected strength and deformation properties of the stabilised soil is one of the key issues in reliable and optimum SM design. Stiff, rigid columns interact in a different way with the soil than the more flexible columns. It is therefore important to account for these differences in the geotechnical design of Soil Mixing.

### REFERENCES

- M. Topolnicki, Low height reinforced embankments supported on piles: application, design and reliability – a panel report, Proc. XII European Conference on Soil Mechanics and Foundation Engineering, Amsterdam, Vol. 2, s. 1191-1194, 1999.
- R. Massarsch, M. Topolnicki, Regional Report: European Practice of Soil Mixing Technology, Proc. of Int. Conference on Deep Mixing – Best Practice and Recent Advances, Stockholm, Vol. I, pp. R19-R45, 2005.
- M. Topolnicki, In situ Soil Mixing, Chapter 9 in Ground Improvement book, Editors M. Moseley and K. Kirsch, Spon Press, pp. 331-428, 2004.

Annexure II Technical paper on “Quality Control of Wet Deep Soil Mixing with reference to Polish Practices and Applications” by Michal Topolnicki,2002



# Quality Control of wet Deep Soil Mixing with Reference to Polish Practice and Applications

**Michal Topolnicki,**

*Prof. Ph. D. Civ Eng.,*

*Head of Marine Civil Eng. Department  
at the Technical University of Gdansk;*

*Managing Director and Chief Designer  
of Keller Polska Ltd., Gdynia, Poland*

*Phone: +48 58 629 7510,*

*Fax: +48 58 629 7470,*

*topolnicki@keller.com.pl*

Presented by

**Keller Grundbau GmbH**

Kaiserleistr. 44

D-63067 Offenbach

Tel. +69 8051 - 0

Fax +69 8051 - 244

E-mail [Info@KellerGrundbau.com](mailto:Info@KellerGrundbau.com)

[www.KellerGrundbau.com](http://www.KellerGrundbau.com)

**Deep Mixing Workshop, Tokyo, 15.–18.10.2002**

**Technical Paper 32-52E**

# Quality Control of Wet Deep Soil Mixing with Reference to Polish Practice and Applications

Michal Topolnicki<sup>1</sup>

## Abstract

With reference to Polish application of wet Deep Soil Mixing, begun in 1999, three selected projects are presented relating to quality control issues. The first case reflects the importance of adequate soil investigation when dealing with soil improvement. The second refers to the evaluation procedure of strength data obtained from laboratory tests on cubic samples, indicating that the standard approach used for concrete should not be automatically applied for DSM. The last case concerns highway bridge support founded on DSM columns and describes quality control by means of a preloading test.

## Introduction

Application of wet Deep Soil Mixing started in Poland in 1999. The first project, designed and conducted by Keller Polska Ltd., comprised the execution of intersecting DSM columns forming a sealing wall along an old dam of the Vistula River in Krakow, as a part of a major food protection program for this historical city. Since then more than 30 projects have been completed in Poland so far, indicating growing importance of this technology. Despite a relatively short period of application, the range of executed DSM projects already covers quite a broad spectrum of difficult geotechnical cases, including the following: improvement of organic soils for a new city road, the foundation of several multi-story buildings on slabs supported by DSM columns, strip and pad foundations of industrial and municipal buildings, foundation supports of highway bridges, the sealing walls and temporary protection of excavation walls.

In Polish foundation practice, DSM columns with a diameter of 80 cm and a length of 3 to 10 m have been executed (in a few cases also 60 cm dia. columns were used, but mainly for sealing walls). This limitation led to a requirement for higher internal column strength than usually applied elsewhere, as compared for instance to Keller's practice in the USA, where large diameter columns are frequently executed.

In the following, three different DSM applications are briefly presented in order to illustrate important quality control issues. All reported cases were designed and executed by Keller Polska Ltd.

---

<sup>1</sup> Prof. Ph. D. Civ Eng., Head of Marine Civil Eng. Department at the Technical University of Gdansk; Narutowicza 11, 80-952 Gdansk, Poland; Phone: +48 58 347 2611; Fax: +48 58 347 1436  
Managing Director and Chief Designer of Keller Polska Ltd.; Rdestowa 51a, 81-577 Gdynia, Poland;  
Phone: +48 58 629 7510; Fax: +48 58 629 7470; topolnicki@keller.com.pl

### Pad and strip foundations with strongly varying loading

This case has been selected in order to illustrate how insufficient soil investigation data may influence performance of foundations supported on DSM columns.

Strip foundations of varying width between 1.0 and 1.7 m were designed for loads ranging from 230 to 729 kN/m, with a resulting unit pressure of 230 to 430 kPa. There were also 12 types of rectangular pad foundations, loaded from 1170 kN up to 5670 kN, with resulting unit pressure of 310 to 677 kPa. This challenging geotechnical project, originally designed for CFA piles because of expected settlement differences, has been changed to modern soil improvement with wet DSM. Pad and strip foundations were designed as shallow foundations supported on DSM columns with an 80 cm diameter. Assumed column layout under the footings is shown in Fig.1. The number of columns under pad foundations ranged from 3 to 14 and was selected taking into account expected internal strength of DSM columns and allowable settlement difference of 5mm over 6 m span, specified by the client. The maximum design load acting on a single column was limited to 512 kN. This corresponds to compression stress of 1330 kPa for a column with reduced diameter due to slightly aggressive groundwater.

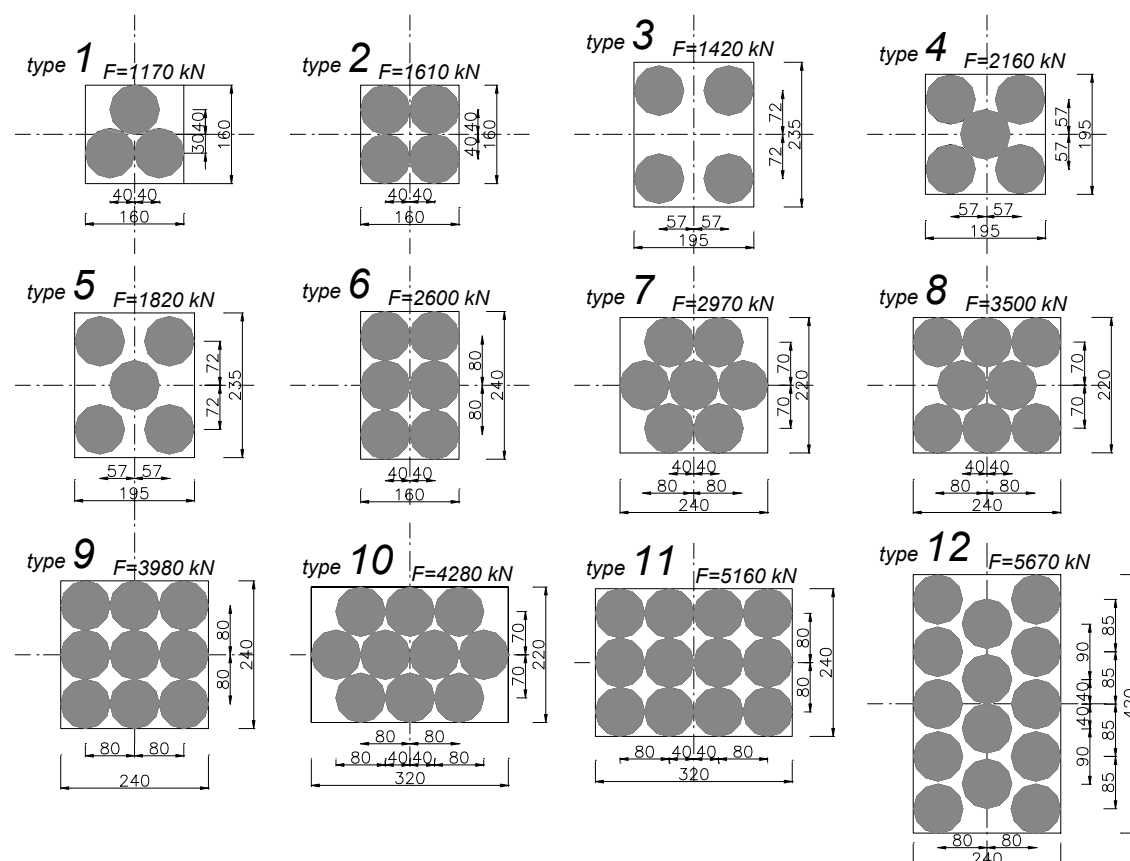


Fig. 1. Arrangement of DSM columns under pad foundations



Fig. 2. Trimmed DSM columns at the bottom of a foundation pit

An initial soil investigation report, ordered by the client and used at the design stage, included soil profiles and parameters evaluated from classical borings and dynamic penetration tests. In general, bearing strata comprised of coarse sand and stiff clay were indicated at the depth of 5 to 6 m below the foundation level. In the case of pad foundation No 9, for instance, a coarse sand layer with compression modulus of 110 MPa was found at 5.7 m depth and the boring was terminated at 6 m (Fig.3). Consequently, for this footing 6 m long DSM columns were assumed in the design.

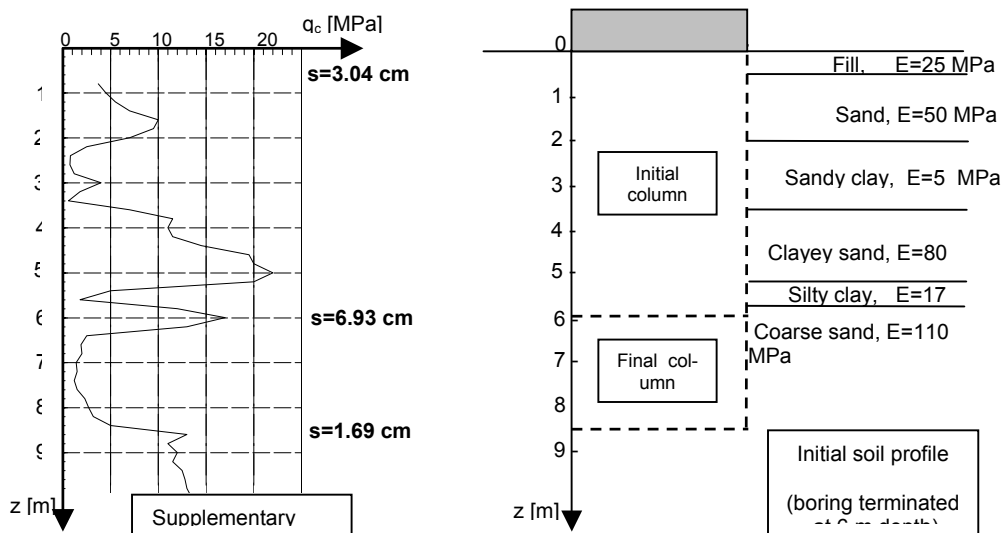


Fig. 3. Initial soil profile at footing No 9 (right) in relation to supplementary cone penetration test (left) and the resulting change in column length

During construction, additional soil investigations were conducted by the contractor in the framework of the quality assurance plan. Close to footing no. 9 a supplementary CPT indicated below 6 m depth a silty clay layer with low stiffness (Fig. 3). Thanks to the immediate reaction of the site engineer it was possible to extend fresh DSM columns to the depth of 8.5m and the whole work was completed successfully.

The reported case was subsequently analysed to see what could actually happen if the initial column length was maintained. Calculations have indicated that with 6 m long columns the expected settlement could reach 7 cm, as indicated in Fig.3. This is because the DSM columns are stiffer than the surrounding soil and most of the load is transferred down to the underlying weak layer. Interestingly, the resulting settlement would be even bigger than for a direct foundation placed on untreated subsoil (ca 3 cm). Consequently, foundation performance would be worse despite the time and money spent on soil improvement. This case underlines the role of adequate soil investigation data and of on-site control of works when dealing with this type of soil improvement.

### Foundation slab on DSM columns

A new multistory building was located in difficult heterogeneous soil conditions. Under superficial mixed fill, organic clay and some peat was present, extending 3.5 to about 6.7 m below the final slab foundation level. Organic soils were underlined by fine sand and silt layers of varying thickness, making ordinary piling very expensive due to necessary pile length. Early calculations indicated also, that direct placement of the foundation slab on the existing soil would lead to large and unequal settlements, ranging from 7 to about 50 cm despite the slab stiffness (Fig.4).

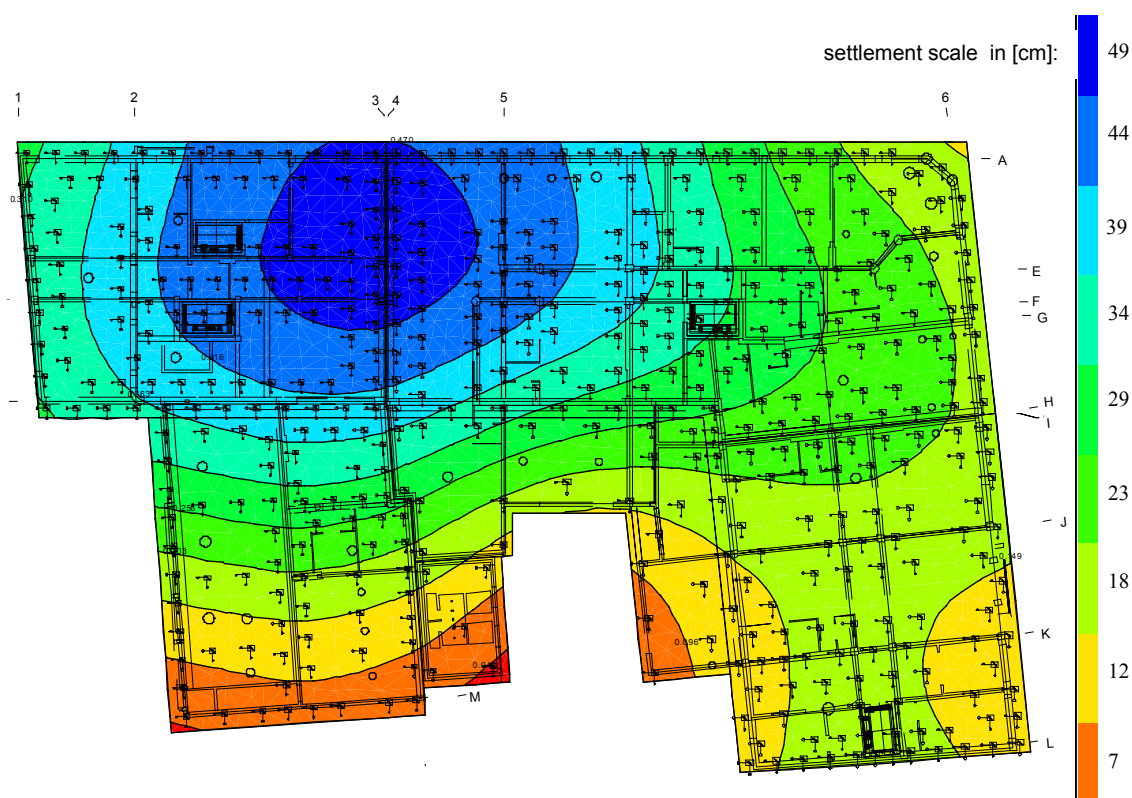


Fig. 4. Calculated settlement of the slab founded directly on untreated subsoil

In these circumstances a wet DSM option was investigated and finally accepted by the client. The design was based on 3D finite element calculation, allowing for slab-soil interaction and elastic behaviour of columns. The resulting arrangement of DSM columns in the plan view and in a cross-section is shown in Figs. 5 and 6, respectively.



Fig. 5. Arrangement of DSM columns under the foundation slab (size of each circle indicates column load in kN)

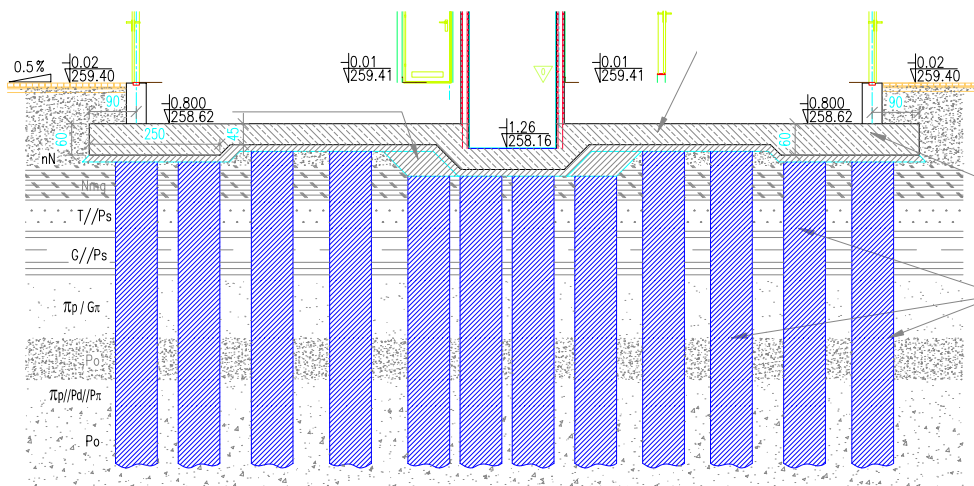


Fig. 6. Cross-section of the foundation slab and DSM columns

For the outlined design, comprised of 461 DSM columns with a total length of about 3280 m, it was essential to make a good estimate of the expected compression strength of the grouted soil, referred to as internal column strength. Due to heterogeneous soil and the presence of organic layers, significant differences in column strength was anticipated. For this reason, maximum factored load acting on a single column was limited to 430 kN, resulting in design compression stress of 0.86 MPa, as well as special mixing procedure was adopted at the construction site. The average unit density of the cement slurry was about 1700 kg/m<sup>3</sup> and the mean consumption rate was about 180 l/m. According to the assumed design criteria, a general safety factor of 2.5 had to be applied to the maximum factored design stress acting on a single column. This led to the required strength of at least 1.9 MPa after 28 days of curing. The actual strength was checked on 32 standard cubic samples, extracted from fresh DSM columns and tested for uniaxial compression at an independent laboratory. The obtained results are presented in Tab. I.

Once the test results became available for control it turned out that three samples (no 2, 3, and 4) had lower strength than required. Although even the minimum strength of 1.11 MPa was higher than the design stress 0.86 MPa, discussion started about the actual margin of safety. Later on it has been also found that the first series of samples were left unprotected during a chilly night and got partly frozen. This observation has not been duly reported, however, and all samples were brought to the laboratory for testing.

The outlined case is reported in order to illustrate that the classical evaluation procedure of sample strength data, based on 95% of confidence as prescribed for ordinary concrete (e.g. Polish Standard PN-88/B-06250), should not be mechanically applied to DSM. The calculations presented in Tab. I show that standard deviation for DSM material can be very large, and generally exceeds 20% of the mean value (in case of concrete this would require additional inspection of concrete quality). Consequently, the classical evaluation approach may lead to overly strong restrictions for DSM applications. It is also demonstrated by evaluations C and D in Tab. I that truncation of the obtained strength to, for example, 6 MPa yields automatically higher calculation strength  $R_{cd}$ . This however should not lead to the conclusion that a reduced amount of cement in the slurry would lead to increased safety of soil improvement. Therefore, a new evaluation procedure for DSM strength data, carefully tailored to this technology, is actually needed. One possibility is to introduce fixed safety factors in relation to mean and minimum obtained strength, like for jet grouting, or to reduce the level of confidence.

### **Highway bridge supports founded on DSM columns**

Recent works for the A2 highway in Poland have initiated new, interesting applications for wet DSM. After careful analyses it turned out that certain road bridges, originally designed on large diameter piles, could be founded on DSM columns fulfilling all technical requirements with respect to stability and settlement of supports and at the same time offering substantial economical savings.

For illustration the solution adopted for bridge VWD-105 is presented. The design included soil improvement for 5 bridge supports using 168 DSM columns. A typical layout is shown in Fig. 7 for support P3 with 30 columns. Allowed maximum factored load for a single column was 458 kN, resulting in compression stress of 916 kPa. The requested compression strength was 2.3 MPa, applying a partial safety factor of 2.5. Predicted settlement for the whole support was 0.95 cm.

Tab.1 Results of compression tests of DSM samples and four evaluation procedures

Compression test results				Evaluation A	Evaluation B	Evaluation C	Evaluation D		
No.	Date of sampling	Strength [MPa]	Mean strength [MPa]	Strength [MPa]	Strength [MPa]	Strength [MPa]	Strength [MPa]		
1.	21.03.2002	3,11	1,87	3,11	samples partly frozen	3,11	samples partly frozen		
2.		1,60		1,60		1,60			
3.		1,11		1,11		1,11			
4.		1,64		1,64		1,64			
5.	27.03.2002	6,76	5,07	6,76	6,76	<b>6,00</b>	<b>6,00</b>		
6.		3,20		3,20	3,20	3,20			
7.		6,36		6,36	<b>6,00</b>	<b>6,00</b>			
8.		3,96		3,96	3,96	3,96			
9.	28.03.2002	3,96	4,34	3,96	3,96	3,96	3,96		
10.		4,09		4,09	4,09	4,09			
11.		4,53		4,53	4,53	4,53			
12.		4,80		4,80	4,80	4,80			
13.	30.03.2002	7,60	7,04	7,60	7,60	<b>6,00</b>	<b>6,00</b>		
14.		8,27		8,27	<b>6,00</b>	<b>6,00</b>			
15.		8,44		8,44	<b>6,00</b>	<b>6,00</b>			
16.		3,87		3,87	3,87	3,87			
17.	02.04.2002	8,18	7,32	8,18	8,18	<b>6,00</b>	<b>6,00</b>		
18.		8,13		8,13	<b>6,00</b>	<b>6,00</b>			
19.		7,64		7,64	<b>6,00</b>	<b>6,00</b>			
20.		5,33		5,33	5,33	5,33			
21.	05.04.2002	7,91	8,04	7,91	7,91	<b>6,00</b>	<b>6,00</b>		
22.		8,04		8,04	<b>6,00</b>	<b>6,00</b>			
23.		8,44		8,44	<b>6,00</b>	<b>6,00</b>			
24.		7,78		7,78	<b>6,00</b>	<b>6,00</b>			
25.	08.04.2002	6,67	6,08	6,67	6,67	<b>6,00</b>	<b>6,00</b>		
26.		6,49		6,49	<b>6,00</b>	<b>6,00</b>			
27.		5,38		5,38	5,38	5,38			
28.		5,78		5,78	5,78	5,78			
29.	09.04.2002	6,36	5,98	6,36	6,36	<b>6,00</b>	<b>6,00</b>		
30.		6,00		6,00	6,00	6,00			
31.		6,22		6,22	<b>6,00</b>	<b>6,00</b>			
32.		5,33		5,33	5,33	5,33			
Calculation according to Polish Standard PN-88/B-06250 (confidence 95%)		Rm = Mean value:		5,72	6,27	4,99	5,44		
		SD = Standard Deviation:		2,14	1,63	1,47	0,87		
		Rcg = Guaranteed strength		Rcg = Rm-1,64*SD (95%)		2,21	3,60	2,57	4,01
		Rck = Characteristic strength		Rck = Rcg/1,25:		1,77	2,88	2,06	3,21
		Rcd = Calculation strength		Rcd = Rck/1,8:		0,98	1,60	1,14	1,78
Maximum factored design stress in DSM column:				0,86	0,86	0,86	0,86		
Additional calculation for 90% of confidence:		Rcg = Rm-1,28*SD (90%)		2,98	4,19	3,10	4,32		
		Rck = Rcg/1,25:		2,39	3,35	2,48	3,46		
		Rcd = Rck/1,8:		1,33	1,86	1,38	1,92		
Evaluation A: All data, as measured in the laboratory									
Evaluation B: Samples 1 to 4 excluded from analysis									
Evaluation C: as A, with strength limited to 6.0 MPa for all samples having strength exceeding 6.0 MPa									
Evaluation D: as B, with strength limited to 6.0 MPa for all samples having strength exceeding 6.0 MPa									

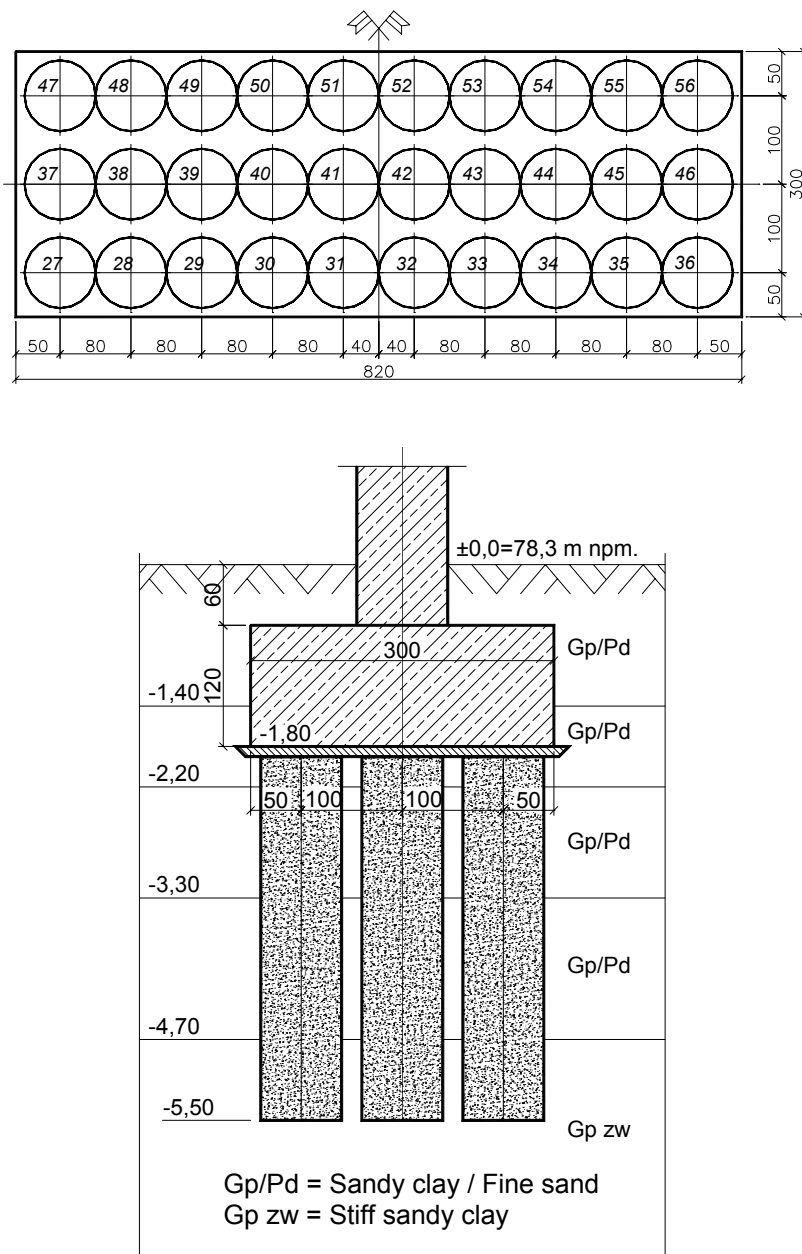
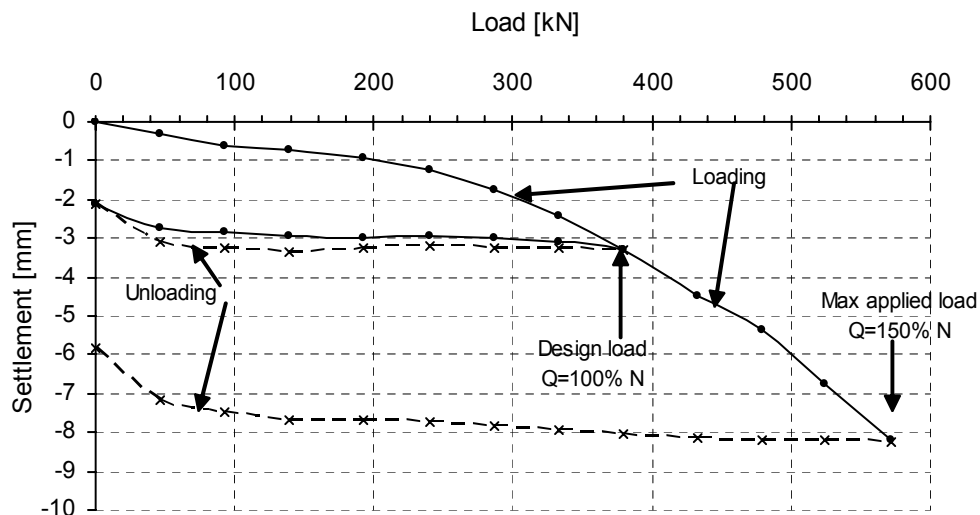


Fig. 7. Typical arrangement of DSM columns (support P3, bridge WD-105)

In order to convince the client and the independent engineer of the merits of this new foundation solution it was recommended that two loading tests of selected single DSM columns were performed. The test was not intended to check the bearing capacity of a column, as it would be required in case of piles, but rather to verify the load-settlement characteristic of DSM column and to confirm the applied design method and the predicted settlement. Pre-loading was conducted in 12 steps up to 572 kN, which is 150% of the value of characteristic maximum load for a single column, equal to  $458/1.2=382$  kN. Each loading step was maintained for at least 30 minutes or until the observed settlement was less than 0.05 mm in 10 min. The obtained settlement curve is presented in Fig. 8.



As can be observed, the total settlement corresponding to the design characteristic load was 3.28 mm, and 2.11 mm after unloading. Under the maximum applied load the behaviour was still far from an ultimate condition and the total settlement was only 8.22 mm and 5.83 mm after full unloading.

The above test results were also reanalysed with the same calculation method in order to check the settlement prediction. For a single column loaded with 100% load the calculated settlement was 6.0 mm, while the observed value was 3.28 mm. This gave evidence that the applied calculation approach is on the safe side and that the predicted settlement for the whole support can be considered as the upper bound estimate. Further settlement observations, collected during subsequent construction stages of the bridge and afterwards, will be also used for future back analysis.

## Conclusions

Increasing applications of the wet Deep Soil Mixing in Poland have shown that this method of soil improvement is very versatile and can be used with technical and economical success. Quality control measures applied so far were closely related to individual project requirements and were based on active control during work execution, including the recording of production parameters and additional soil testing, as well as on post execution tests, including column inspection, sampling and even preloading, if necessary.

The DSM technology still needs optimisation in relation to the equipment, mixing procedure and energy as well as with respect to type and amount of binders applied for different soils, in particular. Moreover, internationally accepted standards for DSM would be very helpful to assure rational and responsible application of this technology in the future.

Annexure III Technical paper on the project case study on “Deep Soil Mixing in Mine tailing for 8m Deep Excavation”, Y.W Yee, V.R.Raju, H K Yandamuri, Kuala Lumpur.



# Deep Soil Mixing in Mine Tailings for a 8 m Deep Excavation

Y.W. Yee, V.R. Raju and  
H.K. Yandamuri

*Keller (M) Sdn. Bhd., Kuala Lumpur*

Presented by

**Keller Grundbau GmbH**  
Kaiserleistraße 44  
D-63067 Offenbach  
Tel. +49 69 8051-0  
Fax +49 69 8051 244  
E-mail: [Info@KellerGrundbau.com](mailto:Info@KellerGrundbau.com)  
[www.KellerGrundbau.com](http://www.KellerGrundbau.com)

Presented at the 16th Southeast Asian  
Geotechnical Conference, 2007, Kuala Lumpur,  
Malaysia

Technical paper 32-57 E

# Deep Soil Mixing in Mine Tailings for a 8m Deep Excavation

Y. W. Yee, V. R. Raju & H. K. Yandamuri  
Keller (M) Sdn. Bhd., Kuala Lumpur, Malaysia  
ywyee@keller.com.my

## Abstract:

Soil improvement using mixing technology has advanced appreciably and can now solve a broad spectrum of geotechnical problems. The method basically involves the introduction and mechanical mixing of binder (cement or lime) with the in-situ soils to improve the strength, deformation and permeability characteristics of the problematic soils. The process procedure and operating parameters suitable for use in the delivery and mixing of cement in the ground would depend on the ground conditions such as soil type, density, water content and the end product required. This paper describes the design and construction methods carried out to enable an 8m deep excavation in very soft ex-mining slime using Deep Soil Mixing (DSM) technique for a sewage treatment plant in Kuala Lumpur. It is demonstrated that cement mixing increased the shear strength of the soil by more than 50 times within a short period which enable the excavation to be carried out at a steep 45 degrees whilst excluding groundwater. This procedure proved to be more cost and time effective compared to the original idea of using sheet piles, anchor tie-backs and grouting. The design process is explained touching on soil investigation to derive engineering and process parameters and subsequent computer simulations. The importance of quality control measures during construction stage are emphasized and available proving methods for the post construction stage are also discussed.

## I BACKGROUND

The Sewage Services Department of the Ministry of Housing and Local Government, Malaysia proposed to construct a Sewage Treatment Plant in Kuala Lumpur. As part of the treatment process, four (4) numbers of 23m diameter digesters were constructed at equi-distance from each other (see Fig. 1). Each digester is essentially a 15m high tank with a coned shaped (45 degree) base buried 8m below ground.

To construct the cone shaped base, it was necessary to firstly, excavate the soil. Being a former tin mining land, the ground is underlain by very soft slime. Conventional excavation method would require multiple handling of installing anchored sheet piles and subsequent removal of soft slime before replacement with competent soil formed at 45 degrees. An alternative method was realised using deep soil mixing technique which involved treating the

soft ground beneath the tank footprint and subsequent excavation of the cone shaped base without the need of any excavation support system.

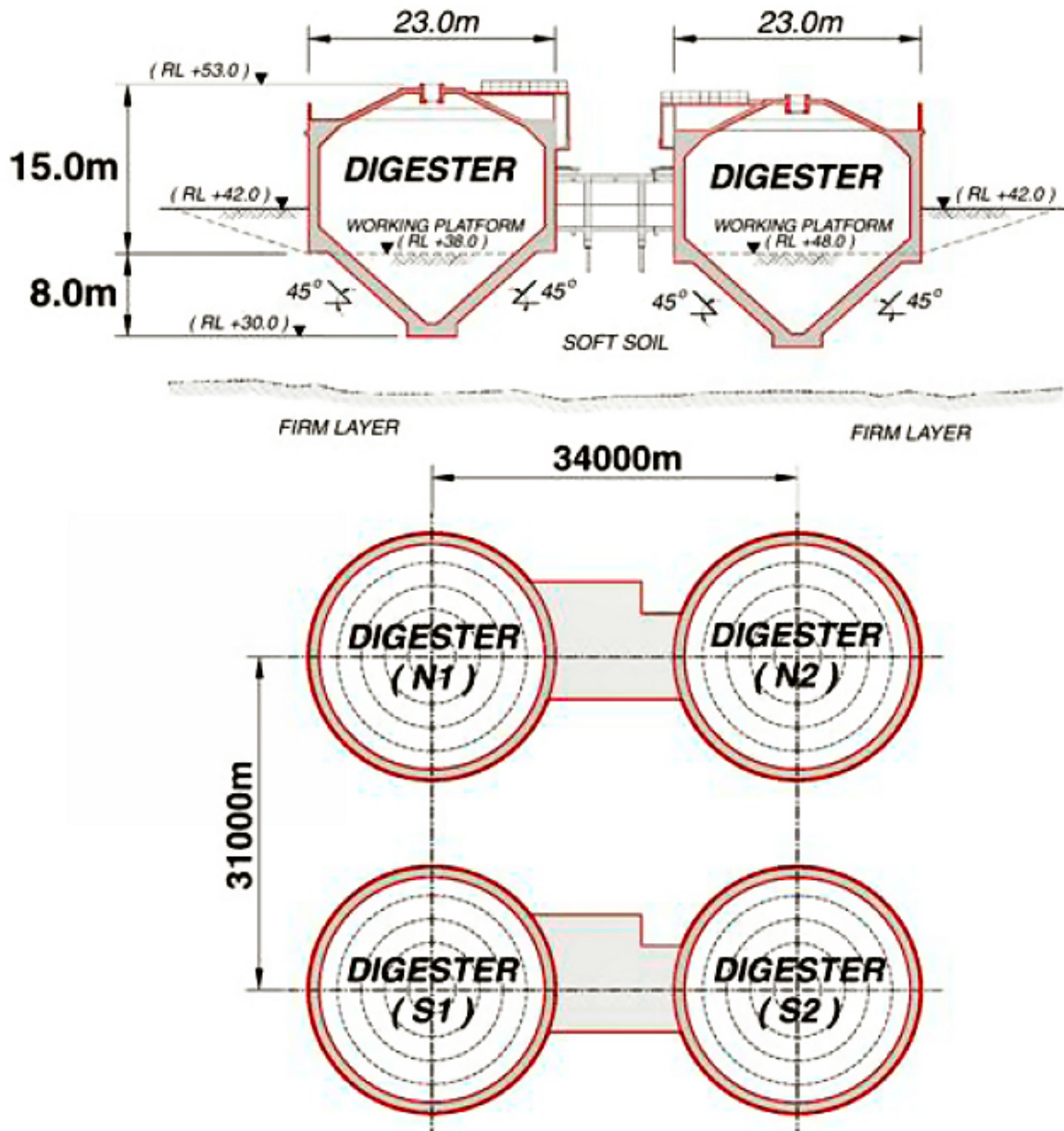


Fig.1 Typical view of four digesters

## 2 SITE LOCATION

The site is located off Tasik Titiwangsa in Kuala Lumpur. The site is a former tin mining land and situated adjacent to private dwellings. Construction works were required to cause minimal disruption to these surrounding properties, especially with regards to ground movement and noise pollution. The four digesters are located at the north-east corner of the site. As shown on the aerial view (Fig. 2), the four digesters are arranged at equal distance from each other and named N1, N2, S1 and S2.



Fig.2 Arial view of the site showing location of digesters

### 3 SUBSOIL CONDITIONS

Being a former tin mining area, the site is underlain by highly variable soil conditions. Very soft slime was found at the foot-prints of 3 of the digesters (N1, S1 and S2) while loose sand with slime layers was found at one of the digesters (N2). The depth of limestone bedrock typically varied between 7m and 13m below ground. The groundwater table was about 2m below ground.

The slime has typically the following characteristics: unit weight  $1.5\text{t/m}^3$ ; moisture content 80% - 100%; liquid limit 70% - 80%; plasticity index 30% - 40%. Geonor vane shear test showed undrained shear strength ( $C_u$ ) of between 5kPa and 10kPa. Typical result of dynamic penetration test (DPT) showing extent of slime (essentially zero blow count) is shown in Fig. 3.

The loose sand (beneath N2) has typically the following characteristics: unit weight  $1.7\text{t/m}^3$ ; moisture content 50%. Typical result of dynamic penetration test (DPT) showing the mixed soil conditions is shown in Fig. 4, generally less than 10 blows / 10cm. Limited SPT tests done on the loose sand, which showed SPT N between 3 to 8 blows / 30cm. Table 1 summarises the typical subsoil conditions for the four digesters.

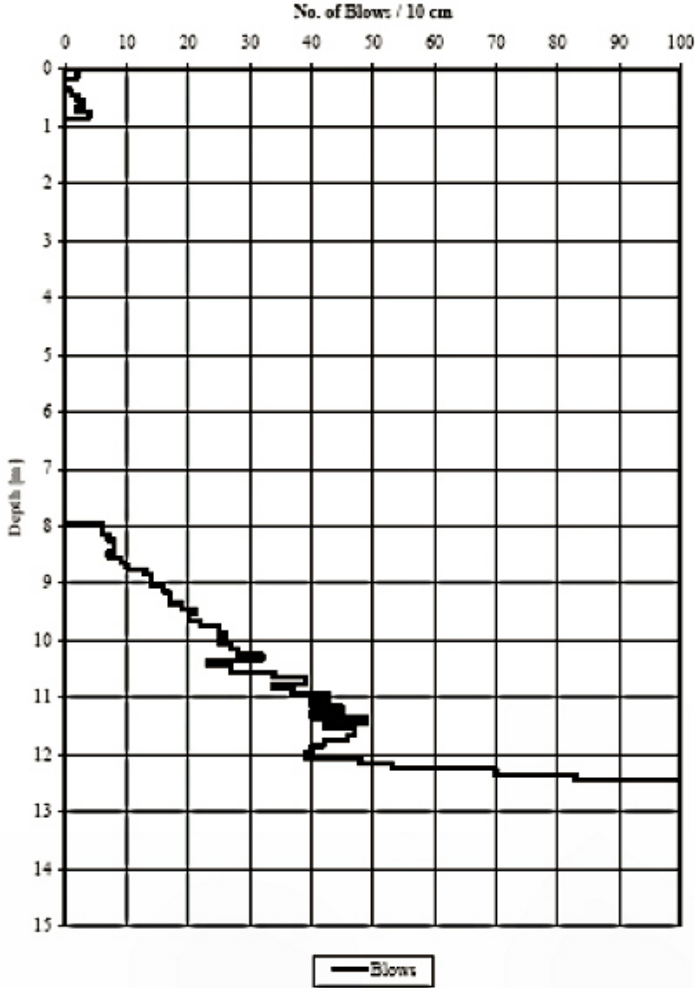


Fig. 3 Typical result of DPT showing slime below N1, S1 and S2

Digester Reference	Typical Subsoil Conditions	
	Top level	Description
Digesters N1, S1 and S2	0m	Fill material
	1m	Very soft slime
	8m	Soft to firm sandy clay
	7 – 13m	Weathered limestone
Digester N2	0m	Fill material
	1m	Loose silty sand (with slime layers)
	12m	Weathered limestone

Table 1 Summary of typical subsoil conditions

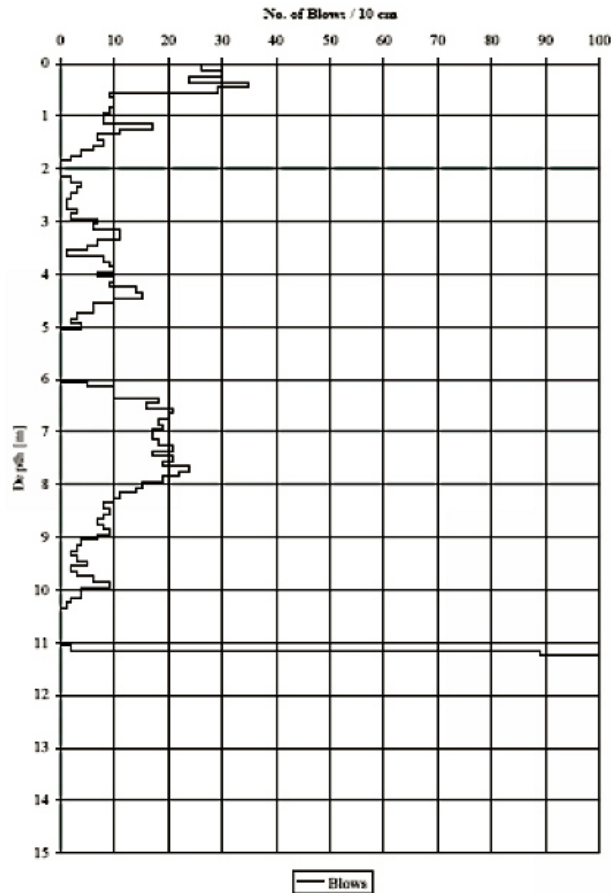


Fig. 4 Typical result of DPT showing loose sand with inter-bedded slime layers below N2

#### 4 GROUND IMPROVEMENT CONCEPT

The objective of ground improvement was to treat the soft ground by improving its strength and stiffness characteristics such that excavation could be carried out safely. The soil was also required to be made fairly impermeable to water to reduce risk of piping and ground loss.

After reviewing many options, it was found that Deep Soil Mixing (DSM) presented the most technically acceptable and cost effective solution.

The soft soil would be mechanically mixed with cement and the end product would be a stiff stabilised soil to allow the required 8m deep excavation. A schematic drawing showing the DSM treated block and geometry of excavation is shown in Fig.5.

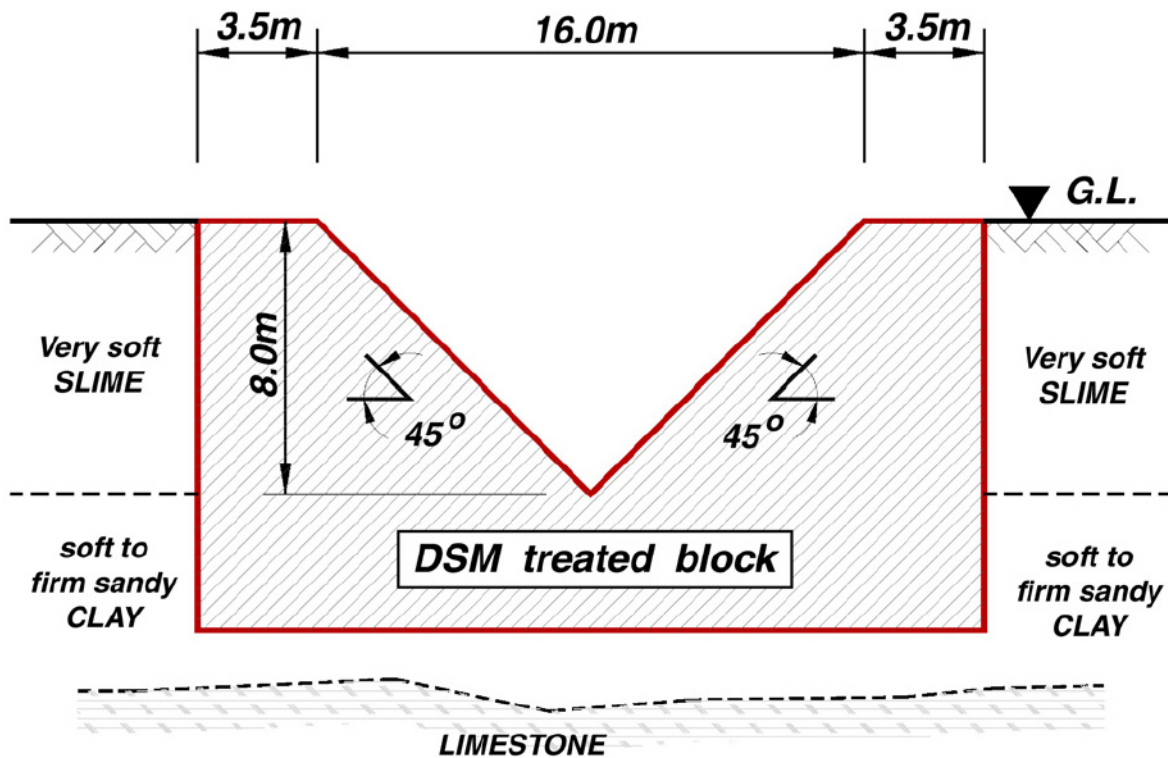


Fig. 5 Schematic of DSM treated block

## 5 DEEP SOIL MIXING TECHNIQUE

Deep Soil Mixing (DSM) technology was invented almost 30 years ago and is a form of ground improvement involving the introduction and mechanical mixing of in-situ soft soils with cementitious compound (CDIT 2002). The compound (which is of-ten referred to as the binder) can be injected into the ground in dry or wet form. A mixing tool is drilled to the intended depth and then withdrawn to form individual columns (diameter can range from 0.5m to 1.5m). The tool is lowered and withdrawn at pre-determined rate of rotation, rate of penetration and rate of withdrawal while delivering the design binder content at a specified flow rate and pressure. The end product is an improved soil with undrained shear strength ranging from 0.1MPa to 6.0MPa, depending on the soil type, mixing process and binder content. Typical applications of deep soil mixing include foundations of embankment fill for roads and highways, stabilization of excavations, foundations for structures and subgrade improvement (Topolnicki 2004; Raju & Abdullah, 2005).

The 'dry' method is more suitable for soft soils with very high moisture content and hence, it was used at digesters NI, SI and S2. Typical picture showing 'dry' DSM rig is shown in Fig. 6.



*Fig. 6."Dry" DSM rig*

The 'wet' method is more appropriate in mixed soil conditions which are generally stiffer, with lower water content. Hence, the 'wet' method was adopted at digester N2. Typical picture showing 'wet' DSM rig is shown in Fig. 7.



*Fig. 7."Wet" DSM rig*

## 6 ENGINEERING ANALYSES

The excavation was designed to satisfy the following conditions:

- a) A 45 degree slope was to be excavated down to 8m depth below ground.
- b) Water seepage into the excavation from the sides and base was required to be minimal.
- c) The treated block was to be able to resist flotation forces.

The DSM design (in terms of cement content and mixing parameters) was determined using theory established by Broms (2004) and in accordance to the design methodology developed by Swedish Geotechnical Society (SGF Report 4:95E 1997).

Slope stability analyses were carried out employing the composite improved parameters. The following Fig. 8 shows critical slip circles from the slope stability analyses (Bishop modified method) to achieve factor of safety above 1.4.

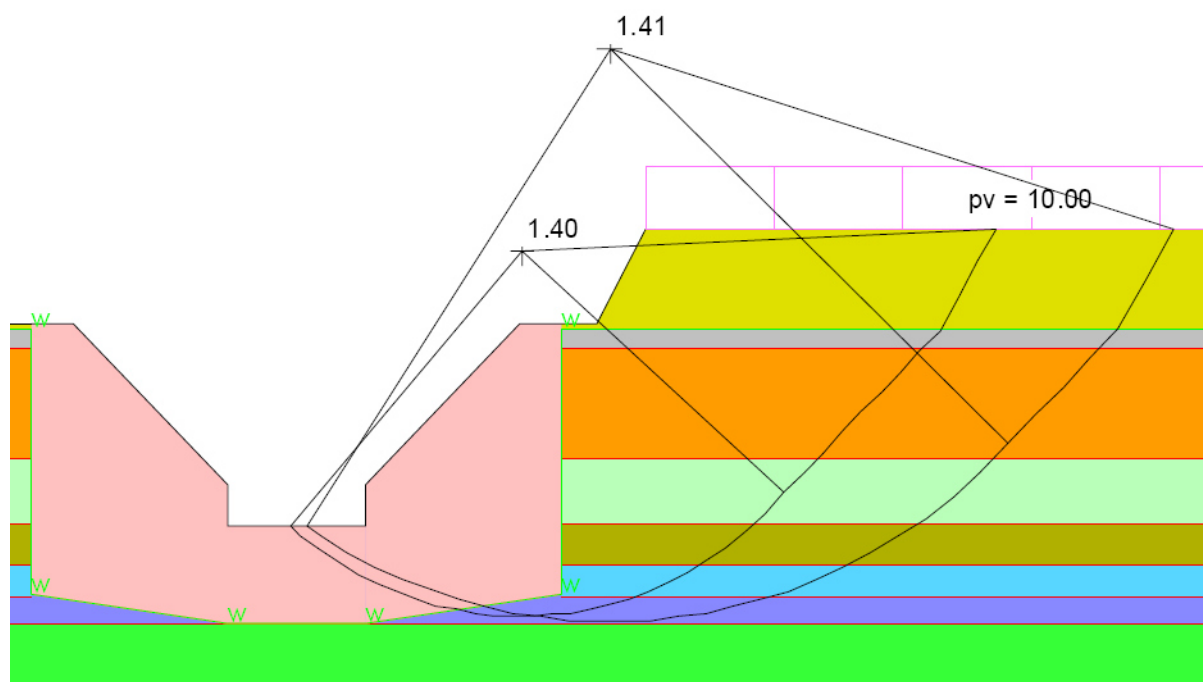


Fig. 8 Typical slope stability analyses

The columns were generally designed to be contiguous (touching columns representing 87% treatment) in the slime soils to minimise water infiltration i.e. at N1, S1 and S2. In the more permeable mixed soils of N2, greater precautionary measure was taken by overlapping the columns (100% treatment).

The DSM block was also designed to be sufficiently massive to overcome potential uplift forces (see Fig. 9). Besides, the block was checked to be adequately stiff to prevent any shear type failure. It was also ensured that no tension forces developed within the block using FEM analyses.

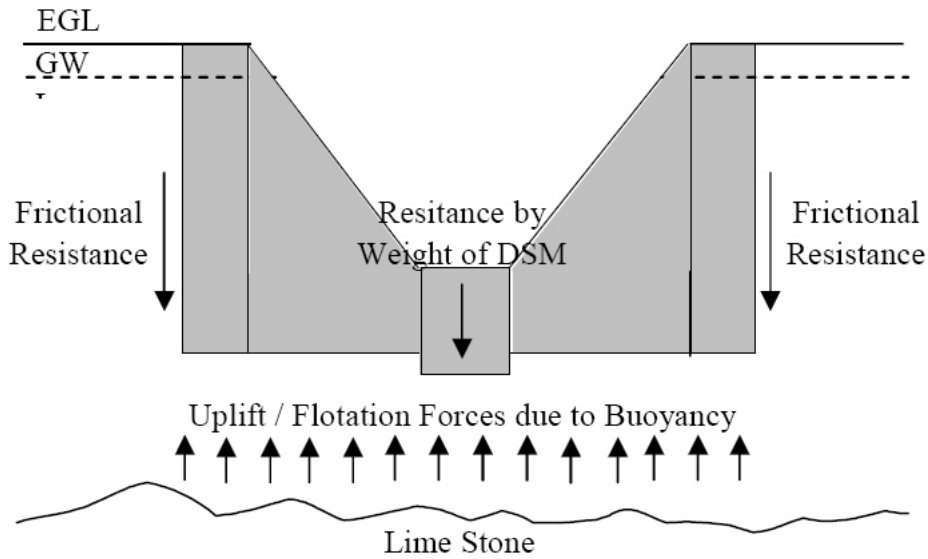


Fig. 9 Design model against flotation forces

## 7 CONSTRUCTION

The soil beneath the digester footprint was essentially treated to form a massive block with conical shape geometry. Individual columns of soil were mixed with cement in contiguous fashion (or with overlap for N2). A typical layout of the treatment scheme is shown in Fig. 10.

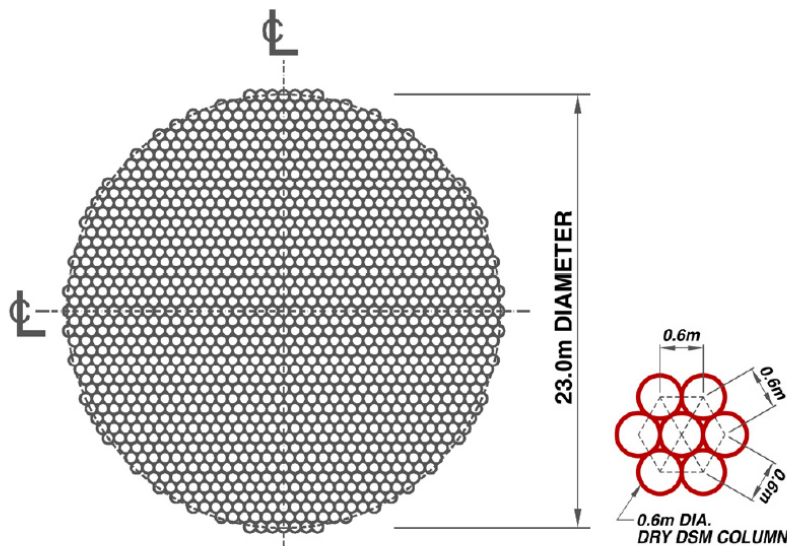


Fig.10 Typical Layout showing DSM treatment scheme

As explained in section 5, both the 'dry' and 'wet' methods of installation were used, due to the variable soil conditions. Basic parameters of 'wet' and 'dry' DSM are summarized in Table 2.

Parameters	'Dry' DSM	'Wet' DSM
Column diameter	0.6m	0.87m
Grid pattern	Triangular	Triangular
Grid spacing	0.6m	0.75m
Depth of treatment	7 to 13m	10 to 12m
Design undrained shear strength (Cu)	150kPa	150kPa
Binder type	Dry cement (OPC)	Grout slurry (w/c ratio = 1.0 to 1.5)
Volume of binder	150 to 200 kg/m <sup>3</sup>	150 to 200 kg/m <sup>3</sup>
Curing time	About 3 to 4 weeks	About 3 to 4 weeks

Table 2 Summary of 'dry' and 'wet' DSM parameters

Construction was carried out with one 'dry' rig and one 'wet' rig. The mixing tools of 'dry' and 'wet' DSM is shown in Fig. 11 and Fig. 12, respectively. The DSM works were commenced in November 2004 and completed in February 2005.



Fig. 11 Process of 'dry' DSM



Fig. 12 Process of 'wet' DSM

## 8 QUALITY CONTROL AND MONITORING DATA

Numerous quality control measures (pre, during and post construction) were implemented which included:

- a) Additional soil investigation to confirm actual soil conditions prior to commencement of soil improvement works as high lighted in section 3.
- b) Trial columns on site prior to construction of working columns.

- c) Real-time computerised monitoring of operating process parameters during construction.
- d) Post construction testing using Standard Penetration Test (SPT) in the field and horizontal coring and subsequent unconfined compressive strength (UCS) test in a laboratory.
- e) Monitoring of lateral displacements using inclinometers during excavation works.

Prior to construction of working columns, trial columns were constructed at designated locations to confirm operating parameters (cement content, rotation speed, withdrawal rate, etc.). After allowing for sufficient curing time, the columns were exposed by excavation for examination. The trial 2.5m deep excavation clearly demonstrated that the previously very soft / loose soil has been successfully treated to allow a vertical cut (see Fig. 13). The diameter and consistency of the columns were also proven.

After initial trials, installation of working columns was commenced with appropriate operating process parameters. The process parameters were closely monitored during installation using real time computer and printout. A typical real-time computerized installation record during construction stage is shown in Fig. 14.



*Fig. 13. Exposed trial columns and subsequent excavation*

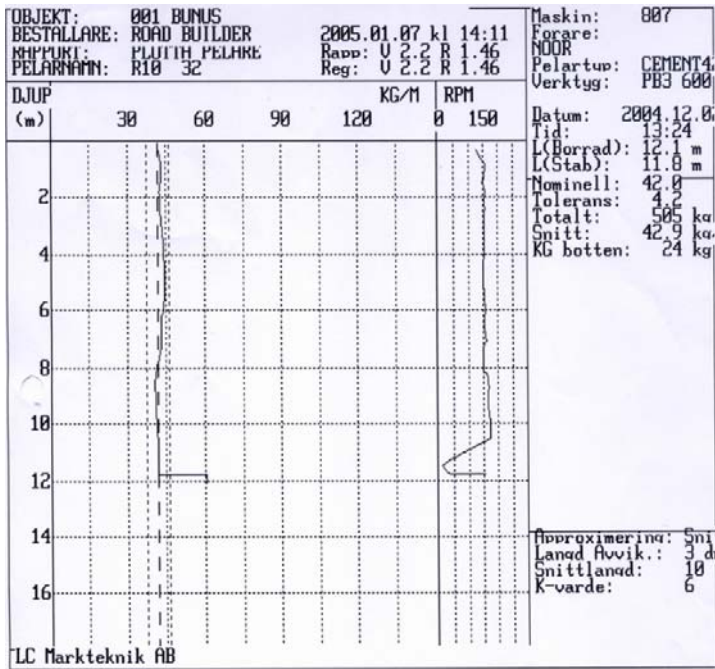


Fig 14 Typical real-time computerised installation record

After sufficient curing period, selected working columns were cored vertically using conventional soil investigation rig (see Fig. 15) to recover samples of 50mm to 60mm diameter. It was observed that it was difficult to retrieve continuous intact cores samples, probably because the columns were relatively low strength. Hence, such coring processes were mostly useful only for visual examination of samples. Standard Penetration Tests (SPT) were carried out for some columns and were used to confirm increase in stiffness of the soil. Typical results are presented in Fig. 15.

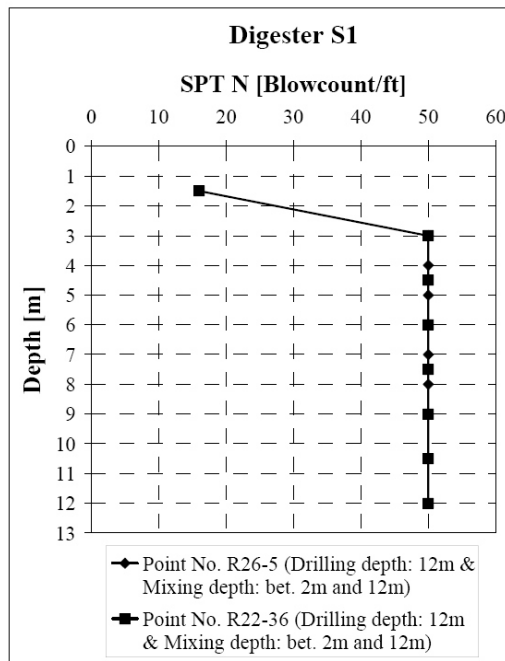


Fig. 15. Vertical coring and SPT result

Horizontal coring was found to be more effective in recovering continuous intact samples. After localised excavation, selected working columns were cored horizontally using hand-held coring machine to recover 100mm diameter samples (see Fig. 16). The solid cored samples were tested in a laboratory and showed more than acceptable UCS (Unconfined Compressive Strength) between 1MPa and 3MPa about 1 to 2 months after installation



*Fig. 16 Horizontal coring and UCS testing*

Cone Penetration Tests (CPT) were attempted but generally gave misleading results. It is noted that within each column cross section there was strength variability and the CPT probe was too small to provide representative result for the entire cross section. Such limitation of the testing method has been observed by others (Larsson 2005).

## **9 EXCAVATION**

Excavation was supposed to have been carried out about one month after installation. However, this was delayed by 3 months due to other outside factors. Typical exposed DSM columns during excavation works are shown in Fig. 17. The intended depth of excavation was reached safely without incident (see Fig. 18).



*Fig. 17 Typical exposed DSM columns during excavation*



*Fig. 18 Completed excavation*

Water infiltration into the excavation was minimal for N1, S1 and S2. At digester N2, localised compaction grouting was implemented to arrest water inflow where weathered rock was found and where mixing had to be terminated prematurely. Inclino-meters were installed to monitor lateral displacement during excavation works which showed minimal lateral movement in the range of 1mm to 3mm (see Fig. 19).

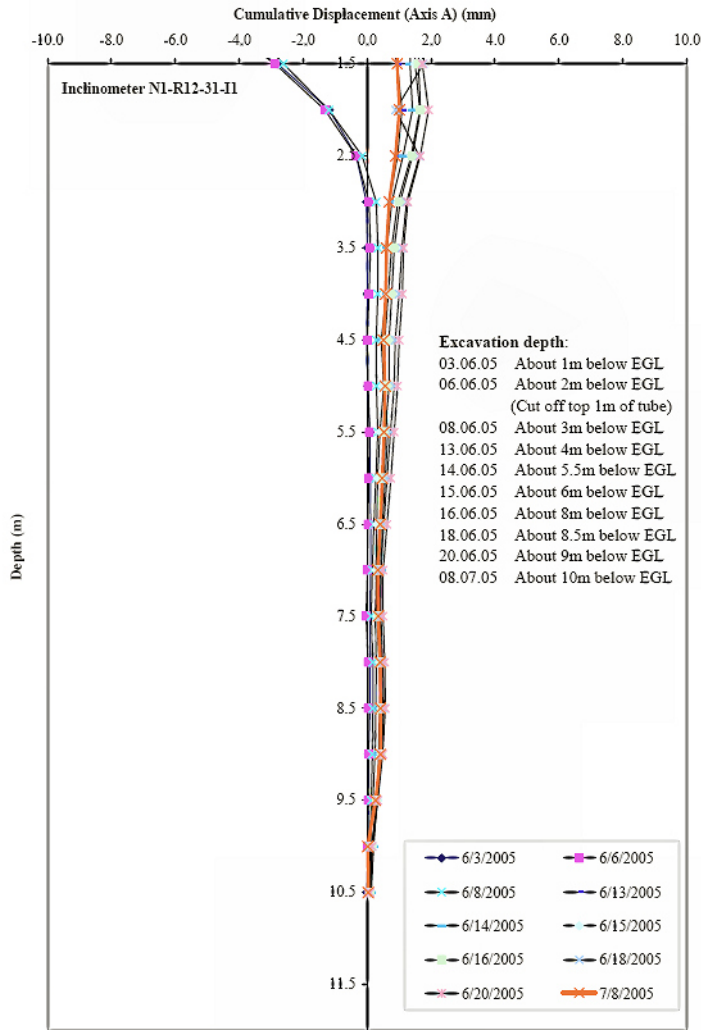


Fig. 19 Results of inclinometer during excavation

## 8 CONCLUSIONS

Deep Soil Mixing technology has been shown to be effective in the treatment of very soft mine tailings. The shear strength of the soil was increased by more than 50 times within a curing period of about 1 to 2 months. The soil treatment enabled 8m deep excavation to be carried out at a steep 45 degrees slope for four (4) digesters. Water infiltration, within the high groundwater environment, was largely excluded without the need for any cut-off wall. The DSM method was proven to be able to provide significant savings in construction cost and time compared to the conventional method of using sheet piles, anchor tie-backs and grouting.

## ACKNOWLEDGMENTS

The authors wish to thank the Main Contractors, Road Builder Bhd for allowing new engineering ideas to be implemented in this project. The support provided by the Project Consultant, Minconsult Sdn. Bhd. is also gratefully acknowledged. Contribution from Keller's staff has been significant, notably Dr. How Y.C. & Mr. D. Schrader (design), Mr. U.P. Raju (project management) and Mr. N. Peterzen (site superintendent).

## REFERENCES

- Broms, B.B. 2004. Lime and lime/cement columns. *Ground Improvement (2<sup>nd</sup> Edition)*, Edited by Moseley, M.P. & Kirsch, K. Spon Press: 252–330.
- Coastal Development Institute of Technology (CDIT). 2002. *The Deep Mixing Method – Principle, Design and Construction*, A.A. Balkema Publishers, Japan.
- Larsson, S. 2005. On the Use of CPT for Quality Assessment of Lime Cement Columns. *Proceedings of the International Conference on Deep Mixing Best Practice and Recent Advances*, Stockholm, Sweden.
- Raju, V.R. & Abdullah, A. 2005. Ground Treatment Using Dry Deep Soil Mixing for a Railway Embankment in Malaysia. *Proceedings of the International Conference on Deep Mixing Best Practice and Recent Advances*, Stockholm, Sweden.
- Swedish Geotechnical Society (SGS): SGF Report 4:95E. 1997. *Lime and Lime Cement Columns – Guide for Project Planning, Construction and Inspection*, Linkoping, Sweden.
- Topolnicki, M. 2004. In situ soil mixing. *Ground Improvement (2<sup>nd</sup> Edition)*, Edited by Moseley, M.P. & Kirsch, K. Spon Press: 331–428.

Annexure IV Technical paper on the project case study on “Excavation Support for TBM Retrieval Shaft using Deep Soil Mixing Technique, Kuala Lumpur”, Ir. Yew Weng, Yee and Ir. Yean Chin & Tan.

# Excavation Support for TBM Retrieval Shaft using Deep Soil Mixing Technique, Kuala Lumpur

Ir. Yew Weng, Yee<sup>1</sup> and Ir. Yean Chin, Tan<sup>2</sup>

<sup>1</sup> Keller (M) Sdn Bhd, Kuala Lumpur

<sup>2</sup> G&P Professionals, Kuala Lumpur

Email: info@keller.com.my

**ABSTRACT:** As part of the construction for the Klang Valley Mass Rapid Transit (KVMRT) Line 1, the South Portal structure at Taman Maluri acted as the shaft to retrieve the Tunnel Boring Machine (TBM) from Cochrane Station. An earth retaining system was required to retain the 15m deep shaft. Deep soil mixing (DSM) columns were used to provide excavation support instead of conventional secant bored pile walls in limestone. The DSM columns were constructed to form a gravity block which has no steel reinforcements and allowed excavation to be carried out without lateral supports. This enabled the TBM to be driven through and retrieved without the need to cut through reinforcing bars or having to design complex placement of struts.

**KEYWORDS:** Deep Soil Mixing, Limestone, Excavation, Cement

## 1. INTRODUCTION

The Klang Valley Mass Rapid Transit (KVMRT) Project when completed will cover a distance of 51km and comprise of 31 passenger stations. The South Portal structure at Taman Maluri, Kuala Lumpur (KL) acted as the transition point between the elevated and underground sections of the Sungai Buloh - Kajang line and also, as the shaft for retrieval of the Tunnel Boring Machines (TBM) from Cochrane Station. The rail level is about 15m below the existing ground level. The ensuing 15m deep excavation required an earth support system. Conventional secant pile retaining walls in limestone have to be designed to resist bending moments and minimise lateral deflection. This is normally done using steel reinforcing bars and steel struts (or anchors). These steel elements do not provide convenient exit for the TBM and hence, an alternative retention system had to be devised.

Deep Soil Mixing (DSM) walls have been used with increasing regularity in Kuala Lumpur (Yee & Chua, 2008), especially over KL limestone formation. The advantages stem not only from the omission of steel reinforcement and lateral bracings, but when designed as a gravity structure, the DSM wall does not need to be socketed into limestone rock. However, there is no prior record of use of this type of wall for mass-transit station boxes and TBM retrieval shafts.

This paper explains the design philosophy adopted for the DSM retention system. The ensuing construction technique, including quality control and safeguards, are also explained. Subsequent performance, during and after TBM break-out, is assessed, together with suggested improvements for future application.

## 2. SITE LOCATION

The site is located within a commercial hub and beside a very busy Jalan Cheras, in Taman Maluri, Kuala Lumpur (see Figure 1). The site was a former petrol station. 3-storey commercial buildings are found just off the south of the site. Construction logistics issues included limited movement of construction vehicle during traffic peak hours and tight space constraint.

## 3. SUBSOIL CONDITION

Based on Geological Map of Selangor, Sheet 94 Kuala Lumpur 1976 and 1993, published by the Mineral and Geoscience Department, Malaysia, the proposed site is located over Kuala Lumpur limestone formation. Ground conditions in limestone areas are known to be exceptionally challenging (Chan, 1986). Due to the inherent karstic feature of limestone bedrock, depth of the limestone

bedrock is highly irregular. Adding to the natural complexity of the ground, the site was a former tin mining area and hence, highly variable soil composition is to be expected.



Figure 1a Location Plan (aerial view)

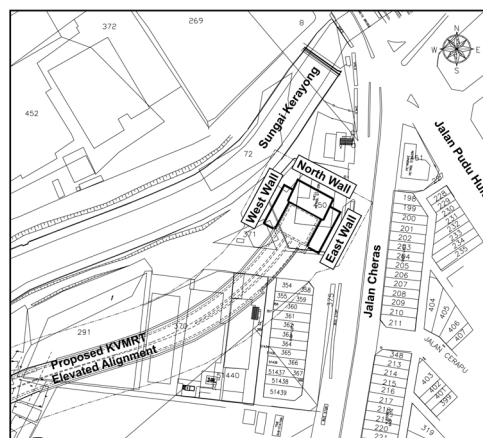


Figure 1b Location Plan (drawing)

Seven (7) boreholes were conducted on the site during the design stage. These showed that thickness of overburden soil varied between 7m and 10m below existing ground level. The soil

generally comprised of sandy silt with interbedded layers of soft clay. This is typical of former tin mining soil. The soil was of soft to stiff consistency with SPT blow-counts typically in the range from 2 to 12 blows/ft.

Before commencement of site work, further information on the rock head profile was gathered by conducting a series of probes along the perimeter of the wall and also, perpendicular to the excavation. This enabled a profile of the rock head to be generated for the purpose of design (see Figure 2).

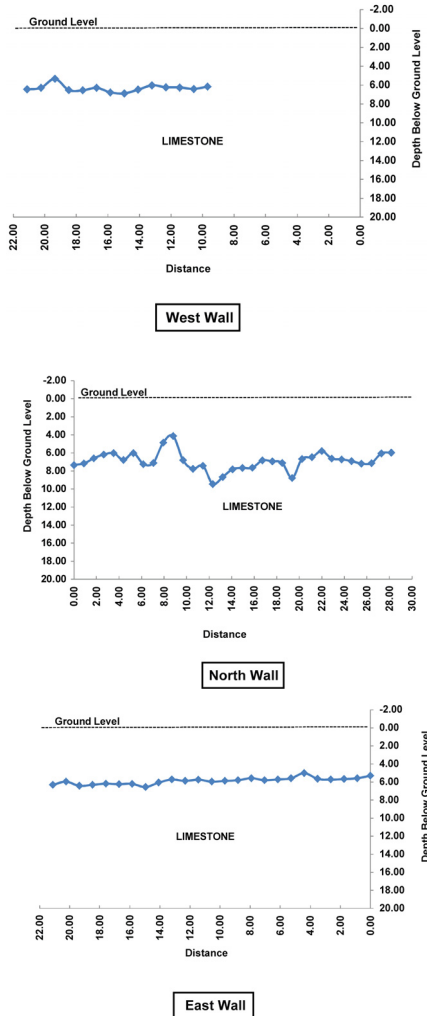


Figure 2 Rock Profile along Wall Perimeter

#### 4. PROPOSED STRUCTURE

At the Maluri South Portal, two numbers of TBM crossed beneath the ground (invert level about 15m below ground surface). At the end of the tunnelling route, a retrieval shaft was required to retrieve the two TBMs. The retrieval shaft was to be formed by vertical excavation retained by an earth support system. As shown in Figure 3, three faces of the wall need to be retained, the most critical being the TBM drive exit. The retaining wall was not only required to resist active earth (and water) pressures but also the TBM thrust pressures at the drive face induced as the TBM daylight into the shaft. Figure 4 shows the cross section of the TBM drive exit face.

Conventional station boxes for the KVMRT were formed using secant bored piles and braced by horizontal struts (or anchors where space permits). Secant piles have advantages in the limestone geology as (i) each pile element can be terminated at different depth (depending on the rock head) after adequate rock socket is achieved, (ii) the interlocking pile elements minimise groundwater ingress into the excavation shaft. However, secant pile retaining walls have to be designed to resist bending moments and minimise lateral deflection. This is usually achieved by means of dense steel reinforcing bars and steel struts (or anchors). When it

comes to TBM exit point, these steel elements do not provide a convenient passage. Hence, an alternative retention system was devised for this retrieval shaft.

Deep Soil Mixing (DSM) walls are becoming more common in Kuala Lumpur (Yee & Chua, 2008), especially for excavation over KL limestone formation. When designed as a gravity block, steel reinforcements and lateral steel bracings are not required; and rock socketing is also not needed. DSM walls have not been used for KVMRT station boxes mainly due to lack of case history for such application. There was concern of medium term durability of the unreinforced wall elements (as the excavation may be kept opened for more than 2 years).

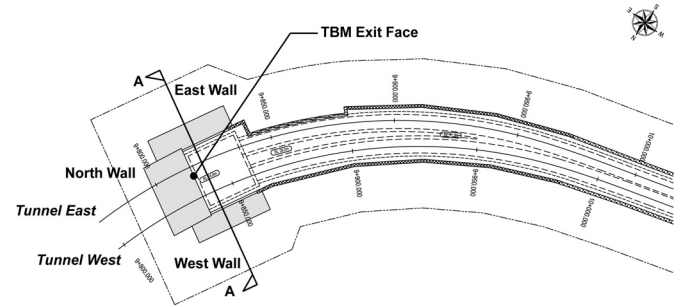


Figure 3 Layout Plan of Shaft

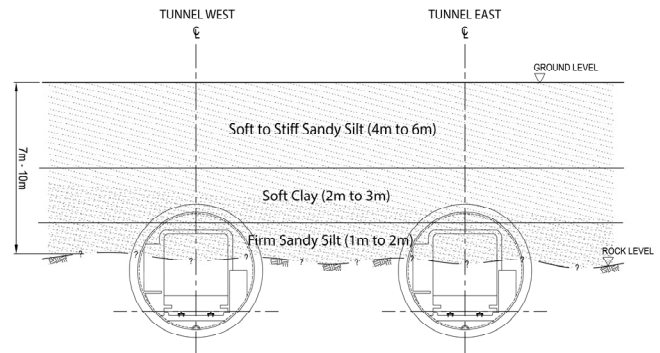


Figure 4 Cross Section of Shaft (Section A-A)

#### 5. DESIGN CONSIDERATIONS FOR A DSM WALL

DSM technique involves the process of mixing soil with cement slurry by using a mechanical tool, which is drilled into the ground. The mixing tool has cutting blades which are rotated as the tool is pushed into the ground. Pre-mixed cement grout is pumped at high pressures through the mixing tool and injected into the soil during penetration and withdrawal, such that the cement paste and in-situ soil are well blended. Through this process, the in-situ soil is improved by cement hydration hardening, bonding of soil particles and filling of voids by pozzolanic hardening (CDIT, 2002). The end product will have greatly enhanced strength, low permeability and low compressibility compared to the original soil. Typical mixing tool is shown in Figure 5.

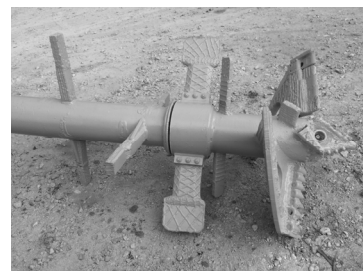


Figure 5 DSM Mixing Tool

For application at the Maluri Retrieval Shaft, the design requirements for the composite wall were reviewed from past projects and literature. Various column configurations were considered.

**5.1 Discrete Columns Arrangement**

Individual DSM discrete columns have been shown to perform well to support vertical load for say, railway embankments (Raju and Abdullah, 2005) and even foundation rafts (Topolnicki, 2002). However, such discrete columns are not suitable when required to resist lateral forces and cases of failure have been documented. Topolnicki (2004) reported that tensile strength may be as low as 8% of UCS and unlikely to be higher than 200 kPa. Since the material is rather brittle, lateral shear forces, uneven movements, or bending stresses may result in failure of the column; and if a series of discrete columns are lined up together, progressive failure may ensue (see Figure 6). Hence, the design has to ensure that compressive stress acting on the columns should not be exceeded and tensile stress avoided.

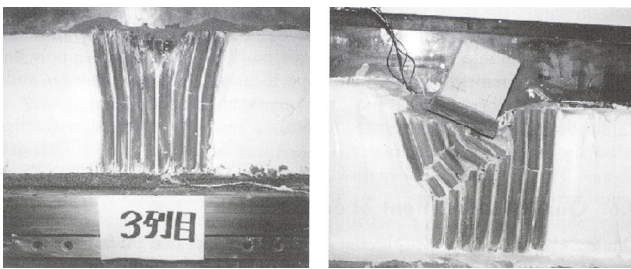


Figure 6 Typical Modes of Failure Observed in Centrifuge Tests (Kitazume et al, 2000)

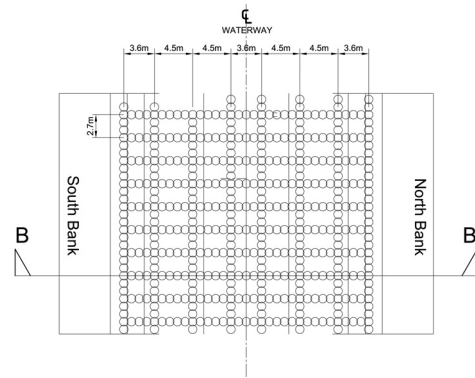
**5.2 Column Grids Arrangement**

Topolnicki (2004) describes applications where grids of columns are constructed and tied together, primarily, to increase rigidity and reduce risks of progressive failure. Since the risks of subjecting the DSM wall to bending forces and movements are increased, detailed analyses using finite element need to be carried out. Strain compatibility between the soil (to mobilise peak shear strength), the structure being supported and the DSM elements would need to be assessed carefully. For example, the failure strain of soft clay is generally 2% to 5%, whilst the DSM column is less than 1% as reported by Topolnicki (2004). Leong W.K. et al (2012) describe such detailed considerations for a slope stabilisation application in soft soils in Singapore. 3D FE analyses were carried out to derive a DSM wall configuration (about 50% replacement ratio) that not only fully utilises the advantages of the composite wall but also isolates the development of tensile stresses (Figure 7). The constructed wall performed efficiently with only 6mm deflection. It should be noted that the Mohr-Coulomb soil model should be used with caution for DSM wall design. At high stress levels, large volumetric change or strain softening may occur, which cannot be captured in the model (Lee, 2011).

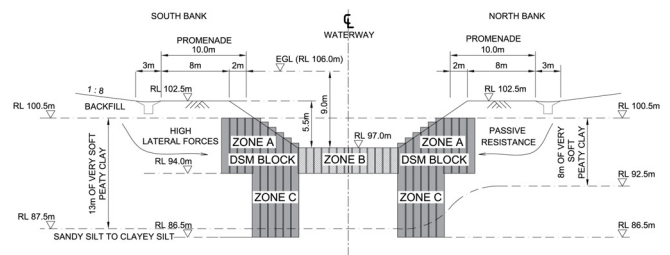
**5.3 Block Arrangement**

The Maluri Shaft was designed to retain a vertical cut face up to 10m high. Together with rock excavation beneath, the total excavated shaft was 15m deep. The consequences of failure were severe and such risks had to be minimised. As such, the design intent was to mix the entire block of soil (100% replacement) using interlocking columns rather than a more economical grid pattern. Having said that, this DSM wall type was still found to be less expensive than conventional secant pile wall. The DSM block was formed by 1m diameter columns overlapping each other by 0.12m thickness in a honeycomb pattern (see Figure 8). Such a configuration ensures that the columns experience less stress;

minimises uneven movements; and there is less concern of the effect of non-uniformity within the block.

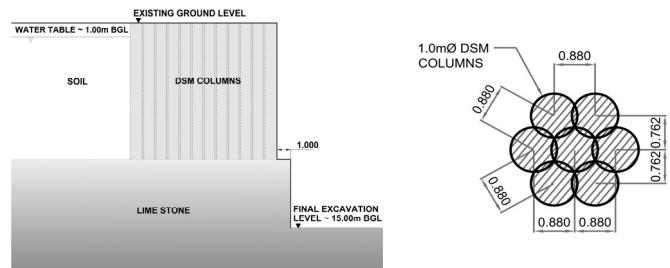


Plan View



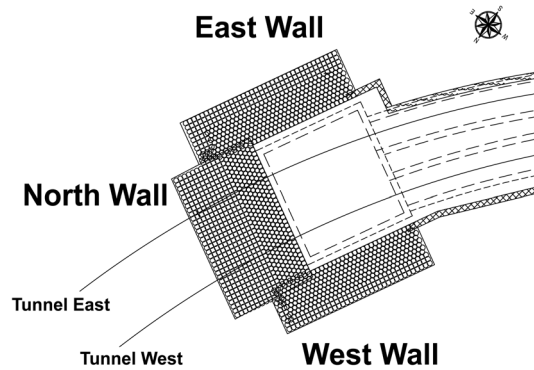
Section B-B

Figure 7 DSM Configuration for Slope Stabilisation (Leong W.K. et al. 2012)



(a) Cross Section

(b) Column Pattern



(c) Wall Layout

Figure 8 (a) Cross Section of DSM Block at the Maluri Shaft (b) Column Pattern (c) Wall Layout

## 6. DSM WALL ANALYSES

The DSM block design was checked against the following failure modes:

### 6.1 Wall overturning stability

The wall had to be sufficiently wide to ensure that it will act like a gravity block. No element of the wall will be subjected to tension or bending forces. Although not an issue on this project site, construction of the wall requires sufficient space (width) behind the excavation face. Generally, if the depth of soil face is  $H$ , then a block width of  $0.6H$  to  $0.8H$  would be required. A factor of safety against overturning of 3.0 was established (see Figure 9).

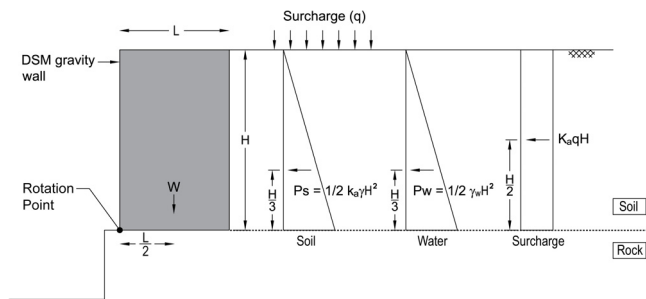


Figure 9 Check for Wall overturning

### 6.2 Wall sliding resistance

Once again, the wall has to be wide enough to provide resisting surface against lateral forces. In the limestone, the uneven rock surface provides excellent interface friction against lateral movement. However, it should be checked that the rock head profile does not incline toward the excavation, which may result in lower resistance than assumed. Sliding check assumed a safety factor of 2.0 (see Figure 10). A check was also made for reduced resistance should the interface be poorly mixed and portions of soils remain.

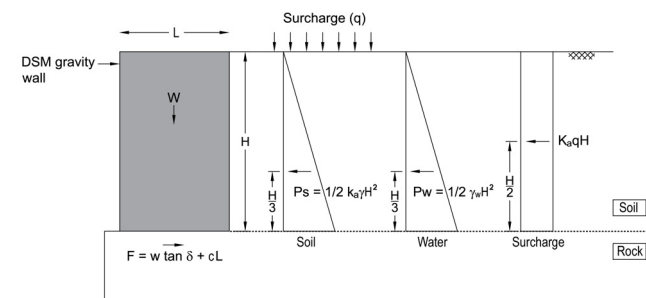


Figure 10 Check for Sliding along Rock Interface

### 6.3 Vertical load support

The block will be carrying temporary construction load. Since the block is supported on limestone rock, bearing capacity to support the load was not an issue. A temporary reinforced concrete slab was cast on the block to spread the load, and avoid any concentrated point load. Short anchor bars were drilled into the DSM block at certain designed grids to tie the slab onto the DSM block. A surcharge load of 20 kPa was assumed.

### 6.4 Inter-locking bond between column elements

The design relies on the effective distribution of soil, water and surcharge loads from the back of the wall into the entire block. For this to happen, load has to be transferred from one element to another via their contact bond (by shear). During construction, it was ensured that “cold joints” were avoided and each column was constructed within 48 hours of the preceding column.

### 6.5 Toe stability

The wall needs to be taken to a sufficient depth to prevent toe “kick out” and basal heave. However, for this project, the rock head is found at a higher level than the excavation level and hence, this check was not relevant.

### 6.6 Groundwater cut-off

The wall has to be effective in reducing water inflow into the excavation, both across the wall and also, the interface between the DSM and rock. Construction of the block was very effective in excluding water, as the size of the block and also, the jagged rock head decreased permeability manifold. The bigger concern of water infiltration stemmed from the untreated rock below the DSM block, with natural fissures and cavities (see Figure 11). It is common to treat the rock by grouting to reduce water infiltration (see Raju and Yee, 2006). Rock fissure grouting was carried out before construction of DSM block at 4m intervals along the excavation perimeter.



Figure 11 Rock Fissures where Water may Ingress into Excavation

### 6.7 Bedrock stability

Pre-construction soil investigation would need to establish that the rock is stable after excavation (against block failure). This is established indirectly, by means of examining the rock quality designation and core recovery ratio. Advice from a geologist is normally sought. During mining of the rock, the exposed rock face was examined at each excavation stage. Rock bolts were installed where there were localised defects found in the rock. Contingency measures to underpin the block using micropiles were planned but not found to be necessary for this project.

### 6.8 Movements (lateral strain)

The DSM block was not designed to withstand high levels of strain. The design had to minimize risks of uneven wall movement.

### 6.9 Blasting force during rock excavation

Mining of the rock within the excavation block is mainly done by controlled blasting. Adjacent to the wall, less invasive mechanical breakers were used. Past work in DSM wall has found that the cement-soil composite structure can tolerate peak particle velocity as high as 50 mm/sec without suffering damage. As a general guide, blasting was not carried out within 3m of the wall face.

### 6.10 TBM thrust pressure

The North DSM wall block had to be wide enough to resist the thrust forces from the TBM. Besides this, TBM operational requirements necessitated extended treatment. Hence, this block was eventually designed to be wider than the others.

Table 1 Dimensions of the DSM Walls

Wall Location	Depth to Rock (m)	Width of DSM Block (m)	Column Dia (m)	Column Interlock (m)	Remarks
North (TBM drive)	4.0 to 10.0	16.7	1.0	0.12	Design governed by TBM operation requirements. As-built DSM column depth varies between 3.5 to 10.5m
East	5.0 to 7.0	9.7	1.0	0.12	Design assumed worst case of 10m soil depth. As-built DSM column depth varies between 3.5 to 7.5m
West	5.0 to 7.0	8.8	1.0	0.12	Design assumed worst case of 10m soil depth. As-built DSM column depth varies between 3.0 to 10.0m

From the above considerations, it is clear that the design of the DSM wall has to consider many practical factors; has to be robust; and with allowance for a fair amount of redundancies. The installed DSM columns were required to have a shear strength of 0.75MPa (UCS = 1.5MPa). The final design dimensions of the wall are summarised in Table 1.

**7. CONSTRUCTION**

Construction of the wall began with site trials to determine the required cement content and mixing parameters. Based on work by Topolnicki (2004) and previous experience in KL, a design cement content between 300 and 350 kg/m<sup>3</sup> was adopted. The operating parameters (e.g. rotation speed, rate of penetration & withdrawal, blade rotation number, flow rate, grout pressure, binder content, etc.) were monitored using real-time computerised recording systems to ensure adequate and uniform mixing of the soil (see Figure 12). Blade rotation number T, defined as the total number of mixing blade passing during 1m of single shaft movement through the soil, was kept above 700 [T = ΣM x (R/V), where M = total number of mixing blades per m depth; R = rotational speed of mixing tool; V = penetration or withdrawal rate m/min]. Most practitioners recommend T > 400 for adequate mixing in normal application.

The formation of “cold joints” had to be avoided. It was ensured that corresponding columns were constructed within 48 hours of preceding columns. Where it was anticipated that this was not possible or there were ground complications, jet grouting was used to form larger columns. For example, in one localized areas, old timber pile foundations were encountered during installation, which required jet grouting to be instituted.

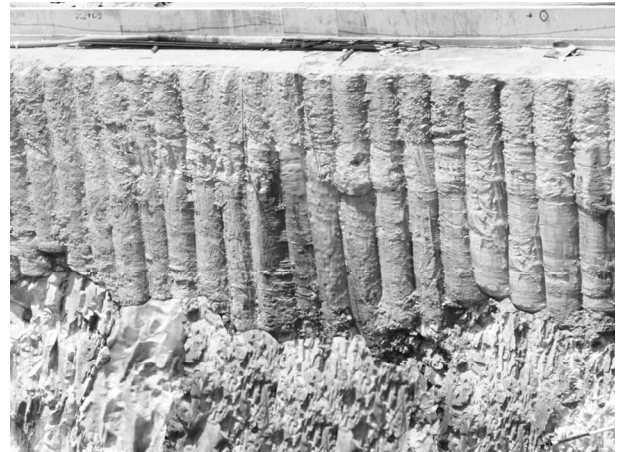


Figure 13 Exposed DSM Columns

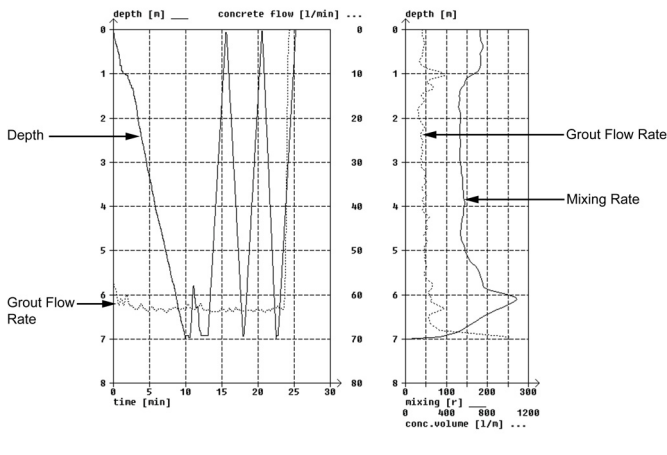


Figure 12 Typical Operation Parameters Monitored by Computer in Real Time during Installation

Figure 13 shows the exposed DSM column and the interface between the column and rock head. Good contact was achieved by keeping the tool at the deepest penetration level for at least 0.5 min whilst jetting and rotating.

There are layers of clay within the soil mass. To avoid formation of soil “bulb”, which impedes thorough soil-cement mixing, a free blade was introduced (see Figure 14).

It was imperative that the columns were interlocked such that the individual columns combined to act as a single block.

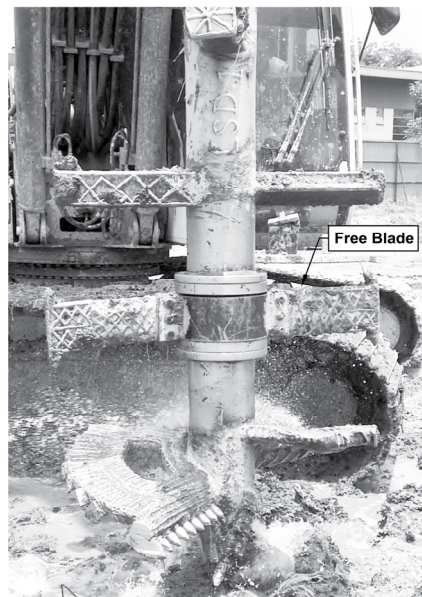


Figure 14 Free Blade in Mixing Tool to Avoid Formation of Soil Bulb

The advancement of DSM technology has resulted in the availability of machines using multiple shafts. Recently, the advent of cutter-soil mixing has also been met with optimism. However, such multiple shaft mixing is not suitable for use in limestone given the pinnacle nature of rock. "Gaps" would result in the soil-rock interface as the blades will be stopped at the highest peak in the limestone. Hence, to ensure proper mixing down to limestone rock head level, a single shaft mixing tool is preferred.

**8. QUALITY CONTROL**

The execution practice and quality control of DSM works follow the British Standard BS EN 14679:2005. A quality plan was drawn up, which included the methods and frequency of checks to be made during construction.

As mentioned before, the operating parameters were monitored using real-time computerised recording systems. Verification process included daily review of these computer records and any deviations were investigated and rectified to the satisfaction of the supervisory team.

Core samples were collected to examine consistency of the columns and to recover sections for unconfined compressive strength (UCS) tests. Cores were done in both the centre and the edge of the columns (where the columns intercept). As shown in Figure 15, test results show UCS strength consistently above 1.5 MPa after 28 days.

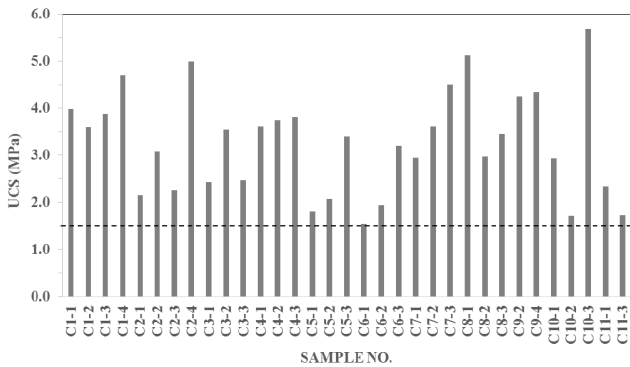


Figure 15 DSM Core Sample UCS Strength Test Results

**9. PERFORMANCE**

Excavation was carried out after completion of the DSM block (subsequent to a curing period exceeding 28 days). Bedrock was mined beneath the block using hydraulic breakers. Rock blasting was carried out nearby and the wall was monitored to ensure that the vibrations induced did not do any damage.

Wall movement was monitored during excavation works using both inclinometers and settlement markers. Three inclinometers were installed, one on each wall face, and twenty-one settlement markers on the ground surface (see Figure 16). Maximum wall movement was observed at East wall, showing a reading of 10 to 15mm (less than 0.15% wall height). The shape of the deflection implied that there was some sliding movement, albeit small. This is well within widely accepted wall deflection criterion of 0.5%. The maximum ground subsidence of 2mm to 6mm was observed behind West wall, and this was probably caused by construction load. Back-analyses imply a stiffness modulus of the block between 35 and 100 x UCS.

Safety precautions were taken during tunnel break-out. This included reducing the TBM slurry pressure to very low levels from usual pressure. The speed of boring was slowed to 30% to 40% of normal speed. In addition to the above, 2 layers of temporary soil nails were installed to strengthen the front face of the DSM block during TBM break-out. The actual TBM break-out occurred on April 8, 2014 (West Tunnel) and April 24, 2014 (East Tunnel). It was reported by the TBM Operators that both break-outs occurred smoothly without incident. There were many spectators viewing the emerging TBMs and they were requested to stand

behind barricades 20m away from the TBM wall face. A video of the break-out is available for view at <http://my.mrt-underground.com.my/videos/breakthrough>. Figure 17 shows the wall during and after TBM exit.

With regards to wall durability, the DSM wall has been standing for 2 years (at the time of writing). Visual examination has found no signs of distress or degradation. For longer term application, weathering resistance can be enhanced with higher cement content (and higher strength of end product). Additional surface protection measures such as applying a gunite surface (with or without steel mesh) may also be implemented. In the permanent stage, structural walls and slabs will be constructed in front of the wall for long term serviceability requirements.

In future, for such applications, the designer could consider economising the design by reviewing the wall width, blade rotation number and other TBM-related parameters.

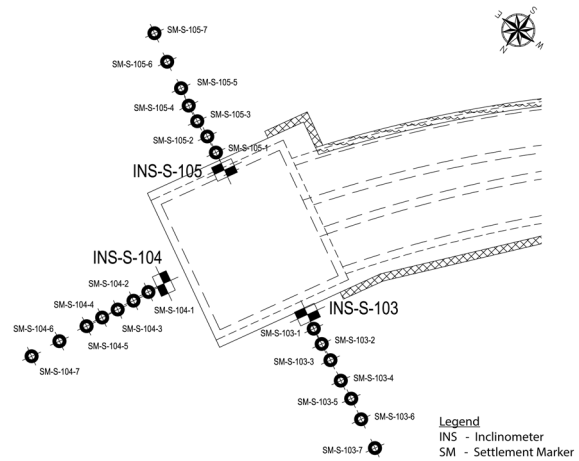


Figure 16 Location of Inclinometers and Settlement Markers



Figure 17 DSM Wall during and after TBM exit

## **10. CONCLUSION**

The Maluri TBM Retrieval Shaft required an excavation of 15m deep. DSM walls comprising 1m diameter columns interlocked with each other were constructed to form a gravity block over three faces of the excavation pit. The DSM block was formed over soil up to 10m high and seated on limestone bedrock beneath. The design was approached with caution given the severe consequences of failure. Besides ensuring high safety factors in various wall stability and sliding checks, the block was designed to be fully treated with cement (100%) to avoid any risk of occurrence of tensile and bending stresses. Strains were kept to a minimum. Construction was carried out with high level of supervision and control, especially in ensuring thorough mixing and avoidance of cold joints between columns. Based on previous experience in similar soils in Kuala Lumpur, the mix design ensured that cement content up to 350 kg per m<sup>3</sup> and blade rotation number above 700 were achieved. The DSM block was excavated with maximum 15mm movement and did not display any distress during the further 5m deep rock excavation afterwards. The DSM wall performed well as the TBM break-out events occurred without incident. The DSM wall stood for 2 years before structural walls were constructed as permanent finish.

## **11. ACKNOWLEDGEMENTS**

The authors wish to thank colleagues from G&P and Keller, for contributing significantly to this project. Their ideas and suggestions during design and construction were invaluable. Grateful recognition is given to Dr. Ooi L.H. for his advice during design development of this project. Appreciation is accorded to PVS Prasad for data compilation in the preparation of this paper.

## **12. REFERENCES**

- BS EN 14679 (2005): Execution of special geotechnical works – Deep Mixing
- Chan, S. F., and Hong, L. E. (1986). Pile foundation in Limestone areas of Malaysia, Foundation Problems in Limestone Areas of Peninsular Malaysia, Geo. Eng. Tech. Div., IEM
- Coastal Development Institute of Technology (CDIT). (2002). The Deep Mixing Method, A.A. Balkema Publisher.
- Kitazume, M. , Okano, K. and Miyajima, S. (2000) Centrifuge model tests on failure envelope of column type DMM improved ground, Soils and Foundations, Vol. 40, No. 4, pp.43-55.
- Lee, F.H. (2011). Cement-Soil Treatment in Underground Construction: Some issues and Recent Findings. Seminar on Infrastructures in Soft Ground – Challenges and Solutions. BCA Academy, Singapore.
- Leong, W.K., Soh, K.K., Yeo, L., Chew, S.H., Leong K.W. and He, Z.W (2012). Deep Soil Mixing Columns as Retaining Structure. 18th SEAGC, Singapore.
- Raju, V.R. and Abdullah, A. (2005). Ground Treatment Using Dry Deep Soil Mixing for a Railway Embankment in Malaysia. Proceedings of the International Conference on Deep Mixing Best Practice and Recent Advances, Stockholm, Sweden.
- Raju, V.R. and Yee, Y.W. (2006). Grouting in Limestone for SMART Tunnel Project in Kuala Lumpur. International Conference and Exhibition on Tunnelling and Trenchless Technology, Kuala Lumpur, Malaysia.
- Topolnicki, M. (2002). Deep Mixing Workshop, Tokyo, 15.–18.10.2002
- Topolnicki, M. (2004). In situ Mixing. Ground Improvement. pp. 331-428.
- Yee Y.W. and Chua C.G. (2008). Case Studies: Deep Soil Mixing in Excavation. Seminar on Excavation & Retaining Walls, Kuala Lumpur. Institution of Engineers Malaysia.
- Yee Y.W., Raju, V.R. and Yandamuri, H.K. (2007). Deep Soil Mixing in Mine Tailings for a 8m Deep Excavation. 16th SEAGC, Kuala Lumpur. pp 573-578.



---

## TABLE OF CONTENTS

<b>1</b>	<b>Background</b> .....	<b>1</b>
1.1	General .....	1
1.2	Technical Committee .....	1
1.3	Brainstorming Session .....	1
<b>2</b>	<b>Grouting Technology</b> .....	<b>1</b>
2.1.1	Types of Grout .....	2
2.2	Methods of Grouting .....	3
2.2.1	Rock/ Fissure Grouting.....	3
2.2.2	Permeation Grouting.....	4
2.2.3	Compaction Grouting.....	5
2.2.4	Jet Grouting .....	5
2.3	Quality Control & Grout Test.....	6
<b>3</b>	<b>Applications</b> .....	<b>8</b>
<b>4</b>	<b>Case studies</b> .....	<b>8</b>
4.1	Case study 1: Seepage control works at Teesta Low Dam – IV, West Bengal, India (Permeation Grouting) .....	8
4.2	Case study 2: Soil arching, Delhi Metro Rail Corporation, Newdelhi (Compaction grouting) ...	9
4.3	Case study 3: Rock Grouting for Deep Shaft for SMART Tunnel (Rock/ Fissure Grouting) .	10
4.4	Case study 4: Settlement control for SMART tunnel (Rock/Fissure Grouting).....	11
4.5	Case study 5: Soil Stabilisation for SMART tunnel (Jet grouting) .....	12
<b>5</b>	<b>Bibliography</b> .....	<b>14</b>

## LIST OF FIGURES

Figure 1: Application range of grouting methods .....	2
Figure 2: Penetrability of various grouts.....	2
Figure 3: Typical cross section of Rock/Fissure grouting.....	3
Figure 4: Process of Rock/Fissure grouting using P, S & T grouting.....	3
Figure 5: Improved ground after completion of Rock/Fissure grouting .....	4
Figure 6: Schematic showing permeation grouting methodology .....	4
Figure 7: Automatic Injection Containers – Computerised Grout Pumps .....	5
Figure 8: Process of compaction grouting.....	5
Figure 9: Execution of jet grouting using T & D system .....	6
Figure 10: Process of jet grouting .....	6
Figure 11: Marsh cone on Grout & Hydrometer test on grout and Water .....	7
Figure 12: Slump cone test .....	7
Figure 13 Quality control monitoring devices .....	7
Figure 14 Quality control records .....	8
Figure 15 Cross section of coffer dam & Permeation grouting .....	8
Figure 16: Teesta Low Dam .....	9
Figure 17: Schematic of the NATM tunnels under an abandoned Nallah channel; the required and existing SPT N values are plotted on the right .....	9
Figure 18 Typical layout of NATM and compaction grouting scheme.....	10
Figure 19 Comparison of Design SPT values with Pre and Post SPT Values & Completed structure	10
Figure 20 Typical layout of grout curtain .....	11
Figure 21 NVM shaft & Dry walls after curtain grouting .....	11
Figure 22 Cross section of grout holes below rail track .....	12
Figure 23 Drilling and grouting beneath rail track .....	12
Figure 24 Schematic diagram of grouting schemes at cutter-head intervention locations. ....	13
Figure 25 Plan & Cross section of Treatment scheme & Grout column after Jet grouting .....	13

## LIST OF TABLES

No table of figures entries found.

---

## LIST OF ENCLOSURES

- Annexure 1 Technical paper on “Ground Improvement Techniques for Infrastructure Projects in Malaysia” by Dr.V. R. Raju and Y Hari Krishna.,2008
- Annexure 2 Technical paper on “Application of Ground anchors to support deep excavation and compaction grouting for NATM tunnel construction for Delhi Metro Rail Corporation (DMRC)” by Jitendra Tyagi, Mohan Gupta, Ashit Shah & Y. H. Krishna and B.C. Kanth
- Annexure 3 Technical paper on “Grouting in Limestone for SMART tunnel project in Kuala Lumpur, Malaysia” by Dr.V. R. Raju and Ir.Y.W. Yee,2006

## **1 Background**

### **1.1 General**

The President Indian Geotechnical Society (IGS) has constituted several Technical Committees (TCs) in order to contribute substantial technical innovations to serve the geotechnical community by publishing guidelines in the field of ground engineering. In this endeavour, IGS formed various TCs to seek support in the preparation of guidelines and publish them on behalf of IGS. In order to form the guidelines, the modus operandi suggested by IGS was to conduct brain-storming sessions in local chapters in each of the selected themes and topics and further to record the proceedings. Each member of the committee shall have to make a presentation followed by a detailed discussion. The chairman of each TC will decide the sub-topics on which the theme paper will be presented by a particular member of the committee, followed by a thorough discussion. The individual TC will develop guidelines with regard to various fields of Geotechnology on behalf of IGS who will contribute in a meaningful way to better geotechnical practices in India.

### **1.2 Technical Committee**

With the above background, IGS has identified Ground Improvement and Geosynthetics is one of the TC and the main objective is to prepare an implementable document for practicing engineers covering Ground Improvement technology, limitations, codal provisions, case histories esp. in India with their performances.

### **1.3 Brainstorming Session**

IGS Hyderabad Chapter has taken initiative to support IGS and conducted one-day National Workshop on Ground Improvement and Geosynthetics on 29<sup>th</sup> August 2015 in JNTU premises. Minutes of meeting was prepared and circulated among the TC members. It was agreed in the meeting that design and construction aspects of ground improvement using Grouting techniques shall be addressed by Keller Ground Engineering Pvt. Limited (Keller).

This document describes concept, theory, design & construction, performance of ground improvement (esp. Grouting) for variety of projects executed in Asia.

## **2 Grouting Technology**

Grouting in ground engineering can be defined as controlled injection of material, usually in a temporary fluid phase, into soil or rock, where it stiffens to improve the physical characteristics of the ground for geotechnical engineering reasons. “Grouting techniques started from practice, not from theory”.

Grouting methods are effective in sealing cavities in both coarse and fine fissures in rock, and sealing pores in granular materials typical of all soils short of clays and very silty sands. With the development of high-pressure pumps cement grouts came to predominate, and they were frequently associated with the sinking of mine shafts.

The in situ deep mixing of stabilizers with soft soils to form columns, walls grids or blocks in the foundation has been developed and applied extensively in civil engineering practice since the 1970s.

The two types of mixing methods, namely deep mechanical mixing (DMM) and high-pressured Jet-grout mixing have been used under deep ground conditions. Both methods rapidly spread nationwide in the 1970s. The method of application range is shown in Figure



## 2.2 Methods of Grouting

There are four principal grouting methods as explained below.

- Rock/Fissure grouting
- Permeation grouting
- Compaction grouting
- Jet grouting

### 2.2.1 Rock/ Fissure Grouting

Rock grouting has a long history of use in dam construction and rehabilitation, and can be applicable to challenges in mining, tunnelling, rock mechanics and environmental remediation. Rock grouting is typically performed to reduce the hydraulic conductivity of, or more appropriately, across a rock mass by injection of grout into the rock's joints and fissures. Its purpose is to fill up artificially created or naturally existing caves, joints and pores with remarkable change in the structure of the void system. Rock grouting serves for sealing and for stabilizing rock and soil. This method is often used to prepare the foundations and abutments for dams. It usually is done using cementing grouts. The typical cross section of intrusion grouting is shown in Figure 3.

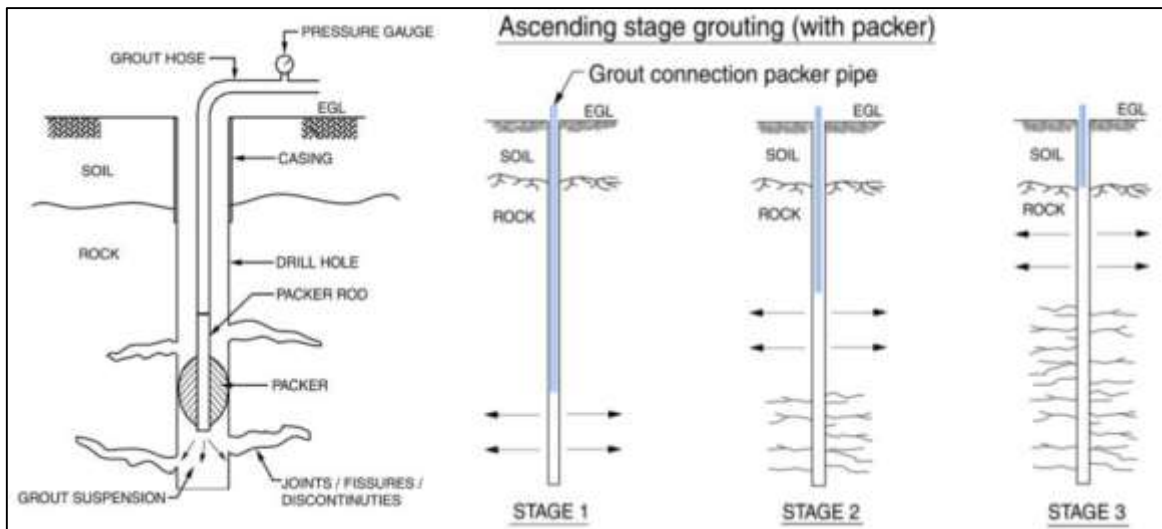


**Figure 3: Typical cross section of Rock/Fissure grouting**

The process of Rock/Fissure grouting using Primary(P), Secondary(S) & Tertiary(T) grouting process is shown in Figure 4.

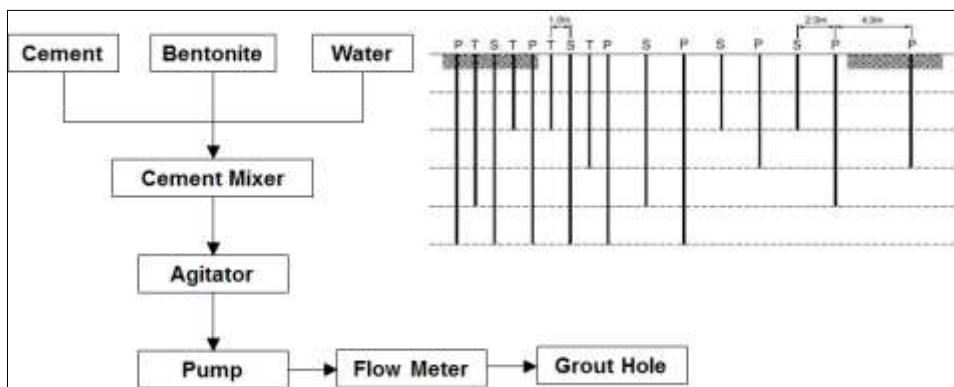


**Figure 4: Process of Rock/Fissure grouting using P, S & T grouting**

The Improved ground after the completion of Rock/Fissure grouting is shown in Figure 5.

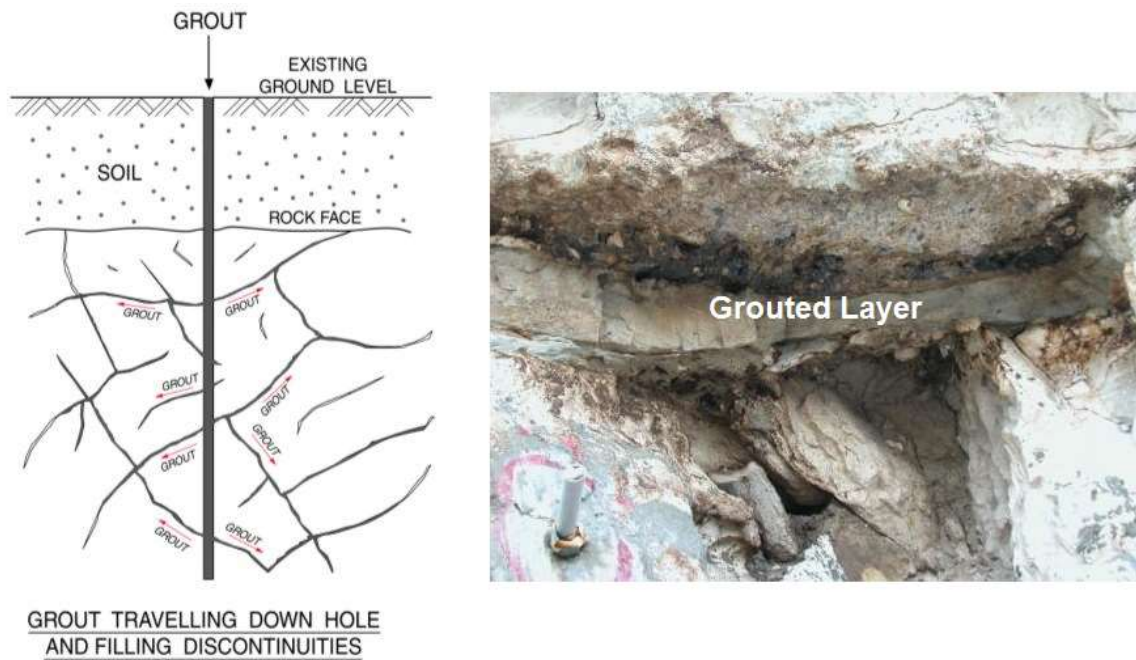


**Figure 5: Improved ground after completion of Rock/Fissure grouting**

### 2.2.2 Permeation Grouting

Permeation grouting is the injection of a fluid grout into granular, fissured or fractured ground to produce a solidified mass by filling grout in voids and fissures to control water flow. Once the grout cures, the porous soil is transformed into a near solid mass. Although this can sometimes be done using cement grouts, the void space in most soils is too much small to permit passage of the Portland cement particles. Hence most permeation grouting is performed using chemical grouts. This is sometimes called chemical grouting also. The treated soil had a much lower hydraulic conductivity and is stronger and less compressible than before. It is often used to form groundwater barriers and to stabilise soils in advance of making excavations or tunnels. The process of permeation grouting and automatic injection containers is shown in Figure 6 and Figure 7.

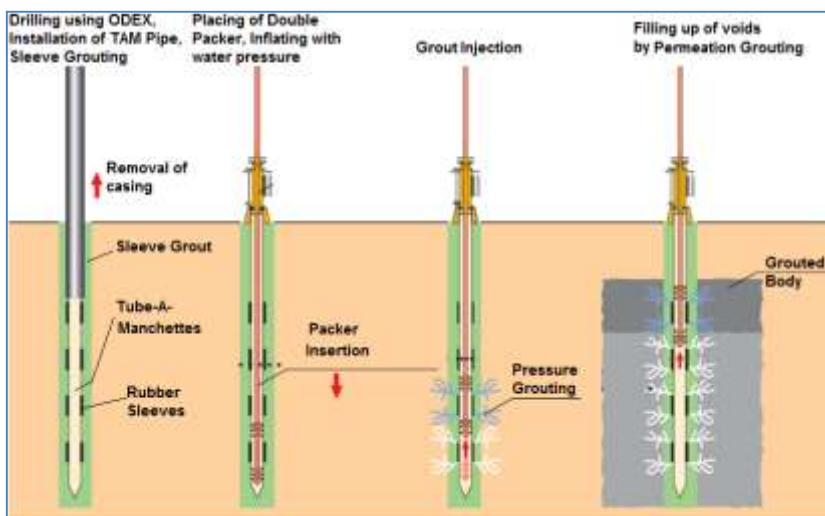


**Figure 6: Schematic showing permeation grouting methodology**



**Figure 7: Automatic Injection Containers – Computerised Grout Pumps**

### 2.2.3 Compaction Grouting

Compaction grouting is the injection of very stiff, low slump (25-75mm) mortar-type grout under relatively high pressures to displace and compact soils in place. It is most effective in cohesionless soils but can also be effective in finer grained soils where disturbance has occurred. Grout mix comprises of Portland cement, sand and bentonite (for workability) or other additives. Compaction grouting is often used to repair structures that had experienced excessive settlement, since it both improves the underlying soils and raised the structure back into position. The typical process of compaction grouting is shown in Figure 8.

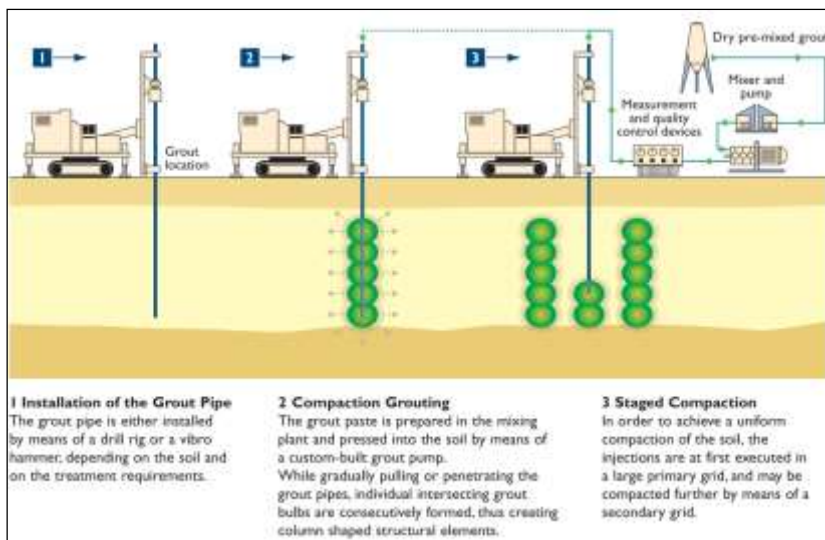


**Figure 8: Process of compaction grouting**

### 2.2.4 Jet Grouting

The jet grouting process consists of the disaggregation of soil or weak rock and its mixing with, and partial replacement by, a cementing agent; the disaggregation is achieved by means of a high energy jet of a fluid which can be the cementing agent itself. Because of the high pressures, this method is usable on a wide range of soil types. This method had been used for ground water control, underpinning, stabilisation prior to tunnelling etc.

Jet grouting can be executed using

- i. T-System (0.8m to 1.2m dia.)
- ii. D-System (1.5m to 2.0m dia.)

The typical cross section of T & D system and process of jet grouting is shown in Figure 9 & Figure 10

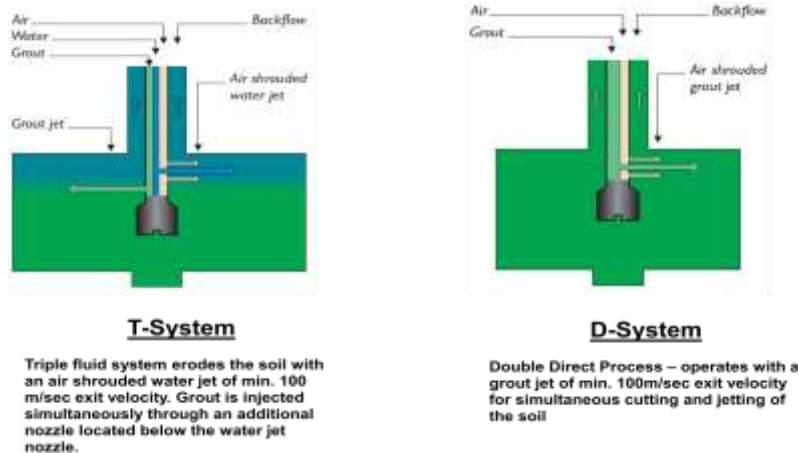


Figure 9: Execution of jet grouting using T & D system

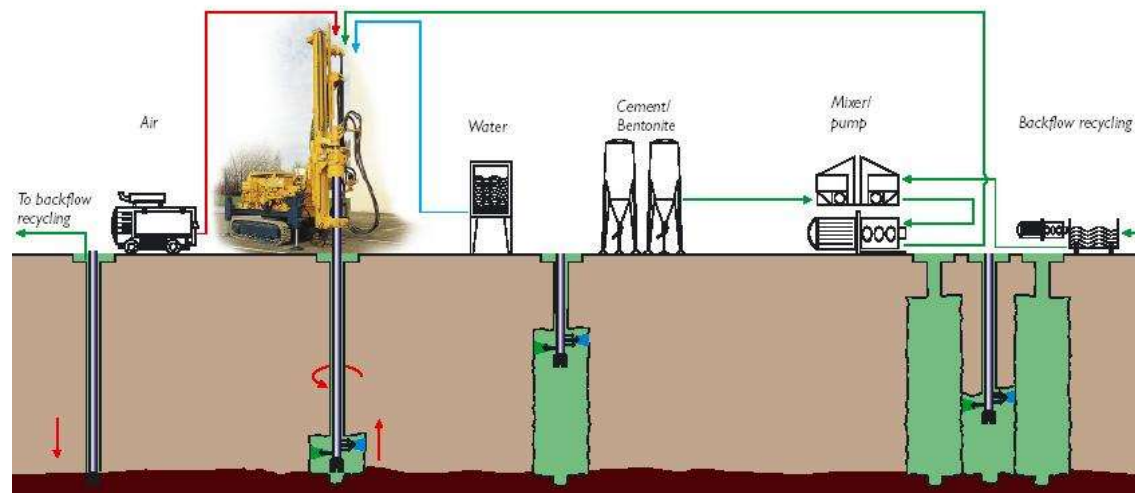


Figure 10: Process of jet grouting

### 2.3 Quality Control & Grout Test.

In all ground improvement techniques quality control during execution is important to ensure uniform improvement of the soil. In grouting techniques appropriate quality assurance and quality control shall be adopted to ensure intended performance of grouting.

The working parameters (e.g. depth, pressure, grout volume, etc.) need to be maintained and recorded at each stage of grouting to determine the appropriate termination criteria. Termination of particular stage is considered, when one of the following conditions achieved:

- Pre-determined grout volume is achieved (in accordance with column diameter)  
– i.e. volume of each bulb
- Pre-determined grout pressure is achieved (in accordance with depth of treatment)  
– i.e. Pressure greater than 20 bars.
- Mortar is overflowing from same grout hole collar

The following test should be done to ensure a good quality of grout

- Density test using hydrometer and mud balance
- Viscosity test using Marsh cone

- Strength tests using hand held pocket penetrometer
- Sedimentation test

The marsh cone test, hydrometer test and slump cone test are shown in Figure 11 & Figure 12. The strength of the grout is also checked by unconfined compressive strength on cored samples. The quality control monitoring devices & records used for grouting are shown in Figure 13 & Figure 14.



Figure 11: Marsh cone on Grout & Hydrometer test on grout and Water



Figure 12: Slump cone test

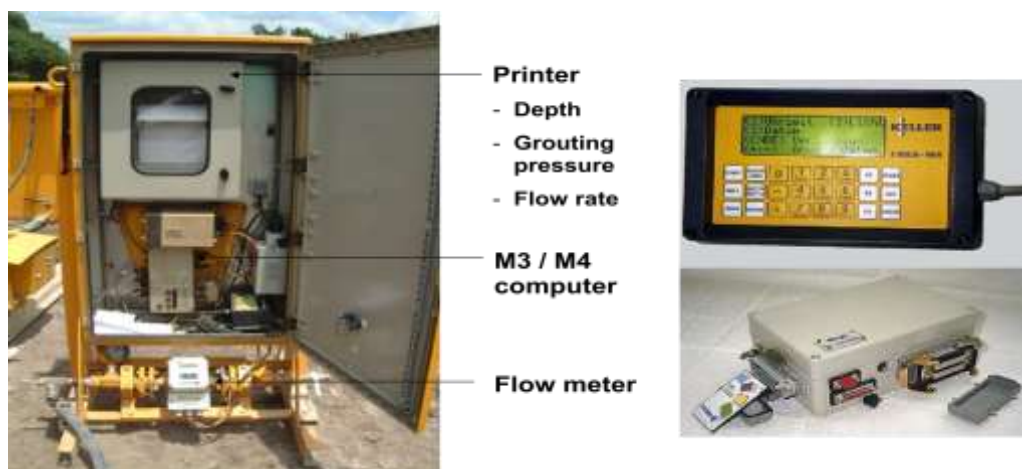


Figure 13: Quality control monitoring devices

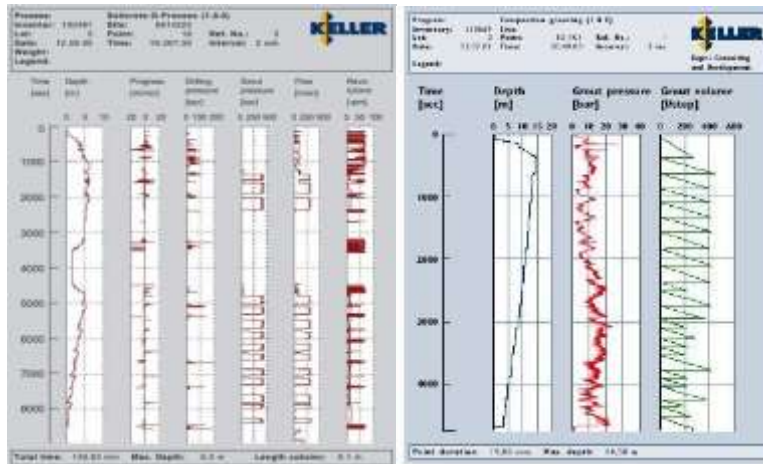


Figure 14: Quality control records

### 3 Applications

The grouting techniques can be adopted for the following ground engineering applications

- Seepage control (Permeation Grouting)
- Soil Arching (Compaction Grouting)
- Rock Grouting for Deep shaft (Rock/Fissure Grouting)
- Settlement Control (Rock/Fissure Grouting)
- Soil Stabilisation (Jet Grouting)

The technical paper explaining the project case studies on “Ground Improvement Techniques for Infrastructure Projects” in Malaysia is enclosed in Annexure 1.

### 4 Case studies

#### 4.1 Case study 1: Seepage control works at Teesta Low Dam – IV, West Bengal, India (Permeation Grouting)

M/s National Hydro Power Corporation proposed the Teesta Low Dam-IV for a Hydro Power Plant (160MW) near siliguri in West Bengal, India. A cofferdam was planned as shown in Figure 15 to divert the river water and allow 20m deep excavation in the river bed.

The river bed alluvium is made of a highly permeable mix of sand, gravels and boulders followed by bedrock. A grout curtain was required to reduce the permeability up to  $10^{-6}$  m/s and to allow the construction of dam foundation in a relatively dry condition. The depth of bedrock varied between 5m and 20m from top of the cofferdam. The cross section of coffer dam and Teesta dam under construction is shown in Figure 16.

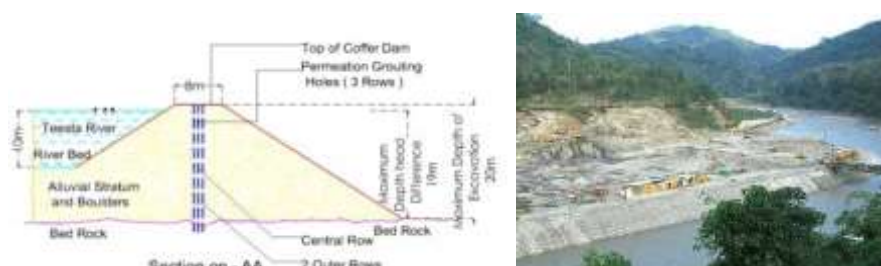


Figure 15: Cross section of coffer dam & Permeation grouting



**Figure 16: Teesta Low Dam**

Maximum excavation depth : 20m  
 Avg Permeability achieved after grouting works :  $10^{-6}$  to  $10^{-7}$  m/s

#### 4.2 Case study 2: Soil arching, Delhi Metro Rail Corporation, Newdelhi (Compaction grouting)

M/s Delhi Metro Rail Corporation (DMRC) is building a metro corridor connecting Central Secretariat and Qutub Minar. New Austrian Tunneling Method (NATM) was adopted to construct the proposed tunnels.

The soils at site generally consist of sandy silt fill to 5m depth. The abandoned *Nallah* channel was excavated and filled with locally available sandy silt to level the ground. SPT N values in the sandy silt fill were in the range of 4 to 17, indicating loose to medium dense. This was followed by medium dense to dense Delhi Silt alluvium layer, with SPT N values between 20 & 30 to about 26m depth. This is underlain by moderately weathered Quartzite bedrock.

The presence of loose filled up sandy soils over a stretch of 100m near Saket station (BC 19C package) posed problems with effective soil arching which is required for NATM construction. Compaction Grouting was adopted to enhance the densities of loose sandy soils to form effective arching. The schematic of tunnel section with required and design SPT N value is shown in Figure 17.

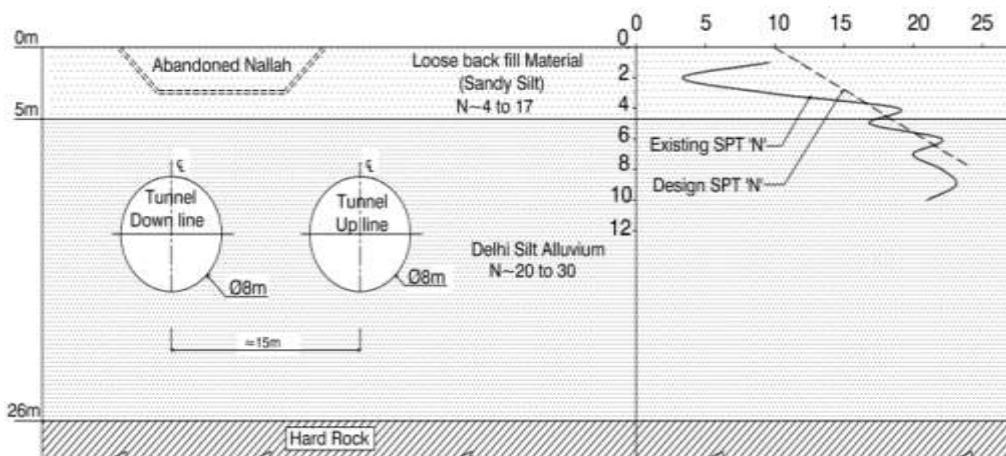


**Figure 17: Schematic of the NATM tunnels under an abandoned Nallah channel; the required and existing SPT N values are plotted on the right**

Figure 18 illustrates the layout and compaction grouting scheme – 2m and 4m square grid of the NATM tunnels. The comparison of design SPT with pre as well as post SPT and the completed structure after grouting are shown in Figure 19.

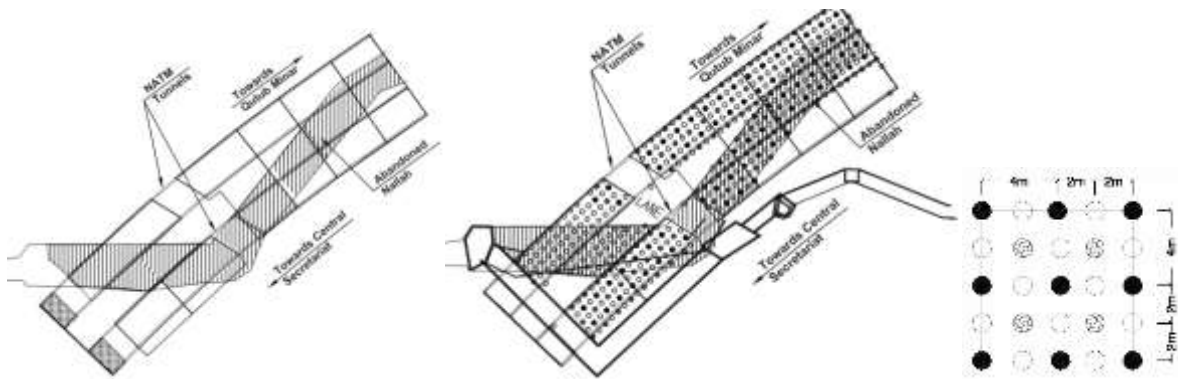


Figure 18 Typical layout of NATM and compaction grouting scheme

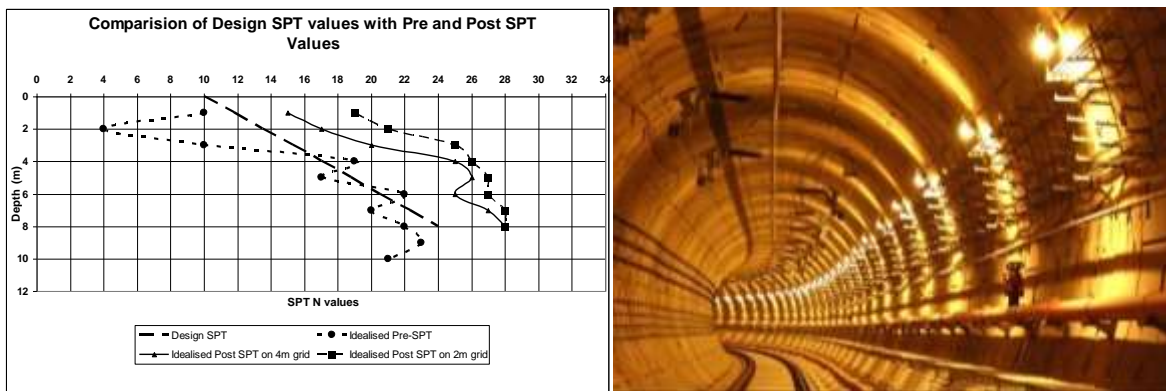


Figure 19: Comparison of Design SPT values with Pre and Post SPT Values & Completed structure

Total linear meters executed : 3000 Lin.m

SPT N value after improvement : 20 to 30

The technical paper explaining the project case study on Application of Ground anchors to support deep excavation and compaction grouting for NATM tunnel construction for Delhi Metro Rail Corporation (DMRC) is enclosed in Annexure 2.

### 4.3 Case study 3: Rock Grouting for Deep Shaft for SMART Tunnel (Rock/ Fissure Grouting)

The SMART tunnel was constructed in very challenging geological terrain comprising cavernous Limestone, with highly permeable subterranean solution channels and cavities. Dewatering activities can result in groundwater lowering which lead to ground subsidence and in some cases, formation of sinkholes. Likewise, actions from tunneling works can cause disturbance to the ground with similar consequence.

The Kuala Lumpur Limestone comprises Upper Silurian marble, finely crystalline grey to cream thickly bedded, variably dolomitic rock. Karstic features are prevalent in the limestone formed by movement of water containing carbonate acid (dissolved carbon dioxide).

The nearly 30m deep launch shaft (named North Ventilation Shaft or NVS) is located at the corner of Chan Sow Lin and Cheras Roads. The two 13m diameter tunnel boring machines were mobilised from this shaft, one north-bound 6km towards Ampang, while the other

headed south 4km to Taman Desa. The depths of the excavation were about 20m and 25m deep. The schematic section of treatment area is shown in Figure 20.

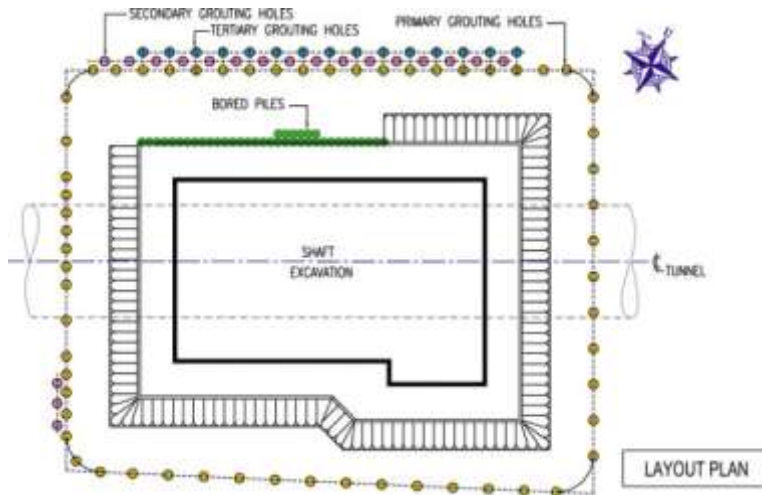


**Figure 20: Typical layout of grout curtain**



**Figure 21: NVM shaft & Dry walls after curtain grouting**

Experience from more than 2 years of grouting at this site has shown that the available technology is effective in minimizing water seepage and ground disturbance.

#### **4.4 Case study 4: Settlement control for SMART tunnel (Rock/Fissure Grouting)**

The SMART tunnel is a project financed by the Government of Malaysia. The proposed tunnel will be about 10km when completed (Figure 3). The launch shaft was located at the corner of Chan Sow Lin and Cheras Roads. Two 12m diameter tunnel boring machines (slurry shield machines) were utilized, one Tunnel Boring Machine (TBM) moving north-bound 6km towards Ampang, while the other TBM will move southwards 4km to Taman Desa. The TBMs will also travel beneath some settlement sensitive areas e.g. rail crossing, bridge crossing, important highway, beside buildings, etc. Grouting works were instituted in these areas as preventive measures to mitigate the risk of ground movement.

There are some structures along the TBM path which were deemed to be sensitive to ground movement that may result from the tunneling works. A program of probing and grouting were implemented with the objective of detecting and filling any natural rock cavities and large fissures, which may otherwise, if untreated, result in collapse and large sudden movement.

One such facility is the Light Rail Transit (LRT) line near Chan Sow Lin Road. The TBM had to pass beneath twin rail tracks some 14m below ground shown in Figure 22. The rock level was about 3 to 8m below ground. Drilling had to be done outside the security fencing beside the track and as such, almost all the holes were drilled at an incline shown in Figure 23. Very strict precautionary measures were implemented during the works which included supervision by the train staff and continuous settlement monitoring of the tracks.

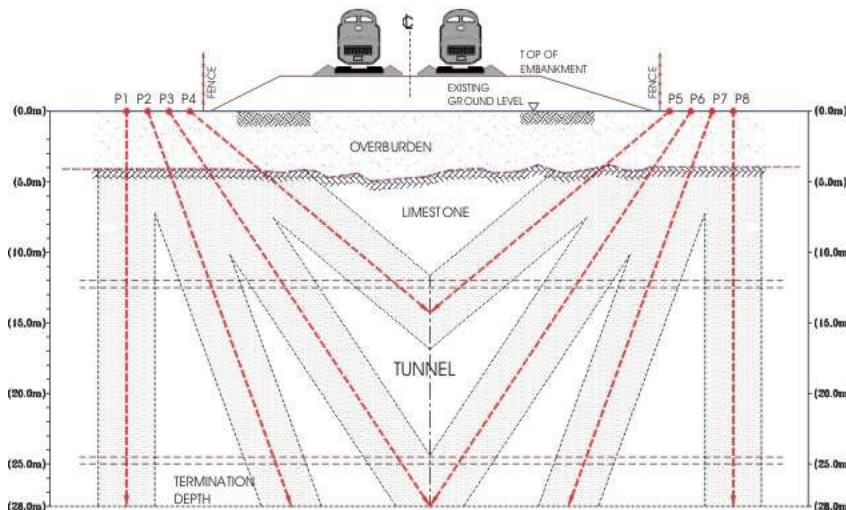


**Figure 22: Cross section of grout holes below rail track**



**Figure 23: Drilling and grouting beneath rail track**

The reported incidences of sinkholes and ground subsidence reduced considerably after grouting works were commissioned.

#### **4.5 Case study 5: Soil Stabilisation for SMART tunnel (Jet grouting)**

A tunnel project in Kuala Lumpur involved the construction of a 13m diameter bored tunnel over approximately 10km stretch. The tunnel will function mainly as a storm water storage and diversion channel but also incorporates a 3km motorway in a triple deck arrangement. The geology encountered along the tunnel path was ex-mining soils and limestone formation.

The subsoil conditions consist of highly variable mixed soils, comprising mainly of loose silty sand and sandy silt underlain by highly variable karstic limestone formation. Groundwater was generally at about 3m to 4m below ground.

The cutter-head of the Tunnel Boring Machine (TBM) required maintenance at regular intervals (about 150m to 200m). Due to the existence of loose sandy material, there was a risk of ground disturbance and subsequent ground subsidence, if left untreated. Most of the cutter-head interventions were located within limestone bedrock and rock grouting was carried out at some locations depending on quality of the bedrock.

At locations, where cutter-head interventions are located partially in soil stratum and partially in bedrock, combination of compaction grouting and rock grouting was utilised and shown in Figure 24. At other locations, where cutter-head interventions are located completely in soil stratum a capping shield made of “Jet Grout block” was designed to ensure face stability whilst maintenance of cutter-head was carried out. The treatment scheme of Jet grouting and grout column is shown in Figure 25. The Jet Grout block was installed from 9m to 28m below existing ground level. The face of the soil gets stabilized after the grouting process.

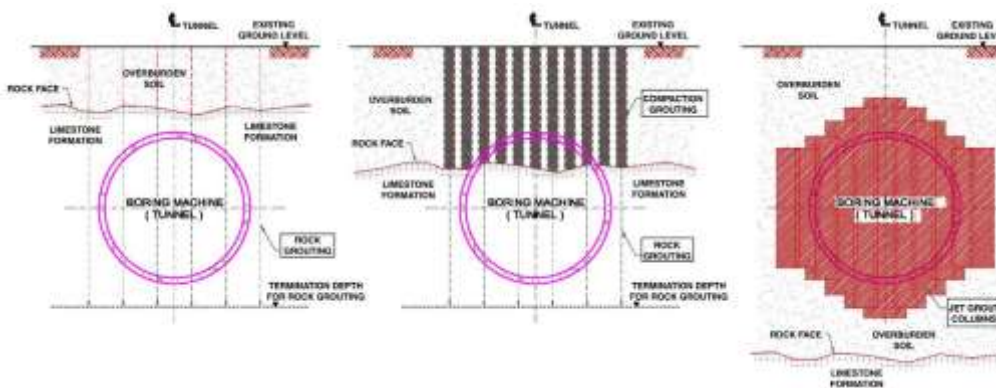


**Figure 24: Schematic diagram of grouting schemes at cutter-head intervention locations.**

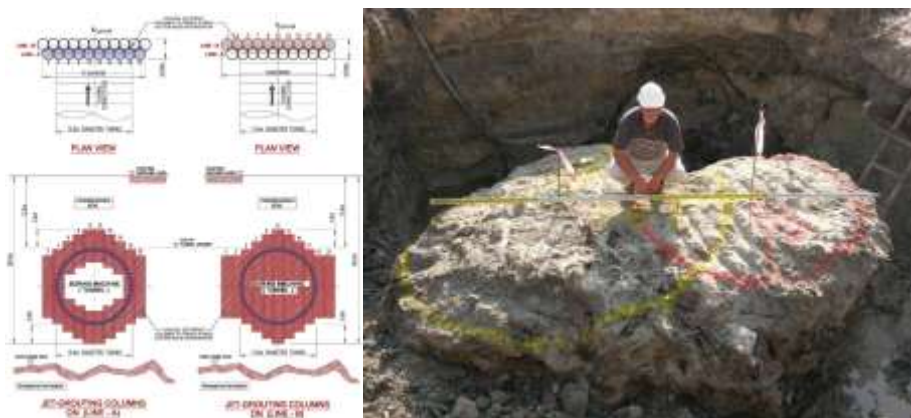


**Figure 25: Plan & Cross section of Treatment scheme & Grout column after Jet grouting**

All the cutter-head interventions which were treated using Jet Grout block performed well. The cutter-head of TBM was parked inside the Jet Grout block and the necessary maintenance was carried out successfully, to withstand an air pressure of 1 to 2 bars without any pressure drop.

The technical paper explaining the project case study on “Recent Experiences with cement grouting and mixing techniques in Kuala Lumpur” is enclosed in Annexure 3.

## 5 Bibliography

1. Dr. A.V. Shroff. "Development in Design & Execution in Grouting Practice", *Indian Geotechnical Society 31<sup>st</sup> Conference (2009)*.
2. Dr Satyendra Mittal "An Introduction to Ground Improvement Engineering", Indian Institute of Technology, Roorke (2013)".
3. Dr. V. R Raju, Ir. Y.W Yee. (2006) "Grouting in Limestone for SMART Tunnel project", *International conference and Exhibition on tunneling and trenches technology*, Kuala Lumpur, Malaysia
4. V.R Raju and Y Hari Krishna, (2008) "Ground improvement Techniques for infrastructure projects in Malaysia", *Proceedings of 12<sup>th</sup> International conference of International Association for computer methods and Advances in Geomechanics*, Goa.
5. Dr. V.R. Raju & Ir. Yee Yew Weng (2005) "Recent Experiences with cement grouting and mixing techniques in Kuala Lumpur" *IEM-GSM Oktoberforum2005: Case Histories in Engineering Geology and Geotechnical Engineering, 4th Oct. 2005, Petaling Jaya*.
6. Y. H. Krishna and B.C. Kanth ,Jitendra Tyagi, Mohan Gupta & Ashit Shah "Application of Ground anchors to support deep excavation and compaction grouting for NATM tunnel construction for Delhi Metro Rail Corporation (DMRC)".

Annexure 1    Technical paper on “Ground Improvement Techniques for Infrastructure Projects in Malaysia” by Dr.V. R. Raju and Y Hari Krishna.,2008.

## Ground Improvement Techniques for Infrastructure Projects in Malaysia

V. R. Raju  
*Keller Far East, Singapore*

Y. Hari Krishna  
*Keller Ground Engineering (India) Pvt. Ltd.*

**Keywords: Vibro methods, Deep Soil Mixing, Grouting techniques, applications in infrastructure projects**

**ABSTRACT:** Ground improvement techniques utilising Vibro methods, Deep Soil Mixing and Grouting technologies are finding increasing application in Malaysia to solve a broad spectrum of geotechnical problems. This paper will describe recent applications in Malaysia for four separate projects – Jet Grouting to form stable cutter-head interventions for a tunnel project; Deep Soil Mixing to support deep vertical basement excavation with limestone interface for a commercial complex; Vibro Concrete Columns to found reinforced concrete tanks in former domestic landfill for a sewage treatment plant; Vibro Stone Columns to support high reinforced soil walls for a highway project. The importance of quality control measures are emphasized and available proving methods are also discussed. The case histories presented demonstrate that the techniques can provide effective solutions to challenging engineering problems.

### 1 Introduction

Malaysia has seen extensive growth for the past one decade with many infrastructure projects in the construction industry. Current technology affords many ground improvement techniques to suit a variety of soil conditions, structure types and performance criteria. These ground improvement techniques can offer alternative foundation systems to the conventional pile foundation systems. For more details on various available ground improvement techniques, the reader is referred to “Ground Improvement 2<sup>nd</sup> Edition” book edited by Moseley & Kirsch (2004).

This paper illustrates four recent case histories in Malaysia, where innovative ground improvement techniques were employed to suit varying needs of application type and performance criteria. The chosen techniques varied from Jet Grouting, Deep Soil Mixing, and Vibro Concrete Columns to Vibro Stone Columns as shown in the Figure 1.

The construction methodology and quality control procedures during execution of works were in accordance with relevant Code of Practices (e.g. BS EN 12716:2001, BS EN 14679:2005, BS EN 14731:2005, etc.). These techniques offered reasonably environmental friendly solutions, especially in urban areas.

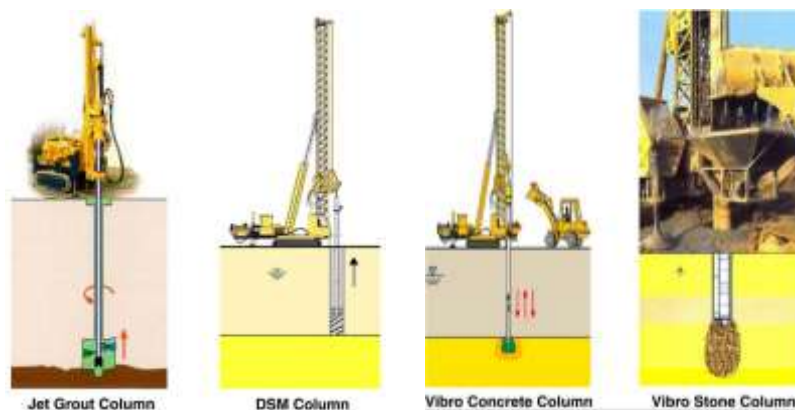


Figure 1. Schematic showing various ground improvement techniques.

## 2 Recent case histories in Malaysia

This paper will describe following four different case histories from four separate projects; where ground improvement techniques were utilised to solve challenging problems in difficult ground conditions:

- Jet Grouting to form stable tunnel boring machine cutter-head interventions for a tunnel project.
- Deep Soil Mixing to support vertical basement excavation over limestone for a commercial complex.
- Vibro Concrete Columns to support reinforced concrete process tanks in a former domestic landfill for a sewage treatment plant.
- Vibro Stone Columns to support high reinforced soil walls for a highway project.

## 3 Application of Jet Grouting

### 3.1 Background

A tunnel project in Kuala Lumpur involved the construction of a 13m diameter bored tunnel over approximately 10km stretch. The tunnel will function mainly as a storm water storage and diversion channel but also incorporates a 3km motorway in a triple deck arrangement. The geology encountered along the tunnel path was ex-mining soils and limestone formation. For more details of the project, the reader is referred to Raju & Yee (2006).

The cutter-head of the Tunnel Boring Machine (TBM) required maintenance at regular intervals (about 150m to 200m). At such TBM stops (referred as “cutter-head intervention”), the slurry pressure will be switched off and the stability of the rock/soil face in front of the TBM relies on air pressure and inherent strength of the in-situ rock/soil. Due to the existence of loose sandy material, there was a risk of ground disturbance and subsequent ground subsidence, if left untreated. Most of the cutter-head interventions were located within limestone bedrock and rock grouting was carried out at some locations depending on quality of the bedrock. At locations, where cutter-head interventions are located partially in soil stratum and partially in bedrock, combination of compaction grouting and rock grouting was utilised. At other locations, where cutter-head interventions are located completely in soil stratum a capping shield made of “Jet Grout block” was designed to ensure face stability whilst maintenance of cutter-head was carried out. Figure 2 represents the schematic of different types of grouting schemes implemented depending on the geological conditions. The subsequent sections explain the details of grouting scheme using large diameter Jet Grout columns to form a stable block in the soil stratum.

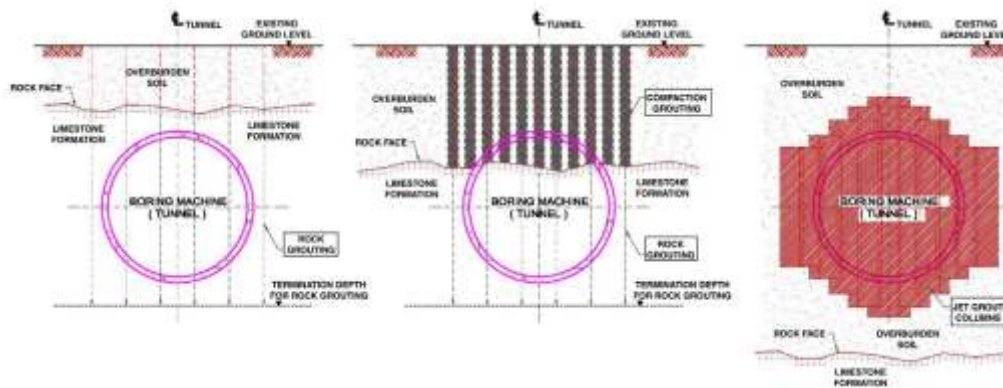


Figure 2. Schematic of grouting schemes at cutter-head intervention locations.

### 3.2 Soil conditions

In general, the subsoil conditions consist of highly variable mixed soils, comprising mainly of loose silty sand and sandy silt underlain by highly variable karstic limestone formation (see Figure 3). Standard penetration test (SPT) blow counts typically vary from 0 blows/0.3m (especially along “slump zones” above rock-head) to 20 blows/0.3m. Historically, mining activities took place at some of the sections which explain the varying nature of the soil. Groundwater was generally at about 3m to 4m below ground.

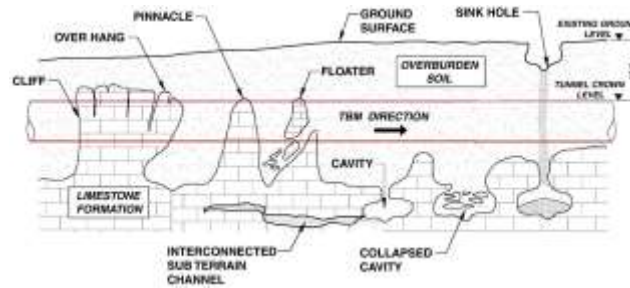


Figure 3. Typical geology along the tunnel path.

### 3.3 Solution

The capping shield made of Jet Grout columns was designed to form a stable block at the cutter-head intervention locations as shown in Figure 4. The shield was formed using 2 rows of 2m diameter Jet Grout columns in front of the cutter-head of TBM. The front row (Line-B) was designed to be full depth section, whereas back row (Line-A) designed to be hollow section to ease the cutting process and also for economy reasons. The Jet Grout block was installed from 9m to 28m below existing ground level.

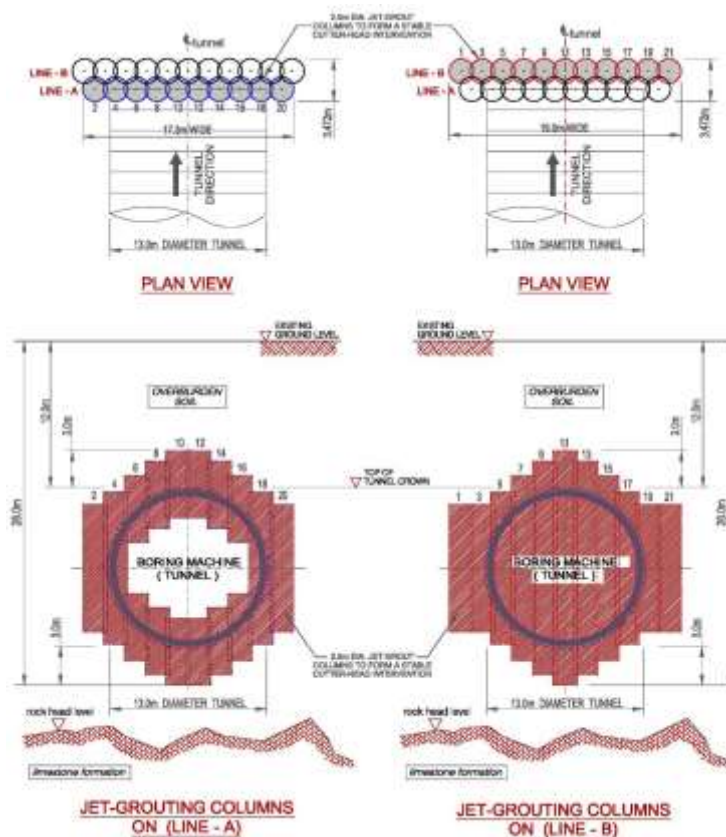


Figure 4. Schematic of Jet Grout block at cutter-head intervention location.

The construction challenges of the Jet Grout block were as follows:

- Formation of consistent 2m diameter Jet Grout columns in the highly variable soil.
- Proper interlocking of each Jet Grout column down to 28m depth which requires the verticality of drilling to be within 0.5% to 1%.
- Required minimum unconfined compressive strength (UCS) of 1MPa for each Jet Grout column.
- Existing underground utilities which required careful attention to avoid damages.
- High power transmission towers which limited the working head-room and associated safety issues.

A trial was performed prior to the commencement of working columns to confirm the erodability of in-situ soils and adequacy of operating parameters. The jetted column was exposed and core samples were taken to verify the as-built diameter and achieved strength. The diameter formed was proven to be more than 2m and UCS was more than 1MPa. The site pictures showing exposed trial columns and execution of working columns using HT 400 pump and D-system are shown in Figure 5.

During construction, as part of quality control measures, the density of backflow from Jet Grouting works were monitored which indirectly reflected the erodability of soil and the diameter of Jet Grout column formed. Based on the laboratory test results, the required CEM soil (i.e. the remaining cement content in the Jet Grout column) to achieve UCS of 1MPa was about 200 to 250 kg/m<sup>3</sup> for sandy soils and 350 to 400 kg/m<sup>3</sup> for clayey soils.



Figure 5. Exposed trial Jet Grout columns (left) and execution of working columns (right).

### 3.4 Performance

All the cutter-head inventions which were treated using Jet Grout block performed well. The cutter-head of TBM was parked inside the Jet Grout block and the necessary maintenance was carried out successfully, to withstand an air pressure of 1 to 2 bars without any pressure drop.

## 4 Application of Deep Soil Mixing

### 4.1 Background

A project comprising 3-storey commercial complex with 2-level basement car park floors (about 7m depth below existing ground level) is under construction in the middle of Kuala Lumpur City Centre. The project site is confined between a newly completed 4-storey commercial lots, light rail transit track and existing old warehouse (see Figure 6). The distance between face of excavation and boundary setback line is in the range of 3m to 10m, hence open sloped excavation was limited to shallow rock-head areas.

The proposed 2-level basement construction required 7m deep excavation with underlying limestone interface for a total perimeter length of about 690m. The conventional solution using contiguous bored piles or anchored sheet piles proved very expensive and needed prolonged construction period. As an alternative, a rigid gravity wall retaining system using interlocked Deep Soil Mixing (DSM) columns was implemented around the perimeter length of about 560m as shown in Figure 6.



Figure 6. Overall layout of proposed basement excavation.

#### 4.2 Soil conditions

The subsoil comprised of loose silty sand deposits and ex-mining soils with SPT values in the range of 5 blows/ft to 12 blows/ft. Underlying this loose soil layers, karstic limestone formation was found with extremely varying rock-head levels ranging between 3m and 15m below existing ground level. Overhanging boulders and pinnacles are common; hence the founding level of the bedrock formation was unpredictable. The ground water table was found to be at about 1m to 2m below existing ground level.

#### 4.3 Solution

The gravity wall block was designed to ensure adequate resistance against lateral earth pressure to support the intended depth of excavation, whilst reducing seepage water inflow and thus, minimise the possible risk of drawdown and consequent ground subsidence to the surroundings. The design of gravity wall required a width of 0.7 times the depth of overburden soil above rock-head level. The gravity wall acted as a temporary retaining structure during the basement excavation works. Wet DSM columns of 0.85m diameter were interlocked at 0.75m centres to form the rigid gravity wall block as shown in Figure 7.

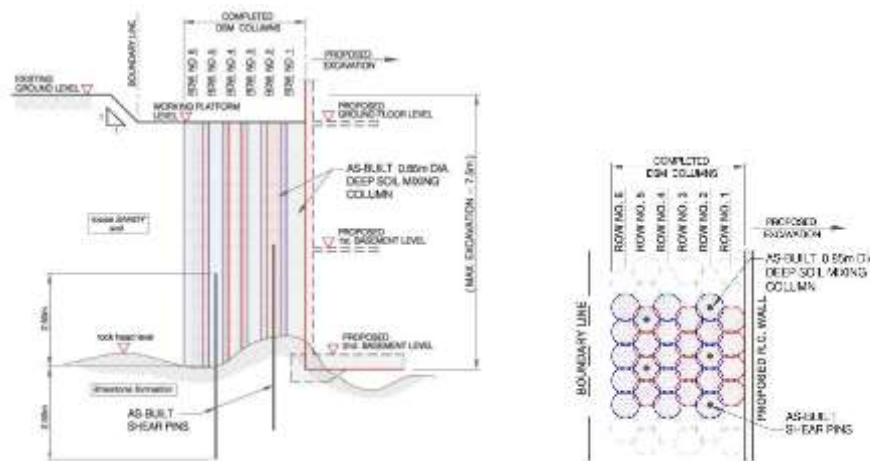


Figure 7. Schematic of DSM gravity wall block.

The columns were designed to achieve an unconfined compressive strength of 1.0MPa with binder content (Ordinary Portland Cement with water-cement ratio of 1:1) in the range of 200kg/m<sup>3</sup> to 250kg/m<sup>3</sup>. The columns were installed to a maximum depth of 12m below existing ground level. For locations, where there was space constraint, shear pins were installed to provide wall stability. A picture of the site with on-going installation works is shown in Figure 8. The operating parameters (e.g. rotation speed, rate of penetration and withdrawal, blade rotation number, flow rate, grout pressure and binder content, etc.) were monitored using real-time computerised recording systems to ensure adequate and uniform mixing of the soil.



Figure 8. Execution of DSM works.

#### 4.4 Performance

Excavation works proceeded upon completion of DSM installation works and subsequent curing period of only 14 days due to tight schedule of the project. Bedrock underneath the DSM columns was excavated using the hydraulic breaker and blasting works. The installed DSM columns were able to withstand the high vibration induced by rock excavation works. At the time of writing this paper, approximately 60% of the excavation works have been completed (see Figure 9). As part of quality control procedure, cores from DSM columns were extracted and tested in a laboratory for UCS. The test results indicated an UCS in the range of 1MPa to 3MPa. In addition, wall movement was monitored during excavation works, which showed a maximum horizontal movement of about 30mm to 40mm.



Figure 9. Completed excavation.

### 5 Application of Vibro Concrete Columns

#### 5.1 Background

A Sewage Treatment plant is under construction in Penang Island and when completed will cater for an ultimate capacity of 1.2 million population equivalent. The project will serve as a centralized sewage treatment facility and will include 12 nos. of Sequential Batch Reactor (SBR) tanks and associated process tanks (see Figure 10).



Figure 10. Overall plan layout of sewage treatment plant.

The SBR tanks are major process tanks in the entire plant and were designed as twin tanks made up of reinforced concrete (total 6 nos. of twin tanks separated by very narrow gap) supported on treated ground. The dimension of each twin tank is approximately 90m x 60m x 7m high. One of the twin tank (SBR 1&2) has additional 2 floors on top of the tank to accommodate administration office and storage area for process equipment. At the time of writing this paper, the building works are almost completed, whilst mechanical and process installation works are ongoing.

## 5.2 Soil Conditions

The site is located on the north-eastern part of Penang Island in Jelutong, about 5 km from Georgetown. The site was reclaimed from the sea and approximately, half of the SBR tanks area was covered by former domestic landfill (3m to 5m thick) waste dumps. The subsoil primarily consists of 3m to 5m thick reclaimed fill / domestic waste dumps followed by 5m to 7m thick soft marine clay. This is followed by stiff to very stiff cohesive deposits to over 50m depth. The ground water table varied between 1m and 2m below existing ground level.

## 5.3 Solution

The original foundation design was piled foundation to over 40m depth; but this was later found to present a few undesirable construction limitations like noise pollution during pile driving; requirement of pre-boring and removal of landfill material; and transportation and storage of pre-cast piles on a congested site; as well as relatively high cost. As an alternative, ground improvement techniques (Vibro Concrete Columns and Deep Soil Mixing) were utilised to support the SBR tanks. Vibro Concrete Columns (VCC) were constructed for 3 nos. of twin tanks (namely; SBR 1&2, SBR 3&4 and SBR 7&8) in the former landfill area, forming concrete pile-like elements by displacing the domestic waste dumps rather than requiring removal. DSM columns were constructed for remaining 3 nos. of twin tanks (namely; SBR 5&6, SBR 9&10 and SBR 11&12) in the non-landfill area.

The alternative foundation system was designed to ensure adequate bearing capacity (to support loading intensity of 92kPa), limit the total settlement of the structure to be less than 75mm and differential settlement to be less than 1(V):360(H). The diameter of Vibro Concrete Columns varied between 0.6m and 0.75m with working loads of 35tons and 50tons, respectively. Typical spacing of columns (0.6m diameter) ranged between 1.8m c/c and 1.6m c/c to support foundation loads of 90kPa and 130kPa, respectively. The depth of columns varied from 8m to 14m. The design mixture of concrete as follows:

- a) Cement content ~ 200kg/m<sup>3</sup>
- b) Water-cement ratio (w/c) ~ 0.5
- c) Grading of aggregates ~ 8mm to 20mm

The picture showing execution of Vibro Concrete Columns using custom-built machine (Vibrocat) is shown in Figure 11. During execution works, appropriate quality control procedures (e.g. cube strength tests, concrete consumption and adequate compaction effort, etc.) were implemented on site.



Figure 11. Picture showing execution of VCC.

## 5.4 Performance

After successful execution of VCC works, the columns were exposed and it was demonstrated that the domestic waste material was displaced sideways during installation and did not contaminate the concrete. Selected working columns were tested up to 1.5 times the working load using plate load tests in 3-cycles.

As part of quality control, coring was carried out through selected working columns to retrieve the samples of 50mm to 100mm diameter. The retrieved samples were tested for UCS and results of tests showed UCS in the range of 10MPa to 40MPa, which is much more than design strength of 5MPa (see Figure 12).

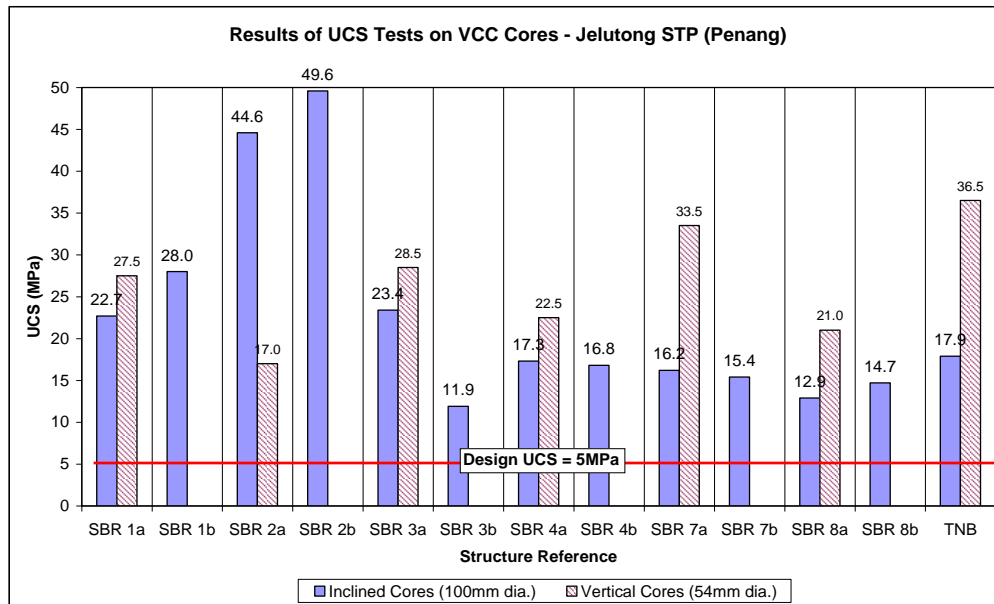


Figure 12. Typical results of UCS tests.

After quality control and testing works, the concrete structures were constructed according to the specifications incorporating a load distribution layer (150mm thick well compacted crusher run) between foundation and super structure. A Hydro test was carried by filling the water into the twin tank with uniform water levels in each tank. The geotechnical objective of the Hydro test was aimed to check the settlement performance of the foundation system under full water load prior to the actual operational stage. The rate of water filling was about 0.5m per day and the design load was maintained for minimum 2 weeks rest period after reaching to the full height. Upon completion of Hydro test, half of the twin tank was emptied, whilst maintaining the full water load in the other half to simulate the loading and unloading sequences during operational stage. Pictures showing completed tanks before and during Hydro test are shown in Figure 13.



Figure 13. Completed SBR tanks – before and during Hydro test (Left: SBR 7&8 and Right: SBR 3&4 in the foreground and SBR 1&2 with 2 floors on top in the background).

The settlements were monitored using precise survey instruments during and after Hydro tests. The Hydro tests for 3 nos. of twin tanks (SBR 1&2, SBR 3&4 and SBR 7&8) supported on VCC foundation have been successfully completed. The settlement monitoring data over the past 10 months period (Sept'06 – Jul'07) has indicated good performance with maximum settlements in the range of 5mm to 20mm. The typical results of settlement monitoring for SBR 7&8 are shown in Figure 14. As expected, a marginal elastic rebound was observed during unloading process (see Figure 14).

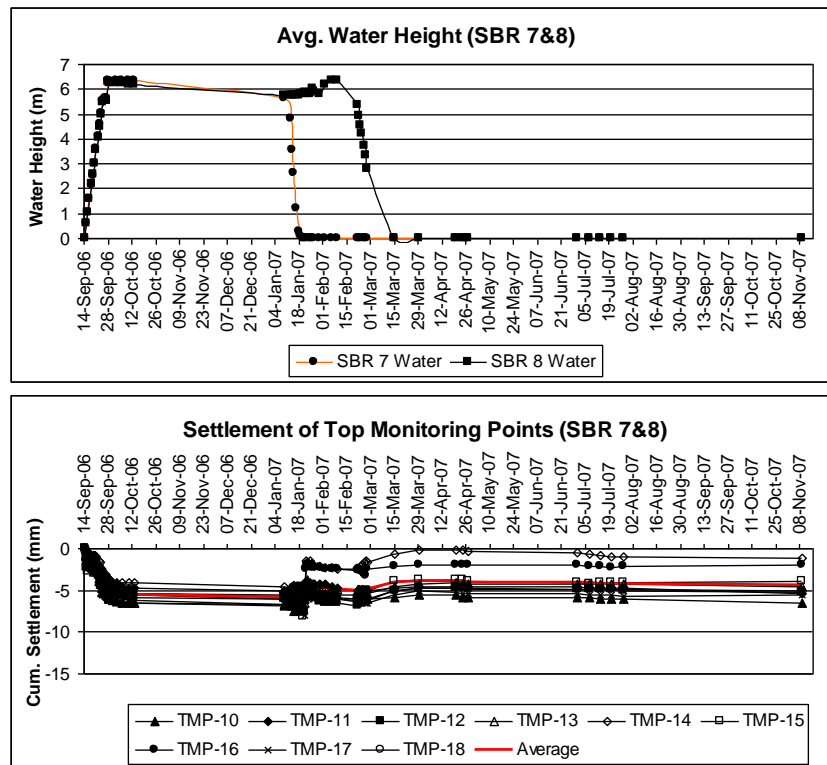


Figure 14. Typical results of settlement monitoring (SBR 7&8).

## 6 Application of Vibro Stone Columns

### 6.1 Background

The highway network in the capital city of Malaysia (Kuala Lumpur) has seen remarkable growth in the recent years. Most of the modern expressways were constructed on a Build, Operate and Transfer (BOT) basis. One such modern expressway with dual three-lane carriageway was opened to the traffic in April 2004. The expressway forms the main interchange at Kampung Pasir Dalam (referred as Pantai Dalam Interchange) to connect three distinct routes in the city (namely; Subang Jaya, Jalan Bangsar and Jalan Kuchai Lama). Due to site constraints at the interchange, high reinforced soil walls were constructed to form the bridge approaches and other ramps to the required design heights (maximum up to 13m). The following Figure 15 represents the detailed plan layout of Pantai Dalam Interchange including instrumentation monitoring scheme. For more details of the project, the reader is referred to Yandamuri & Yee (2006).

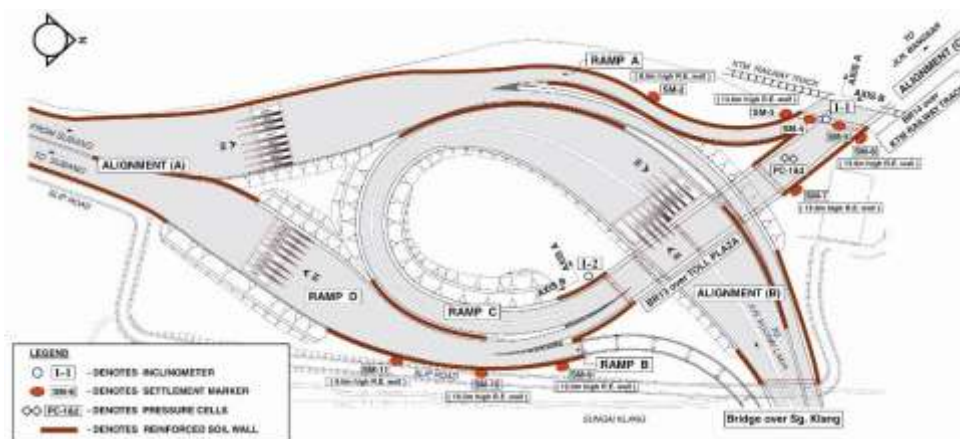


Figure 15. Plan layout of interchange.

## 6.2 Soil Conditions

The subsoil conditions at Pantai Dalam Interchange varied from very soft silts to soft sandy silts down to a depth between 5m and 12m followed by hard sandy silts. Typical plot showing results of cone penetration tests is shown in Figure 16.

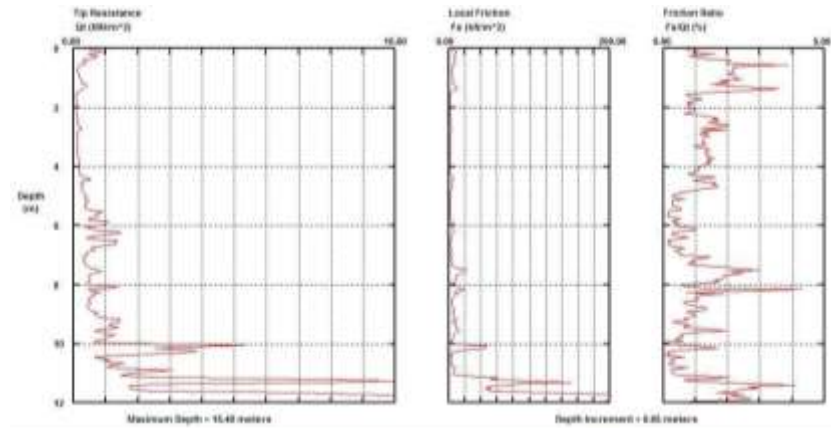


Figure 16. Result of typical cone penetration test at Ramp C.

## 6.3 Solution

Increasingly, Vibro Stone Columns are used to support reinforced soil walls. The combination has proven economy and has intrinsic technical advantages, i.e. the stone columns ensures relatively quick consolidation as the embankment is built; while the wall is constructed in stages (lifts) with the wall panels placed progressively and adjusted for any movement. For details of past Vibro applications in Malaysia, the reader is referred to Yee & Raju (2007).

For Pantai Dalam Interchange, the design scheme comprised of 1.0m diameter columns spaced at 1.5m to 1.8m c/c under reinforced soil walls and 2.0m to 2.3m c/c under earth fill embankments (i.e. area replacement ratios in the range of 15% to 35%). The columns were installed to a depth between 5m and 12m to treat very soft silts and soft sandy silt deposits. The following Figure 17a shows the site conditions during installation of Vibro Stone Columns, whereas Figure 17b shows completed reinforced soil wall (about 13m high) at the same location.



Figure 17a. During construction.



Figure 17b. After completion.

In total, an area of approximately 23,000m<sup>2</sup> was treated with proper quality control measures to ensure design diameter and compaction effort throughout the construction process. The installation works were successfully carried out even adjacent to existing dwellings and very close to the constructed bridge abutments. Vibration monitoring was carried out for such locations and the measured vibration levels in terms of peak particle velocity were less than 20mm/s even when Keller's Mono vibrator was working 1.0m away from the monitoring point (see Figure 18). The British and Australian standards (BS 5228 Part 4 and AS 2187) accept vibration levels between 20mm/s and 50mm/s for normal structurally sound structures.

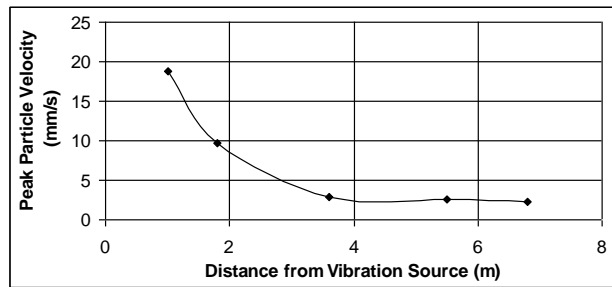


Figure 18. Vibration monitoring during installation works using Keller's Mono vibrator.

#### 6.4 Performance

After completion of ground improvement works using Vibro Stone Columns in June 2003, construction of reinforced soil walls and embankments were commenced. The long-term performance of the treated ground to support high reinforced soil walls is evaluated based on the results of instrumentation monitoring for more than 3 years, both during construction of embankment and operational stages. The data of settlement measurements showed that the Vibro Stone Columns has provided effective drainage paths to dissipate excess pore water pressures under the newly placed fill loads by means of radial and vertical consolidation processes. The time rate of consolidation was also relatively quick; 90% degree of consolidation was achieved within construction period of embankment itself.

The embankments and reinforced soil walls were constructed with a rate of filling of about 1m per week and the highest sections (about 13m high) were completed in about 3 months period. Most of the predicted settlements occurred during the construction period (see Figure 19) leaving minimal residual settlements for the post construction stage. The treated ground settled to a maximum of about 100mm only even under 13m high reinforced soil wall.

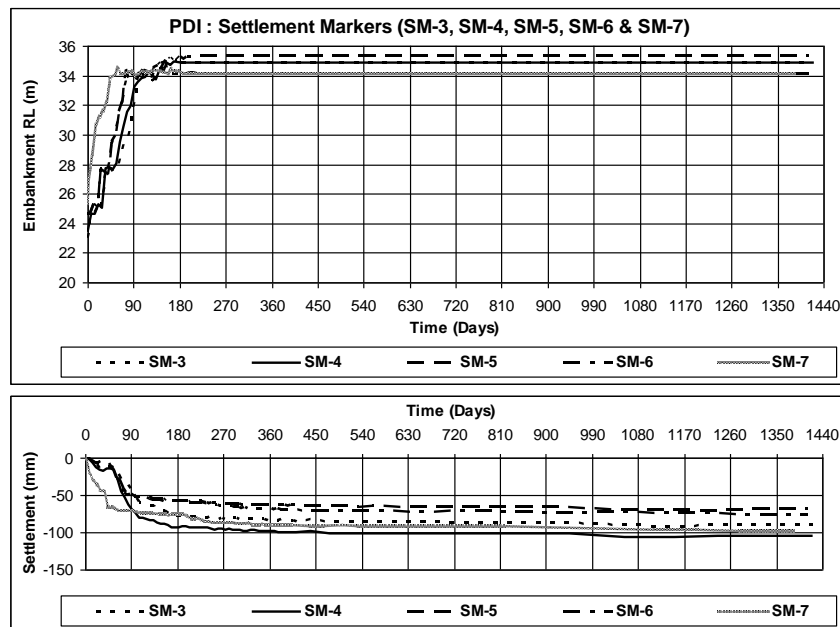


Figure 19. Summary of results of settlement markers.

Inclinometers were installed at highest reinforced soil wall locations to monitor lateral displacements below original ground level, both during construction of the wall and post construction stages. Figure 20 below shows the results of inclinometer measurements at two different locations (near bridge approaches), the results of which indicated less than 30mm lateral displacement (i.e. less than 1/3<sup>rd</sup> of vertical displacement).

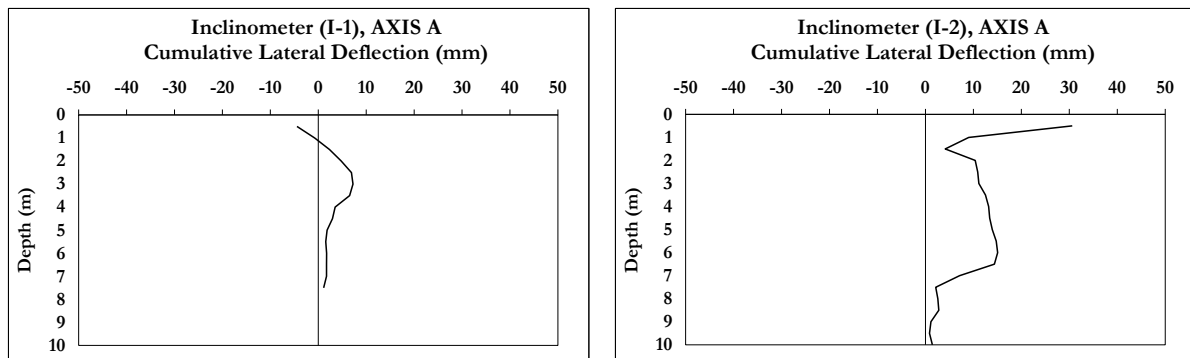


Figure 20. Results of inclinometers (lateral displacements).

## 7 Conclusions

In Malaysia, ground improvement techniques are finding increasing applications in infrastructure projects. Many ground improvement techniques are available to suit the particular needs of soil type, structure type, application type and performance criteria. These techniques offer cost effective solutions, whilst reducing construction period considerably. Furthermore, these techniques also offer environmental friendly systems, which is important for urban areas.

The case histories presented in this paper have demonstrated their effective usage. A Jet Gout block was successfully utilised to form stable ground for a 13m diameter tunnel boring machine cutter-head interventions. Gravity retaining wall formed using Deep Soil Mixing was utilised for a 7m deep basement excavation support (strut free) over pinnacled limestone. Vibro Concrete Columns supported concrete process tanks in a former landfill area without need for removal of domestic waste dumps. Last but not least, Vibro Stone Columns supported reinforced soil walls up to 13m height over formed tin-mined soils. The techniques enabled innovative solutions to be applied, which relied on design according to methods recommended in relevant Code of Practices; proper quality control measures during construction, suitable post construction testing methods and long-term instrumentation monitoring.

## 8 Acknowledgements

The author wish to acknowledge the management and staff of Main Contractors and Consults for their valuable contribution in the implementation of the ground improvement works. The author also wishes to acknowledge colleagues in Keller who contributed immensely in the design and construction, and not forgetting: Mr. Saw Hong Seik, Mr. Chua Chai Guan, Mr. P. Sreenivas and Mr. Joe Chang for their valuable input in the preparation of this paper. The review of this paper by Mr. Yee Yew Weng is also greatly acknowledged.

## 9 References

- Australian Standard: AS2187:1993. *Explosive Code*.
- British Standard: BS 5228-4:1992. Noise and Vibration Control on Construction and Open Sites. *Code of Practice for Noise and Vibration Control applicable to Piling Operations*.
- British Standard: BS EN 12716:2001. *Execution of special geotechnical works – Jet grouting*.
- British Standard: BS EN 14679:2005. *Execution of special geotechnical works – Deep mixing*.
- British Standard: BS EN 14731:2005. *Execution of special geotechnical works – Ground treatment by deep vibration*.
- Moseley M.P., Kirsch K. 2004. *Ground Improvement (2<sup>nd</sup> Edition)*. Published by Spon Press.
- Raju V.R., Yee Y.W. 2006. Grouting in Limestone for SMART Tunnel Project in Kuala Lumpur. *International Conference and Exhibition on Tunneling and Trenchless Technology*, Kuala Lumpur, Malaysia.
- Yandamuri H.K., Yee Y.W. 2006. Performance of A High Reinforced Soil Wall Supported on Vibro Stone Columns. *GSM-IEM Oktoberforum 2006 on Engineering Geology and Geotechnical Engineering*, Petaling Jaya, Malaysia.
- Yee Y.W., Raju V.R. 2007. Ground Improvement Using Vibro Replacement (Vibro Stone Columns) – Historical Development, Advancements and Case Histories in Malaysia. *16<sup>th</sup> Southeast Asian Geotechnical Conference*, Kuala Lumpur, Malaysia.

Annexure 2 Technical paper on “Application of Ground anchors to support deep excavation and Compaction Grouting for NATM tunnel construction for Delhi Metro Rail Corporation (DMRC)” by Jitendra Tyagi, Mohan Gupta, Ashit Shah & Y. H. Krishna and B.C. Kanth.

# APPLICATION OF GROUND ANCHORS TO SUPPORT DEEP EXCAVATION AND COMPACTION GROUTING FOR NATM TUNNEL CONSTRUCTION FOR DELHI METRO RAIL CORPORATION (DMRC)

Authors: *Jitendra Tyagi, CPM, Delhi Metro Rail Corporation,  
Mohan Gupta, Divisional Director, Mott MacDonald Pvt Ltd,  
Ashit Shah, Project Director, Mott MacDonald Pvt Ltd,  
Y. H. Krishna and B.C. Kanth, Keller Ground Engineering India Pvt. Ltd.*

## ABSTRACT

Metro rail construction is planned and is underway in several cities in India, including New Delhi, Mumbai, Chennai and Bengaluru. In New Delhi, the Delhi Metro Rail Corporation (DMRC) has successfully completed and commissioned the 1<sup>st</sup> phase of the metro network covering 65 km. As part of its 2<sup>nd</sup> phase, construction of about 121 km of metro network is almost complete. This includes an exclusive "Airport Metro Express Line", which is under final phase of commissioning. As part of the Airport Metro Express Line, an underground metro station is planned next to the existing New Delhi Railway Station, which required deep excavations in range of 11 m to 19 m. A retaining wall system comprising of soldier pile walls and multi-level ground anchors was adopted to support the deep vertical excavation., A different geotechnical challenge was faced at one of the underground metro corridors near Saket Station. Here the presence of loose sandy silts along an abandoned *Nallah* channel posed problems with regard to effective soil arching, which is necessary for tunnel construction using the proposed NATM method. Compaction Grouting was used to increase the stiffness in the in-situ soils and to enable effective soil arching above the tunnel crown. This paper presents the construction methodology, QA/QC measures and performance testing results related to Ground Anchors and Compaction Grouting.

## 1. INTRODUCTION

Delhi Metro Rail Corporation (DMRC) has successfully completed the 1<sup>st</sup> 65 km phase of metro network in New Delhi. As part of its 2<sup>nd</sup> phase, construction of about 121 km of metro network is almost complete. This includes an exclusive link, namely the “Airport Metro Express Line”, which is under final phase of commissioning.

As a part of this project, an underground metro station, a multi-level car park and a cut-and-cover tunnel have been constructed, which required 11 m to 19 m deep excavation. The designed retaining wall system includes soldier pile walls and multi-level ground anchors to support the vertical deep excavation. Fig. 1 shows part of the DMRC network and the location of the Airport Metro Express Line.

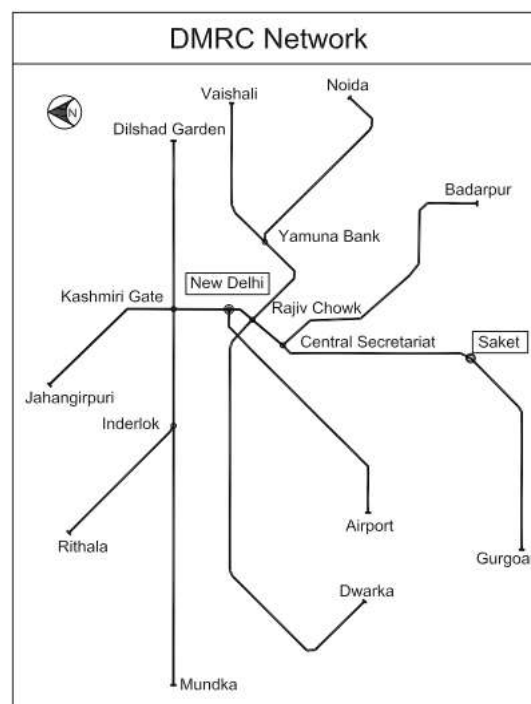


Fig. 1: DMRC network showing Airport Metro Express Line and Saket Station

On the link connecting Central Secretariat Station with Gurgaon, at one of the underground tunnel section (near Saket Station, Fig. 1) connecting Central Secretariat and Qutub Minar, the New Austrian Tunnelling Method (NATM) was adopted for tunnel construction. The presence of loose sandy silts along an abandoned *Nallah* channel posed problems with regard to effective soil arching, which is required for safe tunnel construction. To address this problem, compaction grouting was chosen to increase the stiffness of the in-situ soils to allow effective soil arching above the tunnel crown.

## 2. CASE STUDY 1: GROUND ANCHORS AT NEW DELHI METRO STATION

### 2.1 Introduction to Ground Anchors

A ground anchor is a structural element installed in soil or rock that is used to transmit an applied tensile load (as a result of horizontal earth pressure) into the ground. The basic components of the anchor include (a) the anchorage, (b) the free (or un-bonded) length and (c) the fixed (or bonded or grouted) length. Depending on the application, the anchors may be classified as (a) permanent anchors, (b) temporary non-retrievable anchors or (c) temporary retrievable anchors.

Fig. 2 illustrates the schematic of the types of anchors according to method of installation (BS 8081, 1989).

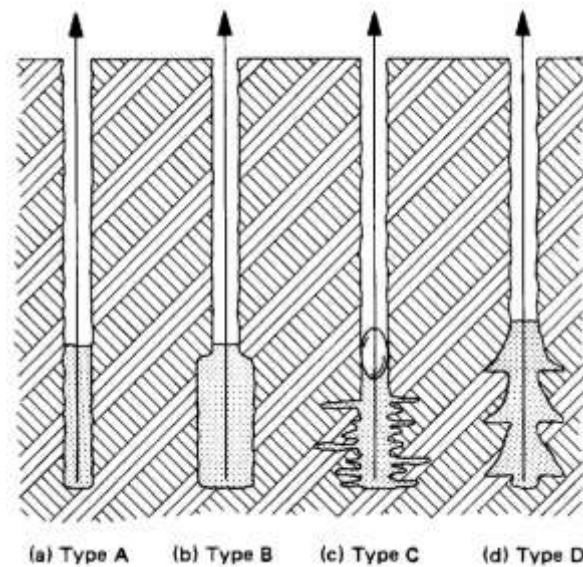


**Fig. 2:** Type of Anchors according to method of installation (BS 8081, 1989). (a) Straight shaft gravity-grouted anchors, (b) Straight shaft pressure grouted anchors, (c) Post grouted anchors (d) Under-reamed anchors.

In general anchor capacity and performance are influenced by four main factors, namely (a) the number of strands to achieve the desired structural capacity, (b) ground characteristics, especially shear strength, to achieve the desired geotechnical capacity, (c) installation techniques and (d) workmanship attained in the field.

## 2.2 Soil conditions

In general site consists of silty clay (Delhi Silt Alluvium) with depth of bedrock varying from as low as 5m to as deep as 18m. The rock can be described as highly to moderately weathered Quartzite. The following profiles (Fig. 3) describe the general stratigraphy with respect to varying depth of bedrock.

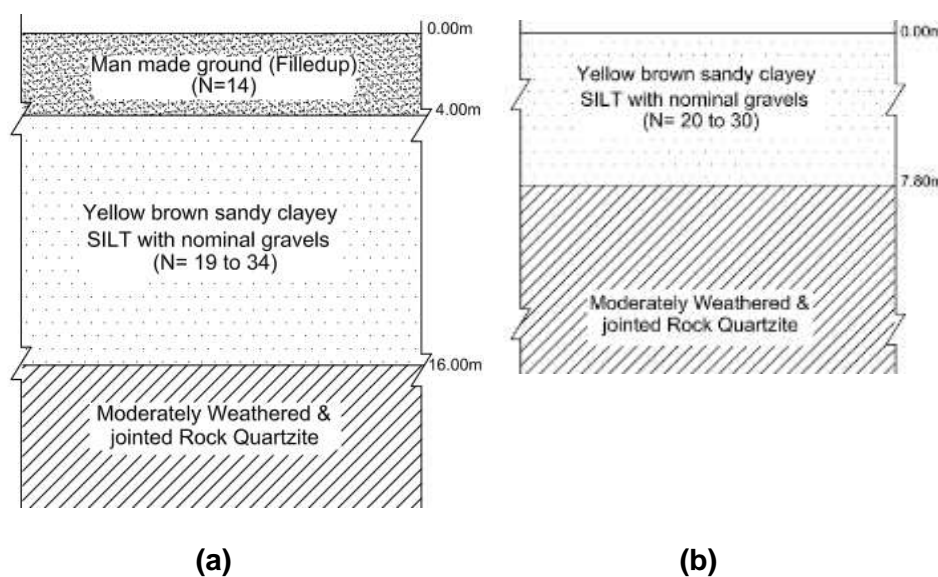


**Fig. 3:** a) Typical soil profile at New Delhi Station b) Typical soil profile at cut & cover tunnel site

### 2.3 Geotechnical problem

For the construction of the underground metro station, multi-level car park and cut-and-cover tunnel on Airport Metro Express Line stretch, an 11 m to 19 m deep excavation was required. The site is next to the existing New Delhi Railway Station and is surrounded by other structures like hotels and hospitals. Therefore, deep vertical excavations were necessary. Fig. 4 shows the layout of station building & car park location.

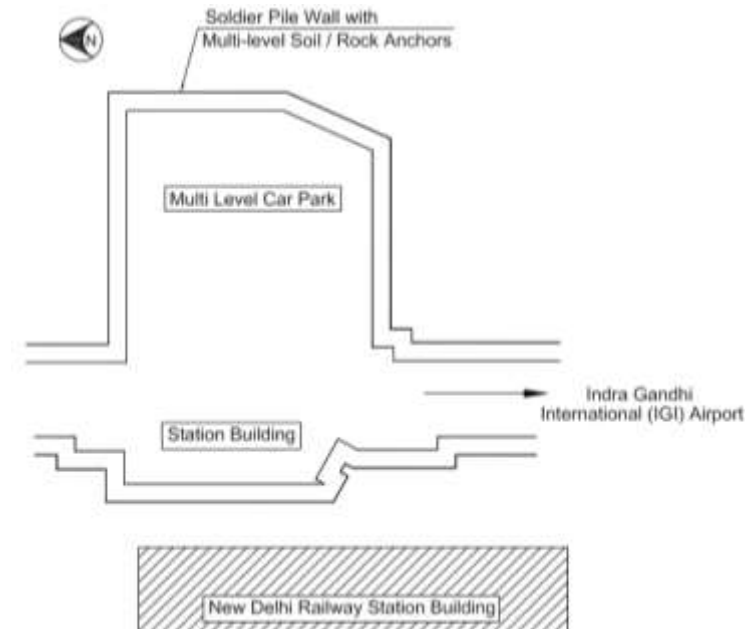


Fig. 4: Layout showing station building and multi-level car park

To retain the soil of the 11 m to 19 m deep vertical excavation, a retention system comprising of soldier pile walls in combination with multi-level soil and rock anchors was proposed. Two to three levels of ground anchors (60 tons and 80 tons) were installed depending upon the depth of excavation. Where the rock level was high, only a single level of anchors was installed.

Fig. 5 shows the schematic of the three levels of soil anchors and rock anchors.

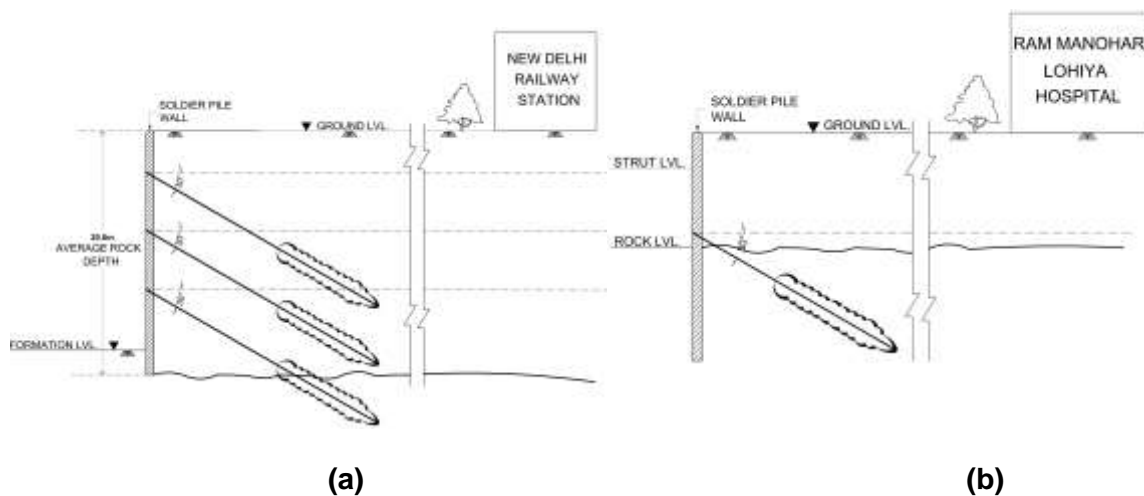


Fig. 5: a) Schematic showing three levels of soil and rock anchors at New Delhi Station site  
b) Schematic showing one level of strut followed by rock anchors at cut & cover tunnel site

## 2.4 Structural and Geotechnical Capacity of Anchors

### 2.4.1 Structural Capacity

To achieve the desired structural capacity of the anchors i.e., say 80 tons, the anchors are fabricated using 6 Nos. of each 12.7mm diameter steel strands (7 ply) LRPC conforming to IS: 14268-1995, clause-II, were used as per the following calculations:

Design capacity of the anchor	= 80 T
Capacity of each strand of 12.7mm dia. (As per IS 14268:1995 For 7 ply, 12.7 mm nominal dia., LRPC strands, clause II)	= 18.74 T
No. of strands	= 6nos (say)
Total Structural capacity of the anchor	= 18.74T x 6nos = 112.44T
Factor of safety against STRUCTURAL capacity of the anchor	= Theoretical capacity / design capacity = 112.4 T / 80T = <b>1.41 &gt; 1.4 (as per BS 8081: 1989)</b>

### 2.4.2 Geotechnical Capacity

The main components of the geotechnical capacity of the anchor are free and fixed length, which are arrived at based on the following calculations:

Design Capacity of the anchor	= 80T
Length of anchor in the active wedge zone	= 10.5m (as per to failure wedge analysis)
Free length of anchor	= 12.5m (incl. 2m additional buffer length)
Fixed length of the anchor, L	= 9.5m (say)
Geotechnical capacity of the anchor	= $\pi \times D \times L \times \tau_{f(\text{Sandy silt})}$
D, Dia of drill hole	= 0.152m
$\tau_{f(\text{Sandy silt})}$ is theoretical skin friction ( <b>&gt; 400 kN/sq.m</b> ) for <b>Sandy Silts having Consistency Index, <math>I_c=1.25</math>, according to BS 8081: 1989, clause 6.2.5.3, Fixed Length in Type C Anchorages</b>	
Considering, theoretical skin friction $\tau_{f(\text{Sandy silt})}$	= 400 kN/sq.m
The ultimate geotechnical capacity of anchor	= $(\pi \times 0.152 \times 9.5) \times 400$ = 1,815 kN ~ 182T
Factor of safety against geotechnical capacity of the anchor	= Theoretical capacity / design capacity = 182 T / 80T = <b>2.3 &gt; 2 (as per BS 8081: 1989)</b>
Total length of the anchor	= Free length + Fixed length = 12.5m + 9.5m = 22m

## 2.5 Installation method

Installation of ground anchors consists primarily of drilling, installation of fabricated anchor, cement grouting and finally by pre-stressing after a curing period of 7 to 10 days. Fig. 6 shows anchor installation works in progress and construction of underground New Delhi metro station in full swing after the successful excavation to the desired depth.



(a)

(b)

**Fig. 6:** a) Installation of ground anchors using Casagrande C6 Hydraulic drill rig  
b) Construction of underground New Delhi metro station after successful excavation to the desired depth (New Delhi railway station is also seen in the back ground)

## 2.6 Testing results

After a curing period of 7 to 10 days, each and every anchor was tested / pre-stressed using a 100 ton multi-strand pre-stressing jack. The anchors are stressed to a test load of 1.1 times of the working load. The working loads were 60 tons at station building and 80 tons at cut-and-cover tunnel location. Every anchor was tested to confirm the respective design capacities. Fig. 7 shows the stressing activity in progress.



**Fig. 7:** Pre-stressing using 100T capacity multi strand jack

## 2.7 Quality Assurance and Control

State-of-the-art of anchor installation includes appropriate QA-QC procedures throughout the construction process. The following QA-QC parameters were monitored and recorded on site, during the installation of anchor:

- Drilling
  - Drilling logs consisting of type of soil encountered with depth were kept
  - (It must be ensured that the soil / rock encountered is not significantly different from the assumptions made during the design. Any significant deviations would trigger a design review.)
- Anchor fabrication parameters
  - Components such as fixed length, free length, length of grout pipes, etc. were checked before the anchor was installed in the drill hole
- Primary Grouting
  - Volume of the grout pumped in and the flow rate was recorded
- Secondary Grouting
  - Volume of the grout pumped in and the flow rate was recorded
  - Grout pressures (> 20kg/sq.cm) at which the grout is pumped was recorded
- Pre-stressing
  - All the ground anchors were pre-stressed (100% frequency)
  - All anchors were tested to 1.1 times the design load
  - Elongation of steel were recorded and checked to be under acceptable limits
  - Staged loading and deformations were recorded

## 2.8 Performance of Ground Anchors

For the New Delhi Railway station excavation, multi-level carpark and cut-and-cover tunnel, a total of 600 ground anchors were installed. Excavation was completed successfully in before the middle of 2010.

## 3. CASE STUDY 2: COMPACTION GROUTING FOR NATM TUNNEL AT SAKET

### 3.1 Introduction to Compaction Grouting

The compaction grouting technique uses displacement and compaction to improve ground conditions. A very viscous (low-mobility), aggregate grout is pumped in stages, forming grout bulbs, which displace and densify the surrounding soils. Significant improvement can be achieved by correctly sequencing the grouting work from primary to secondary to tertiary grids.

The compaction grouting method may be used for the improvement of non-cohesive soils, especially in cases, where soils of loose to medium density are encountered. This method is also used in fine-grained soils in order to install elements of higher strength and bearing capacity, thus improving the load bearing behaviour of the soil.

### 3.2 Soil conditions

The soils at site generally consist of sandy silt fill to 5m depth. The abandoned *Nallah* channel was excavated and filled with locally available sandy silt to level the ground. SPT N values in the sandy silt fill were in the range of 4 to 17, indicating loose to medium dense.

This was followed by medium dense to dense Delhi Silt alluvium layer, with SPT N values between 20 & 30 to about 26 m depth. This is underlain by moderately weathered Quartzite bedrock.

### 3.3 Geotechnical problem

Tunnel excavation by NATM was proposed at a depth of about 9 m below existing ground level. The soil above the tunnel crown is fill material (along the *Nallah* alignment) consisting of sandy silt/silty sand in the top 5 to 6 m. This was followed by Delhi silt alluvium down to the tunnel crown. Fig. 8 illustrates the layout of the NATM tunnels and the alignment of *Nallah* channel.

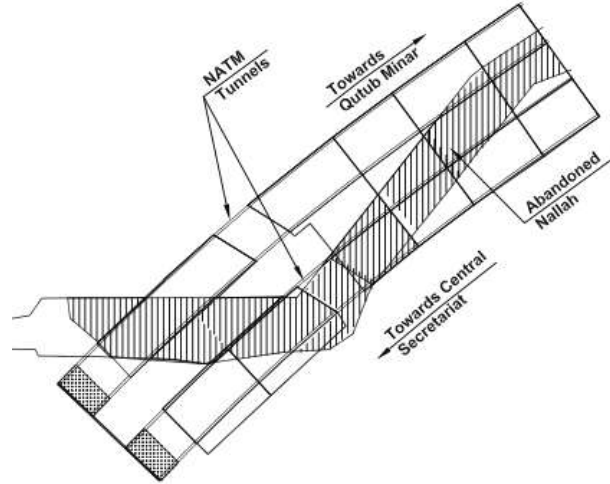


**Fig. 8:** Layout of the NATM Tunnels and abandoned *Nallah* channel

NATM is a method where the surrounding rock or soil formations of a tunnel are integrated into an overall ring-like support structure, thus the supporting formations will themselves be part of this supporting structure. But the pre-improvement soil conditions (loose to medium dense sandy silt/silty sand) was not expected to allow effective arching.

### 3.4 Geotechnical Requirement

Hence, in order to permit safe and stable NATM tunnel excavation and primary lining construction, it was necessary to carry out a combination of shallow and deep ground treatment by compaction grouting. An theoretical SPT 'N' value profile between 10 and 18 with respect to depth was proposed by using the correlation,  $SPT\ N = 10 + 1.75Z$ , where, Z is depth, to form effective soil arching during tunnel construction.

Fig. 9 illustrates the proposed NATM tunnels under a filled up soil strata at abandoned *Nallah* channel location along with the existing and required SPT N value profile.

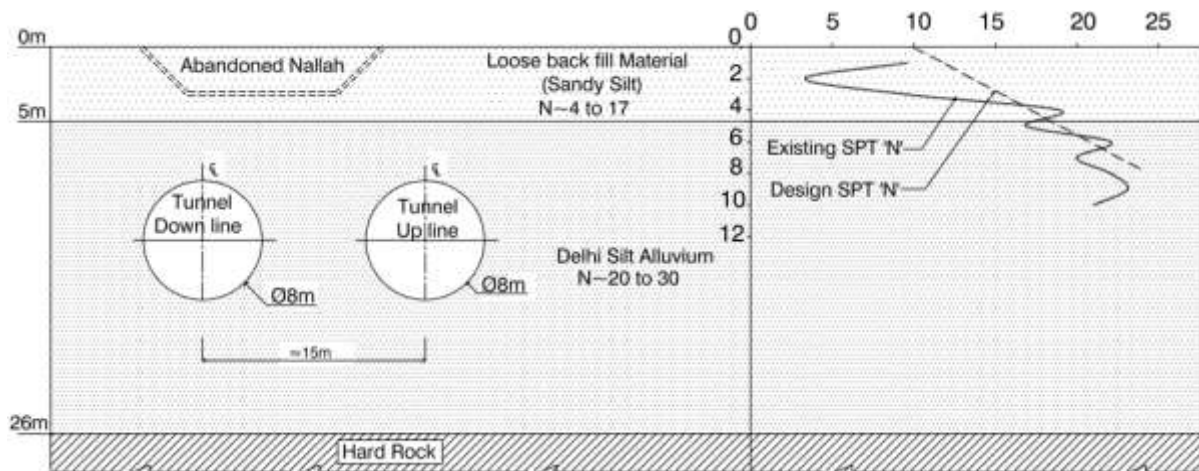


**Fig. 9:** Schematic of the NATM tunnels under an abandoned *Nallah* channel; the required and existing SPT N values are plotted on the right

### 3.5 Installation method

Generally construction consists of drilling, installation of stinger rods and pumping the low slump grout mix from the bottom of the treatment depth to the working platform in steps. For compaction grouting, a low slump cement with a mix proportion of 1:3, water-cement ratio of 0.5 and admixtures like Bentonite and Glenium are used as a plasticizer to increase the workability of grout mix. The slump value of grout mix is about 120 to 150 mm. A truck mounted hydraulic drill rig was used to drill a nominal diameter hole of 90 mm to a depth of about 8 m through the over burden soils. After drilling, the grout mix was pumped through the stinger rods, to form a bulb like element in the loose soils, in stages (0.5 m each) from bottom to the top of the working platform. Fig. 10 shows the compaction grouting works at site.



Fig. 10: a) Picture illustrating the progress of compaction grouting works at site b) Measurement of slump as QA-QC procedures

### 3.6 Testing results

Field trials were carried out to establish a suitable grid pattern to achieve the intended post compaction grouting SPT 'N' values. Trials were carried using 2 m and 4 m square grids. Pre and post compaction grouting SPT 'N' values were recorded and analysed.

Fig. 11 illustrates the typical layout of the compaction grouting – 2m and 4m square grid:

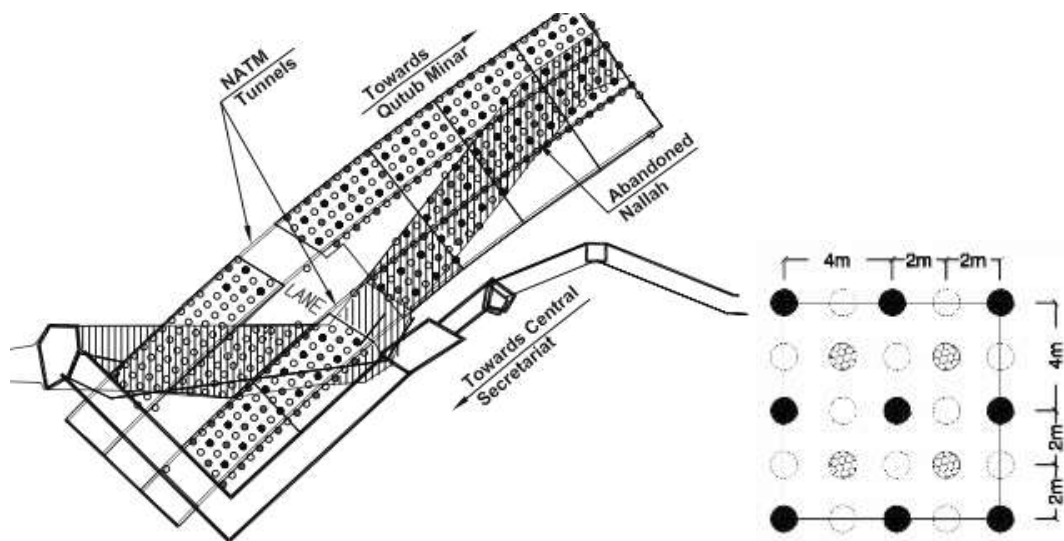


Fig. 11: Layout illustrating the compaction grouting grid – 2 m and 4 m

Pre and post treatment analysis are also done to find the strength of the improved ground. Post treatment SPT 'N' values in the filled up soil increased and ranged between 20 & 30. Both 2 m and 4 m grids were generally able to achieve the required design SPT N values. Fig. 12 shows the Comparison between Design SPT values with Pre and Post-improvement SPT values.

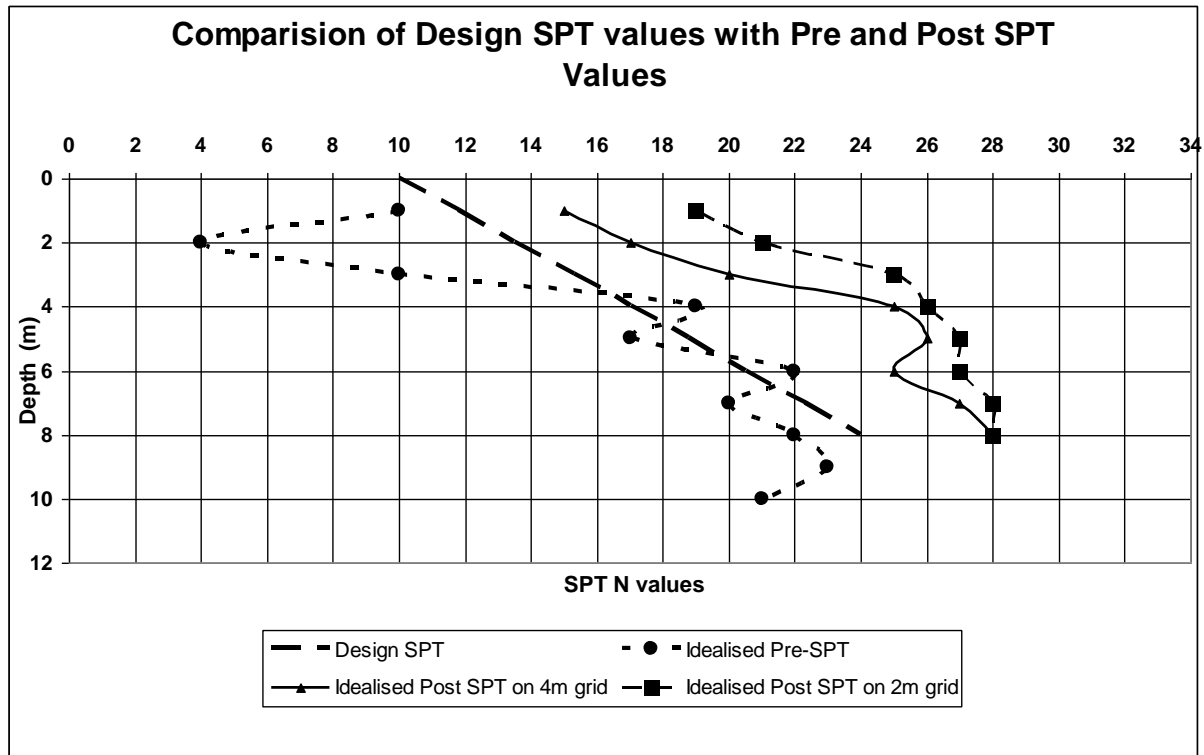


Fig. 12: Comparison of Design SPT values with Pre and Post SPT Values

### 3.7 Quality Assessment and Control

As with other ground improvement techniques, proper quality assurance and quality control (QA-QC) procedures were adopted. The working parameters (e.g depth, pressure, grout volume, heave etc) were maintained and recorded at each stage of compaction grouting process to determine the appropriate termination point. Termination of particular grouting stage was considered when one of the following conditions achieved:

- Pre-determined grout volume is achieved (in accordance with bulb diameter i.e., 0.5 m)
- Pre-determined grout pressure is achieved (in accordance with depth of treatment i.e., 12 kg/sq.cm to 18 kg/sq.cm)
- Mortar is overflowing from same grout hole collar
- Excessive ground heave is measured i.e. greater than or equals to 15 mm

Working parameters (grout volume, pressure, depth, etc.) were monitored using automated quality control systems, which are recorded and printed real-time during the installation of the compaction grouting columns.

### 3.8 Performance of improved ground

A total of 296 grout points were drilled with over 420 m<sup>3</sup> of grout pumped. 19 pre-improvement and 17 post-improvement SPT boreholes were drilled. The NATM tunnel excavation was successfully completed in the middle of 2009.

#### 4. CONCLUSIONS

Soldier pile walls in combination with ground anchors as a retention system was successfully carried out to support the 11m to 19m deep excavations for the underground station and tunnelling works Delhi Metro Rail Project sites. This retention system facilitated the space for construction activities of the underground station and cut & cover tunnel. The construction of these underground structures is now complete (Fig. 13).



**Fig. 13:** Pictures illustrating the regular traffic movement over completed underground **a)** New Delhi Metro Station Building **b)** Cut & Cover Tunnel at Ram Manohar Lohia Hospital

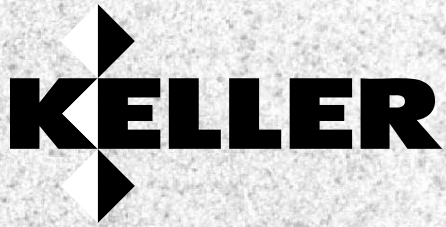
Similarly, Compaction Grouting proved to be effective in densifying the loose silty sandy deposits above the tunnel crown. This facilitated the construction of tunnel by NATM method as the loose silty sandy soils densified after the compaction grouting there by forming self arching which is required for NATM method of construction. This was for the first time Delhi Metro Rail Corporation has constructed a tunnel in loose deposits using NATM method.

#### References

BS 8081: 1999, "British Standard Code of Practice for Ground Anchorages", British Standards Institute, London.

IS 14268: 1995, "Specification for uncoated stress relieved low relaxation seven ply strand for prestressed concrete", Bureau of Indian Standards, New Delhi.

Annexure 3    Technical paper on “Grouting in Limestone for SMART tunnel project in Kuala Lumpur, Malaysia” by Dr.V. R. Raju and Ir.Y.W. Yee,2006.



# Grouting in Limestone for **SMART Tunnel** Project in Kuala Lumpur, Malaysia

**Dr. V.R. Raju and  
Ir. Y. W. Yee**  
*Keller (M) Sdn. Bhd.,  
Malaysia*

Presented by

**Keller Grundbau GmbH**  
Kaiserleistraße 44  
D-63067 Offenbach  
Tel. +49 69 8051-0  
Fax +49 69 8051 244  
E-mail: [Info@KellerGrundbau.com](mailto:Info@KellerGrundbau.com)  
[www.KellerGrundbau.com](http://www.KellerGrundbau.com)

**International Conference and  
Exhibition on Tunneling and Trenchless  
Technology,**  
March 2006, Kuala Lumpur, Malaysia

**Technical paper 60-53 E**

# Grouting in Limestone for SMART Tunnel Project in Kuala Lumpur

Dr. V.R. Raju and Ir. Y. W. Yee  
*Keller (M) Sdn. Bhd.*  
*Kuala Lumpur, Malaysia*  
*(ywyee@keller.com.my)*

## ABSTRACT

The SMART tunnel was constructed in very challenging geological terrain comprising cavernous Limestone, with highly permeable subterranean solution channels and cavities. Dewatering activities can result in groundwater lowering leading to ground subsidence and in some cases, formation of sinkholes. Likewise, actions from tunneling works can cause disturbance to the ground with similar consequence. This paper describes grouting works that were carried out to reduce water inflow into open excavations and to minimize ground disturbance for the SMART Tunnel project. It also details the program of preventive grouting that was implemented, comprising mainly of rock fissure grouting and compaction grouting, and also, jet grouting. The planning and design of the grouting activities, which were carried out to suit specific site conditions are explained. Demanding aspects of working in public areas, beneath sensitive structures like rail track, mitigating heavy water flow and under tight time schedules are discussed.

## 1.0 INTRODUCTION

The SMART tunnel was constructed through Kuala Lumpur Limestone, home to cavernous and karstic features with highly permeable subterranean solution channels. This presented one of the most challenging geological terrains for the construction team. Construction activities during initial construction of the launch shaft led to higher than expected groundwater inflow into the excavation through these solution channels. Systematic grouting was carried out which mitigated the situation. Subsequently, the Main Contractor, MMC-Gamuda JV implemented a grouting program primarily aimed at minimising water inflow into open excavations and also involved ground treatment along the tunnel corridor at areas identified to be prone to ground subsidence.

The following pages will describe the variety of grouting methods selected depending on ground conditions and site constraints, including fissure grouting, compaction grouting and jet grouting. The systematic approach adopted in the design, execution and monitoring was crucial to achieve the desired end result. This required close working relation between engineers and technicians from the Main Contractor and Specialist Contractor to implement the appropriate solution. This paper demonstrates that the grouting program was successful in reducing ground disturbance due to the tunneling activities.

## 2.0 GEOLOGICAL FEATURES OF KUALA LUMPUR LIMESTONE

### 2.1 General

According to Gobbett & Hutchinson (1973), the Kuala Lumpur Limestone comprises Upper Silurian marble, finely crystalline grey to cream thickly bedded, variably dolomitic rock. Karstic features are prevalent in the limestone formed by movement of water containing carbonate acid (dissolved carbon dioxide). As water flows downwards, the bedrock profile near the surface is eroded to form sharply varying pinnacles, cliffs and ravines. Cavities in the rock (infill or empty) seldom exist in isolation but as part of a complex matrix of solution channels. Over time the roof of some cavities may dissolve or collapse which may trigger sinkholes or depressions on the ground surface. Under some conditions, the soil overburden may arch around the cavity (slump zone) and a quasi-stable condition may persist for years (see Figure 1). The occurrences of ground subsidence and formation of sinkhole in limestone are frequently associated with construction activities i.e. when the ground water is lowered, rock/ soil is removed or triggered by vibrations (Tan, 2005).

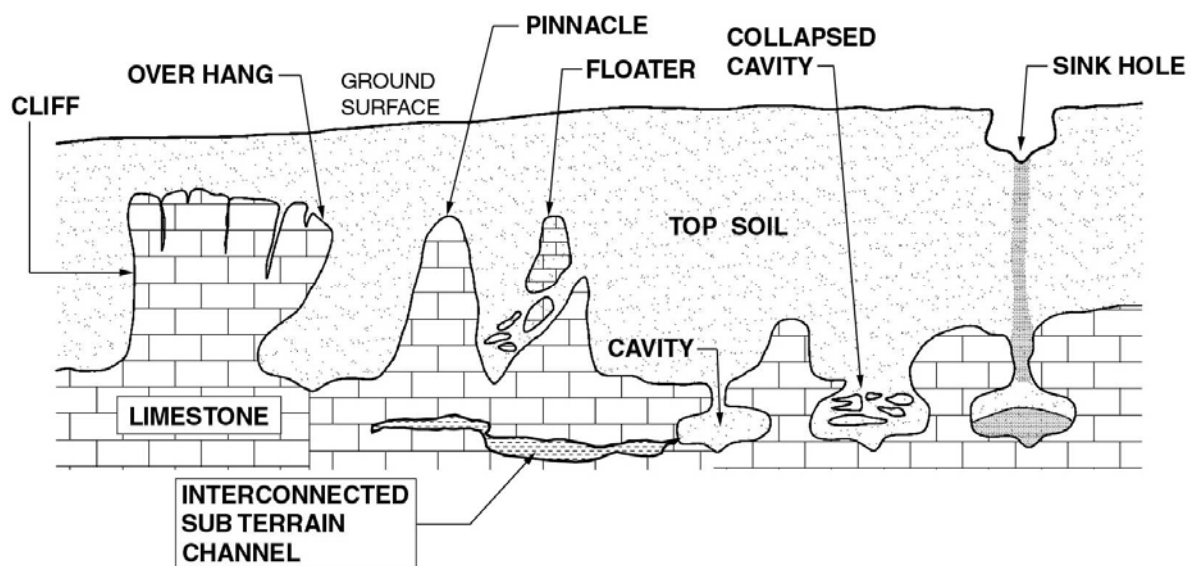


Figure 1: Limestone Rock Profile

### 2.2 The Tunnel Path

The tunnel is located approximately between 10m and 16m below existing ground level. In most areas along the tunnel corridor, the TBM bored almost entirely within the rock mass. Tunneling activities were hence, largely shielded from disturbing the ground surface by the relatively strong rock mass. However, where cavities or rock fissures are of significant proportions or where the rockhead is at greater depths, drilling activities could trigger ground movement. Significant ground displacement could lead to the formation of sinkholes at the surface.

Various interesting geological features were exposed during the SMART Tunnel construction works including steep cliffs, potholes and cavities (see Figure 2). They underline the complex ground conditions in which the tunnel had to be built.



Figure 2: Variable Features in Limestone

### 3.0 OBJECTIVES OF DRILLING AND GROUTING WORKS

Grouting works were initially commissioned to reduce water inflow into the excavated launch shaft (described in section 6.2). Thereafter, a program of “preventive” grouting works was designed and purposefully implemented by the Main Contractor.

The objectives of preventive grouting works were mainly to reduce groundwater lowering and minimize disturbance to the overburden soil, which were achieved by the following means:

- (i) fill solution channels or cavities in rock with slurry and mortar grout
- (ii) grout behind any gaps of retaining walls
- (iii) compact loose overburden using thick mortar grout

In addition, the Main Contractor set up “emergency grouting teams” which were on-call to quickly carry out any remedial works due to ground movement.

### 4.0 PARTICULAR AREAS REQUIRING GROUTING TREATMENT

#### 4.1 Open Excavated Deep Shafts

- (i) The nearly 30m deep launch shaft (named North Ventilation Shaft or NVS) is located at the corner of Chan Sow Lin and Cheras Roads. The two 13m diameter tunnel boring machines were mobilised from this shaft, one north-bound 6km towards Ampang, while the other headed south 4km to Taman Desa.
- (ii) Besides the NVS, open excavations were dug at the North Junction Box (NJB), South Ventilation Shaft (SVS) and South Junction Box (SJB), all typically down to between 25m and 30m below ground.
- (iii) As part of the route will incorporate a traffic tunnel, open excavations were also carried out to form the north and south ingress/ egress traffic entry/ exit points (NIE and SIE). The depths of the excavation were about 20m and 25m deep.

The rockhead level was generally found to be about 5m to 10m below ground. Hence, grout treatment for these open excavation pits mainly comprised of rock fissure grouting to form “grout curtain” around the excavation shafts (Figure 3). The spacing between grout holes was typically 4m, deemed to be reasonable having taken practical constraints into considerations. The depth of drill holes were normally taken to 2m below the depth of the excavation. Where fracture rock was encountered or where the grout take was high, depth of drilling was extended further down and drill holes were added. The grout holes were drilled at least 6m behind the excavation face to be clear of rock bolts.

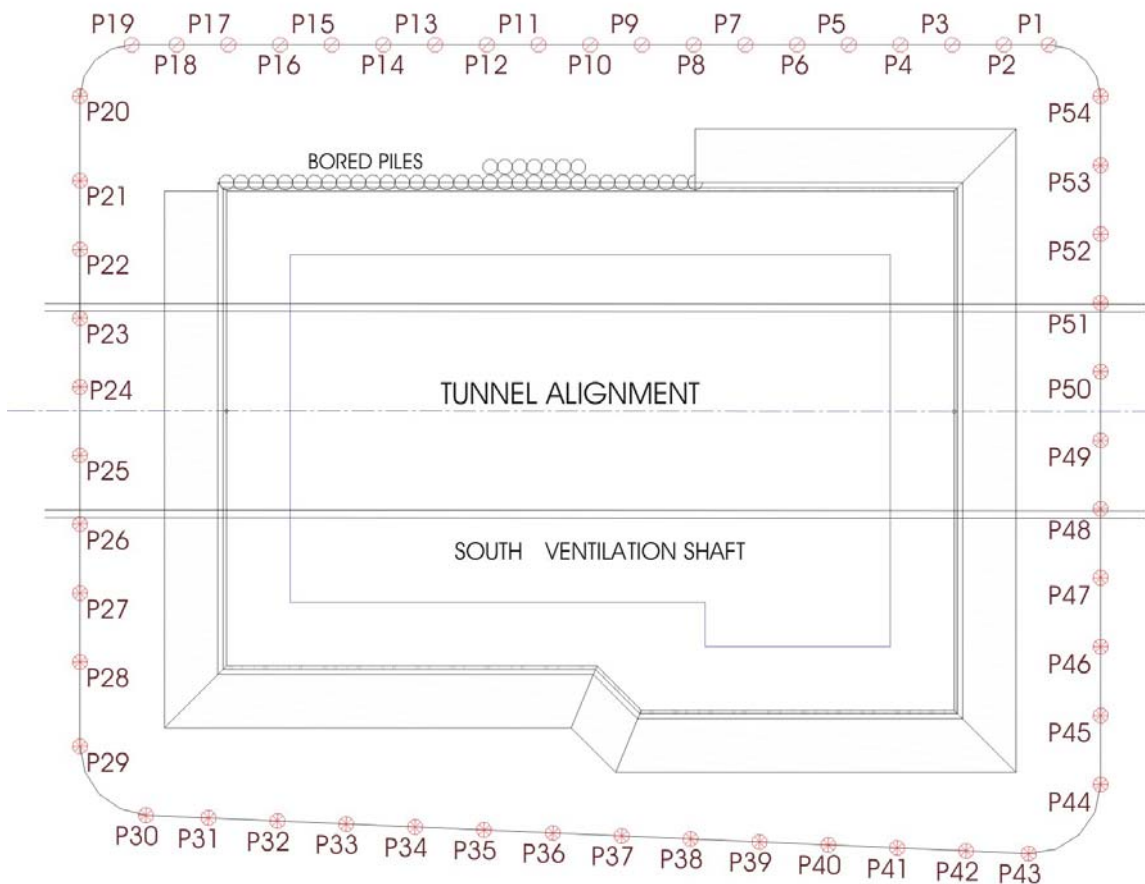


Figure 3: Typical Grout Holes Around Excavation Shaft

#### 4.2 Subterranean Excavation

The tunnel also required the construction of nine Cross Passages as safety exit points along the 3km stretch of traffic tunnel. All Cross Passages were formed by excavation in rock, dug underground from within the tunnel shaft.

Ground treatment consisted of rock fissure grouting to form “grout curtain” around the sides and roof of the proposed box-like underground excavation (Figure 4). The spacing between grout holes was typically 4m. Where fracture rock was encountered or where grout-take was high, drill holes were added in between holes.

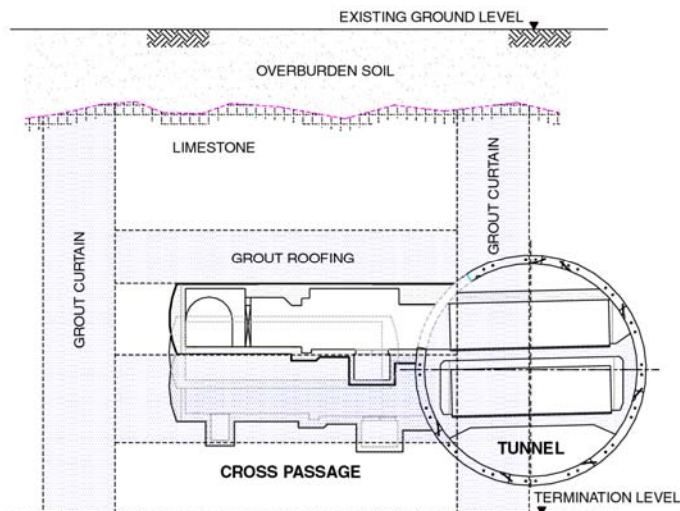


Figure 4: Typical "Grout Curtain" Around Cross Passage

### 4.3 Settlement Sensitive Areas

The TBMs also traveled beneath some settlement sensitive areas e.g. rail crossing, bridge crossing, important highway, beside buildings, etc. These sites were firstly investigated by "exploratory drilling" to ascertain the depth and quality of rock. Depending on the findings, grouting works were carried out, primarily to fill cavities and seal large solution channels.

### 4.4 Cutter-head Intervention Locations

The TBM cutter-head required maintenance at regular intervals. At such TBM stops, there was a risk of ground disturbance. These locations were carefully selected by the Main Contractor based on known soil data. Grouting works were usually specified as a precautionary measure to form a "grout block" where the cutter-head could be parked whilst maintenance was carried out (Figure 5).

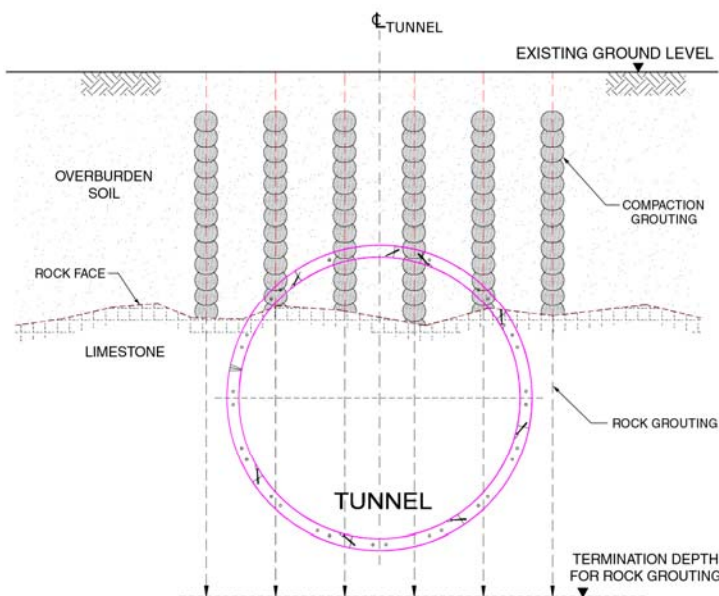


Figure 5: Typical Grout Treatment of Cutter-head Intervention Locations

#### 4.5 Areas of Deep and Cavernous Rock

The Main Contractor carried out detailed geophysical survey and soil investigation ahead of the TBM, along the proposed tunnel path. Particular features which were deemed to pose certain risks to the tunnel mining activities were identified. These features included:

- (i) deep rockhead (or thick soil overburden), especially where soft/ loose soil is found within the tunnel path
- (ii) high density of fractured rock
- (iii) sizeable caverns in the rock mass

Rock fissure grouting and compaction grouting were then instituted (Figure 6).

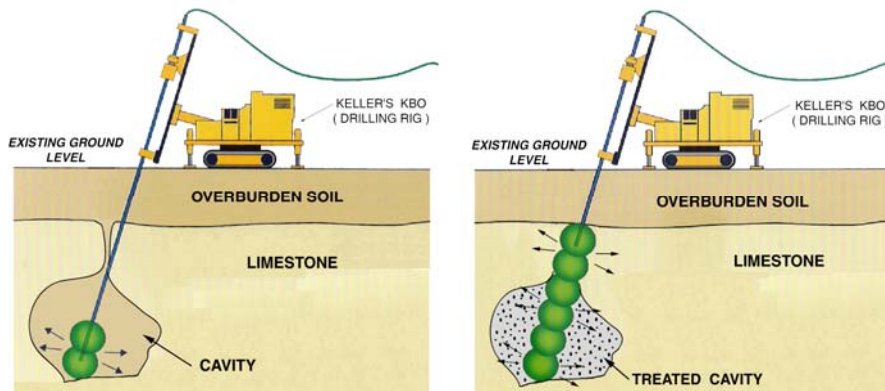


Figure 6: Artist Impression of Cavity Treatment

#### 4.6 Grouting Behind Retaining Walls

The soil encountered on the site was highly variable including loose sand, very soft slime, soft peaty clay and man-made dumping ground. The groundwater was generally at about 3m to 4m below ground. Typically, such mixed soils were highly permeable. The construction of some of the deep excavation shafts (described in section 4.1) required retaining piled wall (usually contiguous bored piles).

Jet grouting was instituted behind some of these walls to minimize water seepage and also to reduce lateral active earth pressures. Figure 7 shows typical detail of the treatment scheme.

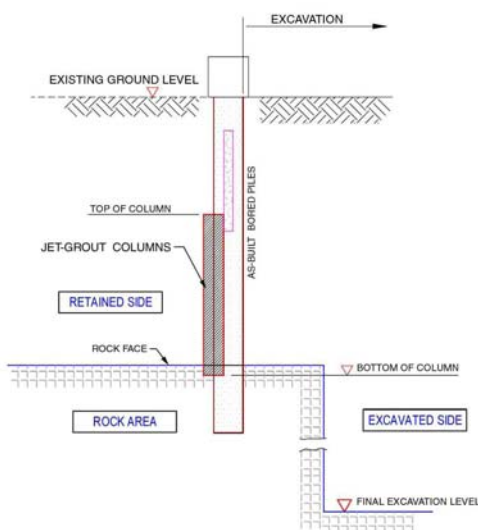


Figure 7: Typical Jet Grout Treatment Behind Contiguous Bored Pile

## 5.0 GROUTING TECHNIQUES

Various grouting techniques were applied for different site conditions on this project including the following:

- (i) Rock fissure grouting
- (ii) Compaction grouting
- (iii) Jet Grouting

The techniques are described below.

### 5.1 Rock Fissure Grouting

Rock fissure grouting was used widely across the site. It was primarily used to form “grout curtain” around excavations to minimize water seepage and was applied at the NJB, SVS, SJB, NIE, SIE and Cross Passages. Besides these, the sites for all cutter-head interventions and other settlement sensitive locations were grouted to minimize potential ground movement.

Description of the methodology involved is given below. In general, they are in line with guidelines given in BS\_EN 12715 (2000).

#### 5.1.1 Drilling

The overlying soil strata was drilled and retained with casing with adequate diameter for the following rock drilling. Drilling in rock was mostly carried out using down-the-hole hammer (DTHH) with drill hole diameter of about 95 to 115mm. The drilling air pressure was controlled to ensure that excessive pressure is not introduced into the ground.

#### 5.1.2 Materials and Properties

Grout comprised Ordinary Portland Cement with some bentonite. Washed sand is added into the mix when the grout take in the hole exceeded 10m<sup>3</sup>. Bentonite was added mainly to reduce shrinkage and aid pumpability. In some cases, additives were included to reduce shrinkage. In general, water cement ratio was kept below 1.5, as thinner mixes were found to segregate under the conditions of use.

#### 5.1.3 Grouting Parameters

Typical grout pressures are as shown in Table 1. The selection of appropriate pressure is crucial to ensure adequate distance of grout flow without causing hydrofracture.

Depth ( m )	Min. Pressure ( bar )	Max. Pressure ( bar )
0 – 5	1	3
5 – 10	3	6
10 – 20	6	10
20 - 30	10	20

Table 1 – Typical Grouting Pressure

Grout mix was prepared by adding pre-determined volume of water and bentonite to cement and mixing using high speed colloidal mixer. Since much of the work was carried out in public areas or within tight space constraints where a silo batching system was not suited, the process was relatively labour intensive. The bentonite used was allowed to soak 24hr before utilization.

#### 5.1.4 Grout Delivery

Delivery of the grout was generally carried out using hydrostatic pumps with pumping pressures of up to 15 bars and flowrates up to 60 lit/min. Where high grout take was anticipated, mono pumps with flowrates exceeding 100 lit/min were used. When grouting large cavities or where there was a need to compact the in-fill material, concrete pumps with capacity of 200 lit/min were used.

Grout was delivered down the grout hole through high pressure grout hoses. In general, pneumatic packers were used to inject grout following an ascending staged grouting process at 5m lift intervals. Where cavities or large fissures were encountered, these are normally grouted immediately and left for 24hrs. The affected hole was then re-drilled and grouting was continued for the next stage (Figure 8).

Mechanical packers were used only where grouting was required near the ground or excavation wall surface.

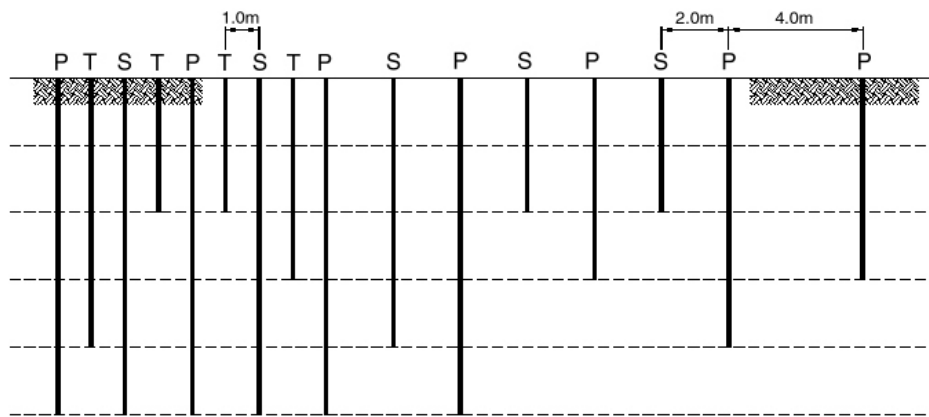


Figure 8: Depiction of Fissure Grouting and End Product

#### 5.1.5 Closure Method

The following *closure grouting technique* was performed as part of the rock grouting works (Figure 9):

- i) *Primary exploration holes* were drilled generally at 4.0m centers around the perimeter of the excavation box.
- ii) In stable boreholes, grouting was carried out in stages, ascending from the base of the grout hole.
- iii) When the grout take in the primary holes exceeded certain volume, *secondary grout holes* were drilled midway between the primary holes and grout injected.
- iv) The next injection sequence (if required) involves drilling *tertiary holes*, located midway between the previous grout holes, to depths indicated by previous local grout takes and grout injected.
- v) The above process is repeated, with grout injections from grout holes at gradually reduced spacing, resulting in overlapping of grout from different injection phases, which enabled the grout to fill progressively finer fissures and discontinuities.



Closure grouting of rock formations ( P: primary S: secondary T: tertiary )

Figure 9: Grouting Using Closure Method

### 5.1.6 Grout Termination Criteria

For grouting in the fissured rock mass one of the following termination criteria had to be satisfied:

- i) Final pressure (max. pressure) to be maintained for a predetermined period (about 5 to 10 minutes) with a reduced flow rate of 2 to 3 lit./min.
- ii) Suspend the grouting if the grout volume reaches a pre-determine amount (normally  $10\text{m}^3$ ) for at least 24 hours in order to allow setting of the grout. After this time lapse, grouting was resumed. (Where suspension of grouting occurred, secondary grout holes were usually added thereafter).

### 5.1.7 Quality Control

#### i) Material Suitability

The quality and consistency of the grout slurry were monitored on site by way of the following means:

- density test using hydrometer and mud balance
- viscosity test using Marsh cone
- strength tests using hand held pocket penetrometer
- sedimentation test

#### ii) Monitoring during Execution

The volume of grout used and flowrate of grout delivery were recorded using grout flowmeter connected to a computer. A hardcopy of the data was printed in real time and was inspected frequently by the supervision personnel.

#### iii) As-built Records

As-built records were necessary not only for recording what has been done but were important to aid the design engineer determine whether additional works were required (e.g. need for secondary holes or deeper grouting depths). These included:

- drilling logs showing duration of drilling and depths where fractured rock were encountered
- grouting logs indicating grout volume consumed versus depth and grouting pressures
- plan layout drawing showing grout take at each point
- other data such as ground monitoring data during grouting was also kept

Figure 10 shows typical as-built records of the grouting procedure.

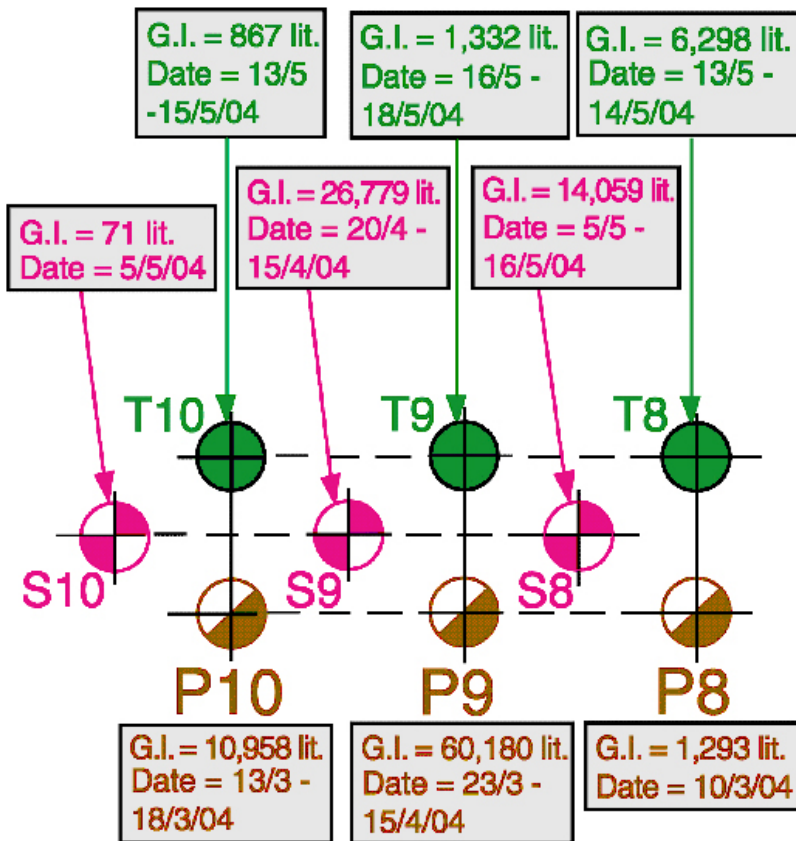


Figure 10 – Typical As-built Grouting Record

#### iv) Water Tests

Where required by the Main Contractor, water tests were carried out on selected grout holes in accordance to BS5930:1999. The grouted zone was required to demonstrate water loss of less than 5 Lugeon.

### 5.2 Compaction Grouting

Compaction grouting was implemented mainly to fill cavities and compact very loose soil overburden on site. Compaction grouting process was first applied in the USA in the 1950s and has developed to include a wide range of applications (Rubright and Bandimere, 2004). Compaction grouting is now the preferred method for soil improvement in the USA (replacing slurry injection), primarily because the grouting process can be better controlled within the localized treatment area. Traditional slurry grouting tends to result in extensive grout travel, often to a distance far beyond the treatment zone and normally wastes large volumes of expensive grout. Whether the targeted soil zone is repaired or not, is uncertain.

The execution method of the compaction grouting process is governed by the European Standard of BS\_EN12715 (2000).

### 5.2.1 Drilling

The technique involves the installation of a grouting pipe (“stinger rod”) to the required depth. The spacing between grout points was varied depending on area of treatment. For overburden compaction, this was typically at 3m centres. Where grout take was high, treatment points were added at appropriate distance.

### 5.2.2 Materials

The grout material comprised of stiff mortar grout (cement, water and sand mix) which was mixed at batching plant and delivered to site. To aid flowability, bentonite and lime were sometimes added. Typical slump suitable for soil compaction is less than 100mm. More flowable mix was used for cavity grouting or treatment at soil/ rock interface to allow greater grout travel.

### 5.2.3 Compaction Process

The stiff mix is pumped into the soil under high pressure until a pre-determined termination criteria is met. The overburden soil was treated as the grout pipe was withdrawn in steps upwards. The end product is a homogeneous grout bulb or series of linked bulbs, formed near the tip of the grout pipe as the pipe is withdrawn in steps (Figure 11). The grout bulbs formed compacts the surrounding ground by displacing loose soil and closing voids existing within the soil (without causing hydrofracture).

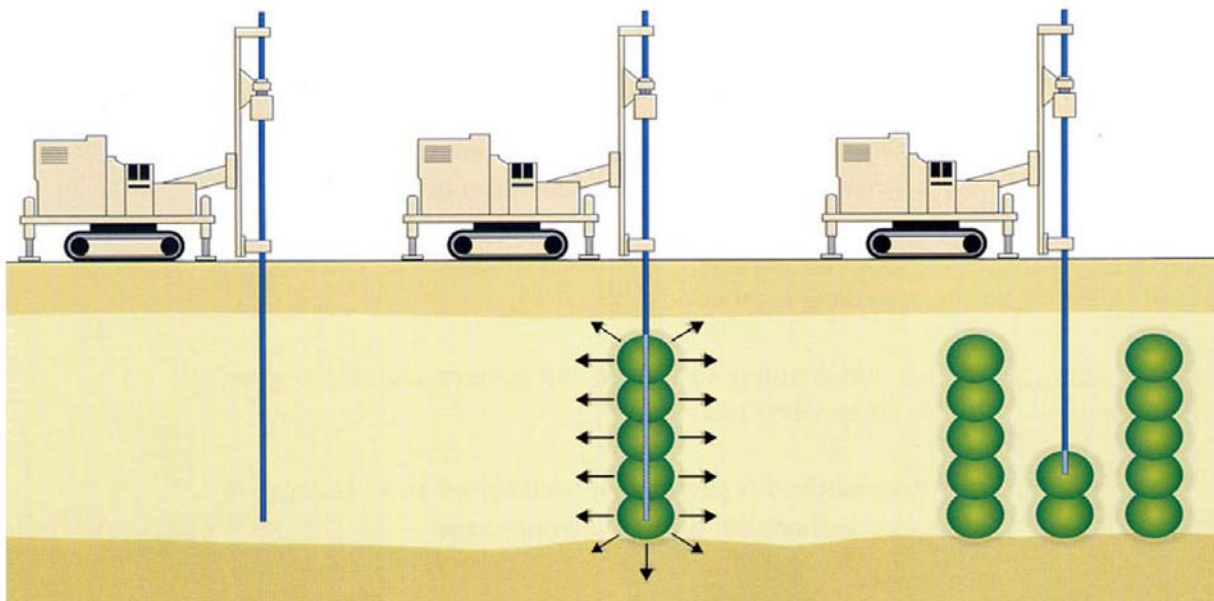


Figure 11: Schematic Drawing of Compaction Grouting Process

The displacement ability of the compaction bulbs also raised the subsided ground surface, thereby remedying any previous ground settlement. For such treatment, several grouting points were normally required in each subsided zone. The method is most effective in non-cohesive soils. When using this technique in saturated fine-grained soils, care should be exercised as temporary increase of pore pressure can result which may lead to temporary reduction in soil shear strength.

#### 5.2.4 Grouting Parameters

Typical compaction grouting parameters are listed in Table 2.

Description	Parameter	Remarks
Grout Point Spacing	2m to 3m grid	Depending on soil conditions, displacement ratio and compaction effort (improvement) required
Sequence of Grout Injection	0.5m steps upwards	Downward grouting used only when grouting near surface or where sensitive structures nearby
Injection Pressure	10 to 20 bar	Grout pressure must be high enough to overcome line losses
Injection Rate	50 to 100 lit/min	Slower rate applied for slow draining soil; Higher rate acceptable for treating "slump" ground or cavities
Injection Volume	Varies	Depending on soil conditions, displacement ratio and compaction effort required.

Table 2: Typical Parameters for Compaction Grouting

#### 5.2.5 Compaction Grouting Termination Criteria

Grouting at each step (depth) was terminated when one of the following criteria was achieved:

- (i) surface ground heave was observed exceeding prescribed limit
- (ii) refusal of further grout flow at pre-determined pressure (e.g. overburden stress + line losses + 5-10 bars)
- (iii) volume of grout exceeded pre-determined volume

#### 5.2.6 Cavity Filling

Almost all the so-called "cavities" encountered on site were actually infilled with very loose soil. The compaction grouting process involved pumping thick mortar which remained localized around the grout pipe and cavity being targeted. The loose soil within the cavity was hence displaced and compacted which helped stabilize the cavity.

One treatment feature to be noted is that high slump compaction grout was also injected at the interface of rock and loose soil, which formed a grouted mass which flowed to fill voids on the rock surface and created a grout cover to minimize downward migration of soil.

#### 5.2.7 Overburden Soil Compaction

Compaction grouting was used widely to treat soil for sinkhole prevention. This was carried out by drilling and injection at pre-determined grids of grouting points at various locations along the project corridor. The insitu loose soil was thereby compacted. The treatment was similar to that shown in Figure 5.

#### 5.2.8 Quality Control

During the installation process, the drilling and grouting parameters were monitored carefully. The pressure and grout volume were measured at every step of grout placement. Ground heave was also monitored throughout the grouting process to ensure that the ground was not over-remedied which could otherwise lead to uplift damages. Post-treatment settlement monitoring was also carried out to ascertain that ground movement has been arrested.

Tests can be done in the ground to verify that the soil has actually achieved the desired level of compaction. Figure 12 shows a typical plot of pre and post treatment SPT results conducted at the project site for compaction grouting points carried out at 3m centres grid. Generally, in the silty and sandy soil encountered, the soil was compacted appreciably from a loose state to a medium dense soil with SPT N values improving by 5 to 10 blows/ft. Naturally, closer spaced grouting points would achieve greater compaction.

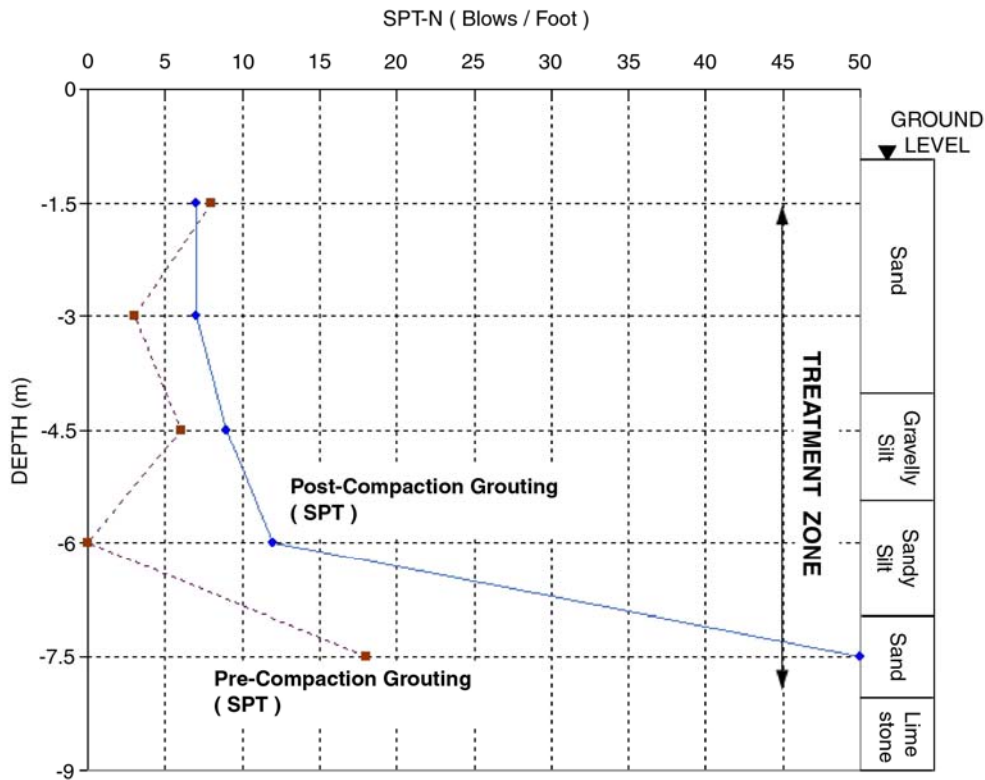


Figure 12: Typical Plot of Pre and Post Compaction Grouting Treatment SPT

### 5.3 Jet Grouting

Jet Grouting is a well-established type of cement soil stabilization. Publications on its usage are numerous (Essler and Yoshida, 2004) and include foundation underpinning, excavation support and props, water sealing slabs, etc. It is a versatile method that can be used for a wide range of soils. For the SMART project, the method was applied to seal gaps between retaining wall piles and reduce lateral earth pressures acting on the walls (see Figure 7).

#### 5.3.1 Drilling and Jetting

The triple tube jetting method was used for this project. This involves jets of water and cement grout being introduced into the soil at high pressures exceeding 400 bar and flowrates above 100 lit/min to erode the soil around the drill hole. The high pressure water is shrouded in a cone of air to concentrate and increase the erosion capability. The eroded soil is rearranged and mixed with the cement grout (Figure 13). Some of the soil will be flushed out to the top of the drill hole through the annular space around the drill rod. The erosion distance (diameter of the grout column formed) varies according to the design and the soil type being treated. This was typically 1.0 to 1.4m diameter.

Factors like the size of the columns, proportion of interlocking columns, as well as construction verticality tolerance were taken into consideration in the design. The execution method of the jet grouting process was in compliance to the European Standard of BS\_EN12716 (2001).

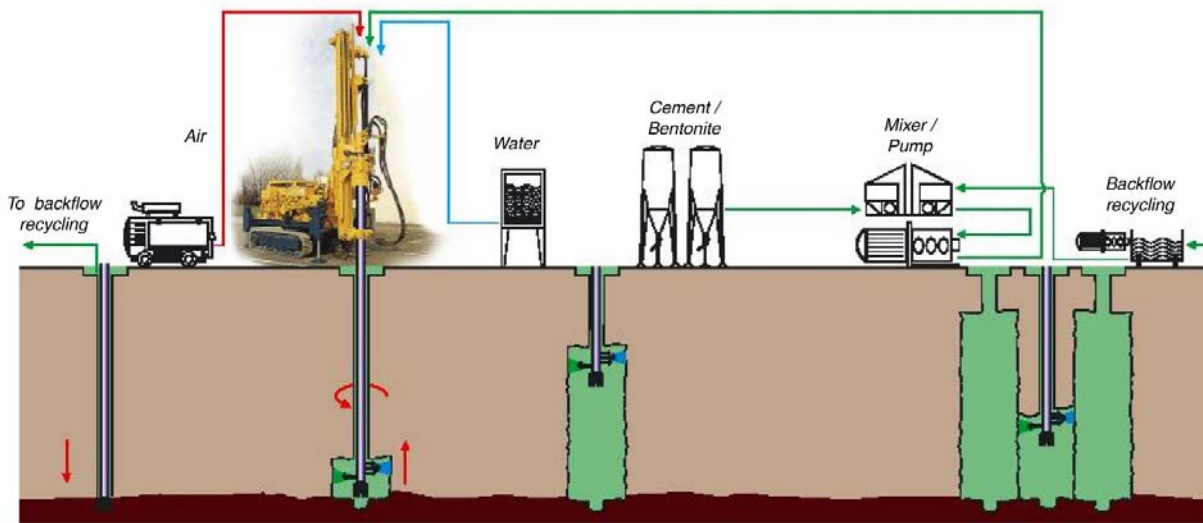


Figure 13: Schematic Drawing of Jet Grouting Process

### 5.3.2 Materials

The sealing effect of jet grout columns to minimize water ingress was primarily determined by the grout composition (with addition of bentonite if necessary) and the quantity injected into the ground. Compressive strength was generally specified by the Main Contractor to be between 0.5 and 1.0 MPa, which was determined by the cement content and the remaining portion of soil in the treated mass.

### 5.3.3 Jetting Parameters

The triple tube system was employed which enabled formation of 1.0m to 1.4m diameter columns required. The typical parameters used are shown in Table 3.

Ref.	Description	Values
1	Grout Pressure	>1.5 MPa
2	Grout Flow Rate	50-200 ltr/min
3	Water Pressure	30-40 MPa
4	Water Flow Rate	80 – 150 ltr/min
5	Water/Cement Ratio	0.67 – 1.0

Table 3 Typical Working Parameters for Triple-tube Jet Grout Columns

### 5.3.4 Quality Control

During the installation process, drilling and grouting parameters were measured in real time. The lifting speed and the rotation of the jetting string, the depth, the pressure and the volume of the erosive and placement jets were automatically recorded in a customized computer and printed out simultaneously. Figure 14 shows the typical print-out from the computer.

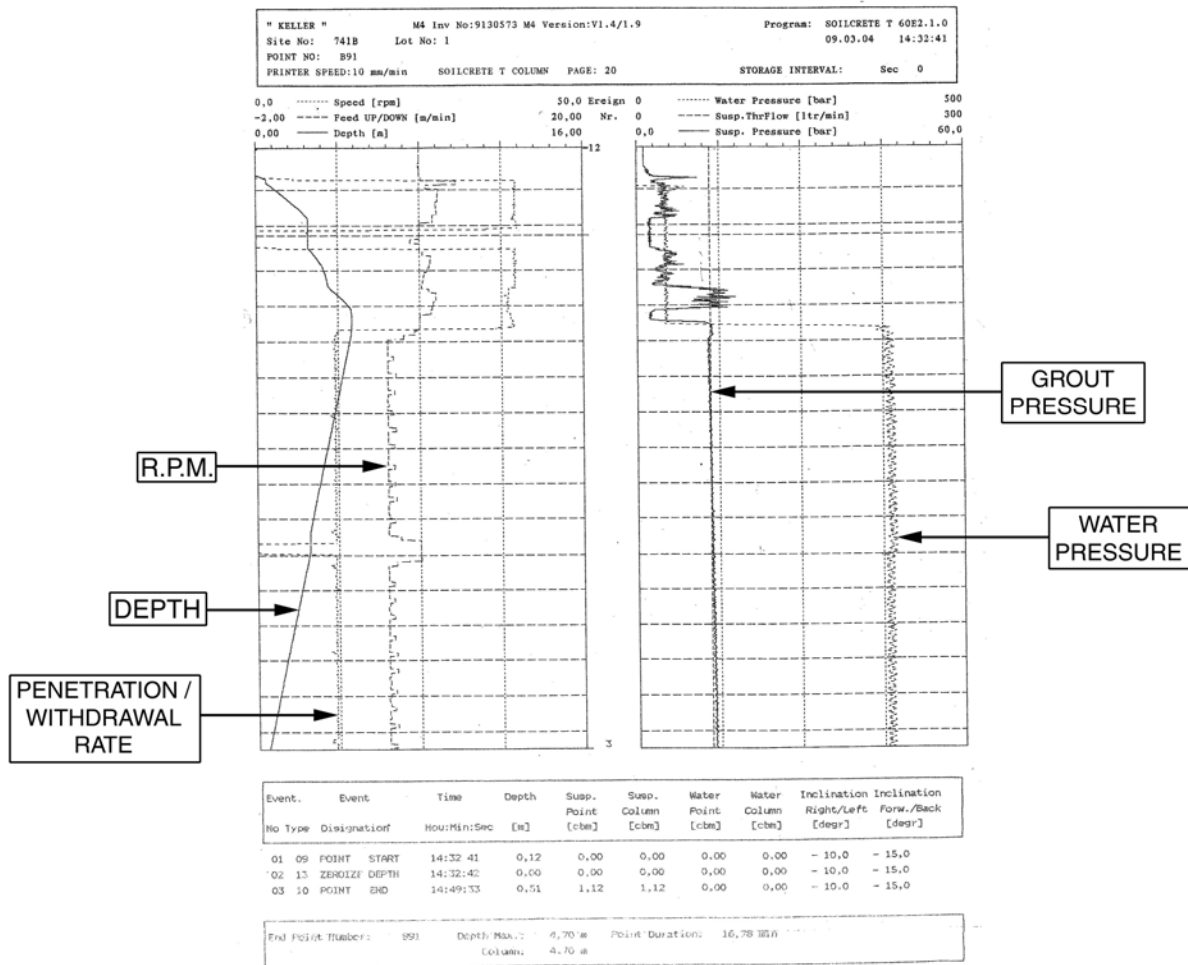


Figure 14: Typical Jetting Parameters Computer Printout

Another important parameter monitored during jet grout columns installation was the spoil return. It gave direct indication of the quality of the treatment in terms of soil erodibility, mixability and column diameter. Low spoil return generally means that the column is not being properly formed. The density of the spoil at the said site was typically 1.6 t/m<sup>3</sup>. Cube samples were retrieved, cured and subjected to compression tests to verify strength. In general, the cube test showed strength of 1.0 to 2.0 MPa after 28 days.

## 6.0 EXAMPLES OF CHALLENGING ASPECTS OF THE WORK

### 6.1 “Emergency Grouting”

Throughout the tunneling works, there were some occurrences of ground depression and sinkholes. Where these features formed over public areas, quick action was required to minimise propagation of the disturbed zone. This necessitated almost immediate mobilization of the required personnel and equipment (see Figure 15).

Where the slump ground “daylighted” on the ground surface (i.e. sinkhole), the area was normally cordoned off from the public. The Main Contractor would then fill the hole with

aggregates. Subsequently, compaction grouting was carried out to infill remaining cavities through a grout pipe drilled to the base of the slump zone. Depending on the extent of the damage, grout holes were added until the ground recovered (usually observable through ground heave).



Figure 15: Treatment of Sinkhole and Ground Depression

## 6.2 Grouting to Stop Heavy Water Flow

The launch shaft (North Ventilation Shaft) for the TBM was the first shaft excavated for the SMART project. The shaft was located at the corner of Chan Sow Lin Road and Cheras Road. The depth of excavation was about 27m below ground and the width of the shaft about 25m. The plan layout of the shaft is shown in Figure 16. Limestone bedrock was generally found 5m below ground but deep ravines were found on the south-east and south-west corners of the shaft.

Water inflow into the excavation was mainly found to be coming through the SE corner of the shaft and was measured to exceed 120 m<sup>3</sup>/hr. The heavy water inflow made it almost impossible to construct the base slab for the TBM launch structure. At that stage, the concrete floor of the excavation had been constructed over the entire pit except for this 360m<sup>2</sup> (20m x 18m) area of exposed rock.

Initially, the Main Contractor tried chemical grouting. However, the flow of water was too high which did not permit time for the grout to set. Subsequently, the Main Contractor decided to use systematic grouting to arrest the problem. This was successfully carried out after working

over an intense 2 week period over 24 hrs. The step-by-step method employed is described below.



Figure 16: Location of Grouting Works at Launch Shaft

*(i) Identify Problem Area*

The area of highest water inflow on the shaft floor was identified. 3 holes were drilled in this region down to a depth about 3m to 6m deep. Water exiting these holes was then channeled through steel pipes into a water sump at a corner of the shaft.

*(ii) Cast Concrete Slab*

A 600mm thick concrete slab was cast to cover the entire exposed rock area (with the exception of the sump). This allowed water flow to be channeled only through openings cored in the slab. The slab also would act as reaction slab for subsequent pressure grouting.

*(iii) Drill and Grout Perimeter “Curtain”*

Grout holes were determined based on an arbitrary spacing of 4m centres. Using closure method, the initial grout holes furthest away from the sump were drilled down to 12m and grouted. These perimeter holes were grouted to form a “grout curtain” to limit lateral flows from outside the area to be grouted. Generally, grouting was carried out using the ascending method, grouting with pneumatic packer placed at 3m intervals.

*(iv) Grouting at Slab/ Rock Interface*

The gap between the slab and the rock was grouted with the aid of mechanical packers.

*(v) Rock Grouting*

Where fractured rock was encountered, grouting was carried out using descending method at 3m intervals, with a 24 hr time lapse between each step to allow for the grout to cure. Through closure method, groundwater inflow was eventually confined to exit from 3 holes at one

corner of the site. Water was flowing at high pressures and when confined to flow through a 140mm casing, the resultant water fountain reached 4 to 5m high (see Figure 17).



*Figure 17: Confined Water Inflow into Shaft During Grouting*

#### *(vi) Compaction Grouting*

Compaction grouting was used to treat the final 3 holes. Ready-mix Grade 30 concrete was utilized and was delivered using a grout pump primed at up to 10 bar. After delivering almost 75m<sup>3</sup> of concrete, the water flow was brought to a manageable level.

The Main Contractor decided not to completely stop water inflow due to concern of water uplift which may damage the base slab. The groundwater level rose significantly after grouting, to a level which was thought to be sustainable and not detrimental to surrounding areas. With the grouting works completed, subsequent construction works were able to proceed accordingly.

### **6.3 Grouting Beneath Rail Tracks**

The TBM had to pass about 14m beneath twin rail tracks near Chan Sow Lin Road (see Figure 18). The rock level was about 3 to 8m below ground but there were concerns that cavities and solution features in the rock may be unstable. Hence, ground treatment was implemented by the Main Contractor.

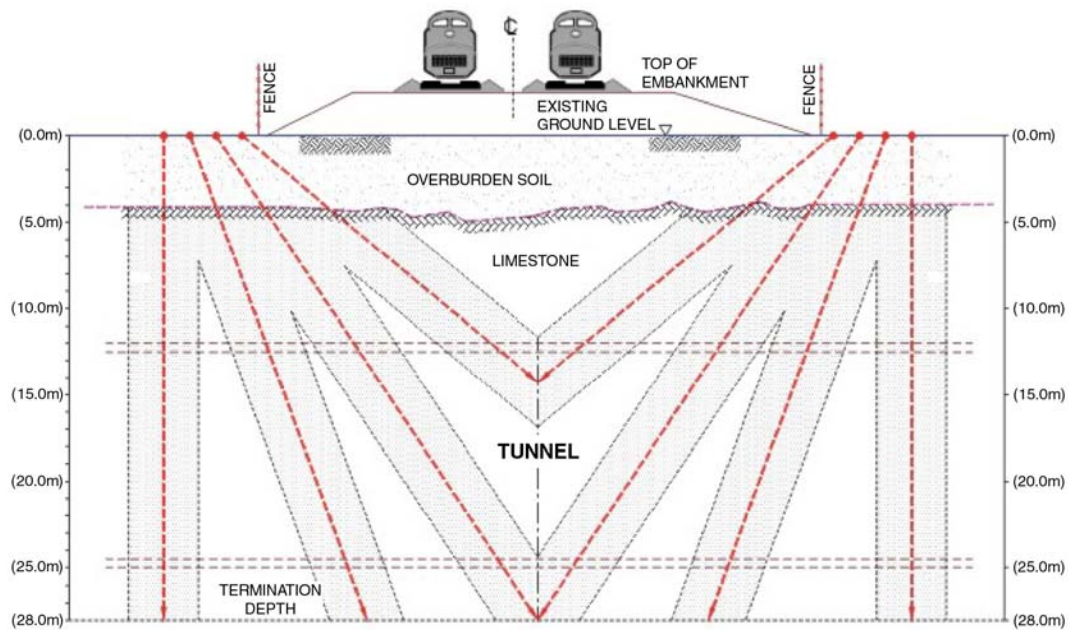


Figure 18: Schematic Section of Treatment Area

Drilling had to be done outside the security fencing beside the track and as such, almost all the holes were drilled at an incline (Figure 19). Very strict precautionary measures were implemented during the works which included continuous supervision by the train staff and settlement monitoring of the tracks. The methodology employed was briefly:

- (i) Investigative probing using continuous rotary coring to recover rock samples to understand geological conditions beneath the track.
- (ii) Perimeter holes were drilled and grouted to form a “grout curtain” to limit lateral flows from beyond the area to be grouted.
- (iii) Inclined holes at various angles were drilled and grouted to cover almost the entire footprint beneath the tracks. Grouting was carried out at relatively low pressures (2 to 5 bars) basically to fill fissures and cavities, not to compact the ground.
- (iii) The grout was allowed 1 to 2 weeks to cure before the TBM passed beneath the tracks without incident.



Figure 19 Grouting Beneath the “Live” Rail Track

## **7.0 PERSONNEL AND EQUIPMENT**

Experienced engineers from the Main Contractor were involved from the onset of the project to identify the problems and potential pitfalls ahead of TBM arrival. The Specialist Contractor aided in suggesting the techniques available to carry out the required works. It was important that engineers and technicians from both Main Contractor and Specialist Contractor worked closely together to implement the appropriate solution.

It was ensured that the correct “tools” were employed for the job. The following lists some of the equipment used on the Project:

- Drilling Rigs – equipped with computer measuring depth, rotation speed and drilling rate
- Drilling Tools – down-the-hole hammer, percussion hammer, rotary bits
- Mixing Plants – colloidal Mixer (>1400 rpm), bentonite mixer, agitator, water tank
- Grouting Plants – concrete pump, hydrostatic pump, mono pump, pneumatic & mechanical packers
- Monitoring Devices – grout flowmeter, grout density measurement devices, testing tools, survey equipment

## **8.0 SAFETY**

Many precautions were taken for working in public area which included:

- (i) Provision of safety gear for personnel such as safety helmet, harness and reflective garment
- (ii) Placement of safety barricade, lighting and warning signages
- (iii) Identification of location of buried services in the area to avoid damaging them during the works
- (iv) Monitoring of ground or property movement to ensure no sudden downward movement or excessive ground heave

## **9.0 PERFORMANCE OF GROUTING WORKS**

### **9.1 Systematic Design and Implementation**

Grouting works implemented at the SMART project have demonstrated that they can be successfully carried out provided that they are properly engineered. This would include the following steps:

- (i) understand the problem and define clearly the desired result
- (ii) apply the appropriate grouting method by using the proper equipment
- (iii) program the sequence of work systematically with constant review of findings on site
- (iv) monitor the work with the aid of experienced eye and quality control tools

### **9.2 General performance**

The “success” of the grouting program could be inferred from the following:

- (i) The heavy water inflow at the launch shaft (North Ventilation Shaft) was reduced from a high level of 120 m<sup>3</sup>/hr to a manageable level.
- (ii) Such large inflow of ground water was not observed at excavation pits at the NJB, SVS, SJB, SIE and NIE shafts, where pre-excavation grouting programs were implemented. All these shafts have been excavated without water inflow problems (Figure 20).

- (iii) The reported incidences of sinkholes and ground subsidence were uncommon in areas where grouting works were commissioned.



Figure 20: Dry Walls of Excavated Shaft

There were a few incidences of water seepage reported in certain areas where grouting was done. This is to be expected since it would be impossible to totally stop water flow given such highly variable fissured rock. Water seepage in these treated areas was mainly observed in the following situations:

- (a) excavation floor where the depth of grouting was not taken to sufficient depth or where there was design change in excavation level (deeper)
  - (b) excavation wall face where secondary grout holes were not carried out
  - (c) excavation wall where rock bolts/ anchors have been drilled through or where blasting works have had a detrimental effect
  - (d) ceiling of cross passages where grout material became dislodged during excavation
- Remedy action, in most cases, has been fairly straightforward.

## **10.0 CONCLUSION**

Like most ground improvement works, grouting works are mainly carried out by specialists and involve more than just simply drilling a hole in the ground and injecting grout slurry. The design of the treatment (e.g. spacing between grout holes, pumping pressure and appropriate mix for the given soil, etc.) needs to be given sufficient consideration. The requirements of existing standards should be adhered to, especially with regards to quality control procedures (e.g. BS\_EN12715 (2000)).

The SMART project afforded ground engineers with the unique challenge of mitigating ground disturbance associated with construction work in Limestone, using grouting technology. Experience from more than 2 years of grouting at this site has shown that the available technology is effective in minimizing water seepage and ground disturbance. It has demonstrated that the success of grouting depended on proper identification of the problem by experienced engineers and subsequent implementation of appropriate mitigating measures (using suitable type of grout, grout parameters, etc.). Proper equipment and tools have to be used and such specialised works required close supervision by experienced personnel. Since grouting works cannot be assessed visually, a strict quality control system was essential to ensure the desired end result was achieved.

## **ACKNOWLEDGEMENTS**

The authors would like to record their gratitude to Jabatan Pengairan dan Pembetungan for permission to publish this paper. The opportunity granted by the Main Contractor, MMC-Gamuda JV to work on this prestigious project is gratefully acknowledged; in particular Mr. Paramsivalingam, Mr. S.K. Ho, Cik Aswana, Mr. Koo K.S., Mr. Tioh, Mr. Gus Klados, Mr. Yeo H.K., Mr. Andrew Yeow, Dr Ooi L.H. and many others. Special thanks are afforded to Mr. Satkunaseelan and Mr. Doraisingam for sharing their knowledge in dealing with the challenging environment. The support provided by the Consultants, SSP and Mott MacDonald is also valued.

The authors wish to thank Keller's SMART Project Team, especially the Project Manager Mr. Sreenivas P. and Project Engineer, Mr. Gobiramanan. Mr. Toth, Mr. Schrader and Mr Saw H.S. also provided significant assistance. It is noted that some of the grouting works were carried out by other sub-contractors to the JV and their contributions to the understanding of the ground conditions are acknowledged.

## REFERENCES

BS 5930. Code of Practice for Site Investigations. 1999

BS EN 12715. Execution of Special Geotechnical Work – Grouting. 2000

BS EN 12716. Execution of Special Geotechnical Work – Jet Grouting. 2001

Essler, R. and Yoshida, H. Jet Grouting. Ground Improvement (2<sup>nd</sup> Edition). Edited by Moseley & Kirsch. Spon Press. 2004

Gobbett, D.J. and Hutchinson, C.S. Geology of the Malay Peninsular, New York: Wiley Interscience. 1973

Rubright, R. and Bandimere, S. Compaction Grouting. Ground Improvement (2<sup>nd</sup> Edition). Edited by Moseley & Kirsch. Spon Press. 2004

Tan S.M. Karstic Features of Kuala Lumpur Limestone. Bulletin of the Institution of Engineers, Malaysia. June 2005

## GEOSYNTHETICS – Glossary & Description

The word Geosynthetics is a generic term encompassing all the polymeric (synthetic or natural) materials used in contact with soil/rock and/or any other geotechnical material in civil engineering applications. These products are used for several purposes in civil engineering applications like reinforcement, drainage, filtration, erosion control, etc. The geosynthetics includes a broad range of products which are as follows:

- ✓ Geotextiles
- ✓ Geogrids
- ✓ Geonets
- ✓ Geomembranes
- ✓ Geofoams
- ✓ Geocomposites
- ✓ Geocells
- ✓ Geopipes
- ✓ Geotubes
- ✓ Geobar
- ✓ Geomat
- ✓ Geomesh
- ✓ Geofabric
- ✓ Geonatural
- ✓ Geostrip
- ✓ Geomatress
- ✓ Electrokinetic geosynthetic
- ✓ Geosynthetic clay liner.

### TERMINOLOGY AND DESCRIPTION of different geosynthetics:

**Geotextile** is a sheet like material made up of natural or synthetic fibres. These sheets are flexible and permeable. It has an appearance similar to a regular fabric. Classification of geotextiles based on the manufacturing process is as follows:

- *Woven geotextiles*- these are made from yarns by a conventional weaving process with a regular textile structure.
- *Non-woven geotextiles*- these are made from directionally or randomly oriented fibres in a loose web by bonding with partial melting, needle punching or chemical bonding agents like glue, rubber, latex, cellulose derivative, etc.
- *Knitted geotextiles*- these are produced by interlocking one or more yarns together.
- *Stitch-bonded geotextiles*- these are formed by the stitching together of fibres or yarns.

**Geogrids** are polymeric, mesh like planar products formed by ribs which are joined at the junction in the same plane. The opening between the longitudinal and transverse ribs are called apertures, are large enough to create interlocking with the surrounding soil particles. The ribs are linked by extrusion, bonding or interlacing.

The extruded geogrids (also called as stretched grids) are classified into two categories based on the direction of stretching during the manufacturing process.

- *Uniaxial geogrids*- these are made by stretching the punched polymer sheets in longitudinal direction, the tensile strength in the longitudinal direction is higher than in the transverse direction.
- *Biaxial geogrids*- these are made by stretching the punched polymer sheets in both the longitudinal and the transverse direction, and, therefore possess considerable strength in both the principal directions.

**Geonets** are thick planar products consisting of ribs in different direction at two different planes. The apertures are in the shape of diamond. Geonets are also termed as geospacers.

**Geomembrane** is an impermeable sheet made up of one or more synthetic materials. They are flexible in nature. Due to its extremely high impermeability properties, it is used as a fluid barrier.

**Geocomposites** are materials, which are made of two or more combinations of geosynthetics to meet advantages of both materials. Examples: Geotextile-geonet, geotextile-geogrid, prefabricated vertical drains (PVD), Geosynthetic clay liners, pavement overlays, etc.

- *Geosynthetic clay liner* is a geocomposite. In this the bentonite clay layer is sandwiched between thick non-woven geotextiles. Geotextile-encased GCLs are stitched or needle punched through the bentonite core to give higher shear resistance. When hydrated they are effective as a barrier. Often used in conjunction with geomembranes.
- *Prefabricated vertical drains* are made of corrugated plastic sheets surrounded by geotextile filters used as a drain in soft clays to accelerate the consolidation process.

**Geocell** is a three dimensional honeycombed structure formed by joining the polymeric sheet strips in a cellular manner. The geocells can be collapsed like an accordion during transport and stretched during the installation. The pockets of the geocells are filled with granular materials to form a semi-rigid base to support load bearing elements like flexible roads, container yards, etc. The geocells help in spreading the applied loads over a large area and provide excellent support even under cyclic loads.

**Geopipes** are perforated or solid-wall polymeric pipes placed beneath the ground surface and backfilled.

**Geofoam** are low density network of closed, gas filled cells made by expansion of polystyrene foam.

**Geotube** is a geotextile fabric with an oval cross section filled with sediment used for shoreline protection and dewatering process.

**Geobar** is a polymeric material in the form of bar.

**Geoblanket** is a permeable blanket which is biodegradable in nature. It is used in slopes where vegetation is possible thereby protecting the slopes.

**Electrokinetic geosynthetic** is a mesh made from a metal wire stringer coated in a conductive polymer; it resembles a reinforcing geomesh, and is available also in the form of sheets, strips or tubes. In addition to electrical conduction it also provides drainage, filtration, and reinforcement functions.

**Geomat** is a three dimensional, polymeric structured made of bonded filaments which are permeable. Used as reinforcement to roots of grass and small plants which provides in turn permanent erosion control.

**Geomatress** is a three dimensional, permeable geosynthetic structure which is filled with soil or concrete after placing over a soil layer to prevent erosion.

**Geostrip** is a strip of polymeric material.

## FUNCTIONS AND APPLICATIONS

Basic functions of Geosynthetics are,

- ✓ **Barrier** - some of the Geosynthetics are impermeable in nature thus it acts as a barrier to fluids or gases. For example, geomembrane, geosynthetic clay liner, thin film geotextile composites and field coated geotextiles are used as fluid barrier to restrict flow of liquids or gases. This function is also used in encapsulation of swelling soils, asphalt pavement overlays and waste containment.
- ✓ **Drainage**-some geosynthetics allow in plane flow of fluid which serves the function as drains. For example Prefabricated vertical drains (PVDs) have been used to accelerate the rate of consolidation of soft clays under foundations. Due to this function geosynthetics are used as pavement edge drains, slope interceptor drains, and abutment and retaining wall drains.
- ✓ **Surficial erosion control**- soil erosion caused by rainfall and runoff on slopes are reduced by providing either temporary geosynthetics or permanent light weight geomat.
- ✓ **Filtration** – geosynthetics allow only fluids to pass across them this function helps in filtration. For example geotextiles prevents migration of soil particles in drains.
- ✓ **Protection**- geosynthetic is used as a localised stress reduction layer to prevent damage to a given surface or layer this termed as protection function.
- ✓ **Reinforcement** – the major function of geosynthetics is to increase the strength of soil mass by its inclusion and thus it maintains the stability of soil mass, which is called reinforcement. As a reinforcement geosynthetics takes the tensile load. Geosynthetics as reinforcement enables the embankments to be constructed over the soft clays and to build embankment with steeper slopes.
- ✓ **Separation** -The geosynthetic are used to separate two layers of soil that have different particle size distributions. For example, geotextiles are used to prevent road base materials from penetrating into soft underlying soft subgrade soils, thus maintaining design thickness and roadway integrity. Separators also help to prevent fine grained subgrade soils from being pumped into permeable granular road bases.

Table 1: Functions served by different geosynthetics

Type of geosynthetic	Functions served by the geosynthetic						
	<i>Barrier</i>	<i>Drainage</i>	<i>Erosion control</i>	<i>Filtration</i>	<i>Protection</i>	<i>Reinforcement</i>	<i>Separation</i>
Woven Geotextile				√		√	√
Non-woven Geotextile		√		√	√	√	√
Geogrid						√	
Geonet		√	√				
Geomembrane	√						
Geocell			√			√	
Geocomposite	√	√	√	√	√	√	√
Geopipes		√					
Geofoam		√			√		

**Some Common Types of polymers used for geosynthetics**

Polyethylene (PE) – used for manufacture of geotextiles, geomembranes, geogrids, geopipe, geonets, geocomposites

Polyvinyl chloride (PVC) – geomembranes, geopipes, geocomposites

Polyester (PET) – Geotextiles & geogrids

Polypropylene (PP) – geotextiles, geomembranes, geogrids, geocomposites

Polystyrene (PS) – geocomposites, geofoam

**Standard Graphical Illustrations for Different Geosynthetics:**

NAME	SYMBOL	GRAPHICAL REPRESENTATION
Geotextile	GTX	-----
Geomembrane	GMB	=====
Geobar	GBA	#####
Geoblanket	GBL	~ ~ ~ ~ ~
Geocomposite drain with geotextile on both sides	GCD	~ ~ ~ ~ ~
Geocell	GCE	
Geocomposite clay liner	GCL	~~~~~
Surficial geosynthetic erosion control	GEC	#####
Electro-kinetic geosynthetic	GEK	#####
Geogrid	GGR	—●—●—●—●—●—●—
Geomat	GMA	~~~~~
Geomattress	GMT	=====
Geonet	GNT	XXXXXXXXXXXXXXXXXXXX
Geospacer	GSP	□□□□□
Geostrip	GST	—●—●—●—●—●—●—

# DESIGN MONOGRAPH FOR DESIGN OF SHALLOW FOUNDATION WITH GEOSYNTHETICS

By

Satyendra Mittal,

Department of Civil Engineering, IIT Roorkee, Email: [satyendramittal@gmail.com](mailto:satyendramittal@gmail.com)

## 1. INTRODUCTION

Foundation is the integral part of any superstructure. Foundations are required to be dependable, intact, firm and sound. Two types of foundations are well known that is shallow foundations and deep foundation. Sometimes shallow foundations have to be provided due to site constrains, limited budgets etc. Size of shallow foundation has to be in commensurate to the loads of the superstructure. There may be such situations where it may be difficult to provide that much space on ground as per design loads. The reason could be the neighbors' property, some water body, historical monuments etc. In such cases, if the size of foundation can be restrained suiting to site conditions but its bearing capacity be increased by use of reinforced element, the purpose gets solved. These days many reinforcing material made of polymers, textiles are available which have made the foundation designs quite innovative, economical and effective. The construction of shallow footings supported on geosynthetic reinforced foundation soils has considerable potential as a cost-effective alternative to conventional deep foundations. In this technique, one or more layers of geosynthetic reinforcement (geotextile, geogrid, geocell or geocomposite) are placed inside a controlled granular fill beneath the footings, to create a composite material with improved performance characteristics. The geosynthetic-reinforced foundation soils provide improved bearing capacity and reduced settlements by distributing the imposed loads over a wider area of weak subsoil. In the conventional construction techniques without the use of any reinforcement, a thick granular layer is needed which may be costly or may not be possible, especially in the sites that have a limited availability of good-quality granular materials. Moreover, the simplicity of the basic principles and the economic benefits over the conventional approaches make the geosynthetic-reinforced foundation soil very attractive to the designers.

Geosynthetics is a generic term for all synthetic materials used in conjunction with soil, rock and/or any other civil-engineering-related material as an integral part of a man-made project, structure or system. A geosynthetic shows its reinforcement function by increasing the strength of a soil mass as a result of its inclusion, thus it maintains the stability of the soil mass. It includes a broad range of synthetic products; the most common ones, used for reinforcement are:

- Geotextiles
- Geogrids
- Geocells

These products are almost exclusively polymeric, and those based on natural fibres (jute, cotton, wool, silk, etc.) are generally not included.

## **2. GEOSYNTHETICS PRODUCTS USED FOR REINFORCEMENT**

Following are popular geosynthetics products:

**2.1 Geotextiles** are permeable, polymeric textile products in the form of flexible sheets.

Currently available geotextiles are classified into the following categories based on the manufacturing process:

- **Woven geotextiles** - They are made from yarns (made of one or several fibers) by conventional weaving process with regular textile structure.
- **Non-woven geotextiles** - They are made from directionally or randomly oriented fibres into a loose web by bonding with partial melting, needle punching or chemical binding agents (glue, rubber, latex, cellulose derivative, etc.).
- **Knitted geotextiles** - They are produced by interlooping one or more yarns together.
- **Stitch-bonded geotextiles** - They are formed by the stitching together of fibres or yarns.

**2.2 Geogrid** is a polymeric, mesh-like planar product formed by intersecting elements, called ribs, joined at the junctions. The ribs can be linked by extrusion, bonding or interlacing, and the resulting geogrids are called extruded geogrid, bonded geogrid and woven geogrid,

respectively. Extruded geogrids are classified into the following two categories based on the direction of stretching during their manufacture:

- **Uniaxial geogrids** - They are made by the longitudinal stretching of regularly punched polymer sheets and, therefore, possess a much higher tensile strength in the longitudinal direction than in the transverse direction.
- **Biaxial geogrids** - They are made by both the longitudinal and the transverse stretching of regularly punched polymer sheets and, therefore, possess equal tensile strength in both the longitudinal and the transverse directions.

**2.3 Geocell** is a three-dimensional honeycomb-like cellular confinement system, which acts as a foundation reinforcement mat for improvement of load bearing capacities of weak soils and as an erosion control barrier for unstable slope surfaces.

### **3. SOIL-GEOSYNTHETIC INTERACTION MECHANISMS**

Soil- geosynthetic interaction is of the utmost importance in several applications of geosynthetics, especially when they act as soil reinforcement. Soil reinforcement consists of the placement of elements duly oriented in the soil, which, by their character, improve the mechanical properties of the new material (reinforced soil) when compared with that of the unreinforced soil. The main target of reinforcement is to inhibit the development of tensile strains in the soil and, consequently, to support the tensile stresses that the soil cannot withstand. The tensile stress imparted by reinforcement improves the soil mechanical properties by reducing the shear stress that has to be carried by the soil and by increasing its available shearing resistance, as the normal stress acting on potential shear surfaces increases. The effectiveness of reinforcement depends on its alignment, it being most effective when aligned in a direction of tensile strain in the soil, so that tensile reinforcement stress develops (McGown et al., 1978; Jewell and Wroth, 1987; Jewell, 1996). The behavior of the reinforced soil depends on several factors, such as:

- Soil and reinforcement mechanical characteristics
- Soil-reinforcement interaction mechanism and properties

- Geometry of the reinforced system
- Shape, number, location and alignment of reinforcements
- Process of construction, etc.

Three mechanisms of interaction can be identified in reinforced systems:

- Skin friction along the reinforcement
- Soil-soil friction
- Passive thrust on the bearing members of the reinforcement.

Skin friction is the only mechanism with geotextiles and strips. In the case of geogrids, the passive thrust on the bearing members of the grids must also be considered as soil-soil friction, if relative movement occurs in the soil along the grids' apertures. Shear strength mobilization between granular soils and geotextiles is a two-dimensional phenomenon, where soil dilatance is allowed, strongly affected by the extensibility of geotextiles. In the case of strips, the phenomenon is three-dimensional and greatly dependent on the characteristics of soil dilatance and on the roughness of the reinforcement surfaces. In fact, the volume of soil shearing around the reinforcement is influenced by its geometry and roughness. With regard to geogrids, the phenomenon can also be considered three-dimensional, mobilizing skin friction for small displacements and progressively mobilizing the passive thrust on the bearing members of the grid as displacement increases. Figure 1 shows the stress distribution in the cases of free soil dilatance (two-dimensional phenomenon) and restricted soil dilatance (three dimensional phenomenon).

Since geogrids are less extensible than geotextiles, the improvement in soil strength and the mobilization of shear resistance along the interface with the soil increase when the reinforcement used is a geogrid.

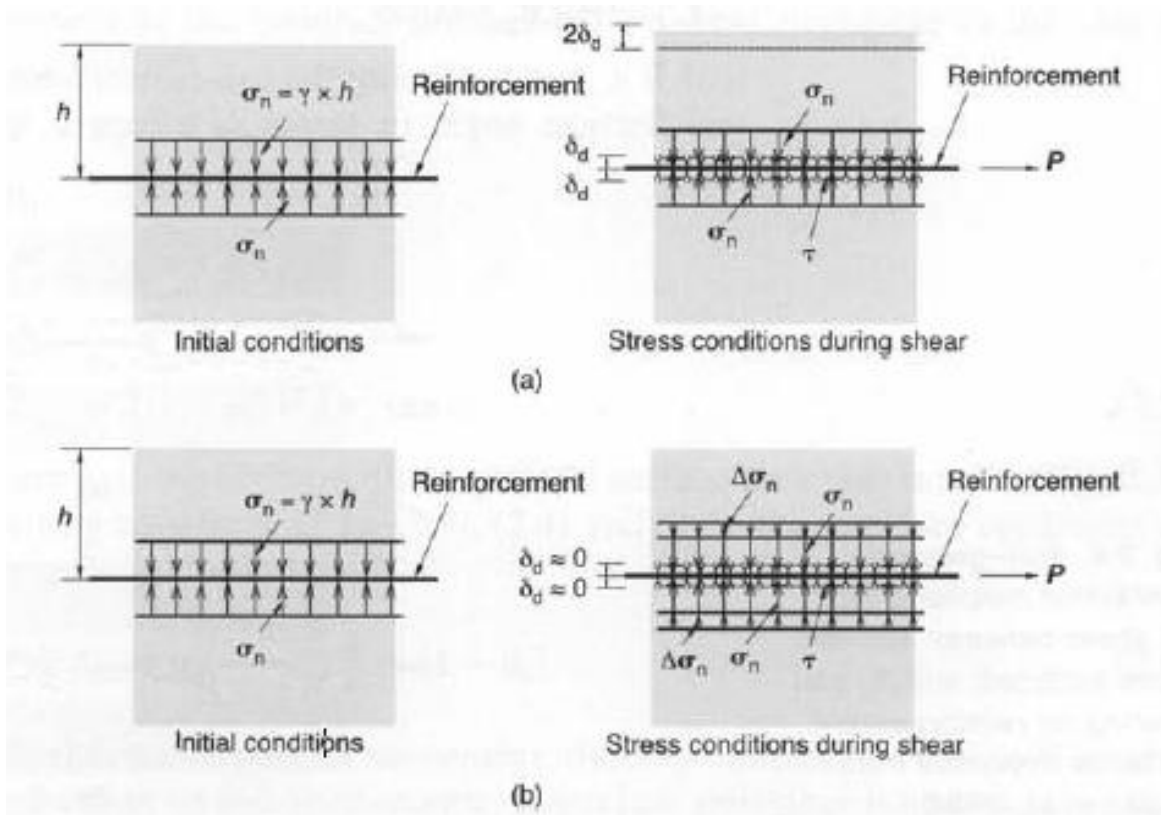


Fig. 1 Stress conditions in reinforced soil: (a) free dilatance; and (b) restricted dilatance  
(after Hayashi et al., 1994)

The geosynthetics, in conjunction with foundation soils, may be considered to have five different roles in improving their load-carrying capacity and settlement characteristics.

(a) Geosynthetics reduce the outward shear stresses transmitted from the overlying soil/fill to the top of the underlying foundation soil. This action of geosynthetics is known as the shear stress reduction effect. This effect results in a general-shear failure, rather than a local-shear failure (Fig. 2a), thereby causing an increase in the load-bearing capacity of the foundation soil (Bourdeau et al. , 1982; Guido et al., 1985; Love et al. , 1987; Espinoza, 1994; Espinoza and Bray, 1995; Adams and Collin, 1997). The reduction in shear stress and the change in the failure mechanism is the primary benefit of the geosynthetic layer at small deformations.

(b) Geosynthetic redistributes the applied surface load by providing restraint of the granular fill if embedded in it, or by providing restraint of the granular fill and the soft foundation soil if

placed at their interface, resulting in reduction of applied stress (Fig. 2b). This is referred to as the slab effect or confinement effect of geosynthetics (Bourdeau et al., 1982; Giroud et al. , 1984; Madhav and Poorooshasb, 1989; Sellmeijer, 1990; Hausmann, 1990). The friction mobilized between the soil and the geosynthetic layer plays an important role in confining the soil.

(c) The deformed geosynthetic, sustaining normal and shear stresses, has a membrane force with a vertical component that resists applied loads, i.e. deformed geosynthetics provide a vertical support to the overlying soil mass subjected to loading. This action of geosynthetics is popularly known as its membrane effect (Fig. 2c) (Giroud and Noiray, 1981; Bourdeau et al. , 1982; Sellmeijer et al. , 1982; Love et al. , 1987; Madhav and Poorooshasb, 1988; Bourdeau, 1989; Sellmeijer, 1990; Shukla and Chandra, 1994a). Depending on the type of stresses - normal stress and shear stress - sustained by the geosynthetics during their action, the membrane support may be classified as 'normal stress membrane support' and 'interfacial shear stress membrane support', respectively (Espinoza and Bray, 1995). Edges of the geosynthetic layer need to be anchored in order to develop the membrane support contribution that results from normal stresses, whereas the membrane support contribution resulting from mobilized interfacial membrane shear stresses does not require any anchorage. The membrane effect of geosynthetics causes an increase in the load-bearing capacity of the foundation soil below the loaded area, with a downward loading on its surface either side of the loaded area, thus reducing its heave potential. It is to be noted that both the geotextile and geogrid can be effective in membrane action in case of high deformation of the reinforced foundation soils (Hass et al., 1988).

(d) The use of geogrids has another benefit due to the interlocking of the soil through the apertures of the grid, which is known as the anchoring effect (Guido et al., 1986). The transfer of stress from the soil to the geogrid reinforcement is made through bearing at the soil to the grid cross-bar interface.

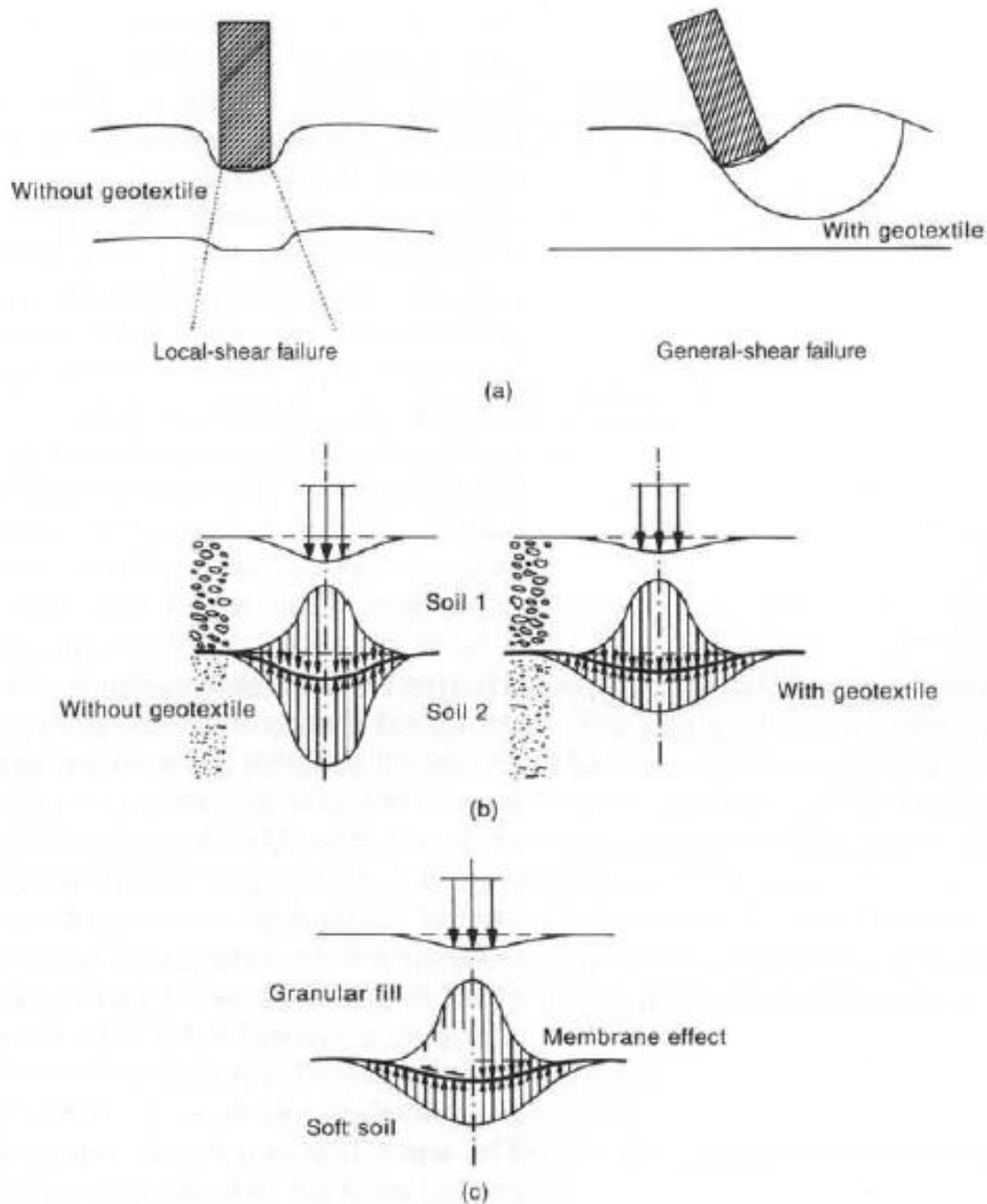


Fig. 2 Influence of geotextile inclusion on a two-layer soil system: (a) change of failure mode; (b) redistribution of the applied surface load; and (c) membrane effect (after Bourdeau et al., 1982; Espinoza, 1994)

(e) Geosynthetics (particularly, geotextiles, but perhaps also geogrids) improve the performance of the reinforced soil system by acting as a separator between the soft foundation soil and the

granular fill. This influence is known as the separation effect of geosynthetics (Guido et al., 1986; Nishida and Nishigata, 1994). The separation can be an important function compared to the above functions (which may collectively be called the reinforcement function) when the ratio of the applied stress ( $\sigma$ ) on the subgrade soil to the shear strength ( $c_u$ ) of the subgrade soil has a low value (less than 8), and it is basically independent of the settlement of the reinforced soil system (Fig. 3).

In general, the improved performance of a geosynthetic-reinforced foundation soil can be attributed to an increase in shear strength of the foundation soil from the inclusion of the geosynthetic layer. The soil geosynthetic system forms a composite material that inhibits development of the soil-failure wedge beneath shallow spread footings .

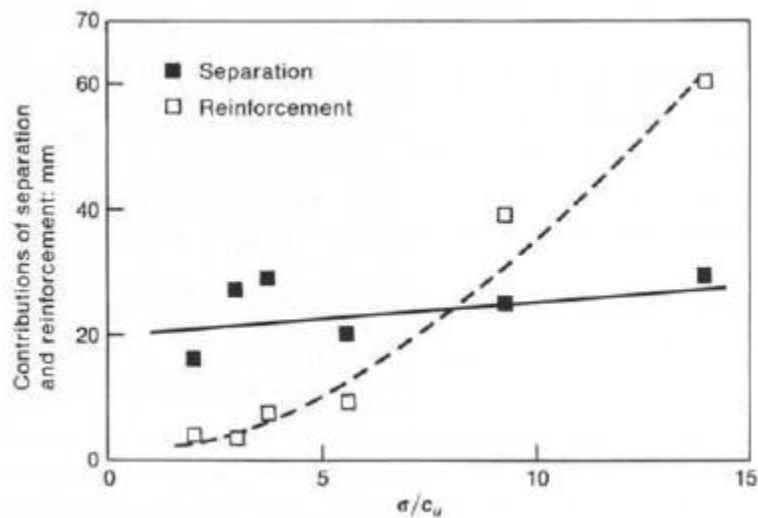


Fig. 3 Relationship between the separation and the reinforcement functions (after Nishida and Nishigata , 1994)

#### 4. MODES OF FAILURE

There are four possible modes of failure for geosynthetic-reinforced shallow foundations. They are as follows.

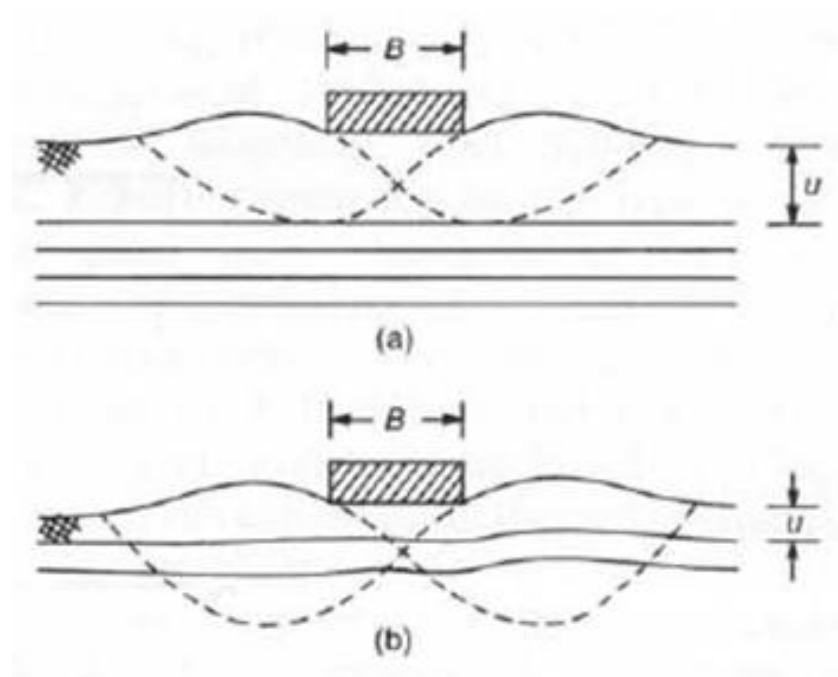
(a) Bearing capacity failure of soil above the uppermost geosynthetic layer (Fig. 4a) - this type of failure is likely to occur if the depth of the uppermost layer of reinforcement ( $u$ ) is greater than about  $2/3$  of the width of the footing ( $B$ ), i.e.  $u/B > 0.67$ , and if the reinforcement concentration in this layer is sufficiently large to form an effective lower boundary into which the shear zone

will not penetrate. This class of bearing-capacity problem corresponds to the bearing capacity of a footing on shallow soil overlying a strong rigid boundary.

(b) Pullout of geosynthetic layer (Fig. 4b) - this type of failure is likely to occur for a shallow and light reinforcement ( $u/B < 0.67$ , and the number of reinforcement layers,  $N < 3$ ).

(c) Breaking of geosynthetic layer (Fig. 4c) - this type of failure is likely to occur with long, shallow and heavy reinforcement ( $u/B < 0.67$ ,  $N > 3$  or 4). The reinforcement layers always break approximately under the edge or towards the centre of the footing. The uppermost layer is most likely to break first, followed by the next deep layer, and so forth.

(d) Creep failure of the geosynthetic layer (Fig. 4d) - this failure may occur due to long-term settlement caused by sustained surface loads and subsequent geosynthetic stress relaxation. The first three modes of failure were first reported by Binquet and Lee (1975a, 1975b) on the basis of the observations made during laboratory model tests (on a footing resting on a sand layer reinforced by metallic reinforcements). The fourth mode of failure, i.e. creep failure, was explained by Koerner (1990).



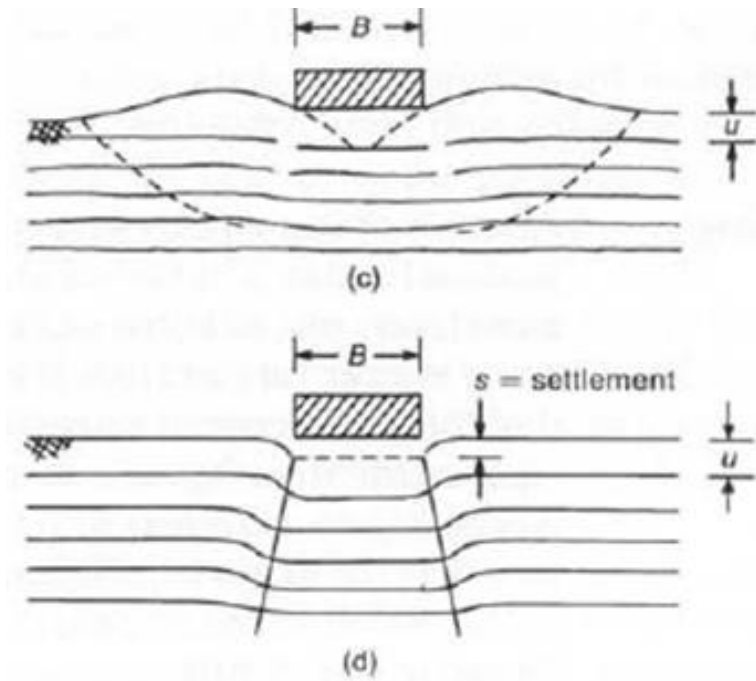


Fig. 4 Possible modes of failure of geosynthetic reinforced shallow foundations (after Binquet and Lee, 1975b; Koerner, 1990)

## 5. STATE OF ART IN BRIEF

A large number of model tests have been conducted in order to evaluate the beneficial effects of reinforcing the soils with geosynthetics, as related to the load-carrying capacity and the settlement characteristics of shallow foundations .

### 5.1 Reinforced granular soil

Guido *et al.* (1985) conducted laboratory model tests to study the bearing capacity of a square footing (side  $B = 0.31$  m) resting on loose sand (relative density = 50%) reinforced with geotextiles of strength varying from 0.67 to 2.16 kN/m. The tests were performed in a square stiffened plexiglass box of dimensions shown in Fig. 5(a). The square sheets of

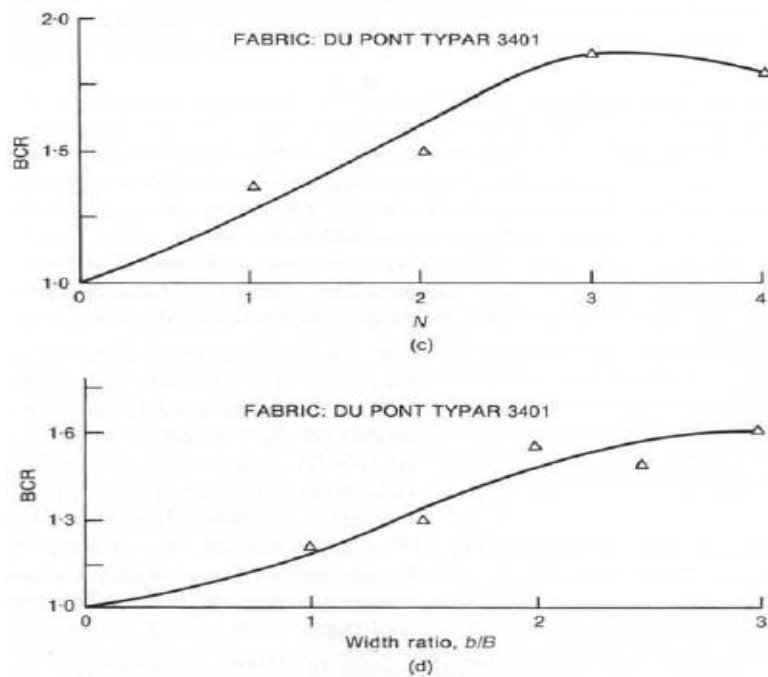
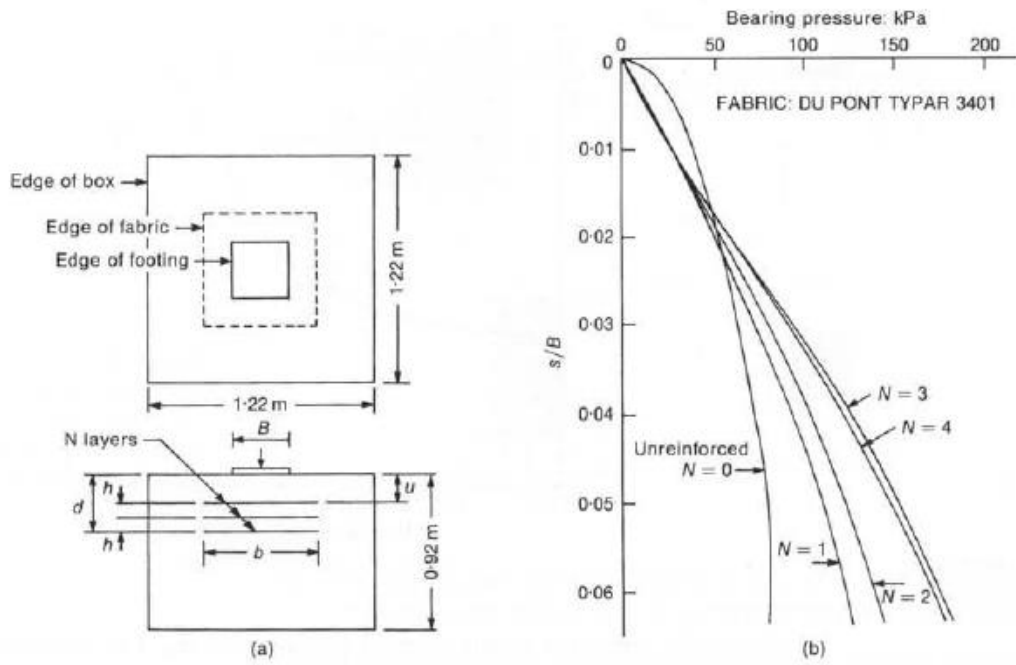


Fig. 5 (a) Geometry of model; (b) load-settlement curves ( $u/B = 0.5$ ,  $h/B = 0.25$ ,  $b/B = 2$ ); (c) BGR variation with  $N$  ( $u/B = 0.5$ ,  $h/B = 0.25$ ,  $b/B = 2$ ); (d) BGR variation with width ratio ( $u/B = 0.5$ ,  $h/B = 0.25$ ,  $N = 2$ ); and (e) BGR variation with tensile strength ( $u/B = 0.5$ ,  $h/B = 0.25$ ,  $b/B = 3$ ) (after Guido et al., 1985)

geotextile were placed concentrically under the square footing. For these tests, several parameters were varied -- the depth below the footing of the first layer of geotextile,  $u$ ; the

vertical spacing of the layer of geotextile,  $h$ ; the number of layers of geotextile,  $N$ ; the width of the square sheet of geotextile,  $b$ ; and the tensile strength of geotextile. For convenience in expressing and comparing test data, the results were presented in terms of a bearing capacity ratio (BCR), a term introduced by Binqet and Lee (I 975a). This term is defined as follows:

$$\text{BCR} = \frac{q_R}{q_u}$$

where  $q_u$  is the ultimate bearing capacity of the unreinforced soil, and  $q_R$  is the bearing capacity of the geotextile reinforced soil at a settlement corresponding to the settlement  $S_u$  at the ultimate bearing capacity  $q_u$  for the unreinforced soil.

Based on the test results, the following generalized conclusions can be made.

- (a) All the parameters stated above have a substantial effect on the load-bearing capacity of the geotextile-reinforced foundation.
- (b) When the geotextile layers are placed within a depth equal to the width of the foundation, they increase the load bearing capacity of the foundation - but only after a measurable settlement has occurred.
- (c) The presence of the geotextile layers changes the failure mode from one of local shear to one of general shear. The trends of variation for BCR have been reported to be independent of the soil type.

Small-scale laboratory model test results for the ultimate bearing capacity of strip and square footings supported by sand reinforced with geogrid layers, as shown in Fig. 6, have been presented by Omar et al. (1993). The general conclusions from the test observations are as follows.

- (a) For development of maximum bearing capacity ratio ( $\text{BCR}_{\text{max}}$ ), the effective depth of geogrid layer  $z$  is about  $2B$  for strip footings and  $1.4B$  for square footings .
- (b) The maximum width of geogrid layers  $b_{\text{max}}$  required for mobilization of maximum bearing capacity ratio is about  $8B$  for strip footings and  $4.5B$  for square footings .
- (c) The maximum depth of placement  $u_{\text{max}}$  of the first layer of geogrid should be less than about  $B$  for the geogrid to be effective.

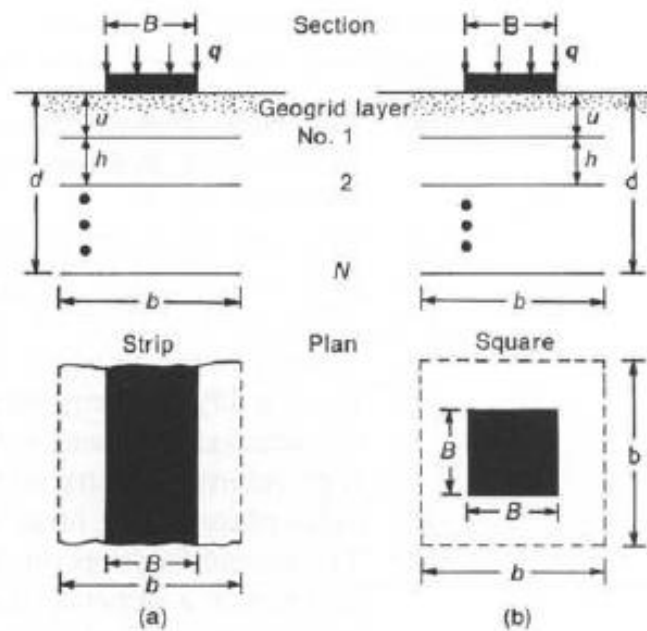


Fig. 6 Strip and square footings supported by sand reinforced with layers of geogrid ( $q =$  load per unit area) (after Omar et al., 1993)

Yetimoglu et al. (1994) investigated the bearing capacity of rectangular footings on geogrid-reinforced sand by performing laboratory model tests. From the test results, the following generalized conclusions can be drawn.

(a) The bearing capacity of rectangular footings can be increased significantly by incorporating geogrid layers at strategic elevations in the foundation soil. However, the settlement at failure may not be affected significantly by the geogrid layer.

(b) For single-layer reinforced sand, the optimum embedment depth (the depth of the reinforcement layer at which the bearing capacity is highest) is approximately  $0.3$  times the footing width  $B$ . For multi-layer reinforced sand, the highest bearing capacity occurs at an embedment depth (for the first layer of reinforcement) of approximately  $0.25B$ . The optimum vertical spacing of the reinforcement layer is between  $0.2B$  and  $0.4B$ .

(c) The bearing capacity of reinforced sand increases significantly with the size of the geogrid reinforcement and the number of reinforcement layers within a certain effective zone. The extent of the effective zone lies approximately within  $1.5B$  from both the base and edges of the footing.

Ju et al. (1996) performed a series of bearing capacity tests on reinforced sand with strip footings. The sand was reinforced with a geonet of relatively weak tensile strength. The types of reinforcement used were one layer, multi-layer, and mattress. Of the three reinforcing methods, the greatest ultimate bearing capacity was obtained from the multilayer type, the optimum layer number was 4, and the ultimate bearing capacity ratio was 3.65.

A total of 34 large model load tests were conducted by Adams and Collin (1997) in order to evaluate the potential benefits of reinforcing the sand with geosynthetic layers below the shallow spread footings. The tests were performed in a reinforced concrete box 5.4 m wide by 6.9 m long by 6 m deep. One to three layers of the geogrid reinforcement, or one layer of geocell, were placed beneath the 0.30, 0.46, 0.61 and 0.91 m square footings. The depth of the reinforcement layers varied between 0.25 and 1.5 m. In the tests, precast, steel reinforced, concrete footings were loaded with a hydraulic ram jacked against a reaction frame. The generalized conclusions from the tests are as follows.

(a) The use of geosynthetic-reinforced soil foundations may increase the ultimate bearing capacity of shallow spread footings by a factor of 2.5.

(b) The maximum improvement in bearing capacity at low strains ( $s/B = 0.5\%$ ;  $s$  is settlement, and  $B$  is footing width) occurs when the top layer of reinforcement is within a depth of  $0.25B$  from the bottom of the footing.

(c) For one layer of reinforcement, improvement in the bearing capacity occurs if the sand within the reinforced zone is compacted to a high relative density so that stress transfer to the reinforcement takes place before large soil strains occur.

(d) The spread footings on the reinforced soil foundation are likely to experience a general-shear plunging failure, if the first layer of reinforcement is placed  $0.4 B$  beneath the base of the footing.

Small-scale laboratory model test results of the ultimate bearing capacity of a strip footing supported by sand reinforced with multiple layers of geogrid were presented by Shin and Das (2000). The tests were conducted with one type of sand compacted at two relative densities and only one type of geogrid. The foundation depth was varied from zero to  $0.75B$  ( $B$  is the footing width). The test results indicated that the  $BCR$  value determined from the surface footing tests

would provide conservative estimates of the ultimate bearing capacity for footings at depths greater than zero.

## 5.2 Reinforced clay

One of the possibilities for increasing the ultimate bearing capacity of a shallow footing supported by a saturated clay foundation under undrained conditions is by reinforcing it by means of geosynthetic layers. Ingold and Miller (1982) reported model test results conducted on geogrid-reinforced clay. The apparatus consisted of a rigid steel box 150mm wide, 150mm deep and 710 mm long, in which the clay was, loaded under undrained plane strain conditions using a rigid strip footing 50 mm wide. Figure 7 shows some model footing test results. It is noted from Fig. 7(a) that the bearing capacity ratio, in general, increases with the number of reinforcing layers ( $N$ ); however, at low settlement ratios (namely  $s/B = 5\%$ ;  $s$  is the footing settlement,  $B$  is the width of footing) and for a number of reinforcement layers less than 5, the reinforcement appears to weaken the foundation as indicated by bearing capacity ratios less than unity. This tendency is repeated in Fig. 7(b), which shows that BCR is  $< 1$  for depth ratio,  $u/B > 0.65$  ( $u$  is the the depth below the footing to the top of the reinforcement layer), and settlement ratio  $s/B = 5\%$ .

Sakti and Das (1987) reported some model test results on the bearing capacity of a strip footing on saturated clay. They used a heat-bonded non-woven geotextile as reinforcement. From their tests, the following general conclusions can be drawn.

- (a) Beneficial effects of geotextile reinforcement are realized when reinforcement is placed within a depth equal to the width of the footing.
- (b) For maximum benefit, the first layer of geotextile should be placed at a depth of about 0.35 times the width of the footing.

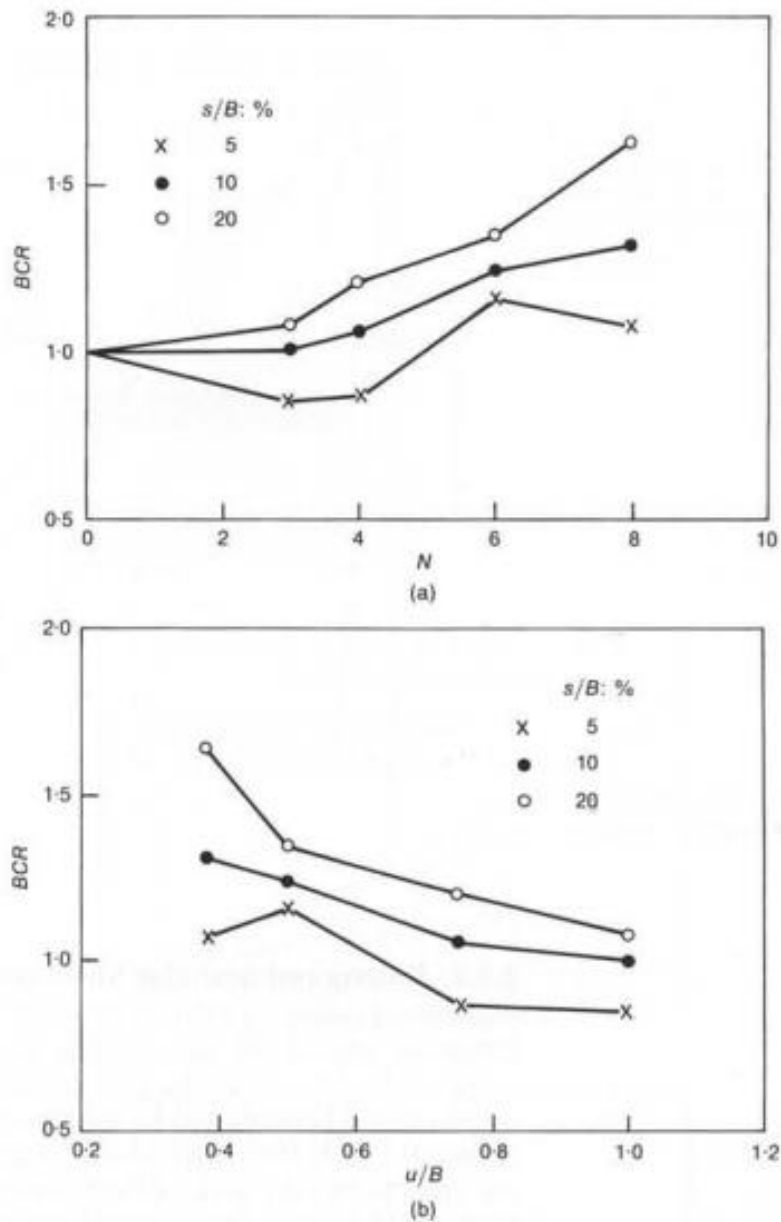


Fig. 7 Model footing test results: (a) BCR versus  $N$ ; and (b) BCR versus  $u/B$  (after Ingold and Miller, 1982)

(c) The minimum length of the reinforcing geotextile layer for maximum benefit is about four times the width of the footing.

(d) Geotextile reinforcements do not have much influence on the foundation settlement at ultimate load.

Koerner (1990) reported the results of model tests conducted at Drexel University's Geosynthetic Research Institute. The loading tests were carried out on 6 inch round footings resting on soft

saturated clay silt, at saturation above the plastic limit and reinforced with woven slit-film geotextile layers at 1.5 in. spacings (Fig. 8). Some improvement in the load-bearing capacity is noted throughout, but the improvement is noteworthy only at large deformations.

Bearing capacity tests on model footings resting on clay subgrades reinforced with horizontal layers of geogrids were conducted by Mandal and Sah (1992). The test results show that the geogrid reinforcement increases the bearing capacity of subgrades, with improvements being observed at nearly all levels of deformation. The maximum percentage reduction in settlement with the use of geogrid reinforcement below the compacted and saturated clay is about 45% and it occurs for the geogrid layer at a depth of  $0.25B$  ( $B$  is the footing width) from the base of the square foundation.

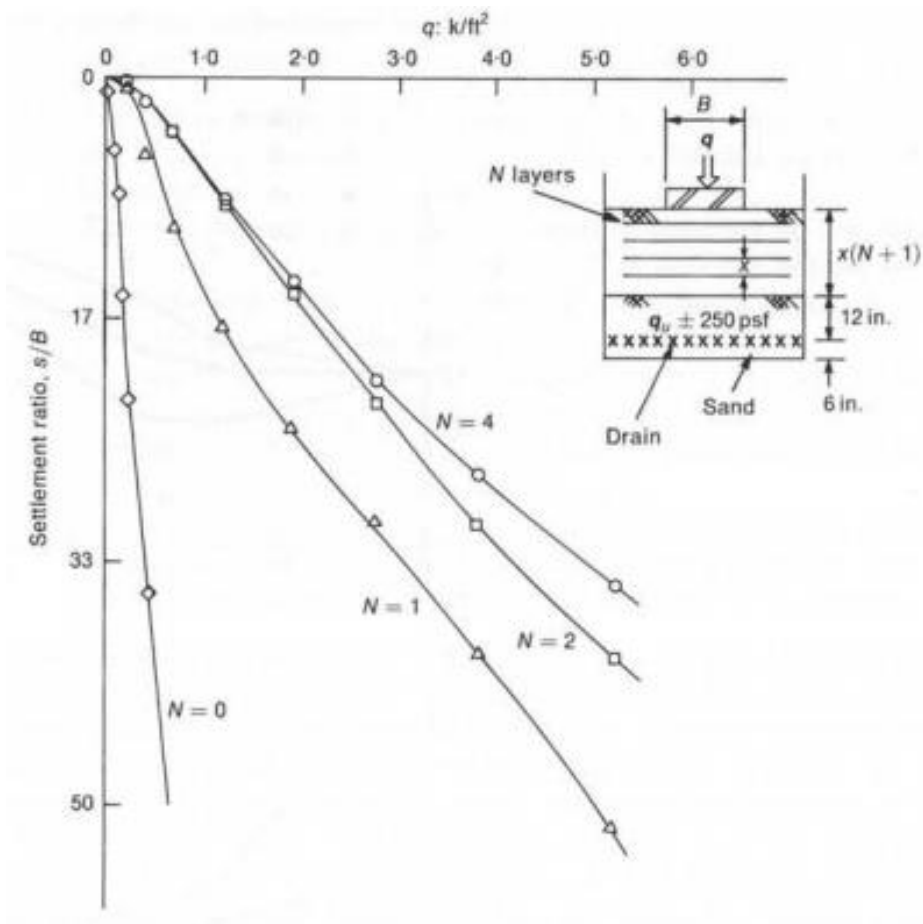


Fig. 8 Model footing test results (after Koerner, 1990)

## 6. DESIGN METHODOLOGY

### 6.1 Reinforced Granular fill

Binquet and Lee (1975a; 1975b) performed a pioneering study on the load-bearing capacity of footings resting on sandy ground reinforced with aluminium foil strips, and proposed a design method based on an assumed failure mechanism as shown in Fig. 9. According to this mechanism, the tensile force, developed in the vertically bending part of the reinforcement across the assumed shear band, increases the bearing capacity of the reinforced sandy ground. When the length of the reinforcement is short, e.g. equal to the width of footing (B), as shown in Fig. 10 (Huang and Tatsuoka, 1990), the model proposed by Binquet and Lee (1975b) is invalid. Schlosser et al. (1983) proposed a failure mechanism, shown in Fig. 11, for the reinforced ground. Based on this failure mechanism, the bearing capacity of a strip footing resting on reinforced ground can be expressed as:

$$q_{u(\text{reinforced})} = \gamma \times D_R \times N_q S_q d_q + 0.5(B + \Delta B) \times \gamma \times N_f \times S_f \quad \dots(1)$$

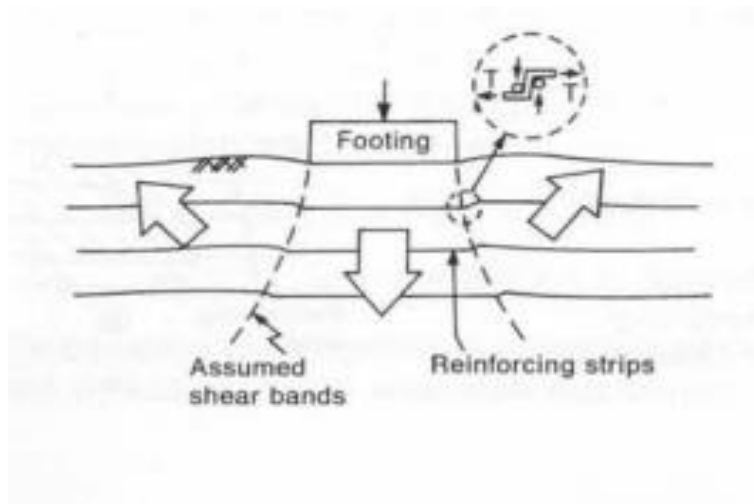


Fig. 9 Failure mechanism for reinforced sandy ground assumed by Binquet and Lee (1975b)

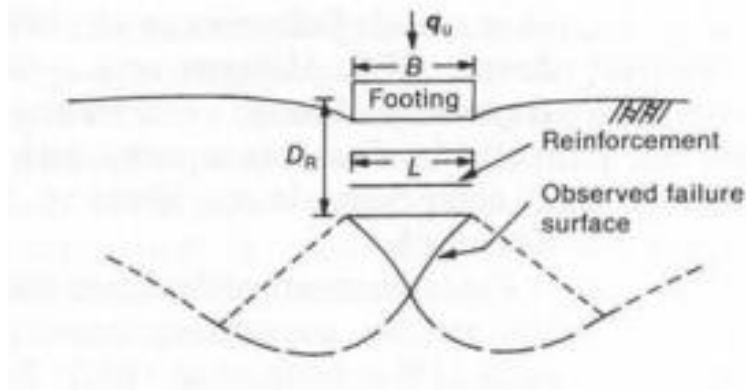


Fig. 10 Failure surface observed by Huang and Tatsuoka (1988; 1990)

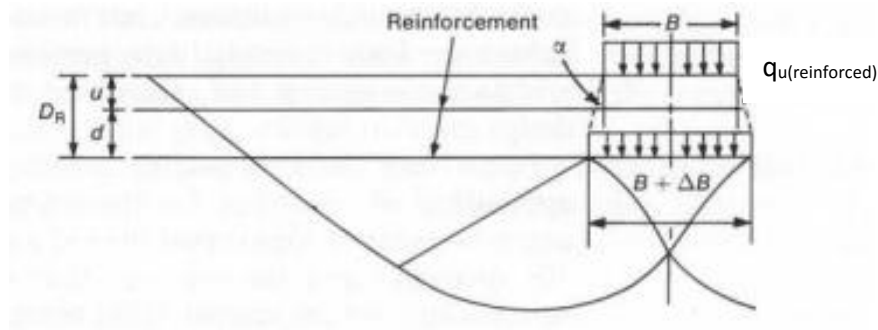


Fig. 11 Failure mechanism of reinforced ground proposed by Schlosser et al. (1983)

where  $q_{u(\text{reinforced})}$  is the ultimate bearing capacity of footing resting on reinforced ground,  $\gamma$  is the unit weight of sand,  $N_q$ ,  $N_y$  are bearing capacity factors,  $D_R$  is the depth of the reinforced zone from the ground surface,  $s_q, s_y$  are shape factors,  $d_q$  is the depth factor,  $B$  is the width of surface footing,  $\Delta B$  is the increase of footing width at the depth of  $D_R$  due to the wide slab effect expressed by  $2D_R \tan \alpha$ , and  $\alpha$  is the load-spreading angle as described in Fig. 11. According to equation (1), the following two mechanisms account for the increase in the bearing capacity of footings resting on densely reinforced sandy ground:

- deep-footing mechanism
- wide-slab mechanism.

The deep-footing mechanism is applicable when a quasi-rigid zone is developed beneath the footing (Huang and Tatsuoka, 1988; 1990). The wide-slab mechanism is applicable only when a quasi-rigid earth slab below the footing extends beyond the width of the footing. For densely reinforced conditions (for either short or long strips), shear bands starting from the edges of the footing extend straight down approximately to the depth  $D_R$ , then form a wedge beneath the

reinforced zone (Fig. 12a). In this case, the bearing capacity of the reinforced ground is controlled by the strength of the zone, including the wedge denoted by B in Fig. 12(a).

For lightly reinforced conditions, the shear bands that start from the edges of the footing form a wedge within the reinforced zone, but the apex of the wedge is deeper than that for the unreinforced ground (Fig. 12b). In this case, the bearing capacity of the reinforced

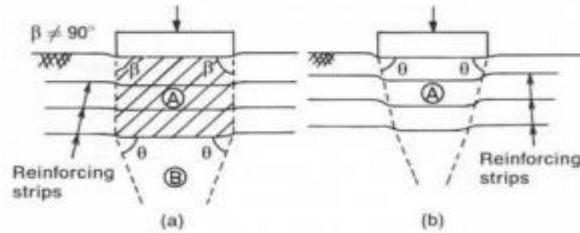


Fig. 12 Failure modes of reinforced sand: (a) densely reinforcing; and (b) lightly reinforcing (after Huang and Tatsuoka , 1988)

ground is controlled by the strength of the block A immediately beneath the footing. In this situation, the failure may occur because of one of the following factors:

- (a) Bond failure between the sand and reinforcement.
- (b) An insufficient CR (covering ratio, which is the width of the reinforcing strip/centre-to-centre horizontal spacing of the reinforcing strips) of reinforcement.
- (c) Rupture failure of reinforcement (Huang and Tatsuoka, 1990).

For estimating the ultimate bearing capacity of a deep footing ( $0 < D_f/B < 2.5$ ;  $B$  = width of footing;  $D_f$  = depth of footing) placed on a homogeneous dry sand, the following equation has been suggested by Terzaghi (1943):

$$Q_{u(\text{unreinforced}, D_f > 0)} = \eta \times B \times \gamma \times N_\gamma + \gamma \times D_f \times N_q \quad \dots(2)$$

where  $q_{u(\text{unreinforced}, D_f > 0)}$  is the ultimate bearing capacity for unreinforced deep footing,  $\eta = 0.5$  for strip footing and  $\eta = 0.4$  for square footing.

Equation (2) can be extended for the reinforced ground based on the deep-footing and wide-slab mechanisms as:

$$Q_{u(\text{reinforced})} = \eta \times (B + \Delta B) \times \gamma \times N_\gamma + \gamma \times D_f \times N_q \quad \dots(3)$$

The tangent of the load-spreading angle from the vertical, namely  $\tan \alpha$ , can be obtained as follows:  $\tan \alpha = \Delta B / 2D_R$  ....(4)

Based on comparisons of measured and multiple-variable data regression for several model test results, the following relationship between the load spreading angle,  $\alpha$ , and the factors that control the scheme for reinforcement were presented by Huang and Menq:

$$\tan \alpha = 0.680 - 2.071d/B + 0.743CR + 0.030L/B + 0.076 \quad \dots(5)$$

where  $d$  is the vertical spacing between two reinforcing layers,  $B$  is the footing width,  $L$  is the length of reinforcing layers, and  $n$  is the total number of reinforcing layers. This relationship is valid under the conditions:  $\tan \alpha > 0$ ;  $0.25 \leq d/B \leq 0.5$ ;  $0.02 \leq CR \leq 1.0$ ;  $1 \leq L/B \leq 10$ ;  $1 \leq N \leq 5$ .

## 7. DESIGN EXAMPLE 1 (For cohesionless soils)

A design example is being given below for cohesionless soil.

A shallow square foundation of width 2m, with its base at a depth of 1 m, is resting on a dry sand stratum having properties as:

$$\gamma_d = 17 \text{ kN/m}^3, \phi = 28^\circ \text{ \& } c=0$$

Geogrid sheets are used as means of reinforcement. Compare the results of bearing capacity of shallow foundation in reinforced and unreinforced case.

### Solution:

#### 7.1 Unreinforced case

The equation 2 in modified form can be written as below:

$$q_{\text{ultimate}} = \gamma D_f N_q + 0.5 \gamma B N_\gamma \quad \dots (2a)$$

Where,

$D_f$  = depth of foundation from ground surface = 1m

$N_q, N_\gamma$  = Bearing capacity factors

$$N_q = 15.30 \quad N_\gamma = 17.79 \quad \text{(Mittal \& Shukla, 2014)}$$

$$\gamma = 17 \text{ kN/m}^3 \quad B = 2\text{m}$$

from Equation (2a),

$$q_{\text{ultimate}} = 17 \times 1 \times 15.30 + 0.5 \times 17 \times 2 \times 17.79 = 260.1 + 302.43$$

$$= 562.63 \text{ kN/m}^2$$

Applying a factor of safety = 3

$$q_{\text{allowable}} = q_{\text{ultimate}} / \text{F.O.S} = \frac{562.63}{3} = 187.54 \text{ kN/m}^2 \quad (\text{Say } 18 \text{ t/m}^2)$$

## 7.2 Reinforced case

Equation for ultimate bearing capacity for the reinforced ground based on the deep footing and wide slab mechanism is given as below in modified form of equation 1:

$$q_{u(\text{reinforced})} = \eta \times (B + \Delta B) \times \gamma \times N_\gamma + \gamma \times D_R \times N_q \quad \dots (1a)$$

$$\eta = 0.4 \text{ (for square footing)}$$

$$B = \text{width of footing} = 2 \text{ m}$$

$$D_R = \text{depth of the reinforced zone from the ground surface} = 3 \text{ m (PLATE 'A')}$$

$\Delta B$  = increase of footing width at the depth of  $D_R$  due to the wide slab effect.

$$= 2D_R \tan \alpha \quad [\alpha = \text{load spreading angle, given by Eq. 5}]$$

$N_q, N_\gamma$  = Bearing capacity factors.

$$\tan \alpha = 0.680 - 2.071d/B + 0.743 CR + 0.030 L/B + 0.076 N \quad \dots (5)$$

[after Huang & Menq, 1997]

Equation (5) is valid under the conditions:

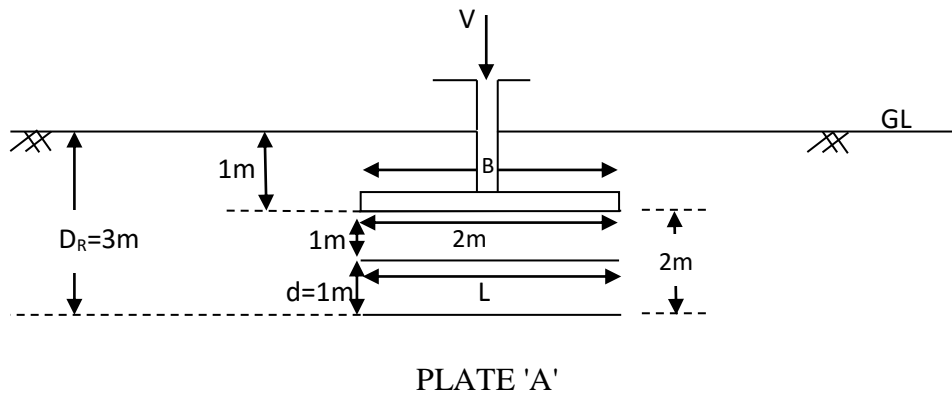
$$\tan \alpha > 0 ; 0.25 \leq d_f/B \leq 0.5 ; 0.02 \leq CR \leq 1.0 ; 1 < L/B \leq 10 ; 1 \leq N \leq 5$$

$d$  = vertical spacing between two Reinforcing layer = 1 m.

$L$  = length of Reinforcing layer

$N$  = total no. of Reinforcing layer, = 2

$$CR = \text{Covering Ratio} = \frac{\text{width of Reinforcing strip}}{\text{centre to centre horizontal space of Reinforcement strips}}$$



**from equation (5)**

$$\tan\alpha = 0.680 - 2.071 \times \frac{1}{2} + 0.743 \text{ CR} + 0.030 \times 6 + 0.076 \times 2 = 0.01365.$$

[say, CR = Covering ratio = 0.05 , L/B = 6]

$$\begin{aligned}\Delta B &= 2 D_R \tan\alpha = 2 \times 3 \times 0.01365 \\ &= 0.0819 \text{ m.}\end{aligned}$$

for  $\phi = 28^\circ$  ,  $N_q = 15.30$   $N_\gamma = 17.79$  (Mittal & Shukla, 2014)

**Therefore, from equation (1a)**

$$\begin{aligned}q_{u(\text{reinforced})} &= \eta \times (B + \Delta B) \times \gamma \times N_\gamma + \gamma \times D_R \times N_q \\ &= 0.4 \times (2 + 0.0819) \times 17 \times 17.79 + 17 \times 3 \times 15.30 \\ &= 1032.38 \text{ kN/m}^2\end{aligned}$$

Applying a factor of safety = 3,

$$q_{\text{allowable}} = \frac{q_{\text{ultimate}}}{F.O.S.} = \frac{1032.38}{3} = 344.13 \text{ kN/m}^2 \quad (\text{Say } 34 \text{ t/m}^2)$$

**Note 1:** *The available literature reveals that practically there is no inclusion of tensile strength factor (related to reinforcing element) in the equation pertaining to cohesionless soil. However, this factor is included in case of cohesive soil (discussed later in Para 7.3).*

**Note 2:** *The above computations clearly show that when soil is reinforced with geogrid, the bearing capacity increases from 18t/m<sup>2</sup> to 34 t/m<sup>2</sup> (which is almost doubled ) for just two layers of reinforcement. It may further increase as the number of reinforcing layers increase ( within the influence zone ). Research work (Mittal, 2013) indicates that when the geogrid is included in soil, not only the angle of internal friction is increased, but there is development of pseudo cohesion also, developed within the composite soil mass. However, that part is ignored in above design example. The users are advised to conduct the tests in the laboratory to determine revised value of  $\phi$  and  $c'$  (apparent cohesion ) developed between soil at site and the reinforcement material, being used for shallow foundations (Mandal & Mhaiskar, 1994).*

For clayey soils, the method for load bearing capacity analysis is defined as below:

### 7.3 Reinforced granular fill-soft foundation soil system

A bearing capacity analysis, presented by Espinoza and Bray (1995) for a single layer geotextile-reinforced granular fill - soft foundation soil, is described here. The bearing capacity equation derived, satisfies both vertical force and horizontal force equilibrium along the geotextile reinforcement and incorporates two important membrane support contributions, namely normal stress membrane support and interfacial shear stress membrane support. The subgrade shear stress reduction effect of geotextile is also included in the equation.

By considering the vertical force equilibrium of a differential geotextile element of unit area as shown in Fig. 13(a), one gets a general equilibrium equation as:

$$q_{app}(x) = q_s(x) + q_g(x) \quad \dots (6)$$

where  $q_{app}(x)$  is the force per unit area above the geotextile,  $q_s(x)$  is the vertical soil reaction per unit area,  $q_g(x)$  is the membrane support contribution per unit area, and  $x$  is the horizontal coordinate.

Assuming plane-strain conditions and considering the vertical and horizontal force equilibrium of the deformed geotextile (Fig. 13(b)), it can be shown that (Espinoza, 1994):

$$q_g(x) = T_h(x) \frac{d^2 y(x)}{dx^2}$$

with:

$$T_h = T(x) \cos \beta(x)$$

$$T(x) = J \varepsilon(x)$$

$$\tan \beta(x) = \frac{dy}{dx} \quad \dots (7)$$

where  $y(x)$  is the vertical deflection of the geotextile,  $\beta(x)$  is the angle that the deformed geotextile makes with the horizontal line at a distance  $x$

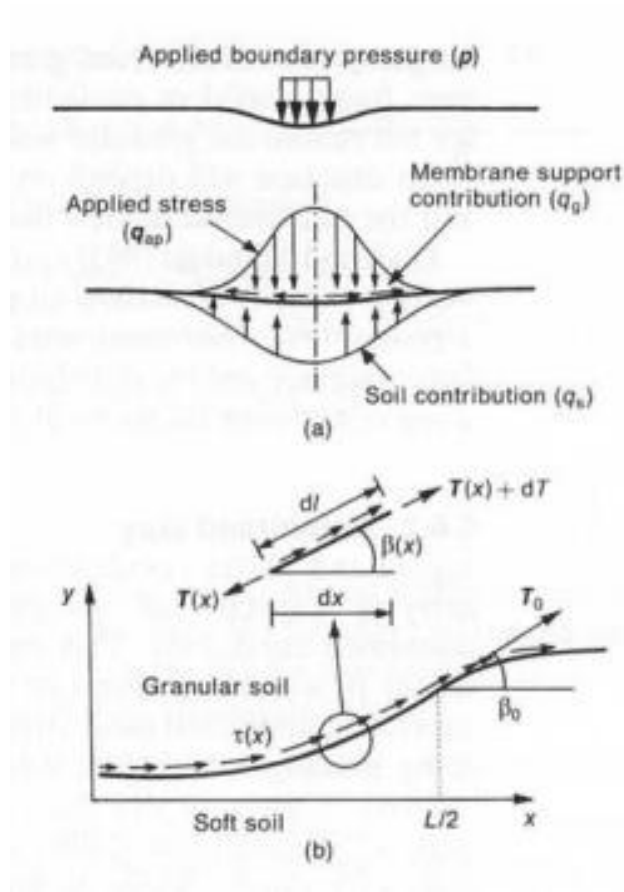


Fig. 13 Forces on a geotextile: (a) membrane contribution provided by geotextile; and (b) vertical and horizontal force equilibrium of the deformed geotextile (after Espinoza and Bray, 1995)

from the centreline,  $T(x)$  is the geotextile tensile force,  $J$  is the geotextile stiffness modulus,  $\epsilon(x)$  is the geotextile strain, and  $T_h(x)$  is the horizontal component of the tensile force  $T(x)$ .

Espinoza (1994) defined the average membrane support contribution,  $q_g'$  as:

$$q_g = \frac{1}{L} \int_{-L/2}^{L/2} q_g(x) dx = \frac{1}{L} \int_{-L/2}^{L/2} T_h(x) \frac{d^2 y(x)}{dx^2} dx \quad \dots(8)$$

where  $L$  is the effective horizontal length of geotextile (defined by the segment joining the stationary points B and D as shown in Fig. 15). This equation satisfies global vertical and horizontal force equilibriums.

The geotextile located outside the effective length (i.e. AB and DE in Fig. 14) exerts a vertical pressure,  $q_{lat}$ , due to membrane support, thus reducing the heave potential of the subgrade soil.

Considering an average surcharge lateral load ( $q_{lat} + \gamma h$ ), the subgrade bearing capacity is given by:

$$q_s = cN_c + \gamma h + q_{lat} \quad \dots(9)$$

where:

$$q_{lat} = \frac{1}{L} \int_{L/2}^{L_c+L/2} q_g(x) dx \quad \dots (10)$$

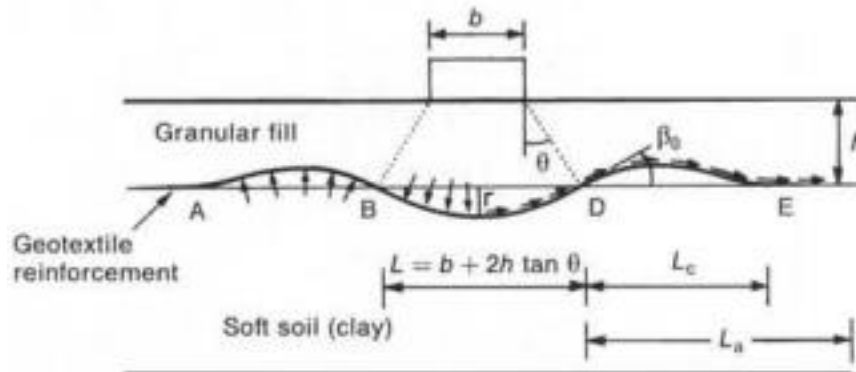


Fig. 14 Failure mechanism (after Espinoza and Bray, 1995)

Table 1 Load spreading angle (note, h is expressed in cm)

Method	Spreading angle, $\theta$ : °	
	Without geotextile	With geotextile
Barenberg (1980)	$\tan^{-1}(0.3 + 5/h)$	$\tan^{-1}(0.6 + 5/h)$
Giroud and Noiray (1981)	$(\pi/4 - \phi/2)$	26.6–35.0
Raumann (1982)	28.8	33.0
Sellmeijer <i>et al.</i> (1982)	26.6–45.0	26.6–45.0
Love <i>et al.</i> (1987)	–	26.6–31.0

and :

$$N_c = 1 + \frac{\pi}{2} + \alpha + \sin \alpha \quad \dots (11)$$

where  $\alpha = \cos^{-1}(\tau_c/c_u)$ ,  $\tau_c$  is the shear applied on the clay surface,  $c_u$  is the undrained shear strength of clay,  $N_c$  is the bearing capacity factor,  $h$  is the thickness of the granular fill,  $\gamma$  is the unit weight of the fill, and  $L_c$  is the length of geotextile preventing heave (Fig. 14).

Equation (11) is based on the lower bound plasticity theory for undrained loading on a semi-infinite saturated clay layer (Bolton, 1979). If the shear above the clay surface is zero (smooth

footing), then  $\alpha = \pi/2$  and  $N_c$  becomes  $(\pi + 2)$ , which is the classical bearing capacity factor for vertical loads on rigid-perfectly plastic material. An  $N_c$  factor larger than  $(\pi + 2)$  may be used for rough footings that transmit inward shear to the clay.

The average vertical stress within the fill can be estimated using a load spreading angle,  $B$ . The average pressure applied to the geotextile is given by:

$$q_{ap} = \gamma h + \alpha_b p \quad \dots (12)$$

where  $\alpha_b = b/L$ , width factor, and  $L = b + 2h \tan \theta$ . Table 1 shows different empirical values of the load spreading angle,  $\theta$ , as reported in literature.

Combining equations (6), (8), (9) and (12), an average equilibrium equation is obtained as:

$$\alpha_b p = c_u N_c + q_t \quad \dots (13)$$

where:

$$q_t = \frac{2}{L} \int_0^{L/2} q_g(x) dx + \frac{1}{L} \int_{L/2}^{L_c+L/2} q_g(x) dx \quad \dots(14)$$

where  $q_t$  is the total membrane support contribution, which includes both normal stress membrane support (membrane contribution obtained from outside the effective length) and interfacial shear stress membrane support (membrane contribution obtained from within the effective length). Normal stress membrane support depends on proper anchorage outside the effective length. Interfacial shear stress membrane support depends upon the applied load and the mobilized interface friction.

Assumptions regarding the geotextile strain distribution and deformation are necessary to numerically evaluate the integral expression given by equation (14). An equation for the admissible surface pressure,  $P_{adm}$ , can be estimated as:

$$p_{adm} = \frac{c_u N_c + T_0 \sin \beta_0 / L + 2\alpha_r \gamma h \tan \psi_m}{\alpha_b (1 - 2\alpha_r \tan \psi_m)} \quad \dots (15)$$

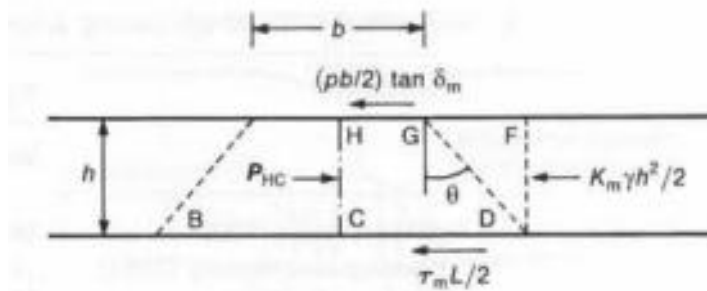


Fig. 15 Mobilized shear (after Espinoza and Bray, 1995)

where  $\alpha_r = r/L$  , rutting factor,  $r$  is the rutting depth (Fig. 14),  $T_0$  is the tensile force in the geotextile layer at point D,  $\beta_0$  is the inclination of geotextile layer at point D, and  $\psi_m$  is the mobilized interface friction angle. The normal stress membrane support is reflected in the tensile force  $T_0$  , and the angle of deflection  $\beta_0$  developed at the stationary points B and D in Fig. 14. In many practical field situations, proper anchorage cannot be ensured at all times during construction (i.e. there is not enough anchorage length,  $L_a$ , or surcharge load,  $\gamma h$ , or a combination of both). In such cases,  $T_0 = 0$  should be used to estimate the admissible pressure. Even in cases where proper anchorage is provided (i.e.  $T_0 > 0$ ), its effect will not be felt until large deformations are induced (i.e.  $\beta_0 \gg 0$ ).

An expression can also be derived for the mobilized interface friction angle based on the strict equilibrium between the membrane and sliding block above it. An expression for this, valid for the situation shown in Fig. 15, is:

$$\tan \psi_m = \frac{[\alpha_h(K - K_{pm}) + M_c(\eta K - \tan \delta_m)]}{[1 + M_c + 2\alpha_r\{\alpha_h(K - K_{pm}) - \eta K + \tan \delta_m\}]} \quad \dots (16)$$

where  $K$  is an earth pressure coefficient,  $K_{pm} = \tan^2(\pi/4 + \phi_m/2)$ , the mobilized passive earth pressure coefficient,  $\phi_m$  is the mobilized soil friction angle,  $\delta_m$  is the mobilized interface friction angle at the footing base, and  $\alpha_h = h/L$  and  $M_c = (c_u N_c + T_0 \sin \beta_0/L) \gamma h$  are dimensionless parameters.

Equations (15) and (16) have been used to predict admissible pressures for a small-scale model test setup and the results are compared with the footing pressures measured by Love et al. (1987) and Milligan et al. (1989) for a series of model tests with various granular fill thicknesses and subgrade strengths. Overall, the computed values of the admissible pressures compare favourably with those measured, and this finding provides support to the validity of the proposed equations (15) and (16).

Ochiai et al. (1994) described a conventional approach for the assessment of the improvement of the bearing capacity due to placement of the geogrid-mattress foundation . In this approach, a vertical load of intensity  $p$  and width  $B$ , applied on the mattress, is transmitted widely to the supporting foundation soil with the corresponding intensity  $p_m$  and width  $B_m$  (Fig. 16).

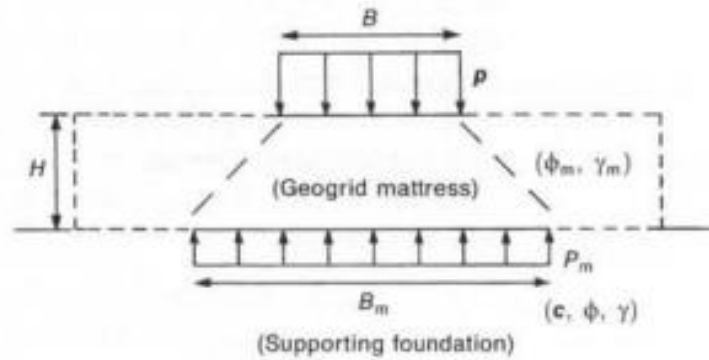


Fig. 16 Effects of the use of a geogrid mattress (after Ochiai et al., 1994)

The ultimate bearing capacity  $q$  without the use of the mattress may be given by Terzaghi's equation, as follows:

$$q = cN_c + 1/2 \gamma B N_\gamma \quad \dots (17)$$

where  $c$  is cohesion and  $\gamma$  is the unit weight of the supporting foundation soil. On the other hand, the ultimate bearing capacity,  $q_m$ , with the use of a mattress, may be given as follows (assuming that the placement of the geogrid mattress has a surcharge effect on the bearing capacity of the supporting foundation)

$$q_m = cN_c + \gamma_m H N_q + 1/2 \gamma B_m N_\gamma \quad \dots (18)$$

where  $\gamma_m$  is the unit weight of the mattress, and  $H$  is the thickness of the mattress. Therefore, the increase in the bearing capacity  $\Delta q$  due to the placement of the mattress can be given as follows:

$$\Delta q = \gamma_m H N_q + 1/2 \gamma (B_m - B) N_\gamma \quad \dots (19)$$

It is therefore found that the evaluation of the bearing capacity improvement requires the estimation of the width  $B_m$ . The experimental studies have revealed that the width of the supporting foundation soil over which the vertical stress is distributed becomes larger as the thickness of the geogrid mattress becomes greater, and as the vertical stiffness of the supporting foundation soil becomes lower. It was suggested, from a design point of view, that the width of the geogrid mattress should be at least large enough to accommodate the vertical stress distribution which takes place under the mattress.

Several authors analysed the geosynthetic-reinforced granular fill - soft soil system by finite element method (Love et al. , 1987; Koga et al. , 1988; Poran et al., 1989; Floss and Gold, 1994; Otani et al. , 1998). The advantage of such an analysis is that displacement distribution, and

stress distribution, can both be obtained in the subsoil as well as in the soil- geosynthetic layer system. Nevertheless, it should be realized that the accuracy of the finite element results depends on the appropriate material properties used and the type of modelling adopted for the analysis. In the finite element analysis, the complete soil- geosynthetic layer system can be modelled using individual elements, such as bar elements for the geosynthetic layer, continuum elements for the soil and joint elements for the interface behaviour, or by using composite elements that comprise the soil- geosynthetic system as whole. In the latter case, the properties of the composite element can be evaluated either experimentally or by a separate numerical analysis.

The bearing capacity analysis of a geosynthetic-reinforced cohesive foundation loaded by a flexible uniform strip footing was carried out by Otani et al. (1998) using a rigid plastic finite element formulation . This method is based on the upper bound theorem of the theory of plasticity, and the bearing capacity is obtained as a load factor at the ultimate limit state. The geosynthetic reinforcement and the surrounding sand layer (constructed around the geosynthetics in the cohesive ground for the purpose of increasing the friction between the geosynthetics and the adjacent soil) are modelled as a single composite material with an equivalent cohesion. The underlying soft ground is also assumed to be purely cohesive and, hence, both the reinforced soil and soft ground are modelled using the von-Mises failure criterion. The method of analysis proposed was checked against the field measurements or the model test results. The analysis indicated that the bearing capacity of the ground of the geosynthetic-reinforced foundation is increased as the depth and the length of the reinforcement are increased, but there is an optimum depth for which the maximum reinforcing effect is obtained. There is also an optimum number of geosynthetic layers. Figure 17 shows a simple design chart for the estimation of the bearing capacity of geosynthetic-reinforced foundations on soft ground. In this chart,  $L$  is the half length of geosynthetic layer,  $B$  is the half width of footing,  $D$  is the depth of geosynthetic layer,  $T$  is the tensile strength of geosynthetic layer,  $q_u$  is the ultimate bearing capacity of unreinforced foundation soil and  $q_{uR}$  is the ultimate bearing capacity of reinforced foundation soil.

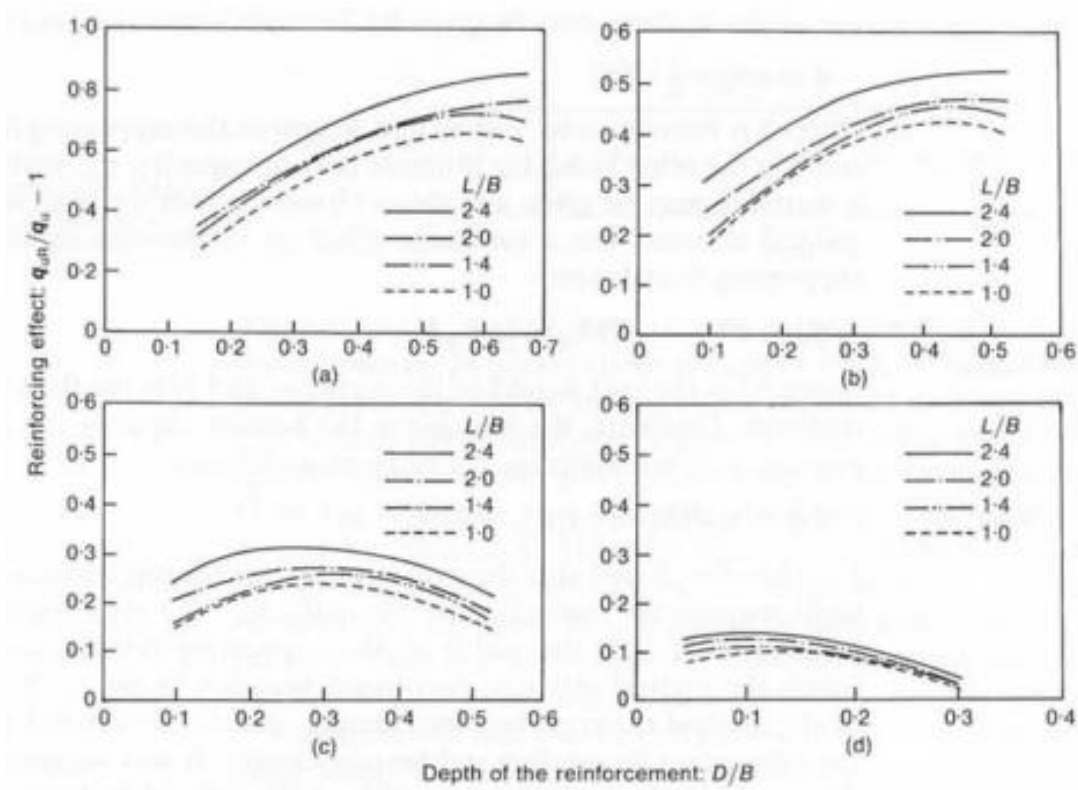


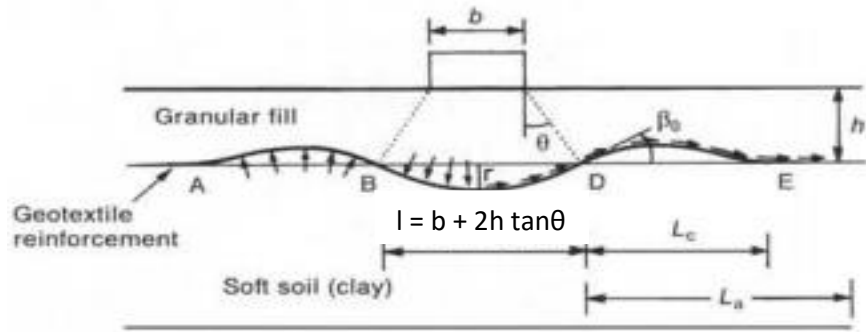
Fig. 17 Effects of the geosynthetics on the bearing capacity of the foundation: (a)  $T = 80$  kN/m; (b)  $T = 55$  kN/m; (c)  $T = 35$  kN/m; and (d)  $T = 15$  kN/m (after Otani et al., 1998)

## DESIGN EXAMPLE 2 (For Cohesive soils)

Perform the bearing capacity analysis of a geosynthetic reinforced foundation loaded by a flexible uniform strip footing of width 1.5m. The geotextile layer having tensile strength as 55 kN/m is placed at a depth of 0.40 m from the base of footing and at the interface of granular fill and soft soil.

**Solution:** The failure mechanism in such cases is illustrated in Fig. 14 which is reproduced

below:



Failure mechanism (after Espinoza and Bray, 1995)

The geosynthetic layer located outside the effective length (i.e. AB and DE in Fig. 15) exerts a vertical pressure,  $q_{lat}$ , due to membrane support, thus reducing the heave potential of the subgrade soil.

Where,  $l$  = Effective horizontal length of geotextile (defined by the segment joining the stationary points B and D as shown in Fig. 15).

$$l = b + 2h \tan \theta$$

Where,

$b$  = width of footing = 1.5 m

$h$  = Thickness of granular fill = 0.40 m

$\theta$  = Load spreading angle (degrees) with geotextile = 26.6 to 31.0 (Love et al. 1987)

$$= 27^{\circ} \text{ (say)}$$

Now,  $l = 1.5 + 2 \times 0.40 \times \tan 27^{\circ} = 1.91 \text{ m}$

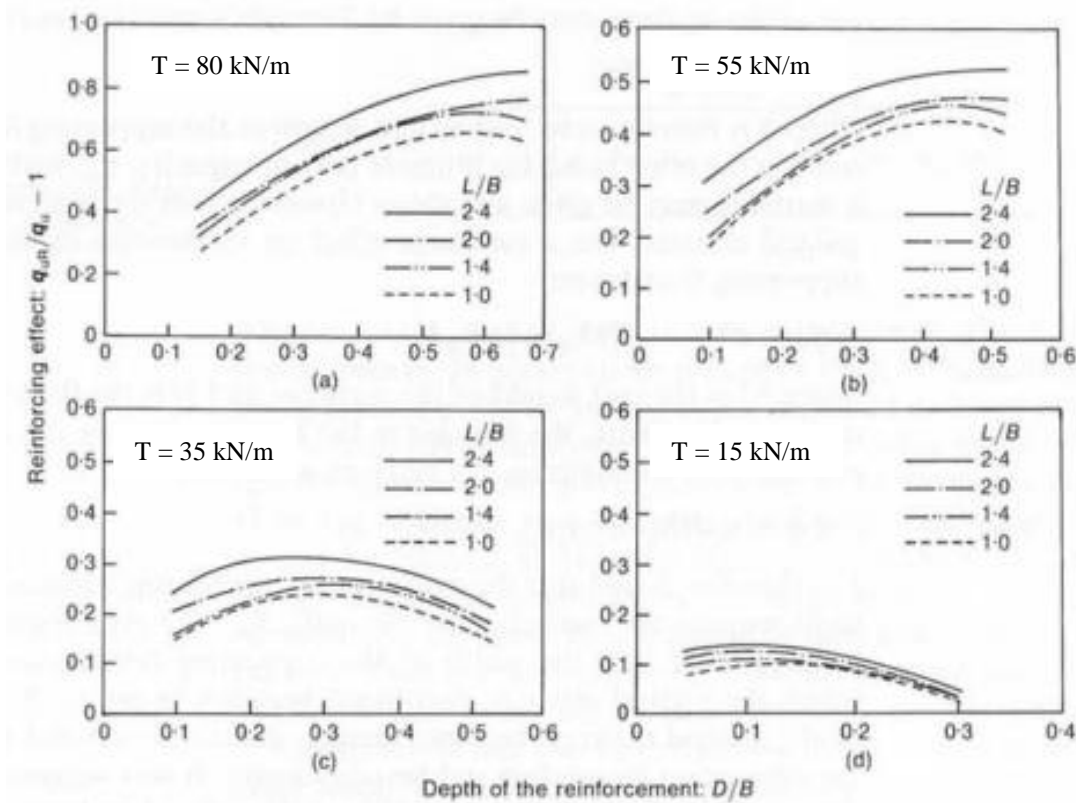
The bearing capacity analysis was carried out by Otani et al. (1988). This method is based on :

1. Upper bound theorem of the theory of plasticity, and the bearing capacity is obtained as a load factor at the ultimate limit state.
2. The geosynthetic reinforcement and the surrounding sand layer (constructed around the geosynthetics in the cohesive ground for the purpose of increasing the friction between

the geosynthetics and the adjacent soil) are modeled as a single composite material with an equivalent cohesion.

3. The underlying soft ground is also assumed to be purely cohesive and, hence, both the reinforced soil and soft ground are modelled using the von-Mises failure criterion.
4. The method of analysis proposed was checked against the field measurements or the model test results.

**Design charts (Fig. 17) for the estimation of the bearing capacity of geosynthetic reinforced foundation on soft ground are reproduced as below for ready reference:**



Effects of the geosynthetics on the bearing capacity of the foundation (after Otani et al., 1998)

In these charts,

$L$  = half length of geosynthetic layer =  $l/2 = 0.95 \text{ m}$

$B$  = half width of footing =  $0.75 \text{ m}$

$D$  = the depth of geosynthetic layer = 0.40 m

$T$  = Tensile strength of geosynthetic layer = 55 kN/m (say)

$q_u$  = ultimate bearing capacity of unreinforced foundation soil.

$q_{uR}$  = ultimate bearing capacity of reinforced foundation soil.

From above design charts,

For  $D/B = 0.53$  m ,  $L/B = 1.26$  and  $T = 55$  kN/m (Fig. 18 b)

$$(q_{uR}/q_u) - 1 = 0.43$$

$$q_{uR}/q_u = 1.43$$

The above computations clearly show that the bearing capacity increases by 1.4 times with the use of only one geosynthetic layer at the interface of granular fill and soft soil.

## **8. CONCLUSION**

In this chapter the results give an idea for the use of geosynthetics in field applications for shallow foundations based on small scale model footing tests. In most practical situations, the improvement in the load bearing

capacity will be due to membrane shear effects (both the interfacial shear stress membrane support and the subgrade shear stress reduction effect) without the need of full anchorage. Users may draw sufficient guidelines and directions from above discussions for design of shallow foundations by use of geosynthetics.

## **ACKNOWLEDGEMENT**

Ms Disha Joshi, PG student, Geotechnical engg, IIT Roorkee helped the author in compilation of material and design examples. Author expresses his sincere thanks to her.

## REFERENCES

1. Adams, M. T. and Collin, J. G. (1997). Large model spread footing load tests on geosynthetic reinforced soil foundations. *Journal of Geotechnical and Geoenvironmental Engineering*, 123, No. I, 66- 72.
2. Adams, M. T. and Collin, J. G. (1997). Large model spread footing load tests on geosynthetic reinforced soil foundations. *Journal of Geotechnical and Geoenvironmental Engineering*, 123, No. I, 66- 72.
3. Binquet, J. and Lee, K. L. (1975a). Bearing capacity tests on reinforced earth slabs. *Journal of Geotechnical Engineering Division, ASCE*, 101, No. 12, 1241 -1255.
4. Binquet, J. and Lee, K. L. (1975b). Bearing capacity analysis of reinforced earth slabs. *Journal of the Geotechnical Engineering Division, ASCE*, 101, No. 12, 1257- 1276.
5. Bolton, M. D. (1979). *A guide to soil mechanics*. Macmillan Press, London.
6. Bourdeau, P. L. (1989). Modeling of membrane action in a two-layer reinforced soil system. *Computers and Geotechnics*, 7, 19- 36.
7. Bourdeau, P. L., Harr, M. E. and Holtz, R. D. (1982). Soil-fabric interaction - an analytical model. *Proceedings of the 2nd International Conference on Geotextiles*. Las Vegas, USA, Nevada, pp. 387- 391.
8. Espinoza, R. D. (1994). Soil-geotextile interaction: evaluation of membrane support. *Geotextiles and Geomembranes*, 13, 281 - 293.
9. Espinoza, R. D. and Bray, J. D. (1995). An integrated approach to evaluating single-layer reinforced soils. *Geosynthetics International*, 2, No.4, 723- 739.
10. Espinoza, R. D. and Bray, J. D. (1995). An integrated approach to evaluating single-layer reinforced soils. *Geosynthetics International*, 2, No.4, 723- 739.
11. Floss, R. and Gold, G. (1994). Causes for the improved bearing behaviour of the reinforced two-layer system. *Proceedings of the 5th International Conference on Geotextiles, Geomembranes and Related Products*. Singapore, pp. 147- 150.
12. Giroud, J. P. and Noiray, L. (1981). Geotextile-reinforced unpaved road design. *Journal of the Geotechnical Division, ASCE*, 107, 1233- 54.

13. Giroud, J. P., Ah-Line, C. and Bonaparte, R. (1984). Design of unpaved roads and trafficked areas with geogrids. Proceedings of the Symposium on Polymer Grid Reinforcement in Civil Engineering, Paper No. 4.1, London.
14. Guido, V. A., Biesiadecki, G. L. and Sullivan, M. J. (1985). Bearing capacity of a geotextile-reinforced foundation. Proceedings of the 11th International Conference on Soil Mechanics and Foundation Engineering. San Francisco, California, USA, pp. 1777-1780.
15. Guido, V. A., Dong, K. G. and Sweeny, A. (1986). Comparison of geogrid and geotextile reinforced earth slabs. Canadian Geotechnical Journal, 23, No. 1, 435- 440.
16. Haas, R., Walls, J. and Carroll, R. G. (1988). Geogrid reinforcement of granular bases in flexible pavements. Transportation Research Record, No. 1188, 19- 27.
17. Hausmann, M. R. (1990). Engineering principles of ground modification. McGraw-Hill, New York.
18. Huang, C. C. and Menq, F.Y. (1997). Deep-footing and wide-slab effects in reinforced sandy ground. Journal of Geotechnical and Geoenvironmental Engineering, 123, No. 1, 30- 36.
19. Huang, C. C. and Tatsuoka, F. (1988). Prediction of bearing capacity in level sandy ground reinforced with strip reinforcement. Proceedings of the International Geotechnical Symposium on Theory and Practice of Earth Reinforcement. Fukuoka, Japan, pp. 191 - 196.
20. Huang, C. C. and Tatsuoka, F. (1990). Bearing capacity of reinforced horizontal sandy ground. Geotextiles and Geomembranes, 9, 51 - 82.
21. Ingold, T. S. and Miller, K. S. (1982). Analytical and laboratory investigations of reinforced clay. Proceedings of the 2nd International Conference on Geotextiles. Las Vegas, Nevada, USA, pp. 587- 592.
22. Jewell, R. A. (1996). Soil reinforcement with geotextiles, CIRIA and Thomas Telford Publishing, London.
23. Jewell, R. A. and Wroth, C. P. (1987). Direct shear tests on reinforced sand. Geotechnique, 37, No. 1, 53- 68.
24. Ju, J. W., Son, S. J., Kim, J. Y. and Jung, I. G. (1996). Bearing capacity of sand foundation reinforced by geonet. Proceedings of the International Symposium on Earth Reinforcement. Fukuoka, Japan, pp. 603- 608.
25. Koerner, R. M. (1990). Designing with geosynthetics, second edition, Prentice Hall, New Jersey, USA. Omar, M. T., Das B. M., Puri, V. K. and Yen, S. C. (1993). Ultimate

- bearing capacity of shallow foundations on sand with geogrid reinforcement. *Canadian Geotechnical Engineering*, 30, 545- 549.
26. Koga, K., Aramaki, G. and Valliappan, S. (1988). Finite element analysis of grid reinforcement. *Proceedings of the International Geotechnical Symposium on Theory and Practice of Earth Reinforcement*. Fukuoka, Japan, pp. 407- 411.
  27. Love, J. P., Burd, H. J. , Milljgan, G. W. E. and Houlsby, G. T. (1987). Analytical and model studies of reinforcement of a layer of granular fill on soft clay subgrade. *Canadian Geotechnical Journal*, 24, 611 - 622.
  28. Love, J. P., Burd, H. J. , Milljgan, G. W. E. and Houlsby, G. T. (1987). Analytical and model studies of reinforcement of a layer of granular fill on soft clay subgrade. *Canadian Geotechnical Journal*, 24, 611 - 622.
  29. Madhav, M. R. and Poorooshasb, H. B. (1988). A new model for geosyntheticreinforced soil. *Computers and Geotechnics*, 6, 277- 290.
  30. Madhav, M. R. and Poorooshasb, H. B. (1989). Modified Paternak model for reinforced soil. *Mathematical and Computational Modelling, an International Journal*, 12, 1505- 1509.
  31. Mandal, J.N and Mhaiskar, S.Y. (1994), "An Overview of Pavement Design Methods With Geosynthetics ", *Geosynthetic world*, Wiley Eastern limited , Mumbai
  32. MandaI, J. N. and Sah, H. S. (1992). Bearing capacity tests on geogrid-reinforced clay. *Geotextiles and Geomembranes*, 11, 327- 333.
  33. McGown, A. , Andrawes, K. Z. and Al-Hasani, M. M. (1978). Effect of inclusion properties on the behaviour of sand. *Geotechnique*, 28, No.3, 327- 346.
  34. Milligan, G. W. E., Jewel, R. A. , Houlsby, G. T. and Burd, H. J. (1989). A new approach to the design of unpaved roads - Part I. *Ground Engineering*, 25- 29
  35. Mittal (2013), " An Introduction to Ground Improvement Engineering", SIPL Publication, Delhi.
  36. Mittal, S. and Shukla, J.P. (2014), "Soil Testing for Engineers", Khanna Publishers, Delhi.
  37. Nishida, K. and Nishigata, T. (1994). The evaluation of separation function for geotextiles. *Proceedings of the 5th International Conference on Geotextiles, Geomembranes and Related Products*. Singapore, 1994.
  38. Ochiai, H., Tsukamoto, Y., Hayashi, S., Otani, J. and Ju, J. W. (1994). Supporting capability of geogrid-mattress foundation . *Proceedings of the 5th International*

Conference on Geotextiles, Geomembranes and Related Products. Singapore, pp. 321 - 326.

39. Otani, J., Ochiai, H. and Yamamoto, K. (1998). Bearing capacity analysis of reinforced foundations on cohesive soil. *Geotextiles and Geomembranes*, 16, 195- 206
40. Poran, C. J., Herrmann, L. R. and Romstad, K. M. (1989). Finite element analysis of footings on geogrid-reinforced soil. *Proceedings of the Geosynthetics '89 Conference*. San Diego, USA, pp. 231 - 242.
41. Sakti, J. P. and Das, B. M. (1987). Model tests for strip foundation on clay reinforced with geotextile layers. *Transportation Research Record*, No. 1153, 40- 45.
42. Schlosser, F., Jacobsen, H. M. and Juran, I. (1983). Soil reinforcement. General Rep., *Proceedings of the 8th European Conference on Soil Mechechanics and Foundation Engineering*. Helsinki, pp. 83- 103.
43. Sellmeijer, J. B. (1990). Design of geotextile reinforced unpaved roads and parking areas. *Proceedings of the 4th International Conference on Geotextiles, Geomembranes and Related Products*. The Hague, Netherlands, pp. 177- 182.
44. Sellmeijer, J. B. , Kenter, C. J. and Van den Berg, C. (1982). Calculation method for fabric reinforced road. *Proceedings of the 2nd International Conference on Geotextiles*. Las Vegas, Nevada, USA, pp. 393- 398.
45. Shin, E. C. and Das, B. M. (2000). Experimental study of bearing capacity of a strip foundation on geogrid-reinforced sand. *Geosynthetics International*, 7, No. I, 59- 71.
46. Shukla, S. K. and Chandra, S. (1994a). A generalized mechanical model for geosynthetic-reinforced foundation soil. *Geotextiles and Geomembranes*, 13, 813- 825.
47. Shukla S. K. (2002), “ Geosynthetics and their applications”, Thomas Telford publications, 1 Heron Quay, London E14 4JD.
48. Yetimoglu, T. , Wu, J. T. H. and Saglamer, A. (1994). Bearing capacity of rectangular footings on geogrid-reinforced sand. *Journal of Geotechnical Engineering*, 120, No. 12, 2083- 2099.

# Cellular Confinement Systems

**Gali Madhavi Latha**

Professor, Department of Civil Engineering, Indian Institute of Science, Bangalore - 560 012,  
E-mail: madhavi@civil.iisc.ernet.in

## 1. INTRODUCTION

Synthetic material usage in civil engineering has, after years of research and successful installations, gained a level of confidence with the engineering community. The generic term 'geocell' refers to three-dimensional, polymeric, honeycomb like cellular material. A structure of these cells interconnected by joints to form cellular network could be used for the confinement of soil. These geocells completely encase the soil and provide all-round confinement, thus preventing the lateral spreading of the soil. Because of this, the soil-geocell layer acts as a stiff mat, distributing the load over much larger area of the subgrade soil. This helps in reducing vertical and lateral deformations of the foundation soil to a large extent besides increasing the overall bearing capacity of the foundation soil.

The concept of cellular confinement was first developed by US Army Corps of Engineers in late seventies (Rea and Mitchell 1978). The primary application was surface stabilization of granular soils under vehicular loading. Now these geocells have found a wide range of applications, which include:

- Embankment base reinforcement
- Foundation support
- Subgrade stabilization
- Erosion control and slope protection
- Channel protection
- Multi-layer reinforcement for retaining walls
- Reinforcing soil covers over flexible conduits

The planar geosynthetics like geotextiles and geogrids interact with the soil through surface friction and interlocking with soil particles. They prevent the lateral flow of soil only through these two mechanisms. Hence, these forms of reinforcement cannot be applied when lateral

flow tendency is severe such as under heavy loads or in flowing water conditions. For such applications, three dimensional confinement of soils is preferred. The three-dimensional confinement of soils is provided either through pre-fabricated geocells or geocells made at the site using geogrids/geotextiles of various grades. The schematic of the three-dimensional confinement of geocells is illustrated in Figure 1.

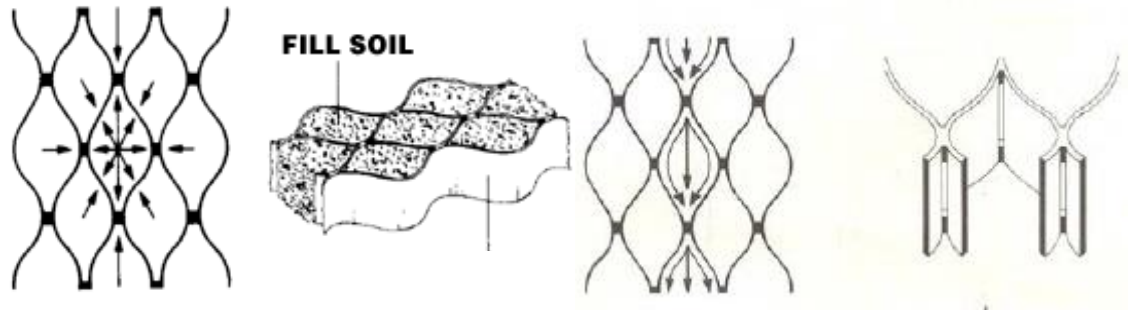


**Figure 1.** Schematic of geocell confinement system

Geocells can be either prefabricated or constructed on site using geogrids. The structure of prefabricated geocell layer is shown in Figure 2. Figure shows both the collapsed and expanded forms of the geocell layer. The collapsed form of the geocell layer, in which the cells are closed, allows the geocell layer to occupy very less space for transportation and handling. Geocell layer is spread on the foundation in expanded form.

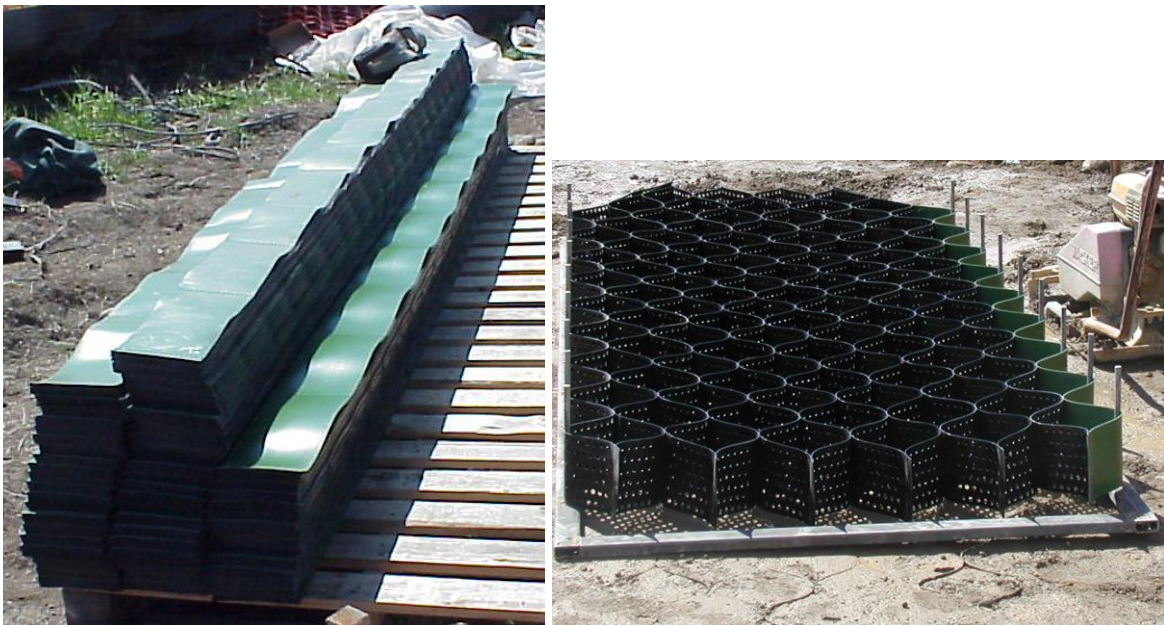


**Figure 2.** Collapsed and expanded forms of geocell layer

Few studies are available on the improvement in strength and modulus of soil due to geocell confinement (Bathurst and Karpurapu 1993; and Rajagopal et al. 1999). Performance of geocell reinforced earth structures is investigated and reported in literature by several researchers (Bathurst and Jarrett 1988; Jenner et al. 1988; Bush et al. 1990; Cowland and Wong 1993; Bathurst and Knight 1998; Krishnaswamy et al. 2000; Madhavi Latha 2000; Dash et al. 2001; Madhavi Latha and Rajagopal 2007; Madhavi Latha et al. 2008, Madhavi Latha et al. 2006; Madhavi Latha and Murthy 2007; Madhavi Latha and Rajagopal 2007; Madhavi Latha et al. 2010; Han et al. 2011).

### ***Construction Procedure***

Initially the level where the first layer of geocell is to be placed is marked and a geotextile layer of high strength is laid at the proposed level to act as a separator between the geocells and the foundation soil. The dimensions and position of geocell layer are marked and stakes are put at the four corners. Above this, the geocell layer is expanded and positioned and anchored over the embedded stakes. A typical geocell layer with anchors looks as shown in Figure 3. Then the first row of cells is filled with a dump truck and the fill sand is pushed into cells using shovels and all the rows are filled subsequently. No cell should be filled completely until the adjacent cell is at least half-filled. No traffic is allowed to move over the unfilled cells. The cells should be overfilled slightly to allow for consolidation. Next, the infill sand inside the cells is compacted through multiple passes by the tracked equipment used to spread the infill (Figure 4). A vibrating roller and/or water may be required to achieve the specified level of compaction. Once the cells are filled and the system is compacted, the geocell layer is ready to withstand moving construction traffic.

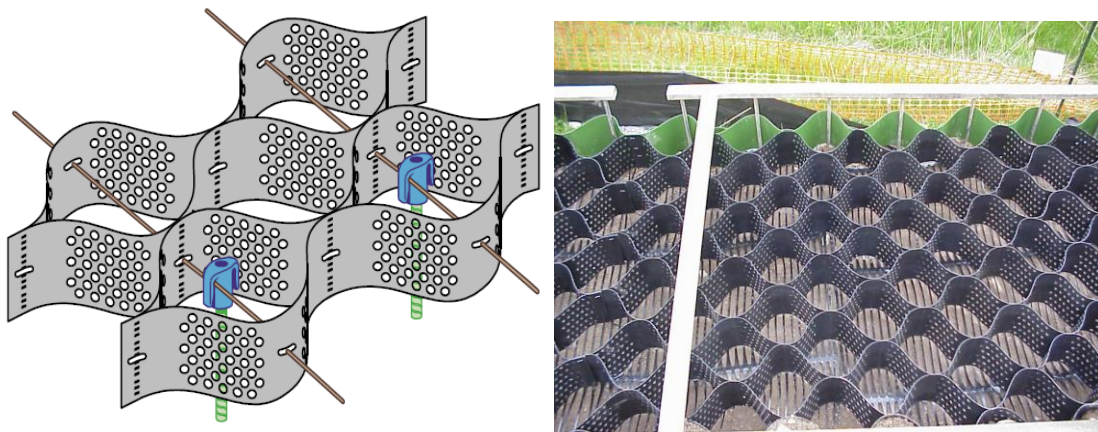


**Figure 3.** Expanded geocell layer with anchors



**Figure 4.** Filling of geocells

This document describes and compiles the laboratory and small scale field studies carried out on geocell reinforced soil structures. Embankments supported on geocell layers, foundations resting on geocell layer and road subgrades stabilized with geocell layer are considered and the beneficial role of geocells in these structures is investigated and explained.

## **2. GEOCELL SUPPORTED EMBANKMENTS**

The embankments constructed on soft clays are prone to excessive settlements and shear failure due to high compressibility and low shear strength of foundation soil. There is also a tendency for lateral spreading because of the horizontal earth pressures acting within the embankment. In view of these factors, construction of embankments over soft soils poses interesting challenges to the geotechnical engineer. Soil reinforcement is accepted as one of the attractive solutions to support the embankments constructed on soft soils due to the savings on time and cost apart from flexibility in space requirements. The advantages of geocell reinforcement, which make it most appealing for the construction of embankments over soft foundation soils, are:

- It acts as an immediate working platform for the movement of construction traffic
- It allows construction of embankments of greater heights and steeper slopes
- It promotes uniform settlements
- It minimizes construction time and required space
- It increases bearing capacity and reduces settlements to a great extent
- It provides short and long term global stability to the embankment

Figure 5 shows the schematic diagram of the basal geocell layer used to support embankment construction over soft clay foundation. Application of geocells for constructing a rail road embankment on soft clay is shown in Figure 6.

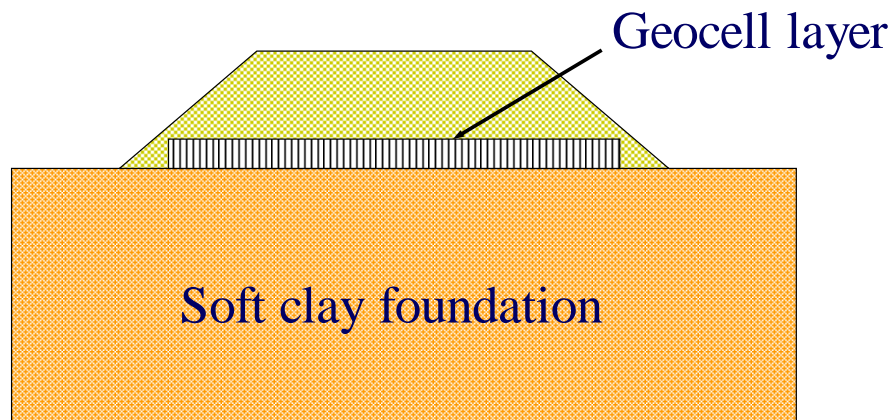


**Figure 5.** Geocell supported embankment



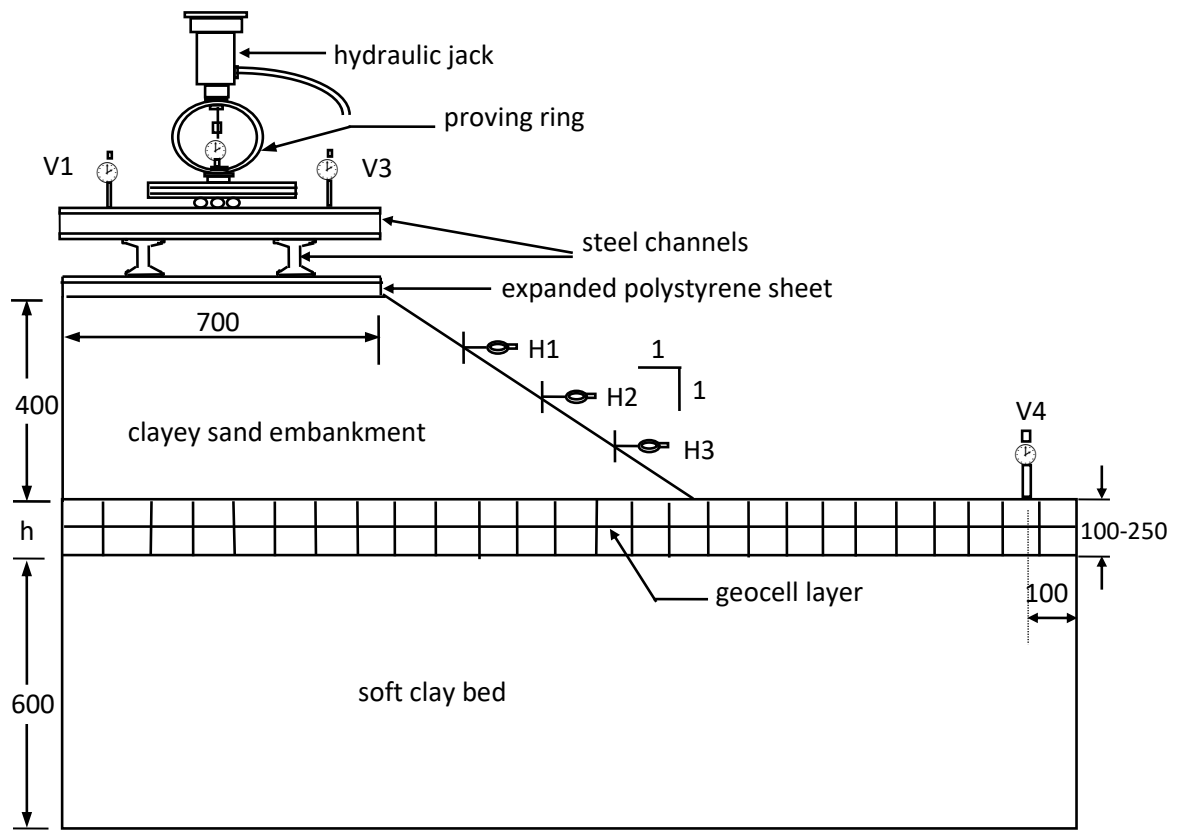
**Figure 6.** Geocells for constructing a rail road embankment on soft clay

A series of load tests on laboratory models of embankments constructed on soft clay foundation were carried out by Madhavi Latha (2000). Steel tank of plan dimensions 1800 mm  $\times$  800 mm and 1200 mm depth was fabricated for conducting the model tests on embankments. The tank was fitted with perspex sheet on one side to visualize the failure of

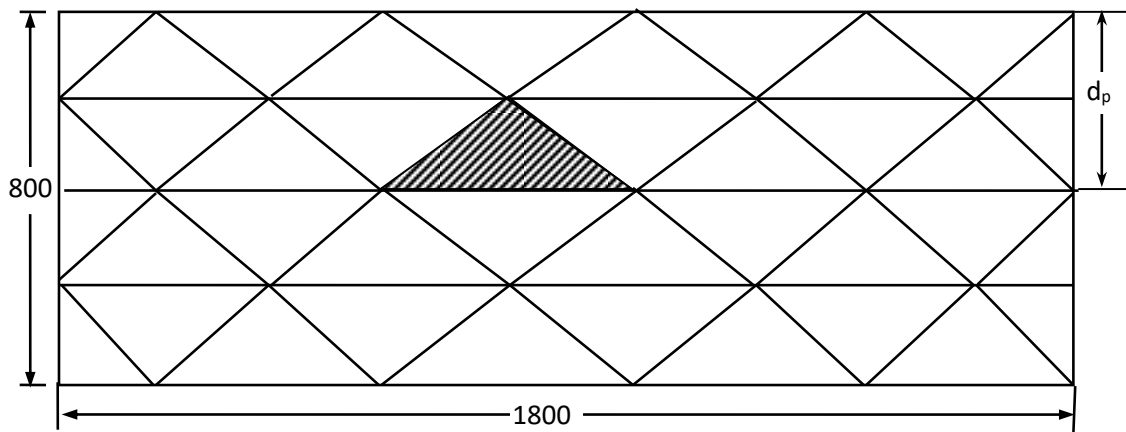
the embankment. The other three sides of the tank were made smooth and rigid to create plane strain conditions in the tank. Soft clay bed of 600 mm depth was prepared in this test tank. For this purpose, clay was mixed with excessive amount of water and consolidated under a surcharge pressure of 10 kPa. The bed was cured for one full week to achieve uniform properties of void ratio of 0.9 and density  $1.7\text{Mg/m}^3$ , which resulted in CBR value 0.5 and vane shear strength of 20 kPa.

After leveling the clay bed, a layer of geocells was formed on top of the clay bed. This was done by cutting the geogrids to required length and breadth from full rolls and placing them in transverse and diagonal directions with bodkin joints inserted at the connections. The tensile strength properties for various geogrids used in the model tests are determined from wide width tensile strength tests and presented in Table 2. The order of geogrids in the order of increase in their tensile strength/stiffness is NP-1, NP-2, BX and UX. After the formation of geocell layer, pockets of geocells were filled with soil and this soil was compacted using a steel rod. The unit weight of the infill soil was maintained at  $17\text{ kN/m}^3$  for all the tests. The compaction quality of this layer was verified by testing undisturbed core samples collected from at least six individual cells. Above the geocell layer, symmetrical half of the embankment was constructed using clayey sand in lifts. Each layer was compacted with calculated number of blows to achieve an average density of  $1.9\text{ Mg/m}^3$ . The properties of the soil in the constructed embankment, determined by taking undisturbed samples are given in Table 3. The embankments were subjected to uniform surcharge pressure on the crest until the failure. The physical dimensions of the embankment and the set up used to apply uniform surcharge on its crest are shown in Figure 7. The slip surfaces were observed to pass through the soft foundation soil with deeper slip circles for embankments with stiffer geocell reinforcement as shown in Figure 8. The soil beyond the embankment was observed to heave up as the embankment settled into the soft clay soil.

The vertical and horizontal deformations and the strains developed within the geocell layer were measured during the test. The influence of various parameters such as tensile stiffness of geogrids used to fabricate the geocell layer, height and pocket-size of geocell layer and the type of fill material inside the geocell on the behaviour of the embankments were studied in detail. Results from the tests on unreinforced and geocell supported model embankments indicated that the geocell reinforced embankments exhibited improved load carrying capacity and reduced deformations. Geocell reinforcement was found to be beneficial in pushing the failure envelope deeper, helping in mobilizing higher shear strength compared to the unreinforced embankment. The efficacy of the geocell layer mainly depended on the tensile modulus of the geocell material ( $M$ ) and the aspect ratio (height to diameter ratio) of geocells. Even clay-filled geocells provided moderate support to the embankment. As long as the dimensions and tensile modulus of the geocell material and infill soil remained the same, the pattern of geocell formation did not affect the performance of the embankment. Important findings from these studies are presented in Figure 9.



(a) Sectional Elevation



(b) Plan view

all dimensions are in mm

**Figure 7.** Test set-up of model embankment

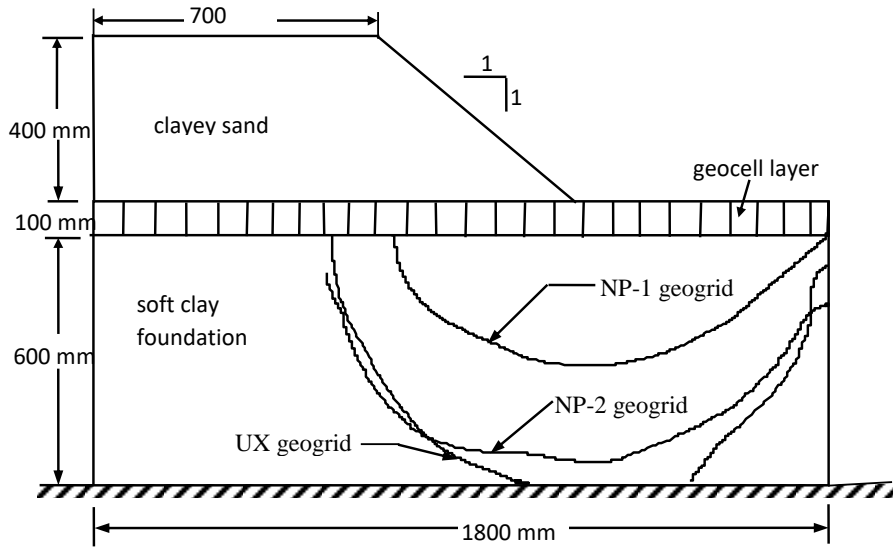


Figure 8. Failure surfaces observed in model embankments

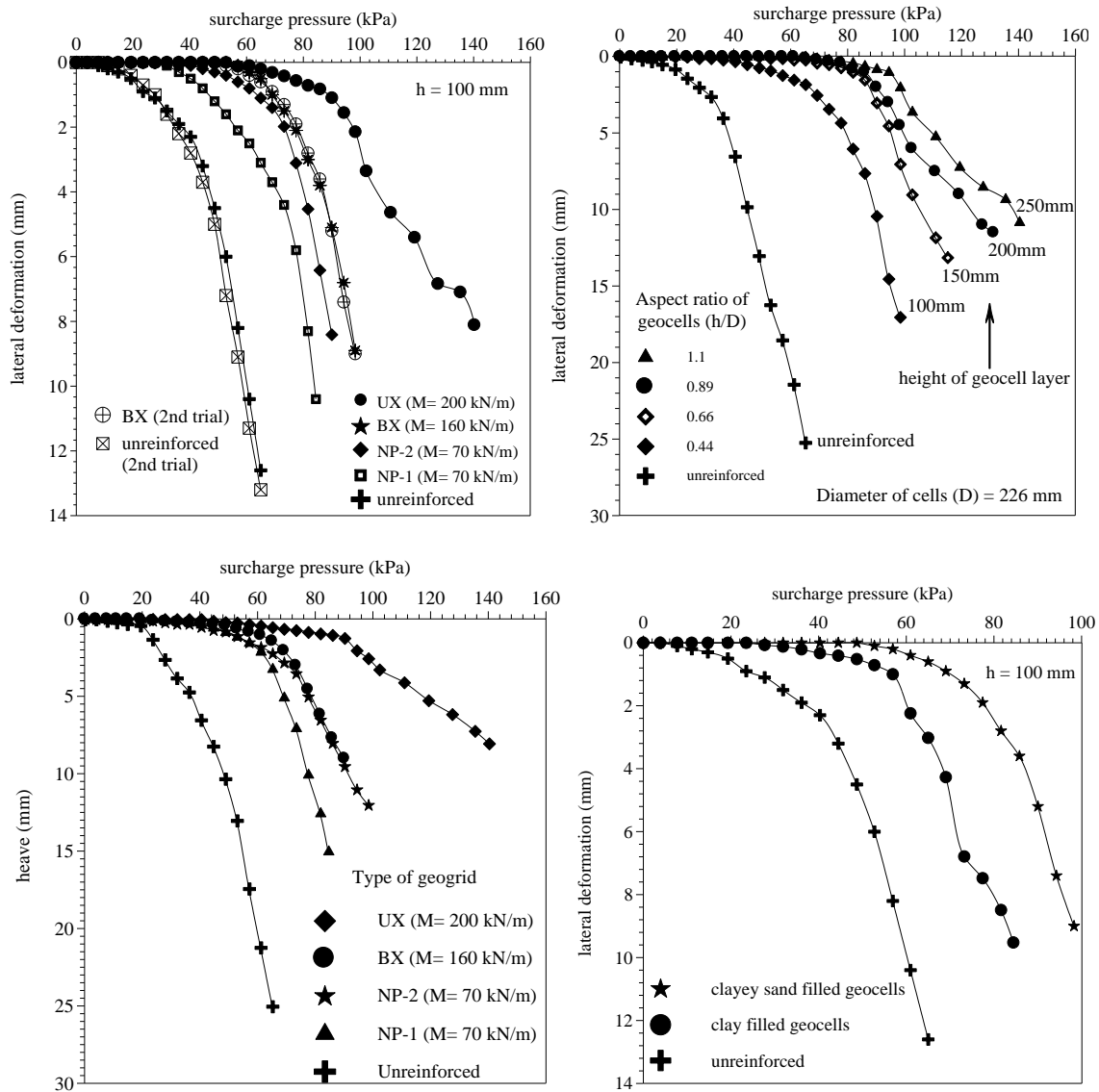


Figure 9. Results from the load tests on model embankments constructed on soft clay bed

### ***Guidelines for the Construction of Geocell Supported Embankments***

Based on the laboratory experiments and finite element simulations on geocell supported embankments, the following guidelines are suggested for the construction of these embankments on soft foundation soils (Madhavi Latha, 2000).

- A layer of planar geogrid has to be spread over the soft foundation soil layer to act as working platform for the formation of geocells and also to avoid penetration of cells into the soft soil.
- Granular soils are preferred for fill inside the geocells because the confinement effect is more pronounced in these soils, leading to greater reduction in overall deformations. However, in the absence of granular fill, locally available soils may also be used if found suitable from other considerations like drainage.
- Even the geogrids having moderate secant modulus (not less than 200 kN/m) may be used for forming the geocells as the influence of the modulus was found to be marginal beyond a limit of about 200 kN/m.
- Geogrids with large aperture openings offer lesser confinement to the soil. Very small aperture makes the geogrid unsuitable for the insertion of joints. The aperture size should be medium for achieving significant confinement effect and better interfacial friction along with ease in construction.
- A height to diameter ratio of 1.0 is recommended for the geocells. The height of the geocell layer could be determined from trial finite element analysis or other simple analyses such as slope stability analysis. In both the cases, the geocell layer could be treated as an equivalent composite soil layer.
- The geocells can be formed in either diamond or in the chevron patterns, both of which were observed to give similar performance.
- The geocell layer can be truncated at the toe of the embankment.

## **DESIGN METHODS FOR GEOCELL SUPPORTED EMBANKMENTS**

The methods of design available for geocell-supported embankments are very few. Two of them are discussed in detail in this document. The first method is the slip line method proposed by Jenner et al. (1988). The second method is based on slope stability analysis, proposed by Madhavi Latha et al (2006).

### ***Design Based on Slip Lines***

Jenner et al. (1988) suggested a method for designing geocells for supporting embankments. In this design, plastic bearing failure of the soil was assumed instead of slip circle failure. This type of failure was expected for embankments, whose width is more than four times the depth of the foundation soil. The methodology developed by Johnson and Mellor (1983) for the compression of a block between two rough, rigid plates was used for determining the bearing capacity of the soft foundation soil. The soft soil, which was analogous to the block, was assumed to get compressed between the geocell mattress at the top and the hard stratum at the bottom. This analogy was used for developing a non-symmetric slip line field in the soft foundation soil.

The concept of this design is that the geocell mattress exerts a degree of restraining influence on the deformation mechanism of the soft soil, thus rotating the direction of principal stresses. The direction of maximum shear stress also rotates correspondingly, pushing the failure surface deep in to the foundation soil. A  $15^\circ$  slip line field was used to determine the bearing resistance of the soft soil. Figure 10 shows the slip line field used in the design and corresponding bearing pressure diagram. The bearing capacity diagram was developed by working from the outer edge of the slip line field inwards to the boundary of the 'rigid head', defined on the slip line field by the ratio of geocell width to the depth of the soft layer. The 'rigid head' is term used to denote the soil zone, which remains in the active condition and so does not experience plasticity. Thus the slip line field is used to define the maximum allowable pressure distribution within a zone of limiting plasticity.

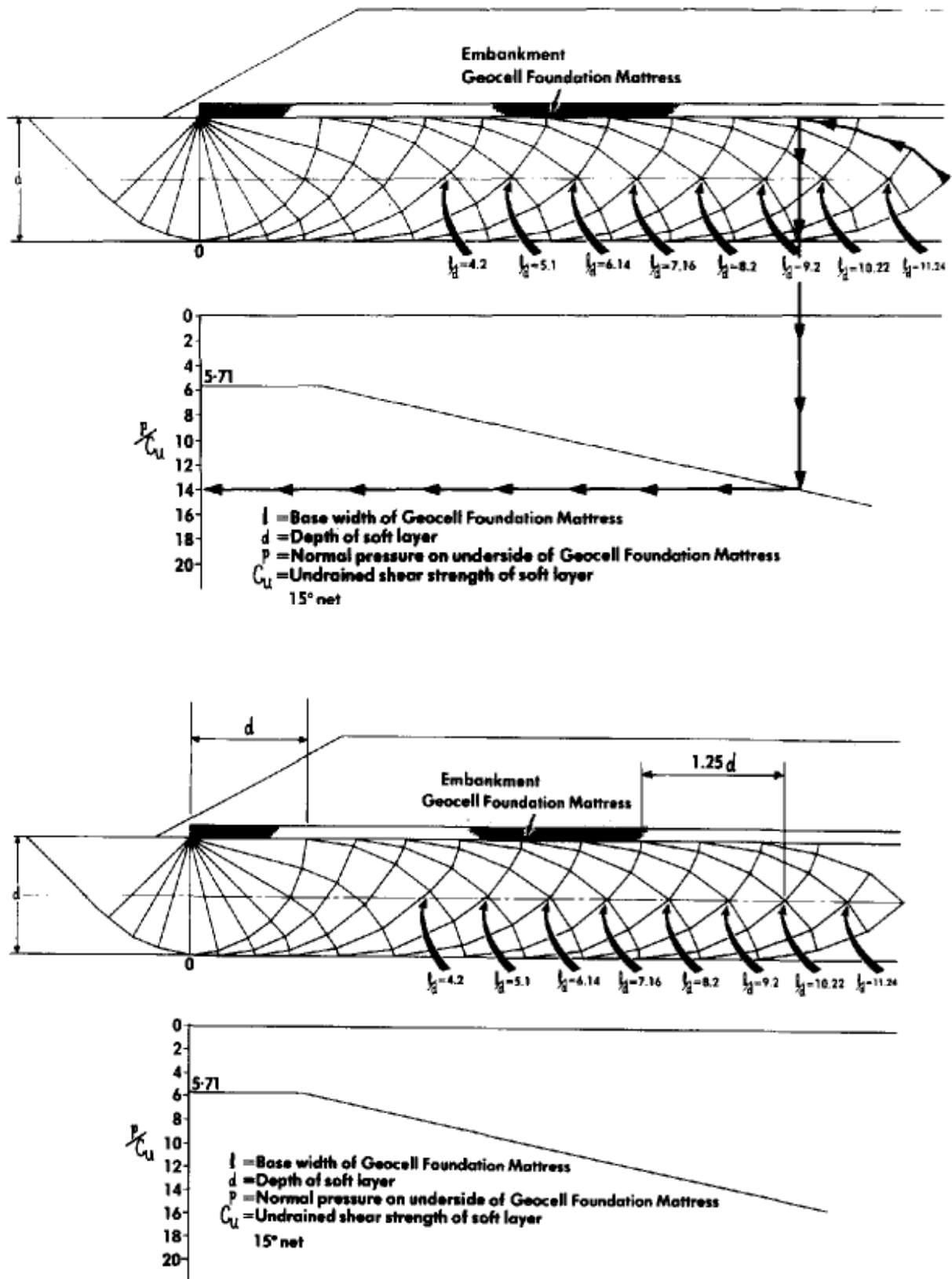


Figure 10. Method of design of geocell mattress for supported embankments  
(Jenner et al. 1988)

The stress distribution across the ‘rigid head’ can be determined by considering the rotations of each of the chords of the stress field bounding the rigid field. An average pressure across the rigid head can be calculated as

$$\frac{P'}{C_u} = \frac{2(2I + 0.5d)}{2X} + \frac{P}{C_u} \quad (1)$$

where  $P/C_u$  is the value read from the stress field at the extreme end of the rigid head

$P'$  is the average stress over the rigid head

$I = \Sigma(\text{horizontal chord lengths} \times \text{rotation})$

$X = \Sigma(\text{horizontal chord lengths})$

$d = \text{depth of soft soil layer}$

A typical calculation of average stress across the rigid head for the slip line field shown in Figure 11 is given in Table 1.

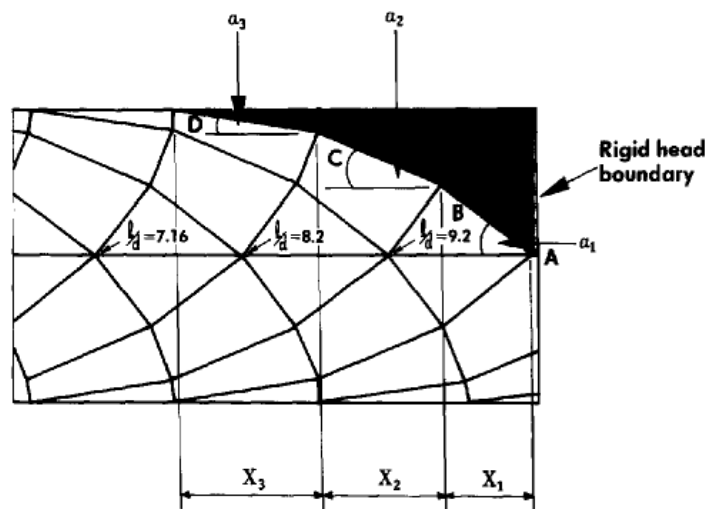


**Figure 11.** Conditions across rigid head boundary

Table 1. Calculation of average stress over ‘rigid head’

	Slip line			
	A-B	B-C	C-D	A-D
Chord	$X_1 = 1.6$	$X_2 = 2.2$	$X_3 = 2.6$	$X = 6.4$
Rotation (deg.)	$a_1 = 37.5^\circ$	$a_2 = 22.5^\circ$	$a_3 = 7.5^\circ$	
Rotation (radians)	0.654	0.395	0.431	
Chord $\times$ rotation	1.05	0.86	0.34	$I=2.25$

From Table 1,

$$\frac{P'}{C_u} = \frac{2(2 \times 2.25 + 0.55)}{2 \times 6.4} + \frac{P}{C_u} = 1.094 \frac{P}{C_u} \quad (2)$$

Hence the additional resistance due to the average pressure across the rigid zone can be taken as  $C_u$ . This value can be applied for all ratios of width of the geocell mattress to a depth of soft layer greater than four. For values less than four, the additional resistance over the rigid head will be greater and should be calculated for each case. The bearing capacity diagram can be drawn as shown in Figure 12.

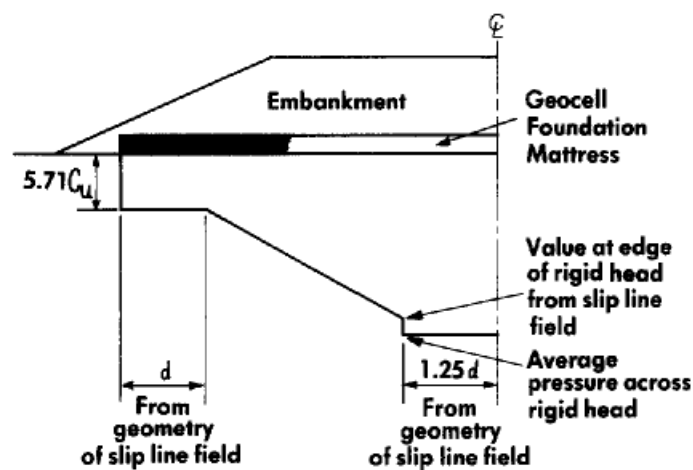


**Figure 12.** Bearing capacity diagram

The allowable bearing capacity is now checked against the overburden stresses and the factor of safety against bearing capacity failure is calculated. If the factor of safety is less than one, the following options can be considered (Bush et al., 1990).

- Adding a steep sided berm to the outer edge of the original embankment to cause additional downward pressure on the outer passive wedge thus increasing the overall bearing capacity of the foundation
- Increasing the strength of soft foundation soil due to consolidation can be used in the analysis as the geocell layer filled with granular soil acts as excellent drainage blanket and allow for the quick strength gain in soft soil during construction.
- Constructing embankment in stages, the height in each stage is a limit equilibrium height corresponding to the strength of soft soil at that stage.

## DESIGN EXAMPLE 1

It is proposed to construct a 6 m high embankment over 6 m thick layer of soft cohesive soil with undrained shear strength of  $15 \text{ kN/m}^2$ . The cross section of embankment is shown in Figure 13. A surcharge of  $20 \text{ kN/m}^2$  will be applied. Design suitable geocell mattress for this case.

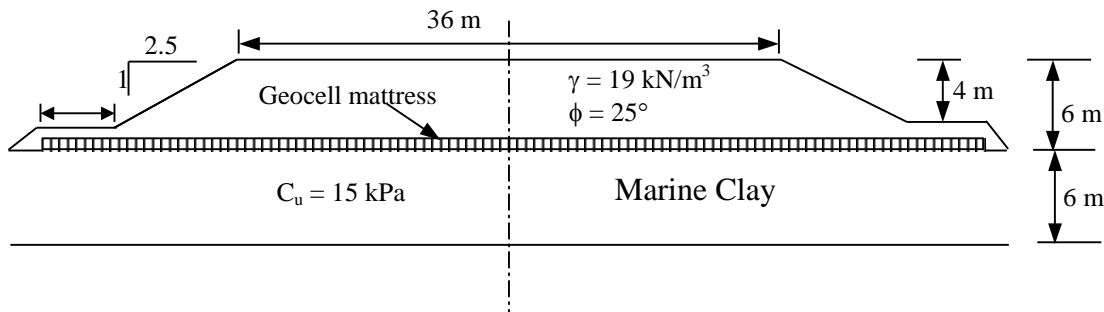


**Figure 13.** Cross section of the embankment in design example 1

To design a geocell mattress for the above problem, slip line method can be adopted as follows:

Embankment base width = 66 m

Width of geocell mattress =  $66 \text{ m} - 4 \text{ m}$  (leaving 2 m offset either side) = 62 m

Width of geocell/depth of soft soil layer =  $62/6 = 10.33$

From stress field diagram shown in Figure 1,  $P/C_u = 12$

Average pressure across rigid head  $P' = 12 C_u + C_u = 13 C_u$

Hence the bearing capacity diagram can be drawn as shown in Figure 14.

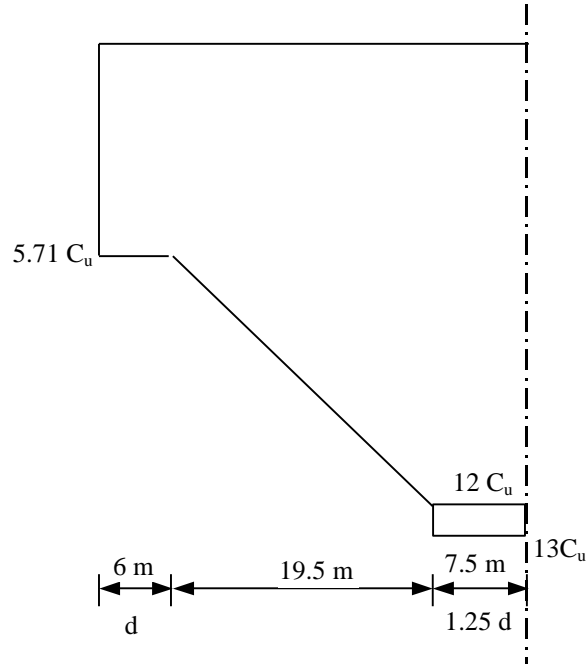


**Figure 14.** Bearing capacity diagram for the design example

Load from the embankment allowing a surcharge pressure of 20 kN/m<sup>2</sup>:

$$(18+28)/2 \times 4 \times 19 + (18 \times 20) + 33 \times 2 \times 19 = 3362 \text{ kN/m}^2$$

Bearing capacity from the pressure diagram :

$$6 \times 5.71 C_u + (5.71+12)/2 \times C_u \times 19.5 + 7.5 \times 13 C_u = 304.43 C_u$$

$$C_u \text{ required for equilibrium} = 3362/304.43 = 11.04 \text{ kN/m}^2$$

$$\text{Actual } C_u = 15 \text{ kN/m}^2$$

Factor of safety against bearing capacity failure = 15/11.04 = 1.35 (against 1.25 required).

Hence safe.

For designing the geocell mattress, consider an element of soil within the granular cellular mattress, but interfacing with the soft layer. The stress condition in element can be obtained from a Mohr-circle construction as shown by Jenner et al (1988).

The horizontal stress on the element:

$$\sigma_h = \sigma_n - 2x \quad (3)$$

Where  $\sigma_n$  is the vertical stress on the element.

$$x = \frac{2\sigma_n \sin^2 \phi' \pm \left[ 4\sigma_n^2 \sin^4 \phi' - 4(\sin^2 \phi' - 1)(\sigma_n^2 \sin^2 \phi' - \tau^2) \right]^{1/2}}{2[\sin^2 \phi' - 1]} \quad (4)$$

$\tau =$  shear stress at the interface =  $C_u$  in limiting condition =  $11.04 \text{ kN/m}^2$

$\sigma_n$  under highest part of the embankment =  $6 \times 19 + 20 = 134 \text{ kN/m}^2$

$\phi = 40^\circ$  for the geocell fill material

$\therefore x = 51.36 \text{ kN/m}^2$

$\therefore \sigma_h = \sigma_n - 2x = 134 - 2 \times 51.36 = 31.28 \text{ kN/m}^2$

The rotation of principal stress occurs within the mattress depth. Therefore mattress strength required =  $31.28 \text{ kN/m}$ . Hence a geocell mattress with long term tensile strength more than  $31.28 \text{ kN/m}$  should be used to support the embankment, with a geogrid base.

### ***Design Based on Slope Stability Analysis***

This method uses a general-purpose slope stability program to design the geocell mattress of required strength for embankment. The computer program developed for conducting slope stability analysis of geocell supported embankments reads the slope parameters, height of geocell layer, depth of foundation soil, shear strength parameters of embankment soil and geocell layer, properties of foundation soil, pore pressure co-efficient and the value of uniform surcharge pressure on the crest. The program uses Bishop's method of slices for calculating the factor of safety. The program automatically searches different trial slip circles and gives the minimum factor of safety and coordinates of the center of the critical slip circle. The reliability of the computer program was ensured by running some example problems. The factor of safety obtained from the program was in agreement with the minimum factor of safety obtained from graphical construction.

For designing geocell mattress below an embankment, geocell layer is treated as a layer of soil with cohesive strength greater than the encased soil and angle of internal friction same as the encased soil. This is because; geocells provide all-round confinement to the soil due to the membrane stresses in the walls of geocells, because of which apparent cohesion is developed in the soil. Using the rubber membrane theory proposed by Henkel and Gilbert (1952), Bathurst and Karpurapu (1993) analyzed the cohesive strength of soil encased in a single geocell in triaxial compression. The same analysis was extended for multiple geocells and also for geocells made of geogrids by Rajagopal et al. (1999) and Madhavi Latha (2000).

Later Latha and Murthy (2007) applied the same analysis to quantify the strength and stiffness of geocell reinforced sand. Equations developed from the above analyses can be used for estimating the cohesive strength of a layer of geocells. In case of geocells made of geogrids, if we consider individual cells, the soil is not fully confined as in case of geocells made of geotextile, because of apertures in geogrids. However, during loading, the soil in each geocell is subjected to lateral confinement due to interaction mechanism between cells. The validity of equations for cohesive strength based on rubber membrane theory for geocells made of geogrids was verified by Rajagopal et al. (1999) and Madhavi Latha (2000) by testing soil encased in geocell made of open mesh.

The additional confining pressure due to the membrane stresses can be written as (Henkel and Gilbert 1952),

$$\Delta\sigma_3 = \frac{2M\varepsilon_c}{D} \frac{1}{(1-\varepsilon_a)} = \frac{2M}{D_o} \left[ \frac{1-\sqrt{1-\varepsilon_a}}{1-\varepsilon_a} \right] \quad (5)$$

where  $\varepsilon_a$  is the axial strain at failure,  $\varepsilon_c$  is the circumferential strain at failure,  $D_o$  is the initial diameter of sample,  $D$  is the diameter of the sample at an axial strain of  $\varepsilon_a$  and  $M$  is the modulus of the membrane.

The above equation was used to calculate the additional confining pressure due to geocell reinforcement, using the parameters as follows.  $D_o$  was taken as the initial diameter of geocell. The geocell pockets are not circular but are triangular in shape. The equivalent diameter for the triangular shaped geocells can be obtained by equating the area of the triangle to a circle of equivalent area.  $M$  is the modulus of the geocell material at axial strain  $\varepsilon_a$ , determined from the load-strain curves obtained from wide width tensile strength test on geogrids.

The relation between the induced apparent cohesive strength and the additional confining stress due to the geocell can be derived by drawing Mohr circles for the unreinforced and reinforced soil samples as shown in Figure 15.

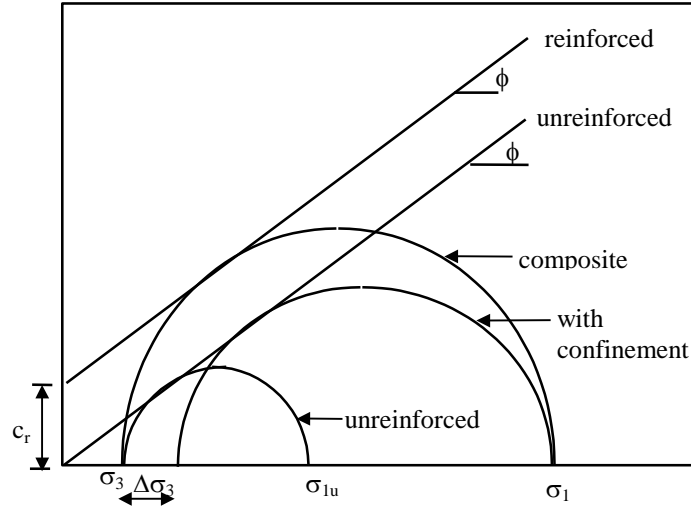


**Figure 15.** Mohr circles for calculating the strength improvement due to geocell reinforcement

From Mohr-Coulomb failure theory, the ultimate stress on soil sample can be calculated by considering the soil as a composite as (large circle)

$$\sigma_1 = k_p \sigma_3 + 2c_r \sqrt{k_p} \quad (6)$$

In which  $k_p$  is the coefficient of passive earth pressure. If the same is considered as an unreinforced soil with an additional confining stress of  $\Delta\sigma_3$ , the failure stress can be calculated as

$$\sigma_1 = k_p (\sigma_3 + \Delta\sigma_3) \quad (7)$$

Equating (6) and (7), the additional cohesive strength due to geocell layer can be obtained as

$$c_r = \frac{\Delta\sigma_3}{2} \sqrt{k_p} \quad (8)$$

Substituting the value of  $\Delta\sigma_3$  obtained from equation (5) in equation (8), we will get the apparent cohesion induced to soil due to geocell confinement. This additional cohesive strength is added to the original cohesive strength of soil encased in geocells to get the cohesive strength of geocell layer ( $c_g$ ).

For preliminary design problems, if the geometry of the embankment, properties of foundation and embankment soils are given, we can perform slope stability analysis with trial values of height of geocell layer and determine the cohesive strength of geocell layer required to get a design value of factor of safety. From this cohesive strength, we can back calculate the modulus of geocell required for assumed values of pocket-size of geocell and axial strain in the walls of geocell.

This design method has been verified for the case of geocell supported model embankments constructed in laboratory with varying pocket sizes of cells, varying height of geocell mattress, for geocell layers made of different geogrids and for sand and clay infill materials by Madhavi Latha et al. (2006). It was observed that the maximum surcharge pressure at which the embankments failed in the model tests was agreeing well with the surcharge pressure at which the factor of safety was obtained as one in the slope stability analysis.

## DESIGN EXAMPLE 2

It is proposed to construct a 4 m high embankment over a 6 m thick layer of soft cohesive soil having undrained shear strength of 15 kPa. A surcharge of 55 kPa will be applied. The embankment soil has got cohesion of 12 kPa and angle of internal friction of  $35^\circ$ . Find out the type and configuration of geocells needed to achieve a desired factor of safety of 3. Cross-section of the embankment in given problem is shown in Figure 16. From slope stability analysis of unreinforced embankment, the minimum factor of safety was obtained as 0.633. The center of critical slip circle was obtained as (7.975, 15.983).

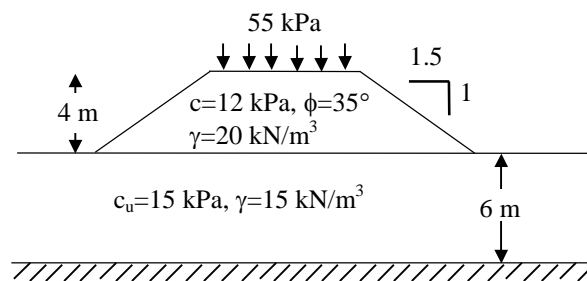


**Figure 16.** Cross-section of the embankment in design example 2

Assuming that the embankment soil itself will be used as fill material inside the geocells and the height of geocell layer is 2 m, geocell layer will have angle of internal friction of  $35^\circ$ . By

conducting slope stability analysis with trial values of cohesion of geocell layer, for a factor of safety of one, the cohesive strength of geocell layer ( $c_g$ ) was obtained as 30 kPa. As the fill soil has original cohesive strength of 12 kPa, additional cohesive strength to be derived from geocell reinforcement ( $c_r$ ) is 18 kPa. For a  $\phi$  value of  $35^\circ$ ,  $k_p$  is 3.69. Substituting the values of  $c_r$  and  $k_p$  as 18 kPa and 3.69 in equation (8),  $\Delta\sigma_3$  is obtained as 18.7 kPa.

Assuming that the axial strain in geocell wall is 5% and the pocket-size of the geocell layer is 1 m, equivalent diameter of cells is calculate as 0.564 m. Substituting the values of  $\Delta\sigma_3$ ,  $D_0$  and  $\varepsilon_a$  in equation (5),  $M$  is obtained as 200 kN/m. Thus a geocell layer of 2 m height and pocket size of 1 m with geocells made of geogrids having secant modulus at 5% strain ( $M$ ) as 200 kN/m could be provided at the base of the given embankment to achieve a factor of safety of three against bearing capacity failure.

### 3. GEOCELL RETAINING WALLS AND SLOPES

Stacking of geocell layers to create retaining walls and slopes has solved several issues like space constraints and complicated designs by allowing flexible design patterns with multifold increase in the load carrying capacity of these structures. Geocell walls are extremely flexible and hence the deformations are independent in each layer to an extent, thus avoiding cumulative deformations piled up at the top of the wall as seen in case of rigid retaining walls. Schematic diagram of a typical geocell retaining walls are shown in Figure 17 and a finished geocell retaining wall is shown in Figure 18.

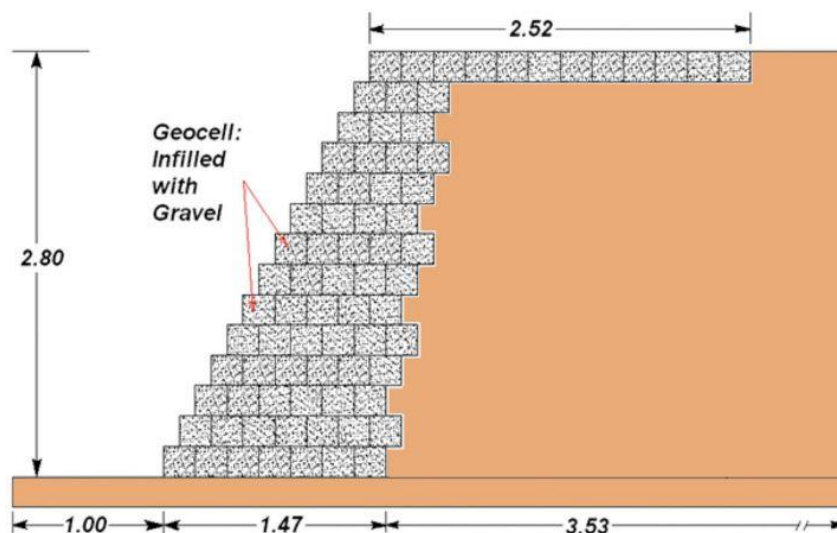


**Figure 17.** Schematic diagram of geocell retaining wall



**Figure 18.** Finished geocell retaining wall

Geocell walls are found to be extremely stable against seismic loads because of their flexibility and wider facia that can render stability against sliding and overturning. Systematic shaking table studies are carried out at Indian Institute of Science, on the seismic response of geocell retaining walls, especially to study their acceleration and displacement response affected by various levels of ground motion parameters. Tensile strength of geocell material is scaled down to suit the similitude requirements of the model tests, keeping in view of the range of tensile strength of geocells typically used in field. Figure 19 shows the photograph of a typical geocell wall tested in shaking table (Latha and Manju, 2016).

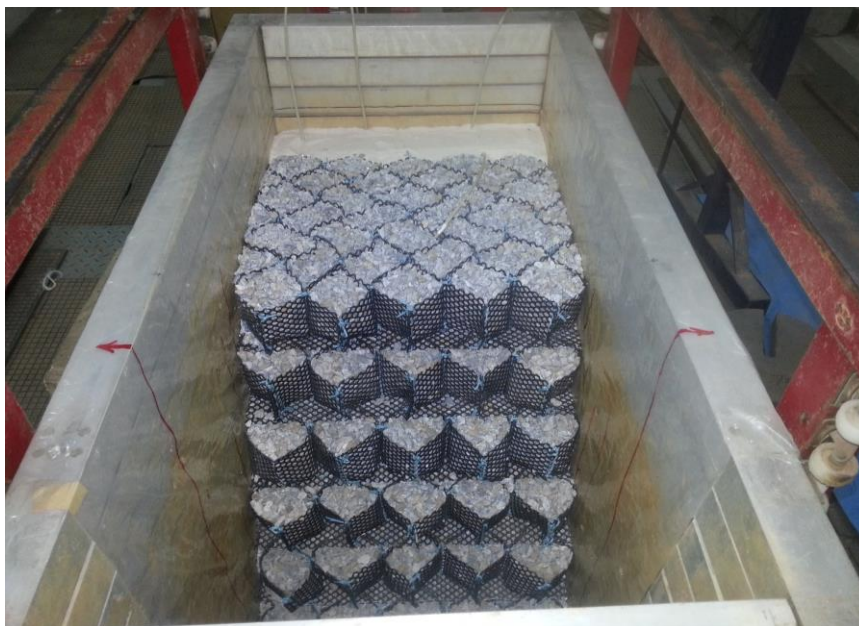


**Figure 19.** Typical geocell wall constructed in a laminar box

The stability of the geocell wall increases with the increase in the number of fascia cells. Figure 20 shows the reduction in displacements of the wall with the normalized height, when subjected to ground motion of acceleration amplitude 0.3g at different frequencies 1,2,3 and 7 Hz in different tests (S1A3F1, S1A3F2, S1A3F3, S1A3F7, S2A3F1, S2A3F2, S2A3F3, S2A3F7), S1 representing 4 fascia geocells, S2 representing 2 fascia geocells, F1-F7 representing frequency range.

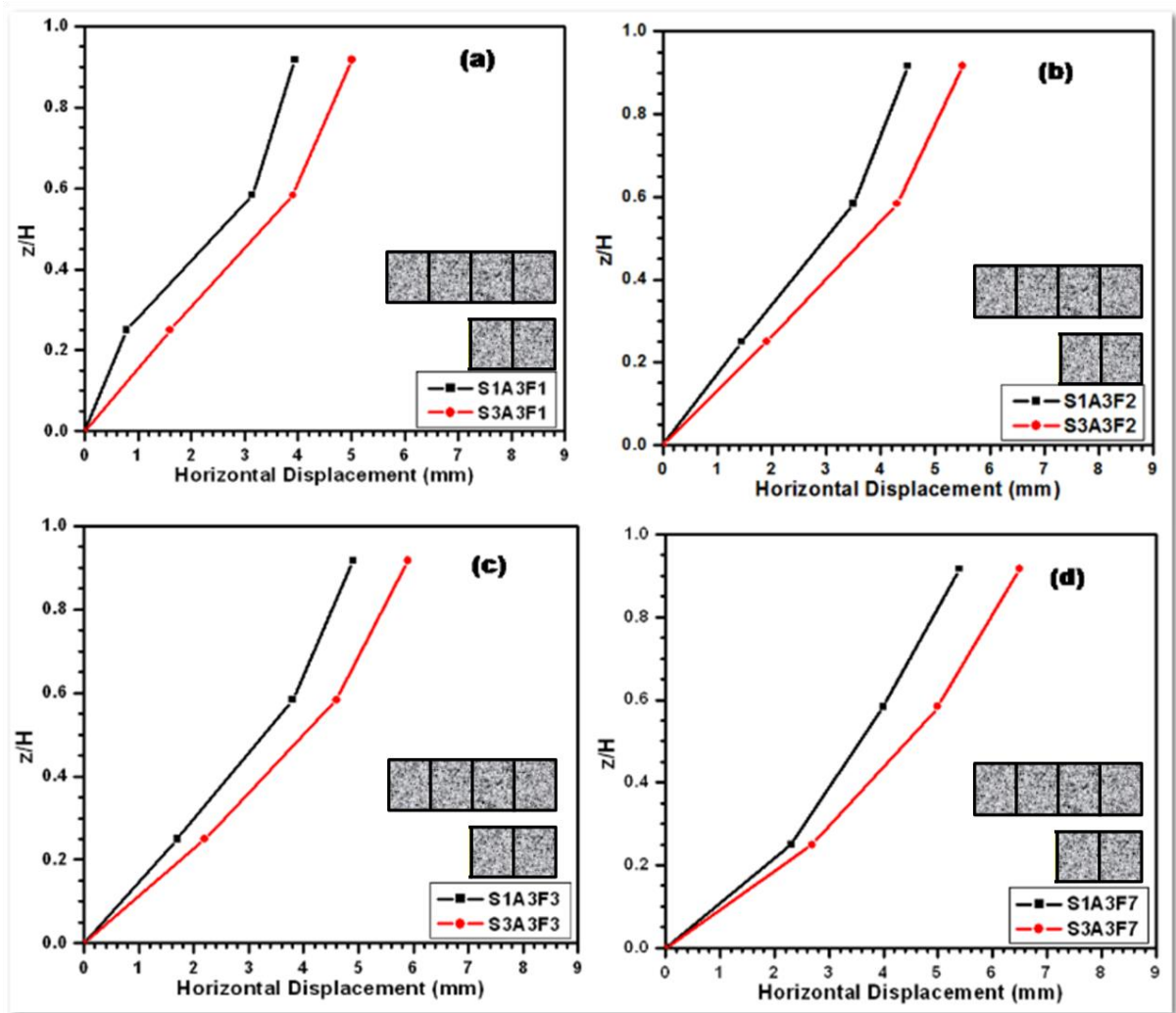


**Figure 20.** Effect of geocell configuration on wall deformations a) 1 Hz b) 2 Hz c) 3 Hz d) 7 Hz (After Latha and Manju, 2016)

#### 4. GEOCELL SUPPORTED FOUNDATIONS

It is the pioneering work of Binquet and Lee (1975) that marked the beginning of systematic research in the field of reinforced earth beds. Subsequently many researchers have reported

the beneficial effects of using soil reinforcement on the performance improvement of shallow foundations. Geocell reinforcement for foundation strengthening has gained lot of attention in recent times. Geocell mattresses provided below the foundation are proved to be effective in distributing the load over larger area compared to other forms of reinforcement and it is established that the bearing capacity can be improved as much as five times by using geocell reinforcement. Increase in lead bearing capacity of sand beds with geocell reinforcement is studied by Latha and Somwanshi (2009). Figure 21 shows the schematic diagram of geocell reinforced foundation bed.

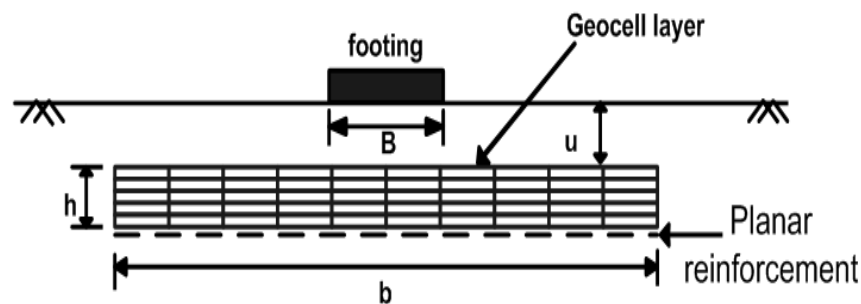


**Figure 21.** Schematic of the model footing on geocell reinforced earth bed

It is well established through laboratory and field studies that among the different forms of geosynthetics, geocell is usually the compact form, which provides better bearing capacity for a foundation bed by providing allround confinement and distributing loads over a larger are. A geosynthetic material, when used in different forms like planar layers, geocells or discrete elements, gives different strength improvements though the quantity of material is same. The mechanism by which the strength is improved varies in different forms. In planar layers and discrete elements, strength improvement is mainly due to friction. Interlocking also adds up to the strength if the material has apertures to hold the soil grains. Randomly oriented reinforcing elements coil around the soil particles which will be additional advantage in some cases. In case of geocells, in addition to the friction and interlocking, allround confinement effect imparts additional strength to the encased soil. A study is undertaken by Latha and Somwanshi (2009) to compare the performance of different forms of geosynthetic reinforcement (i.e. geocell, planar layers and randomly distributed mesh elements) in improving the bearing capacity of square footings and reducing the deformations for exactly same quantity of material. A photograph of polypropylene made geosynthetic material used in different forms for supporting foundation loads is shown in Figure 22.

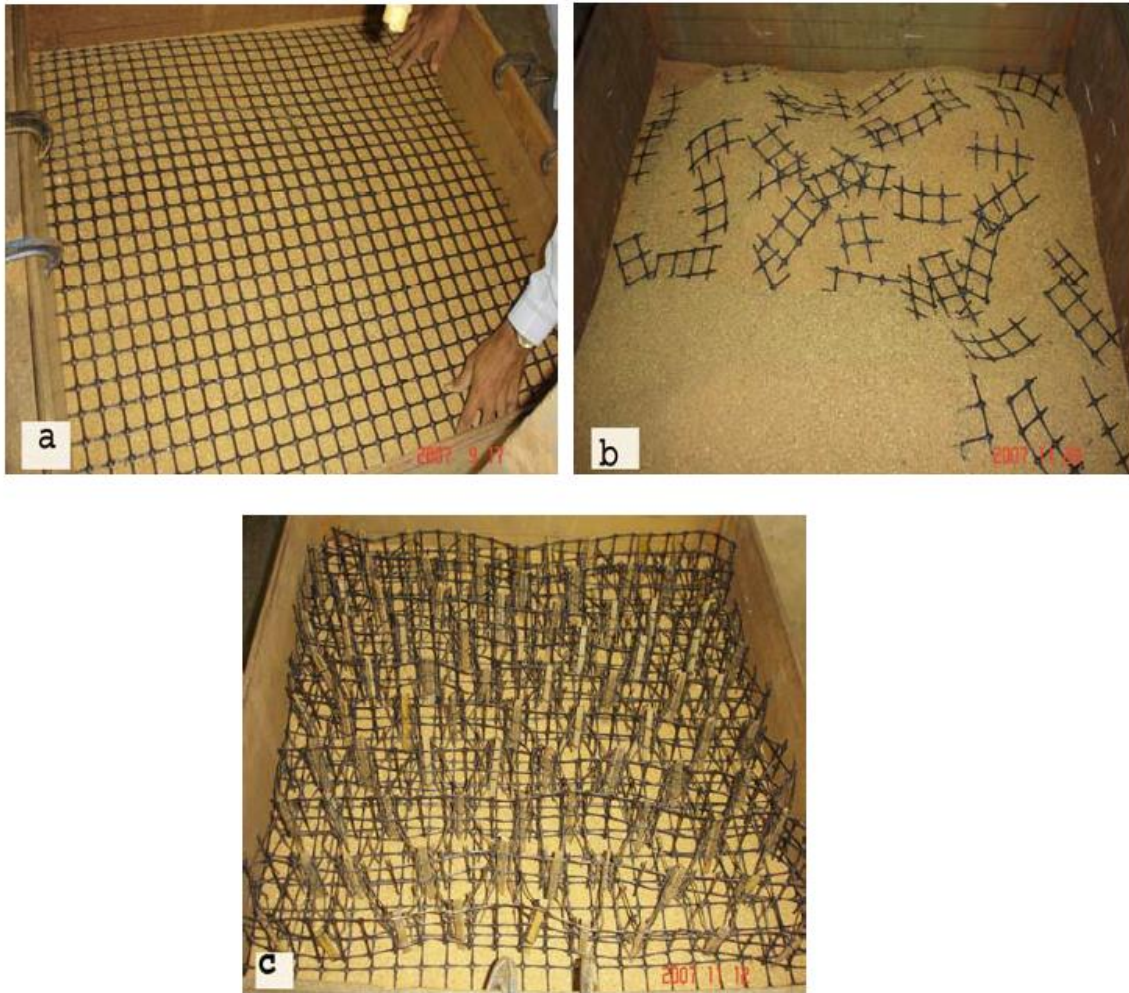


**Figure 22.** Geosynthetics in different forms used for reinforcement: (a) planar layers, (b) randomly distributed mesh elements and (c) geocell layer

Results of model tests carried out on unreinforced sand beds and sand beds reinforced with planar geosynthetics, random fibres and geocells are compared in Figure 23. Sand bed with geocell reinforcement did not show a clear failure even at a large settlement equal to about 35% of the footing width as shown in Figure 23. The response is almost linear up to much larger settlements of about 13% of the footing width. The footing with geocell reinforcement carried load as high as five times the ultimate capacity of footings on unreinforced soil. The footing settlement of 20-30% does not truly represent the possible field situation. However, the tests were continued beyond this settlement so as to show that even at this higher settlement, the load applied is well below the bearing capacity of the footing. At settlements lower than 10% of the footing width, the geocell layer performed almost on par with the planar reinforcing layers.

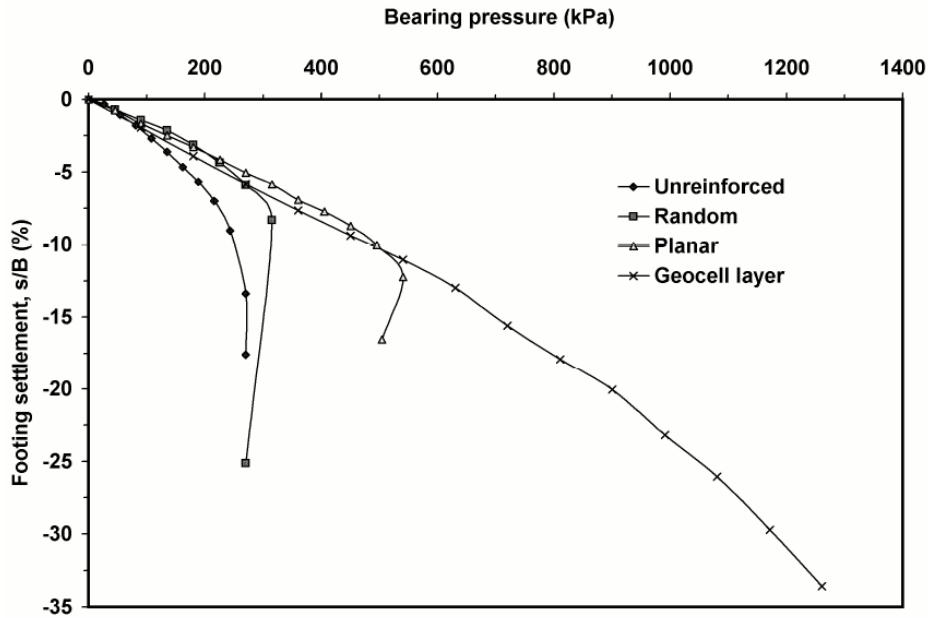


**Figure 23.** Variation of bearing pressure with footing settlement for different forms of biaxial grid reinforcement

The extremely high load bearing capacity exhibited by the footing on geocell layer is probably the result of three factors. First, the geocell mattress due to its cellular structure contains and confines the sand more effectively. As a result a better composite material is formed, which helps to redistribute the footing load over a wider area. Second, geocell reinforcement system acts as an interconnected cage and derives anchorage from both sides of loading area, due to friction and passive resistance developed at the soil/geocell interfaces. Further, because of shear and bending rigidity of the geocell layer, the footing load is carried even after shear failure of the sand inside the geocell pockets beneath footing. Third, the planar layer below geocell mattress resists the downward movement of soil due to footing penetration. In contrast, planar reinforcement layers underwent pullout failure leading to abrupt failure while much of its tensile strength remains immobilized.

## 5. GEOCELL REINFORCED SUBGRADES

Geosynthetics can be effectively used to reinforce road subgrades in soft soils. In general, the geosynthetic layer is placed at the interface of the subgrade and the aggregate base. Sometimes, additional layers are placed within the base course and above the base course to provide extra support to the wheel loads. Geosynthetics can have one or more of the following functions when used for in the construction of roads: separation, filtration, drainage

and reinforcement. Compared to the unreinforced unpaved road, the presence of geosynthetic reinforcement can provide the following benefits:

- Reduction of fill thickness
- Separates aggregate from soft soil if a geotextile is used
- Increases soft soil bearing capacity
- Reduces fill lateral deformation
- Generates a more favorable stress distribution
- Widens the spreading of vertical stress increments
- Reduces vertical deformation due to membrane effect
- Increases the lifetime of the road
- Requires less periodical maintenance
- Reduces construction and operational costs of the road

The following sections briefly describe various laboratory triaxial tests, model plate load tests and field tests carried out on geocell reinforced unpaved road sections and the important observations from these studies.

### **Large Diameter Cyclic Triaxial Tests**

Cyclic loading resistance of geocell reinforced aggregate systems was investigated by Nair and Latha (2014) through large diameter cyclic triaxial tests. Aggregates of different size ranges were mixed in calculated proportions by weight to obtain the gradation specified for rural roads. Triaxial samples of 300 mm diameter and 600 mm height were prepared using this sampled aggregate. The strength and stiffness characteristics of this aggregate inside a geocell made of woven geotextile at different elevations were determined from static and cyclic triaxial tests. The results were compared with the tests using planar geogrid reinforcement. Fig. 24 shows the failure patterns observed in these tests.

Aggregate reinforced with planar geogrids bulged between the layers but the geocell encasement could arrest the bulging. Even a geocell of low seam strength of 7.5 kN/m could provide an increase in confining pressure of 7 kPa for a large diameter triaxial sample.

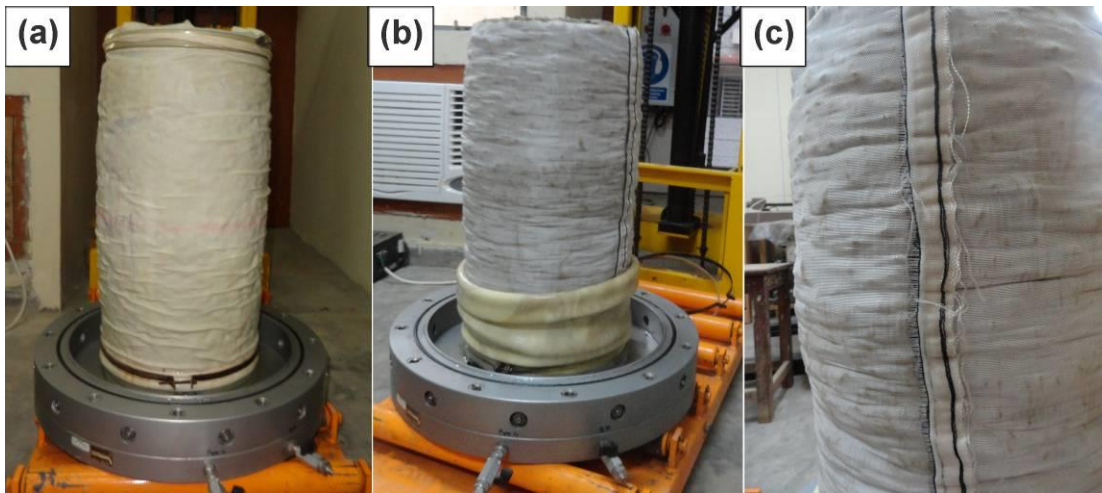


**Figure 24.** Failure modes for samples reinforced with  
 (a) 4 layers of biaxial geogrid and (b, c) geocell

### **Model Plate Load Tests**

Nair and Latha (2015) carried out plate load tests on model pavement sections reinforced with planar and cellular geosynthetic systems. Granular sub-base was constructed over clayey subgrade in a steel tank to simulate field condition. Geogrid and geocell reinforcements were used in the studies. Repeated loading was applied on these unreinforced and reinforced sections to understand the resilient behaviour of these systems. The effect of type, form and position of reinforcement in reducing plastic settlements was also investigated through these experimental studies. The influence of aspect ratio of geocell reinforcement on elastic and plastic strains is also studied. These model studies were carried out in a steel tank of 750 mm × 750 mm cross section and 620 mm height. Load is applied through a circular steel plate of 150 mm diameter and 10 mm thickness. The size of the plate was selected such that there will be no interference with the boundary. A manually operated hydraulic jack of 100 kN capacity was used to push the loading plate to the fill and the applied load was measured using a load cell of 10 kN capacity. Schematic sketch of the experimental set-up is shown in Fig. 25.

Locally available red soil was used, classified as clay of low plasticity (CL) is used as subgrade in the experiments. The red soil used showed maximum dry unit weight of 18.24 kN/m<sup>3</sup> at an optimum moisture content of 15.5% in a standard Proctor test. The subgrade soil had an unsoaked CBR value of 19% at optimum moisture content and maximum dry unit weight corresponding to standard Proctor effort. Granular material of various size ranges was

collected and sampled such that it conformed to Grading III of granular sub-base design as given by IRC (2004). In all the reinforced tests, to prevent the intermixing of granular sub-base with the subgrade a geotextile layer was placed at the interface. The various types of reinforcing materials used in the experiments are strong and weak geogrids and geocells.

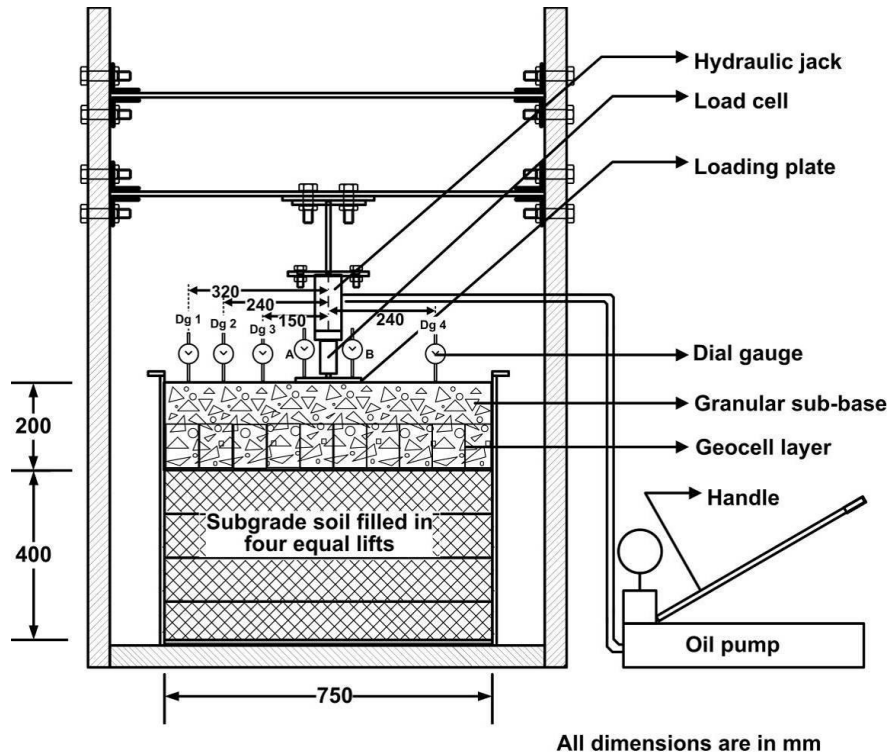


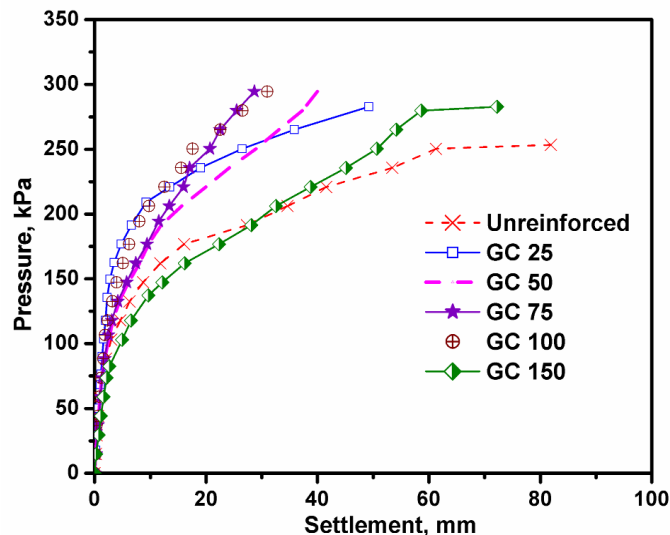
**Figure 25.** Schematic sketch of the experimental set-up of Nair and Latha (2015)

Commercially available geocells were used to reinforce the granular base. Five different heights of geocell reinforcement were used in the experiments viz., 25 mm, 50 mm, 75 mm, 100 mm and 150 mm. Out of this 75, 100 and 150 mm heights were commercially available. Higher height geocell samples were cut to have 25 and 50 mm height geocell samples. Based on the height of geocell used to reinforced granular sub-base they are designated as GC 25, GC 50, GC 75, GC 100 and GC 150. For granular sub-base reinforced with 75 mm high geocell, the position of the geocell was also varied in three of the tests. Photograph of aggregate being filled in commercially available geocell sample is shown in Fig. 26. The total weight of granular sub-base used for filling the 200 mm height was 186 kg in both unreinforced and reinforced cases.



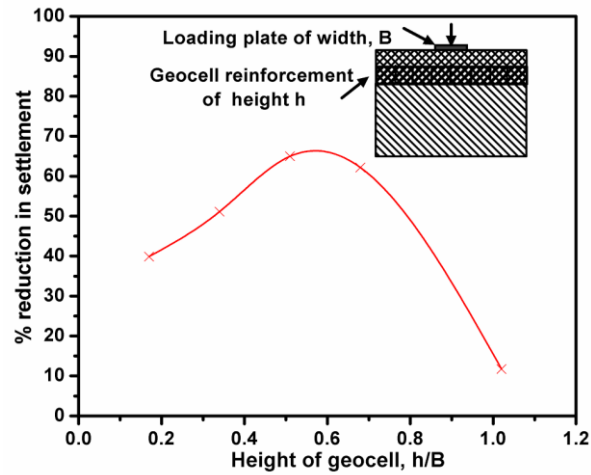
**Figure 26.** Photograph of aggregate being filled in geocell pockets

Repeated load tests were carried out on models of geocell reinforced pavement sections. All the reinforced systems showed punching failure and the pressure-settlement response corresponding to the first loading stage of unreinforced and geocell reinforced sections is shown in Fig. 27.



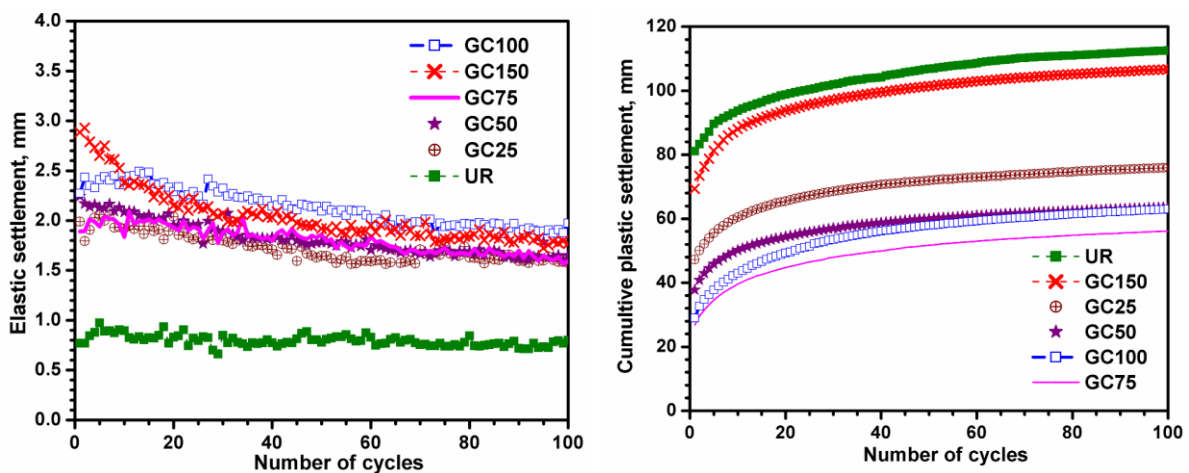
**Figure 27.** Pressure versus settlement for unreinforced and geocell reinforced sections

Fig. 28 shows the variation of percentage reduction in settlement (PRS) with height of geocell reinforcement. From the figure it is seen that when the height of geocell reinforcement is increased from 25 mm to 150 mm initially the PRS increased and the maximum reduction in settlement is observed for geocell of 75 mm height. On increasing the height of geocell beyond 75 mm PRS decreased which implies that those sections developed enormous settlements.



**Figure 28.** Percentage reduction in settlement with height of geocell

The effectiveness of geocell reinforcement is compared in terms of elastic and cumulative plastic settlements developed under repeated loading and are shown in Fig.29. It is evident that geocell reinforced sections reduced the cumulative plastic settlements and the maximum reduction is observed for 75 mm height geocell reinforced section and least reduction for GC 150 mm section. Geocell of 100 mm height developed less plastic settlements initially but increased with number of repetitions and at the end of 100 cycles. GC 100 and GC 50 developed almost same cumulative plastic settlements. The ascending order of performance improvement (in terms of reducing cumulative plastic settlement) for various geocell reinforced sections was GC 150, GC 25, GC 50, GC 100 and GC 75.



**Figure 29.** Cumulative elastic and plastic settlements in unreinforced and geocell reinforced sections

The elastic settlements developed in the geocell reinforced sections depend upon the stiffness of the geocell mattress. Higher the height of geocell section, higher is the elastic settlement.

Though 150 mm height geocell reinforced section developed high elastic settlements initially, it decreased drastically after 10 cycles. As the height of geocell increases the cumulative plastic settlement decreases up to 75 mm height geocell and beyond that it again increases. Similarly when the height of geocell increases, the elastic settlement also increases. But for 25 mm, 50 mm and 75 mm sections the elastic settlement is more or less the same at the end of 100 cycles because when the height of geocell gets reduced, it behaves more or less like a planar reinforcement. The surface profile for unreinforced and geocell reinforced sections of various heights at the end of 50 and 100 cycles is shown in Fig. 30. From the figure it is seen that unreinforced section and 150 mm high geocell reinforced section developed heave compared to any other section. In all other geocell reinforcement sections, an overall settlement of the granular sub-base was observed. This infers that the load applied on the geocell mattress was distributed to a larger area and thus increases the overall stiffness of the sub-base.

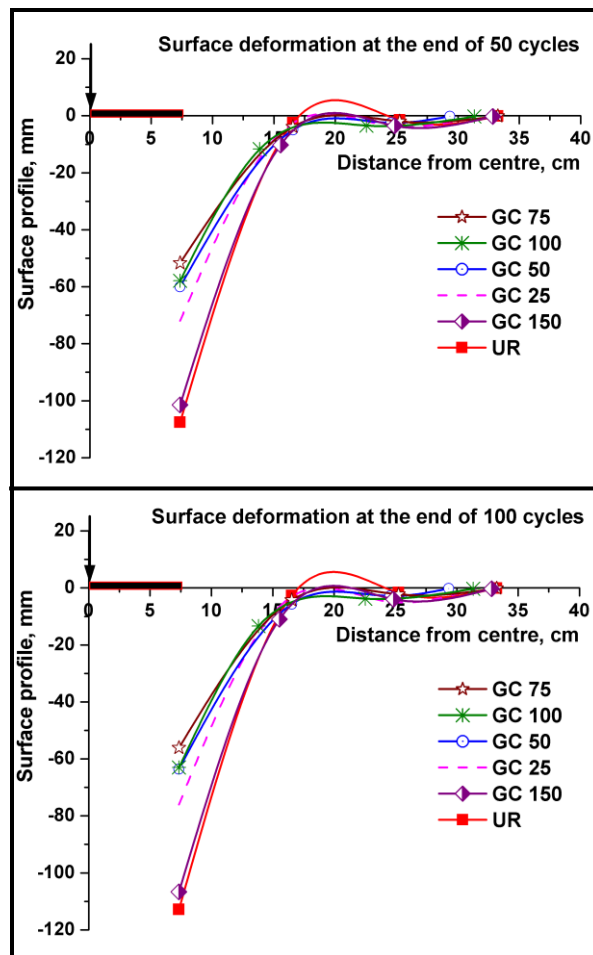


**Figure 30.** Surface profile at the end of 50 and 100 cycles for unreinforced and geocell reinforced sections

The elastic and plastic settlements developed in the 75 mm height geocell reinforced sections at various placement positions are compared in to understand the stiffness of the systems. Fig. 31 compares the improvement factors corresponding to the loading stage of first cycle for the unreinforced and 75 mm height geocell reinforced sections. It was observed that the order of performance of various sections in reducing cumulative plastic settlement is dependent on the height of the granular fill above i.e., higher the height of fill, lesser is the cumulative plastic settlement. On comparing the elastic settlements it can be seen that section with reinforcement placed at top had less elastic settlement compared to other two sections considered. This could be due to the loose packing of the granular material within the geocell pocket that too at a shallow depth from the surface making that section weak and flexible. Section with geocell placed at middle exhibited a stiff behaviour compared to section with geocell placed at interface and hence needed more elastic and plastic settlements to mobilize the tensile force in it.

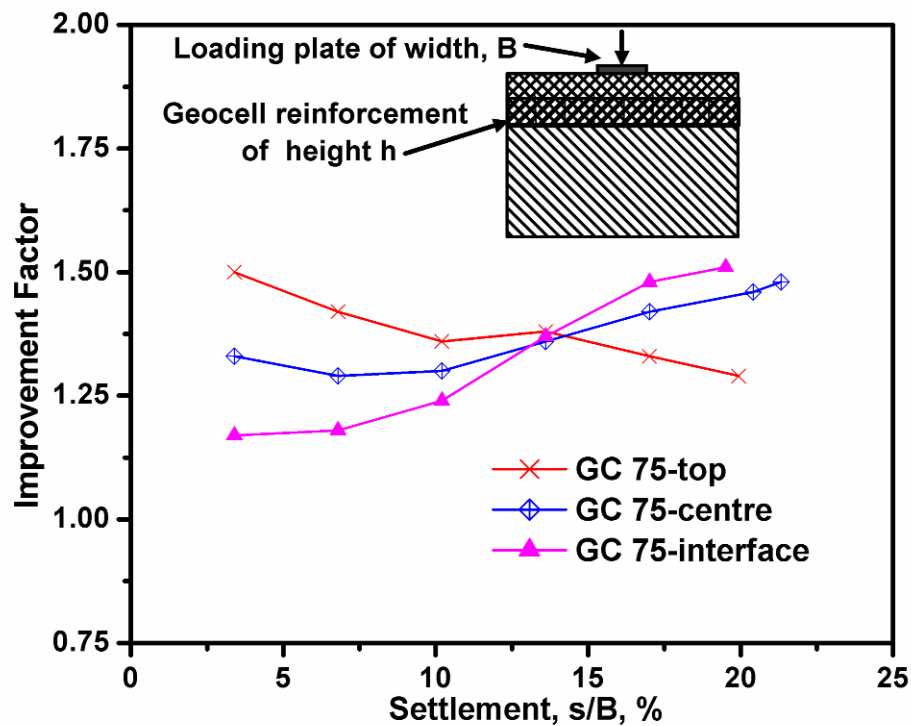


**Figure 31.** Variation of improvement factor for 75 mm height geocell sections at different positions with settlement of plate for loading stage of first cycle,  $s/B$  (%)

### Field Tests

Trafficability tests were conducted on geosynthetic reinforced unpaved roads in field, using prototype materials and vehicle, thus avoiding some of the limitations of small-scale

experiments. Planar geogrids layers and geocell layers fabricated on site using geogrids were used in different tests and the performance of geogrids in these two forms is compared. The site where the experiments were carried out is situated in Indian Institute of Science, Bangalore. The site chosen for constructing model road section was measured  $2\text{ m} \times 1\text{ m}$ . The soil at the location is classified as Sandy Clay with an undrained cohesion of 40 kPa and CBR value of 22%. The original soil at the location was mixed with excess amount of water and made slushy for a depth of 10 cm and leveled. The soil beneath this 10 cm depth will be dry or wet depending on summer or rainy season respectively. This bed was left as such for at least 24 hours so that the soil attained homogeneous consistency. The water content and unit weight of the subgrade were maintained as 30% and  $17\text{ kN/m}^3$  respectively. The prepared subgrade has an undrained cohesion of 12 kPa and CBR value of 1%. The aggregate used for the road section is of average size 12 mm. A biaxial geogrid having ultimate tensile strength of 40 kN/m in both the directions and a uniaxial geogrid having ultimate tensile strength of 60 kN/m in longitudinal direction and 20 kN/m in transverse direction were used as reinforcement.

In case of geotextile and geogrids, a geosynthetic layer was cut from the rolls and placed over the test section, covering the entire test section. The longitudinal direction of geosynthetic layer was coinciding with the length direction of the road for all the tests to achieve maximum benefit. In case of geocell reinforcement, initially a geotextile layer was placed over the subgrade. A layer of geocells was constructed in diamond pattern at the site to a size of  $2\text{ m} \times 1\text{ m}$  using biaxial geogrid and anchor pins of 6 mm diameter and 10 cm effective height and placed above the geotextile as shown in Figure 32. Geotextile layer was needed for this case to separate the subgrade and base course and to avoid mixing of layers during vehicle passage.

Tests were done with geocell layers of two different geometries, with the aspect ratio of cells as one and 0.5. The test with geocells of aspect ratio of 0.5 is compared with the test with planar reinforcement because both the tests use geogrid of  $2\text{ m}^2$  total area, comparing the cellular and planar form of geogrid reinforcement with the usage of same amount of reinforcement, as the area of geogrid used in tests with planar geogrid was  $2\text{ m}^2$ . The aggregate was placed over this bed directly (in case of unreinforced tests) or over the geosynthetic layer placed on top of the leveled soil subgrade (in case of reinforced tests). Total quantity of aggregate required to obtain the desired unit weight of  $13.05\text{ kN/m}^3$  for 10

cm thickness was divided into three portions and after spreading each portion, it was compacted using a hand roller and leveled.



**Figure 32.** Geocell layer prepared at the site

In case of tests with geocell reinforcement, aggregate was filled in geocells itself at the required density. The in-situ dry soil was mixed with 10% water and placed over the aggregate layer to prepare a comfortable riding surface. The thickness of this layer was maintained as 5 cm and it was leveled using a drop hammer. A scooter weighing 106 kg was driven by a person weighing 55 kg at the centre of the finished roadbed. The speed of the vehicle was maintained as 18 to 20 kmph and the vehicle was passed in one direction only. The rut depths were measured at marked grid points after every 20 passes until 200 passes were completed. Then it was passed continuously for 50 times more and the final rut depths were noted. If the vehicle started skidding in any point of time, the test was stopped at that particular stage and the corresponding number of passes and rut depths were noted.

Figure 33 compares the behaviour of geotextile, biaxial geogrid and geocell layer prepared using 5.85 m<sup>2</sup> area of biaxial geogrid (aspect ratio of 1) with the control section in terms of rut formation at different sections. Sections 1, 2 and 3 are spaced at equal distance along the road section, dividing the road into . The aspect ratio of cells was 1, as maintained in most of the field cases. From this plot, it is evident that this geocell layer is the most efficient form of reinforcement compared to all other types tested. Also reduction in heave of adjacent road

surface and more uniform settlements were observed in case of road section reinforced with geocell layer. However, the cost involved in preparing the geocell layer and the construction time are to be considered while assessing the relative beneficial effects of these reinforcing materials.

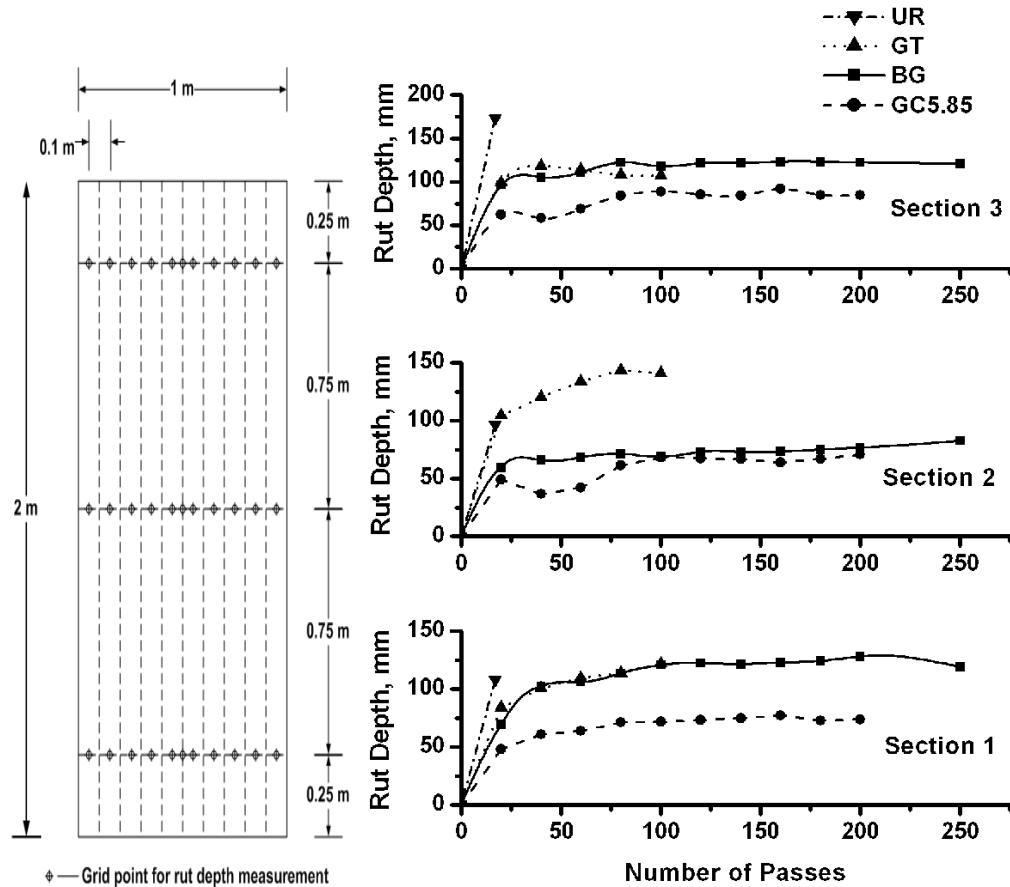


**Figure 33.** Comparison of performance of geocell layer with biaxial geogrid and geotextile at different sections

Note - UR: Unreinforced; BG: Biaxial Geogrid reinforced; GT: Geotextile reinforced; GC: Geocell reinforced

## 6. GEOCELLS FOR FLOOD PROTECTION

Geocells are being successfully employed for building flood protection systems. In catastrophic rain and emergency flood situations, these geocell flood walls offer stronger and effective control of holding back water. geocell flood wall offers quick set-up in comparison to sandbags and other traditional flood control techniques. The cellular system for these walls is made up of a strong geotextile and the cells are expanded and filled with sand or other suitable ballast material to provide structural support. These systems could be made use to constructed flood barriers of any shape and size in very less time. One more advantage of these systems compared to the traditional sand bags is that these systems function as a

cohesive singular structure as opposed to separate sandbag units that are susceptible to structural failure. Specific advantages of these systems are: Easy installation, quick removal, workability with tough terrains, durability and strength and economic pricing. Figure 34 shows geocell flood protection systems.



**Figure 34.** Geocell flood protection systems

These geocell flood protection systems have all the essential components such as speed, structural strength, low seepage rates, and reuse, each factor contributing equally to overall performance of a flood barrier. These flexible barrier systems can be designed to be used in various circumstances common in flood fight arenas. Applications include road building over unstable soils, levee seepage and boil control, mudslide diversion and control, and beach erosion. If these flood protection systems can be deployed in regional and strategic locations nationwide, we can ensure enhanced preparedness measures for floods in various parts of the country. These systems are a cheaper replacement to the traditional sand bags, but are extremely robust and suitable for rapid and easy installation. A highly successful case study of these geocell flood protection systems was reported in Smithland, Kentucky, USA in May 2011. Within 48 hours after receiving the flood warning, the installation teams were formed

from volunteers including local citizens, city employees, National Guard support, and even inmates from nearby correctional facilities. They could install more than 10,500 linear feet of Flood Walls, stretching over one mile in length stacked two units high, almost four feet of additional flood protection height to a key stretch of the levee to help raise the town levee to meet the pending flood projections

## **7. GEOCELLS FOR EROSION CONTROL IN SLOPES AND CHANNELS**

Soil slopes are prone to erosion due to wind or water forces. These forces form rills in the exposed soil. Over the time, these forces get concentrated within the rills, which accelerate the erosion process. Geocells could be successfully substituted for more costly conventional erosion control systems such as riprap, revetment mats, armour stones and gabions. To protect a slope from erosion, a layer of geocells is placed over the slope and anchored to the slope at specified intervals. These geocells confine the fill material and protect it from being moved by wind or water. Each cell acts as a dam that allows wind or water to pass over the top while holding the fill in place. The cell wall inhibits the formation of rills, thus preventing the erosive process. Grass can be grown in the pockets of geocell, making the slope more stable and attractive. On vegetated slopes, geocell system increases erosion resistance by encapsulating and protecting the vegetated root zone. As construction budgets tighten and environmental concerns rise, synthetic materials used to prevent soil transport have seen a rapid gain in popularity. Since natural surfaces are susceptible to large soil loss due to the kinetic energy generated by precipitation impact and flowing water, the magnitude of the erosion damage is a function of the surface's resistance to transport. Geocell erosion control systems have been developed specifically to strengthen the soil surface for these types of applications. These materials vary in size, shape and composition, but are all designed to decrease soil disturbance and increase soil moisture.

Since any increase in the tensile strength and/or density of the soil results in a greater resistance to applied forces, a dimensionally stable containment system is an attractive way of protecting a slope. Geocells are three-dimensional polyethylene structures that physically contain the infill material desired and resist the soils' natural weakness to detach and move downslope. These products are economical, aesthetically pleasing and quite easy to design and work with when involved in erosion control and channel lining projects. A variety of

materials can be used to build these erosion control systems into a three dimensional cellular network and they can be filled with choice of infill materials ranging from sand to gravel. Geocell layers provide protection for open channels and hydraulic structures. This type of protection is ideal for channels exposed to severe erosive conditions as well as channels with continuous flows. The hydraulic performance of conventional protection materials such as concrete, gravel, riprap and vegetation is greatly improved by confining them within the cellular structure.

A geocell channel protection system can be designed for a particular site based upon the factors like compatibility with local environment, ecological and aesthetic requirements, maximum anticipated flow conditions, associated hydraulic stresses and surface roughness. Geocell layer with a nonwoven geotextile under-layer combined with custom outlet ports assures effective subgrade drainage and subsoil protection. Vegetated soil can be used as infill material in geocell pockets for swales, ditches and on upper slopes of large channels, where low to moderate, intermittent flows occur. Geocell walls, which contain the topsoil infill, form a series of check-dams, extending throughout the channel protection system. Rill and gully development is restricted since the flow is continuously redirected to the surface. Figure 35 shows the schematic and photograph of geocell erosion control systems.



**Figure 35.** Schematic diagram and photograph of geocell erosion control system

## 8. GEOCELLS FOR DEFENSE APPLICATIONS

The geocell barrier system can be utilized to provide personnel and infrastructure protection in military and security applications. These systems are extremely light in weight, man portable and non-metallic with a small logistical footprint. They are commercially available

in various flexible and modular configurations and can be installed rapidly. These systems can be installed as defense barriers to provide protection from fire, blasts and bullets. They offer significant logistical advantages over sandbags and other barriers systems. Each unit is man portable, with section length close to 5m and weighing less than 10 kg. These cells can be filled with locally available materials, the system is modular in height and width allowing construction to meet the differing threat requirements. All parts are man portable and air droppable, facilitating deployment in hostile environments. Geocell security barriers (Defencell™) have been installed in many locations in UK and abroad to provide effective but discreet protection to infrastructure. Construction can be tailored in height, width and configuration to meet operational force protection requirements. Cellular structure provides considerable strength combined with built-in redundancy so if one cell is damaged the one behind will continue to provide protection and stability. The completely non-metallic structure has been extensively tested and protects against vehicle attack as well as blast and ballistic threats yet is easy to install and maintain. These systems are 5-10 times lighter than gabions and their all-textile construction minimizes risk of secondary fragmentation and RF interference sometimes caused by wire mesh gabions. These geocell barriers are tested for a wide range of ballistic threats and different explosive charges, and meet the protection requirements.



**Figure 36.** Applications of cellular confinement systems in military and security operations  
(from Defencell™ Website)

## **9 SUMMARY**

The beneficial use of geocell reinforcement for embankment basal reinforcement, reinforcing earth beds to support foundations, subgrade reinforcement for unpaved roads, retaining walls, flood protection and erosion control systems is reviewed. Laboratory and field experiments on geocell reinforced soil structures are presented and results showed that the geocell reinforcement is effective in improving the load carrying capacity of these structures and in reducing the deformations. Compared to the planar geosynthetic reinforcement, cellular reinforcement is many times effective in supporting the loads because of the all-round confinement effect. Major factors that influence the efficacy of the geocell layer are the aspect ratio of cells, tensile modulus of the geocell material and the infill material. In case of embankments, geocell layer helped in pushing the failure surface deep into the foundation bed, thus mobilizing more shear strength. In case of foundation beds, geocell reinforcement redistributed the load over wider area and provided resistance to the downward movement of the soil. In case of subgrades, geocell layer substantially improved the traffic benefit ratio. Other applications of cellular confinement systems, including slope erosion control, channel protection, flood protection and military barrier systems are briefly discussed.

## **REFERENCES**

- Bathurst, R.J. and Jarrett, P.M. (1988). "Large scale model tests of geocomposite mattresses over peat subgrades." *Transportation Research Record*, 1188, 28-36.
- Bathurst, R.J. and Karpurapu, R. (1993). "Large scale triaxial tests on geocell reinforced granular soils." *Geotechnical Testing Journal*, 16(3), 296-303.
- Bathurst, R.J. and Knight, M.A. (1998), "Analysis of geocell reinforced soil covers over large span conduits." *Computers and Geotechnics*, 22, 205-219.
- Binquet, J. and Lee, K.L. (1975). "Bearing capacity analysis on reinforced earth slabs." *Journal of Geotechnical Engineering Division, ASCE*, 101(12), 1257-1276.
- Bush, D.I., Jenner, C.G. and Bassett, R.H. (1990). "The design and construction of geocell foundation mattress supporting embankments over soft ground." *Geotextiles and Geomembranes*, 9, 83-98.
- Cowland, J.W. and Wong, S.C.K. (1993). "Performance of a road embankment on soft clay supported on a geocell mattress foundation." *Geotextiles and Geomembranes*, 12, 687-705.

- Dash, S. K., Krishnaswamy, N. R. and Rajagopal, K. (2001). "Bearing capacity of strip footings supported on geocell-reinforced sand." *Geotextiles and Geomembranes*, 19, 235–256.
- Han, J., Pokharel, S. K., Yang, X., Manandhar, C., Leshchinsky, D., Halahmi, I., and Parsons, R.L. (2011). "Performance of geocell-reinforced RAP bases over weak subgrade under full scale moving wheel loads", *ASCE Journal of Materials in Civil Engineering*, 23(11), 1525-1535.
- Henkel, D.J. and Gilbert, G.D. (1952). "The effect of the rubber membrane on the measured triaxial compression strength of clay samples". *Geotechnique*, 3, 20-29.
- Jenner, C.G., Bush, D.I. and Bassett, R.H. (1988). "The use of slip line fields to assess the improvement in bearing capacity of soft ground given by a cellular foundation mattress installed at the base of an embankment." *Proc. Int. Geotech. Symp. Theory and Practice of Earth Reinforcement*, Balkema, Rotterdam, 209-214.
- Johnson, W. and P.B. Mellor (1983). *Engineering Plasticity*. Ellis Marwood Ltd., Chichester. Van Nostrand Reinhold, UK.
- Krishnaswamy, N.R., Rajagopal, K. and Madhavi Latha, G. (2000), "Model studies on geocell supported embankments constructed over a soft clay foundation." *Geotech. Testing J., ASTM*, 23(2), 45-54.
- Latha, G.M. and Manju, G.S. (2016). "Seismic Response of Geocell Retaining Walls Through Shaking Table Tests". *International Journal of Geosynthetics and Ground Engineering*, 2(7), 1-15.
- Latha, G. M. and Somwanshi, A. (2009). "Effect of reinforcement form on the bearing capacity of square footings on sand", *Geotextiles and Geomembranes*, 27(6), 409-422
- Madhavi Latha G., Rajagopal K. and Krishnaswamy N.R. (2006). "Experimental and theoretical investigations on geocell supported embankments." *Int. J. of Geomechanics*, 6(1), 30-35.
- Madhavi Latha, G. (2000). "Investigations on the behavior of Geocell supported embankments." Ph.D. Thesis, Indian Institute of Technology Madras, Chennai, India.
- Madhavi Latha, G. and Rajagopal, K. (2007). "Parametric finite element analyses of geocell supported embankments." *Canadian Geotechnical Journal*, 44(8), 917-927.
- Madhavi Latha, G. and Vidya S. Murthy. (2007). "Effects of reinforcement form on the behaviour of geosynthetic reinforced sand." *Geotextiles and Geomembranes*, 25, 23-32.

- Madhavi Latha, G., Asha M Nair and Hemalatha, M.S. (2010). "Performance of geosynthetics in unpaved roads." *International Journal of Geotechnical Engineering*, 4(2), 151-164.
- Madhavi Latha, G., Dash, S. K. and Rajagopal, K. (2008). "Equivalent continuum simulations of geocell reinforced sand beds supporting strip footings." *Geotechnical and Geological Engineering*, 26(4), 387-398.
- Madhavi Latha, G. Asha M Nair and Hemalatha, M.S. (2010) "Performance of geosynthetics in unpaved roads", *International Journal of Geotechnical Engineering*. 4(2), 151-164
- Nair, A.M. and Latha, G.M. (2014). "Large diameter triaxial tests on geosynthetic-reinforced granular sub-bases", *Journal of Materials in Civil Engineering*, ASCE, 04014148:1-8.
- Nair, A.M. and Latha, G.M. (2016). "Repeated load tests on geosynthetic reinforced unpaved road sections", *Geomechanics and Geoengineering*, 11(2), 95-103.
- Rajagopal, K., Krishnaswamy, N.R. and Madhavi Latha, G. (1999), "Behavior of sand confined in single and multiple geocells." *Geotextiles and Geomembranes*, 17, 171-184.
- Rea, C., and Mitchell, J.K., (1978). "Sand reinforcement using paper grid cells", Preprint 3130, ASCE spring convention and exhibit, Pittsburgh, PA, 644-663.

## **Ground improvement Case studies**

Minimol Korulla

Chief Technical Officer at Maccaferri Environmental Solutions Pvt. Ltd.

*Case Study -1: Road Over Bridge connectivity between Mundra and NH8A near PMC Building, Port Road, Mundra, Gujarat.*

Mundra Special Economic Zone is located in Kutch district, Gujarat and is one of the largest SEZ in India. An ROB was proposed over the railway line that cuts across the connectivity road between Mundra and NH8A. The approaches of ROB were proposed to be retained by Reinforced soil wall system (granular fill soil unit weight 20KN/m<sup>2</sup> and angle of internal friction 32). Maximum height of reinforced soil wall was 9m. However, foundation soil comprising primarily of sandy silt with clay was found to have inadequate load bearing capacity to bear the load of retaining walls. The soil upto 3m depth was clayey silt followed by silty sand upto 4.5m depth. And sandy silt with traces of clay till 9m depth.

Keeping in mind the high water table and high consolidation settlements, such a ground improvement technique was to be proposed which would improve bearing capacity of soil, reduce post construction settlement and also facilitate process of implementation. By providing conventional solutions of soil replacement other such techniques was not warranted and would have had made the structure commercially unviable. Thus, considering all these factors, stone column technique with a geosynthetic raft i.e. basal reinforcement was adopted.

High strength geogrids having mono axial array of geosynthetic strips, which has planar structure were used as basal reinforcement to improve the strength of underlying soil with a drainage layer and geotextile in between. The uni directional ultimate strength of mono axial geogrid was 200KN/m. Stone columns were used to reduce the settlement of approach road at higher heights. The high strength geogrids placed were effectively able to distribute the stress uniformly to foundation soil, thereby decreasing the differential settlement. Maximum tensile load was calculated as sum of loads needed to transfer the vertical embankment lading on the stone columns and load needed to resist lateral sliding. Since the load was transmitted to stone columns, settlement of the soil in between the columns was also reduced considerably.

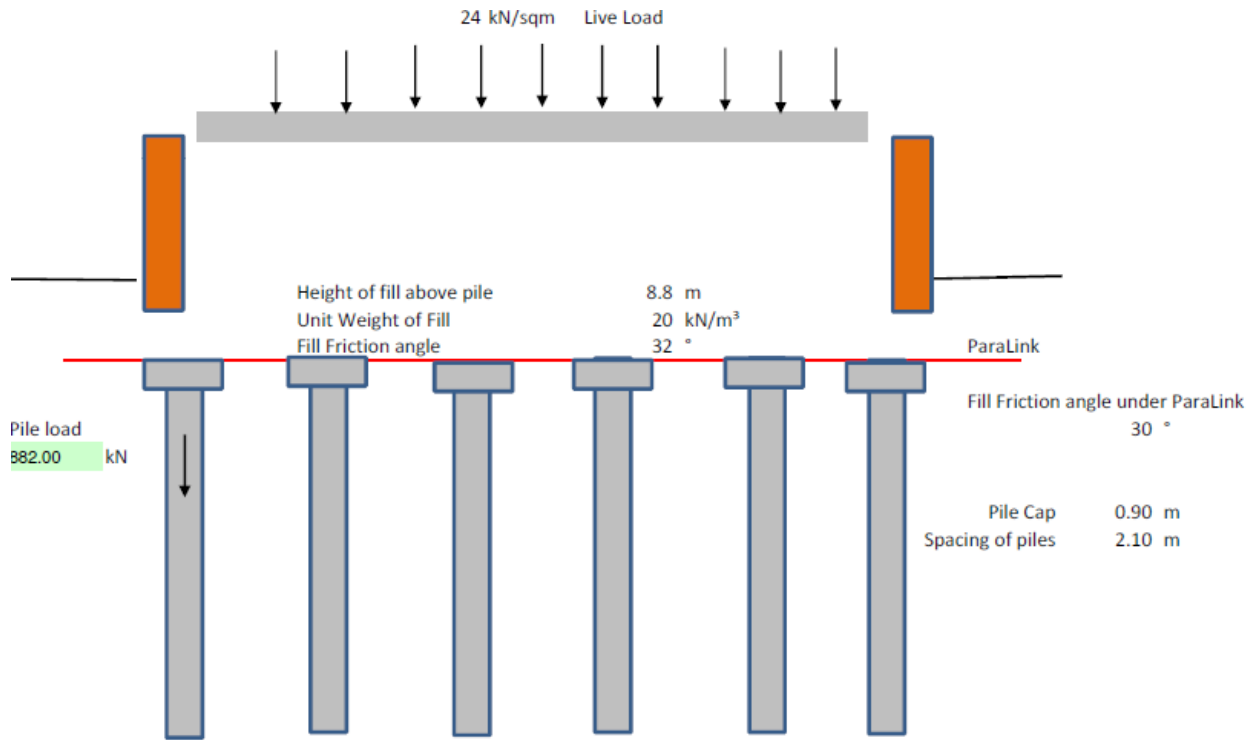


Figure 1. Schematic representation of Ground improvement- Pile (stone columns) supported Basal Reinforcement.

The complete Pile (stone columns) supported Basal Reinforcement was designed as per BS 8006. Ultimate limit state i.e. Stone column group capacity, extent, vertical load shedding onto stone columns caps, lateral sliding stability of embankment fill and over all stability was considered. Serviceability limit state for Excessive strains in reinforcement and settlement of stone column foundation were also checked. In this project the stone columns were designed as per 15284 (Part 1).

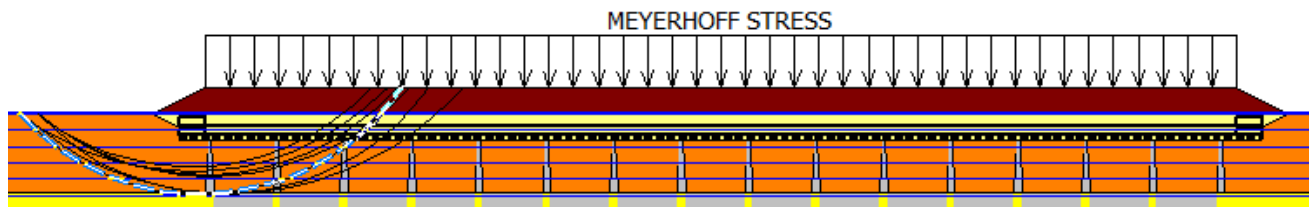


Figure 2. Schematic representation of global stability check output

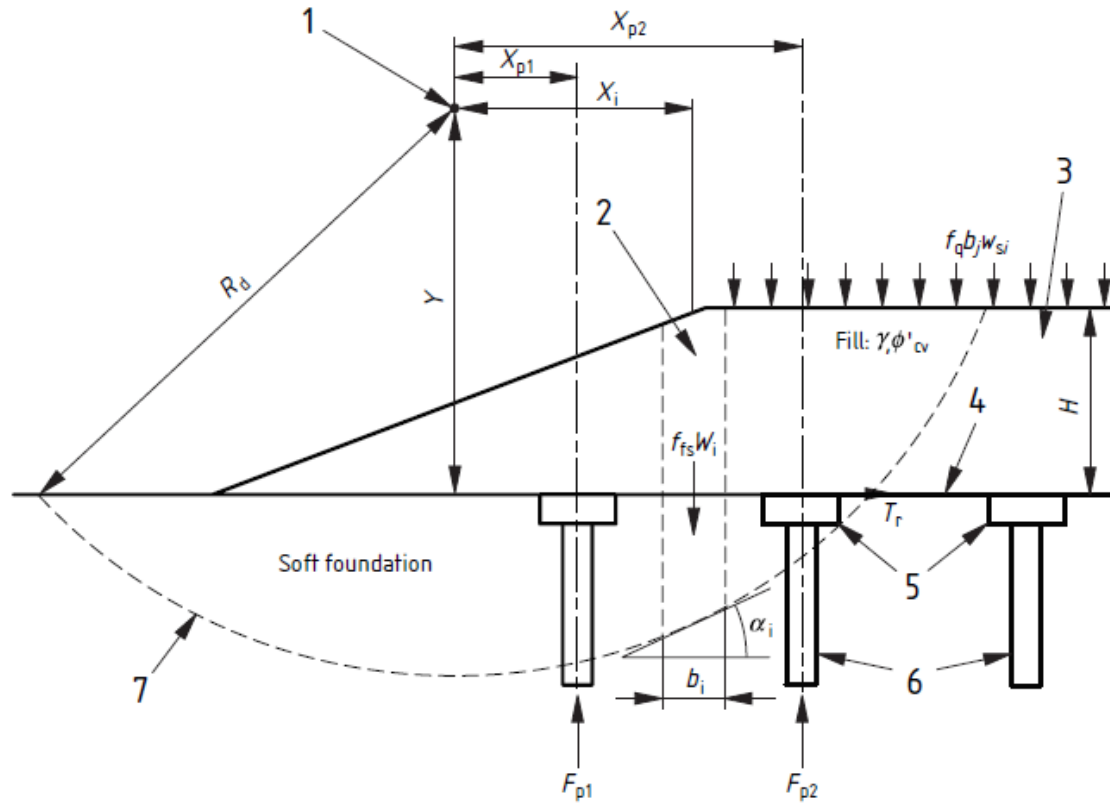


Figure3. Variables used in analysis of overall stability of basal reinforced piled embankments

Note:

1 Slip circle centre, 2 Slice i, 3 Embankment, 4 Reinforcement, 5 Pile caps, 6 Piles, 7 Most critical slip surface

The area is recommended to be excavated till the founding level where the stone columns are installed.

Stone columns:

- South side - entire zone including the reinforced and unreinforced section was improved by stone column technique.
- North side - owing to relatively better quality of soil, stone columns were provided only under reinforced soil.

High strength geogrid was laid throughout the entire zone both in the North and South side of the structure. The surface of the stone column was covered with a free draining granular fill compacted to 95% of Modified Proctor density.

Table Summary of ground improvement

Wall Heights(m)	8.8	8	7.2	6.4	5.2 & down
-----------------	-----	---	-----	-----	------------

Ultimate tensile strength of geogrid (KN/m)	200	200	200	200	200
Stone column Dia(m)	0.6	0.6	0.6	0.6	0.6
Stone column Spacing(m)	1.55	2	2	2.2	2.5

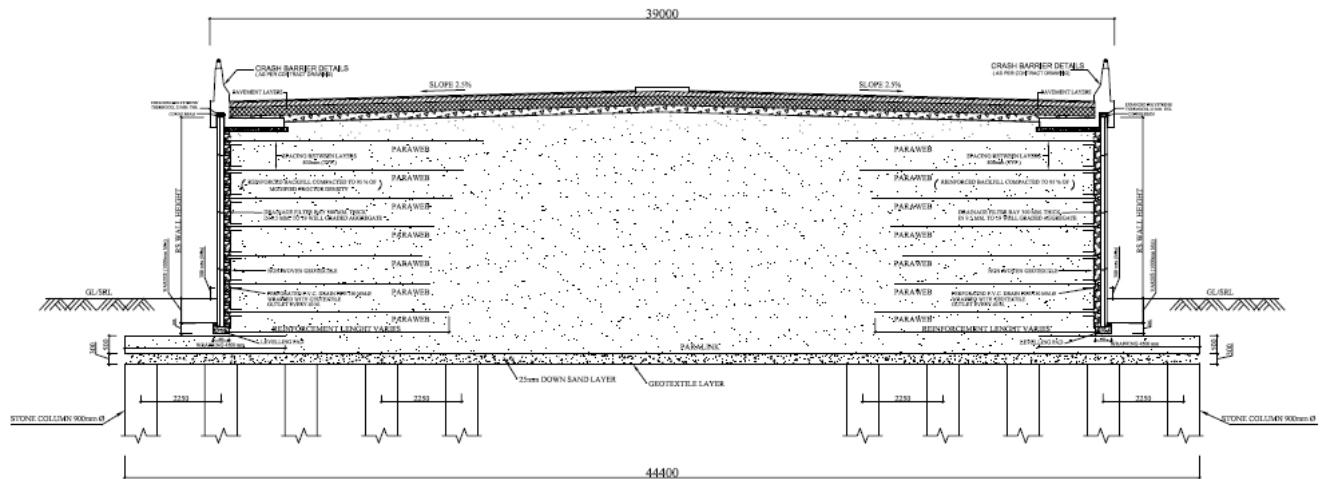


Figure 4. Typical Cross section of Ground Improvement and Reinforced soil wall- North Side

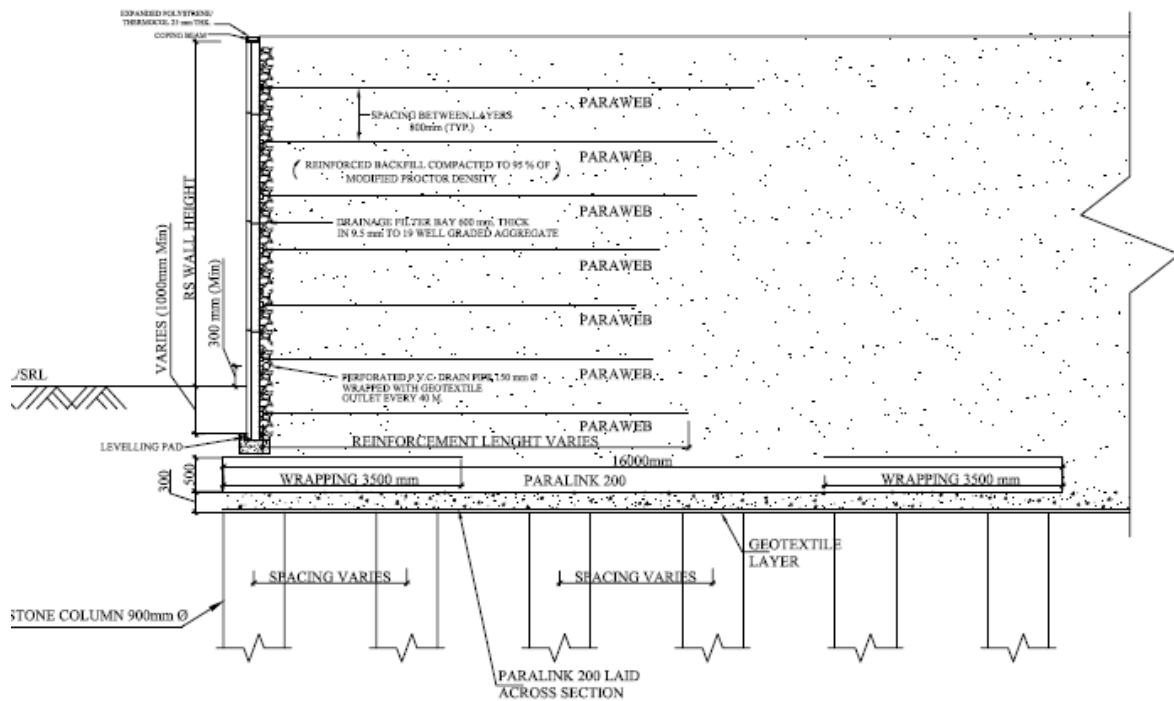


Figure 5. Typical cross section of ground improvement at Cross wall.



Photo 1 Installation of stone column



Photo 2 Installation of drainage layer



Photo 3 Laying of High strength uniaxial Geogrid



## **Case study 2: Ground improvement for ramp at Calcutta riverside, Bhatnagar**

River Bank Developers Pvt. Ltd. was widening the approach ramp that leads to a ROB at the entrance of the project. Existing ramp is an open embankment, however due to scarcity of space Reinforced Soil Wall is to be constructed for the proposed ramp. The proposed road/ ramp will move parallel to the existing road and then will merge with the existing road before the location of the ROB. Length of the ramp was about 160m and the height varies from 1m at the start to about 6.4m near the ROB.

### **Objective**

The subsoil at location of Reinforced Soil wall upto a depth of 10 m is soft to very soft silty clay having S.P.T. value ranging from 0 - 4. Besides this the water table was at a depth of 0.5m. Area to be consolidated was 1691.2 m<sup>2</sup>. Construction without some sort of soil treatment was impractical due to unpredictable long-term settlement. Although surcharging increases pore water pressure, yet settlement can take considerable time, often years, as the water lacks an easy path to leave the soil. Hence the requirement of ground improvement here was such that it is cost effective and time saving.

### **Solution Proposed**

Prefabricated Vertical Drains (PVD) for accelerated consolidation of soft soil was adopted to accelerate settlements, to reduce time for consolidation & to avoid Post Construction settlements. As a surcharge, an embankment of height equivalent to the height of ramp was constructed and was kept for duration of 45 days. During this time consolidation of soft soil has occurred. Consolidation of soft cohesive soils using prefabricated vertical drains reduced settlement times from years to months. Most settlement has occurred during construction, thus keeping post-construction settlement to a minimum. The Prefabricated Vertical Drains are less expensive, are installed more easily and quickly and gave better drainage by providing shortened drainage paths for the water to exit the soil. The spacing of PVD's adopted was 1.2m c/c in a square configuration to achieve 90% consolidation in 45 days. Installation of 13,860 m length of PVD's was completed in 15 days after the sand bed was laid. Above PVD's a drainage blanket of 0.3 – 0.5 m. was placed for drainage purpose

### **Design Considerations**

The following design parameters were considered to find out the required spacing of PVD's to achieve 90% consolidation.

Co-efficient of vertical consolidation ( $C_v$ ) =  $2.31 * 10^{-3} \text{ cm}^2 / \text{sec}$  (Calculated from soil investigation report by referring BH. No. 1)

Co-efficient of radial consolidation ( $C_h$ ) =  $C_v = C_h$  (Assumed)

Average degree of consolidation  $U = 90\%$  (Assumed)

Undrained cohesion of clay =  $31 \text{ kN/m}^2$  (As per soil investigation report)

Plasticity index of soil =  $22\%$  (As per soil investigation report)

Unit weight of clay =  $17.8 \text{ kN/m}^3$  (bulk) (As per soil investigation report)

Depth of clay layer =  $10 \text{ m}$  (As per soil investigation report)

Consolidation Period = Preferred period  $1.5 - 2.0$  Month (Assumed)

Area to be consolidated =  $151 * 11.2 (10+0.6+0.6) = 1691.2 \text{ m}^2$

## Conclusions

Based on the design,

- 1) The spacing of PVD's is calculated  $1.2$  meter center to center (if  $C_h = C_v$ ) to achieve a  $\sim 90\%$  consolidation within  $1.5 - 2.0$  months. The detail calculations are shown in Annexure-II.
- 2) PVD's are provided upto  $1.5 \text{ m}$ . height of RS wall i.e. up to  $151 \text{ m}$ . length of wall. For remaining length of a wall (approx.  $29 \text{ m}$ .) a well granular soil having angle of internal friction  $32$  degree can be placed up to  $1 \text{ m}$ . below levelling pad to take care of safe bearing capacity as well as settlement.
- 3) Above PVD's a drainage blanket of  $0.3 - 0.5 \text{ m}$ . should be placed for drainage purpose.
- 4) The total required length of PVD's is  $13860$  (including  $10\%$  wastage).



**Fig-1: Installed PVD's**



**Fig-2: Installation of PVD**

### **Case study 3: South kasheli creek bridge Thane Bhiwandi Vadapa road, Maharashtra**

Kasheli Bridge built since British time lies on the Old Agra Road over the Thane Creek. This bridge is 460 meters long and connects the Thane mainland to Bhiwandi. For a major bridge across Thane Bhiwandi Vadapa Road, the solid approaches were required to be retained using reinforced soil walls. There was an embankment existing for many years. The road had to be widened to the increased width of the bridge. The subsurface comprised of top 4 to 6 m of very soft to soft dark grey clay. From 7.5 m to 10.0 m soil constituted silty clay. This layer was followed by medium dense dark grey medium sand. As the structures were near the ground water table was at existing ground level. The construction of approaches had to be completed quickly with minimum post construction settlement.

#### **Solution**

In order to achieve the required global and bearing stability, basal reinforcement over piles was implemented for the new embankment. The piled embankment technique allowed embankments to be constructed to the required heights without any restraint on construction rate with control on post construction settlements. Basal reinforcement was used to form a geosynthetic raft over piles and transfer the load to the piles, and thus enabling to maximize the economic benefits of the piles installed in soft foundations. The reinforcement also helped in counteracting the horizontal thrust of the embankment fill and the need for raking piles along the extremities of the foundation could be eliminated. Fill soil properties were considered as: cohesion-0 kN/m<sup>2</sup>, angle of friction-32°, unit weight-20 kN/m<sup>2</sup>. The maximum height of the embankment was 9.6m.

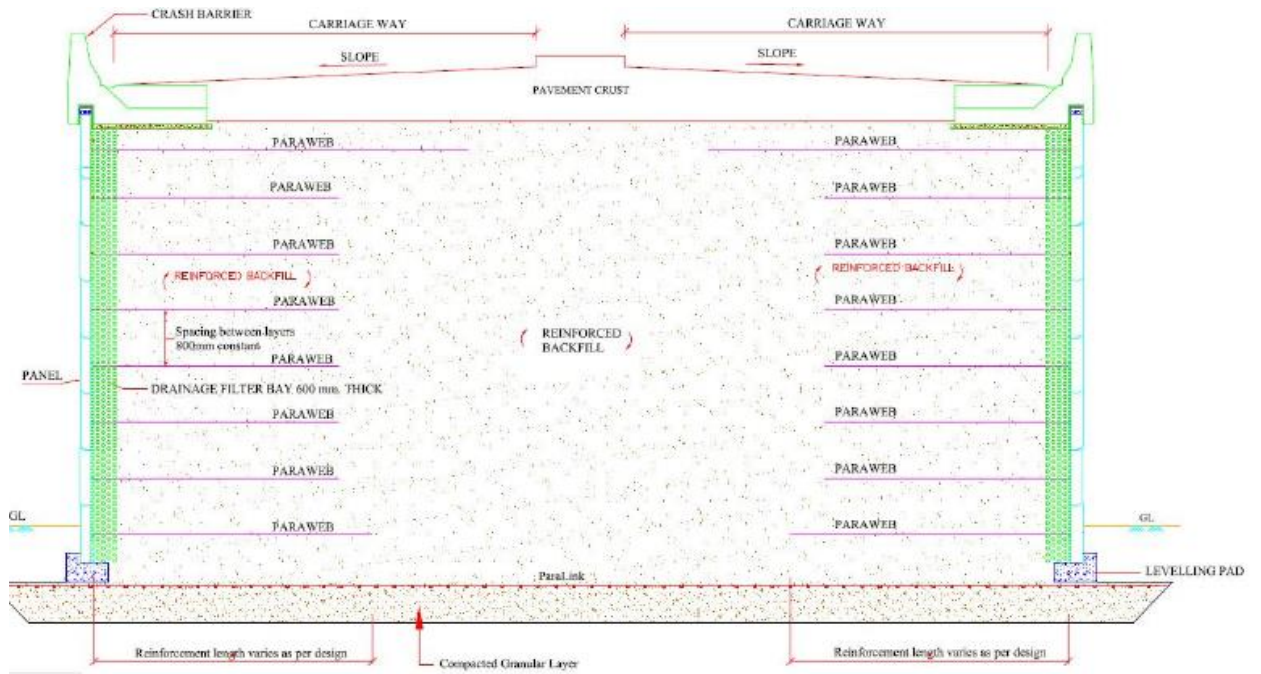


**Fig-1: Typical Cross sectional drawing**

In the direction along the length of the embankment, the maximum tensile load should be there which needed to transfer the vertical embankment loading onto the pile caps. In the direction along the width of the embankment the maximum tensile load should be the sum of the load which needed to transfer the vertical embankment loading onto the pile caps and the load needed to resist lateral sliding. Basal reinforcement proposed here was high strength geogrid which has planar structure consisting of a uni-axial array of composite geosynthetic strips.

Each single longitudinal strip had a core of high tenacity polyester yarns tendons encased in a polyethylene sheath; the single strip was connected by cross laid polyethylene strip which gave a grid like shape to the composite. Two layers of geogrid having uni-axial strength 400 kN/m each along and across the road were given. The design was carried out according to BS: 8006 (1995). The design of piled embankments was not included in the scope of the present document.



**Fig-2: Laying of Geotextile over Pile caps**



**Fig-3: Laying of basal reinforcement over pile caps**



**Fig-4: Completed Reinforced soil wall structure**

## **Case study 4 Road Over Bridge near Dibrugarh (ROB 15) Assam, India**

### **Objective**

A Road Over Bridge was to be constructed in Dibrugarh, district Assam by Northeast Frontier Railway. The approaches of the ROB were to be retained by Reinforced Soil walls. Moreover, the soil at the site was cohesive (CI) for the top 3m, followed by loose to medium dense fine silty sand. After investigation it was found that the shear properties of the soil were weak and hence a major problem of bearing and global instability could be expected.

### **Solution**

For retaining the bridge approaches, mechanically stabilized concrete panel wall using geosynthetic strip as reinforcement was constructed as the vertical retaining wall. In order to avoid deep excavation and replacing the soil, panel wall system with basal reinforcement as ground improvement was constructed.

Basal reinforcement was provided for construction of embankments on soft soils, which is a very efficient technique to improve the bearing capacity and global stability of the foundation as all the stresses on the foundation is taken care by the reinforcement that is provided. Basal reinforcement prevents collapse and limit vertical movement of the embankment surface following the formation of a void in the foundation.

Ground improvement was done for heights ranging from 6m to 5m and 5m to 1m for Seismic and Static conditions present at the site. High strength uni-axial geogrids as basal reinforcement with a tensile strength of 50kN/ m was used for ground improvement.

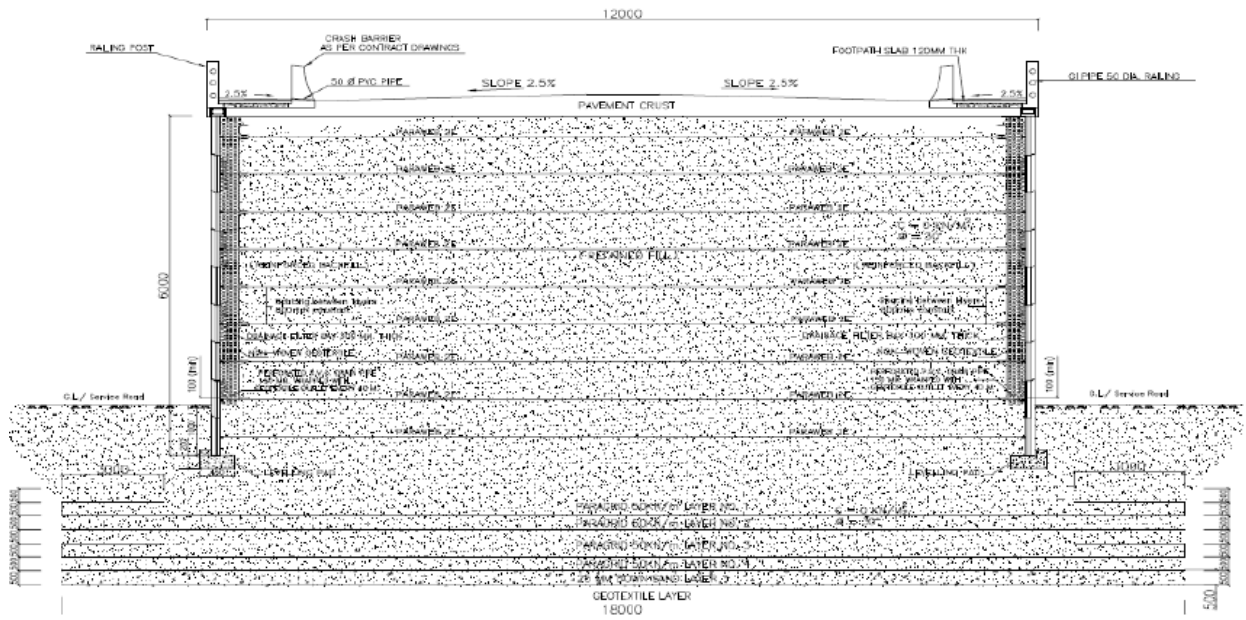


**Fig-1: Cross section of Reinforced soil wall for 6m height near abutment**



**Fig-2: Installation of Geotextile**



**Fig-3: Spreading of fill material over installed Geotextile**



**Fig-4: Compaction of fill material over installed Geotextile**



**Fig-5: Installed high strength uni-axial Geogrid (basal reinforcement)**



**Fig-6: Installation of RS wall system over improved ground**